Characterization of Transverse Profiles

PUBLICATION NO. FHWA-RD-01-024 APRIL 2001

U.S. Department of Transportation
Federal Highway Administration

Research, Development, and Technology
Turner-Fairbank Highway Research Center
6300 Georgetown Pike
McLean, VA 22101-2296

FOREWORD

This report documents a study undertaken to identify and evaluate indices to characterize pavement rutting. As a result of this work, several transverse profile indices have been added to the Long Term Pavement Performance (LTPP) database to facilitate future analysis. In addition, the study has yielded important findings regarding the accuracy and repeatability of three- and five-point rut depth measurements commonly collected for pavement management purposes. It was found that the three-point rut depth measurement does not provide repeatable and accurate measurement of pavement rutting. Also, if a five-sensor rut bar is used for network-level data collection, care should be taken to ensure that the transverse location of the rut bar is consistent from year to year and that the mean values are adjusted to reflect more realistic rut depth values.

This report will be of interest to highway agency engineers involved in the collection, processing, and interpretation of data collected to characterize pavement rutting. The study findings regarding the repeatability and accuracy of three- and five-point rut depth measurements have been summarized in Publication No. FHWA-RD-01-027, which may be found at http://www.tfhrc.gov/pavement/lttpp/library.htm under "TechBriefs."

T. Paul Teng, P.E.
Director, Office of Infrastructure
Research and Development

NOTICE

This document is disseminated under the sponsorship of the Department of Transportation in the interest of information exchange. The United States Government assumes no liability for its contents or use thereof. This report does not constitute a standard, specification, or regulation.

The United States Government does not endorse products or manufacturers. Trade and manufacturers' names appear in this report only because they are considered essential to the object of the document.

Technical Report Documentation Page

1. Report No.	2. Government Accession No.	3. Recipient's Catalog No.
FHWA-RD-01-024		

4. Title and Subtitle	5. Report Date
Characterization of Transverse Profiles	6. Performing Organization Code

7. Author(s)	8. Performing Organization Report No.
A.L. Simpson	

9. Performing Organization Name and Address	10. Work Unit No. (TRAIS)
Fugro-BRE, Inc. 8613 Cross Park Drive Austin, Texas 78754	11. Contract or Grant No. DTFH61-96-C-00003

12. Sponsoring Agency Name and Address	13. Type of Report and Period Covered
Office of Infrastructure Research and Development Federal Highway Administration 6300 Georgetown Pike McLean, Virginia 22101-2296	Final Report, 1997-2000 14. Sponsoring Agency Code

15. Supplementary Notes

Data used in this study was obtained from NIMS release 8.6. The files are dated October 1998.
Contracting Officer's Technical Representative (COTR): Cheryl Richter, HRDI-13
Project Contractor: ERES Consultants, Inc.
Subcontractor: Fugro-BRE, Inc.

16. Abstract

A study of the transverse profile data currently being collected under the Long Term Pavement Performance project was undertaken. The data were collected by three processes: (1) Dipstick®, (2) a photographic method, and (3) straightedge used to collect rut depths.

This study examined several indices for the purposes of quantifying and qualifying the transverse profiles. It is recommended that five indices be added to the National Information Management System. These indices include the area of the rut below a straight line connecting the end points of the transverse profile, the total area below the straight lines connecting the maximum surface elevations, the maximum depth for each wheelpath between a 1.8-m straightedge placed across the wheelpath and the surface of the pavement, and the width of the rut based on a 1.8-m straightedge.

These indices were studied in order to determine typical trends by climate, surface thickness, soil type, and age. In addition, the time-series trends for each test section were studied in order to determine whether any anomalies existed and the potential causes of these anomalies.

17. Key Words	18. Distribution Statement
Transverse profile, permanent deformation, rut depth, asphalt pavement.	No restrictions. This document is available to the public through the National Technical Information Service, Springfield, Virginia 22161.

19. Security Classif. (of this report)	20. Security Classif. (of this page)	21. No. of Pages	22. Price
Unclassified	Unclassified	303	

Reproduction of completed page authorized

SI* (MODERN METRIC) CONVERSION FACTORS

APPROXIMATE CONVERSIONS TO SI UNITS

Symbol	When You Know	Multiply By	To Find	Symbol
	LENGTH			
in	inches	25.4	millimeters	mm
ft	feet	0.305	meters	m
yd	yards	0.914	meters	m
mi	miles	1.61	kilometers	km
	AREA			
in^2	square inches	645.2	square millimeters	mm^2
ft^2	square feet	0.093	square meters	m^2
yd^2	square yards	0.836	square meters	m^2
ac	acres	0.405	hectares	ha
mi^2	square miles	2.59	square kilometers	km^2
	VOLUME			
fl oz	fluid ounces	29.57	milliliters	mL
gal	gallons	3.785	liters	L
ft^3	cubic feet	0.028	cubic meters	m^3
yd^3	cubic yards	0.765	cubic meters	m^3
NOTE: Volumes greater than 1000 l shall be shown in m^3.				
	MASS			
oz	ounces	28.35	grams	g
lb	pounds	0.454	kilograms	kg
T	short tons (2000 lb)	0.907	megagrams (or "metric ton")	Mg (or "t")
	TEMPERATURE (exact)			
°F	Fahrenheit temperature	5(F-32)/9 or (F-32)/1.8	Celcius temperature	°C
	ILLUMINATION			
fc	foot-candles	10.76	lux	lx
fl	foot-Lamberts	3.426	candela/m^2	cd/m^2
	FORCE and PRESSURE or STRESS			
lbf	poundforce	4.45	newtons	N
lbf/in^2	poundforce per square inch	6.89	kilopascals	kPa

APPROXIMATE CONVERSIONS FROM SI UNITS

Symbol	When You Know	Multiply By	To Find	Symbol
	LENGTH			
mm	millimeters	0.039	inches	in
m	meters	3.28	feet	ft
m	meters	1.09	yards	yd
km	kilometers	0.621	miles	mi
	AREA			
mm^2	square millimeters	0.0016	square inches	in^2
m^2	square meters	10.764	square feet	ft^2
m^2	square meters	1.195	square yards	yd^2
ha	hectares	2.47	acres	ac
km^2	square kilometers	0.386	square miles	mi^2
	VOLUME			
mL	milliliters	0.034	fluid ounces	fl oz
L	liters	0.264	gallons	gal
m^3	cubic meters	35.71	cubic feet	ft^3
m^3	cubic meters	1.307	cubic yards	yd^3
	MASS			
g	grams	0.035	ounces	oz
kg	kilograms	2.202	pounds	lb
Mg (or "t")	megagrams (or "metric ton")	1.103	short tons (2000 lb)	T
	TEMPERATURE (exact)			
°C	Celcius temperature	1.8C + 32	Fahrenheit temperature	°F
	ILLUMINATION			
lx	lux	0.0929	foot-candles	fc
cd/m^2	candela/m^2	0.2919	foot-Lamberts	fl
	FORCE and PRESSURE or STRESS			
N	newtons	0.225	poundforce	lbf
kPa	kilopascals	0.145	poundforce per square inch	lbf/in^2

* SI is the symbol for the International System of Units. Appropriate rounding should be made to comply with Section 4 of ASTM E380.

(Revised September 1993)

TABLE OF CONTENTS

CHAPTER **PAGE**

TABLE OF CONTENTS (CONTINUED)

CHAPTER **PAGE**

LIST OF FIGURES

FIGURE **PAGE**

LIST OF FIGURES (CONTINUED)

FIGURE **PAGE**

LIST OF FIGURES (CONTINUED)

FIGURE **PAGE**

LIST OF FIGURES (CONTINUED)

FIGURE **PAGE**

LIST OF FIGURES (CONTINUED)

FIGURE **PAGE**

LIST OF FIGURES (CONTINUED)

FIGURE **PAGE**

LIST OF FIGURES (CONTINUED)

FIGURE **PAGE**

LIST OF FIGURES (CONTINUED)

FIGURE **PAGE**

LIST OF FIGURES (CONTINUED)

FIGURE **PAGE**

LIST OF TABLES

TABLE **PAGE**

CHAPTER 1. INTRODUCTION

BACKGROUND

Rutting is not just a common mode of distress on asphalt pavements, but also a safety hazard because it allows water to pool on the roadway. Many studies have attempted to predict the progression of rutting in asphalt concrete and composite pavements. In some of the studies, rutting or rut depth is referred to as "permanent deformation." However, permanent deformation is layer- or material-dependent, while rutting measured at the surface is the accumulation of permanent deformation in each pavement layer and the subgrade. The terms "rutting" and "rut depth" will be used exclusively within this report.

Rutting measured on the pavement's surface is caused by three different mechanisms. These are:

- One-dimensional vertical permanent or plastic deformation in the asphalt concrete layers (typically referred to as localized densification).

- Lateral flow in the asphalt concrete mixtures (sometimes referred to as accelerated deformation, tertiary or shear flow).

- Mechanical deformation of subsurface layers.

Unfortunately, rut depths measured with a 1.2-m or 1.8-m straightedge (the two lengths most commonly used) do not identify the mechanism of the rutting observed at the surface. Identification of the cause is critical to the development of an accurate rutting prediction model; however, more importantly, it would be highly beneficial for managing pavements and selecting appropriate rehabilitation options.

Within the Long Term Pavement Performance (LTPP) program, transverse profiles have been used to quantify wheelpath rutting and other types of surface distortion. Currently, these profiles exist within the National Information Management System (NIMS) as a series of x-y points defining the pavement surface. Rut depths measured using a 1.2-m straightedge are available in the NIMS, but no indices representing the transverse profile measurements were available when the work reported herein was undertaken.

Different agencies have used different measurement techniques for quantifying the surface rut depths along a roadway for use in managing and evaluating their pavements. The American Society for Testing and Materials (ASTM) has a specification (ASTM E1703-95) for measuring the rut depth of a pavement using a straightedge. ASTM E1656-94 covers the collection of automated transverse profile data. Currently, Texas uses a five-point system in which x-y coordinates are collected adjacent to the lane edge, in each wheelpath, and mid-lane. The rut depth is defined as the vertical distance between a line connecting the points at the edges of the lane and the point in each wheelpath. Many States, such as Kansas and Florida, use a three-point system in which data are collected in each wheelpath and mid-lane. In this case, the rut depth is

defined as the difference in elevation between the mid-lane measurement and the wheelpath measurements.

The use of these various systems (the straightedge, 3.7-m string line, five-point system, three-point system, and the transverse profile) is not conducive to the standardized system that is required for the development of a mechanistic-empirical rutting prediction model. More importantly, a one-parameter index (i.e., rut depth) does not allow one to identify the mechanism or mechanisms that cause the surface distortions.

OBJECTIVES

The objectives for this research were as follows:

- Identify and characterize representative cross-profiles.
- Quantify bias and precision in time-series measurements.
- Select methodology and compute rut indices.

SCOPE OF REPORT

This report is divided into eight chapters. The second chapter provides an overview of how transverse profile data have been collected for LTPP. The third chapter provides the definitions of the indices that were considered in this study and how these indices are calculated. The fourth chapter presents comparisons of the indices. The fifth chapter examines the variability of the indices. It also compares the indices to common materials characteristics and pavement parameters to relate the behavior of the indices to commonly accepted theories of rutting. The sixth chapter evaluates the methods of data collection that are most commonly used by the States. The seventh chapter provides the field-determined bias and precision values that may be expected from each index. The eighth chapter summarizes the investigations and provides recommendations for future research.

CHAPTER 2. DATA USED IN STUDY

Transverse profile measurements are made within the LTPP program using three different procedures. These three procedures are listed below and each of these procedures is described in this chapter.

- PASCO RoadRecon 75
- FACE Dipstick®
- 1.2-m Straightedge

Dipstick® is used whenever a manual distress survey is conducted. These measurements are intended as a backup for the transverse profile measurements collected by RoadRecon 75. The 1.2-m straightedge measurements are required for the SPS-3 projects only, but were obtained on some sections in other experiments.

PASCO RoadRecon 75

Data Collection Equipment

The PASCO RoadRecon system incorporates a van driven across the test section at night. A boom, on which a 35-mm camera has been mounted, extends from the rear of the van at the top of the unit. A strobe projector, mounted on the bumper, contains a glass plate that has a hairline etched onto it. The strobe and the camera are synchronized so that when the camera is triggered to take a picture, the strobe projects a shadow of the hairline onto the pavement surface at a specific angle in relationship to the van (and thus at an approximate angle to the pavement surface). The coordinates along the hairline image for each picture are later digitized and stored on a computer. Photographs are taken approximately every 15.2 m.

Calibration

PASCO follows a rigorous process for calibration, data processing, and data review to ensure data quality for the LTPP database. A more detailed description of these steps may be found in reference 1.

Data Collection

The driver films each General Pavement Study (GPS) test section several times in an attempt to obtain two or three good, complete passes of the section. For the Specific Pavement Study (SPS) projects with multiple test sections, the entire project is filmed several times to obtain two or three good, complete passes of the project. The film is reviewed in the office for the purpose of selecting the best “pass” for entry into the database. For the SPS projects, the best two sets of film are chosen and the project is pieced together by choosing one section from one film and the

next section from the other film. All of the film, whether it is used or not, is retained as a backup by the contractor.

Data Processing

The film is used to create a digital profile, which is a series of x-y points defining the location of the surface of the pavement in a plane. All of the digitizing is performed using the negatives of the film. The point (0, 0) is the outside edge of the lane. A mouse with cross hairs is moved across the line on the film. The technician selects from 24 to 30 points on the line that include the peak highs and lows on the profile. The resulting profile is stored in a computer file that can be loaded directly into the database.

As of October 1998, there were five rounds of PASCO data in the NIMS. This means that for some sections, there may be as many as five or six observations. Figures 1 through 4 illustrate some common sets of PASCO transverse profile data. The legend for these figures provides the longitudinal location along the test section of the profile.

FACE Dipstick®

Data Collection Equipment

The FACE Dipstick® is used as part of a manual distress survey. This equipment is described in the *Distress Identification Manual* as follows:[2]

> "The body of the Dipstick® houses an inclinometer (pendulum), LCD panels and a battery for power supply. The sensor of the Dipstick® is mounted in such a manner that its axis and the line passing through the contact points of the footpads are coplanar. The sensor becomes unbalanced as the Dipstick® is pivoted from one leg to the other as it is moved down the pavement, causing the display to become blank. After the sensor achieves equilibrium, the difference in elevation between the two points is displayed. The Dipstick® is equipped with a choice of hardened steel spike feet or ball-and-swivel footpads. The swivel pads should be used on textured pavements."

Calibration Process

A series of calibration and zero checks are performed prior to data collection.[2] When these checks are completed, the operator may begin transverse profile measurements. The operator "pops" a chalk line to establish a transverse line on the pavement surface every 15.2 m, carefully avoiding any raised pavement markings. Readings are taken every 0.3 m across the lane and back to the starting point so that a closed loop is used at each station. The perfect closed loop results in a difference of 0 between the first reading and the last reading. The difference in the first reading and the last reading is used as a quality control check. The maximum allowable error is 0.076 mm per reading, or 1.8 mm total difference in the first reading and last reading for a transverse run 7.32 m long (3.66 m up and 3.66 m back). When all profile measurements for a

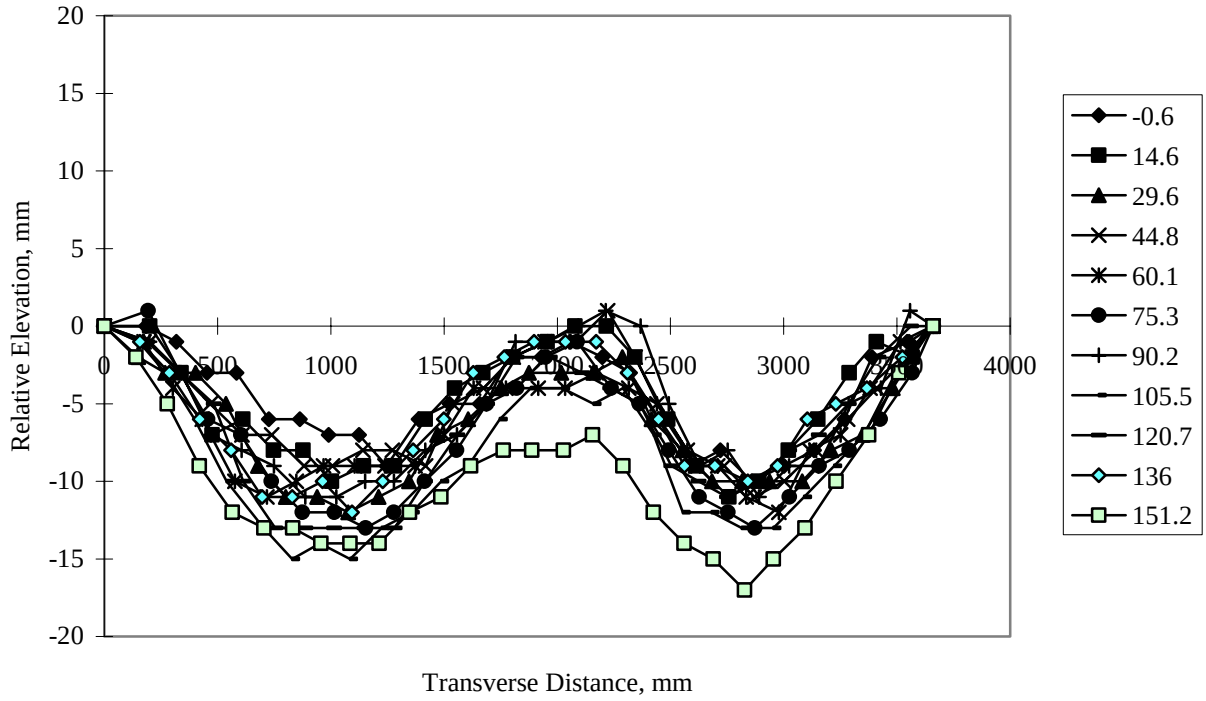

Figure 1. Transverse profiles obtained on test section 491001 on October 30, 1989 by PASCO.

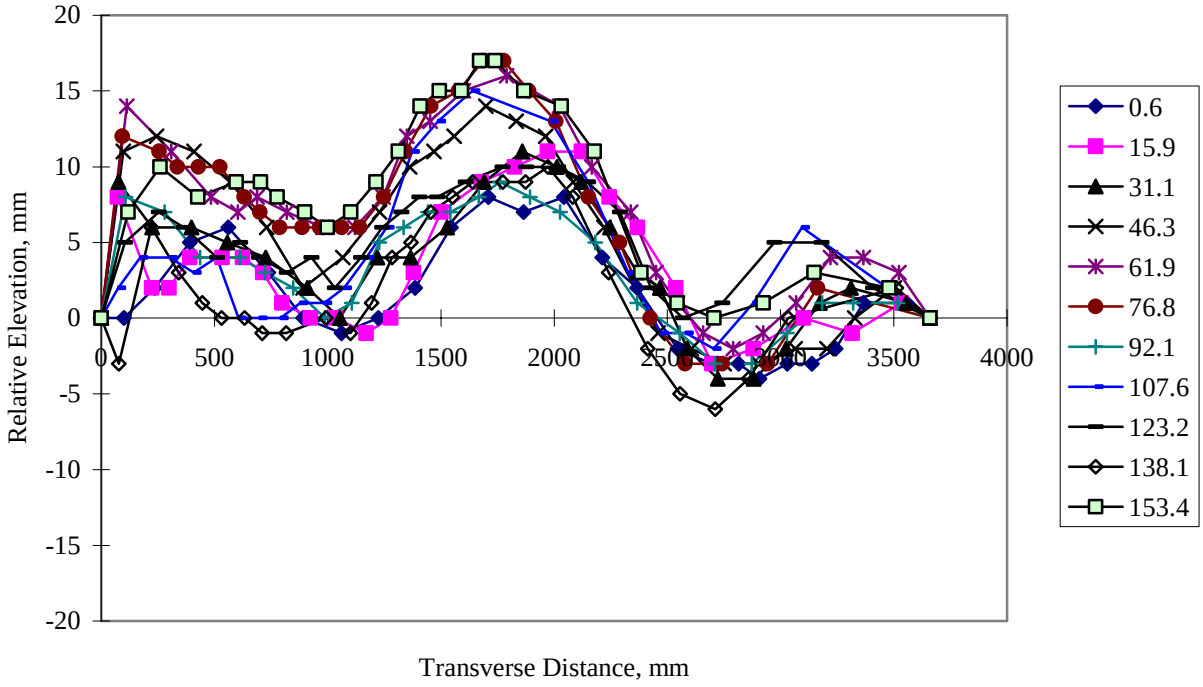

Figure 2. Transverse profiles obtained on test section 501002 on April 27, 1993 by PASCO.

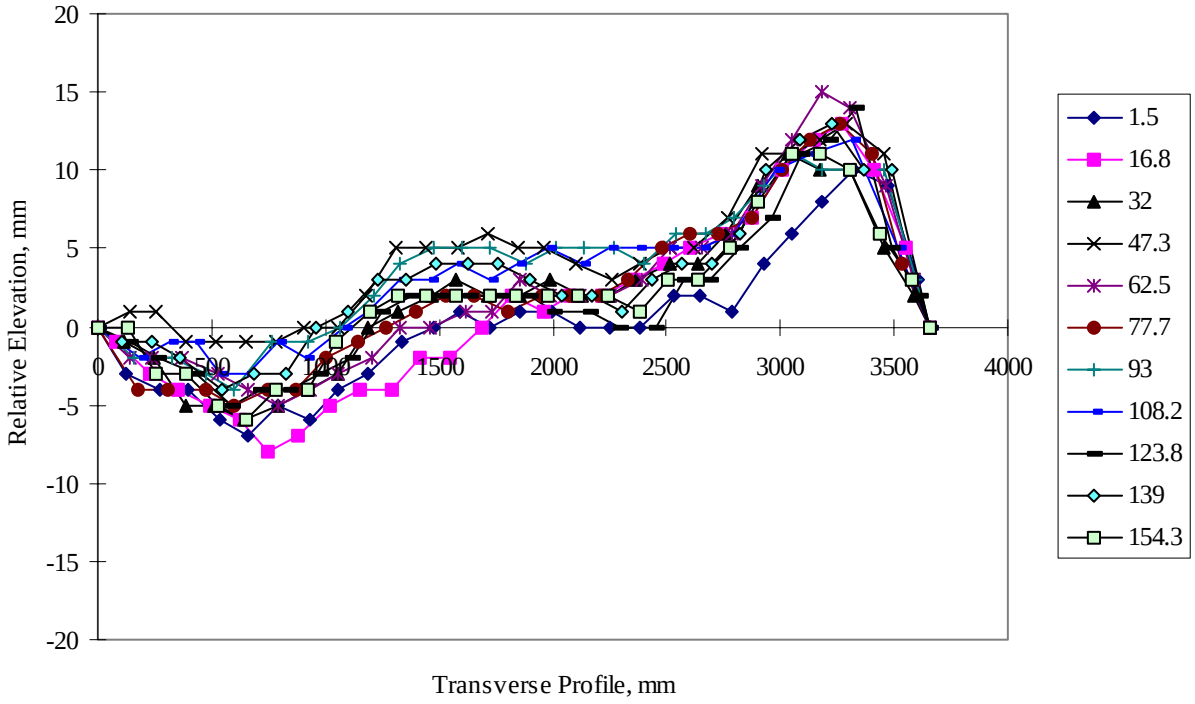

Figure 3. Transverse profiles obtained on test section 811803 on July 5, 1989 by PASCO.

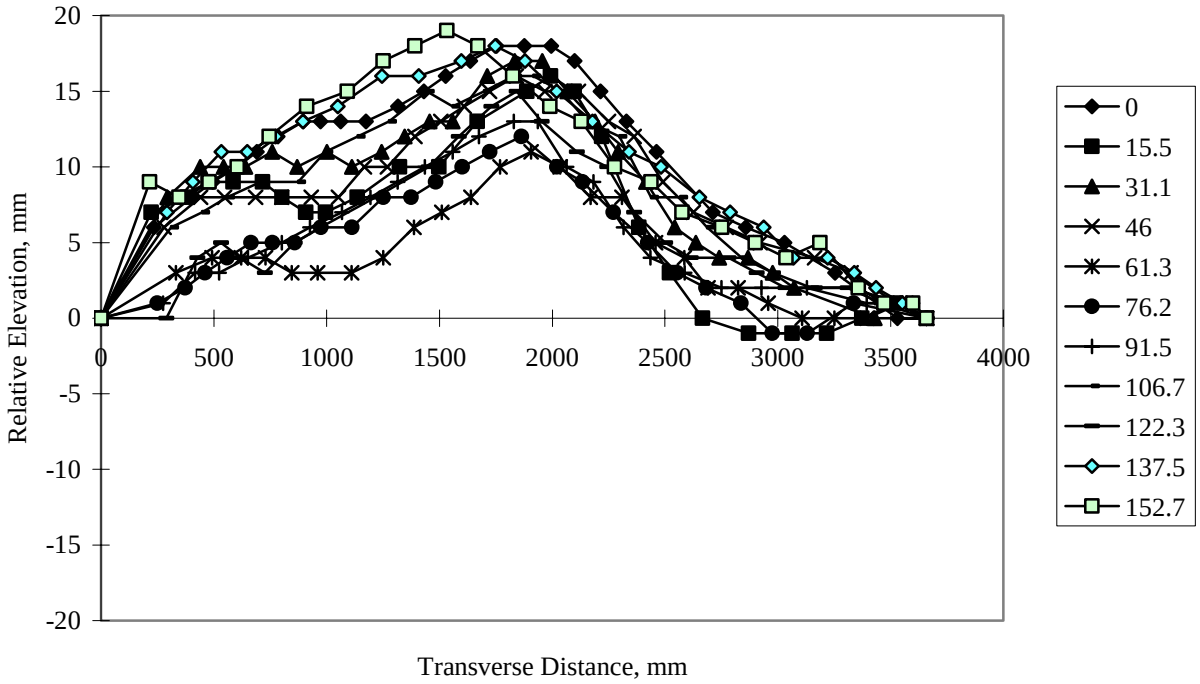

Figure 4. Transverse profiles obtained on test section 124107 on March 9, 1994 by PASCO.

given section have been taken, the operator performs a second set of "zero" and calibration checks to validate the measurements.[2]

Data Processing

The Dipstick® data are entered manually into the PROQUAL software for quality assurance checks.[3] The checks performed by PROQUAL include a user review of a graph of the transverse profile and a check to ensure that the transverse loop falls within acceptable tolerance levels. PROQUAL also calculates a rut depth using the string line method for each wheelpath for each transverse profile entered; however, the rut depth data are not stored in the NIMS. These rut depths are easily recalculated from the data that are stored in the database.

Figures 5 through 8 illustrate typical transverse profiles collected with the Dipstick®. The legends on these figures provide the longitudinal location along the test section of the profile. Prior to February 1997, measuring transverse profiles using the Dipstick® during manual distress surveys was encouraged, but not required, and a limited number of measurements were made. As of February 1997, all manual distress surveys conducted on asphalt-surfaced test sections are required to include transverse profile measurements taken with the Dipstick®. A comparison of the Dipstick® method and the PASCO method is discussed in chapter 3.

1.2-m STRAIGHTEDGE

In the past, lateral distortion differentials generally have been limited to measurements of rut depths using a straightedge (usually 1.2 m in length). The straightedge is placed across a wheelpath so that the vertical distance between the bottom of the straightedge and the pavement surface is maximized. This vertical distance is called the "rut depth." One measurement is taken for each wheelpath every 15.2 m along the test sections. Straightedge measurements are required only on the SPS-3 sections.[2]

DATA AVAILABILITY

All analyses completed for this study are based on data contained in Release 8.6 of the NIMS, dated October 1998. There were 4,127 sets of profiles in this data set, with 45,370 total transverse profiles. A set of profiles includes one profile measurement every 15.2 m. Of the 4,127 sets of observations, 806 were collected by Dipstick® and 3,321 were collected by PASCO.

Usually, 11 profiles are taken per test section. The quality control checks performed on the NIMS do not require that all transverse profiles taken on the same day for a single test section pass the quality control checks at the same time. Therefore, some sets do not include the typical 11 profiles. In addition, throughout the analysis, it was noted that a few of the sets of profiles taken with the Dipstick® only included profiles for every 30.5 m, i.e., these sets of profiles only contained six profiles.

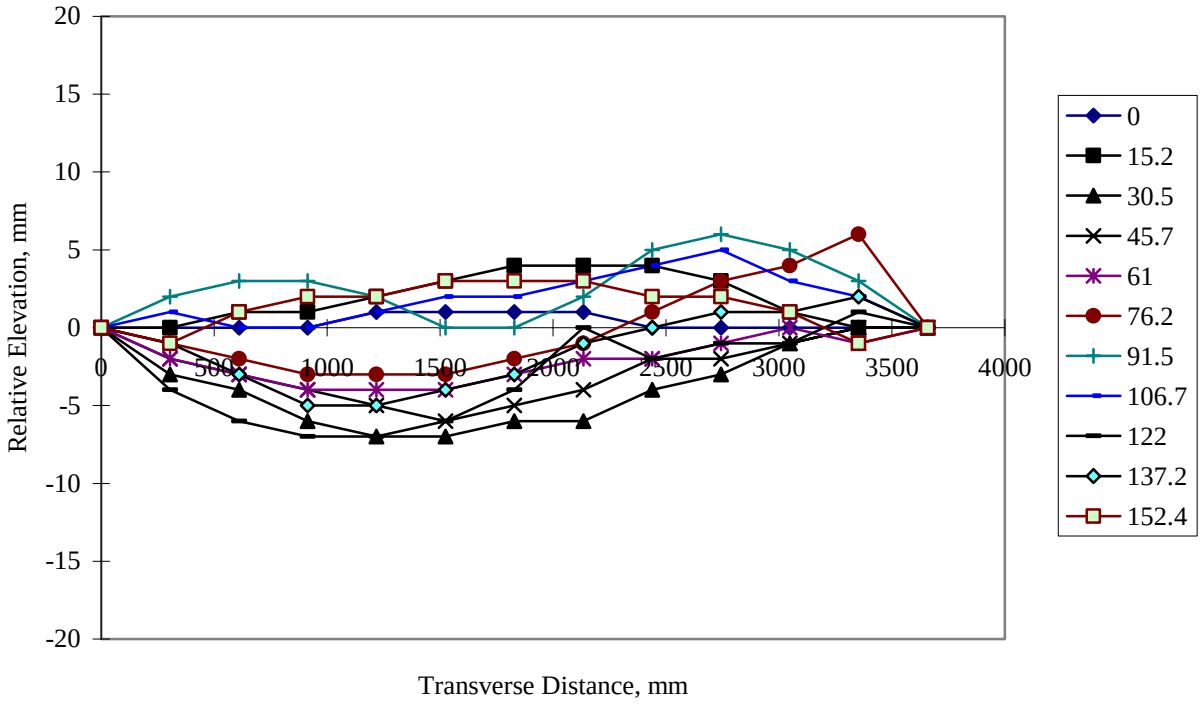

Figure 5. Transverse profiles obtained on test section 151003 on February 20, 1991 with a Dipstick®.

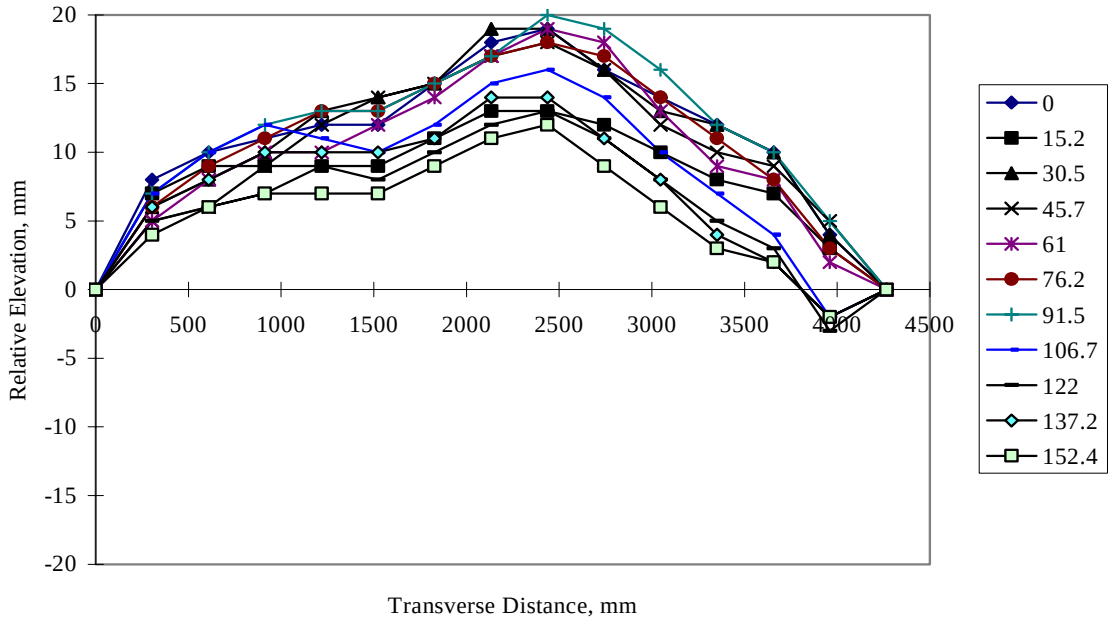

Figure 6. Transverse profiles obtained on test section 161010 on December 16, 1993 with a Dipstick®.

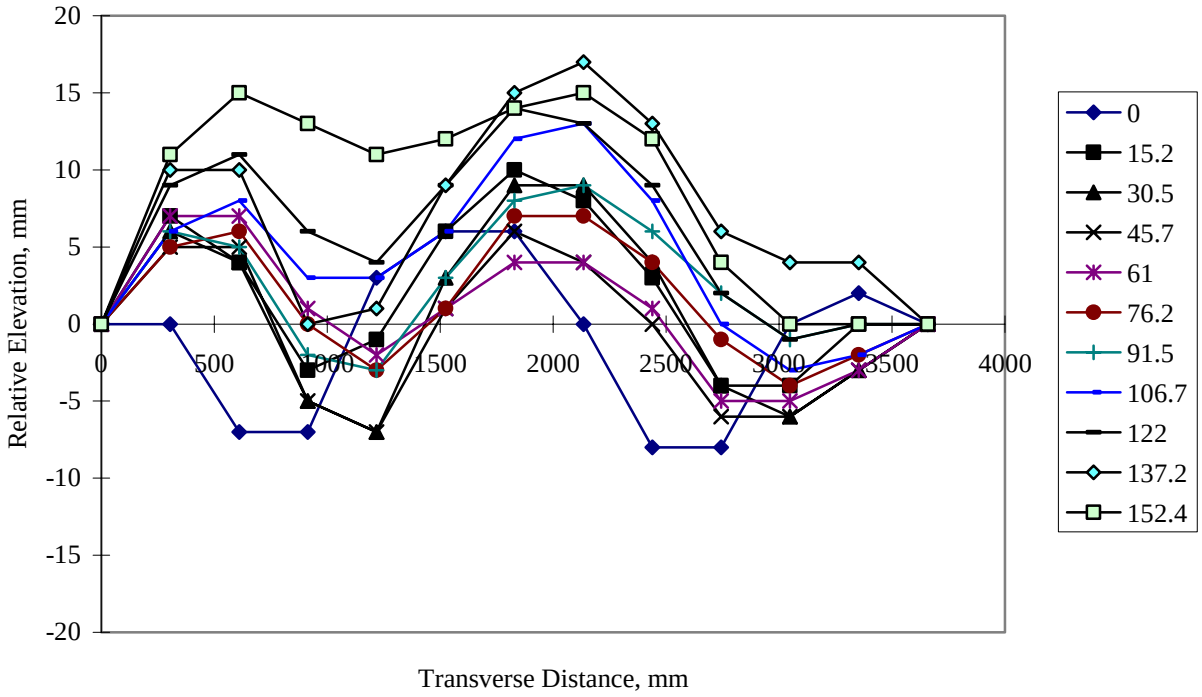

Figure 7. Transverse profiles obtained on test section 201010 on April 22, 1993 with a Dipstick®.

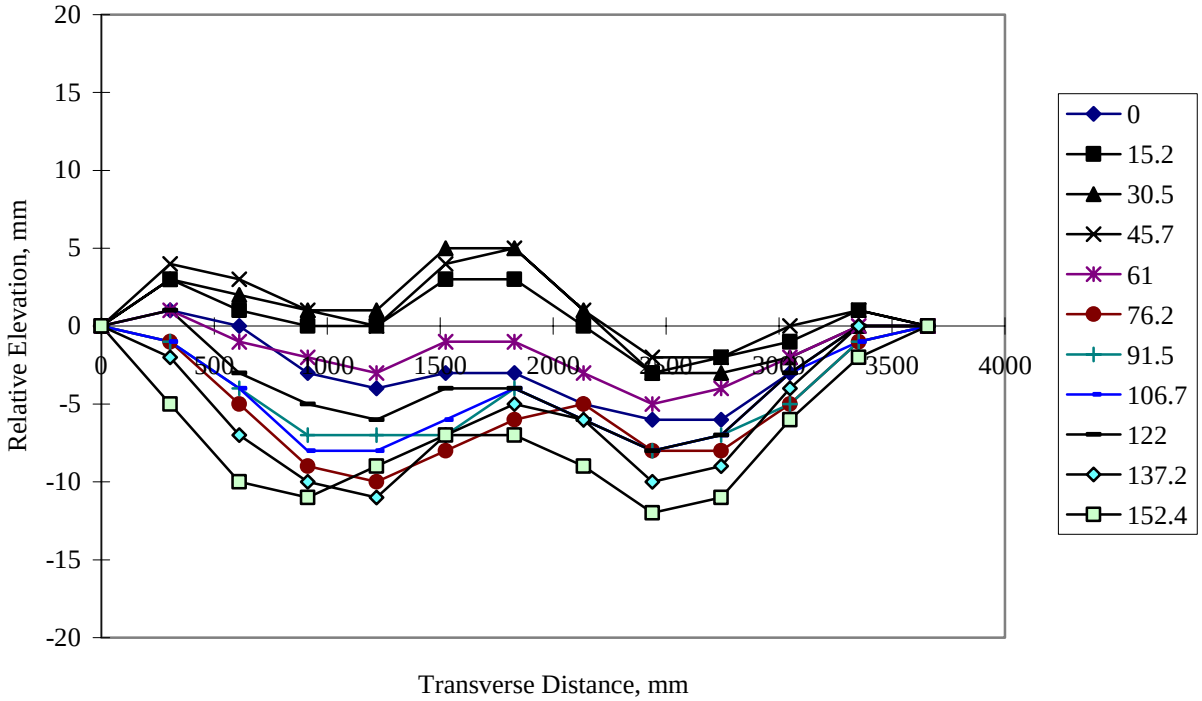

Figure 8. Transverse profiles obtained on test section 561007 on September 8, 1995 with a Dipstick®.

CHAPTER 3. CALCULATION OF INDICES

POTENTIAL INDICES

Ten characterizations or indices of the transverse profile were chosen for study. Figures for these indices are provided in a later section of this chapter, which includes a more thorough description. These indices were selected from discussions with various experts and include the following:

- Area of rut below and area of pavement above a straight line connecting the end points of the transverse profile.
- Area between straight lines connecting the maximum surface elevations and the pavement surface.
- Maximum depth for each wheelpath between a 1.2-m straightedge placed across a wheelpath and the surface of the pavement below the straightedge.
- Maximum depth for each wheelpath between a 1.8-m straightedge placed across a wheelpath and the surface of the pavement below the straightedge.
- Maximum depth for the outside wheelpath between a horizontal line from the edge of the pavement and the pavement surface (i.e., the depth of water that may accumulate before drainage onto the shoulder).
- Maximum depth for the inside wheelpath between a horizontal line from the maximum elevation between the wheelpaths and the pavement surface (i.e., the maximum depth of water that may accumulate before drainage into the outer wheelpath, assuming elevations in an adjacent lane greater than the maximum depth between wheelpaths).
- Maximum depth for each wheelpath between a wire line extended across the entire lane width and the pavement surface.
- Width of rut.
- Radius of curvature of deformation.
- PASCO typecasting as described below.

This list of characterizations includes the ideas of the research team, as well as those obtained during a literature review; discussions with the LTPP Distress Expert Task Group (ETG) at a meeting held in September 1997; discussions with PASCO, USA; and discussions with the Data Analysis ETG. The ETGs are part of an advisory structure operated by the Transportation Research Board (TRB), which advises the Federal Highway Administration (FHWA) on the

conduct of LTPP. As the name implies, the Data Analysis ETG provides guidance and support on issues concerning data analysis. The Distress ETG provides guidance and support on issues concerning the collection and interpretation of distress information.

At the American Association of State Highway Officials (AASHO) Road Test, the rut depth was defined as the maximum depth for each wheelpath between a 1.2-m straightedge and the surface of the pavement below the straightedge.[4] Recent studies of rutting in hot-mix asphalt (HMA) pavements have defined rut depth as the maximum depth for each wheelpath between a 1.8-m straightedge and the surface of the pavement below the straightedge.[5-6] One shortcoming of the straightedge method is that it provides no indication as to the type of surface distortion that is occurring.

ETG RECOMMENDATIONS

Based on the recommendations of the Distress and Data Analysis ETGs, the rut depth and rut width based on a 1.2-m straightedge and the depth of water in each wheelpath were not considered in any further analyses. The positive and negative areas, the fill area, the rut depth and rut width from the 1.8-m straightedge, the rut depth and rut width from the lane-width wire line, and the radius of curvature were considered the most beneficial. The location of the rut depth based on the distance from the edge of the lane was added to serve as a diagnostic tool. For the remainder of the report, the terms "1.8-m rut depth" and "1.8-m rut width" refer to the rut depth or width of the rut based on a 1.8-m straightedge, respectively. In addition, the terms "wire line rut depth" and "wire line rut width" refer to the rut depth and width of the rut based on a lane-width wire line, respectively.

METHOD OF CALCULATION

The physical description of each index was examined with relationship to the transverse profile being collected for the purpose of determining how each index would be calculated. These methods of calculation were incorporated into a VisualBasic program entitled RUTCHAR. The RUTCHAR program, which was used to calculate each index from the transverse profile data, is discussed later in this chapter.

Positive and Negative Areas

As shown in figure 9, positive and negative areas are the areas of deviation between the pavement surface and a straight line connecting the end points of the transverse profile. The outcome from this calculation will be a positive area for the area below the pavement surface and above the straight line, and a negative area for the area above the pavement surface and below the straight line. These areas were easily determined, because the straight line is the x-axis.

A finite integral technique is employed. The best method to use is the trapezoidal rule since the distances between the points on the x-axis are not necessarily equal. This method assumes that a pair of *x*-*y* coordinates provides the four corners of a trapezoid. The area of the trapezoid is:

$$Area = \tfrac{1}{2} (y_{i+1} + y_i) (x_{i+1} - x_i) \quad (1)$$

This value is calculated for each *x*-*y* pair where both y's have the same sign. If the *y*'s change their sign, it is necessary to find the slope between the two points. The *x* coordinate (x_0), where the line connecting the two points cross the x-axis, can be found by the following equation:

$$x_0 = \frac{y_i}{slope} + x_i \quad (2)$$

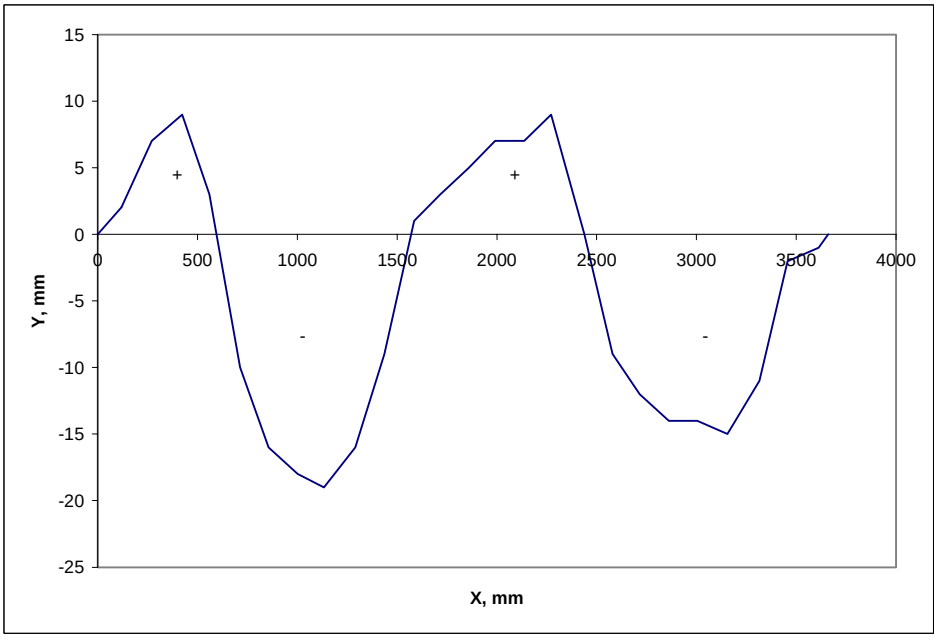

Figure 9. Illustration of the positive and negative area indices.

The area of the triangle between (x_i, y_i) and (x_0, 0) can be determined, and the area of the triangle between (x_0, 0) and (x_{i+1}, y_{i+1}) can be determined.

Finally, the positive area is the sum total area where y_i and y_{i+1} are greater than or equal to 0. The negative area is the sum total area where y_i and y_{i+1} are less than or equal to 0. These two values can be used in conjunction as a sum (positive minus negative) or a ratio to indicate the amount of rutting affecting the pavement.

Area of Fill

The area of fill is the area in millimeters squared below the straight lines connecting the maximum surface elevations and above the pavement surface as shown in figure 10. This value describes the material required to "fill in" the ruts for a unit length of pavement.

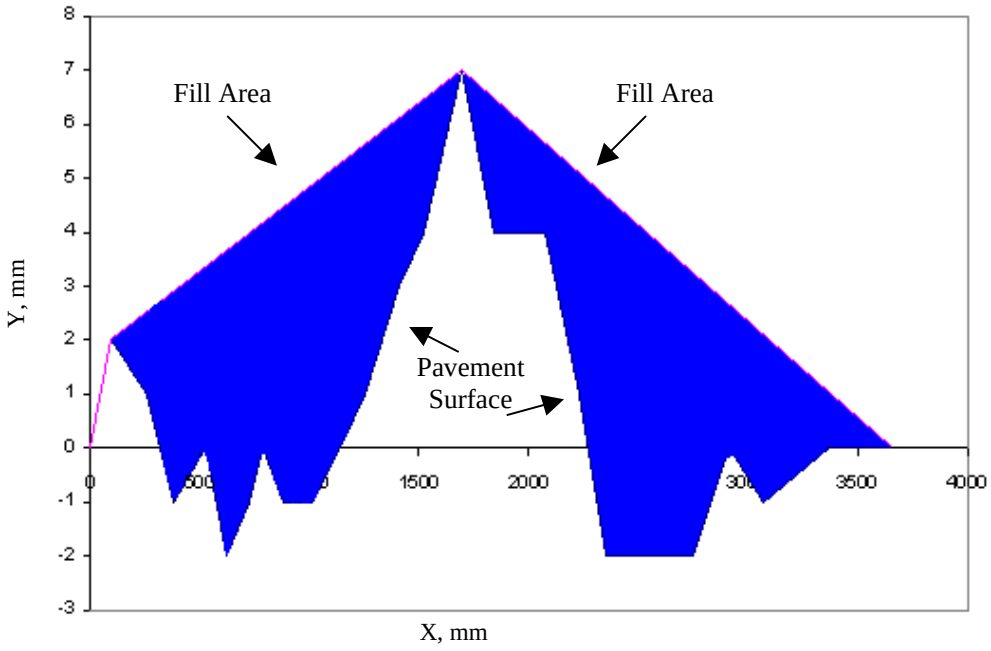

Figure 10. Illustration of the fill area index.

The first step is to stretch an imaginary wire line across the pavement surface (i.e., the lane width). The fill area is defined as the area between the wire line and the pavement surface, and is calculated using the trapezoidal rule previously described.

Calculated Rut Depth Based on a 1.8-m Straightedge

This rut depth is the maximum distance in millimeters in each wheelpath between a 1.8-m straightedge and the surface of the pavement, as shown in figure 11. The procedure described below provides the rut depth, width, and location for the left wheelpath (LWP) and is repeated for the other half of the lane to obtain the values for the right wheelpath (RWP).

An iterative process was used to place the straightedge on each half of the lane. The distance between the points on which the straightedge sat never exceeded 1.8 m. When the maximum rut depth was determined for one-half of the lane, the exact distance between the points on which the straightedge sat and the location at which the maximum rut depth occurred was recorded. The same process was used for determining rut depth in each half of the lane.

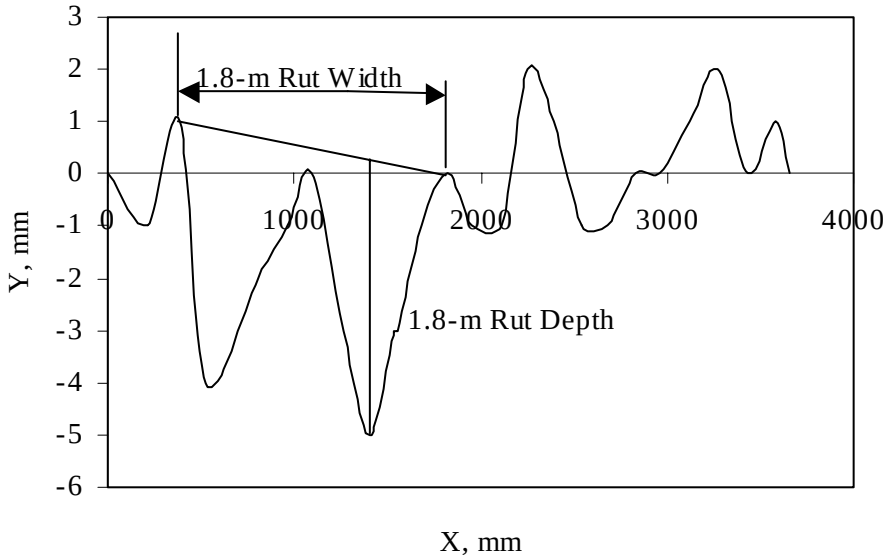

Figure 11. Illustration of the 1.8-m rut depth and 1.8-m rut width.

Calculated Rut Depth Based on a Lane-Width Wire Line

This rut depth, reported in millimeters, is the maximum distance for each wheelpath between a lane-width wire line placed across the lane and the pavement surface, as shown in figure 12. This value can best be visualized by imagining a wire stretched across the pavement surface so that it touches only the maximum elevation, or peaks, of the pavement surface. The rut depth is the distance between that wire and the pavement surface.

The wire line is defined as a series of straight lines. When the wire line is established, the next step is to determine the distance of each *x-y* coordinate from the wire line. The lane is then divided into half. The rut depth in each wheelpath is the maximum distance between the wire line and the *x-y* coordinates in each half-lane.

The rut width is the difference in the *x*'s of the two peak points surrounding the rut depth in each wheelpath. The rut location is the value of *x* at which the maximum rut depth in each wheelpath occurred.

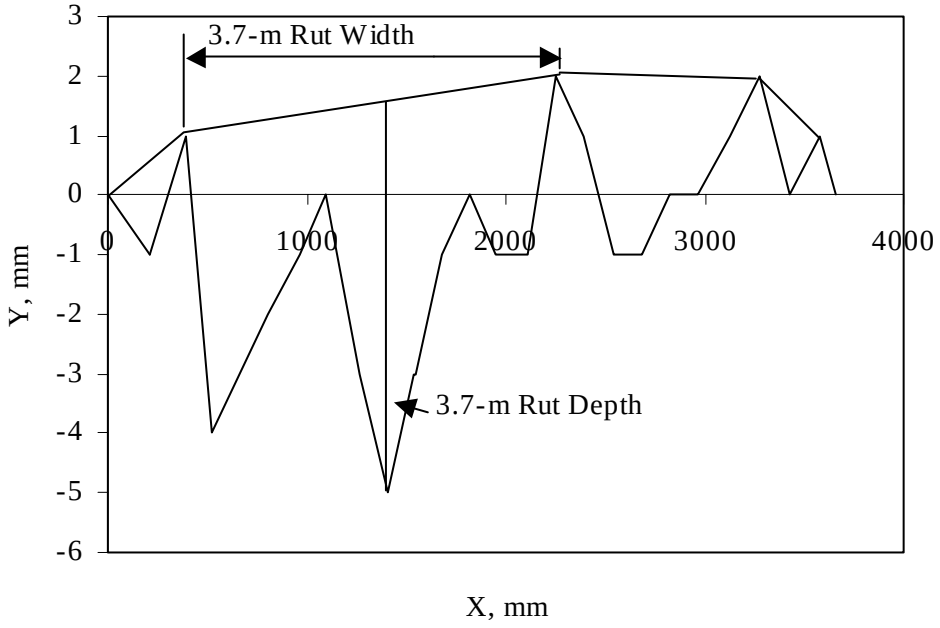

Figure 12. Illustration of the wire line rut depth and the wire line rut width.

Radius of Curvature

The radius of curvature is the minimum radius of curvature of the surface profile in each wheelpath. Three points are required to uniquely define a circle. Initially, the radius of curvature was found by determining the radius of the circle defined by each set of three consecutive points. The radius of curvature reported in each wheelpath was the minimum radius for that half of the lane where the center of the circle was still above the surface of the pavement. Figures 13, 14, and 15 show examples of the circles circumscribed by this method. While these circles are geometrically correct, they do not provide any meaningful measure of the wheelpath.

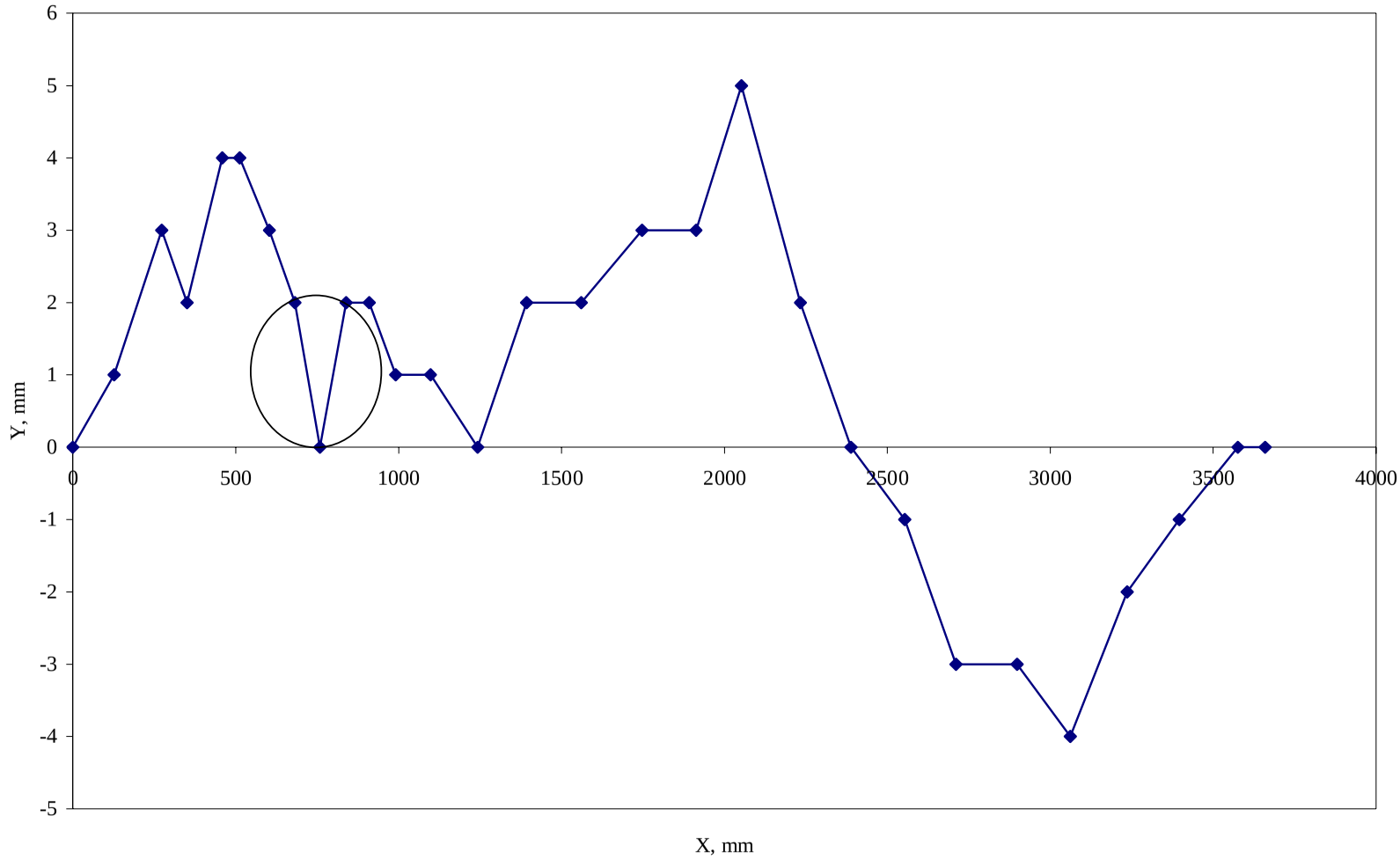

Figure 13. Transverse profile for test section 48A506 obtained on March 9, 1995 by PASCO at station 91.5 m.

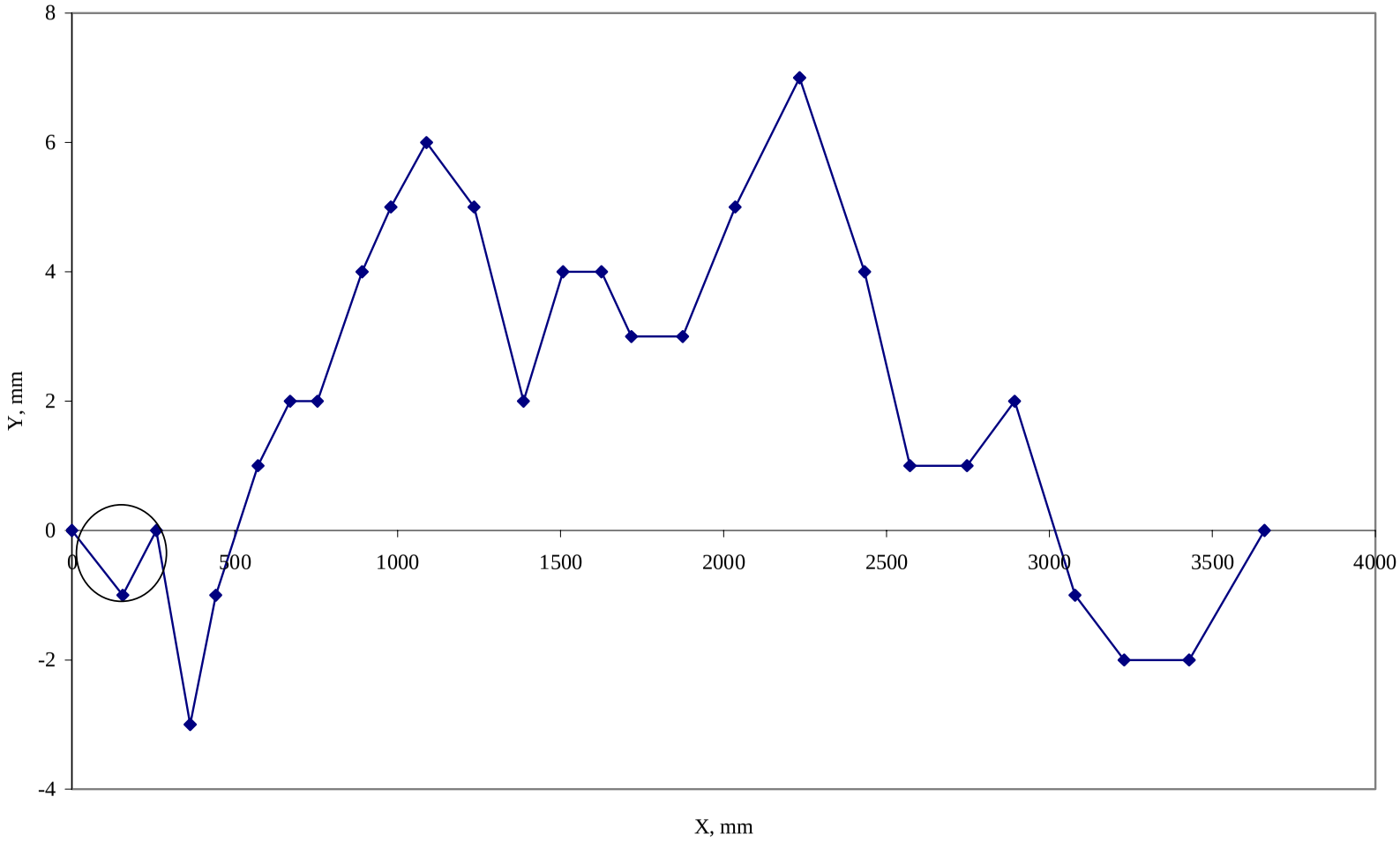

Figure 14. Transverse profile for test section 541640 obtained on September 29, 1992 by PASCO at station 152.4 m.

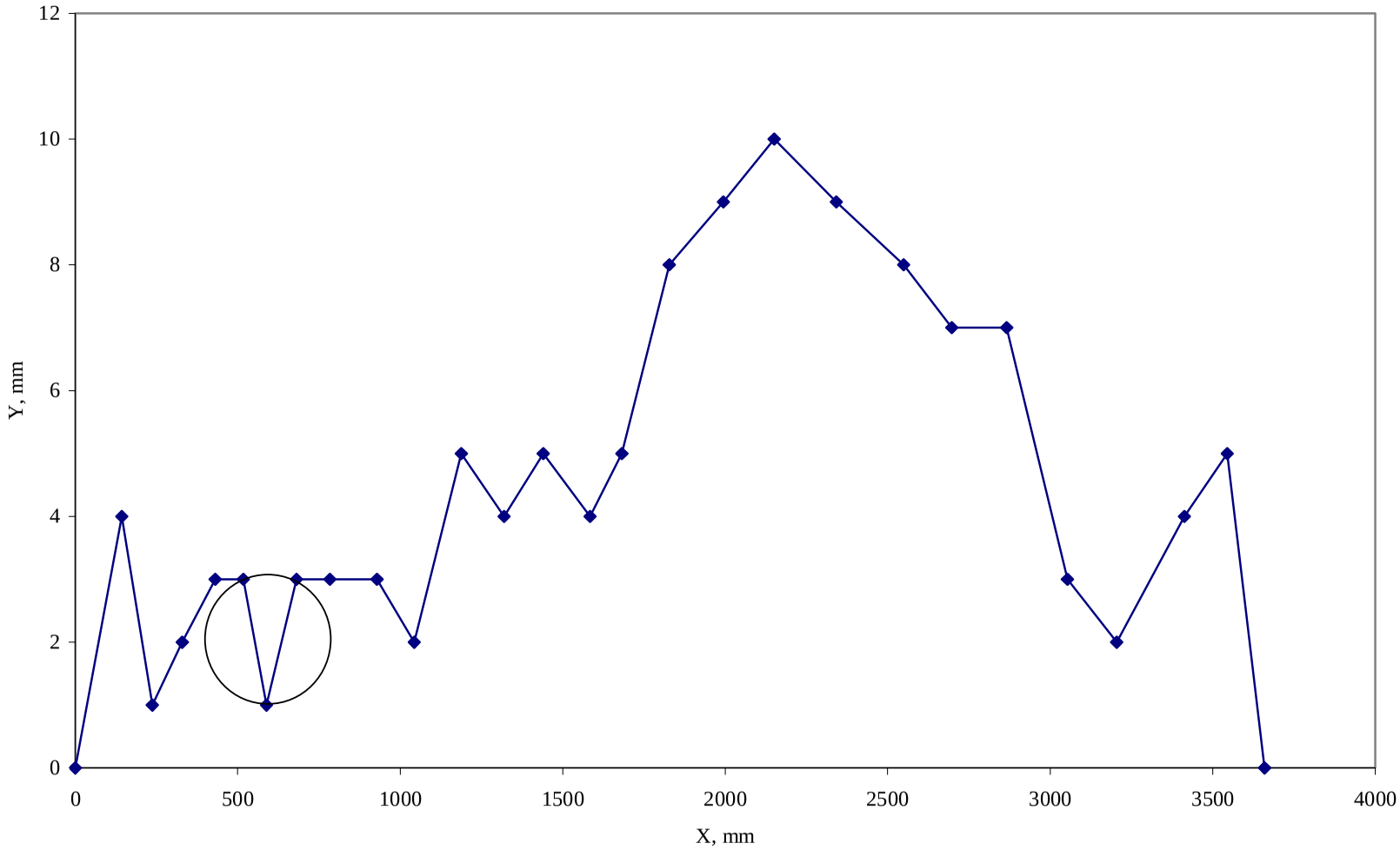

Figure 15. Transverse profile for test section 36B340 obtained on October 9, 1995 by PASCO at station 92.7 m.

A second approach was considered in which a circle would be circumscribed for each wheelpath. If the pavement did not exhibit a definable depression in the wheelpaths, then a circle would be fitted to the mid-lane hump as shown in figure 16. However, in attempting to apply this concept, the profile shown in figure 17 was encountered. The question then became how to apply a circle to the wheelpaths or the mid-lane of this profile. From this evaluation, a decision was made to apply a parabola to each wheelpath rather than a circle. A parabola is defined as follows:

$$(x - h)^2 = 4p(y - k) \tag{3}$$

where:

(h, k) = vertex of the parabola.
p = distance between the focus and the vertex.

Alternatively, one may say that "a parabola is the set of points in a plane that are equidistant from a given fixed point and a fixed line in the plane."[7] The fixed point is the focus and the fixed line is the directrix. The value p is directly related to the width of the opening of the parabola.

Each profile was examined to determine if any of the y values were negative. If at least four consecutive y-coordinates were negative, a parabola was fitted through those negative points. A least-squares regression was used to fit a quadratic equation to the x-y points. The equation fit was of the form:

$$y = B_0 + B_1 x + B_2 x^2 \tag{4}$$

and

$$p = \frac{1}{4B_2} \tag{5}$$

The values reported from the regression were the p-value, the F-statistic, and R^2. The F and the R^2 were reported so that some judgment could be made as to the significance of the fit. This method was applied to the available data, but only 35 percent of the profiles had a statistically significant fit.

The radius of curvature is not commonly used to measure rutting. Hence, to establish a minimum radius would be problematic. If the radius was too small, the value obtained would not necessarily be representative of what was occurring in the wheelpath. If the radius was too large, then some wheelpaths with very narrow rutting would be totally overlooked. Figure 16 does not show any definable wheelpaths; therefore, the proposal was to fit a parabola to the surface of the pavement with the opening of the parabola facing down rather than facing up as it would in a wheelpath. Figure 17 does not have a definable hump in the middle of the lane as seen in figure 16. Neither a parabola nor a circle could be fit to the middle of the lane or the wheelpaths. Due to the difficulties in appropriately defining and calculating this index, no additional analyses were attempted. It is not recommended for inclusion in the database.

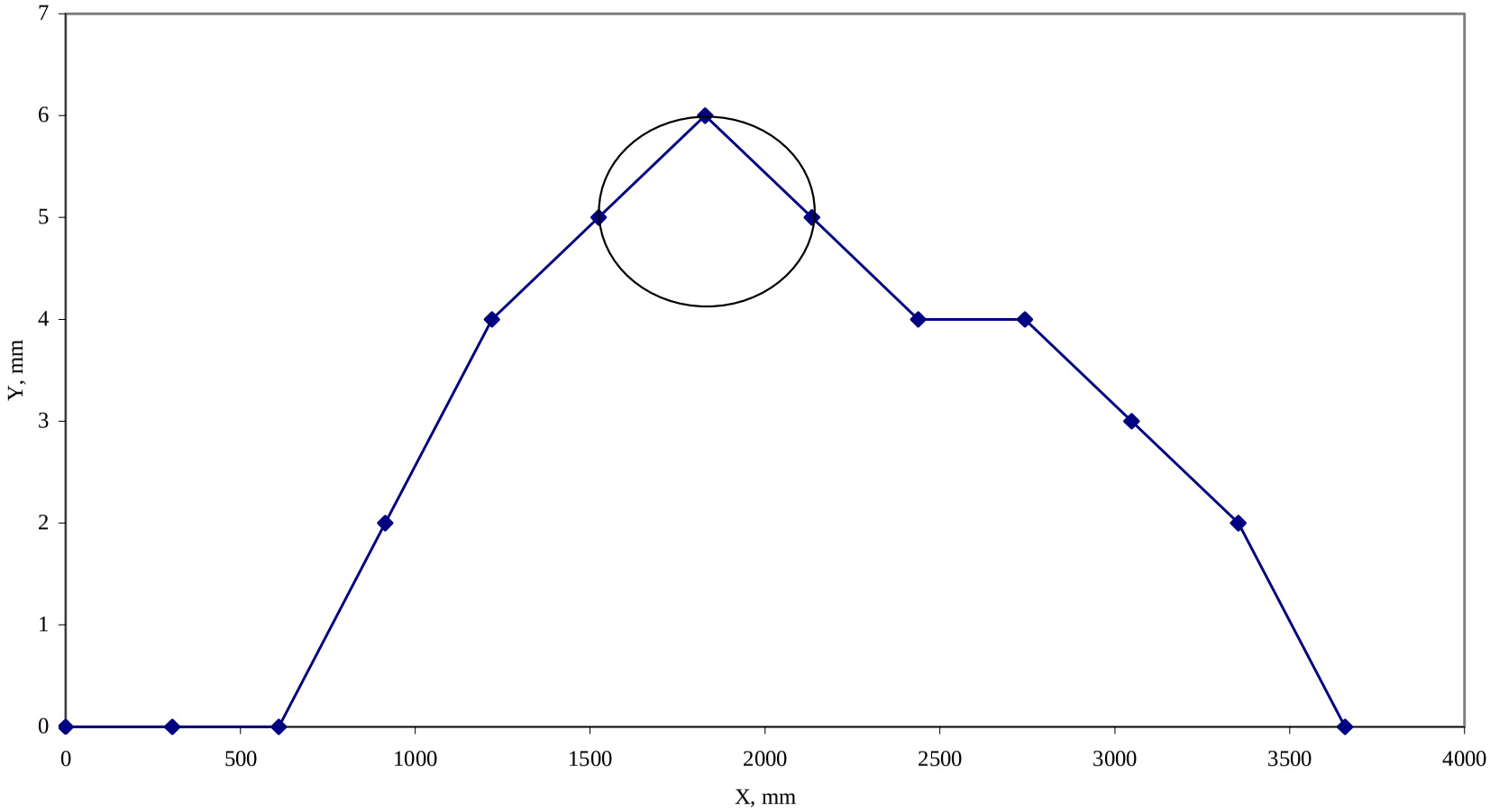

Figure 16. Transverse profile obtained for test section 566032 obtained on August 26, 1996by PASCO at station 61 m.

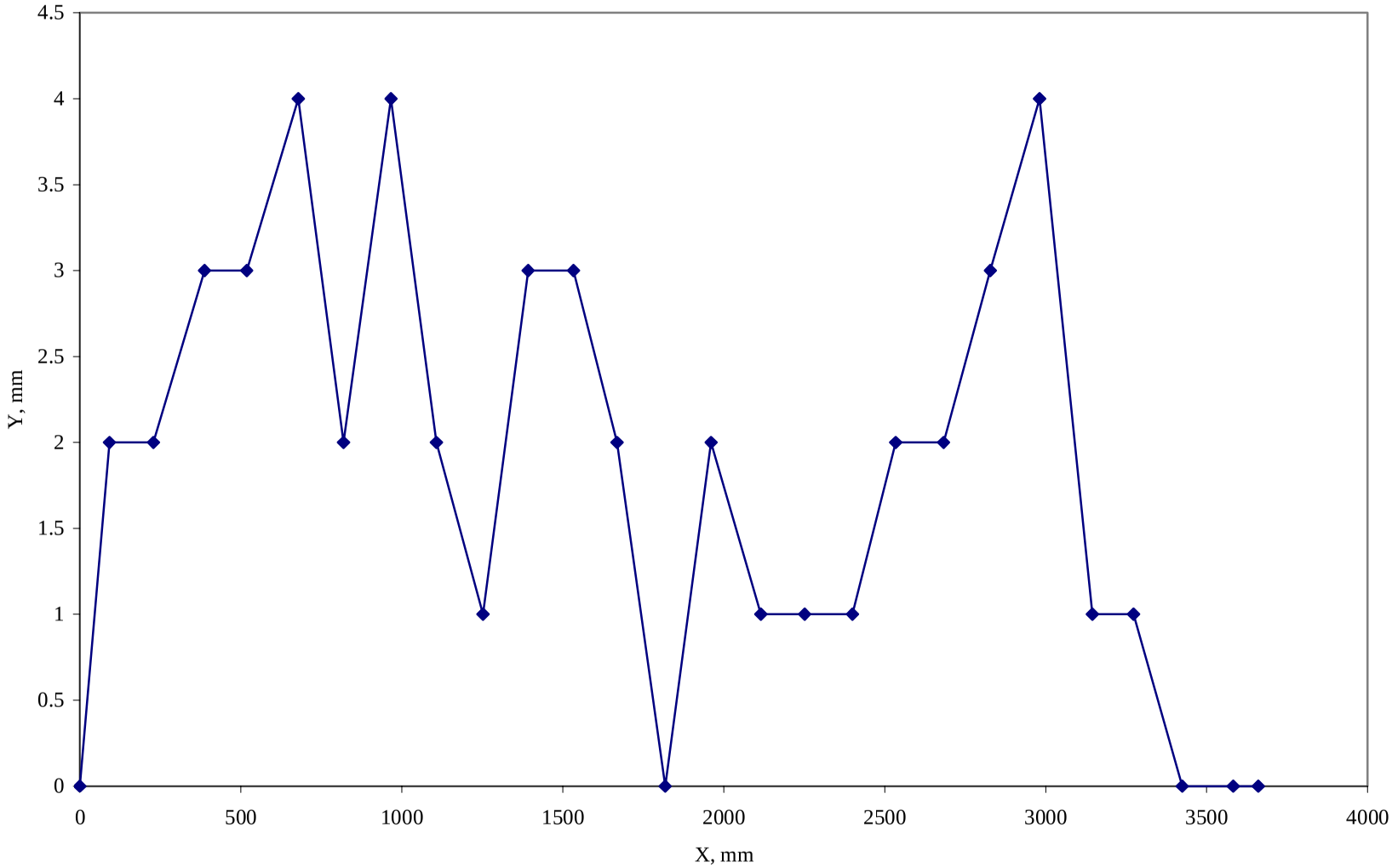

Figure 17. Transverse profile for tests section 421610 obtained on May 17, 1990 by PASCO at station 91.8 m.

PASCO Typecasting

The typecasting method groups the individual profiles into one of 14 shape categories. Each profile in the database fits into one of the 14 categories illustrated in figures 18 and 19. The shape factor is the number shown at the left of each profile category.

The shapes are based on the location of the rut in each half of the lane and the number of ruts present in each half of the lane. These shapes may provide a clue as to the rutting mechanism. However, the number of shapes that have been specified make it difficult to determine the category to which the profile belongs. Figure 17 is a good example of the problems encountered in determining shape factors. The middle of the section is the lowest point on the profile. The difficulty with this profile is deciding whether or not this is dual wheel-track rutting and how to automate this decision. For these reasons, it is recommended that this factor be excluded from the Information Management System (IMS).

RUTCHAR PROGRAM

Program Description

Since there were in excess of 45,000 profiles, a VisualBasic program was written to automate the calculations of the rutting indices noted previously. It also calculates the means and standard deviations of each index. The user's guide is provided in appendix A.

The program provides two output files. The first file includes the indices for each transverse profile contained in the input file. This file also includes the lane width provided by the transverse profile, a flag indicating whether or not the profile was taken within the 152-m section limits, and flags on the individual indices. The second input file contains the mean, standard deviation, minimum, and maximum for each index for each transverse profile survey.

Transverse profile measurements are to be taken every 15 m along the test section. Though the RoadRecon unit generally meets this requirement, it may record a measurement anywhere from 0.2 m prior to the station or 0.1 m after the station. Since some of these profiles fall outside of the 152-m test section, these profiles are flagged and excluded from the section averages.

The flags on the individual indices indicate a potential outlier. The values are flagged if they lie more than two standard deviations away from the mean. These values are still included in the mean and standard deviation calculations. The flag is provided as a tool for analysts.

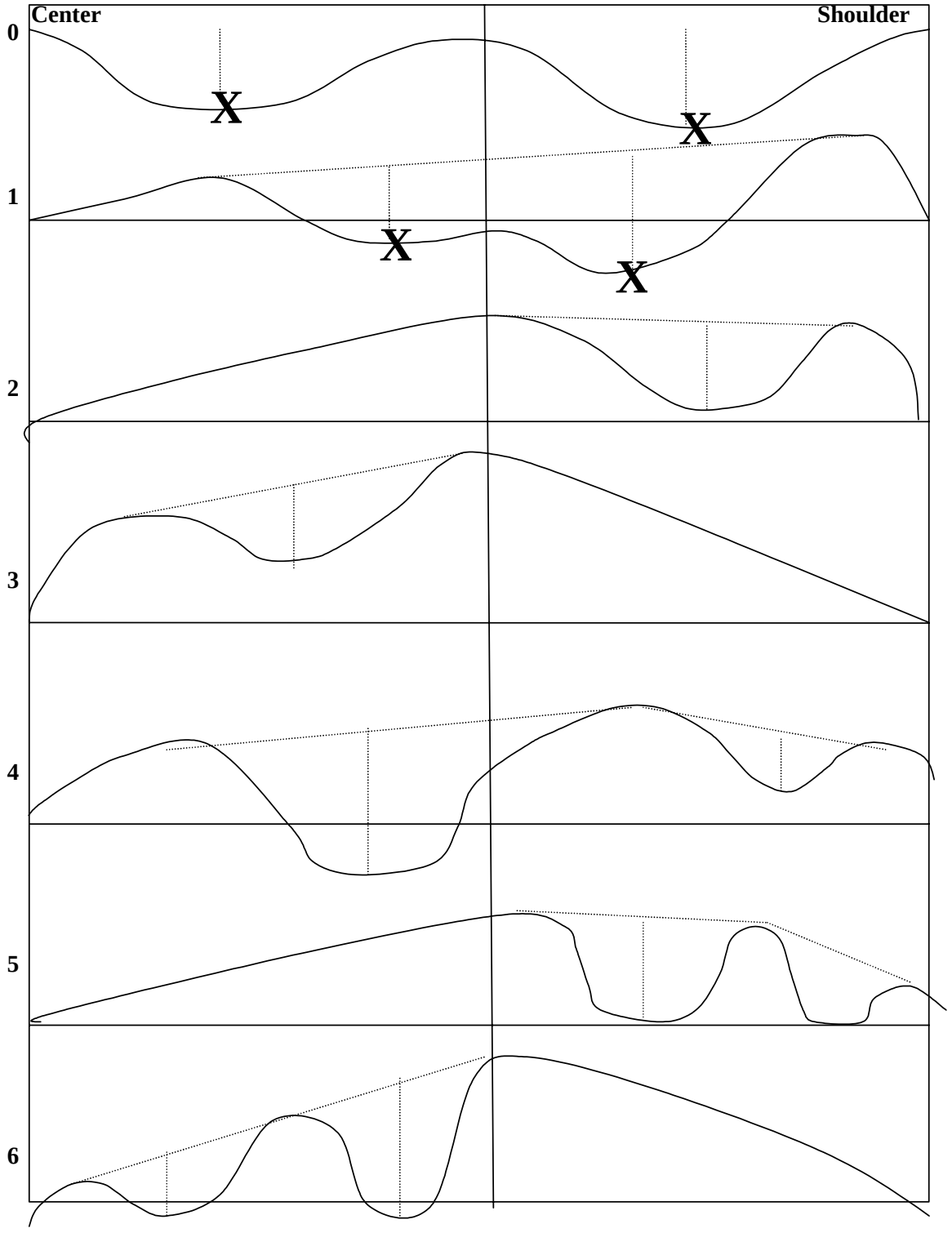

Figure 18. PASCO typecasting shapes (shapes 0-6).

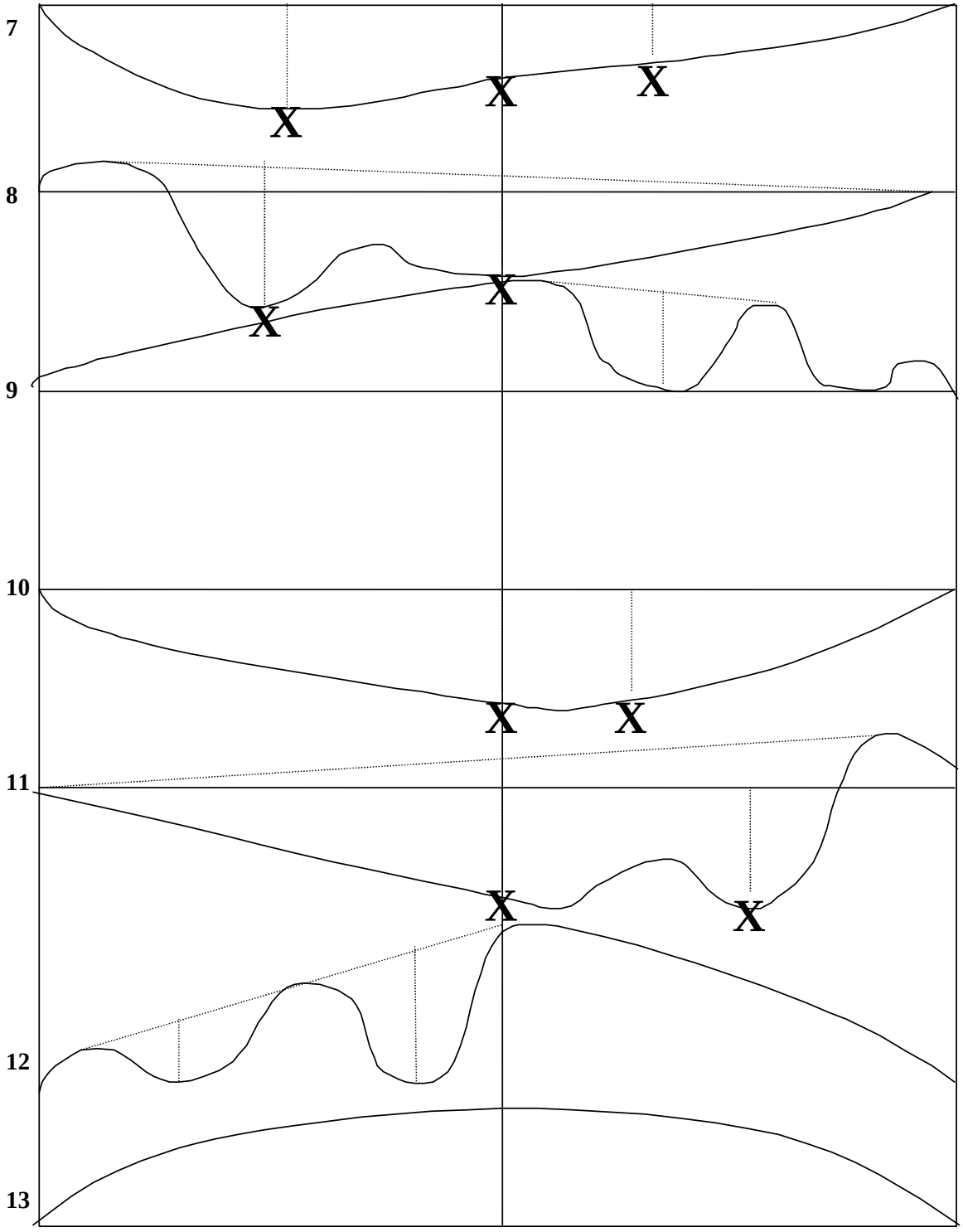

Figure 19. PASCO typecasting shapes (shapes 7-13).

In addition to the output files, the program creates another file, DATCHK.OUT. This file contains the results of checks on the data. In the process of calculating the indices from the data extraction, two discontinuities were noted in the data. These discontinuities were encountered with the PASCO data only and are probably a result of the data processing. The first is a duplicate *x*-*y* point. In this case, the duplicate point was removed and all calculations were performed without the duplicate point. A message is written to DATCHK.OUT, which contains the State code, Strategic Highway Research Program (SHRP) ID, construction number, survey date, station, *x*, and "IS A DUPLICATE POINT."

The second discontinuity occurs when two y-values are shown for the same x-coordinate. In this case, the *x*-value is reduced by 1 mm, so the first *x*-*y* point is moved back by 1 mm. In this case, the same fields are written to DATCHK.OUT except that the message is changed to read "IS A DUPLICATE X". A list of the profiles with these discontinuities was provided to FHWA.

Program Verification

The purpose of the verification process was to ensure that the program accurately calculated the indices, not to validate the physical representation of the indices. One hundred profiles were randomly selected from the data set for program verification. Each of the indices was calculated manually for each of the profiles. This program was used for calculating all of the indices for these profiles. The algorithm for each index was written and the program was run using the test set as the input file. The output was compared to the hand calculations and, if the data were not the same, the algorithm was reviewed. The process was reiterated using the test set until the program was found to accurately calculate each index. Appendix B provides the overall distribution of the indices calculated by the RUTCHAR program for the individual profiles and the section means.

The complete data set was used to provide a final check of the program. Some relationships were known to exist between the indices prior to their calculations (for example, the rut depth calculated based on a lane-width wire line should be greater than the rut depth based on a 1.8-m straightedge). These relationships were used to confirm that the algorithms had been accurately programmed.

CHAPTER 4. INDEX COMPARISONS

In order to identify the index or set of indices that would be most useful to practicing engineers, a set of comparisons were made. First, the indices were examined to determine the number of measurements required along each test section to get an accurate representation of the rutting on each section. Second, the indices were compared to each other. These comparisons allow for the determination of which indices provide the same general information about the transverse profile. Two indices are thought to be providing the same information if they are highly correlated.

MINIMUM NUMBER OF MEASUREMENTS

As previously stated, profiles are collected every 15.2 m. The question arose as to whether the number of profiles taken on each section could be reduced from 11 total observations (one profile every 15 m) to 6 total observations (one every 30 m) without sacrificing the accuracy. An analysis was conducted to determine the consequences of reducing the number of surveys. Specifically, the averages of the indices were determined, but only using the data measured every 30 m. These values were then compared to the averages of all of the stations in a series of pairwise t-tests,[8] using a significance level of 0.05.

The results from these tests are provided in appendix C. As can be seen in table 1, there is little difference between the two data sets. The 1.8-m RWP rut depth, 1.8-m RWP rut width, the wire line RWP rut depth, and the wire line rut width were the only indices for which the t-test was not significant. All of the results for the other indices showed a statistically significant difference. The mean differences for the indices were so small that they were within the capability of the equipment. For example, the difference in the LWP 1.8-m rut depths was 0.02 mm. Finally, the spread around the line of equality, as shown in the figures in appendix C, was quite narrow. The largest spread seen was in the rut widths.

The first set of comparisons noted above included all of the available data. However, the question of the number of measurements necessary to accurately determine the amount of rutting on a test section originally arose with respect to the Dipstick® data. If this reduction is appropriate, then the time required to collect the Dipstick® transverse profiles would be reduced by almost half. Thus, a second set of comparisons was made that included only the Dipstick® data. These results are also shown in appendix C. This reduced data set exhibits exactly the same trends as the complete data set.

The pairwise t-tests showed that using 6 observations (rather than 11) produced no overall bias in the estimate of the average rut depth. The standard deviation of an arithmetic average of n observations is $\sigma/\sqrt{n}$. Hence, the curve $y=\sqrt{n}$ provides the relationship between the precision (y) and the number of observations (n). In this case, the relative precision is $\sigma/\sqrt{6}$. Reducing the sample size from 11 to 6 increases $\sigma/\sqrt{n}$ by 25 percent.

Table 1. Comparison of section means of all versus six measurements for all indices.

Index	p-Value	Mean Difference
Negative Area, mm^2	0.0002	51
Positive Area, mm^2	0.0147	42
Fill Area, mm^2	0.0045	36
1.8-m Rut Depth, LWP, mm	0.0046	0.02
1.8-m Rut Width, LWP, mm	0.0465	2.3
1.8-m Rut Depth, RWP, mm	0.7940	0.00
1.8-m Rut Width, RWP, mm	0.9858	0.00
Wire Line Rut Depth, LWP, mm	0.0019	0.02
Wire Line Rut Width, LWP, mm	0.2825	2.6
Wire Line Rut Depth, RWP, mm	0.1312	0.01
Wire Line Rut Width, RWP, mm	0.6749	1.0

Another approach for examining this question, which addresses sample size, was also investigated. In this approach, one determines the number of observations required to detect the difference in means μ_2 and μ_1. In this case, it is possible to determine the minimum number of samples required to detect, with 95 percent confidence, a specific level of bias.[8] The calculation is as follows:

$$n = \frac{\sigma^2 (z_{1-\alpha/2} + z_{1-\beta})^2}{(\mu_2 - \mu_1)^2} \quad (6)$$

where:

n = sample size.
σ^2 = within-section variance of index.
z = normal distribution statistic associated with α and β.
μ_2-μ_1 = bias or difference in means to be detected.
α = level of significance, 5 percent.
β = probability of false acceptance, 20 percent.

Table 2 presents the results of these calculations for each index. The level of bias used to develop these numbers is provided in the (μ_2 - μ_1) column.

Table 2. Results of sample size analysis, 11 versus 6 measurements.

Index	$(\mu_2 - \mu_1)$	*n*
Positive Area, mm^2	3000	9
Negative Area, mm^2	3000	8
Fill Area, mm^2	3000	8
LWP 1.8-m Rut Depth, mm	2	4
RWP 1.8-m Rut Depth, mm	2	5
LWP 1.8-m Rut Width, mm	100	17
LWP 1.8-m Rut Location, mm	100	29
RWP 1.8-m Rut Width, mm	100	16
RWP 1.8-m Rut Location, mm	100	35
LWP Wire Line Rut Depth, mm	2	6
RWP Wire Line Rut Depth, mm	2	6
LWP Wire Line Rut Width, mm	100	184
LWP Wire Line Rut Location, mm	100	26
RWP Wire Line Rut Width, mm	100	182
RWP Wire Line Rut Location, mm	100	35

The data in this table illustrate that the only indices for which six profiles are acceptable are the rut depths. All other indices require at least 11.

INDEX COMPARISONS

The indices were compared to determine which were most likely to provide consistent information for a specific profile. If two indices provide consistent information, it will not be necessary to consider both indices in future analyses. Correlation between the indices indicates the strength of the relationship between two indices. For example, the 1.8-m rut depth and the wire line rut depth should be highly correlated because these values should be measuring the same information about the surface. Table 3 contains the correlation matrix for the indices.[8] As shown, some of the correlations are much stronger than others. Note that data from the individual profiles were used to generate the correlation matrix and other comparisons shown later in this section. A more detailed discussion of these results follows.

The rut locations were not included in the correlation matrix. These values will be useful to analysts in examining trends in rut depths for individual profiles and sections. However, the location is of little value without the rut depth. It describes nothing about the severity or quality of the rut and it only provides the location of the wheelpath. For this reason, rut location was not included in the correlation matrix.

Table 3. Correlation matrix for indices.

	Negative Area, mm^2	Positive Area, mm^2	Fill Area, mm^2	1.8-m Rut Depth, LWP, mm	1.8-m Rut Width, LWP, mm	1.8-m Rut Depth, RWP, mm	1.8-m Rut Width, RWP, mm	Wire Line Rut Depth, LWP, mm	Wire Line Rut Width, LWP, mm	Wire Line Rut Depth, RWP, mm	Wire Line Rut Width, RWP, mm
Negative Area	1.0000	0.4967	-0.9098	-0.6443	-0.3239	-0.6757	-0.3691	-0.7748	-0.5633	-0.7904	-0.5846
Positive Area	0.4967	1.0000	-0.4225	-0.2694	-0.3971	-0.2640	-0.4067	-0.3428	-0.5247	-0.3269	-0.5311
Fill Area	-0.9098	-0.4225	1.0000	0.8045	0.3906	0.8372	0.4355	0.8985	0.4956	0.9186	0.5220
1.8-m Rut Depth, LWP	-0.6443	-0.2694	0.8045	1.0000	0.3851	0.7392	0.2843	0.9555	0.2339	0.7191	0.2127
1.8-m Rut Width, LWP	-0.3239	-0.3971	0.3906	0.3851	1.0000	0.2390	0.2677	0.4293	0.5707	0.2710	0.3224
1.8-m Rut Depth, RWP	-0.6757	-0.2640	0.8372	0.7392	0.2390	1.0000	0.4070	0.7249	0.1955	0.9639	0.2691
1.8-m Rut Width, RWP	-0.3691	-0.4067	0.4355	0.2843	0.2677	0.4070	1.0000	0.3228	0.3218	0.4420	0.5994
Wire Line Rut Depth, LWP	-0.7748	-0.3428	0.8985	0.9555	0.4293	0.7249	0.3228	1.0000	0.4011	0.7683	0.3697
Wire Line Rut Width, LWP	-0.5633	-0.5247	0.4956	0.2339	0.5707	0.1955	0.3218	0.4011	1.0000	0.3320	0.8541
Wire Line Rut Depth, RWP	-0.7904	-0.3269	0.9186	0.7191	0.2710	0.9639	0.4420	0.7683	0.3320	1.0000	0.4089
Wire Line Rut Width, RWP	-0.5846	-0.5311	0.5220	0.2127	0.3224	0.2691	0.5994	0.3697	0.8541	0.4089	1.0000

Rut Widths

In general, the correlation matrix shows that the 1.8-m rut widths are not very highly correlated with any of the other indices. A paired t-test was performed to compare the values in the two wheelpaths. The results indicate that there is a significant statistical difference between the wheelpaths. The dispersion of the data was so large that it appears that almost any line could be fitted. This shows that there is virtually no relationship between the rut widths of the LWP and RWP. One potential cause of the differences observed in the rut widths between the two wheelpaths is the varying distances between wheels from one vehicle to another. If the drivers of the various vehicles tend to follow a particular path, the rut width for a particular wheelpath could be fairly narrow, while the other is fairly wide.

The 1.8-m rut widths had the highest correlation with the wire line rut widths. Paired t-tests were performed to compare the 1.8-m rut widths to the wire line rut widths. The 1.8-m rut width cannot exceed 1,800 mm as defined by the straightedge length. Generally, where the rut width for the lane-width wire line was less than 1,800 mm, the 1.8-m rut width was the same value. In most cases, the rut width was greater than 1,800 mm as determined by the wire line. Therefore, the 1.8-m rut width is not recommended for widespread use in the analysis of rutting.

A second boundary was observed at approximately 3,700 mm. For computational purposes, the imaginary wire stretched across the pavement surface is the same width as the lane. Most of the sections included in the LTPP program are 3.7 m wide, which is the location of the upper boundary. However, a few of the sections are almost 4.3 m wide, which accounts for data points above the 3,700-mm boundary.

The highest correlation for the wire line rut width was between the wheelpaths. A paired t-test comparing the values for each wheelpath also was conducted. The test was statistically significant. The graph shows a large amount of scatter in the bottom left corner of the graph, though there appears to be a clear upper boundary as shown by the diagonal line. Those points not falling on the line of equality have different rut widths for each wheelpath. The boundary occurs when the sum of the rut widths in each wheelpath equals the lane width. Beyond that point, the rut widths fall exactly on the line of equality. If the sum of the rut widths is greater than the lane width, and the rut widths for the two wheelpaths fall on the line of equality, then the middle portion of the transverse profile is lower than the outside edges.

The 1.8-m rut widths and the wire line rut widths should provide the same general measure of the transverse profile. However, these two indices are not correlated. When the wire line rut width is used, data from either wheelpath may be sufficient to accurately describe the profile.

Rut Depths

The highest correlations shown are between the 1.8-m rut depths and the wire line rut depths. Figures 20 and 21 show the results from a paired t-test for the LWP and RWP, respectively. The figures show that the 1.8-m rut depths are never more than the wire line rut depths. In general, the values are not the same, but they are closely related. The correlation between the wheelpaths

for each rut depth is moderate. The rut depth in one wheelpath is a reasonable indicator of the rut depth in the other wheelpath.

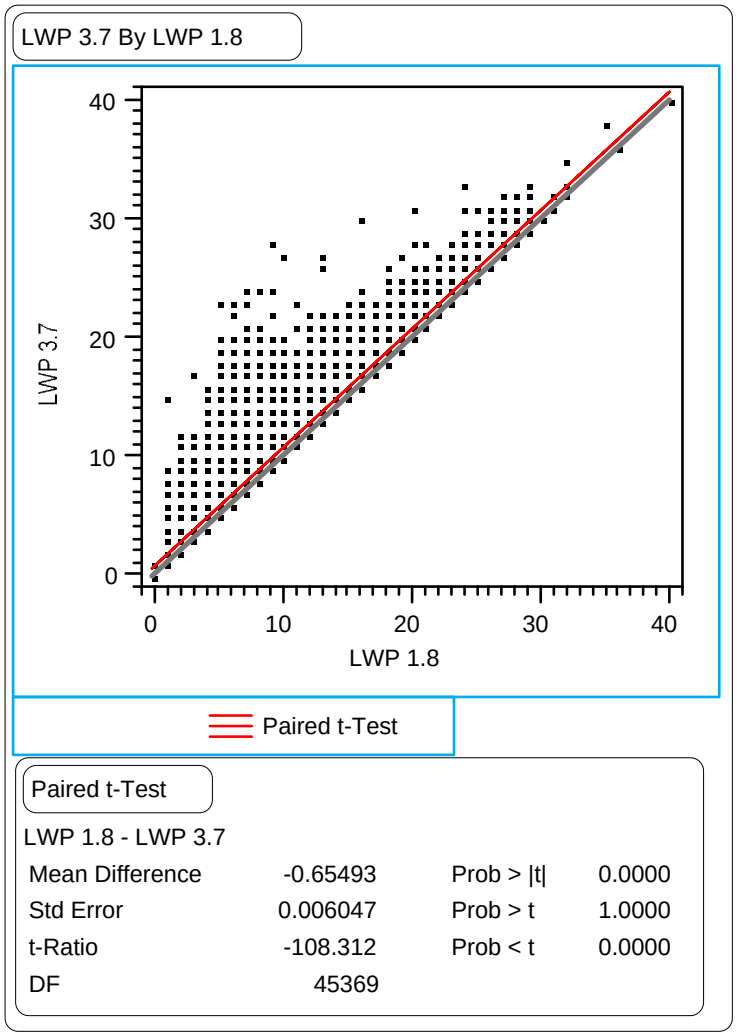

Figure 20. Paired t-test comparing LWP 1.8-m rut depths versus the LWP wire line rut depths.

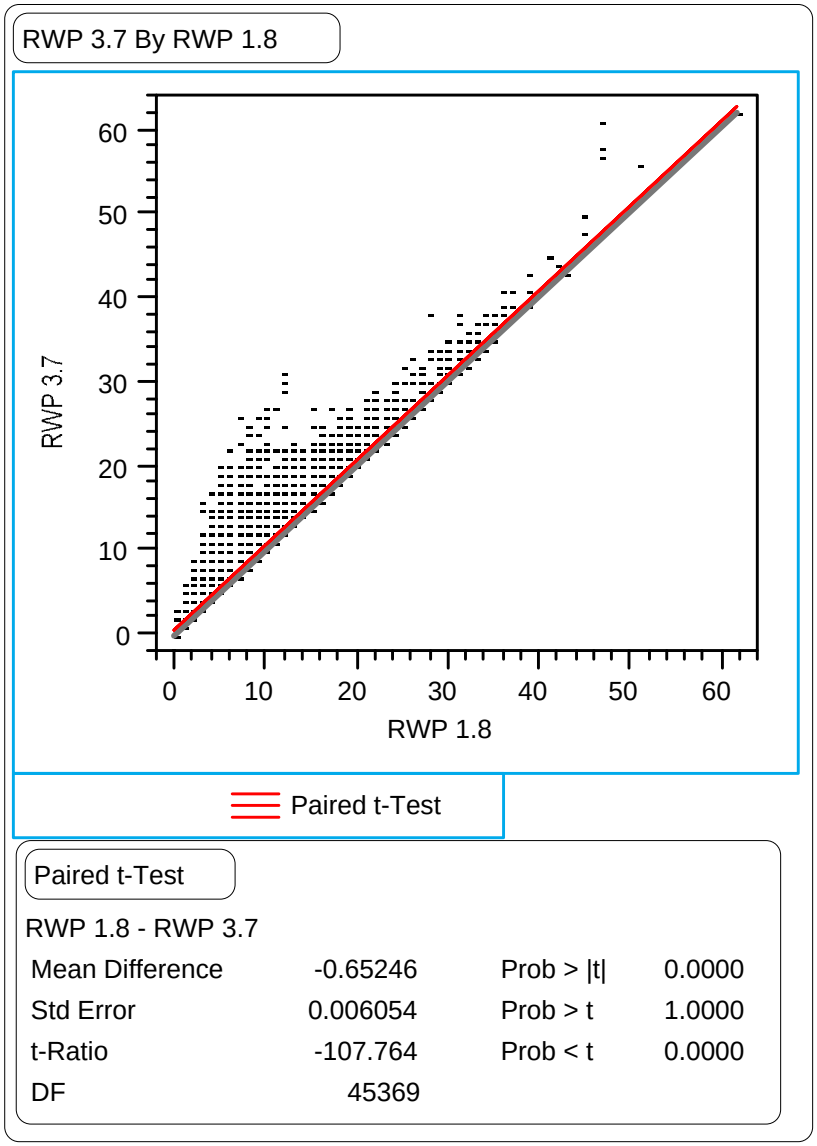

Figure 21. Paired t-test comparing the RWP 1.8-m rut depths versus the RWP wire line rut depths.

Areas

The fill area was fairly highly correlated to the rut depths. As noted previously, fill area is the volume of material required to "fill in" the ruts for a unit length of pavement. This value is essentially a two-dimensional representation of the rut or the rut width multiplied by the rut depth. By definition, it must show good correlation with the rut depths. However, for this reason, it was expected that the wire line rut width would also have a relatively large correlation with the fill area. However, just the opposite was observed when the correlations were examined.

The fill area also had a good correlation with the negative area. Figure 22 illustrates the relationship between these two indices. The fill area can be more than the absolute value of the negative area, but it can never be less. A fairly strong relationship was found between the fill area and the negative area. This is expected, because if the positive area is 0, the fill area and the negative area should be the same. Comparing the fill area to the negative area can be used as a quality control check on the data.

Summary

In general, the 1.8-m rut depth and the wire line rut depths provide the same measure of the rutting. The negative area and the fill area may indicate the same causes of the rutting. The 1.8-m and wire line rut widths generally provide the same type of information, though not highly correlated. The positive area does not provide the same information as any of the other indices.

Each index recommended for inclusion in the IMS has advantages and disadvantages. Rut depth is the most widely used index and many engineers have a good understanding of the range of rut depths typically encountered. However, this value alone provides only a one-dimensional measure of rutting.

The rut width provides data on the second dimension of rutting. Without using the rut depth in addition to the rut width, the severity of rutting is difficult to quantify. Since this parameter is not typically measured, most people may not have a feel for the range of rut widths that they may encounter.

The areas provide a two-dimensional characterization of the rutting. Because none of the area indices have been used widely in the past as with the rut widths, it may take some time to develop a good understanding of the range of values that may be encountered. The fill area could be useful to the State Highway Agencies (SHAs) for determining initial estimates of volumes of material to be used in a leveling course. Because this index is two-dimensional, a deep narrow rut will have the same value as a wide shallow rut. Finally, it is hypothesized that the combined use of the positive and negative areas may be indicative of the cause of the rutting. Trenching would be required to test this hypothesis.

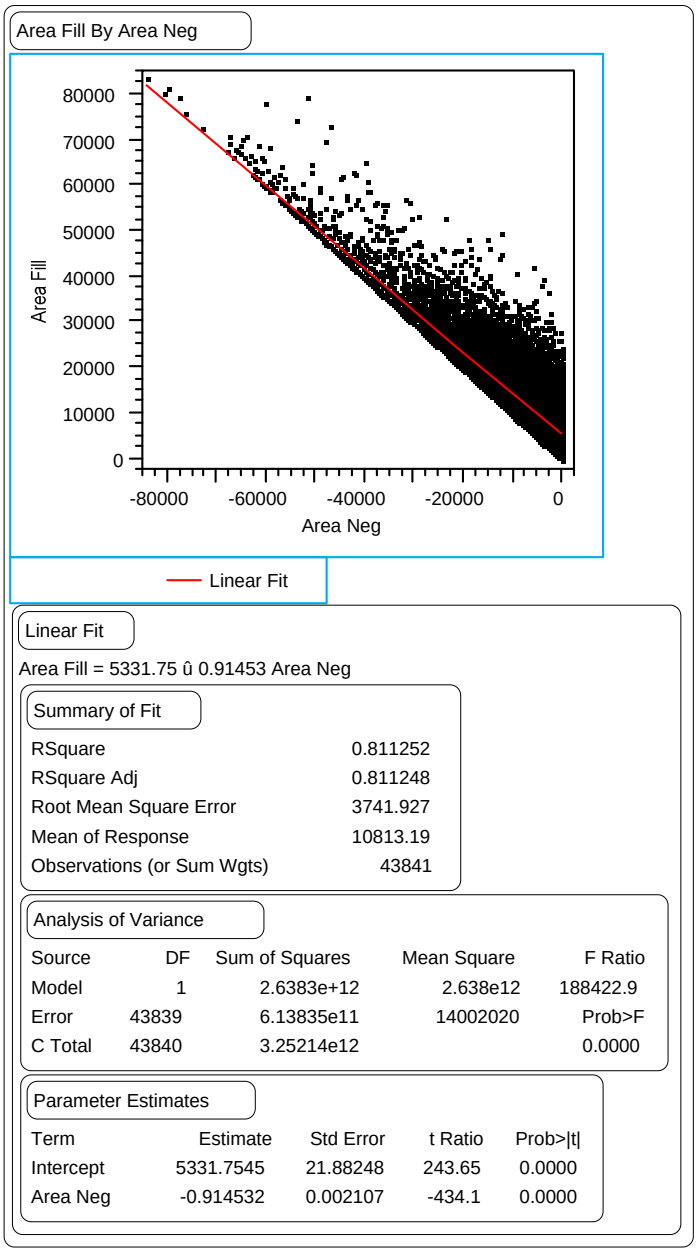

Figure 22. Comparison between the negative area index and the fill area index.

CHAPTER 5. INDEX EVALUATION

This chapter examines the relationship of each index to the other pavement parameters. These parameters include such items as age, base type, and HMA thickness. This analysis examines how the indices behave with respect to the wire line depth. In this way, the reader may gain more familiarity with these unfamiliar values. Furthermore, this analysis begins the process of discerning which indices may be useful in determining the mechanism causing the rutting. Any index that is affected by subgrade type provides information about how the surface rutting is affected by the subgrade.

A preliminary study was conducted to assess the variability of each index since most of the analyses conducted in this chapter use the section mean. Table 4 presents the ranges of the within-section standard deviations. As is evident, the ranges are quite broad. Each index, except the fill area, has some surveys for which the standard deviation is 0. Note that a standard deviation of 0 for the rut depths is the result of rounding off the data. The difference between the minimum and maximum rut depths for the cases where a standard deviation of 0 was found was typically 1 or 2 mm. The rut widths and rut locations that have a standard deviation of 0 were obtained from data that were collected by the Dipstick®. In these cases, the data for that survey were fairly uniform, such that even with the variations in the *y*-values collected, no variation was seen in the calculated indices. Finally, the surveys for which the negative area or the positive area has a 0 standard deviation merely indicates that all 11 profiles for each survey were either all above the horizontal datum or all below the horizontal datum.

Some of the test sections are extremely uniform, as shown by the minimum standard deviation of 0, while other test sections are quite variable. In general, the larger variabilities were seen in test sections with larger amounts of permanent deformation. This is illustrated by the range of the coefficient of variation (COV) shown in table 5. For the positive and negative areas where the standard deviation was 0, the mean was also 0. Because the COV was incalculable, the minimum shown in table 5 for these indices was not 0.

SECTION COMPARISONS

The section means were compared to determine how each index varied with some of the basic pavement parameters, such as surface thickness, climatic zone, subgrade type, and age. While many researchers and State highway personnel are familiar with rut depth (how it develops and the general magnitude of the value), it is anticipated that not nearly as many are familiar with the area indices or rut widths.

Table 4. Range of standard deviations for each index.

Index	Standard Deviation		
	Minimum	Mean	Maximum
Negative Area	0	3,128	19,164
Positive Area	0	3,552	27,616
Fill Area	206	3,096	18,373
1.8-m Rut Depth, LWP	0	2	11
1.8-m Rut Location, LWP	0	213	700
1.8-m Rut Width, LWP	0	181	796
1.8-m Rut Depth, RWP	0	2	18
1.8-m Rut Location, RWP	0	227	737
1.8-m Rut Width, RWP	0	184	774
Wire Line Rut Depth, LWP	0	2	11
Wire Line Rut Location, LWP	0	210	685
Wire Line Rut Width, LWP	0	457	1,915
Wire Line Rut Depth, RWP	0	2	18
Wire Line Rut Location, RWP	0	229	755
Wire Line Rut Width, RWP	0	459	1,915

Table 5. Range of COVs for each index.

Index	Coefficient of Variation, %	
	Minimum	Maximum
Negative Area	-7	-350
Positive Area	5	367
Fill Area	5	329
1.8-m Rut Depth, LWP	0	100
1.8-m Rut Width, LWP	0	124
1.8-m Rut Location, LWP	0	28
1.8-m Rut Depth, RWP	0	200
1.8-m Rut Location, RWP	0	146
1.8-m Rut Width, RWP	0	123
Wire Line Rut Depth, LWP	0	100
Wire Line Rut Location, LWP	0	26
Wire Line Rut Width, LWP	0	135
Wire Line Rut Depth, RWP	0	200
Wire Line Rut Location, RWP	0	146
Wire Line Rut Width, RWP	0	123

The comparisons in this section were used to examine the relationship between each index and standard materials characteristics and pavement parameters. These analyses were limited to simple comparisons of the indices between various groups. In all likelihood, the rutting observed on the surface is not due to just one factor, but rather to a combination of factors. In each case examined, the statements made are broad, sweeping claims that are only true if all the other conditions are equivalent. These supplemental analyses were conducted to determine whether the other indices behave in the same manner as the rut depth, which is better understood.

The test sections were divided into groups based on the parameter of interest, such as the age of the pavement or the thickness of the HMA layer. The group means were then compared using a Student's t-test with an α-level of 0.05. This provides a 95 percent level of confidence that the means are different. A test also was performed to determine whether the variances for each group were the same. All of these results are provided in appendix E. The distributions by GPS and SPS experiments are provided in appendix B.

Pavement Age

A linear regression was performed to determine how each index varied by age. Table 6 provides the results from each of the regressions for the GPS-1 experiment, HMA over granular base. A simple linear regression of the form $y = mx + b$ was used. In this case, y was the rutting index of interest. The coefficient (or slope), m, is provided in table 6. The age was x and the y-intercept was b or the value of the index at time 0. The F-statistic and the "Prob>F" provide the level of significance. The "Prob>F" is the probability of finding a larger F by pure chance. The regression is considered significant for a probability of less than 0.05.[8] The last value in the table is the coefficient of age from the linear regression or the slope of the line fit through the data.

These analyses show that the only indices that do not change significantly with age are the 1.8-m and wire line rut widths. At first, it appears that the negative area improves with age. However, the negative area is a negative number; therefore, a negative coefficient simply indicates that the negative area gets more negative (increases) with age. The sign of the coefficients for all of the other indices with significant regressions is positive. Because these are all positive numbers, these indices increase with time. Note that the coefficients for the 1.8-m and the wire line rut depths are the same and corroborate the fairly large correlation shown between these indices in chapter 4. In summary, the area and rut depth indices all increase with age, as expected.

Table 7 provides the results for the GPS-2 experiment, HMA over stabilized base. These results are similar to those for HMA over granular base. The 1.8-m and wire line rut widths did not have significant results except for the RWP 1.8-m rut width, which had a negative slope. This indicates that the RWP 1.8-m rut width decreases (the width gets narrower) with time. The results for the negative area also were insignificant. The other indices with significant results increased with time. While the coefficients for the 1.8-m and wire line rut depths are not as similar to each other as those for the HMA sections on granular base, these values lie within a narrow range.

Table 6. Results from comparisons with age for the GPS-1 section means.

Index	F	Prob>F	Coefficient
Negative Area	5.5967	0.0182	-105
Positive Area	8.7846	0.0031	142
Fill Area	13.4480	0.0003	162
1.8-m LWP Rut Depth	22.3839	<0.0001	0.10
1.8-m LWP Rut Width	0.0537	0.8168	-0.2
1.8-m RWP Rut Depth	12.8283	0.0004	0.08
1.8-m RWP Rut Width	0.1082	0.7423	-0.4
Wire Line LWP Rut Depth	22.6285	<0.0001	0.10
Wire Line LWP Rut Width	1.8210	0.1775	-4.7
Wire Line RWP Rut Depth	11.9857	0.0006	0.09
Wire Line RWP Rut Width	1.7074	0.1916	-4.7

Table 7. Results from comparisons with age for the GPS-2 section means.

Index	F	Prob>F	Coefficient
Negative Area	0.7411	0.3897	-43
Positive Area	7.6285	0.0059	194
Fill Area	7.0746	0.0080	127
1.8-m LWP Rut Depth	10.5178	0.0012	0.07
1.8-m LWP Rut Width	1.8177	0.1788	-2.3
1.8-m RWP Rut Depth	5.8403	0.0160	0.05
1.8-m RWP Rut Width	5.5479	0.0188	-4.5
Wire Line LWP Rut Depth	11.3622	0.0008	0.08
Wire Line LWP Rut Width	1.6629	0.1977	-6.4
Wire Line RWP Rut Depth	6.9163	0.0088	0.07
Wire Line RWP Rut Width	3.0783	0.0799	-8.9

Experiment Comparisons

Next, the indices for the HMA over granular base experiment were compared to those observed on test sections in the GPS-7 experiment, HMA overlay of portland cement concrete (PCC). These results are provided in appendix E. No significant difference was seen between the two experiments for the positive area and the LWP wire line rut width. For all of the other indices, the test sections with HMA over granular base had greater amounts of rutting than the HMA overlay of PCC sections. It is anticipated that the HMA overlay of PCC sections would have less rutting than the GPS-1 sections. Rutting potentially could occur in any layer of the structure in the HMA over granular base sections. However, since no rutting is expected to occur in the PCC layer, rutting should be limited to the HMA overlay in the GPS-7 sections. This should limit the total amount of rutting that does occur. In this comparison, the positive area does not behave in the same manner as the other indices. This index probably does not provide the same information about the transverse profile as the other indices.

Thickness of Asphalt Concrete Layers

The test sections in the GPS-1 (HMA over granular base) and GPS-2 (HMA over stabilized base) experiments were grouped by the thickness of the HMA surface. If the section had less than 76 mm of HMA surface, it was placed in the thin group. If a section had between 76 mm and 178 mm of HMA, it was placed in the moderate group. If the section had more than 178 mm of HMA, it was placed in the thick group. The thick sections had significantly more negative area and less positive area than the other two groups. The thick sections had larger RWP 1.8-m rut widths than the thin or moderate sections. The thin sections had smaller LWP 1.8-m rut widths than the moderate or thick sections. The thin sections had smaller LWP 1.8-m rut depths and LWP wire line rut widths. In general, the thicker asphalt sections had wider ruts.

Base Stabilization

The sections in the GPS-1 (HMA over granular base) and GPS-2 (HMA over stabilized base) experiments with less than 127 mm of HMA were selected for further study. In general, the rutting of thin asphalt pavements is expected to be governed by base and subgrade properties. Therefore, the set of sections used were limited to those that would be considered thin-surfaced. These sections were divided into two groups based on whether or not the base had been stabilized, and comparisons were made between the two groups. The results are provided in appendix E.

All of the indices, except positive area, were larger for the sections with granular bases than for those with stabilized bases. The test sections with granular bases exhibited smaller positive area than the sections with stabilized bases. In theory, and all else being equal, the stabilized bases will do a better job of distributing the load on the subgrade. The improved load distribution should prevent some of the accumulation of rutting (or permanent deformation) in the lower portion of the structure, such as the base and subgrade. Therefore, the sections with stabilized bases should perform better than those with granular bases.

The sections with stabilized bases subsequently were divided into two groups based on whether the base was portland cement-stabilized (cement) or asphalt-stabilized (asphalt). The test sections in the cement group had larger positive areas, on average, than the sections in the asphalt group. Otherwise, all of the indices were larger, on average, for the sections in the asphalt group than for the sections in the cement group. In general, a cement-stabilized material is expected to be stiffer than an asphalt-stabilized material. The stiffer material should prevent rutting in the underlying layers. Therefore, the sections with a cement-stabilized base should accumulate less rutting than those with an asphalt-stabilized base, assuming that all other conditions are equal. It was expected that the indices would be larger for the sections with an asphalt-stabilized base than for those with a cement-stabilized base.

Climatic/Environmental Zones

For the last set of comparisons, the GPS-7 (HMA overlay of PCC) sections were used to examine the trends of the indices by environmental zones. These test sections were divided into freeze (F) and no-freeze (NF) based on the freeze index. If the freeze index was greater than 56°C-days, the section was considered to be in a freeze zone. If the freeze index was less than 56°C-days, the section was considered to be in a no-freeze zone. These results are also provided in appendix E.

The no-freeze zone had more negative area, more fill area, larger 1.8-m rut depths, larger wire line rut depths, and larger wire line rut widths in the LWP than the freeze zone. There were no significant differences observed in the positive area, 1.8-m rut widths, and RWP wire line rut widths. The rut widths in this case were not larger for the sections in the warmer climate. The positive area is not just a measure of rutting, but also may be a measure of heave. The lack of a significant difference for the positive area and the rut widths should not be a cause for concern as these indices are providing new information about the transverse profile.

Theoretically, larger rutting should occur in the overlay in a warm climate. Those indices most closely related to the severity of rutting increase in the no-freeze environment.

Summary

For most of the groups described above, the indices performed in a manner that is consistent with theory. Sections with a stiff structure exhibited less rutting. The GPS-7 (HMA overlay of PCC) sections had larger indices than the GPS-1 (HMA over granular base) sections. Stiff base types had smaller indices than the less stiff base types. In addition, GPS-7 sections in warm climates had more rutting, or larger indices, than those in cool climates. However, the rut width and positive areas were the least likely to conform to generally accepted, albeit simplistic, theory on how rutting progresses. This indicates that as a rut gets deeper, it does not necessarily get wider.

VARIABILITY COMPARISONS

Table 5 listed the minimum and maximum within-section COV. A check was made to determine how the COVs varied with changes in structure and environment. Table 5 provided the range of COVs for all of the data in the database. Table 8 provides the minimum, mean, and maximum within-section COV for the test sections in the GPS-1 and GPS-2 experiments.

Table 8. Distribution of within-section COVs for GPS-1 and GPS-2 experiments.

Index	Minimum	Mean	Maximum
Negative Area	-7	-87	-350
Positive Area	6	82	367
Fill Area	6	28	329
1.8-m LWP Rut Depth	0	28	100
1.8-m RWP Rut Depth	0	29	200
1.8-m LWP Rut Width	0	14	124
1.8-m RWP Rut Width	0	14	123
Wire Line LWP Rut Depth	0	28	100
Wire Line RWP Rut Depth	0	29	200
Wire Line LWP Rut Width	0	25	135
Wire Line RWP Rut Width	0	26	123

Table 8 illustrates that the distribution of the within-section variation is similar for the indices. The mean COV for the negative and positive areas are larger than the other means, but the rest of the values are close. The sections were then divided into a “thin” group if the HMA surface was less than 127 mm or a “thick” group if the HMA surface was greater than 127 mm. Table 9 provides the ranges of COVs for these two groups.

Not much difference is observed between the two groups. The number of observations in the thin group is 716 and the number of observations in the thick group is 711.

Further examination of the indices variability with structure is based on a comparison between those sections with a thin surface and a granular base and those sections with a thick surface and a stabilized base. Table 10 includes these results. In this table, “weak” refers to a pavement that has less than 76 mm of HMA and a granular base, while “strong” refers to a pavement that has more than 76 mm of HMA and a stabilized base.

Table 9. Distribution of within-section COVs for thin and thick test sections.

Index	Thin			Thick		
	Min.	Mean	Max.	Min.	Mean	Max.
Negative Area	-8	-87	-350	-7	-83	-350
Positive Area	7	82	367	7	85	333
Fill Area	6	29	329	7	26	115
1.8-m LWP Rut Depth	0	29	100	0	27	100
1.8-m RWP Rut Depth	0	29	200	0	29	100
1.8-m LWP Rut Width	0	14	124	0	12	96
1.8-m RWP Rut Width	0	15	123	0	12	102
Wire Line LWP Rut Depth	0	29	100	0	27	100
Wire Line RWP Rut Depth	0	29	200	0	28	100
Wire Line LWP Rut Width	0	25	135	0	24	96
Wire Line RWP Rut Width	0	26	123	0	25	102

Table 10. Distribution of within-section COVs for weak and strong structures.

Index	Weak			Strong		
	Min.	Mean	Max.	Min.	Mean	Max.
Negative Area	-8	-81	-341	-13	-93	-340
Positive Area	8	86	367	8	75	277
Fill Area	7	29	171	9	27	84
1.8-m LWP Rut Depth	0	28	100	0	30	100
1.8-m RWP Rut Depth	0	30	100	0	29	100
1.8-m LWP Rut Width	0	13	124	0	14	54
1.8-m RWP Rut Width	0	12	123	0	15	102
Wire Line LWP Rut Depth	0	29	100	0	30	100
Wire Line RWP Rut Depth	0	30	100	0	29	100
Wire Line LWP Rut Width	0	25	135	0	24	80
Wire Line RWP Rut Width	0	25	123	3	25	102

There were 401 sections in the weak group and 173 sections in the strong group. The maximum COV is lower for the strong group than for the weak group; however, the difference may be due to the number of test sections. No conclusions can be drawn from these data.

TIME-SERIES STABILITY

Each index from each section was plotted by survey date. In this analysis, the section means of the indices were used. A line was fitted through the points. In some cases, only two points in time were available. If more than two points were available, least-squares regression was used to fit the line to the data.[8] Generally, even if the data do not follow a linear trend, if they increase with time, a line fit to the data will have a positive slope. The plots and regressions were used to examine the time-series trends exhibited by the indices.

Slope Comparisons

The slopes of the lines fitted to the data were placed in a separate database. The sign of the slope for each index was compared to the sign on the RWP 1.8-m rut depth. The 1.8-m rut depth is a quantity that has been used on many occasions and its response to various conditions is fairly well documented. The expectation is that the rut depth will usually increase with time. Occasionally, a section of roadway may experience frost heave or swelling soil and, in this case, the rut depth could decrease. The results for these analyses, as well as the distributions of the slopes, are provided in appendix F.

The cross tabs, or contingency tables, provide a count for each of the cells.[8] The –1 indicates a negative slope, 0 indicates a zero slope, and +1 indicates a positive slope. In the first figure in appendix F, the slopes for the negative area are compared to those for the RWP 1.8-m rut depth. Only 20 percent of the test sections had the same slope. The negative area is a negative number. For the size of the negative area to increase over time, the slope of the line has to be negative. This means that for the negative area to exhibit the same trend as the 1.8-m rut depth (i.e., increasing in size when the rut depth increases in size), its slope must be opposite in sign. A second review of the table illustrates that the slopes for the negative area are opposite in sign from the slopes for the RWP 1.8-m rut depth 64 percent of the time. The negative area index should not be expected to behave the same way over time as the RWP 1.8-m rut depth.

The positive area was examined in comparison to the RWP 1.8-m rut depth. For one section of 793 total sections, the positive area exhibited a 0 slope where the RWP 1.8-m rut depth exhibited a positive slope. The slope for the rut depth on this section was 0.0003. In all other instances, if the RWP 1.8-m rut depth exhibited a zero slope, the positive area exhibited a zero slope, and if the positive area exhibited a zero slope, the RWP 1.8-m rut depth exhibited a zero slope. For 39 percent of the sections, the slopes for the two indices had the same sign. For the amount of rutting to increase significantly, the amount of positive area will probably decrease. In this case, the sign of the positive area over time would be the opposite of the sign of the RWP 1.8-m rut depth. A second review of the contingency table shows that 44 percent of the sections are the opposite in sign. Based on this review, the positive area may not exhibit consistent trends with the RWP 1.8-m rut depth.

The fill area, LWP 1.8-m rut depth, and the wire line rut depths were all fairly highly correlated with the RWP 1.8-m rut depth, so the slopes were expected to be similar. In addition, if the rut depth increases, the fill area and other rut depths should increase. The contingency tables for each of these indices reveal that if the RWP 1.8-m rut depth exhibited a zero slope, then the other indices also exhibited a zero slope and vice versa. In addition, the slopes had the same sign for 85 percent of the sections for the fill area, 82 percent of the sections for the LWP 1.8-m rut depth, 95 percent of the sections for the RWP wire line rut depth, and 82 percent of the sections for the LWP wire line rut depth. This analysis indicates that these indices will follow the same general trends as the RWP 1.8-m rut depth.

The 1.8-m rut widths and the wire line rut widths were the last set of indices to be examined. The slopes for these indices were all zero when the slope for the RWP 1.8-m rut depth was zero. The slopes had the same sign for 67 percent of the sections for the RWP 1.8-m rut width, 63 percent of the sections for the LWP 1.8-m rut width, 69 percent of the sections for the RWP wire line rut width, and 66 percent of the sections for the LWP wire line rut width. These values indicate that these indices may not follow the same trend as the RWP 1.8-m rut depth.

Check for Decreasing Ruts

The next step in examining the time-series trends was to review the plots to determine if there were significant decreases or increases on any of the test sections. Again, the section means were used rather than the individual index. A threshold value was set for this examination. The decrease had to be larger than these values before it was reported. An estimate of error of 2 mm was used in the examination of rut depths. An error in the rut widths was allowed to be as high as 100 mm before it was reported. The area indices were all allowed to have an error of 1,000 mm^2. Initially, 4,133 sections were reviewed to obtain the list provided in table 11.

These decreases may be due to a number of causes, such as frost heave or swelling soils. Alternatively, they may be due to maintenance or rehabilitation of the test section. These trends were noted on test sections where both the PASCO RoadRecon unit and the Dipstick® had been used to collect data; however, not all sections where both equipment had been used to collect data exhibited this type of trend. Another factor that might contribute to this trend is the fact that the measurements are never taken at exactly the same station in consecutive surveys. While Dipstick® surveys generally repeat the same stations on each survey, the PASCO RoadRecon unit will not be able to achieve such accuracy. Table 11 includes a list of test sections that exhibited these decreases and possible explanations.

The trends reviewed were of the section averages. When all of the sections with decreasing trends were identified, the trends for the individual stations within each test section were reviewed. With the exception of one or two stations in any given section, the individual stations followed the same trends as the section averages. Next, the longitudinal profile and distress data were identified to determine whether these exhibited a similar decrease. A decrease in the International Roughness Index (IRI) or other distress would have been indicative of a maintenance or rehabilitation event. As seen in the table, many of the trends can be attributed to

Table 11. Time-series stability trends.

Section ID	Index	Potential Explanation
021001	Pos Area	No explanation
041001	All Areas	Use of both PASCO and Dipstick® for measurement
041002	All	Use of both PASCO and Dipstick® for measurement
041003	All	Distress decreased from May 1993 to Jan. 1994, suggesting rehabilitation or maintenance
041006	All	Distress decreased from May 1993 to Jan. 1994, suggesting rehabilitation or maintenance
041007	All	Distress decreased from Sept. 1994 to Feb. 1995, suggesting rehabilitation or maintenance
041015	Fill, Neg Areas; Widths	Use of both PASCO and Dipstick® for measurement
041017	Widths	Use of both PASCO and Dipstick® for measurement
041022	Neg, Fill Areas, Depths, Widths	Appears to be maintenance or rehabilitation, but not enough distress or longitudinal profile data available to verify
041034	Depths	Use of both PASCO and Dipstick® for measurement
068153	Pos, Neg Areas; Depths	Use of both PASCO and Dipstick® for measurement
081029	Depths, Widths	IRI decreased from Nov. 1993 to Sept. 1997, suggesting rehabilitation or maintenance
081047	All Areas, Depths	Decrease is due to use of both PASCO and Dipstick® for measurement
087780	Depths	Appears to be maintenance or rehabilitation, but not enough distress or longitudinal profile data available to verify
161005	Neg, Fill Areas	No explanation
161009	All Areas, Depths	Decrease in IRI from Aug. 14, 1991 to Oct. 24, 1992, suggesting an unrecorded maintenance or rehabilitation event
161010	Pos Area	Use of both PASCO and Dipstick® for measurement
161020	All	No explanation
161021	Pos Area, Widths	Use of both PASCO and Dipstick® for measurement
231001	Depths	No explanation
307066	Pos, Neg Areas	Use of both PASCO and Dipstick® for measurement
341003	RWP Depths	No explanation
341011	Pos, Neg Areas	No explanation
341030	Depths	No explanation
371006	Depths	Use of both PASCO and Dipstick® for measurement
371024	All	Database shows overlaid on Nov. 10, 1992; however, data trend indicates that construction probably took place prior to Oct. 14, 1992
371817	Depths	No explanation
371992	All	Use of both PASCO and Dipstick® for measurement

Table 11. Time-series stability trends (continued).

Section ID	Index	Potential Explanation
421597	Pos Area, Depths	Use of both PASCO and Dipstick® for measurement
421605	Neg, Fill Areas; Depths	Decrease in distress from May 5, 1993 to Oct. 20, 1993, suggesting an unrecorded maintenance or rehabilitation event
491001	Depths, Widths	Use of both PASCO and Dipstick® for measurement
491008	Neg, Fill Areas; Depths	Distress and IRI data suggest that the drop is not due to a maintenance or rehabilitation event
491017	Depths	Use of both PASCO and Dipstick® for measurement
501002	Widths	No explanation available
501004	Depths	No explanation
511002	Depths	IRI data suggest that the drop is not due to a maintenance or rehabilitation event
531008	All Areas, Depths	Decrease in distress from June 16, 1994 to Aug. 31, 1994, suggesting an unrecorded maintenance or rehabilitation event
531801	All Areas	No explanation
811805	Neg, Fill Areas; Depths, Widths	Decrease in distress from May 24, 1995 to Aug. 25, 1995, suggesting an unrecorded maintenance or rehabilitation event
041062	Pos Area, Depths	Use of both PASCO and Dipstick® for measurement
062041	Neg Area, Depths	Use of both PASCO and Dipstick® for measurement
062647	Pos Area	Use of both PASCO and Dipstick® for measurement
087781	Depths	Appears to be maintenance or rehabilitation, but not enough distress or longitudinal profile data to verify
322027	All	Use of both PASCO and Dipstick® for measurement
341638	All Areas, Depths	No explanation
361643	Neg Area, Depths, Widths	Decrease in IRI from May 1996 to Oct. 1997, suggesting rehabilitation or maintenance
361644	Depths	No explanation
371645	Depths, Widths	Use of both PASCO and Dipstick® for measurement
372825	Depths	Use of both PASCO and Dipstick® for measurement
412002	Neg, Fill Areas; Depths, Widths	Decrease in distress from May 5, 1993 to Oct. 20, 1993, suggesting an unrecorded maintenance or rehabilitation event
501681	All	No explanation
541640	All	Decrease in IRI from Sept. 1990 to Nov. 1991, suggesting rehabilitation or maintenance
562015	Depths	IRI data suggest that the drop is not due to maintenance or rehabilitation
562037	Pos, Neg Areas	No explanation
567772	All	Use of both PASCO and Dipstick® for measurement
567773	All Areas	No explanation

Table 11. Time-series stability trends (continued).

Section ID	Index	Potential Explanation
818529	Neg, Fill Areas; Depths	Use of both PASCO and Dipstick® for measurement
871680	Pos Area, Widths	No explanation
881647	Pos Area	No explanation
892011	Pos Area	No explanation
046055	Pos Area, Widths	No explanation
046060	All Areas	Use of both PASCO and Dipstick® for measurement
066044	Depths	Use of both PASCO and Dipstick® for measurement
086002	Neg, Fill Areas; Depths	Use of both PASCO and Dipstick® for measurement
306004	Pos, Neg Areas; Depths	No explanation
416011	Pos Area	Use of both PASCO and Dipstick® for measurement
491005	Depths	No explanation
491006	All Areas	No explanation
536048	All Areas	No explanation
566029	Neg, Fill Areas	No explanation
566031	All Areas, Widths	Decrease in IRI from July 1994 to July 1997, suggesting rehabilitation or maintenance
566032	All Areas	Use of both PASCO and Dipstick® for measurement
826007	Depths	Use of both PASCO and Dipstick® for measurement
846804	Neg, Fill Areas; Depths, Widths	IRI data suggest that the drop is not due to maintenance or rehabilitation
361008	Pos Area	No explanation
371803	Depths	Use of both PASCO and Dipstick® for measurement
511423	Pos Area	No explanation
811804	Fill Area	Use of both PASCO and Dipstick® for measurement
371352	Pos Area	Use of both PASCO and Dipstick® for measurement
826007	Fill Area, Depths, Widths	Use of both PASCO and Dipstick® for measurement
871620	Pos Area, Widths	No explanation
087035	Neg, Fill Areas; Depths, Widths	Appears to be maintenance or rehabilitation, but not enough distress or longitudinal profile data to verify
417018	Neg, Fill Areas; Depths	Use of both PASCO and Dipstick® for measurement
421610	Pos Area	No explanation
547008	All	Decrease in IRI from April 29, 1992 to Nov. 5, 1993, suggesting an unrecorded maintenance or rehabilitation event
872811	Pos Area	No explanation
872812	Pos Area, Depths	No explanation
421614	Depths	No explanation
320103	Pos, Neg Areas	Use of both PASCO and Dipstick® for measurement

Table 11. Time-series stability trends (continued).

Section ID	Index	Potential Explanation
320104	Pos Area	Use of both PASCO and Dipstick® for measurement
320105	Pos Area	Use of both PASCO and Dipstick® for measurement
320107	Pos Area	Use of both PASCO and Dipstick® for measurement
320108	Neg Area	Use of both PASCO and Dipstick® for measurement
320109	Neg, Fill Areas	Use of both PASCO and Dipstick® for measurement
320110	Neg Area	Use of both PASCO and Dipstick® for measurement
320112	Pos Area	Use of both PASCO and Dipstick® for measurement
510114	Pos Area	No explanation
04C340	Depths, Widths	Use of both PASCO and Dipstick for measurement
04C350	Neg, Fill Areas; Depths, Widths	EXPERIMENT_SECTION table shows Out of Study on Feb. 1, 1997; however, data indicate that the construction probably took place prior to Sept. 26, 1996
04D310	Widths	Use of both PASCO and Dipstick® for measurement
08A320	All Areas	Use of both PASCO and Dipstick® for measurement
08A350	Neg, Fill Areas	Use of both PASCO and Dipstick® for measurement
16A310	Pos Area	Use of both PASCO and Dipstick® for measurement
16A320	All Areas	Use of both PASCO and Dipstick® for measurement
16A330	Pos Area	Use of both PASCO and Dipstick® for measurement
16A350	Pos Area	Use of both PASCO and Dipstick® for measurement
16B320	Pos, Neg Areas	Use of both PASCO and Dipstick® for measurement
16B330	Pos Area	Use of both PASCO and Dipstick® for measurement
16B350	Pos Area	Use of both PASCO and Dipstick® for measurement
24A310	Pos, Fill Areas	Use of both PASCO and Dipstick® for measurement
24A311	Pos Area	Use of both PASCO and Dipstick® for measurement
24A331	Pos Area	Use of both PASCO and Dipstick® for measurement
24A350	Pos Area	Use of both PASCO and Dipstick® for measurement
30A310	Pos, Neg Areas; Depths	Use of both PASCO and Dipstick® for measurement
30A330	Pos, Neg Areas	Use of both PASCO and Dipstick® for measurement
32B310	Pos Area	Use of both PASCO and Dipstick® for measurement
32B330	Neg Area	Use of both PASCO and Dipstick® for measurement
32B340	All Areas	Use of both PASCO and Dipstick® for measurement
32B350	Pos, Neg Areas	Use of both PASCO and Dipstick® for measurement
36A310	Depths	No explanation
36A320	All	No explanation
36A321	Neg Area, Depths	No explanation
36A331	Pos, Neg Areas; Depths	Use of both PASCO and Dipstick® for measurement
36A340	Neg Area, Depths	Use of both PASCO and Dipstick® for measurement
36B320	Depths	Use of both PASCO and Dipstick® for measurement
36B350	Pos Area	No explanation

Table 11. Time-series stability trends (continued).

Section ID	Index	Potential Explanation
36B351	Pos Area, Depths, Widths	EXPERIMENT_SECTION table has not been updated to include construction event number 2
36B353	Pos Area	No explanation
42B330	Pos Area	No explanation
42B340	Pos Area, Depths	No explanation
42B350	Pos Area	No explanation
42B351	Pos, Neg Areas, Depths	Use of both PASCO and Dipstick® for measurement
49A320	Pos Area, Depths; Widths	Use of both PASCO and Dipstick® for measurement
49A330	Pos Area	Use of both PASCO and Dipstick® for measurement
49B350	Pos Area	Use of both PASCO and Dipstick® for measurement
49B390	Pos Area	Use of both PASCO and Dipstick® for measurement
49C320	Pos, Neg Areas	Use of both PASCO and Dipstick® for measurement
49C330	Pos, Neg Areas	Use of both PASCO and Dipstick® for measurement
49C350	Pos, Neg Areas	Use of both PASCO and Dipstick® for measurement
51A321	Pos Area	Use of both PASCO and Dipstick® for measurement
53C350	Pos, Fill Areas	Use of both PASCO and Dipstick® for measurement
87A311	Widths	No explanation
87B360	Pos Area, Depths	EXPERIMENT_SECTION table shows no change in construction number
87B361	Depths	Use of both PASCO and Dipstick® for measurement
040503	Depths	Use of both PASCO and Dipstick® for measurement
040505	Depths	Use of both PASCO and Dipstick® for measurement
040506	Depths	Use of both PASCO and Dipstick® for measurement
230503	All	EXPERIMENT_SECTION table has not been updated to include construction event number 2
230504	All	EXPERIMENT_SECTION table has not been updated to include construction event number 2
230505	All	EXPERIMENT_SECTION table has not been updated to include construction event number 2
230506	All	EXPERIMENT_SECTION table has not been updated to include construction event number 2
230507	All	EXPERIMENT_SECTION table has not been updated to include construction event number 2
230508	All	EXPERIMENT_SECTION table has not been updated to include construction event number 2
230509	All	EXPERIMENT_SECTION table has not been updated to include construction event number 2
230559	All	EXPERIMENT_SECTION table has not been updated to include construction event number 2

Table 11. Time-series stability trends (continued).

240559	Pos Area	Use of both PASCO and Dipstick® for measurement
240563	Pos Area	Use of both PASCO and Dipstick® for measurement
240560	All	EXPERIMENT_SECTION table has not been updated to include construction event number 2
300561	Pos Area	Use of both PASCO and Dipstick® for measurement
060603	Pos Area	Use of both PASCO and Dipstick® for measurement
060604	Pos Area	Use of both PASCO and Dipstick® for measurement
060606	Pos Area	Use of both PASCO and Dipstick® for measurement
060607	Pos Area	Use of both PASCO and Dipstick® for measurement
060608	Pos, Fill Areas	Use of both PASCO and Dipstick® for measurement
420603	Pos, Neg Areas	Use of both PASCO and Dipstick® for measurement
420604	Pos, Neg Areas	Use of both PASCO and Dipstick® for measurement
420606	Pos, Neg Areas	Use of both PASCO and Dipstick® for measurement
420607	Pos, Neg Areas	Use of both PASCO and Dipstick® for measurement
420608	Depths	Use of both PASCO and Dipstick® for measurement
300805	Pos Area	Use of both PASCO and Dipstick® for measurement
340801	Neg, Fill Areas	Use of both PASCO and Dipstick® for measurement
340802	Fill Area, Depths, Widths	Use of both PASCO and Dipstick®for measurement
360801	Pos Area	Use of both PASCO and Dipstick®for measurement

the change in devices (i.e., PASCO and Dipstick®) between surveys. Some of the trends, however, cannot be explained by a change in device or by a maintenance or rehabilitation event.

SUMMARY

The comparisons in this chapter are provided in table 12. This summary shows that the positive area, negative area, and LWP rut depths are the most consistently affected of all of the pavement parameters. The 1.8-m rut widths were the least affected indices. The positive and negative areas should be examined further for their potential for identifying the rutting mechanism.

Table 12. Summary of comparisons.

Rutting Index	Age	HMA/Granular Base vs. HMA Overlay of PCC	GPS-1 and GPS-2				GPS-7 Freeze vs. No-Freeze
			Surface Thickness		HMA < 127 mm Stabilized vs. Non-Stabilized	HMA < 127 mm Asphalt Stabilized vs. Cement Stabilized	
			< 76 vs. 76-118	76-118 vs. > 118			
Negative Area	I	S		S	S	S	S
Positive Area	I			S	S	S	
Fill Area	I	S			S	S	S
1.8-m LWP Rut Depth	I	S	S		S	S	S
1.8-m LWP Rut Width		S	S		S	S	
1.8-m RWP Rut Depth	I	S			S	S	S
1.8-m RWP Rut Width		S		S	S	S	
Wire Line LWP Rut Depth	I				S	S	S
Wire Line LWP Rut Width		S	S		S	S	S
Wire Line RWP Rut Depth	I	S			S	S	S
Wire Line RWP Rut Width		S			S	S	S

I = Increase, S = Significant at 95 percent level of confidence

CHAPTER 6. COMPARISONS OF THREE-POINT AND FIVE-POINT RUT DEPTHS

The three-point and five-point systems are used by many SHAs for collecting project- and network-level rut depths. Most of these agencies use a "Rut Bar" mounted on a vehicle with either three or five acoustic sensors. A survey of SHAs on equipment used for transverse profile data collection indicated that among the 39 SHAs responding, 22 SHAs use a three-point system. These data are shown graphically in figure 23.

The acoustic sensors measure the distance, or height, from the sensor to the pavement surface at the locations defined below.

- The three-point systems have one sensor located above each wheelpath and one sensor in the middle. Hence, a rut depth is obtained for each wheelpath by calculating the difference between the height at the center of the pavement and the height over each wheelpath.

- The five-point systems have two extra sensors, usually located approximately 0.30 m from the outside of the two wheelpath sensors.

An analysis was undertaken to determine how measurements from the three- and five-point systems compare and how the measurements compare with rut depths calculated based on a lane-width wire line.

METHOD OF CALCULATION

A software program was written to calculate the three-point and five-point rut depths from the transverse profiles collected by the RoadRecon unit and the Dipstick®. In this program, it is assumed that the data collected by these two methods are connected by straight lines. This is considered to yield a reasonably accurate representation of the transverse profile.

The software used two approaches in generating the data, as illustrated in figure 24. In the "best case" scenario, the transverse placement of the rut bar is identical at each station along the test section at which transverse profiles are collected. This scenario assumes that there is no lateral vehicle movement in the lane within the test section. In the "worst case" scenario, the transverse placement of the rut bar is random for all stations. This scenario assumes that there is variable lateral vehicle movement in the lane within the test section.

Regardless of the scenario, 30 rut depth calculations are made at each station along the highway at a randomly selected transverse location. The left sensor is placed assuming a normal distribution, with an average placement of 914 mm.

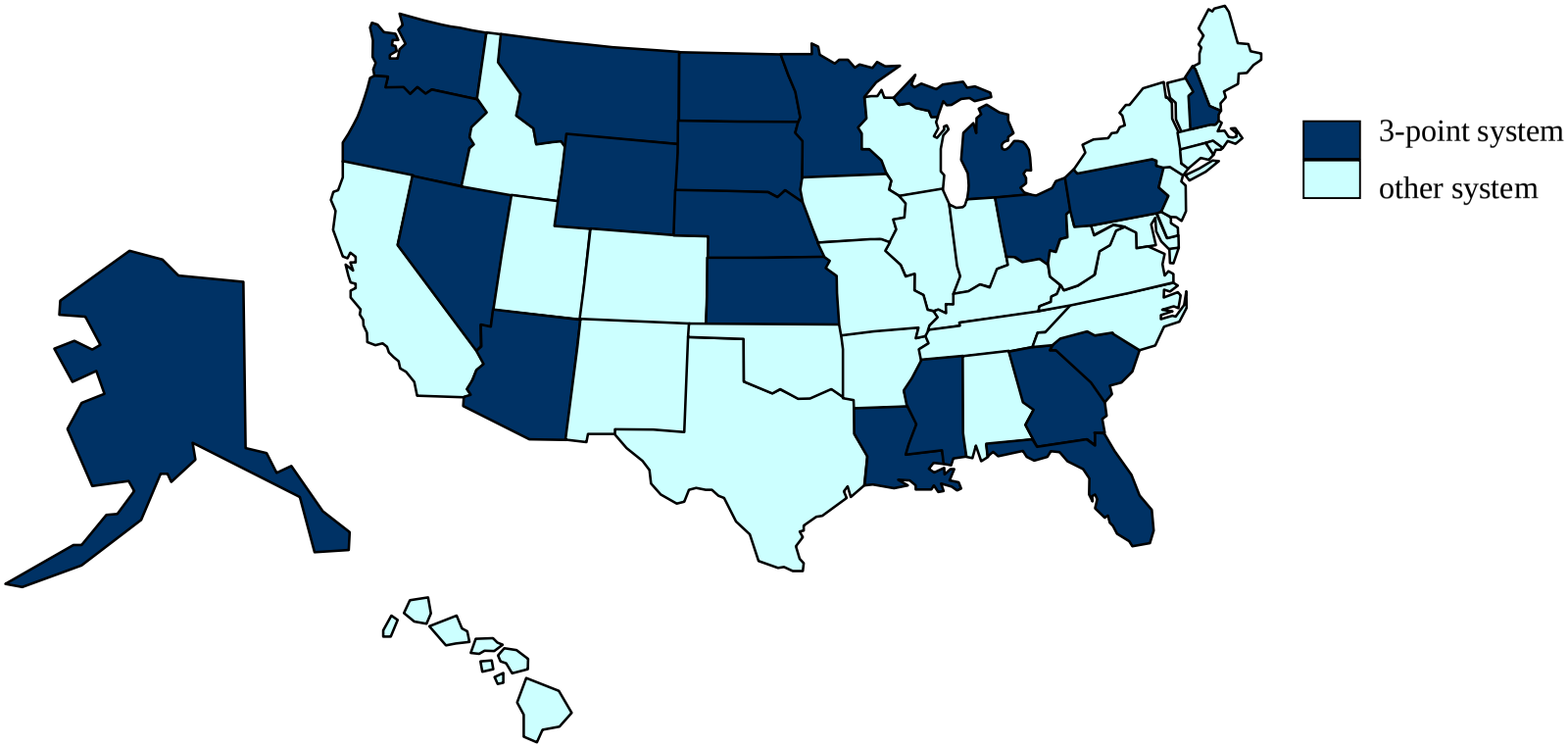

Figure 23. Illustration of those States that use a three-point profiling system.

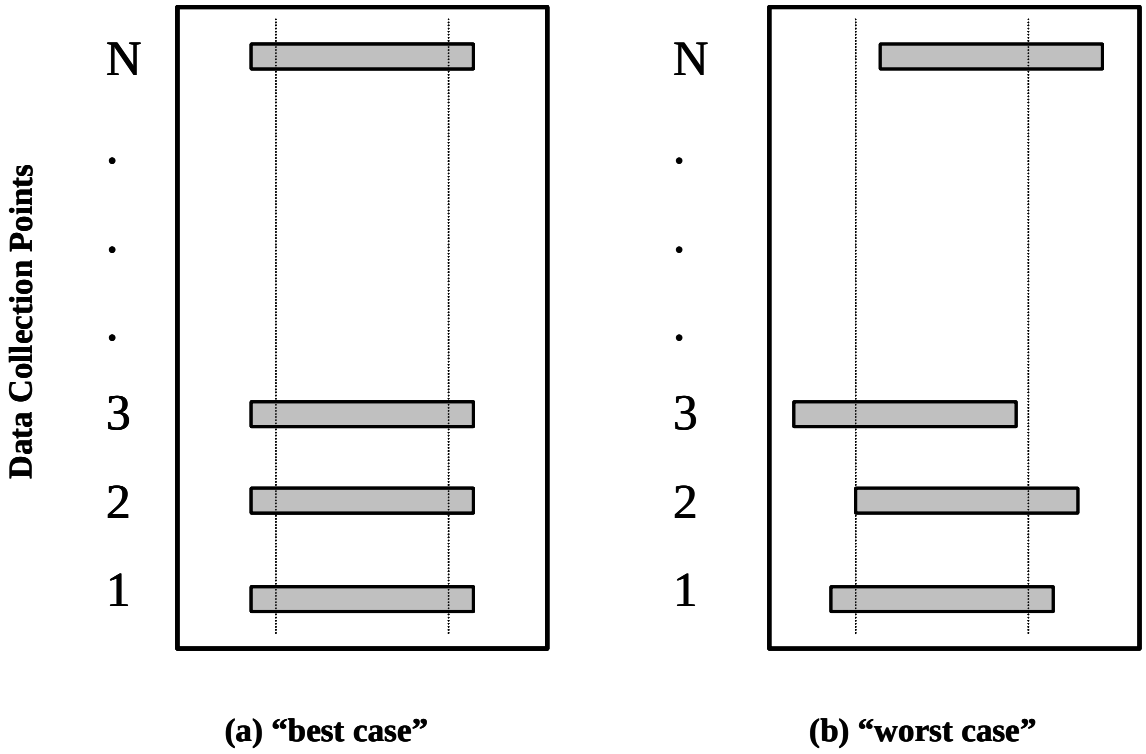

Figure 24. Rut bar measurement.

The lateral standard deviation or "wander" of the survey vehicle used in the computations was 127 mm. This value for the vehicle wander was determined from field data collected at a limited number of sites. On these sites, a five-sensor rut bar was used to obtain five repeat measurements. Elevation measurements were also obtained on these sites. The program was used to generate rut bar data, with the wander ranging from 50 mm to 250 mm. The standard deviation of the five-sensor rut bar results at each level of wander was compared to the standard deviation of the actual measurements. These results are provided for the LWP and the RWP in figures 25 and 26, respectively. Based on these results, a wander of 127 mm is the most suitable value.

The sensors on the three-sensor rut bar are assumed to have a standard spacing of 914 mm. The rut depth is calculated as the difference between the elevation of the pavement in the center of the lane and the elevation of the pavement in each wheelpath, as shown in the lower portion of figure 27.

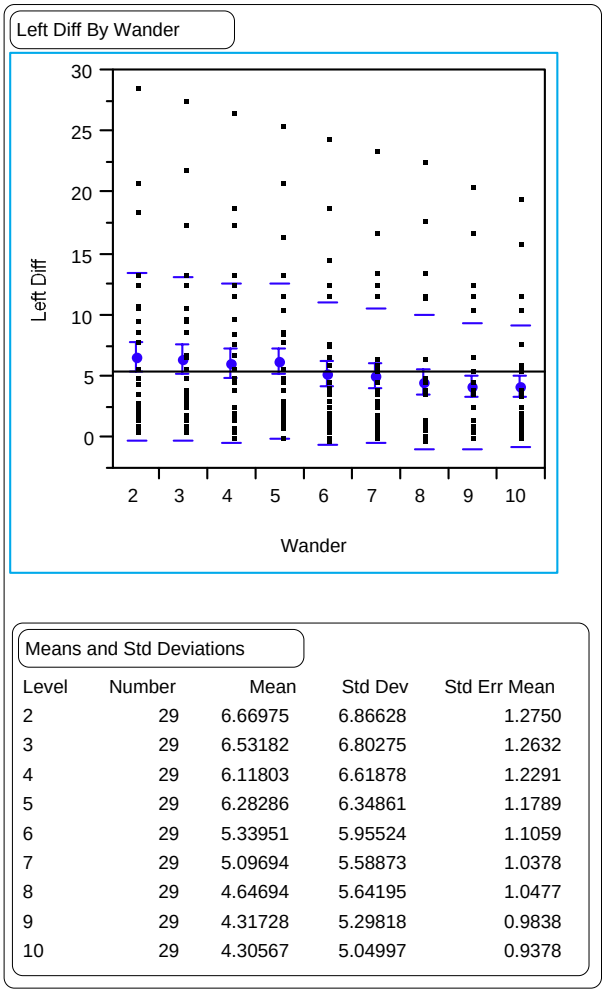

Means and Std Deviations

Level	Number	Mean	Std Dev	Std Err Mean
2	29	6.66975	6.86628	1.2750
3	29	6.53182	6.80275	1.2632
4	29	6.11803	6.61878	1.2291
5	29	6.28286	6.34861	1.1789
6	29	5.33951	5.95524	1.1059
7	29	5.09694	5.58873	1.0378
8	29	4.64694	5.64195	1.0477
9	29	4.31728	5.29818	0.9838
10	29	4.30567	5.04997	0.9378

Figure 25. Means and standard deviations of the differences observed for the LWP versus wander.

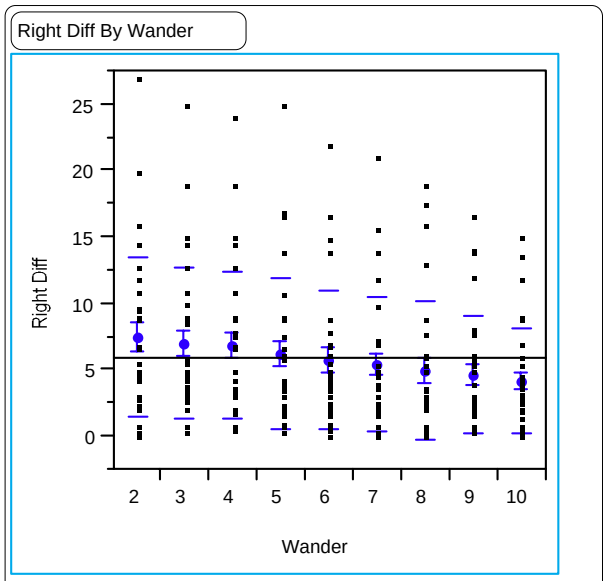

Means and Std Deviations

Level	Number	Mean	Std Dev	Std Err Mean
2	29	7.58147	6.14350	1.1408
3	29	7.05976	5.81465	1.0798
4	29	6.93029	5.67262	1.0534
5	29	6.33562	5.75870	1.0694
6	29	5.79595	5.29036	0.9824
7	29	5.54251	5.09489	0.9461
8	29	5.06599	5.21097	0.9677
9	29	4.67769	4.47739	0.8314
10	29	4.25476	4.04032	0.7503

Figure 26. Means and standard deviations of the differences observed for the RWP versus wander.

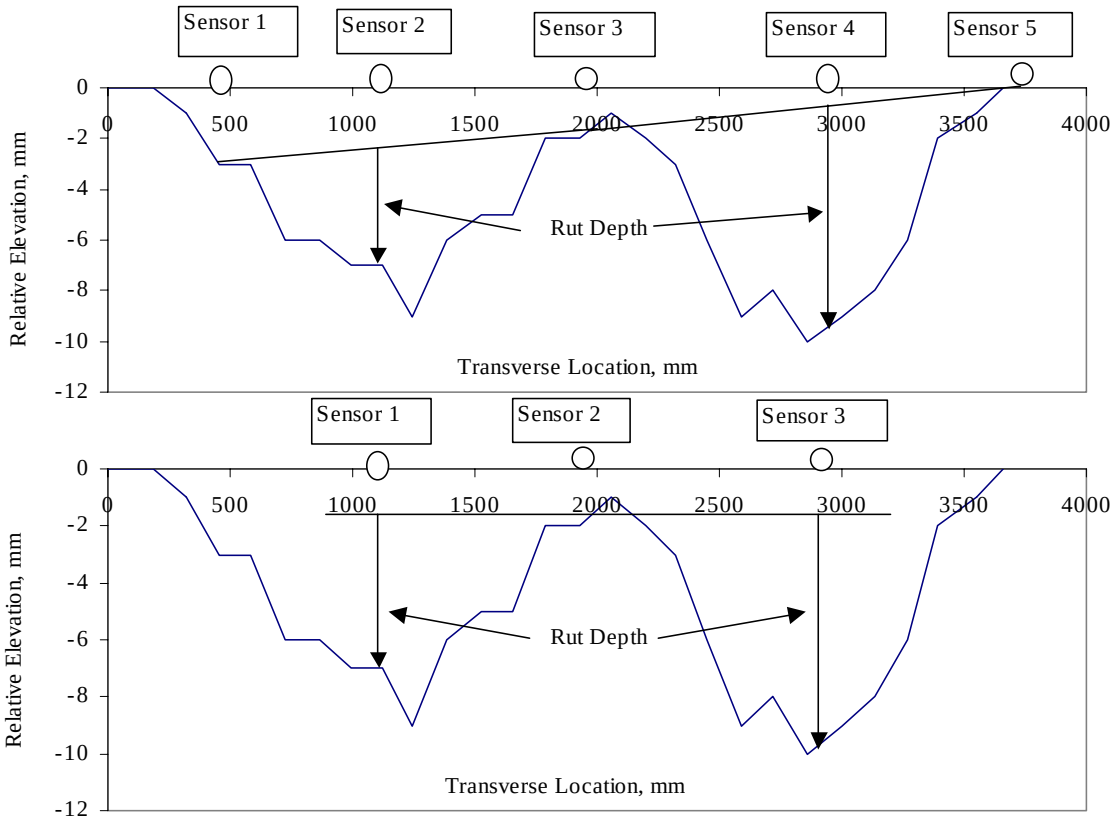

Figure 27. Calculation of rut depth from the rut bar.

The three center sensors of the five-sensor rut bar have the same spacing as the sensors on the three-sensor rut bar. The two outside sensors are located 305 mm from the sensors placed over the wheelpath. The rut depth is obtained by drawing a line from sensors 1 to 3 and sensors 3 to 5. The difference between the line and the pavement elevation at sensors 2 and 4 is the rut depth for the LWP and RWP, respectively. This calculation is illustrated in the upper portion of figure 27.

Both the three- and the five-point calculations can yield a negative rut depth. The three-point system will provide a negative rut depth for transverse profiles, such as that shown in figure 28. The five-point system will provide a negative rut depth for transverse profiles, such as that shown in figure 29. However, other shapes may also yield a negative rut depth.

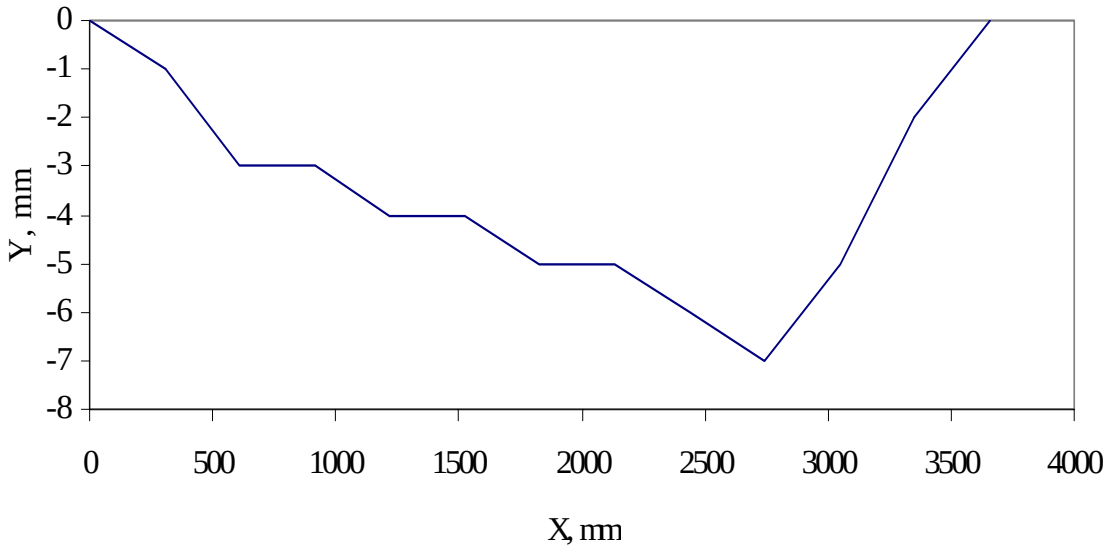

Figure 28. Typical transverse profile providing a negative rut depth from three-point analysis.

Figure 29. Typical profile providing a negative rut depth from five-point analysis.

ANALYSES

To examine the rut depths for the three-point and five-point profiles, a histogram was created for the three-point rut depths, the five-point rut depths, and the wire line rut depths. As a minimum, these histograms illustrate that both the three-point and five-point calculations can provide negative rut depths. The mean, standard deviation, and minimum and maximum values for the three-point rut depths, the five-point rut depths, and the wire line rut depths are all provided in table 13.

Variation

The standard deviations of the simulation runs were pooled across stations to obtain a value for each survey date. The standard deviations provide some indication of the effect of vehicle wander on the calculated rut depth. PASCO corrects for this phenomenon by taking a picture that is slightly larger than the width of the lane. The standard deviation for each wheelpath provides an indication of the range of values (maximum and minimum rut depths) that may be observed for a given transverse profile. These standard deviations were found to be correlated to the mean rut depth for the section. Therefore, it is more appropriate to discuss the variability in terms of COV.

The pooled standard deviation and section mean were used to calculate the COV. These values were used to examine the variability associated with each profile for both the best-case and worst-case scenarios. The values of COV were within round-off error between the two scenarios. For the three-point rut bars, the average COV was 104 percent, while the average for the five-point rut bars was 239 percent. These values indicate that the transverse placement of the rut bar dramatically influences the measurement and, hence, the rut depth calculation.

Combined Data Sets

The correlation matrix for these rut depths shows that the five-point rut depths have a higher correlation with the wire line rut depths (0.8 and 0.6 for the LWP and RWP, respectively) than the three-point rut depths (0.5 and 0.4 for the LWP and RWP, respectively). In addition, the correlations of the LWP for all three rut depths were higher than those for the RWP (table 13). This higher correlation with the LWP rut depth may be partially attributed to the fact that there is typically greater consistency/uniformity in the LWP over time.

Comparisons were then made among the three-point rut depth, the five-point rut depth, and the wire line rut depth by wheelpath. Paired t-tests indicated that there were statistically significant differences, indicating that the different measurement techniques do not provide the same estimate of rutting.

Table 13. Correlation of three-point and five-point rut depths versus the wire line rut depths.

	3-Point, Worst Case			5-Point, Worst Case			Wire Line			3-Point, Best Case			5-Point, Best Case		
	LWP	RWP	Avg.	LWP	RWP	Avg.	LWP	RWP	Avg.	LWP	RWP	Avg.	LWP	RWP	Avg.
Number of Observations	79,616	79,616	79,616	79,616	79,616	79,616	79,616	79,616	79,616	79,616	79,616	79,616	79,616	79,616	79,616
Mean	3.2	3.1	3.2	1.0	-0.1	0.4	5.9	5.9	5.9	3.2	3.1	3.2	1.0	-0.1	0.4
Standard Deviation	4.28	4.68	3.93	2.24	1.91	1.67	4.4	4.6	4.2	4.28	4.68	3.93	2.24	1.91	1.67
Minimum	-37.0	-25.0	-21.5	-14.0	-13.0	-10.0	0	0		-36.0	-25.0	-21.0	-14.0	-13.0	-10.0
Maximum	73.0	64.0	65.5	36.0	22.0	19.0	77	63	70	74.0	65.0	66.0	36.0	22.0	17.5
Correlation to wire line rut depth	0.5363	0.4188	0.4381	0.7761	0.5350	0.7541	---	---	---	0.5364	0.4193	0.4385	0.7754	0.5356	0.7546
R^2	0.288	0.175	0.192	0.602	0.286	0.569	---	---	---	0.288	0.176	0.192	0.601	0.287	0.569
RMSE	3.68	4.18	3.78	2.75	3.89	2.76	---	---	---	3.68	4.18	3.78	2.75	3.89	2.76
Se/Sy	0.84	0.91	0.90	0.62	0.85	0.66	---	---	---	0.84	0.91	0.90	0.62	0.85	0.66
p-value from paired t-test	0.0000	0.0000	0.0000	0.0000	0.0000	0.0000	---	---	---	0.0000	0.0000	0.0000	0.0000	0.0000	0.0000

LWP = Leftt Wheelpath, RWP = Right Wheelpath, RMSE = Root Mean Square Error, Se/Sy = Standard error of the regression divided by the standard deviation of the *y*-value

These data indicate that the five-point rut depth never exceeds the wire line rut depth. However, the three-point rut depth may be larger or smaller than the wire line rut depth. The average difference between the wire line rut depth and the five-point rut depth was 5 mm for the LWP and 6 mm for the RWP. On average, the three-point rut depth was 4 mm smaller than the wire line rut depth in both wheelpaths. These values indicate that the differences are significant, both statistically and from an engineering perspective.

Paired t-tests for the three-point rut depths versus the five-point rut depths yielded statistically significant differences. On average, the three-point rut depths were 2 mm larger than the five-point rut depths; however, some differences were as large as 40 mm.

Finally, a series of linear regressions were used to examine the potential correlation between the rut depths. The results from these regressions are shown in table 13. Figures 30 and 31 show a graphical comparison of the three- and five-point rut depths versus those determined from the lane-width wire line. As is evident, the correlations are weak.

The relationship between the wire line rut depth and the five-point rut depth was stronger than that between the wire line rut depth and the three-point rut depth (i.e., R^2 of 0.38 versus 0.65 and 0.15 versus 0.22, respectively). In all cases, the data included a large amount of scatter.

The relationships between the five-point rut depths and the three-point rut depths were very different between the wheelpaths. The R^2 for the LWP was 0.44 and the R^2 for the RWP was 0.003.

Some States that use these systems use the average rut depth from a given length of pavement. Therefore, the analyses were repeated, examining the average rut depth for the section for both scenarios of the three-point and five-point systems. Table 14 includes the mean, standard deviation, and minimum and maximum values for these rut depths. The table shows that negative values for average rut depths, though smaller than for the individual rut depths, may still be computed.

The correlation coefficients are also provided in table 14. The values are slightly lower than those shown for the five-point rut depth in table 13, but are slightly higher than those for the RWP three-point rut depth. Naturally, the same is true for the coefficients of determination (R^2) also shown in table 14.

The results of the paired t-tests reflect a statistically significant difference between the average three-point versus the wire line rut depths and the average five-point versus the wire line rut depths. The mean difference for the average three-point comparison was 3 mm. The mean difference for the average five-point comparison was 5 mm. Both values are of some concern from an engineering standpoint.

In summary, the average three-point and five-point rut depths did not show a stronger relationship with the wire line rut depth than did rut depths calculated for the individual wheelpaths.

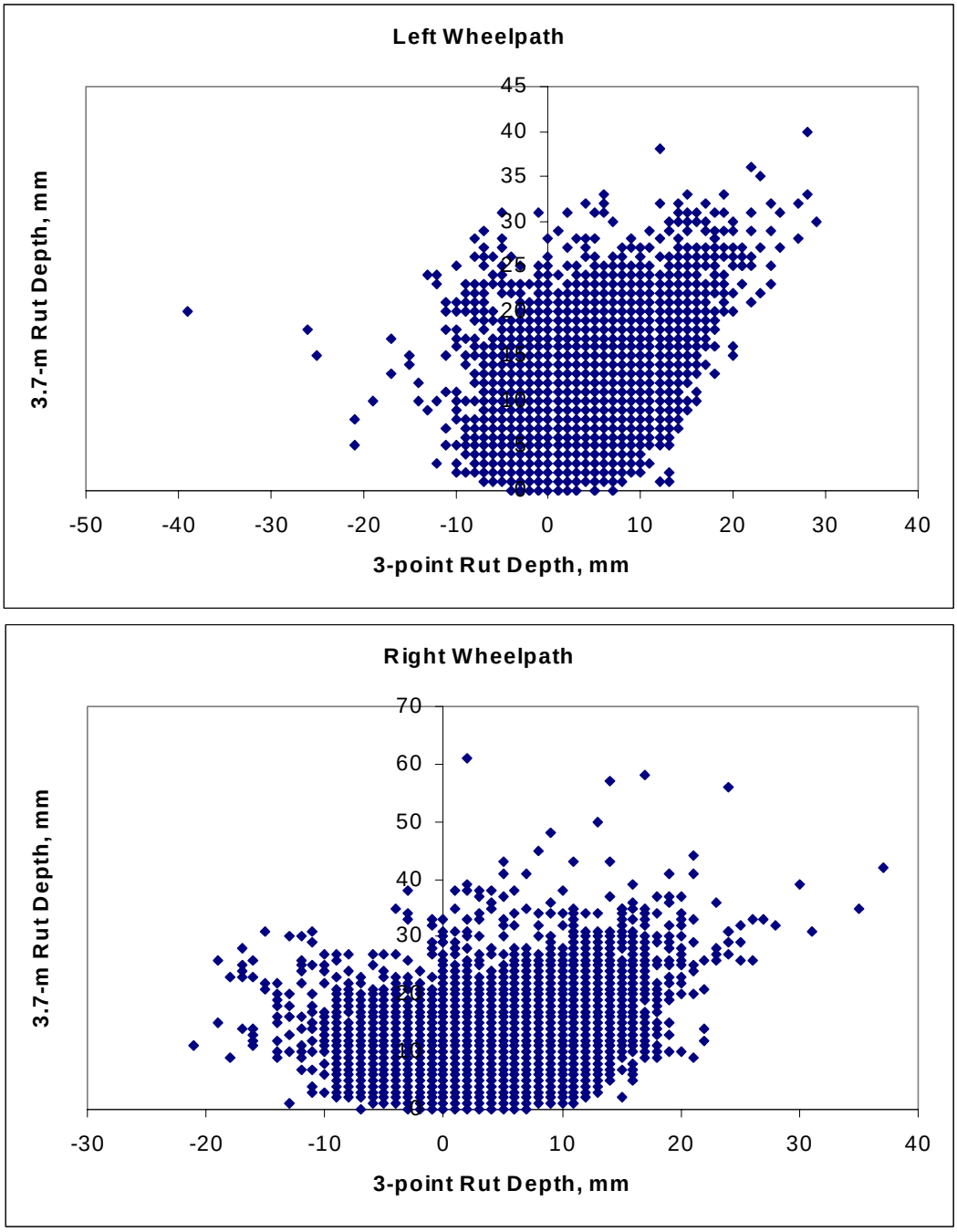

Figure 30. Graphical comparison of the three-point rut depths versus the wire line rut depths.

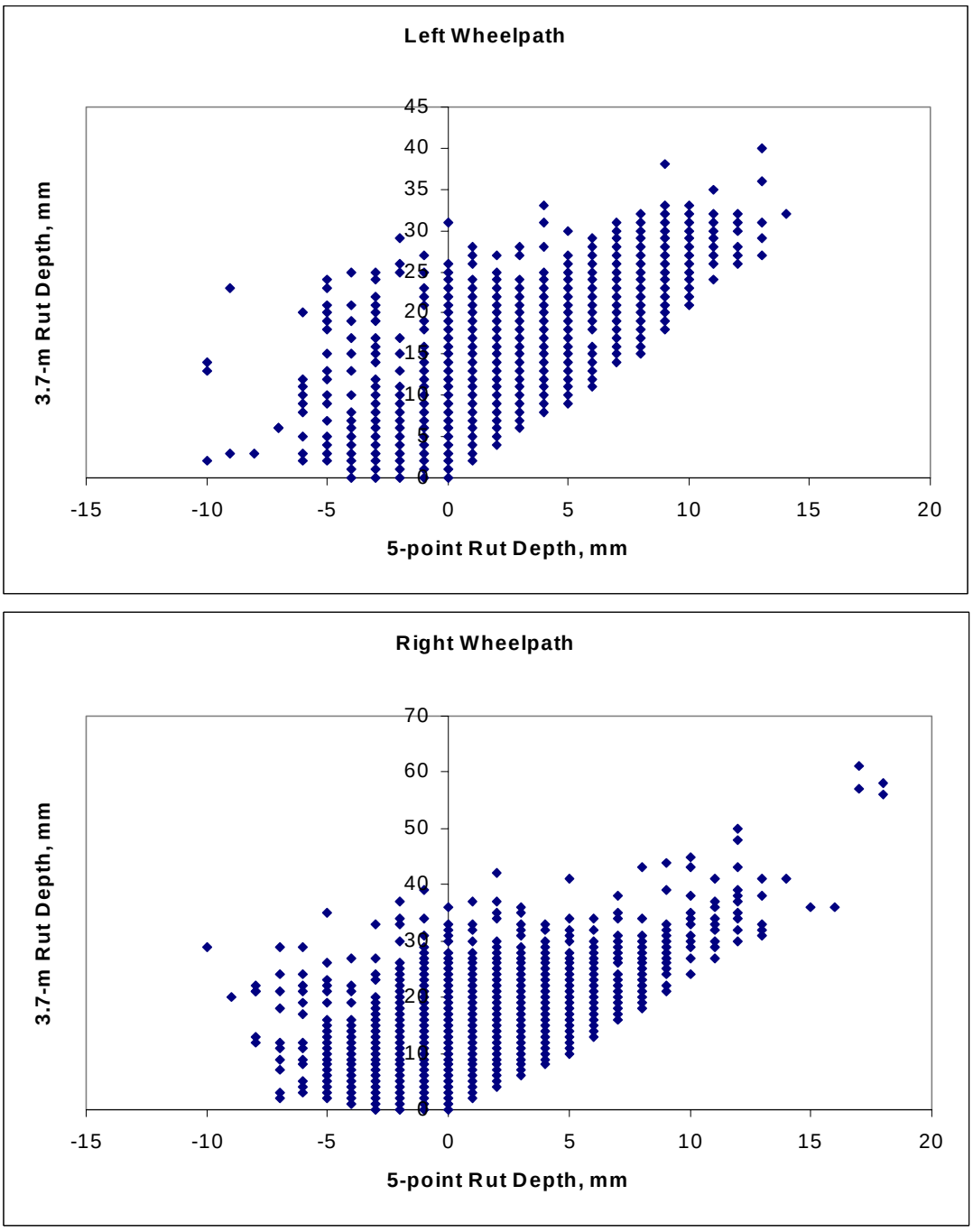

Figure 31. Graphical comparison of the five-point rut depths versus the wire line rut depths.

Table 14. Correlation of average three-point and five-point rut depths versus the wire line rut depths.

	3-Point, Worst Case	5-Point, Worst Case	Wire Line	3-Point, Best Case	5-Point, Best Case
Number of Observations	7,229	7,229	7,229	7,229	7,229
Mean	3.2	0.5	5.9	3.2	0.5
Standard Deviation	3.60	1.48	3.93	3.61	1.49
Minimum	-15.2	-6.9	0.0	-15.7	-6.8
Maximum	52.6	12.4	54.6	54.4	11.9
Correlation to wire line rut depth	0.4636	0.8224	---	0.4623	0.8197
R^2	0.215	0.676	---	0.214	0.672
RMSE	3.48	2.23	---	3.48	2.25
Se/Sy	0.89	0.57	---	0.89	0.57
p-value from paired t-test	0.0000	0.0000	---	0.0000	0.0000

RMSE = Root Mean Square Error
Se/Sy = Standard error of the regression divided by the standard deviation of the *y*-value

Blocked Data Sets Versus Shape

The shape of the transverse profile may affect the correlation between the rut depths. To test for this possibility, the data were divided into categories based on the transverse profile shape using the complete profile information available from the original PASCO and Dipstick® profiles. Four categories were used for this analysis:

- Category 1 - Profiles for which the two outside edges were lower than the rest of the entire profile.
- Category 2 - Profiles that were bowl-shaped.
- Category 3 - Profiles that were all negative, but with a “hump” in the middle.
- Category 4 - Profiles for which the middle portion of the profile was larger than the two outside edges and the portions of the profile in the wheelpaths were lower than the two outside edges.

Examples of each are shown in figure 32. Figure 33 reflects the number of profiles within each category. Category 4, which contained the most data, is considered to be a typical profile. Category 2 included the fewest number of profiles.

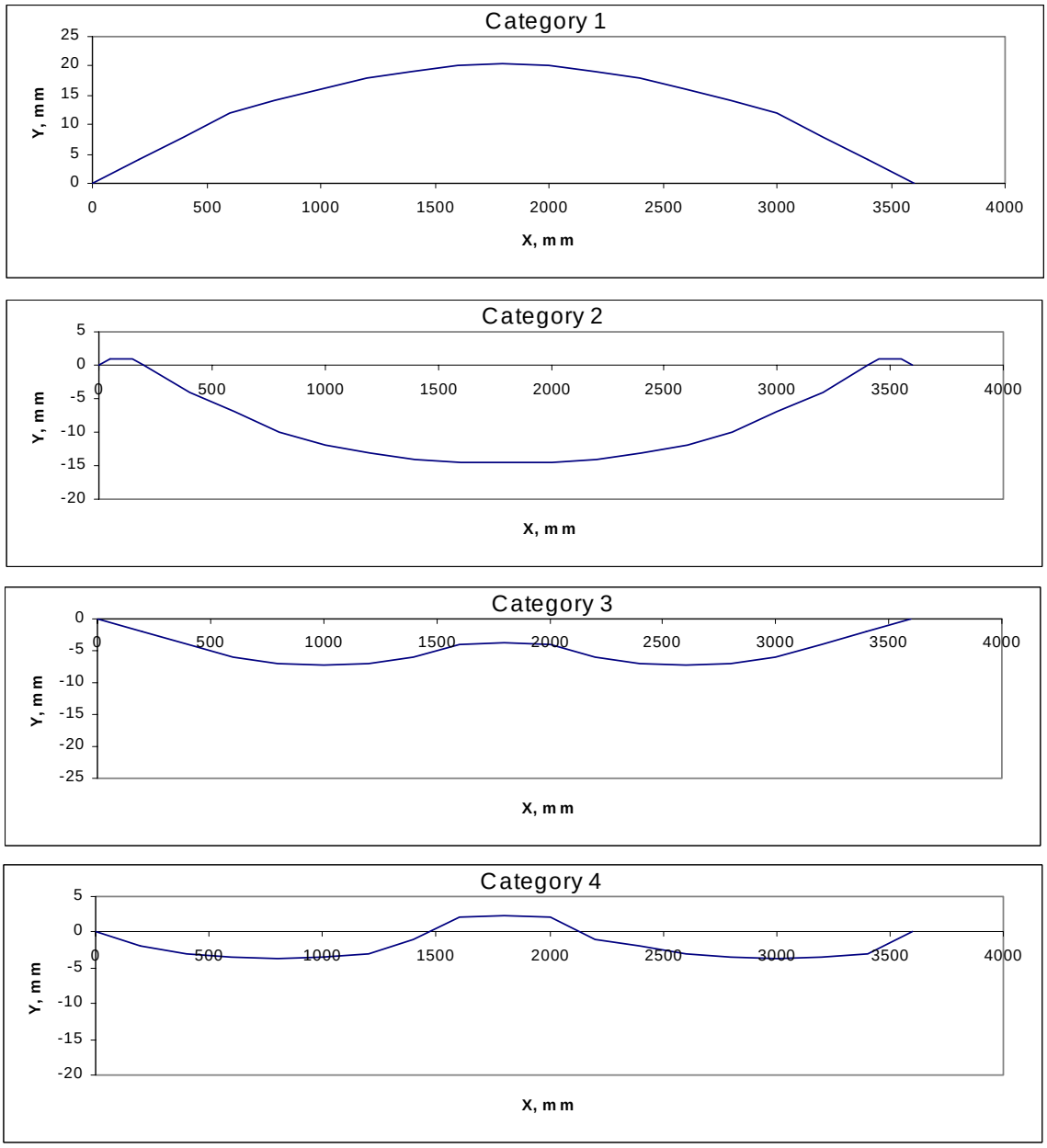

Figure 32. Transverse profile shape categories.

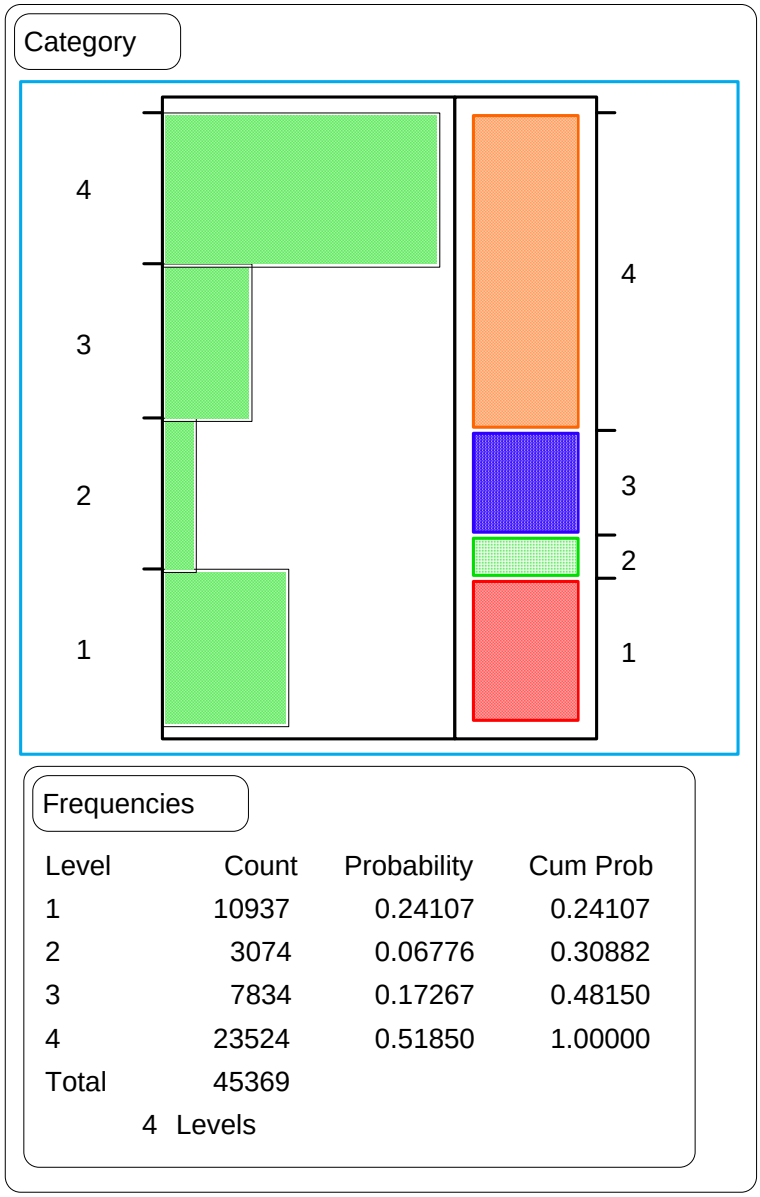

Figure 33. Number of profiles within each shape category.

Table 15 lists the means and standard deviations for each of the profile categories. The differences between the best-case and worst-case scenarios were within round-off error; therefore, only one value is presented. The differences between the means were all significantly different from each other, with the exception of categories 2 and 4 for the RWP five-point rut depth. Considerable overlap existed between the distributions of each category for each rut depth.

Statistical tests conducted on each category were identical to those conducted on the combined data set. These steps included the examination of the histograms, the development of the correlation matrix, a paired t-test between each of the rut depths, and a linear regression between each of the rut depth indices. Table 15 summarizes the comparisons with the wire line rut depths.

Category 1 Profiles

The correlation matrix for category 1 exhibited much weaker correlations than those observed for the combined data set. As with the combined data set, the correlations for the five-point rut depths versus the wire line rut depths (0.57 and 0.42 percent for the LWP and RWP, respectively) were stronger than those for the three-point rut depths versus the wire line rut depths (0.54 and 0.24 for the LWP and RWP, respectively). It is interesting to note that the correlation between the three-point rut depth and the five-point rut depth for the RWP is negative. This means that as the three-point rut depth increases, the five-point rut depth decreases, which is contrary to the expectation.

The results of the paired t-tests for category 1 were all statistically significant. The mean differences between the five-point rut depths and the wire line rut depths (3 mm for the LWP and 4 mm for the RWP) were smaller than those observed for the combined data set. These values are considered significant from an engineering perspective.

The mean differences between the three-point rut depths and the wire line rut depths were also smaller than those for the combined data set. The mean difference for both wheelpaths was 1 mm, suggesting that the significance between the three-point rut depth and the wire line rut depth is questionable.

The differences between the three-point rut depths and the five-point rut depths are also considered significant. These differences averaged 3 mm, but some were as large as 24 mm. The three-point rut depths were generally, but not always, larger than the five-point rut depths.

The regression analyses were all statistically significant. The regressions for the five-point rut depths had higher R^2 values than the regressions for the three-point rut depths. However, the data scatter was extensive. Like the combined data set, the explained variation (i.e., R^2 values) for the LWP three-point rut depth versus the five-point rut depth was higher than for the RWP.

Table 15. Correlation of three-point and five-point rut depths versus the wire line rut depths by category.

	Category 1				Category 2				Category 3				Category 4			
	3-point		5-point		3-point		5-point		3-point		5-point		3-point		5-point	
	LWP	RWP	LWP	RWP	LWP	RWP	LWP	RWP	LWP	RWP	LWP	RWP	LWP	RWP	LWP	RWP
Number of Observations	10,937	10,937	10,937	10,937	3,074	3,074	3,074	3,074	7,834	7,834	7,834	7,834	23,524	23,524	23,524	23,524
Mean	2.4	2.3	-0.4	-0.6	-1.1	-1.8	0.2	0.0	2.7	2.2	2.2	0.7	3.8	4.1	1.4	0.2
Standard Deviation	3.25	3.88	1.29	1.26	3.02	2.76	1.26	1.36	3.75	4.15	2.32	1.88	4.61	5.05	2.32	2.07
Minimum	-14.0	-14.0	-9.0	-10.0	-37.0	-14.0	-7.0	-9.0	-17.0	-23.0	-6.0	-8.0	-28.0	-20.0	-11.0	-13.0
Maximum	25.0	24.0	6.0	9.0	10.0	11.0	8.0	22.0	29.0	26.0	17.0	13.0	34.0	64.0	21.0	22.0
R^2	0.294	0.059	0.328	0.174	0.00	0.01	0.179	0.283	0.367	0.199	0.603	0.215	0.521	0.433	0.696	0.283
RMSE	1.42	1.76	1.42	1.65	3.52	4.23	3.19	3.60	3.81	4.50	3.01	4.45	2.94	3.57	2.34	4.02
Se/Sy	0.82	0.97	0.82	0.91	1.00	1.00	0.91	0.85	0.80	0.90	0.63	0.89	0.69	0.75	0.55	0.85
p-value from paired t-test	<0.0001	<0.0001	0.0000	0.0000	0.0000	0.0000	0.0000	0.0000	0.0000	0.0000	0.0000	0.0000	0.0000	0.0000	0.0000	0.0000

LWP = Left Wheelpath, RWP = Right Wheelpath, RMSE = Root Mean Square Error, Se/Sy = Standard error of the regression divided by the standard deviation of the *y*-value

Category 2 Profiles

The correlation coefficients for the five-point rut depths versus the wire line rut depths were lower than those computed for the combined data set (0.42 and 0.53 for the LWP and RWP, respectively). However, the correlations for the three-point rut depths versus the wire line rut depths were much lower (0.01 and 0.08 for the LWP and RWP, respectively). The correlation coefficients for the three-point rut depths versus five-point rut depths were higher for the LWP than for the RWP.

Results from the paired t-tests were all significant. For this shape category, the three-point rut depths, like the five-point rut depths, were never larger than the wire line rut depths. This yielded greater mean differences than those observed for the combined data set. The five-point rut depths were 6 mm smaller than the wire line rut depths in the LWP and 7 mm smaller in the RWP, on average. The three-point rut depths were 8 mm smaller than the wire line rut depths in the LWP and 9 mm smaller in the RWP, on average.

The regressions for category 2 data were not all significant. The regression for the LWP three-point rut depths versus the wire line rut depths was not significant. The amount of scatter in the data indicates that, although some of the regressions were moderate, i.e., R^2 less than 0.50, there is not a strong relationship between the measurement methods for this category.

Category 3 Profiles

The correlations for these data were generally better than those observed for the combined data set. In fact, the LWP five-point rut depths versus the wire line rut depths had a correlation coefficient of 0.8, which is large.

Results from the paired t-tests were all significant. For this shape category, the three-point rut depths were always less than the wire line rut depths. The mean differences were similar to those observed for the category 2 data. The mean differences observed for the comparison of the three-point versus the five-point rut depths were so small that they should not be considered significant from an engineering perspective.

The linear regressions for these data were all significant. Though the data show considerable scatter, graphical presentation of these data reveals a slight, but identifiable, trend, except for the RWP three-point rut depths versus the five-point rut depths.

Category 4 Profiles

The correlation coefficients for this category were higher than those computed for the combined data set. The correlation coefficients for the five-point rut depths versus the wire line rut depths were 0.83 and 0.53 for the LWP and RWP, respectively. The correlation coefficients for the three-point rut depths versus the wire line rut depths were 0.72 and 0.66 for the LWP and RWP, respectively.

Results of the paired t-tests indicate that the measurements obtained from the different methods were significantly different rut depths, although the mean differences were not as large as those observed for the category 2 and 3 data. The three-point rut depths were generally, but not always, smaller than those obtained using the wire line method.

The linear regressions were all statistically significant. The data showed quite a bit of scatter, but a general trend was detectable from all of the graphs except one. The graph for the RWP three-point rut depth versus the five-point rut depth did not show any trend, even though the regression was significant. The correlations noted here were similar to those observed for the category 3 data set.

Blocked Data Sets Versus Rut Depth

In addition to shape, the data were categorized based on the amount of rutting, since the amount of rutting may affect the correlation between the rut depths. The data for the individual profiles were sorted by mean rut depth for the profile. These data were divided roughly into thirds. The "low rutting" group consisted of profiles with an average rut depth of less than 4.5 mm. The "moderate rutting" groups consisted of profiles with rutting from 4.5 mm to 7.2 mm. The "high rutting" group consisted of profiles with more than 7.2 mm of rutting.

Low Rutting

The results from these comparisons are provided in table 16. The correlation coefficients were less than those observed from the combined data set. The correlation coefficients for the five-point rut depths versus the wire line rut depths were 0.49 and 0.31 for the LWP and RWP, respectively. The correlation coefficients for the three-point rut depths versus the wire line rut depths were 0.41 and 0.15 for the LWP and RWP, respectively.

The paired t-test results indicate that the measurements obtained from the different techniques were significantly different rut depths. The mean differences observed for the five-point rut depths were greater than 2 mm and large enough to be considered significant. The mean differences observed for the three-point rut depths were small enough to be considered insignificant, but the amount of scatter in the data was large enough to be of concern.

The linear regressions were all statistically significant. The data showed quite a bit of scatter, but a general trend was detectable. Even though these regressions were significant, the relationships between the rut depths were limited at best.

Table 16. Correlation of three-point and five-point rut depths versus the wire line rut depths for profiles with less than 4.5 mm of rutting.

	3-Point, Worst Case			5-Point, Worst Case			3-Point, Best Case			5-Point, Best Case			Wire Line		
	LWP	RWP	Avg.	LWP	RWP	Avg.	LWP	RWP	Avg.	LWP	RWP	Avg.	LWP	RWP	Avg.
Number of Observations	34,781	34,781	34,781	34,781	34,781	34,781	34,781	34,781	34,781	34,781	34,781	34,781	34,781	34,781	34,781
Mean	1.9	1.9	1.9	-0.3	-0.7	-0.5	1.9	1.9	1.9	-0.3	-0.7	-0.5	2.7	2.7	2.7
Standard Deviation	2.67	3.06	2.26	1.10	1.03	0.78	2.66	3.06	2.26	1.10	1.03	0.78	1.29	1.26	0.95
Minimum	-9.0	-14.0	-5.0	-7.0	-12.0	-6.5	-9.0	-14.0	-5.0	-7.0	-11.0	-6.0	0.0	0.0	0.0
Maximum	14.0	17.0	13.0	4.0	3.0	2.0	14.0	17.0	13.0	4.0	3.0	2.0	8.0	7.0	4.0
Correlation to Wire Line Rut Depths	0.4110	0.1484	0.0829	0.4886	0.3106	0.3481	0.4090	0.1481	0.0817	0.4872	0.3114	0.3466	---	---	---
R^2	0.169	0.022	0.007	0.239	0.096	0.121	0.167	0.022	0.007	0.237	0.097	0.120	---	---	---
RMSE	1.17	1.25	0.95	1.12	1.20	0.89	1.18	1.25	0.95	1.12	1.20	0.89	---	---	---
Se/Sy	0.91	0.99	1.00	0.87	0.95	0.94	0.91	0.99	1.00	0.87	0.95	0.94	---	---	---
p-value from paired t-test	0.0000	0.0000	0.0000	0.0000	0.0000	0.0000	0.0000	0.0000	0.0000	0.0000	0.0000	0.0000	---	---	---

LWP = Left Wheelpath, RWP = Right Wheelpath, RMSE = Root Mean Square Error, Se/Sy = Standard error of the regression divided by the standard deviation of the *y*-value

Moderate Rutting

The results from the comparisons of the profiles in the moderate rutting category are provided in table 17. The correlation coefficients were lower than those for the combined data set. These values were larger than those for the low rutting data set.

Results from the paired t-test indicate that the measurement techniques do not provide the same value of rut depth. The differences ranged from 2.6 mm to 5.7 mm. These values are large enough to consider the observed differences to be significant from an engineering perspective, as well as a statistical perspective.

The linear regressions were also statistically significant. Although these results were not as good as those for the combined data set, they were better than those for the low rutting data set. The data showed considerable scatter and the value of these regressions have little meaning from the engineering point of view.

High Rutting

The results of the comparisons of the high rutting data set are provided in table 18. The correlation coefficients were smaller than those observed for either the combined data set or the moderate rutting data set.

Results from the paired t-tests indicate that the measurements obtained from the different measurement techniques were not the same. The mean differences were all greater than 5 mm. These differences were greater than those observed for the profiles with moderate rutting.

The linear regressions were statistically significant. However, the R^2 and error terms associated with these regressions indicate that the fit of the lines to the data are very poor.

SUMMARY

In summary, the following conclusions were drawn from these analyses:

- The transverse location of the rut bar dramatically affects the measurement and, hence, the rut depth computation. Thus, consistent lateral placement of the survey vehicle is essential to repeatable rut depth measurements using the three- or five-point rut bars.

- The paired t-tests illustrate that the three rut depth measurement systems (three-point, five-point, and wire line) do not provide the same values (i.e., there are statistically significant differences among them).

- The three-point rut depths underestimate the wire line rut depths for transverse profiles where the middle of the profile is lower than the outside edges of the lane (categories 2 and 3).

Table 17. Correlation of three-point and five-point rut depths versus the wire line rut depths for profiles with from 4.5 mm to 7 mm of rutting.

	3-Point, Worst Case			5-Point, Worst Case			3-Point, Best Case			5-Point, Best Case			Wire Line		
	LWP	RWP	Avg.	LWP	RWP	Avg.	LWP	RWP	Avg.	LWP	RWP	Avg.	LWP	RWP	Avg.
Number of Observations	23,565	23,565	23,565	23,565	23,565	23,565	23,565	23,565	23,565	23,565	23,565	23,565	23,565	23,565	23,565
Mean	3.0	2.7	2.9	0.9	-0.2	0.4	3.0	2.7	2.9	0.9	-0.2	0.4	5.6	5.5	5.6
Standard Deviation	3.60	4.11	3.22	1.42	1.47	1.01	3.56	4.12	3.22	1.42	1.46	1.01	1.67	1.70	0.84
Minimum	-14.0	-13.0	-8.0	-9.0	-11.0	-6.5	-15.0	-13.0	-7.0	-9.0	-10.0	-6.0	0.0	0.0	4.5
Maximum	19.0	20.0	17.5	6.0	7.0	3.5	18.0	20.0	17.5	6.0	6.0	3.5	13.0	12.0	7.0
Correlation to Wire Line Rut Depths	0.5013	0.2762	0.1270	0.4900	0.2961	0.2203	0.4997	0.2768	0.1260	0.4901	0.2949	0.2205	---	---	---
R^2	0.251	0.076	0.016	0.24	0.088	0.049	0.250	0.077	0.016	0.24	0.087	0.049	---	---	---
RMSE	1.44	1.63	0.84	1.45	1.62	0.82	1.44	1.63	0.84	1.45	1.62	0.82	---	---	---
Se/Sy	0.86	0.96	1.00	0.87	0.95	0.98	0.86	0.96	1.00	0.87	0.95	0.98	---	---	---
p-value from paired t-test	0.0000	0.0000	0.0000	0.0000	0.0000	0.0000	0.0000	0.0000	0.0000	0.0000	0.0000	0.0000	---	---	---

LWP = Left Wheelpath, RWP = Right Wheelpath, RMSE = Root Mean Square Error, Se/Sy = Standard error of the regression divided by the standard deviation of the *y*-value

Table 18. Correlation of three-point and five-point rut depths versus the wire line rut depths for profiles with more than 7 mm of rutting.

	3-Point, Worst Case			5-Point, Worst Case			3-Point, Best Case			5-Point, Best Case			Wire Line		
	LWP	RWP	Avg.	LWP	RWP	Avg.	LWP	RWP	Avg.	LWP	RWP	Avg.	LWP	RWP	Avg.
Number of Observations	21,270	21,270	21,270	21,270	21,270	21,270	21,270	21,270	21,270	21,270	21,270	21,270	21,270	21,270	21,270
Mean	5.5	5.6	5.6	3.2	1.1	2.1	5.5	5.6	5.5	3.2	1.1	2.1	11.2	11.6	11.4
Standard Deviation	5.86	6.25	5.43	2.69	2.73	2.00	5.86	6.25	5.43	2.70	2.73	2.00	4.64	4.94	4.18
Minimum	-37.0	-25.0	-21.5	-14.0	-13.0	-10.0	-36.0	-25.0	-21.0	-14.0	-13.0	-10.0	1.0	1.0	7.5
Maximum	73.0	64.0	65.5	36.0	22.0	19.0	74.0	65.0	66.0	36.0	22.0	17.5	77.0	63.0	70.0
Correlation to Wire Line Rut Depths	0.4711	0.3282	0.2941	0.6427	0.4532	0.6066	0.4724	0.3294	0.2955	0.6407	0.4537	0.6074	---	---	---
R^2	0.222	0.108	0.086	0.413	0.205	0.368	0.223	0.109	0.087	0.411	0.206	0.369	---	---	---
RMSE	4.10	4.66	3.99	3.56	4.40	3.32	4.09	4.66	3.99	3.56	4.40	3.32	---	---	---
Se/Sy	0.88	0.94	0.95	0.77	0.89	0.79	0.88	0.94	0.95	0.77	0.89	0.79	---	---	---
p-value from paired t-test	0.0000	0.0000	0.0000	0.0000	0.0000	0.0000	0.0000	0.0000	0.0000	0.0000	0.0000	0.0000	---	---	---

LWP = Left Wheelpath, RWP = Right Wheelpath, RMSE = Root Mean Square Error, Se/Sy = Standard error of the regression divided by the standard deviation of the *y*-value

- Although a better correlation (but still considered poor) existed between the five-point rut depths and the wire line rut depths than between the three-point rut depths and the wire line rut depths, they consistently underestimated the wire line rut depths.

- A better correlation was found between the rut depths for those transverse profile shapes with a “hump” in the middle (categories 3 and 4).

- Generally, the larger the wire line rut depths, the bigger the difference that will be observed between the wire line rut depths and the three-point and five-point rut bars.

As a result of these analyses and comparisons, the analysts concluded that neither the three-point nor the five-point rut depth measurement systems provide reliable and accurate estimates of rut depths as measured with a wire line.

CHAPTER 7. FIELD STUDY

To determine the bias and precision of the PASCO and Dipstick® data collection methods, it was necessary to conduct a field study. The data set housed in NIMS contains several sets of surveys in which the PASCO method and a Dipstick® method were used to collect data for a 1-year time frame. While these data allowed for comparisons between these two methods, they did not allow for a direct computation of the bias and precision of these two measurement methods.

The field study presented here utilized data from only one roadway. The mechanism causing the rutting could potentially affect the bias and precision of the transverse profile and, subsequently, the bias and precision for the indices. This field study provides a good initial estimate of the bias and precision; however, as additional data become available, the data should be used to verify the bias and precision values presented here.

DATA COLLECTION

A site with varying rut depths was selected outside of Thompsontown, Pennsylvania, on the frontage road of U.S. 322. Two 152.5-m test sections were selected along this roadway for use with the field study. The site had minimal traffic because the frontage road was a dead-end road. Profile measurements were made along each section every 15 m. All data were collected within a 2-week time frame.

Four methods were used to collect the data. The first was a straightedge survey. A 3.9-m straightedge was placed on blocks. The distance between the straightedge and the surface of the pavement was measured every 152 mm. Three operators used this method to collect profile data on each profile with eleven profiles measured on each section. Each operator made three replicate measurements, for a total of nine sets of profiles collected. The data collected by this method were considered the benchmark for the bias computation.

The second method used to collect data was the FACE Dipstick®. The Dipstick® collects data every 305 mm across the profile. As with the straightedge method, each operator made three replicate measurements of each profile.

The RoadRecon unit was then used to collect data along each section. These measurements were made using the standard method of taking a picture approximately every 15 m. The images collected of each profile were digitized five times by five different operators. Due to the speed at which the RoadRecon unit is normally operated, the spacing between the images is rarely exactly 15 m. Therefore, a second set of measurements was taken using the RoadRecon unit in a static mode. The unit was driven to the appropriate station and the image was collected. These measurements were taken every 15 m and at the same stations where the dynamic images were obtained. Therefore, twice as many profiles were collected using this method than for any other method. These images were also digitized five times by each of the five operators. All the data were processed to ensure uniformity. The *y*-values were expressed in terms of elevation relative

to a horizontal datum drawn through the end points of the profiles. The x-values were expressed in terms of distance from the outside lane edge.

ANALYSIS

The first step of the analysis was to compute each index using the data collected. All the analyses were conducted by examining differences between the indices. The indices were calculated using the RUTCHAR program. An analysis of variance (ANOVA) was completed to examine the differences by operator, section, and station.[8] Differences were expected to occur between each of the profiles; however, differences between operators may prove to be important in later data collection.

For the straightedge data collection method, the ANOVA results did not show a statistically significant difference between operators for any of the indices. A t-test showed a significant difference of 79 mm for the location of the LWP 1.8-m rut depth. This difference is considered to be fairly small. No differences were observed for the data collected using the Dipstick®.

The dynamic RoadRecon measurements reflect statistically significant differences between operators for the negative area, fill area, LWP 1.8-m rut depth, RWP 1.8-m rut width, and the LWP wire line rut depth. The largest difference observed between operators for the fill area was 3200 mm^2. The largest difference for the LWP 1.8-m rut depth was 2 mm. The difference observed for the LWP 1.8-m rut depth is within the precision limits. The differences observed for both the fill area and the RWP 1.8-m rut width are quite large. Most of the indices obtained from the static RoadRecon unit were significantly different, with the exception of the positive area. The differences observed in the data collected by the RoadRecon unit indicate the importance of trained operators to process the data.

Even though these differences were noted, the remainder of the analyses were conducted using the pooled data set. The precision values noted may be a little larger than are actually seen in practice. Only experienced personnel should process the data. This study incorporated at least one set of data processed by inexperienced personnel. On the other hand, at least one set of data used was processed by very experienced personnel. The data were pooled by operator to provide a between- and within-operator variance, a total variance, and an average for each measurement type. The distributions of each of these values were examined by measurement type.

The first set examined was the measurements collected using the straightedge method. In particular, the within-operator variance for the negative area showed one value to be much larger than the others. A single profile was found to cause the much larger within-operator variance for that one station. Figure 34 shows each of the profiles collected by the straightedge method for all of the operators. One profile in particular does not follow the trend of the other profiles. Tables 19 and 20 provide the precision for each of the indices by measurement method. These are presented by COVs in conjunction with ASTM C670.[9]

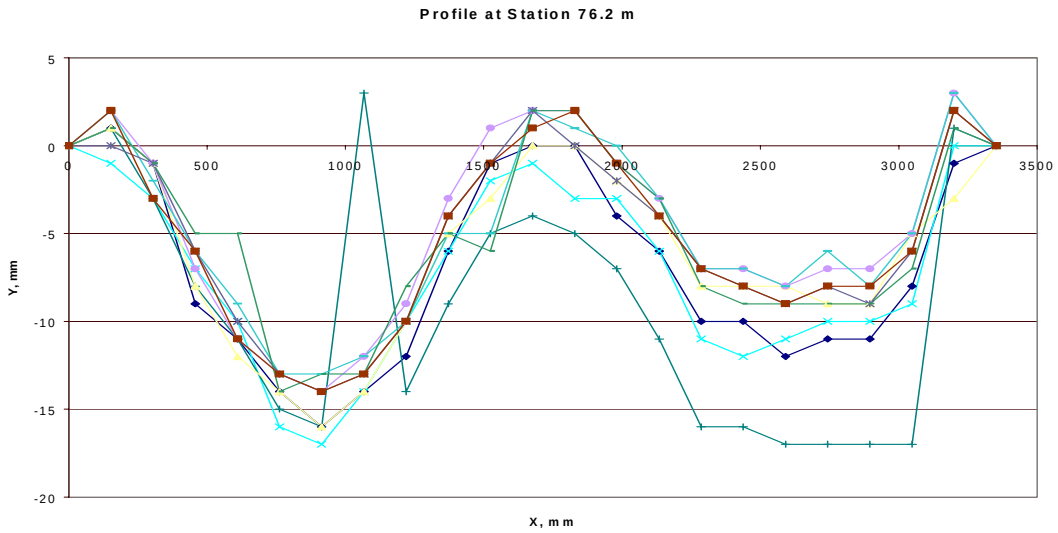

Figure 34. Profiles obtained using the straightedge method at station 76.2 m.

A further investigation was undertaken to determine whether the influential profile was errant or discrepant. The original data were examined and the profile was processed correctly. This profile affects 6 of the 15 indices being examined. No record was made of problems encountered while collecting the profile. Even though the profile may be influential, it was deemed inappropriate to remove it from the analysis simply because it was different from the other observations.

The other measurement methods were examined for similar influential observations. No profiles were found that were significantly different from the other measurements of the same profile.

The within- and between-operator variances were examined to determine whether they were correlated to the average of the index. The within- and between-operator precisions are given in tables 19 and 20, respectively. These are given in terms of COV (as directed by ASTM C670-96) and provide an indication of the repeatability of the data processing by an individual operator and the reproducibility of the data processing between two operators. Only a limited number of the variances for the indices for any of the measurement types were correlated to the average of the index.

The data were reviewed to determine the effect of longitudinal variation on the profile collected. The dynamic measurements were not taken at exactly the same locations as the straightedge and Dipstick® measurements. (It is not possible for the driver to trigger the system to take a measurement at an exact location while the van is moving.) The static RoadRecon measurements were taken at twice as many stations as the other systems. In this case, the unit was driven to the location of interest, stopped, and triggered to take a measurement. This method was used to obtain the data at the stations where the Dipstick® and straightedge methods were used and the stations where the dynamic measurements were taken.

Table 19. Within-operator precision for each index.

Measurement Type	Negative Area	Positive Area	Fill Area	1.8-m LWP Depth	1.8-m LWP Loc.	1.8-m LWP Width	1.8-m RWP Depth	1.8-m RWP Loc.	1.8-m RWP Width	Wire Line LWP Depth	Wire Line LWP Loc.	Wire Line LWP Width	Wire Line RWP Depth	Wire Line RWP Loc.	Wire Line RWP Width
Straightedge	-14	30	6	8	4	5	7	9	4	8	4	11	7	9	10
Dipstick®	-6	12	3	6	1	2	2	2	1	7	1	7	2	2	4
Static PASCO	-17	64	9	11	6	7	11	14	6	11	19	16	11	14	16
Dynamic PASCO	-18	71	9	10	5	7	9	12	6	10	5	14	9	12	13

Table 20. Between-operator precision for each index.

Measurement Type	Negative Area	Positive Area	Fill Area	1.8-m LWP Depth	1.8-m LWP Loc.	1.8-m LWP Width	1.8-m RWP Depth	1.8-m RWP Loc.	1.8-m RWP Width	Wire Line LWP Depth	Wire Line LWP Loc.	Wire Line LWP Width	Wire Line RWP Depth	Wire Line RWP Loc.	Wire Line RWP Width
Straightedge	-13	18	3	5	3	3	4	4	2	5	2	5	4	4	5
Dipstick®	-5	12	2	4	1	1	1	1	1	4	1	4	2	1	2
Static PASCO	-16	41	9	10	3	4	9	9	3	10	3	9	9	9	9
Dynamic PASCO	-12	45	6	9	3	3	6	1	4	9	3	7	6	5	6

The offset stations were compared to the stations that were exactly 15.2 m apart. First, a set of paired t-tests were conducted. The only index for which a significant difference was found was the LWP wire line rut depth, indicating that profiles within a limited distance were very similar.

The data were examined to determine whether the difference in the values of an index increased with increasing distance between the stations where those profiles were observed. The absolute value of the differences at the stations and the indices were checked for a correlation, but none was noted. A correlation between the difference in the index and the difference at the station would provide a means for establishing a limit on the distance from the station the measurement can be taken and still be representative of that location.

A t-test was performed to compare the dynamic PASCO readings to the static PASCO data. In all cases, there were no statistically significant differences. The mean differences shown as part of the results of the test were well within the COV ranges shown in tables 19 and 20. Therefore, the static data were used to assess the bias of the PASCO method of data collection.

A series of paired t-tests were used to determine the bias of the various measurement methods. The straightedge method was used as the benchmark for this analysis. Table 21 presents the minimum and maximum levels of bias found for each index where a statistically significant difference was found by the t-tests. These values are based on the ASTM procedure of providing a 95 percent confidence interval for bias.[9]

The indices calculated from the Dipstick® data versus those from the straightedge show considerable scatter. This scatter presents itself in the bias values determined for the indices that were found to be significantly different from the straightedge indices because the straightedge measurements were taken every 152 mm and the Dipstick® measurements were taken every 305 mm. Therefore, the actual measurements for the Dipstick® could be compared to those taken at the same location. A graph of these data also showed considerable scatter. The bias for these relative elevation measurements lies between –4 and –2.

A direct comparison was made between the indices calculated from the static PASCO data and the indices calculated from the Dipstick® data. The only indices that were significantly different between the two methods were the 1.8-m rut depths, 1.8-m rut widths, wire line rut depths, and wire line rut widths. All of the plots showed a large amount of scatter. For analysis purposes, the data collected by the RoadRecon unit and the Dipstick® may be used interchangeably when the area indices are being considered. However, if the researcher is examining either rut depths or rut widths, only the data from one of the collection methods should be used.

SUMMARY

The precision and bias values for both the Dipstick® and the RoadRecon unit were determined from five repeat runs. These values are presented in tables 19, 20, and 21. Based on these data, the Dipstick® data were more precise, but less accurate than the RoadRecon unit. The Dipstick® and RoadRecon unit provide the same results for the area indices, but the results are different for the rut depths and rut widths.

Table 21. Minimum and maximum levels of bias.

Index	Minimum	Maximum
RoadRecon		
Negative Area	-2135	-5043
Positive Area	-941	-2711
Fill Area	1135	2629
LWP 1.8-m Rut Width	20	85
RWP 1.8-m Rut Depth	0.3	1.3
RWP 1.8-m Rut Location	-20	-75
RWP 1.8-m Rut Width	49	103
RWP Wire Line Rut Depth	0.3	1.3
RWP Wire Line Rut Location	-18	-71
Dipstick®		
Negative Area	2592	-10852
Positive Area	1283	-4775
LWP 1.8-m Rut Depth	-6	-2
LWP 1.8-m Rut Location	-284	132
LWP 1.8-m Rut Width	-222	-40
LWP Wire Line Rut Depth	-6	-2
LWP Wire Line Rut Location	-272	140
RWP Wire Line Rut Depth	0.1	6
RWP Wire Line Rut Width	-37	820

CHAPTER 8. CONCLUSIONS AND RECOMMENDATIONS

The following conclusions can be drawn from these analyses.

- The 1.8-m and wire line rut depths are fairly highly correlated ($R^2 \approx 0.95$) and provide the same type of information, namely the severity of the rutting.

- It was anticipated that the 1.8-m and wire line rut widths would be related. The data do not substantiate this.

- The fill area provides a two-dimensional rut depth. This index exhibited a fairly high correlation with the rut depths ($R^2 \approx 0.85$) and the negative area ($R^2 \approx 0.91$).

- The positive area did not behave in the same manner as any of the other indices; therefore, it may provide additional information about the profile.

- The mean rut depth for a section can be accurately obtained with only six profiles. However, the other indices considered in this study require the 11 measurements that were originally included in the data collection plan.

- Results of the paired t-tests indicate that there are statistically significant differences between three rut depth measurement systems – three-point, five-point, and wire line.

- The transverse location of the rut bar dramatically affects the measurement and, hence, the rut depth computation. Thus, consistent lateral placement of the survey vehicle is essential to repeatable rut depth measurements using the three or five-point procedures.

- Although a better correlation ($R^2 \approx 0.5$), but still considered poor, existed between the five-point rut depths and the wire line rut depths than between the three-point rut depths and the wire line rut depths ($R^2 \approx 0.2$), the five-point rut depths consistently underestimated the wire line rut depths.

- The three-point rut depths underestimate the rut depths for transverse profiles where the middle of the profile is lower than the outside edges of the lane (categories 2 and 3).

- A better correlation was found between the three-point, five-point, and wire line rut depths for those transverse profile shapes with a "hump" in the middle ($R^2 \approx 0.35$ for the three-point and $R^2 \approx 0.6$ for the five-point) (categories 3 and 4).

- These data indicate that the five-point rut depth never exceeds the wire line rut depth. However, the three-point rut depth may be larger or smaller than the wire line rut depth.

- The average three-point and five-point rut depths did not show a stronger relationship with the wire line rut depths calculated for the individual wheelpaths.

- Generally, the size of the difference observed between the wire line rut depths and the rut depths from the three-point and five-point rut bars increases with an increase in the wire line rut depth.

- Neither the three-point nor the five-point rut depth measurement system provides reliable and accurate estimates of rut depths as measured with a wire line.

- The Dipstick® relative elevation measurements are very precise, but not very accurate. The RoadRecon unit relative elevation measurements are not very precise, but are relatively accurate. For example, the coefficient of variation of the rut depth for the RoadRecon unit was approximately three times that of the Dipstick® (11 percent versus 4 percent, respectively). Also, the bias for the LWP rut depth is much larger for the Dipstick® than for the RoadRecon unit (4 mm versus 0 mm, respectively). These trends, as shown in tables 19, 20, and 21, are consistent for all the indices.

- Analysis performed using rut widths or rut depths should be performed using only one method of data collection. Analysis involving any of the other indices could be performed using the combined data set.

The recommendations from this study are as follows:

- Two tables should be added to NIMS. The first table should contain the values of the indices studied for each individual profile. These indices include the positive area, negative area, fill area, LWP and RWP 1.8-m rut depths, LWP and RWP 1.8-m rut locations, LWP and RWP wire line rut depths, LWP and RWP wire line rut widths, and LWP and RWP wire line rut locations. The second table should contain the mean, standard deviation, and minimum and maximum values for each index for each survey. The rut depths are the most commonly used and most widely understood measure of rutting. The rut widths and positive area indices appear to provide additional information about the profile. Until it is proven that this additional information is not useful, these indices should be kept in NIMS. The fill area and negative area are both highly correlated to the rut depths. However, the fill area is a very easily understood index and provides the user an opportunity to segue into viewing the transverse profile from different perspectives.

- Further review needs to be undertaken to determine the cause of the negative trends for the sections provided in table 11.

- The three-sensor rut bar does not provide repeatable and accurate rut depth measurements and, therefore, would not provide adequate network-level rut depths

for pavement management systems. Inconsistent rut depths obtained over time from the highway network would be problematic for determining rehabilitation needs.

- If a five-sensor rut bar is used for network-level data collection, care should be taken to ensure that the transverse location of the rut bar is consistent from year to year and that the mean values are adjusted to reflect more realistic rut depth values.

- A second field study should be undertaken. This field study should examine the relationship between the indices studied and the mechanism causing the rutting. This study should also provide additional information to verify the bias and precision values presented here.

- Indices not recommended for inclusion in the database are: PASCO typecasting, radius of curvature, and maximum water depth in each wheelpath.

- To limit the variability of the area and rut width indices, a transverse profile measurement should be made every 15.2 m on each test section.

APPENDIX A.
RUTCHAR PROGRAM USER'S GUIDE

INTRODUCTION

The purpose of the User's Guide for the RUTCHAR program, developed under the Transverse Profile Data Study by Fugro-BRE, Inc. in Austin, Texas, is: (1) to describe the system so that potential users can determine its applicability, and (2) to provide users with all the information necessary to operate and use the system efficiently and effectively.

One of the objectives of the Transverse Profile Data Study was to provide a method for characterizing the transverse profiles collected on the test sections included in the LTPP project. The characterizations were then to be determined for all of the data that had passed through the Quality Control (QC) process in the NIMS. At that time, 45,370 transverse profiles resided in NIMS for which the rutting characterizations needed to be determined. The RUTCHAR program was written to perform these calculations and to provide a method by which these calculations could be easily performed for all of the transverse profile data to be collected.

This program was intended for the sole purpose of calculating the rutting indices of data collected for LTPP. The output of the program should then be filtered into a table in NIMS.

The program was written in VisualBasic and requires an IBM 486-compatible system or later with Windows 95 or later.

APPLICATION DESCRIPTION

As previously stated, the program was written to calculate the indices used to characterize the transverse profile data for NIMS.

The first step in the program is a check of the input data. This data should be a series of *x*-*y* coordinates that define the transverse profile. Each of the *x*-*y* coordinates is reviewed to determine whether there are any duplicates. If a duplicate set of *x*-*y* coordinates is encountered, one of the duplicates is removed from the data set for all further calculations. A message is written to a file named DATCHK.OUT, which provides the section ID, construction event number, survey data, the *x*-coordinate, and the statement "IS A DUPLICATE POINT."

Next, a check is performed to find duplicate *x*-values. It was found that not all of the problems encountered were due to duplicate *x*-*y* coordinates in the data being used to perform these calculations. In some cases, the *x*-values were the same, but the *y*-values were different. In this case, the first of the duplicate *x*-values is reduced by 1. Furthermore, the section ID, construction event number, survey data, the *x*-coordinate, and the statement "IS A DUPLICATE X" are written to the DATCHK.OUT file.

The input file containing the original data set is not overwritten, but the data being used for the calculation are slightly altered. Once the check has been completed, the computation of the indices is initiated. The following discusses the computation of each index.

SYSTEM OPERATION

In order to run the software, double-click on the RUTCHAR icon. The system will prompt the user for four file names. The first file should be a data extraction of the MON_T_PROF_PROFILE table. The last file should be a data extraction of the MON_T_PROF_MASTER table. Both files should be in a fixed-width format.

The other two file names are the output file names. The first file being created will contain the calculated indices for each profile contained in the MON_T_PROF_PROFILE extraction. This file name should be formatted UR##YYYY.RIP. In this case "##" refers to the number of times these calculations have been performed in the year. "YYYY" is the year. The second file being created will contain the mean, standard deviation, and minimum and maximum values for each index for each survey. This filename should be formatted UR##YYYY.RIS. The format of these files is provided in tables 22 and 23.

While the data is being processed, a message will appear on the screen, "Please wait, your data is being processed."

The second output file is the DATCHK.OUT file, which has been previously discussed. This file will automatically be written in the directory from which the program was run. This file will be written if neither of the two discontinuities discussed are encountered; however, it will be 0-bytes long. If this file already exists in the directory from which the program is run, it will not be overwritten. The program will append information to the DATCHK.OUT file, but will never overwrite it. The user should rename or delete the previously written DATCHK.OUT file if he/she wants to work with a new file.

Table 22. File format output for the UR##YYYY.RIP file.

Item	Format	Units	IMS Field Name	Comments
1	Character(4)		SHRP_ID	1 - 6
2	Numeric		STATE_CODE	8 - 10
3	DD-MMM-YYYY		SURVEY_DATE	12 - 22
4	Numeric	m	POINT_LOC	24 - 29
5	Numeric	mm^2	NEGATIVE_AREA	31 - 39
6	Character(1)		NEGATIVE_AREA_FLAG	41 - 43
7	Numeric	mm^2	POSITIVE AREA	45 - 51
8	Character(1)		POSITIVE_AREA_FLAG	53 - 55
9	Numeric	mm^2	FILL_AREA	57 - 63
10	Character(1)		FILL_AREA_FLAG	65 - 67
11	Numeric	mm	LLH_DEPTH_1_8	69 - 73
12	Character(1)		LLH_DEPTH_1_8_FLAG	75 - 77
13	Numeric	mm	LLH_WIDTH_1_8	79 - 83
14	Character(1)		LLH_WIDTH_1_8_FLAG	85 - 87
15	Numeric	mm	LLH_OFFSET_1_8	89 - 93
16	Character(1)		LLH_OFFSET_1_8_FLAG	95 - 97
17	Numeric	mm	RLH_DEPTH_1_8	99 - 103
18	Character(1)		RLH_DEPTH_1_8_FLAG	105 - 107
19	Numeric	mm	RLH_WIDTH_1_8	109 - 113
20	Character(1)		RLH_WIDTH_1_8_FLAG	115 - 117
21	Numeric	mm	RLH_OFFSET_1_8	119 - 123
22	Character(1)		RLH_OFFSET_1_8_FLAG	125 - 127
23	Numeric	mm	LLH_DEPTH_WIRE_REF	129 - 133
24	Character(1)		LLH_DEPTH_WIRE_REF_FLAG	135 - 137
25	Numeric	mm	LLH_WIDTH_WIRE_REF	139 - 143
26	Character(1)		LLH_WIDTH_WIRE_REF_FLAG	145 - 147
27	Numeric	mm	LLH_OFFSET_WIRE_REF	149 - 153
28	Character(1)		LLH_OFFSET_WIRE_REF_FLAG	155 - 157
29	Numeric	mm	RLH_DEPTH_WIRE_REF	159 - 163
30	Character(1)		RLH_DEPTH_WIRE_REF_FLAG	165 - 167
31	Numeric	mm	RLH_WIDTH_WIRE_REF	169 - 173
32	Character(1)		RLH_WIDTH_WIRE_REF_FLAG	175 - 177
33	Numeric	mm	RLH_OFFSET_WIRE_REF	179 - 183
34	Character(1)		RLH_OFFSET_WIRE_REF_FLAG	185 - 187
35	Numeric	mm	TRANS_PROFILE_MEASURE_LENGTH	189 - 193
36	Character(1)		SECTION_STAT_INCLUDE_FLAG	195 - 197
37	DD-MMM-YYYY		DATA_PROCESS_EXTRACT_DATE	199 - 209

Table 23. File format for the UR##YYYY.RIS file.

Item	Format	Units	IMS Field Name	Comments
1	Character(4)		SHRP_ID	1 - 6
2	Numeric		STATE_CODE	8 - 10
3	DD-MMM-YYYY		SURVEY_DATE	12 - 24
4	Numeric		NO_PROFILES	26 - 27
5	Numeric	mm^2	POSITIVE_AREA_MEAN	29 - 35
6	Numeric	mm^2	POSITIVE_AREA_STD	37 - 43
7	Numeric	mm^2	POSITIVE_AREA_MIN	45 - 51
8	Numeric	mm^2	POSITIVE_AREA_MAX	53 - 59
9	Numeric	mm^2	NEGATIVE_AREA_MEAN	61 - 69
10	Numeric	mm^2	NEGATIVE_AREA_STD	71 - 79
11	Numeric	mm^2	NEGATIVE_AREA_MIN	81 - 89
12	Numeric	mm^2	NEGATIVE_AREA_MAX	91 - 99
13	Numeric	mm^2	FILL_AREA_MEAN	101 - 107
14	Numeric	mm^2	FILL_AREA_STD	109 - 115
15	Numeric	mm^2	FILL_AREA_MIN	117 - 123
16	Numeric	mm^2	FILL_AREA_MAX	125 - 131
17	Numeric	mm	LLH_DEPTH_1_8_MEAN	133 - 137
18	Numeric	mm	LLH_DEPTH_1_8_STD	139 - 143
19	Numeric	mm	LLH_DEPTH_1_8_MIN	145 - 149
20	Numeric	mm	LLH_DEPTH_1_8_MAX	151 - 155
21	Numeric	mm	RLH_DEPTH_1_8_MEAN	157 - 161
22	Numeric	mm	RLH_DEPTH_1_8_STD	163 - 167
23	Numeric	mm	RLH_DEPTH_1_8_MIN	169 - 173
24	Numeric	mm	RLH_DEPTH_1_8_MAX	175 - 179
25	Numeric	mm	MAX_MEAN_DEPTH_1_8	181 - 185
26	Numeric	mm	LLH_WIDTH_1_8_MEAN	187 - 191
27	Numeric	mm	LLH_WIDTH_1_8_STD	193 - 197
28	Numeric	mm	LLH_WIDTH_1_8_MIN	199 - 203
29	Numeric	mm	LLH_WIDTH_1_8_MAX	205 - 209
30	Numeric	mm	LLH_OFFSET_1_8_MEAN	211 - 215
31	Numeric	mm	LLH_OFFSET_1_8_STD	217 - 221
32	Numeric	mm	LLH_OFFSET_1_8_MIN	223 - 227
33	Numeric	mm	LLH_OFFSET_1_8_MAX	229 - 233
34	Numeric	mm	RLH_WIDTH_1_8_MEAN	235 - 239
35	Numeric	mm	RLH_WIDTH_1_8_STD	241 - 245
36	Numeric	mm	RLH_WIDTH_1_8_MIN	247 - 251
37	Numeric	mm	RLH_WIDTH_1_8_MAX	253 - 257
38	Numeric		RLH_OFFSET_1_8_MEAN	259 - 263
39	Numeric		RLH_OFFSET_1_8_STD	265 - 269
40	Numeric		RLH_OFFSET_1_8_MIN	271 - 275
41	Numeric		RLH_OFFSET_1_8_MAX	277 - 281
42	Numeric	mm	LLH_DEPTH_WIRE_REF_MEAN	283 - 287
43	Numeric	mm	LLH_DEPTH_WIRE_REF_STD	289 - 293
44	Numeric	mm	LLH_DEPTH_WIRE_REF_MIN	295 - 299
45	Numeric	mm	LLH_DEPTH_WIRE_REF_MAX	301 - 305

Table 23. File format for the UR##YYYY.RIS file (continued).

Item	Format	Units	IMS Field Name	Comments
46	Numeric	mm	RLH_DEPTH_WIRE_REF_MEAN	307 - 311
47	Numeric	mm	RLH_DEPTH_WIRE_REF_STD	313 - 317
48	Numeric	mm	RLH_DEPTH_WIRE_REF_MIN	319 - 323
49	Numeric	mm	RLH_DEPTH_WIRE_REF_MAX	325 - 329
50	Numeric	mm	MAX_MEAN_DEPTH_WIRE_REF	331 - 335
51	Numeric	mm	LLH_WIDTH_WIRE_REF_MEAN	337 - 341
52	Numeric	mm	LLH_WIDTH_WIRE_REF_STD	343 - 347
53	Numeric	mm	LLH_WIDTH_WIRE_REF_MIN	349 - 353
54	Numeric	mm	LLH_WIDTH_WIRE_REF_MAX	355 - 359
55	Numeric	mm	LLH_OFFSET_WIRE_REF_MEAN	361 - 365
56	Numeric	mm	LLH_OFFSET_WIRE_REF_STD	367 - 371
57	Numeric	mm	LLH_OFFSET_WIRE_REF_MIN	373 - 377
58	Numeric	mm	LLH_OFFSET_WIRE_REF_MAX	379 - 383
59	Numeric	mm	RLH_WIDTH_WIRE_REF_MEAN	385 - 389
60	Numeric	mm	RLH_WIDTH_WIRE_REF_STD	391 - 395
61	Numeric	mm	RLH_WIDTH_WIRE_REF_MIN	397 - 401
62	Numeric	mm	RLH_WIDTH_WIRE_REF_MAX	403 - 407
63	Numeric	mm	RLH_OFFSET_WIRE_REF_MEAN	409 - 413
64	Numeric	mm	RLH_OFFSET_WIRE_REF_STD	415 - 419
65	Numeric	mm	RLH_OFFSET_WIRE_REF_MIN	421 - 425
66	Numeric	mm	RLH_OFFSET_WIRE_REF_MAX	427 - 431
67	Character(1)		T_PROF_DEVICE_CODE	433 - 435
68	DD-MMM-YYYY		DATA_PROCESS_EXTRACT_DATE	447 - 457

APPENDIX B.
DISTRIBUTION OF THE INDICES

This appendix contains distributions of each of the indices by various categories. Each distribution includes a histogram, a normal probability plot, a list of quantiles, the mean, the standard deviation, the confidence interval, the skewness of the distribution, and the kurtosis of the distribution. The histogram provides a distribution of the data collected. The histogram in figure 35 illustrates that the majority of the data for the negative area index lies between 0 and -10,000. The normal probability plot, located to the right of the histogram, is another method for viewing the distribution of the data. This type of plot is often used to determine if the data are normally distributed. The closer the line presented in the plot is to a straight line, the more the data are considered to follow a normal distribution. The quantities are determined by sorting the data in ascending order. The value for the 25^{th} percentile is the value found one-quarter of the way through the data. The skewness and kurtosis are both values that pertain to the normality of the data. Skewness is a measure of the tendency of the deviations to be larger in one direction than in the other. Skewness values that have a large absolute value are likely to be from a non-normal distribution. Kurtosis measures the "heaviness" of the tails of a distribution. A large value of kurtosis indicates a heavy-tailed distribution. Kurtosis and skewness values are usually less than ± 1.0.

Figures 35 through 49 contain the distribution of all of the individual values for each index. Figures 50 through 63 provide the distribution of the section means. All of the sections are included in these distributions. Figures 64 through 79 provide the distribution of the GPS-1 (HMAC over granular base) section means. Figures 80 through 94 provide the distribution of the GPS-2 (HMAC over stabilized base) section means. The GPS-6 (HMAC overlay of HMAC) section mean distributions are provided in figures 95 through 109. The GPS-7 (HMAC overlay of PCC) section mean distributions are provided in figures 110 through 124.

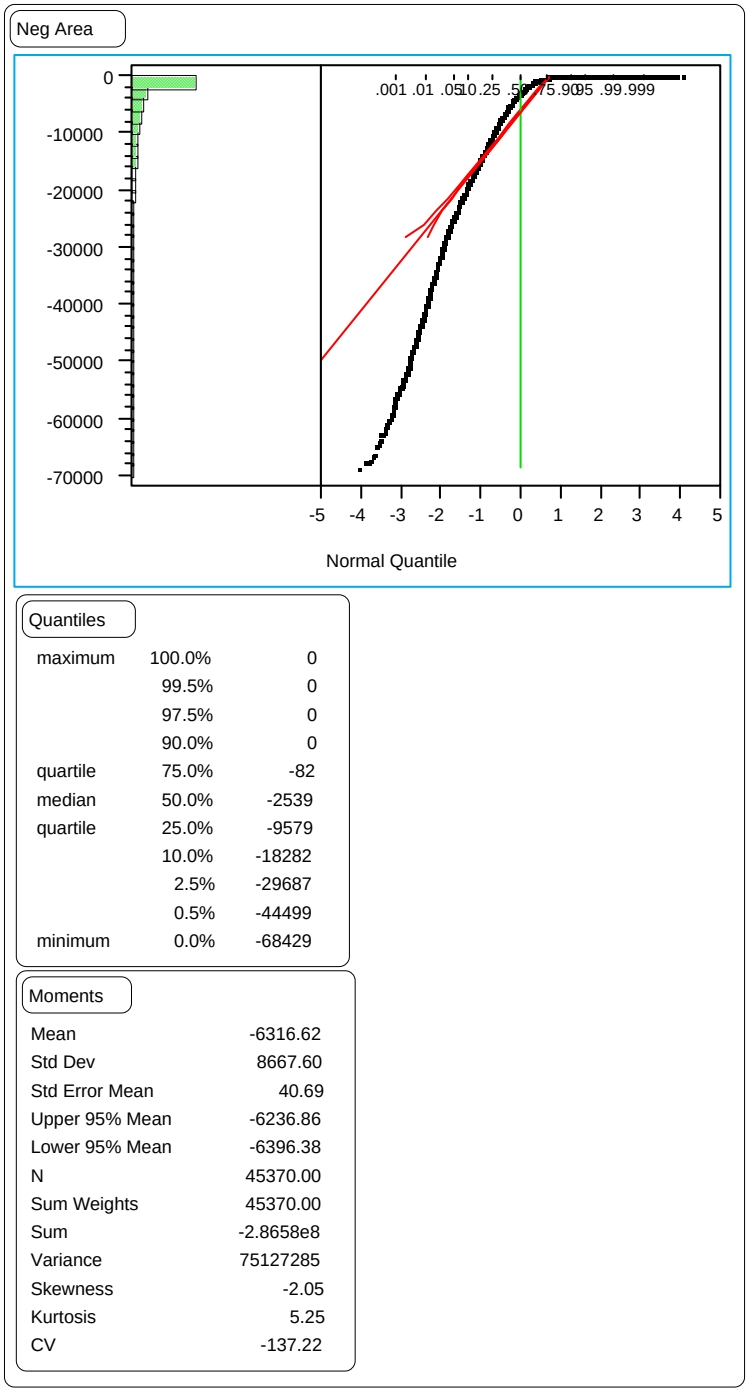

Figure 35. Distribution of the negative area index.

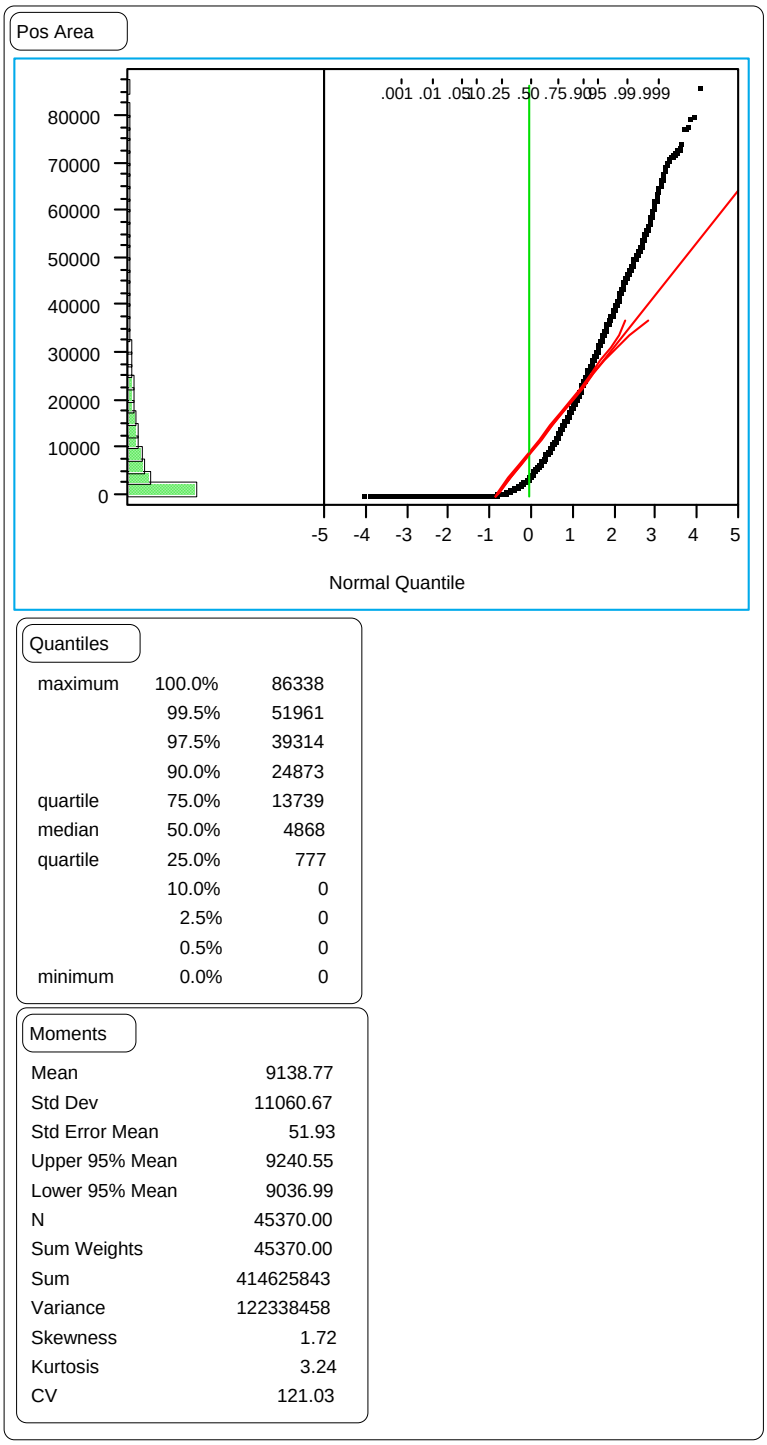

Figure 36. Distribution of the positive area index.

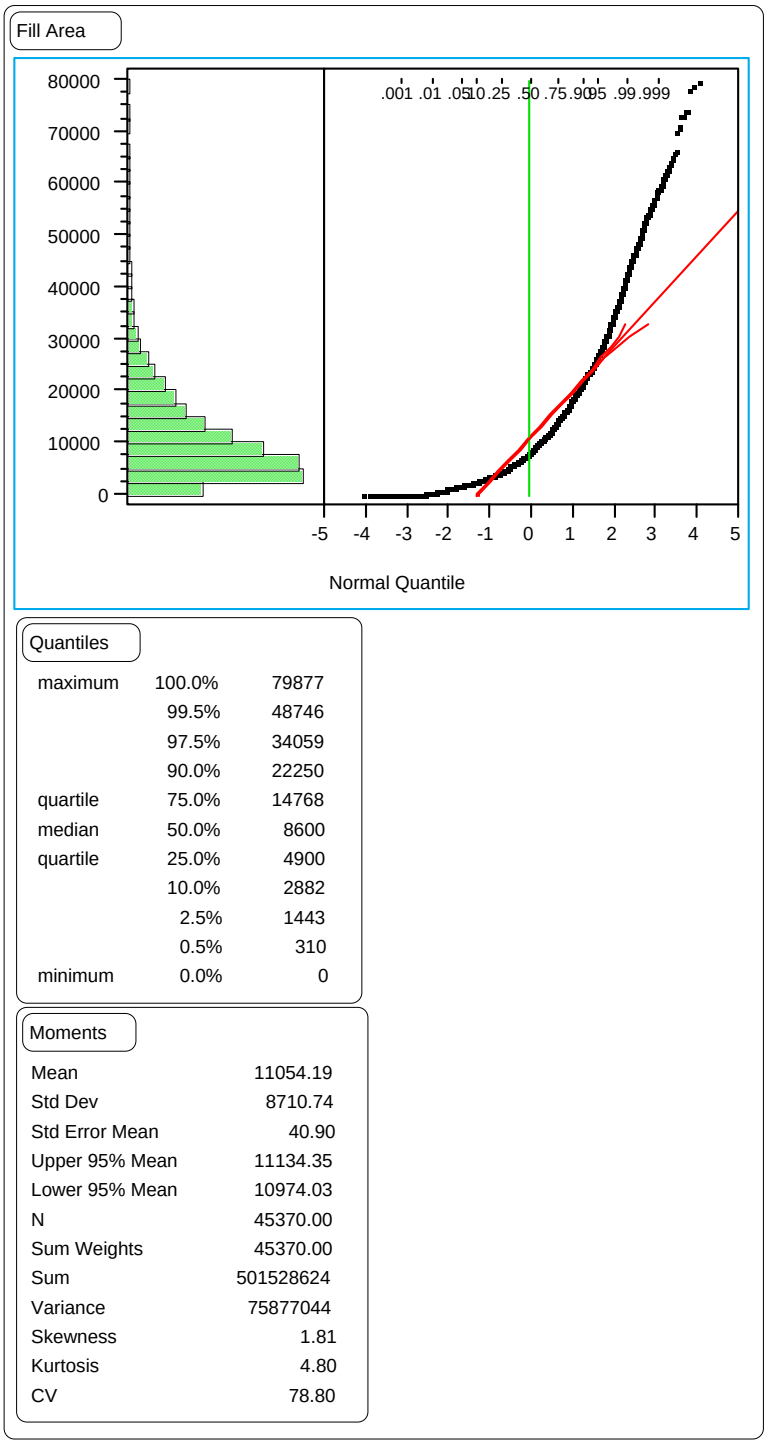

Figure 37. Distribution of the fill area index.

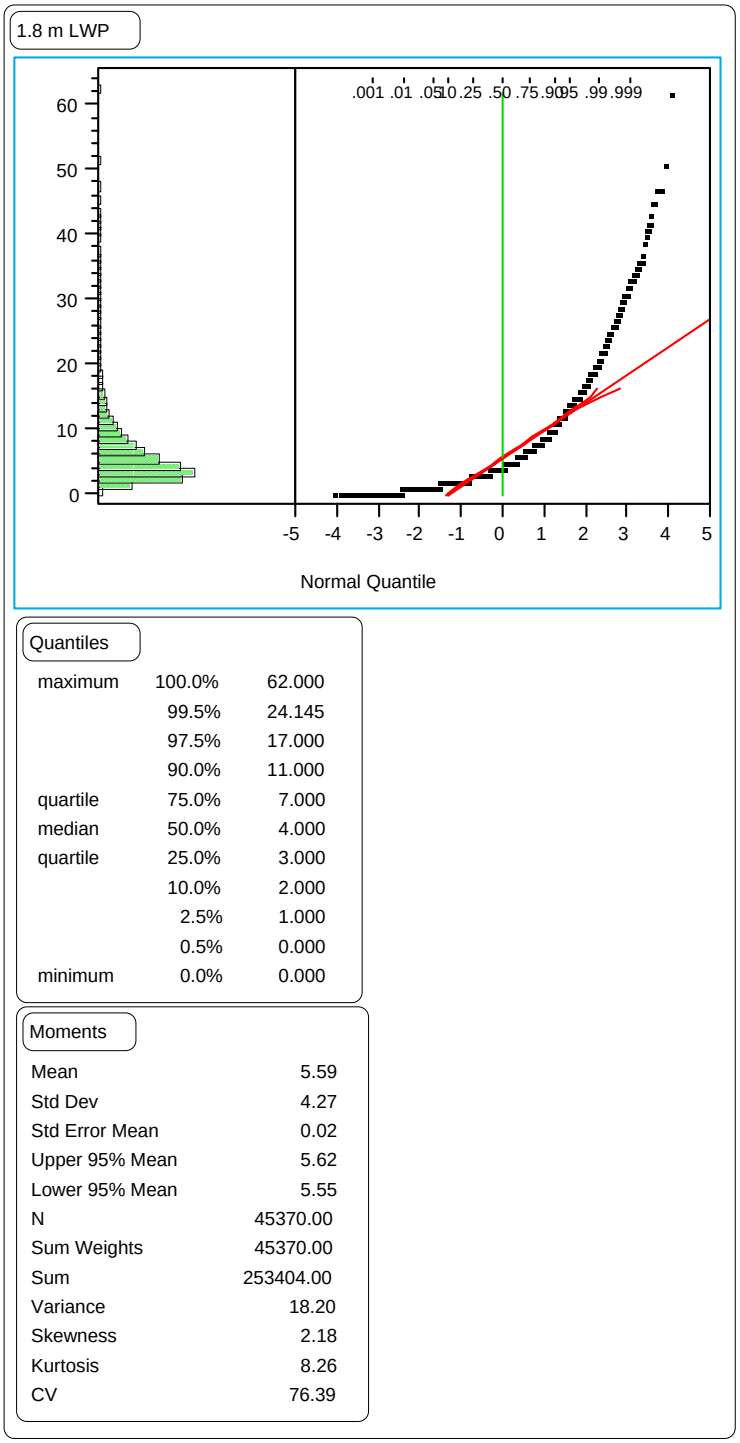

Figure 38. Distribution of the LWP 1.8-m rut depth.

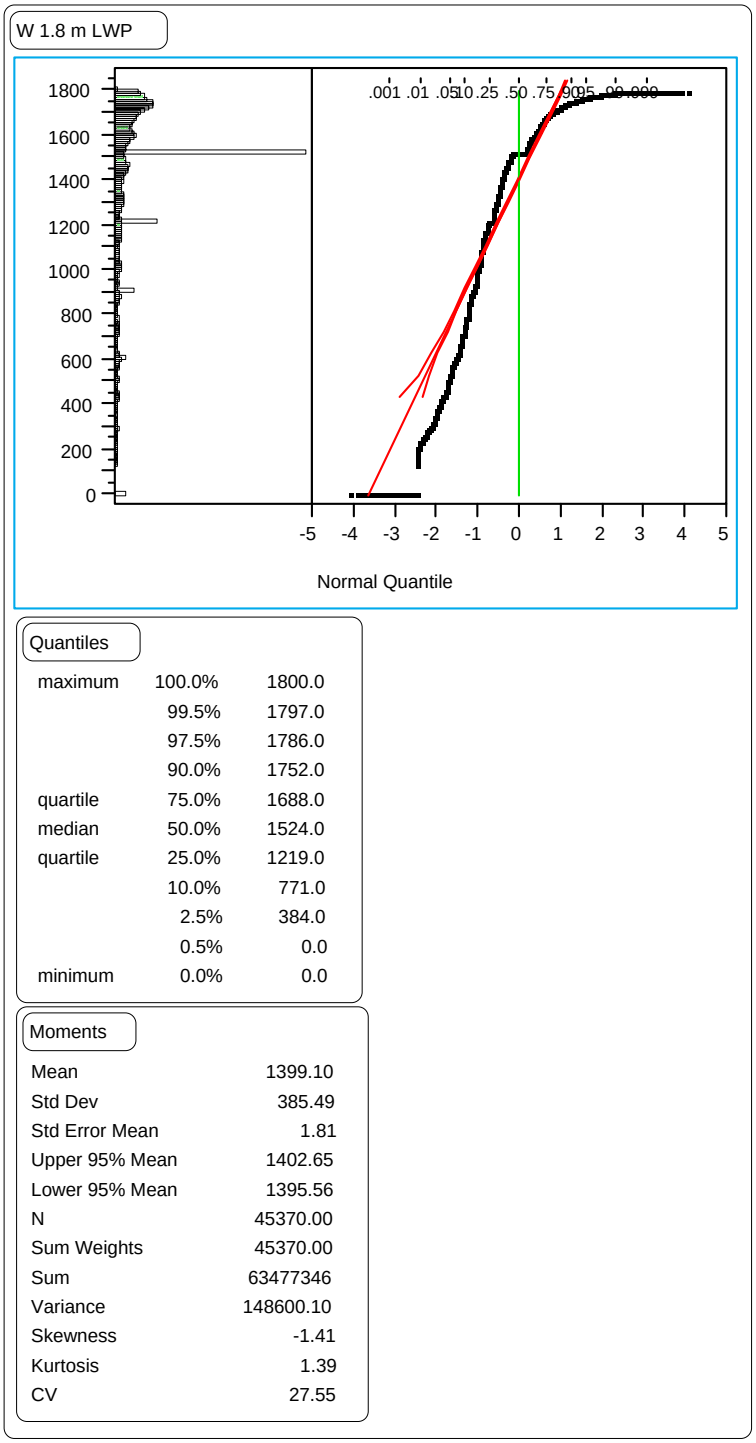

Figure 39. Distribution of the LWP 1.8-m rut width.

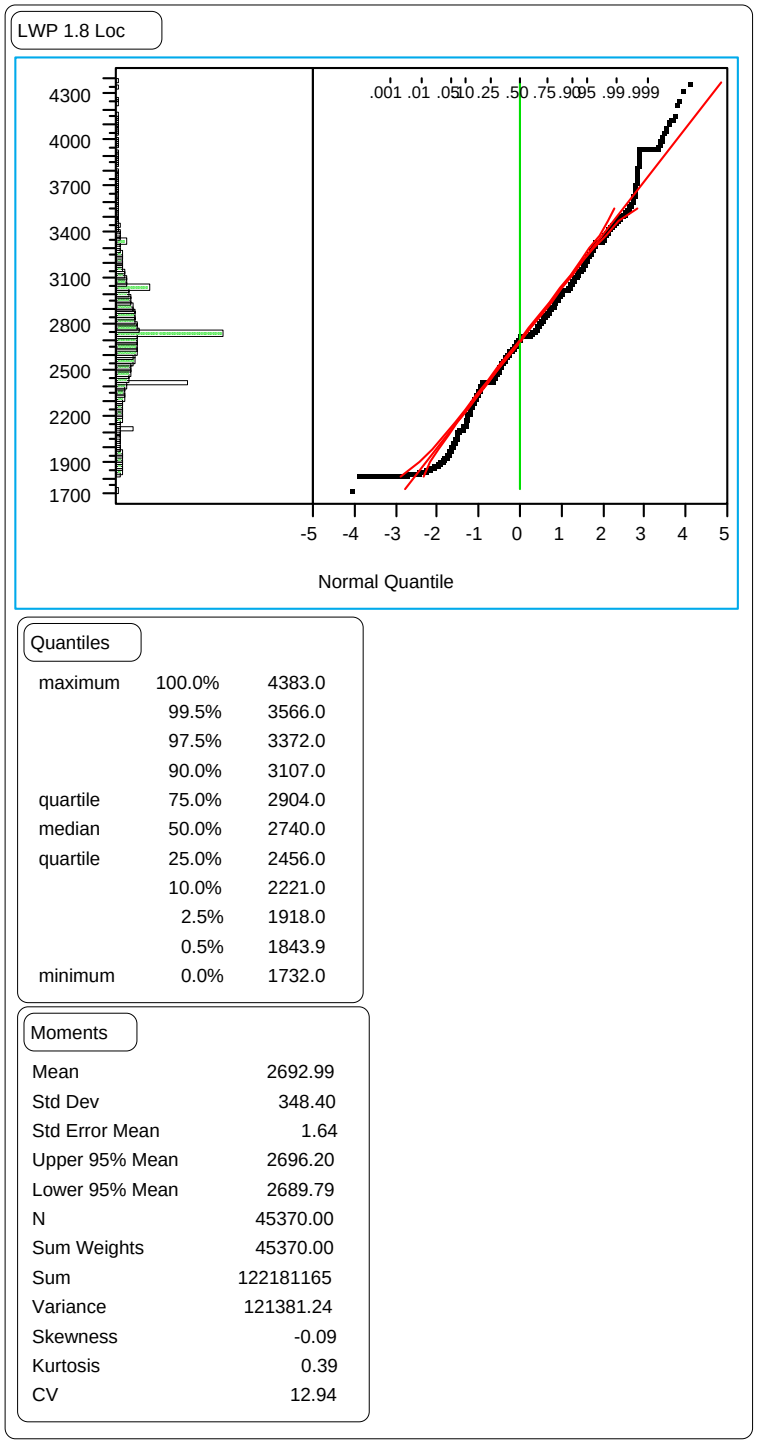

Figure 40. Distribution of the LWP 1.8-m rut location.

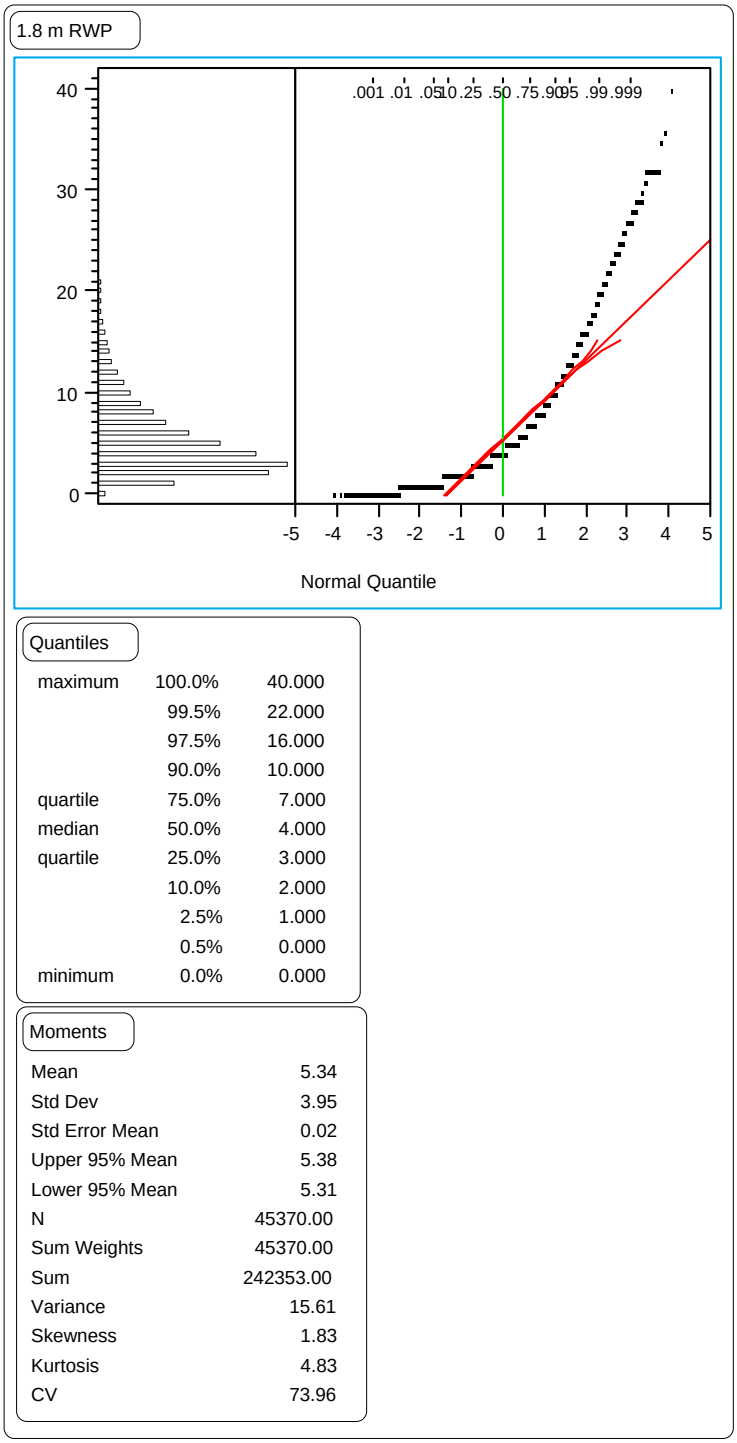

Figure 41. Distribution of the RWP 1.8-m rut depth.

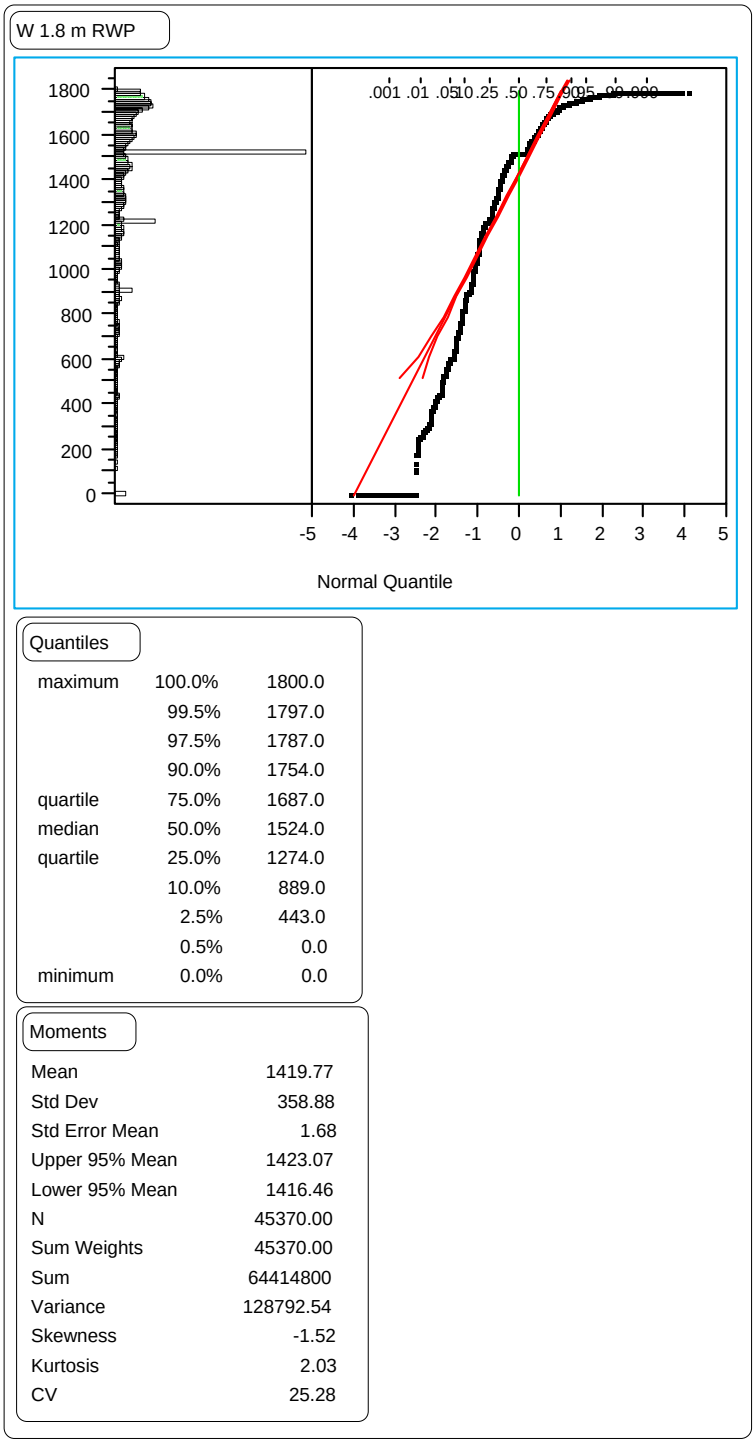

Figure 42. Distribution of the RWP 1.8-m rut width.

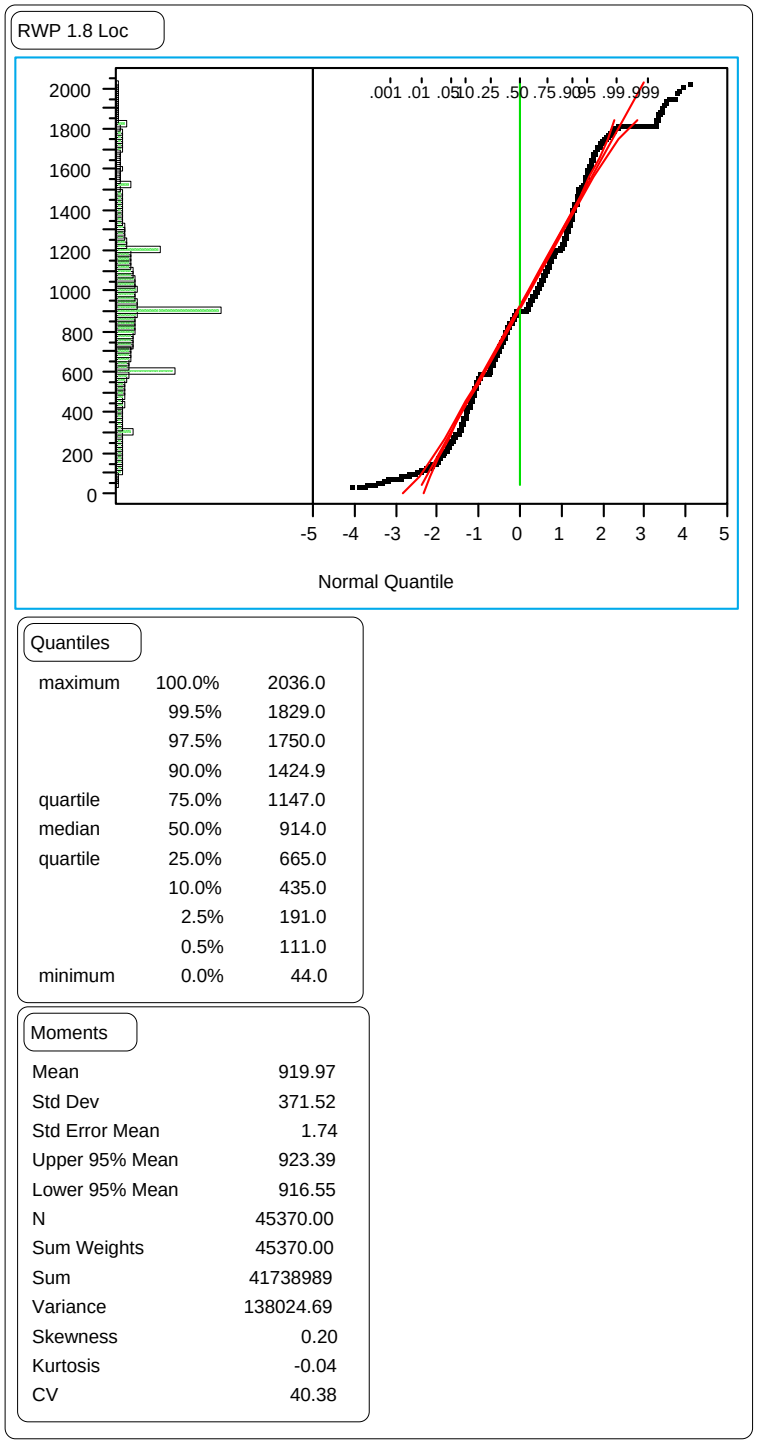

Figure 43. Distribution of the RWP 1.8-m rut location.

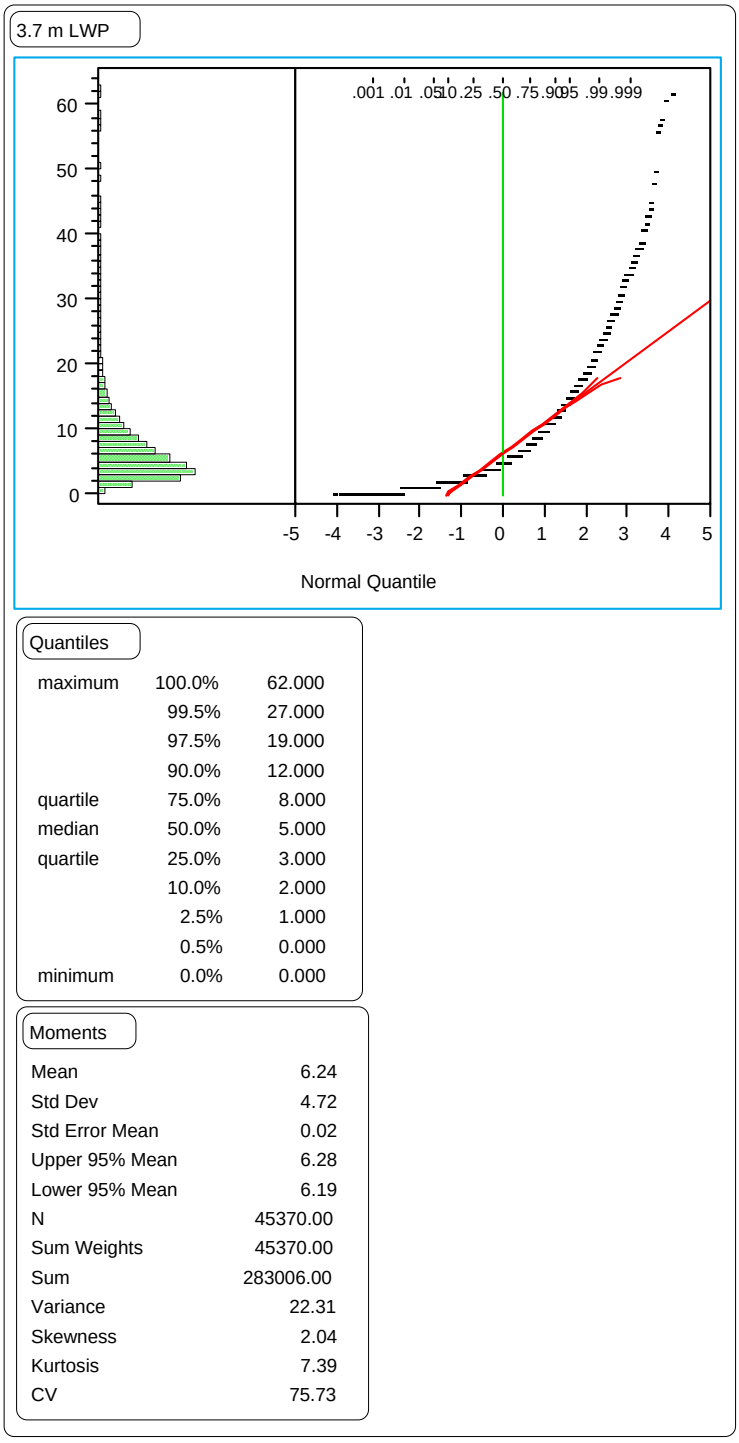

Figure 44. Distribution of the LWP wire line rut depth.

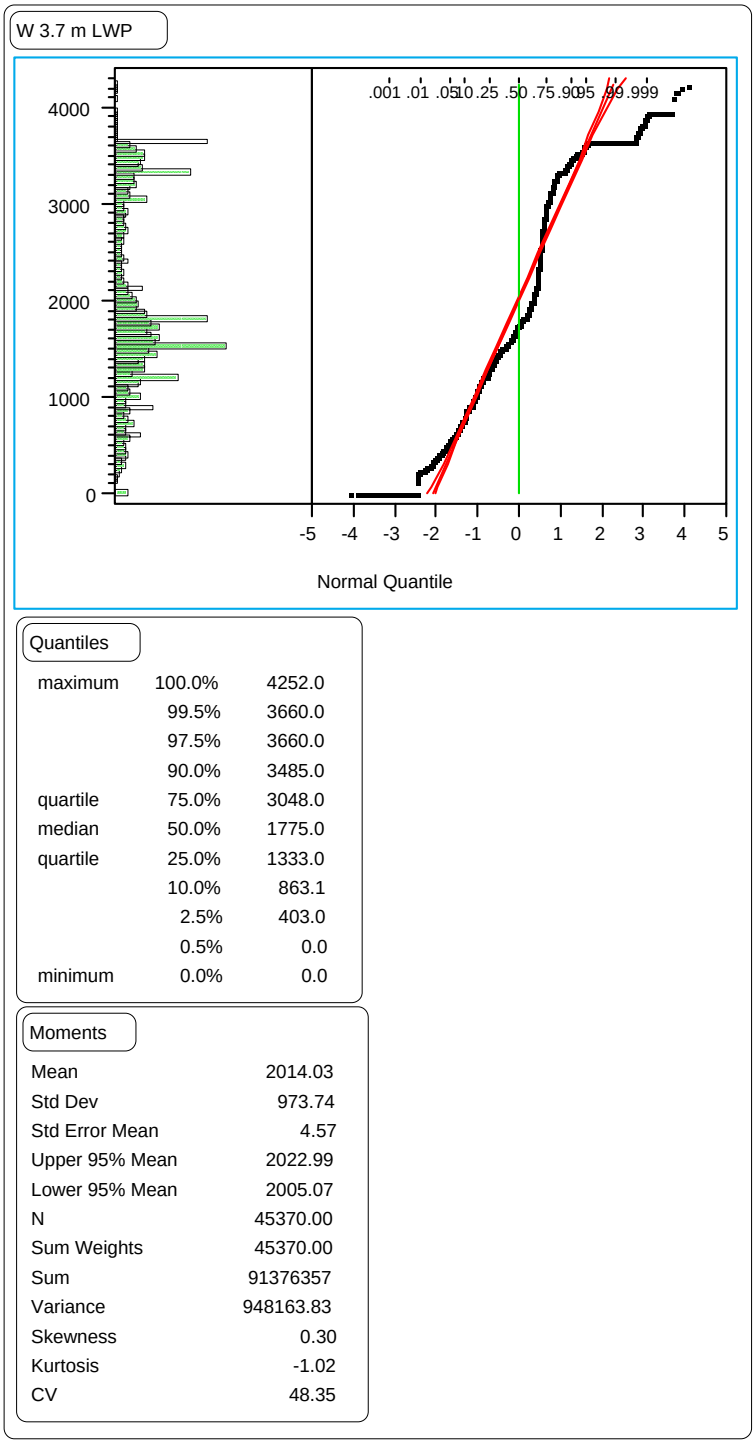

Figure 45. Distribution of the LWP wire line rut width.

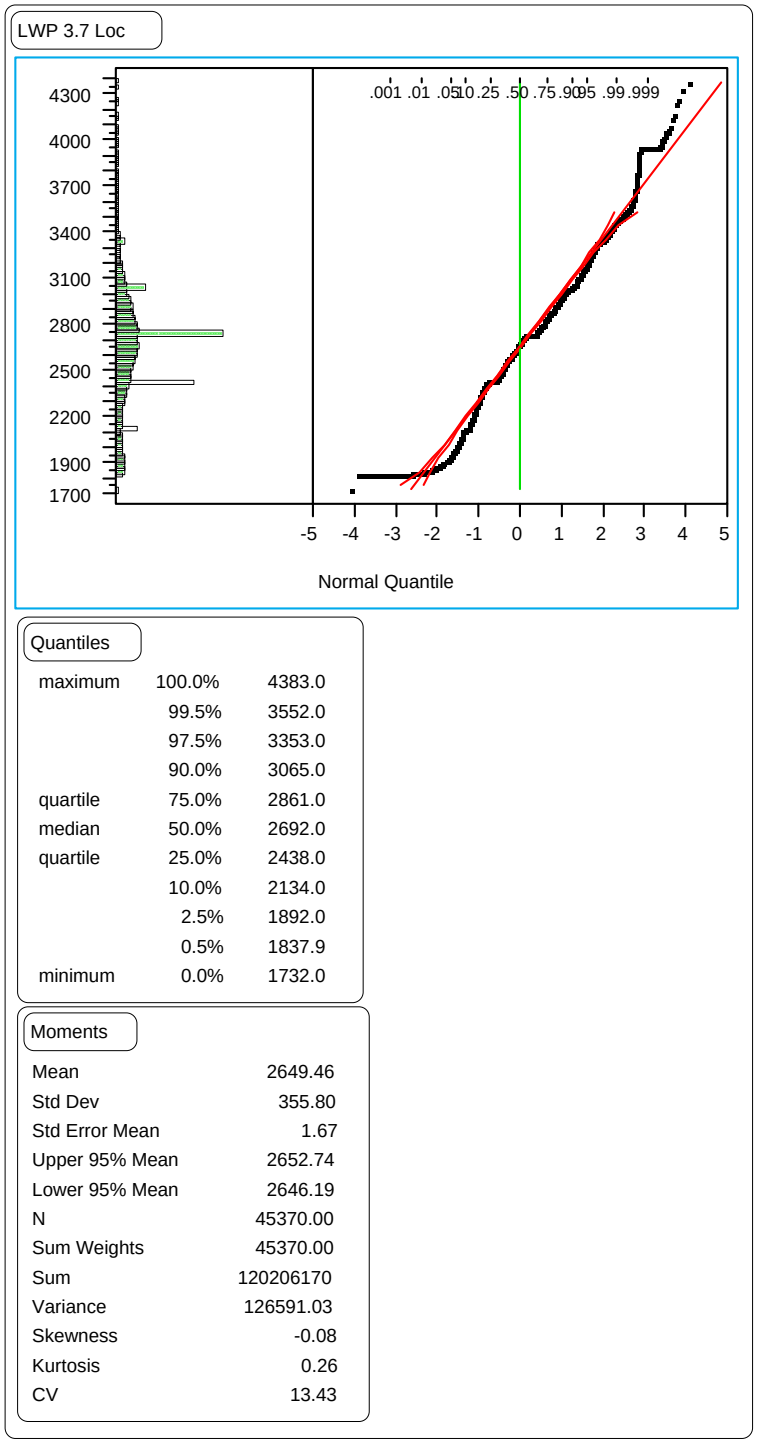

Figure 46. Distribution of the LWP wire line rut location.

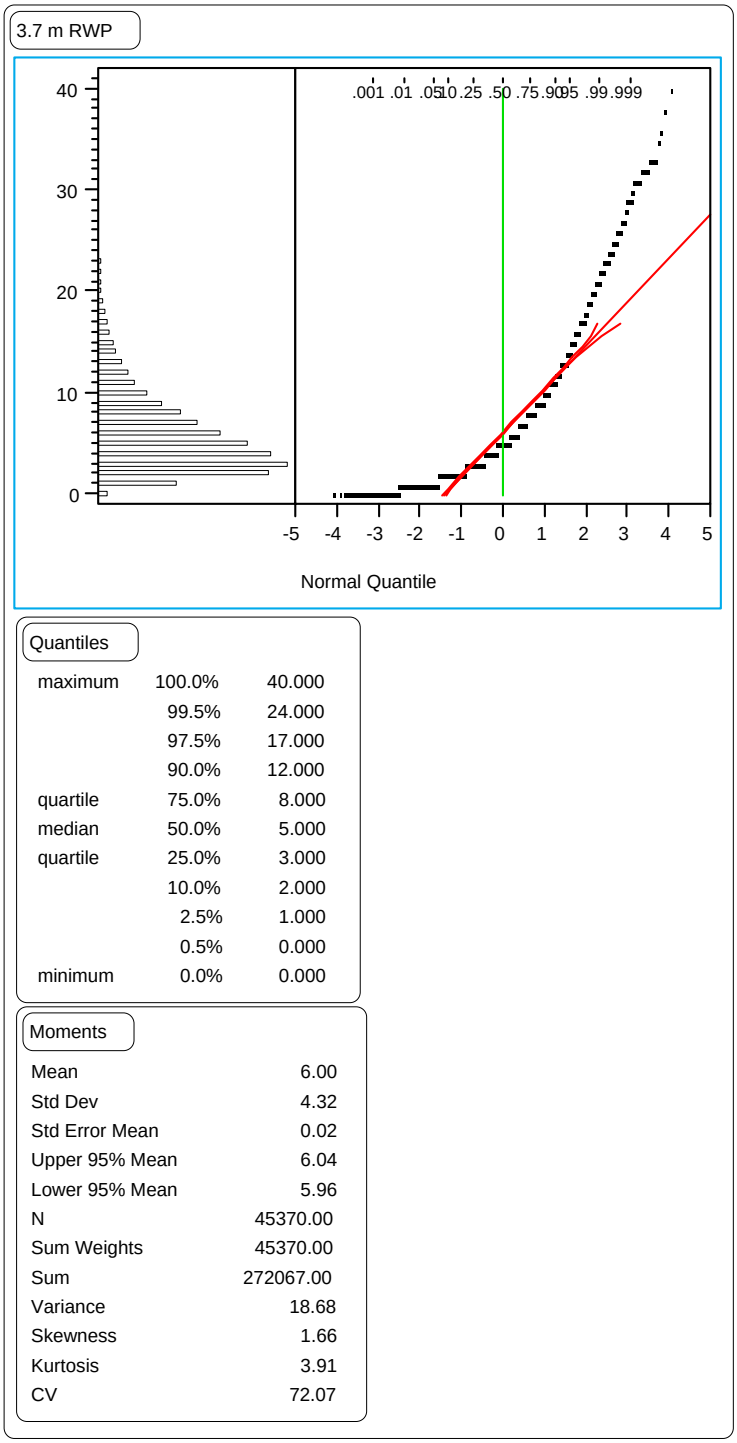

Figure 47. Distribution of the RWP wire line rut depth.

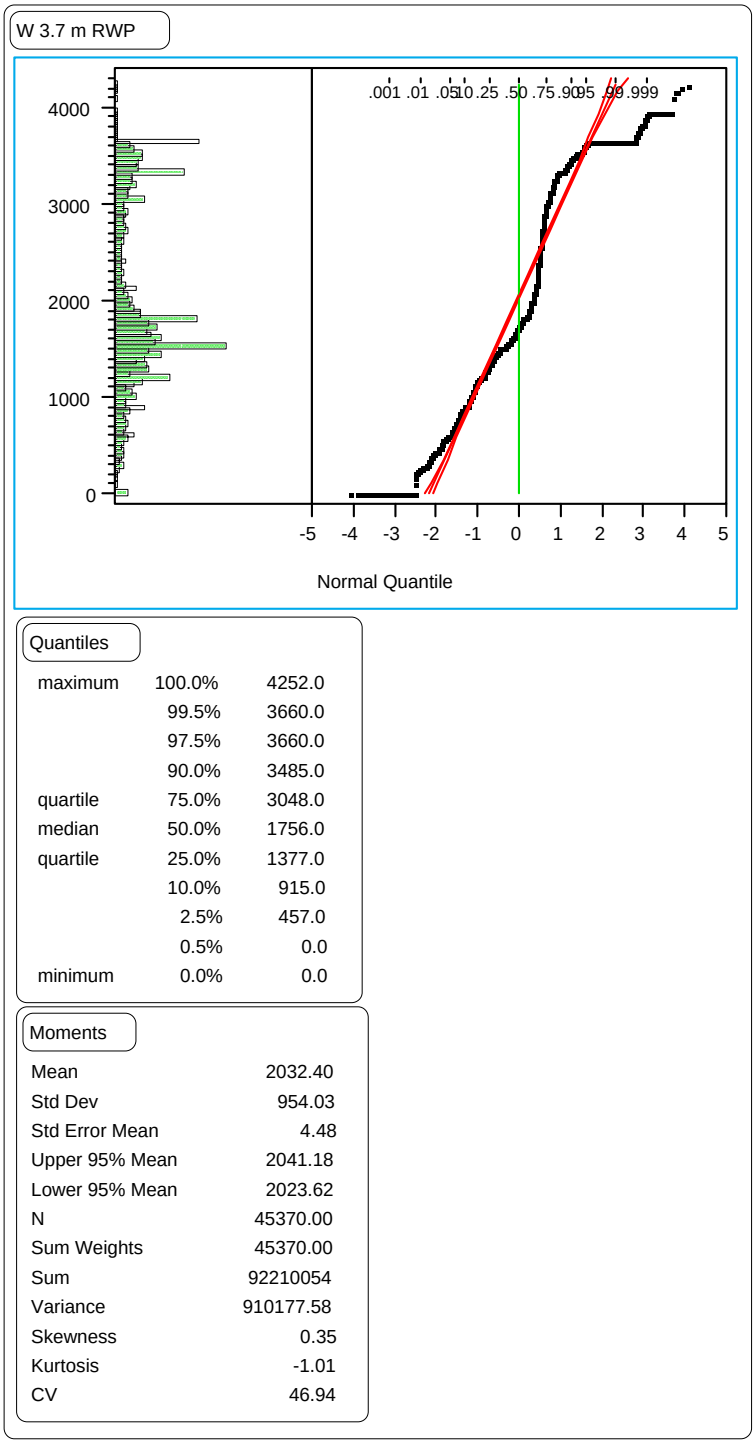

Figure 48. Distribution of the RWP wire line rut width.

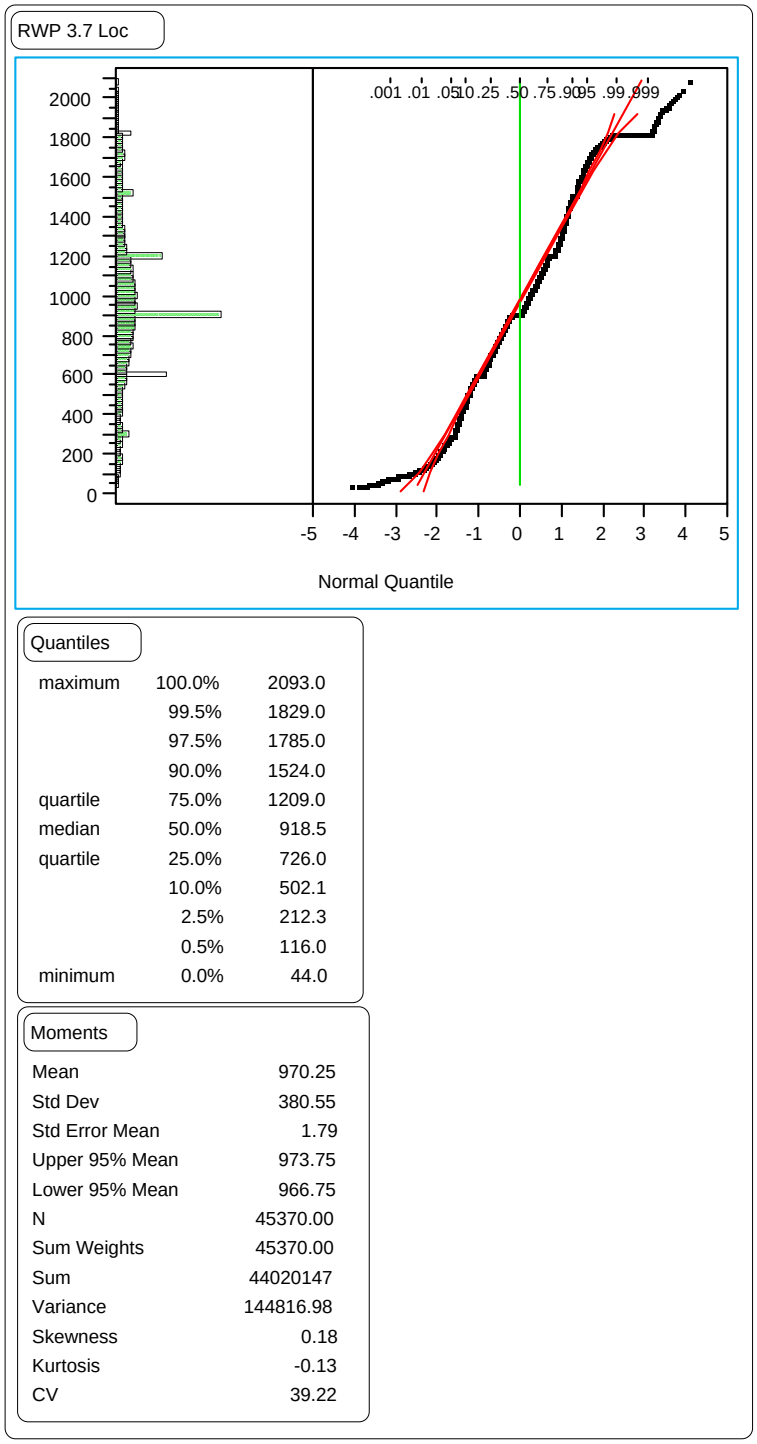

Figure 49. Distribution of the RWP wire line rut location.

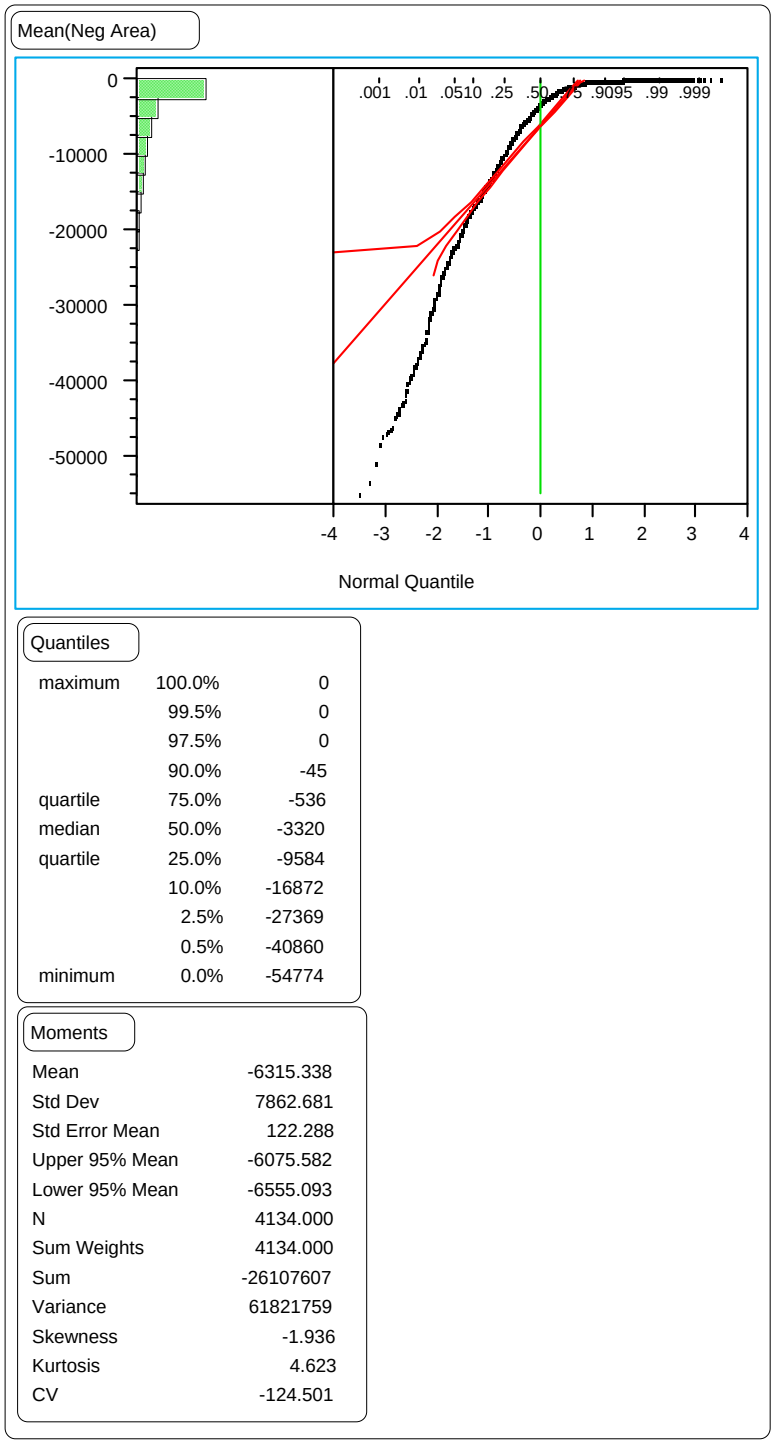

Figure 50. Distribution of the section means of the negative area index.

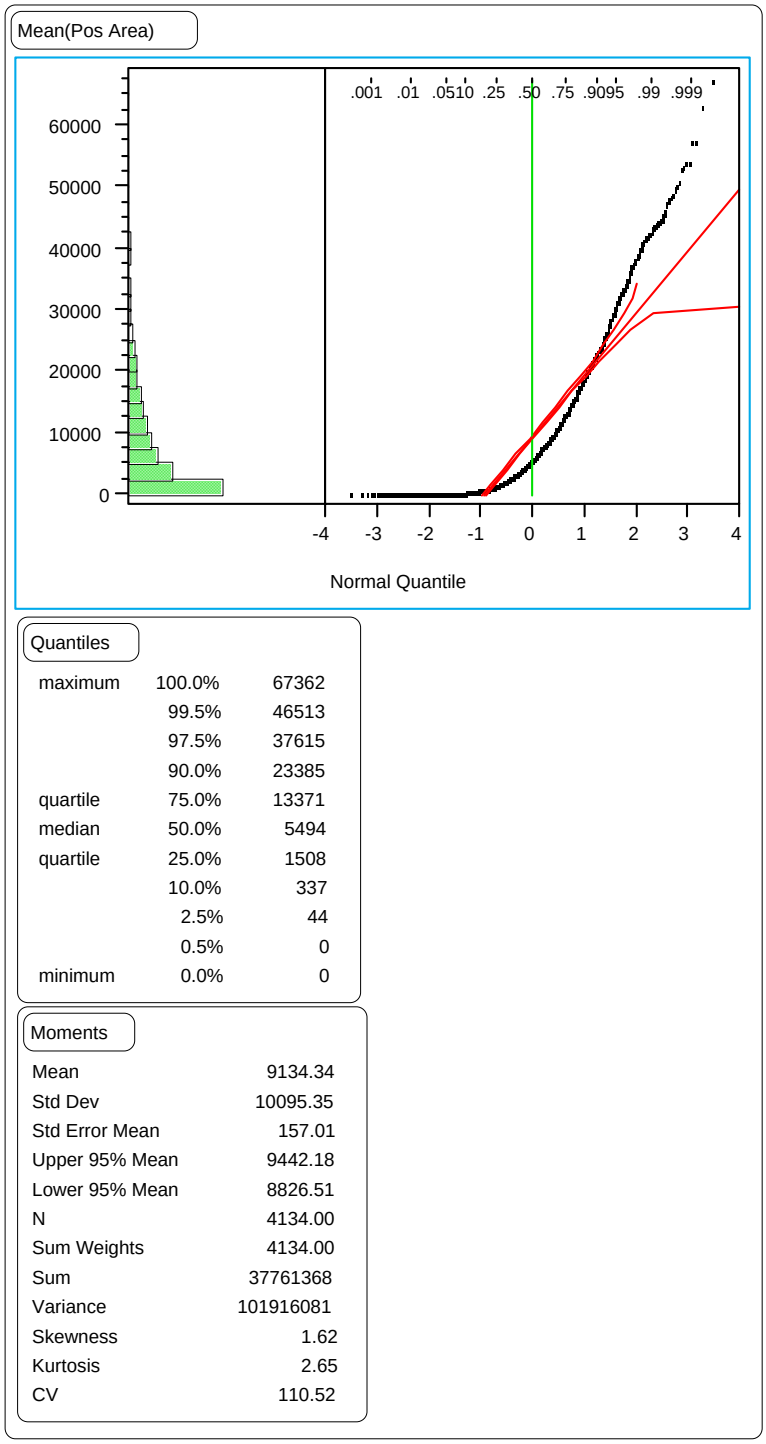

Figure 51. Distribution of the section means of the positive area index.

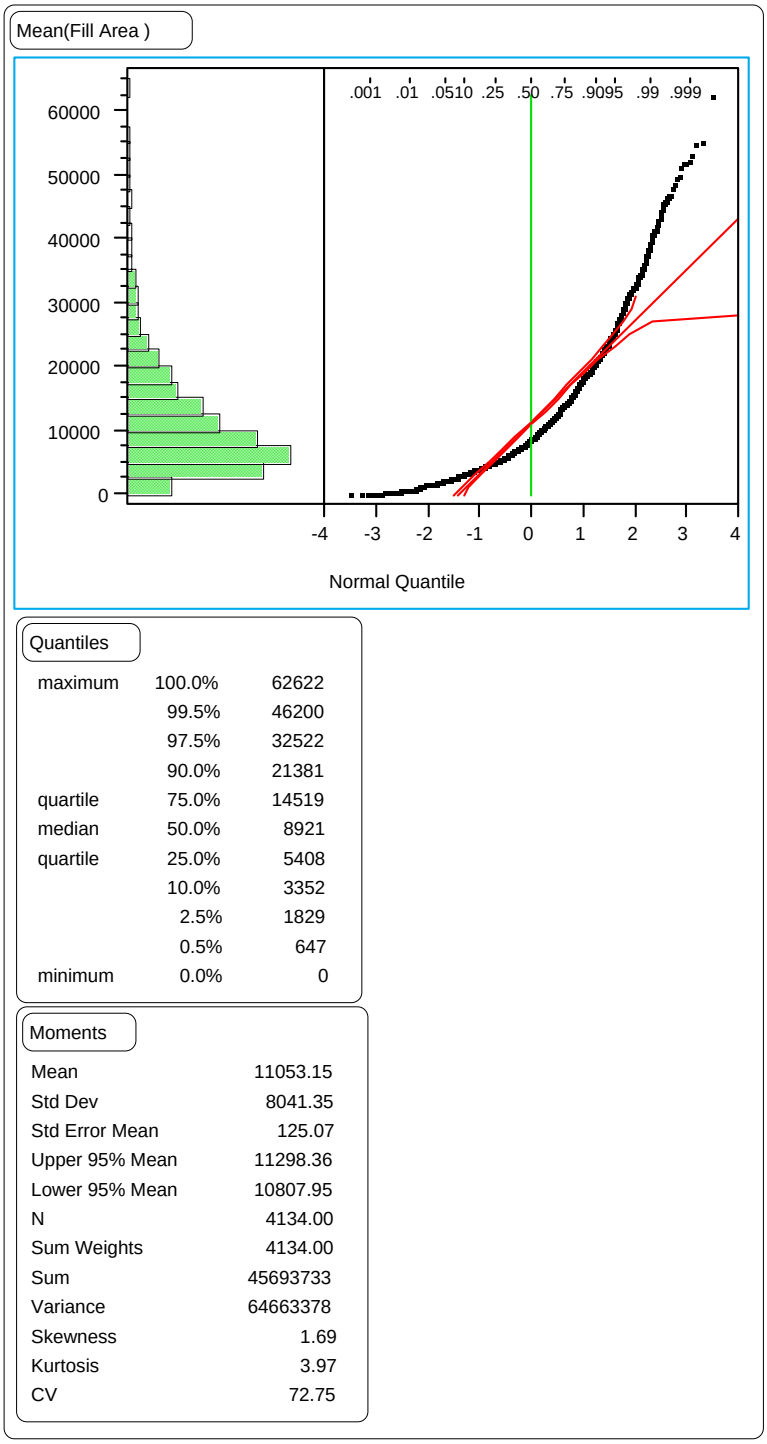

Figure 52. Distribution of the section means of the fill area index.

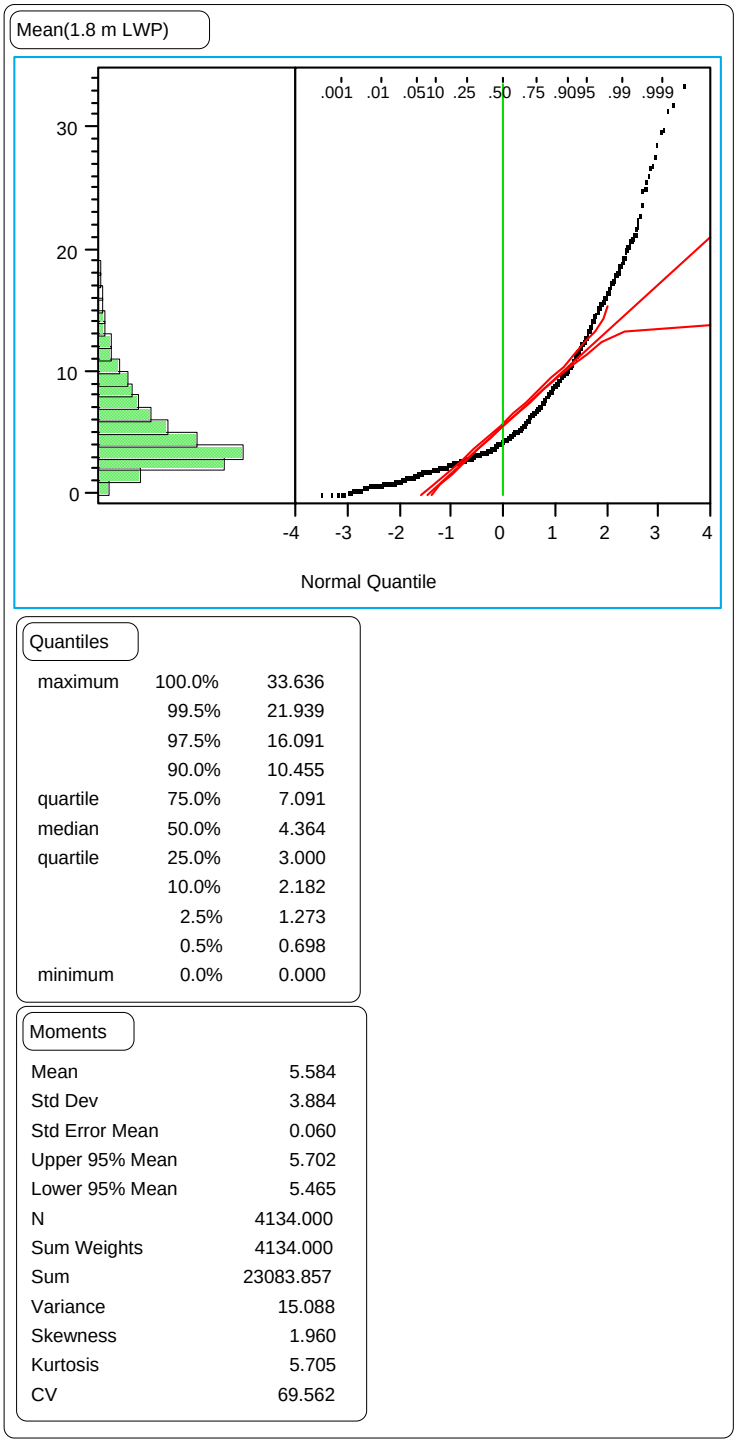

Figure 53. Distribution of the section means of the LWP 1.8-m rut depths.

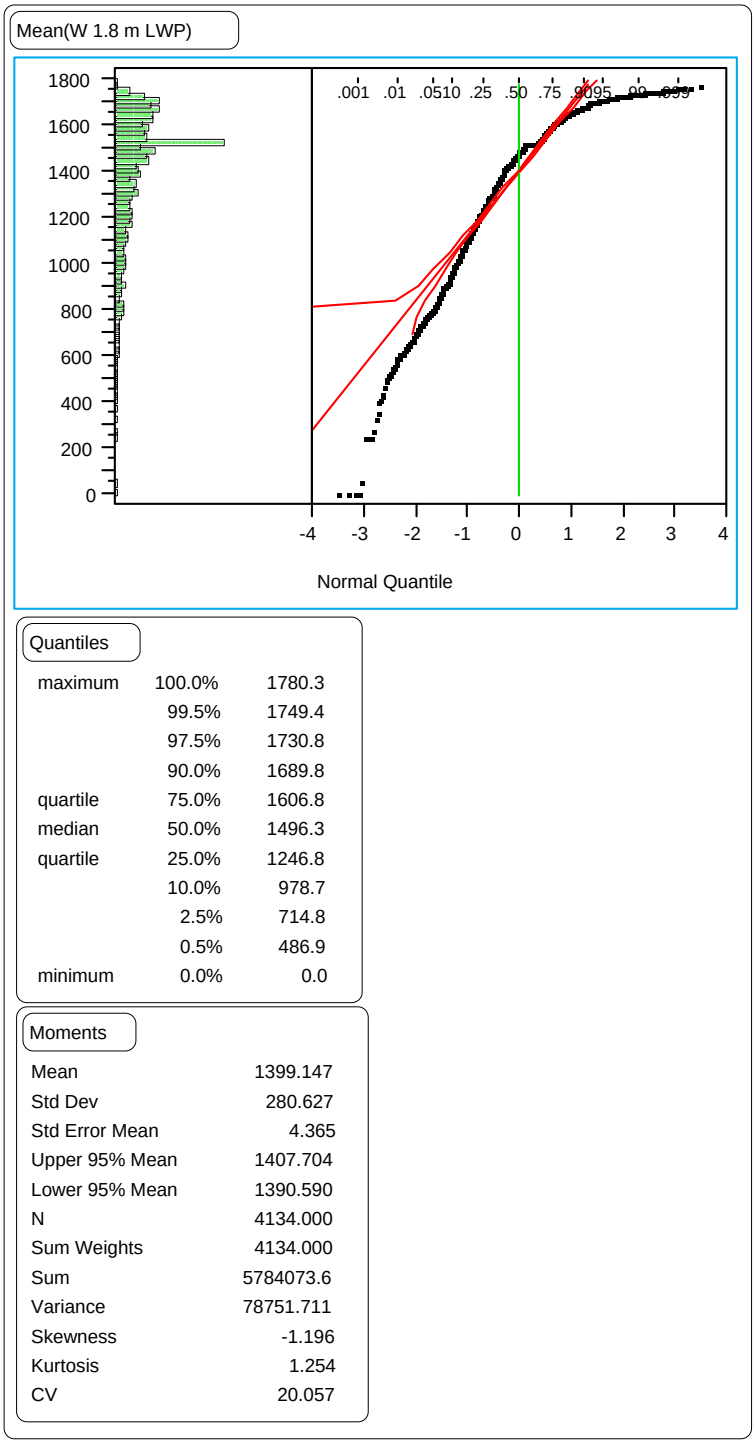

Figure 54. Distribution of the section means of the LWP 1.8-m rut widths.

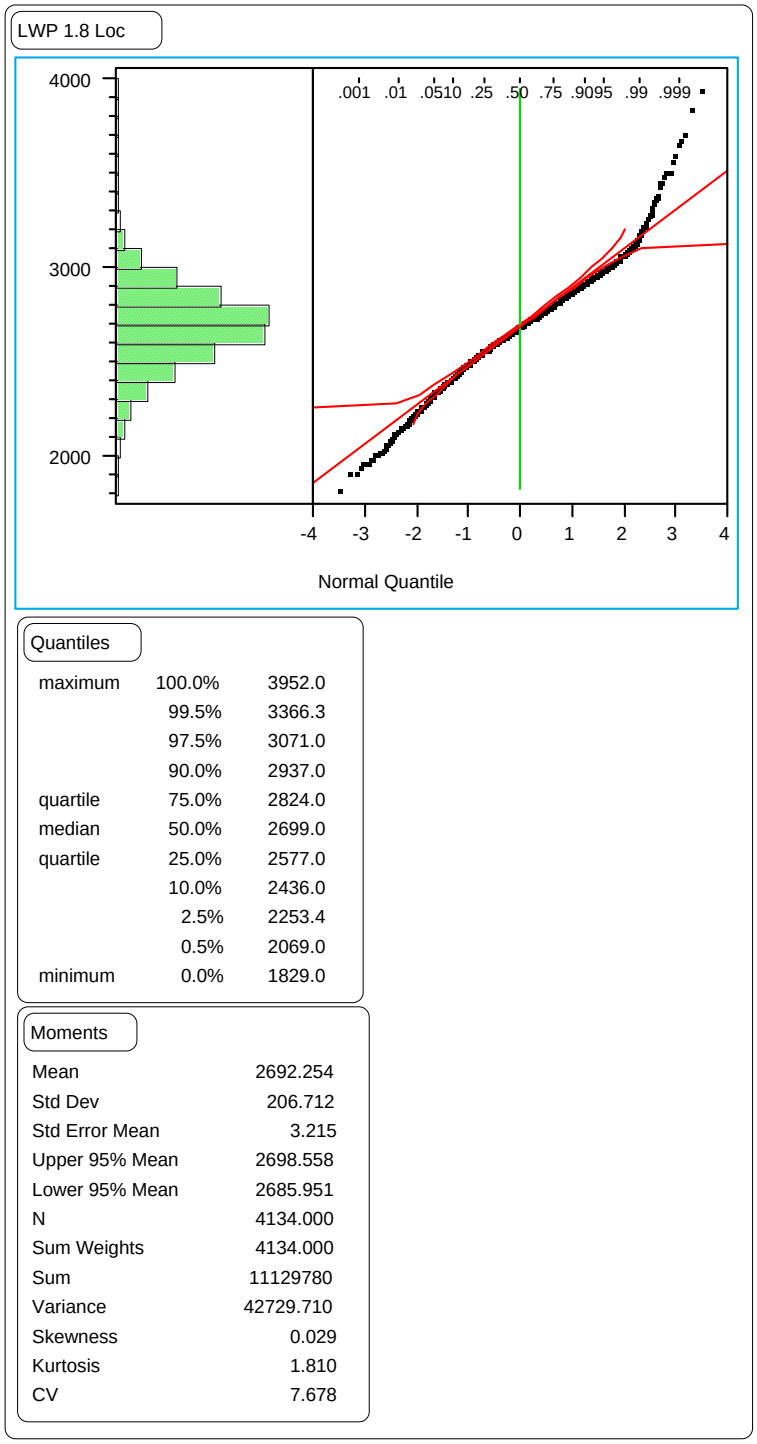

Figure 55. Distribution of the section means of the LWP 1.8-m rut locations.

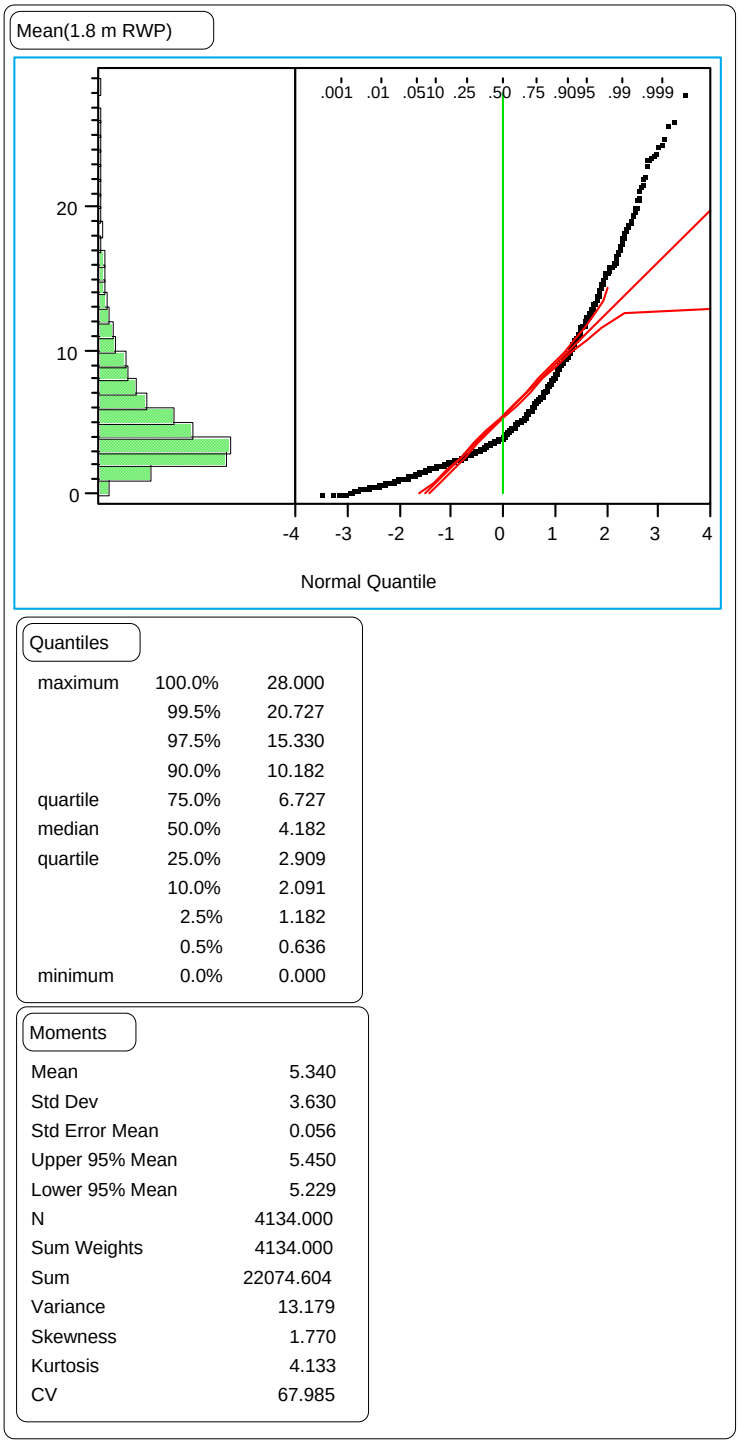

Figure 56. Distribution of the section means of the RWP 1.8-m rut depths.

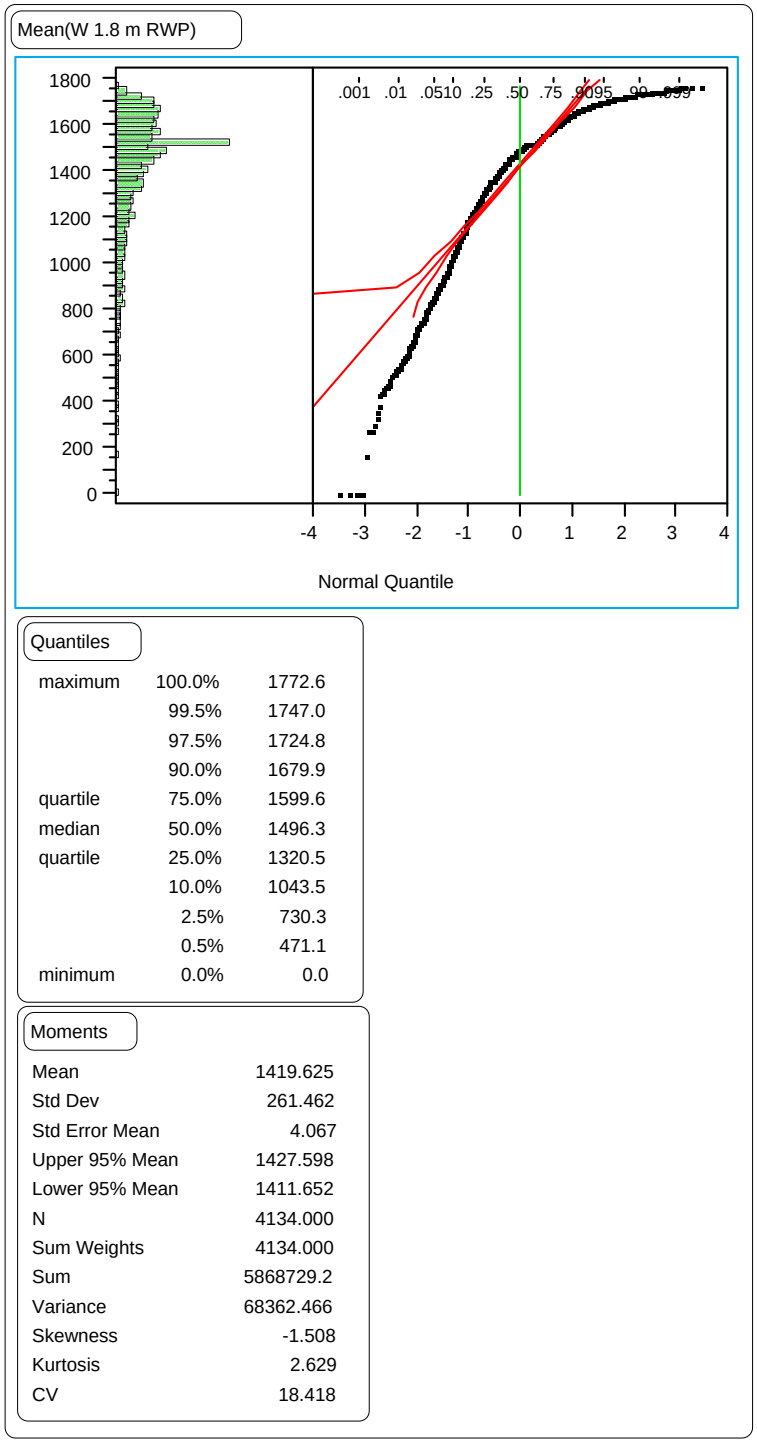

Figure 57. Distribution of the section means of the RWP 1.8-m rut widths.

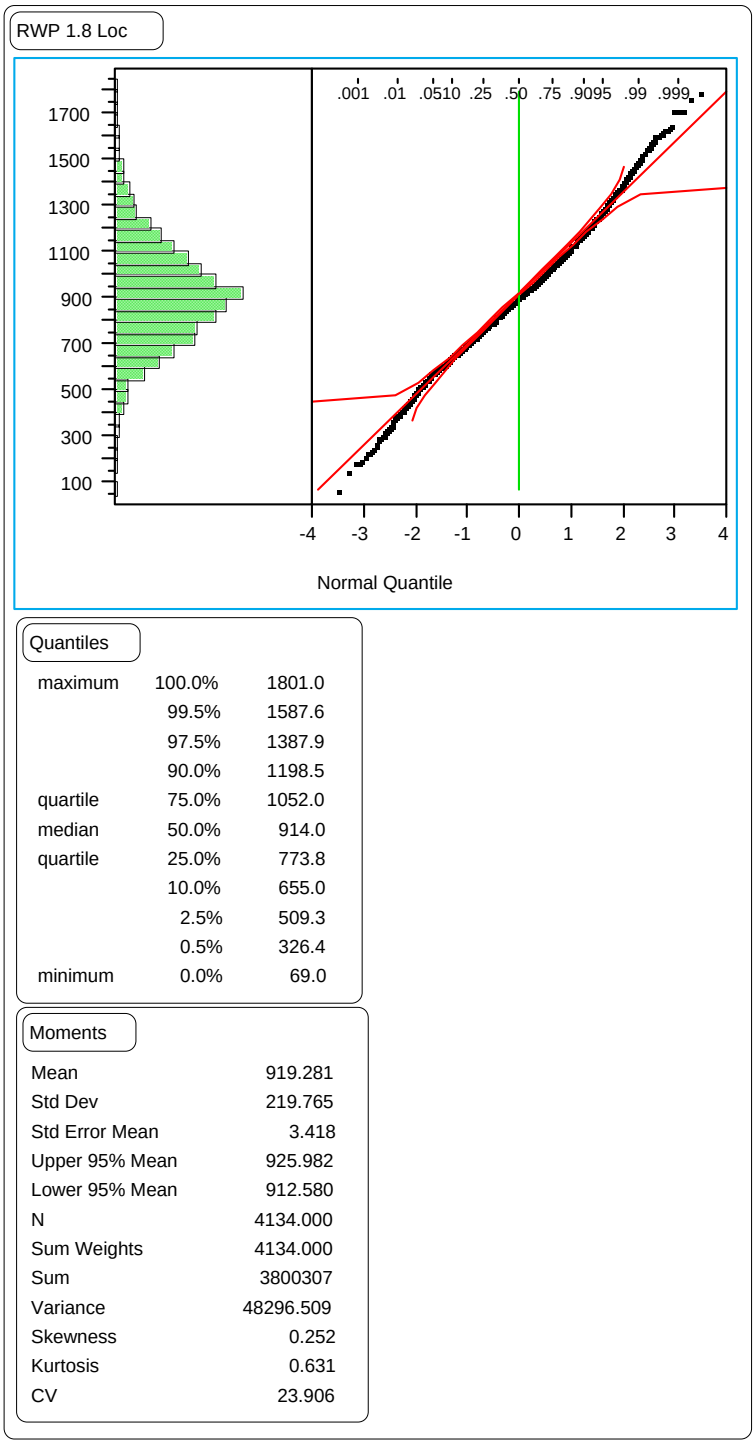

Figure 58. Distribution of the section means of the RWP 1.8-m rut locations.

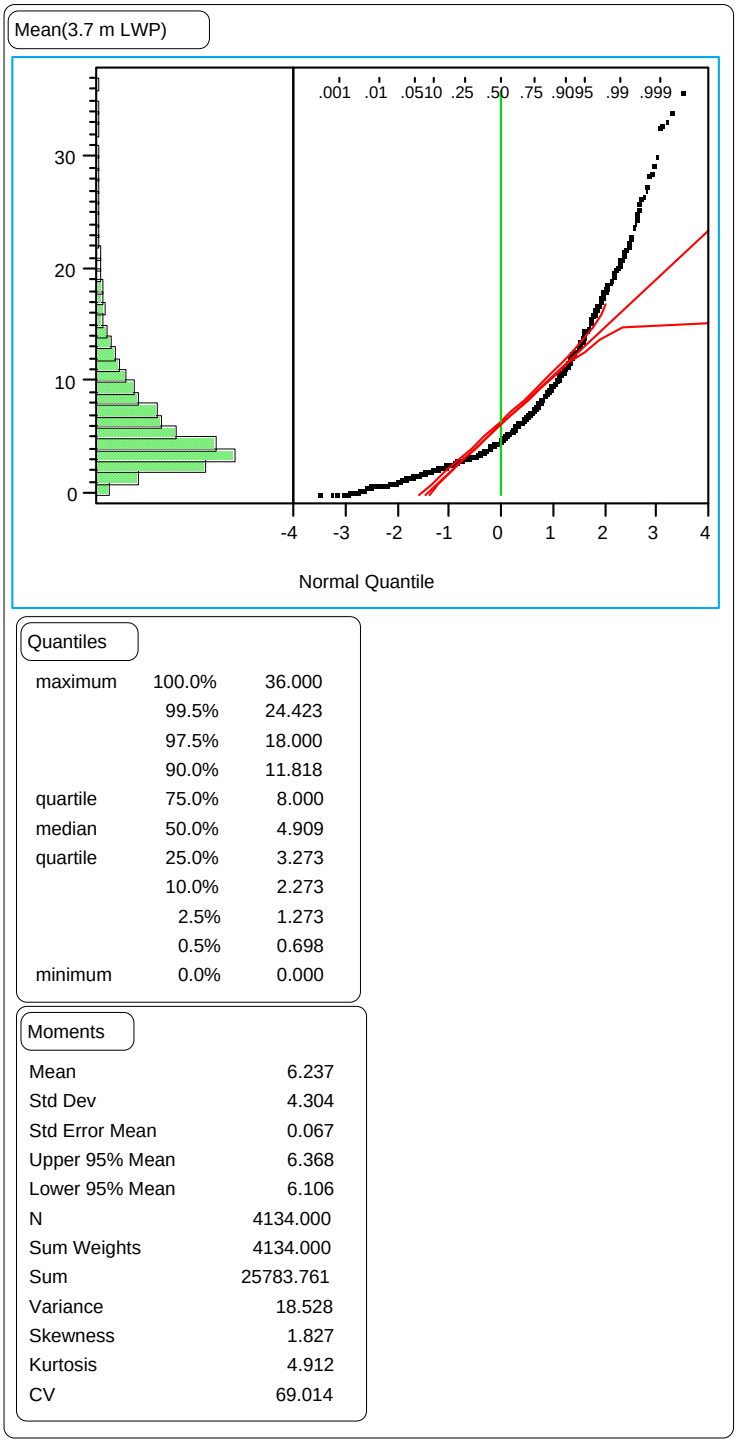

Figure 59. Distribution of the section means of the LWP wire line rut depths.

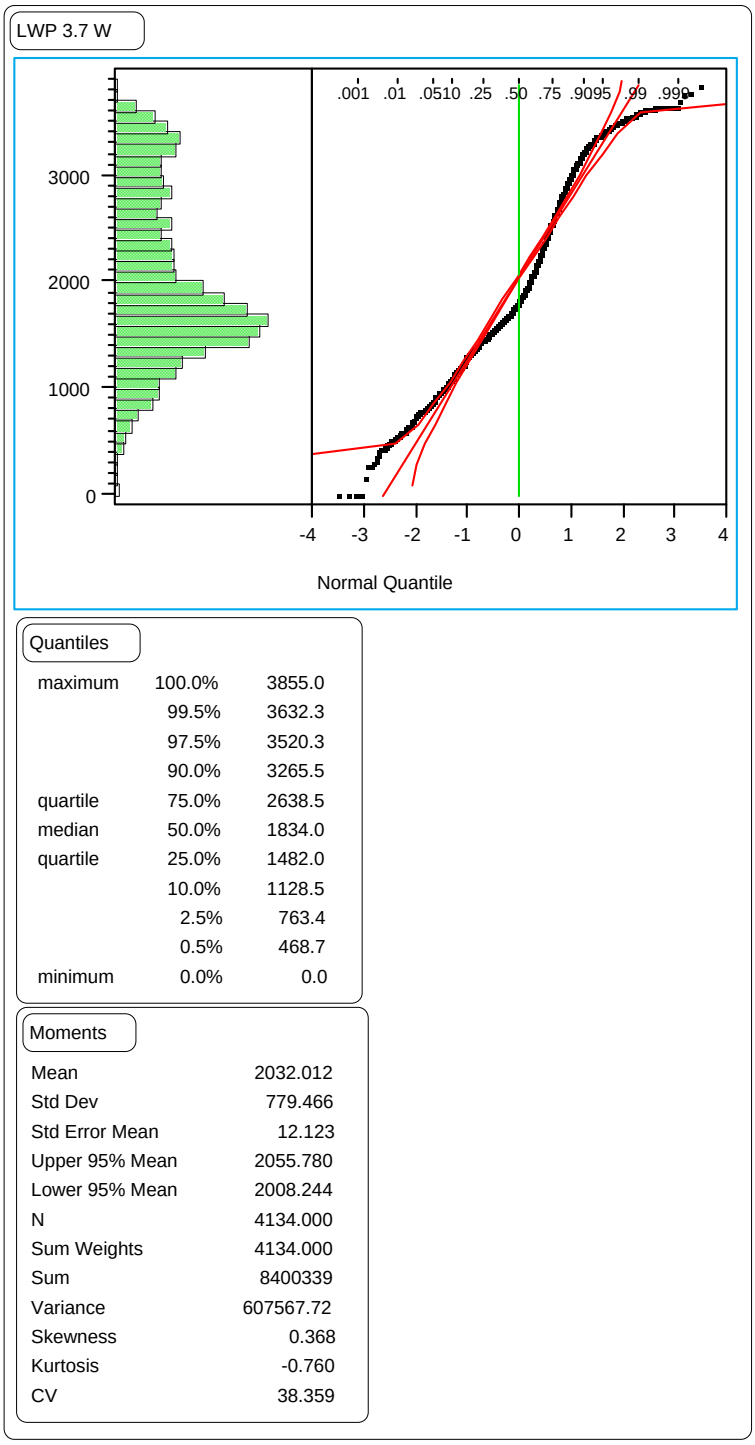

Figure 60. Distribution of the section means of the LWP wire line rut widths.

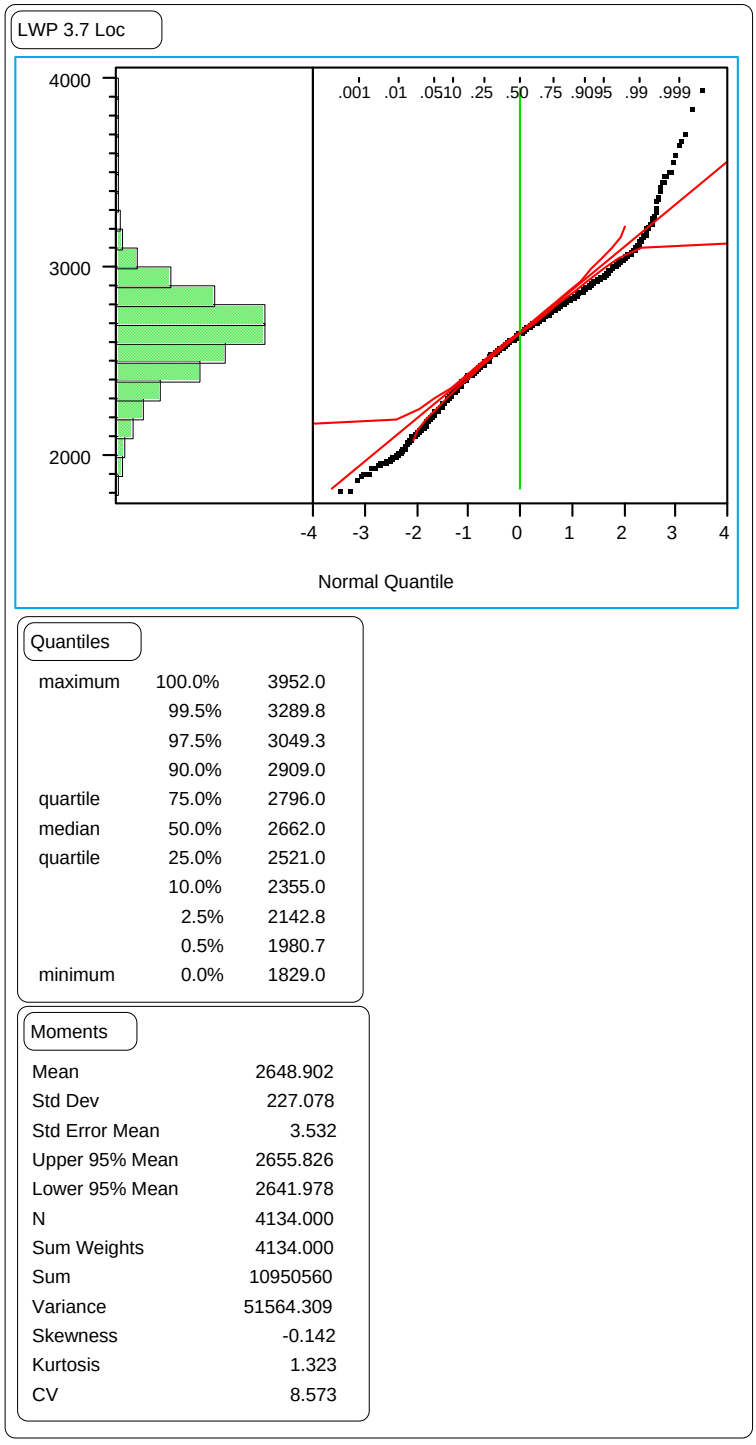

Figure 61. Distribution of the section means of the LWP wire line rut locations.

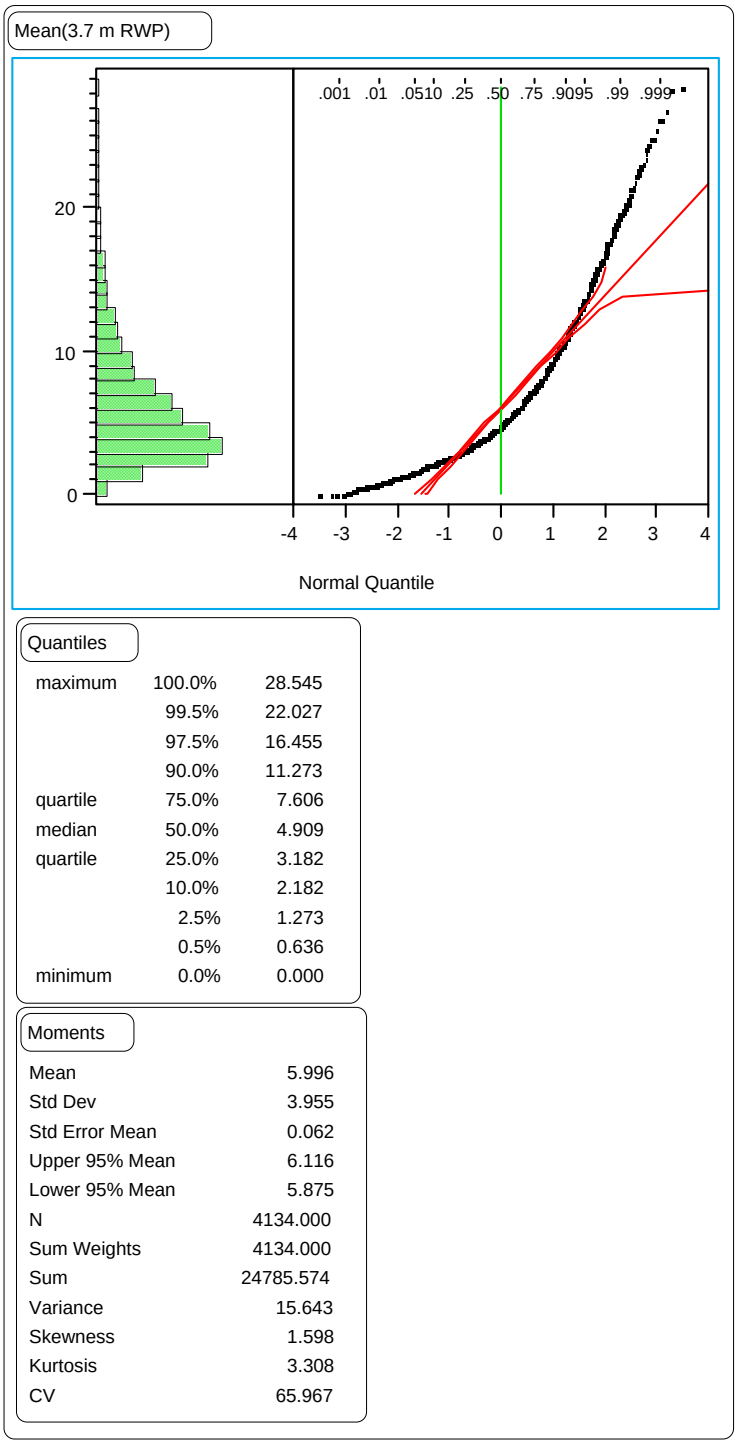

Figure 62. Distribution of the section means of the RWP wire line rut depths.

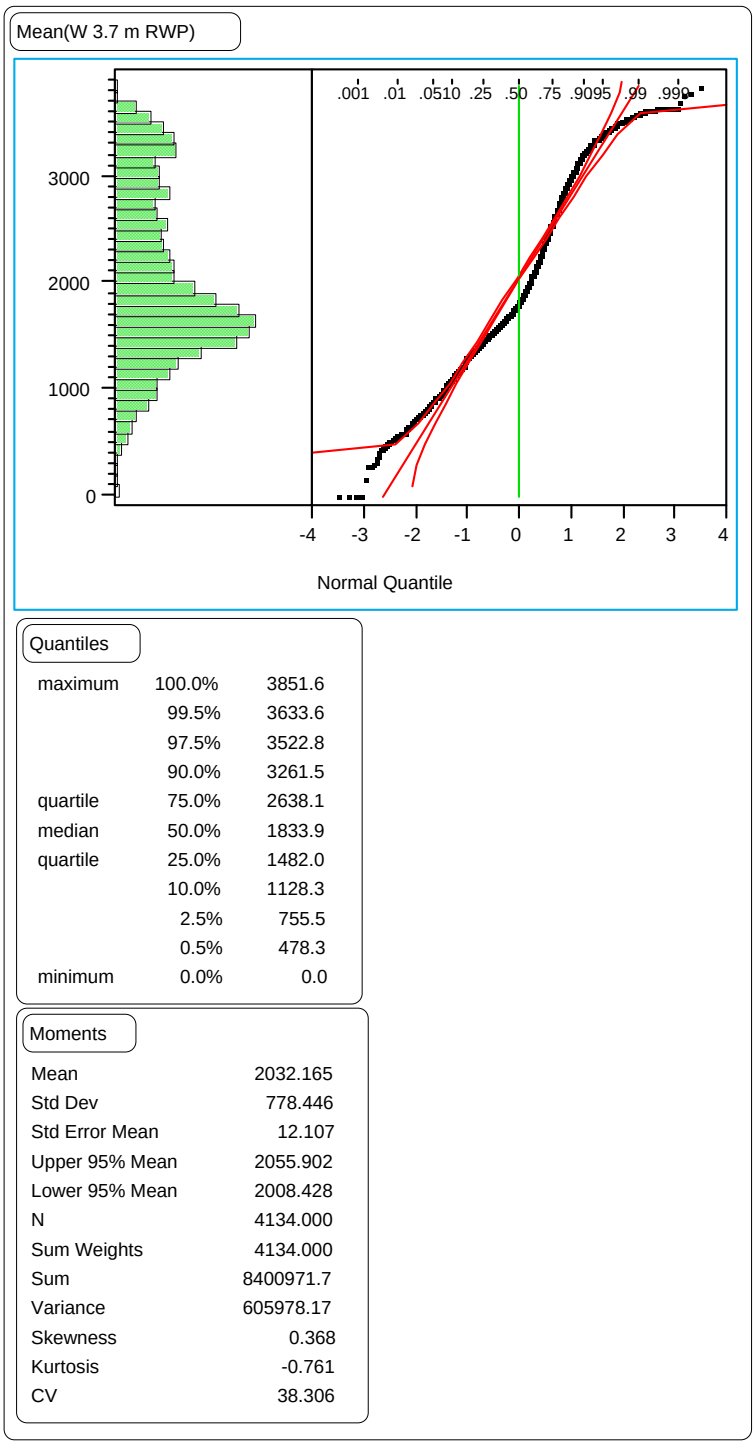

Figure 63. Distribution of the section means of the RWP wire line rut widths.

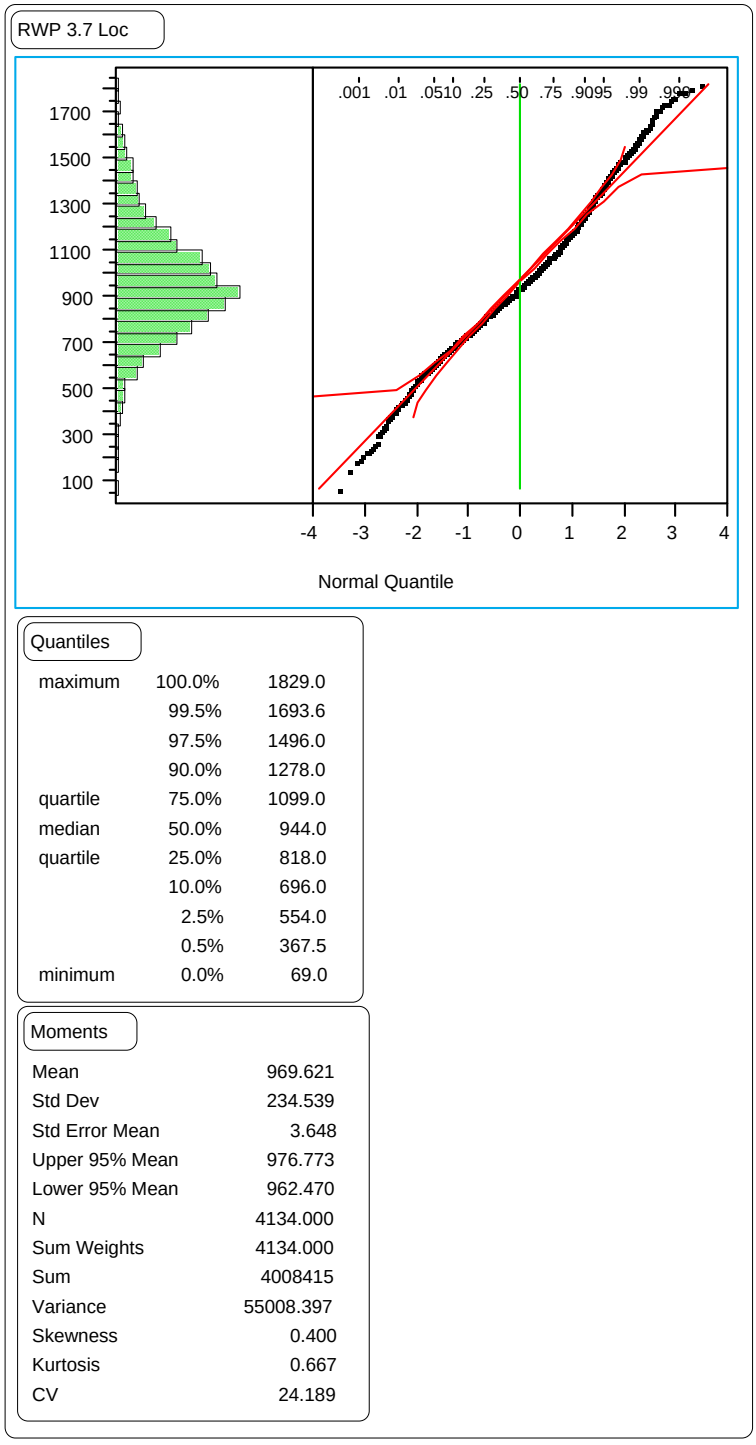

Figure 64. Distribution of the section means of the RWP wire line rut locations.

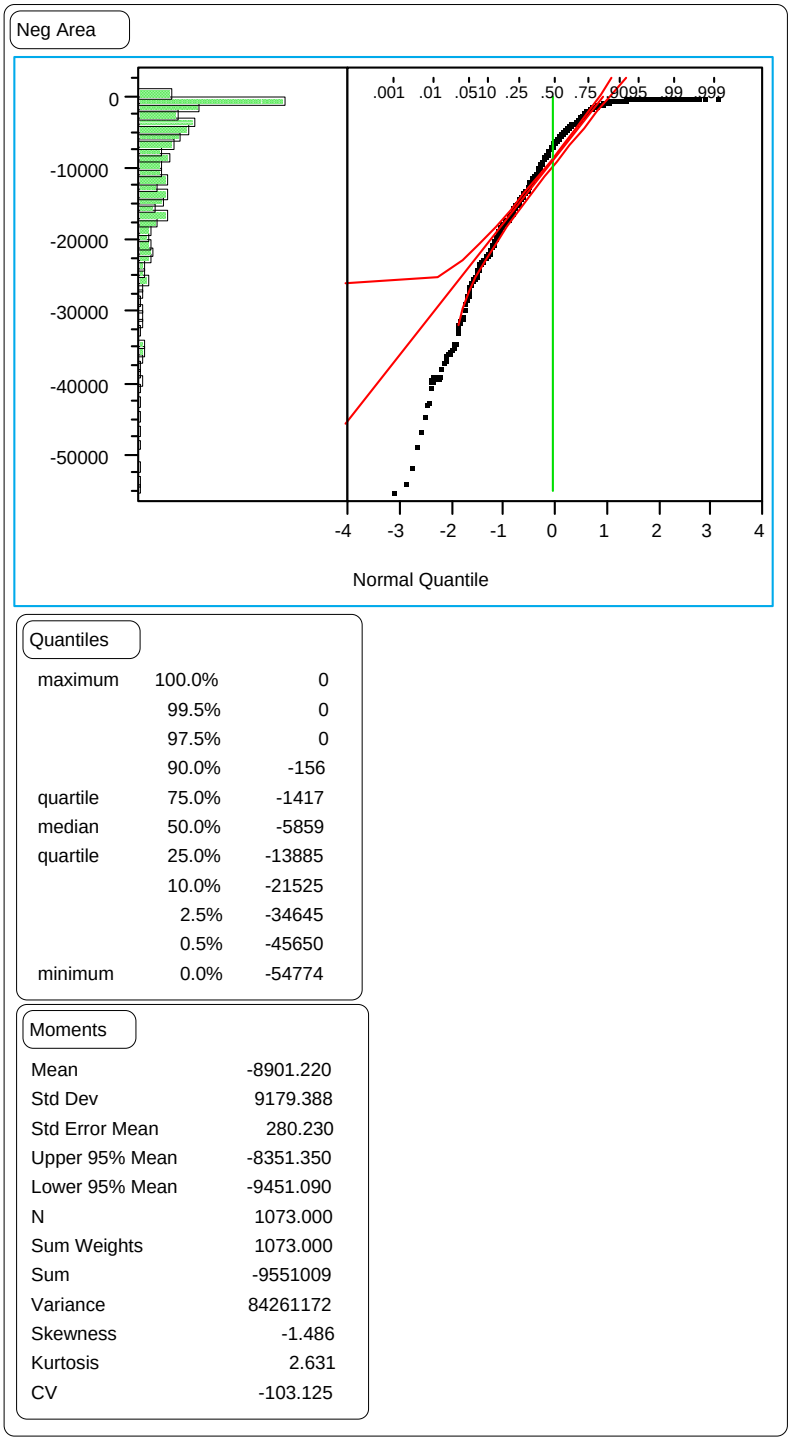

Figure 65. Distribution of the section means of the negative area index on GPS-1 test sections.

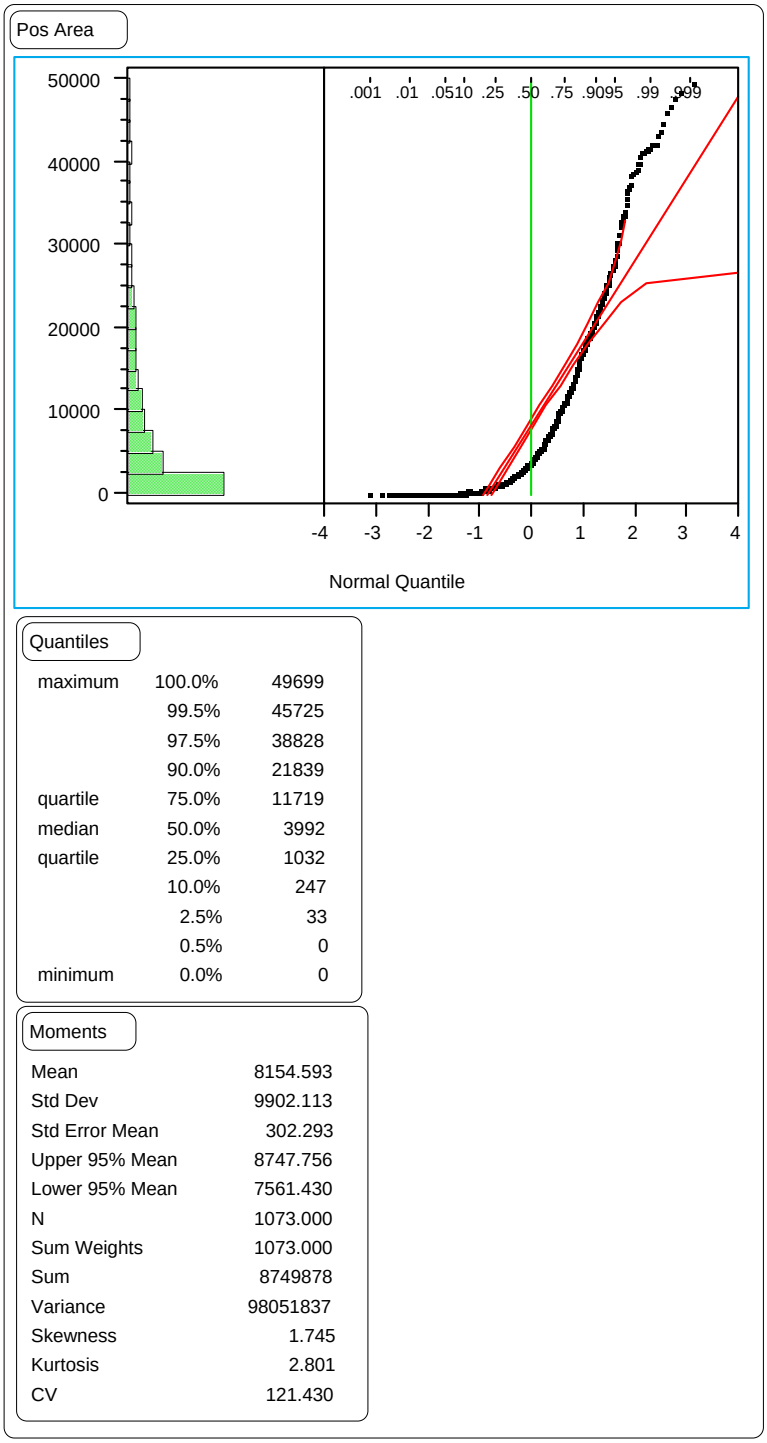

Figure 66. Distribution of the section means of the positive area index on GPS-1 test sections.

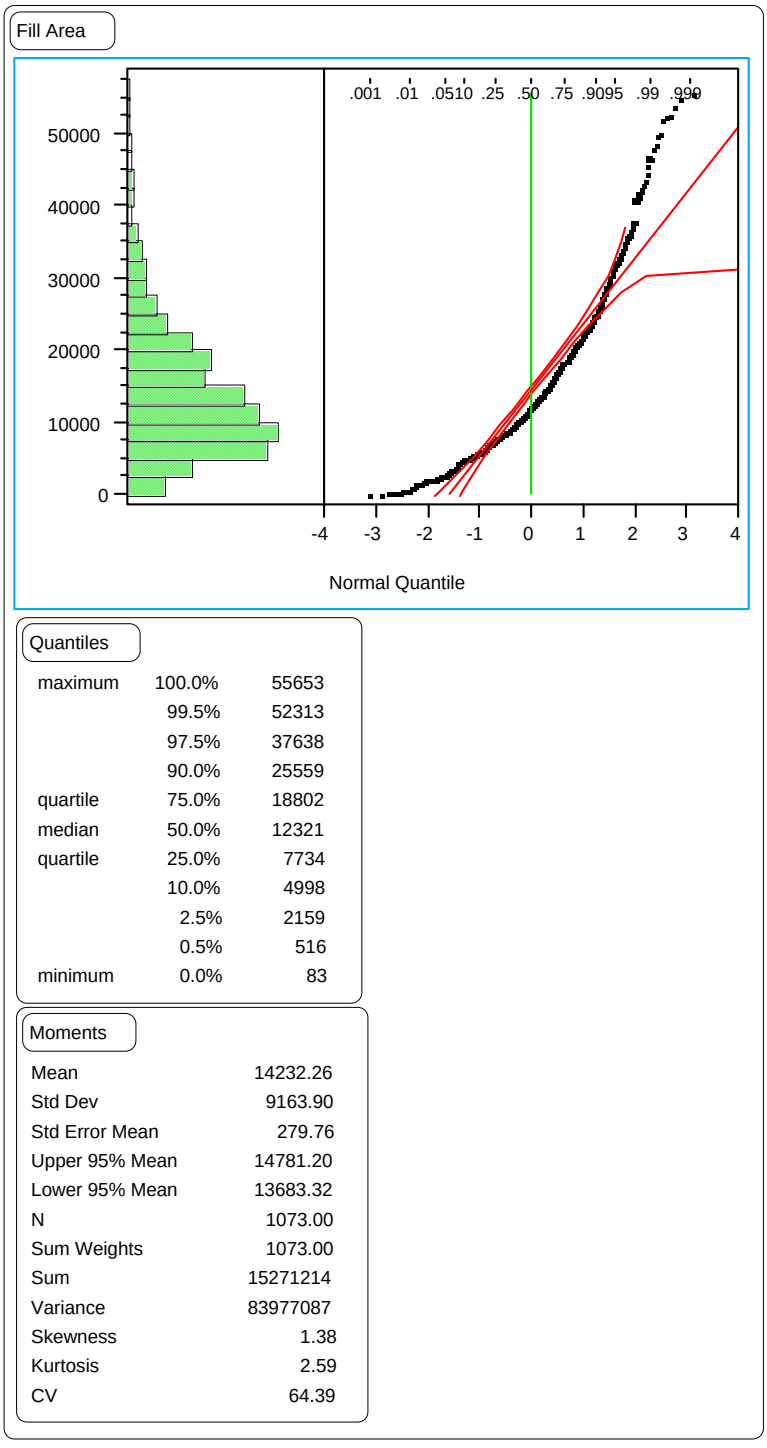

Figure 67. Distribution of the section means of the fill area index on GPS-1 test sections.

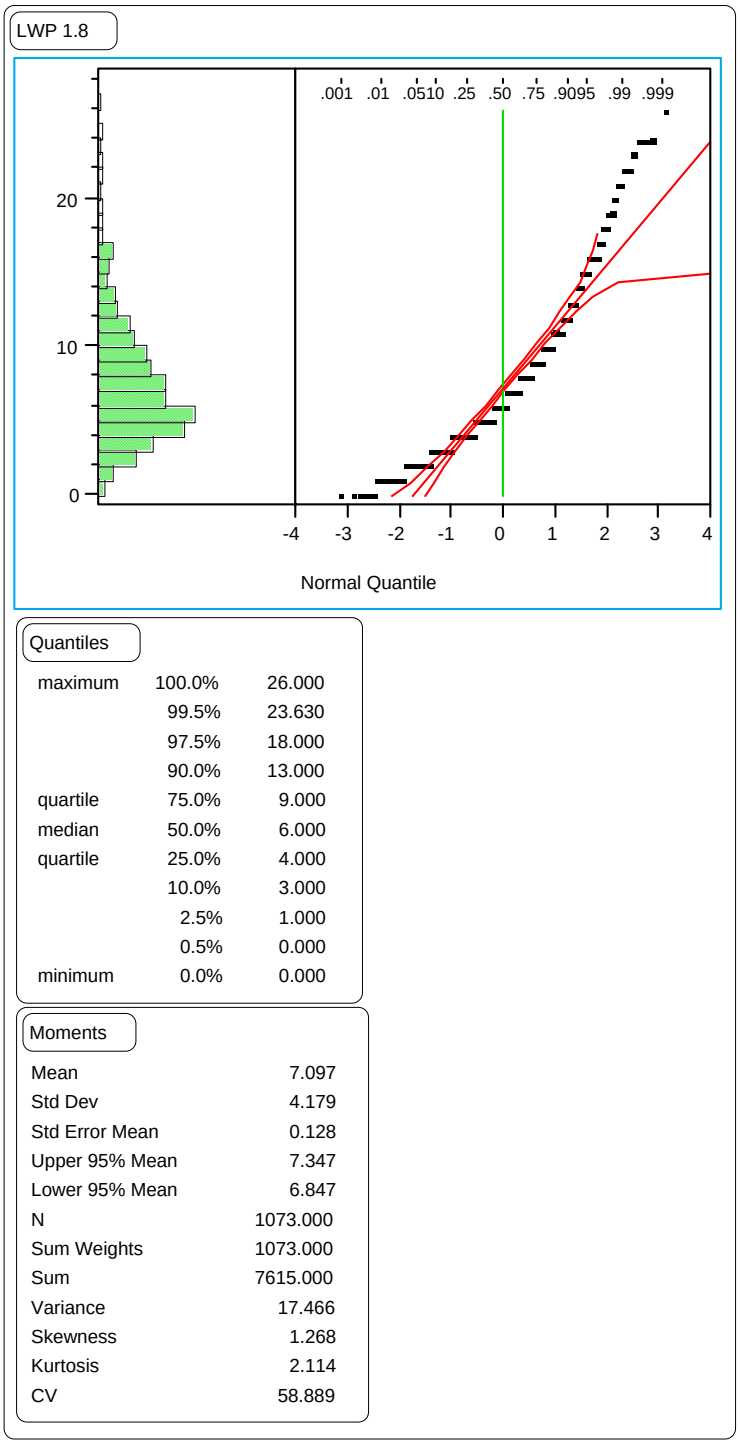

Figure 68. Distribution of the section means of the LWP 1.8-m rut depths on GPS-1 test sections.

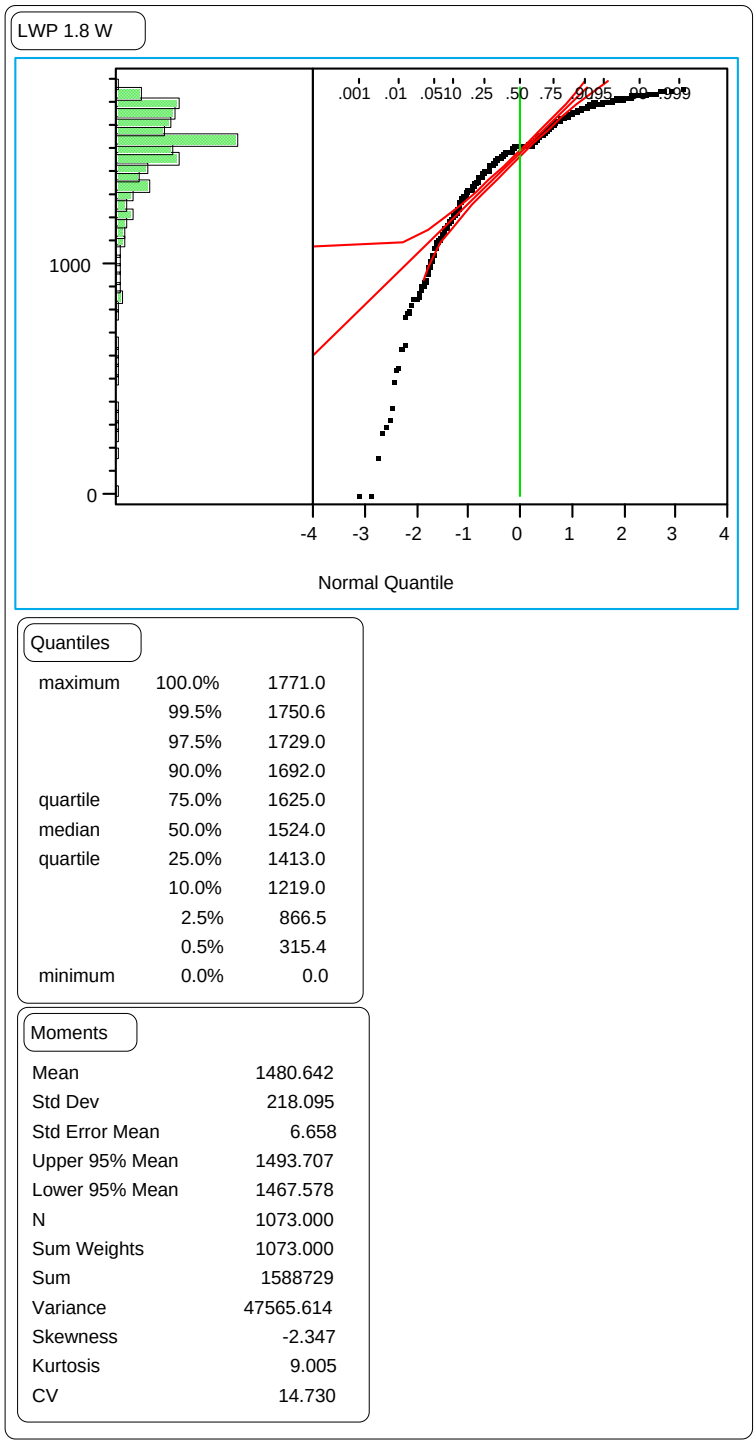

Figure 69. Distribution of the section means of the LWP 1.8-m rut widths on GPS-1 test sections.

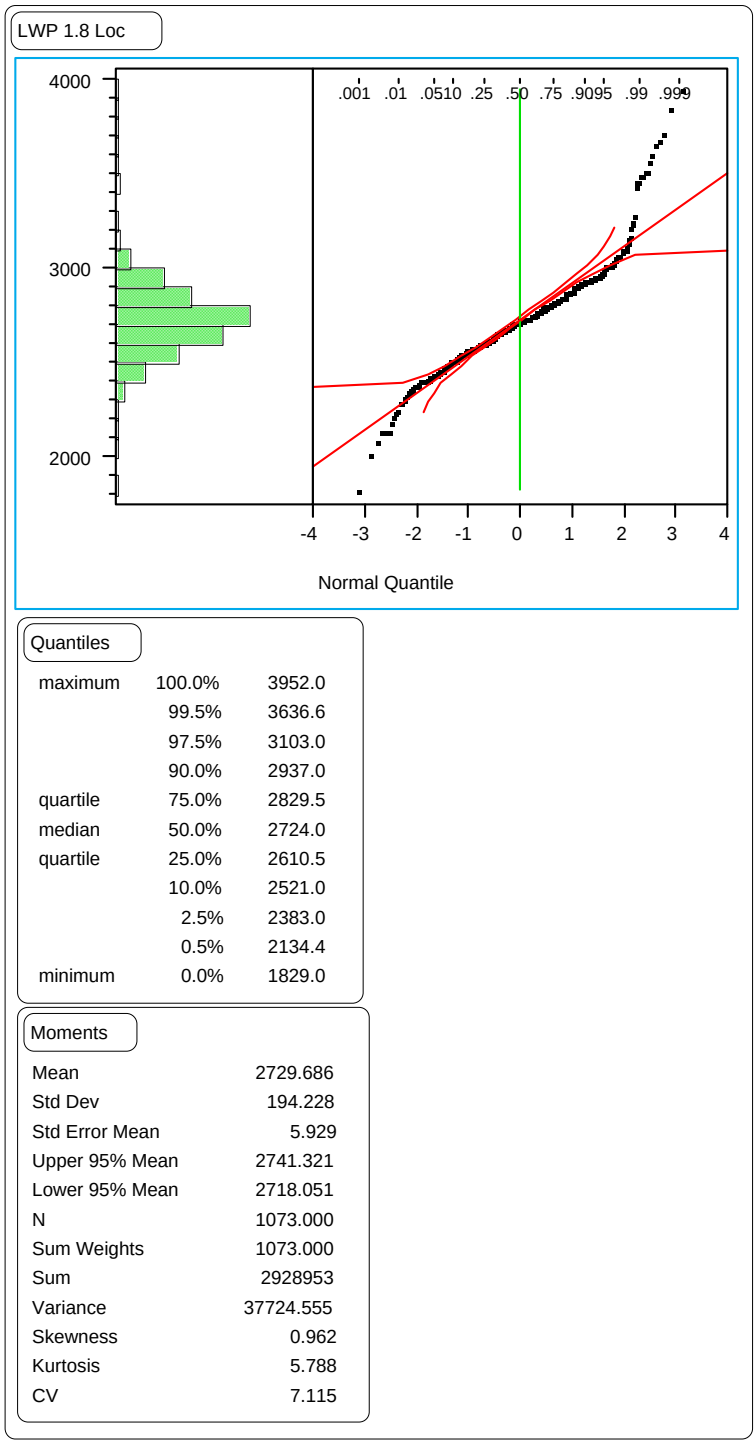

Figure 70. Distribution of the section means of the LWP 1.8-m rut locations on GPS-1 test sections.

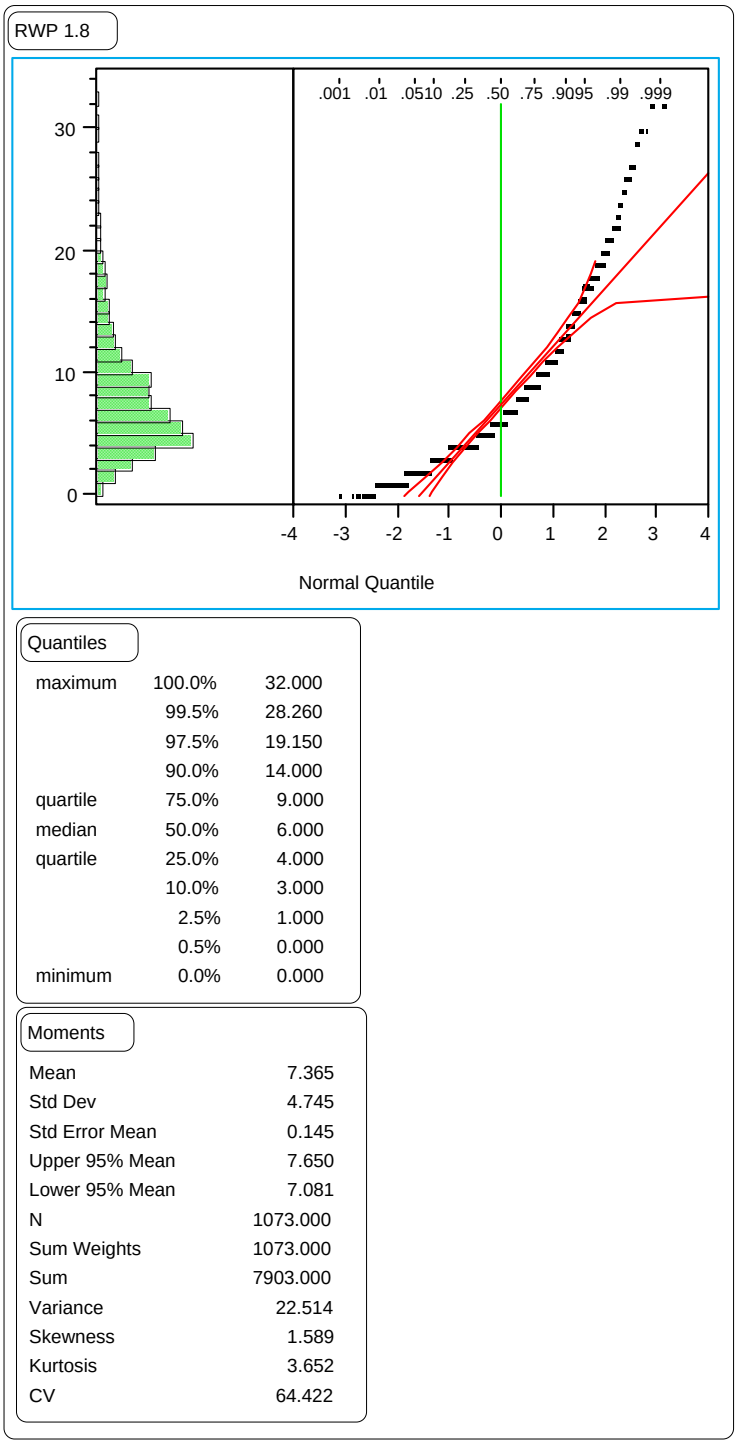

Figure 71. Distribution of the section means of the RWP 1.8-m rut depths on GPS-1 test sections.

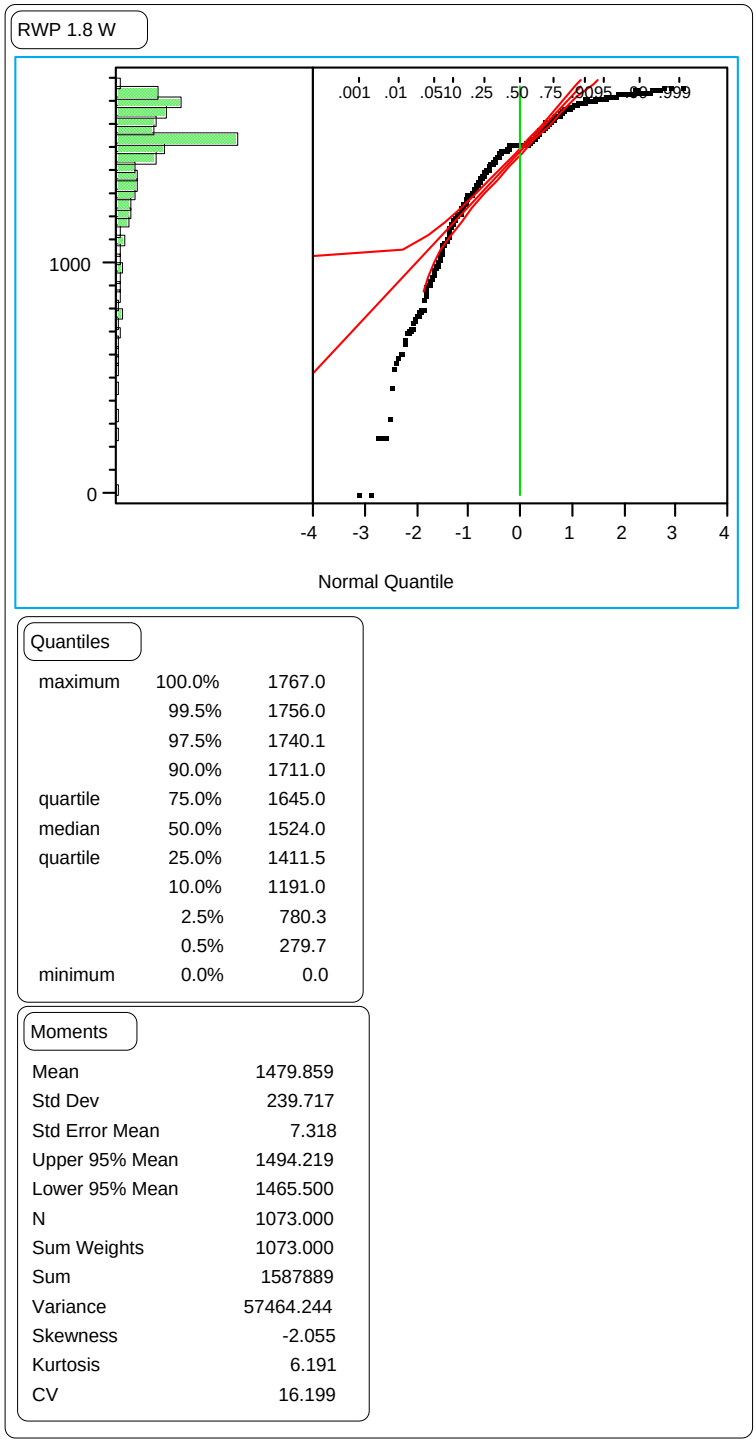

Figure 72. Distribution of the section means of the RWP 1.8-m rut widths on GPS-1 test sections.

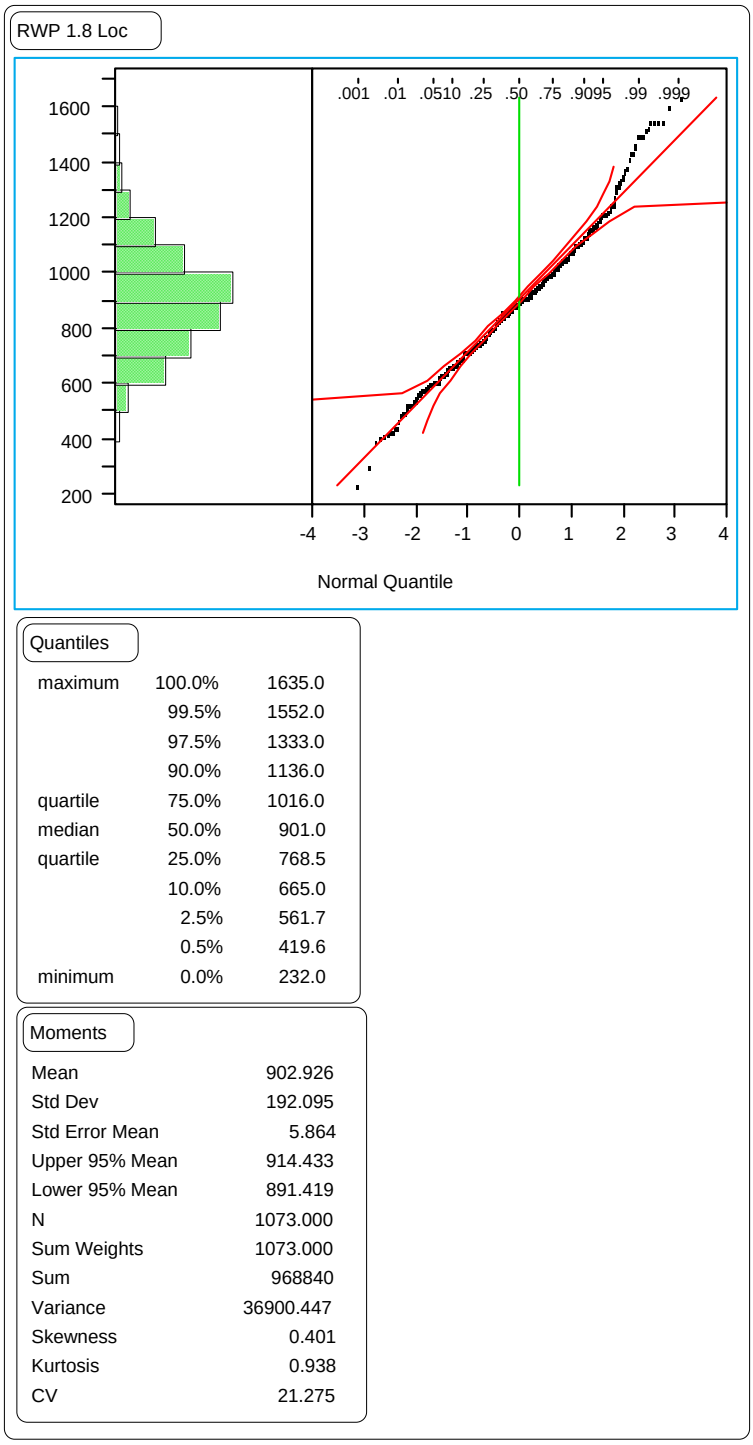

Figure 73. Distribution of the section means of the RWP 1.8-m rut locations on GPS-1 test sections.

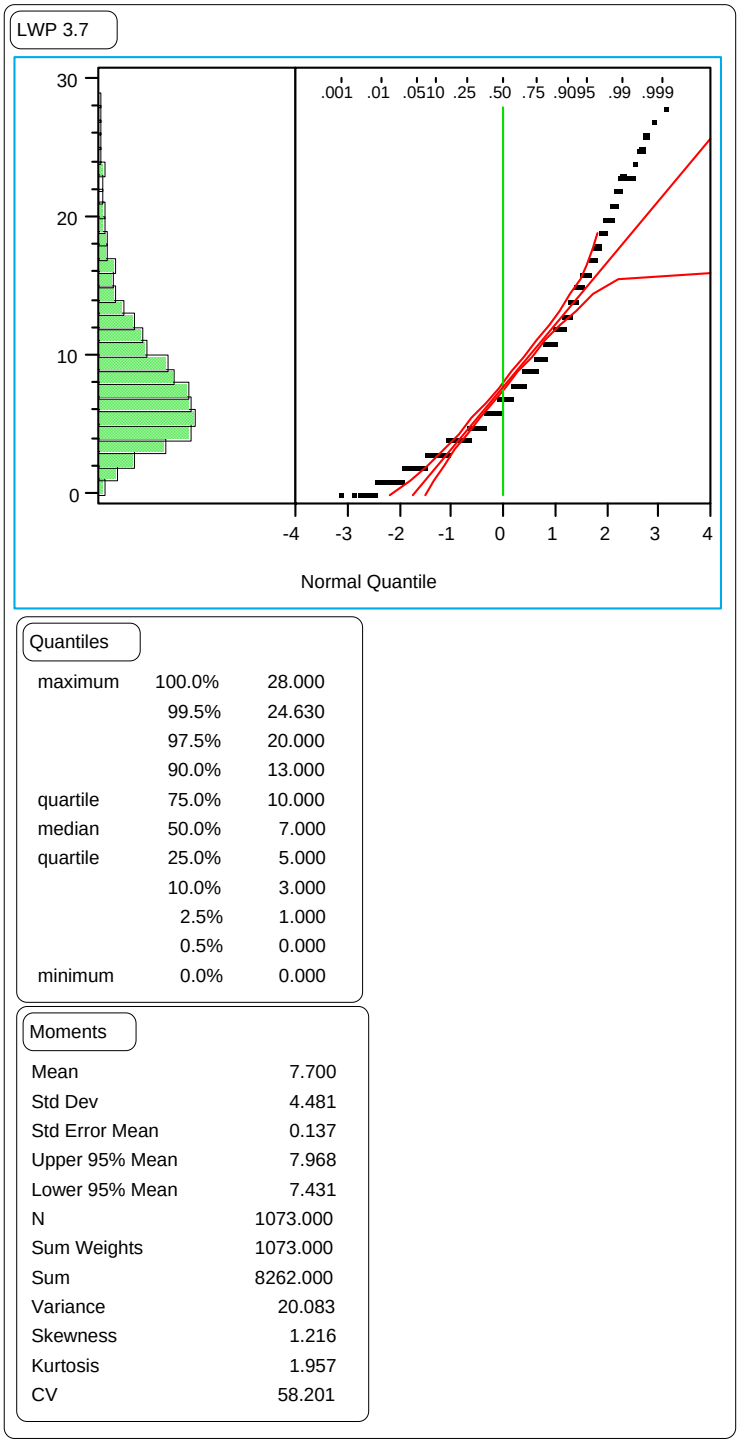

Figure 74. Distribution of the section means of the LWP wire line rut depths on GPS-1 test sections.

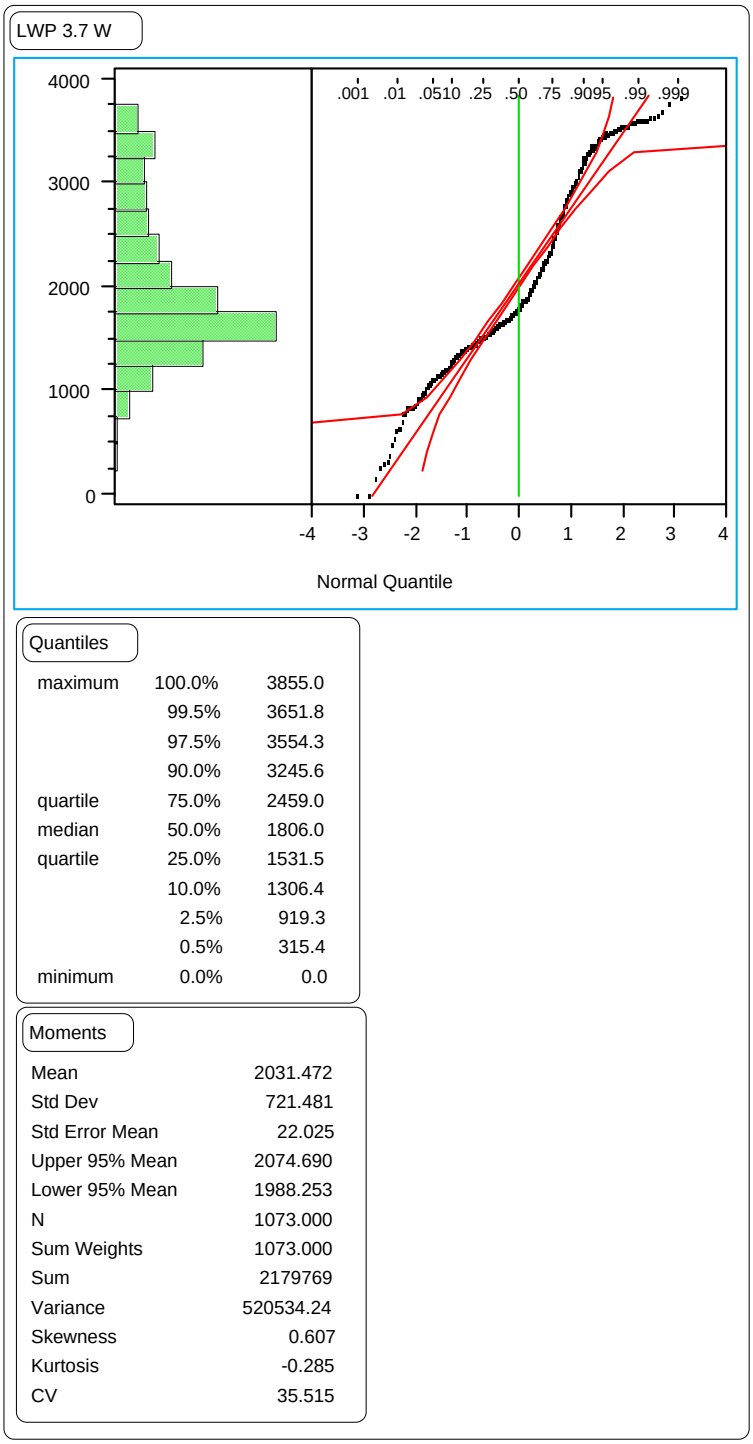

Figure 75. Distribution of the section means of the LWP wire line rut widths on GPS-1 test sections.

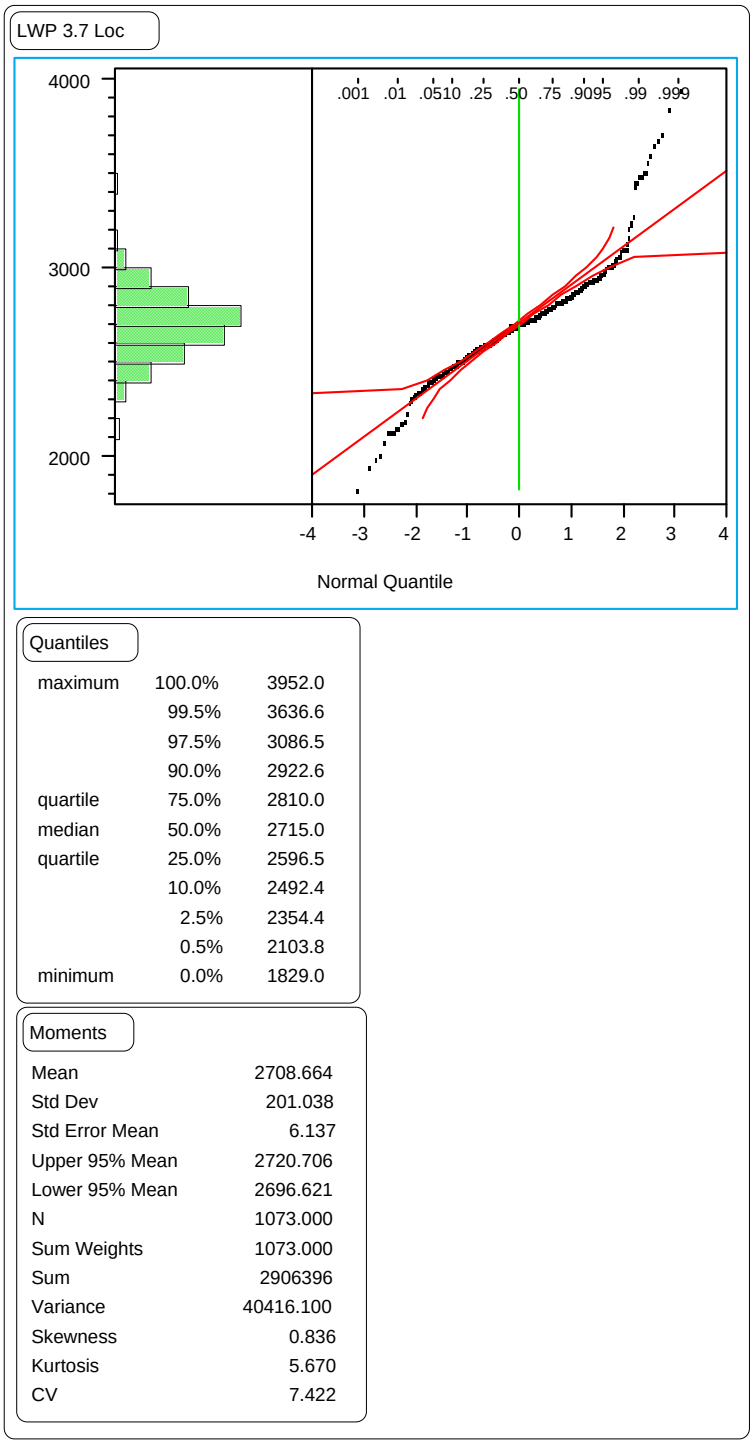

Figure 76. Distribution of the section means of the LWP wire line rut locations on GPS-1 test sections.

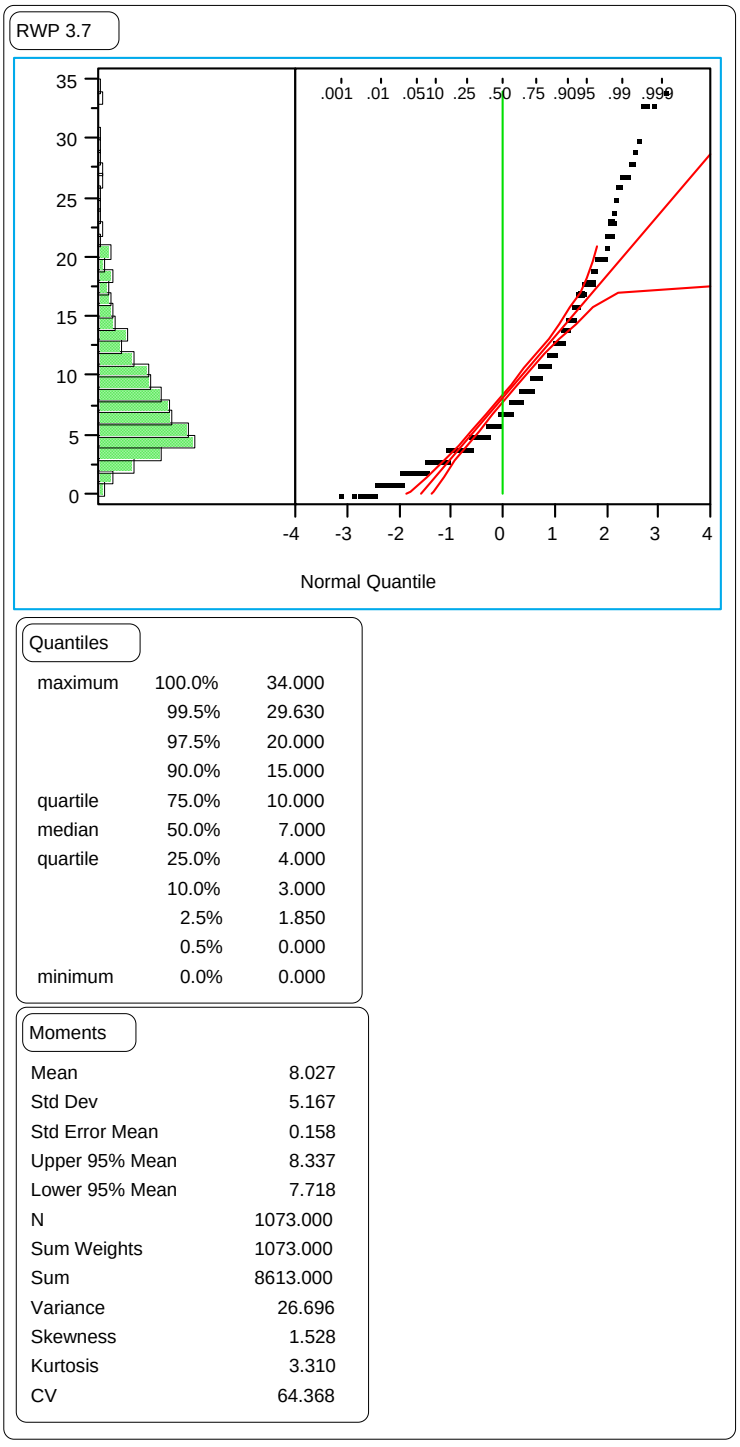

Figure 77. Distribution of the section means of the RWP wire line rut depths on GPS-1 test sections.

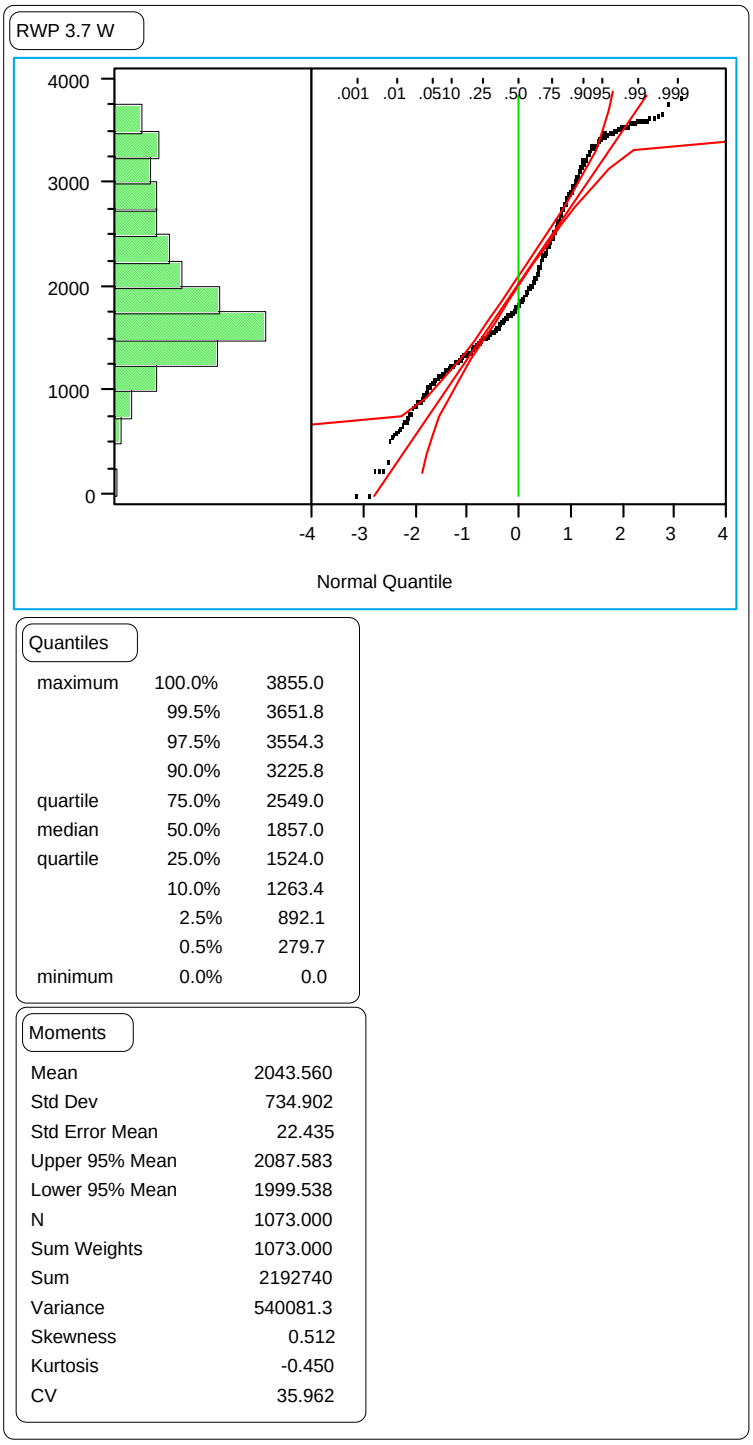

Figure 78. Distribution of the section means of the RWP wire line rut widths on GPS-1 test sections.

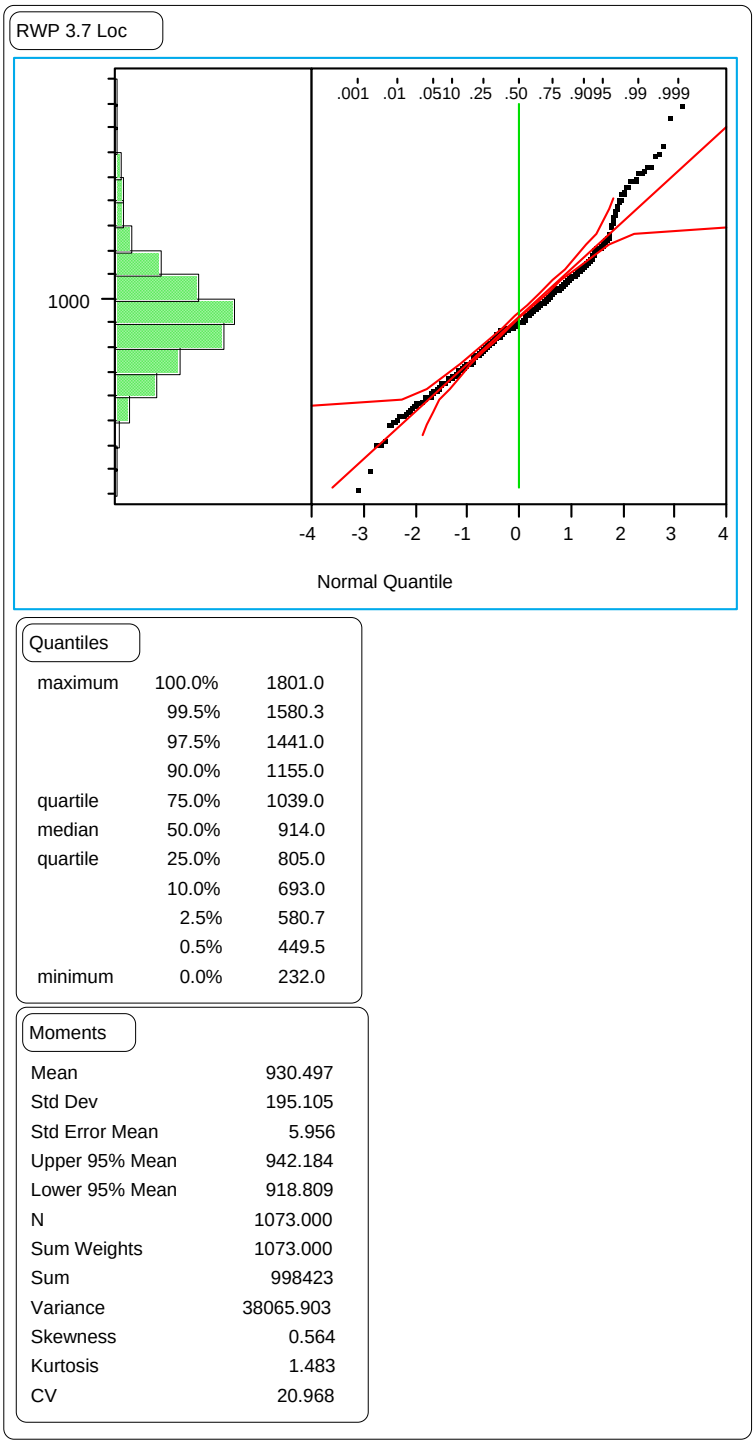

Figure 79. Distribution of the section means of the RWP wire line rut locations on GPS-1 test sections.

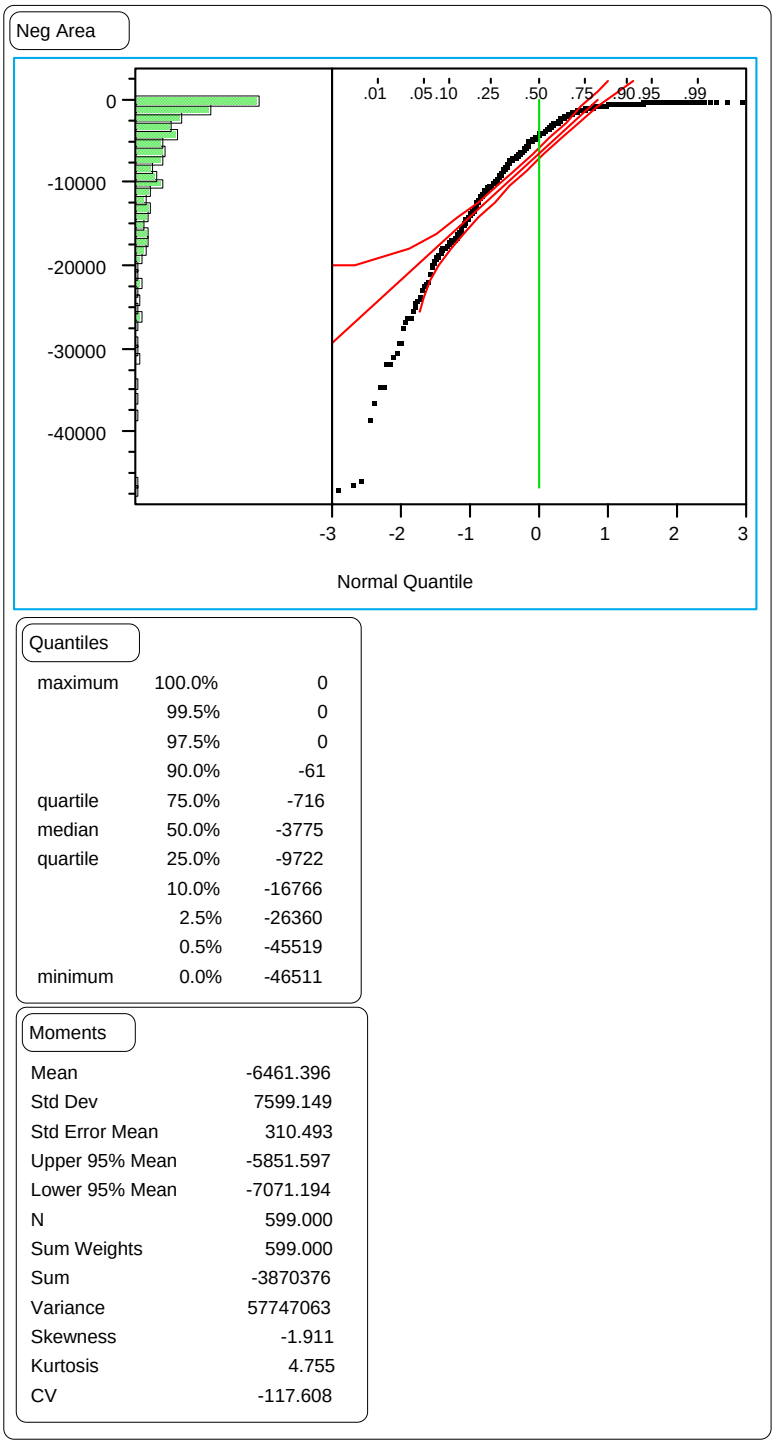

Figure 80. Distribution of the section means of the negative area index on GPS-2 test sections.

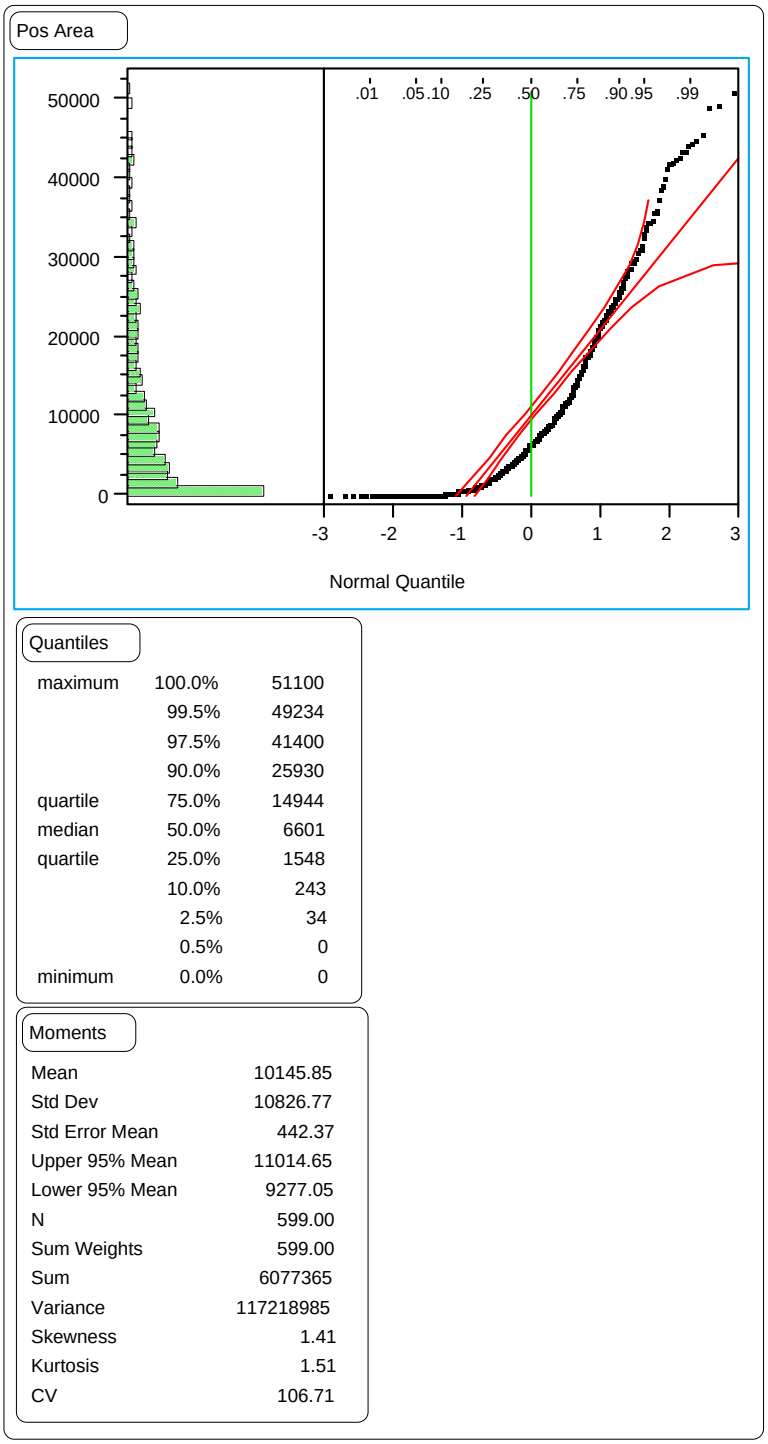

Figure 81. Distribution of the section means of the positive area index on GPS-2 test sections.

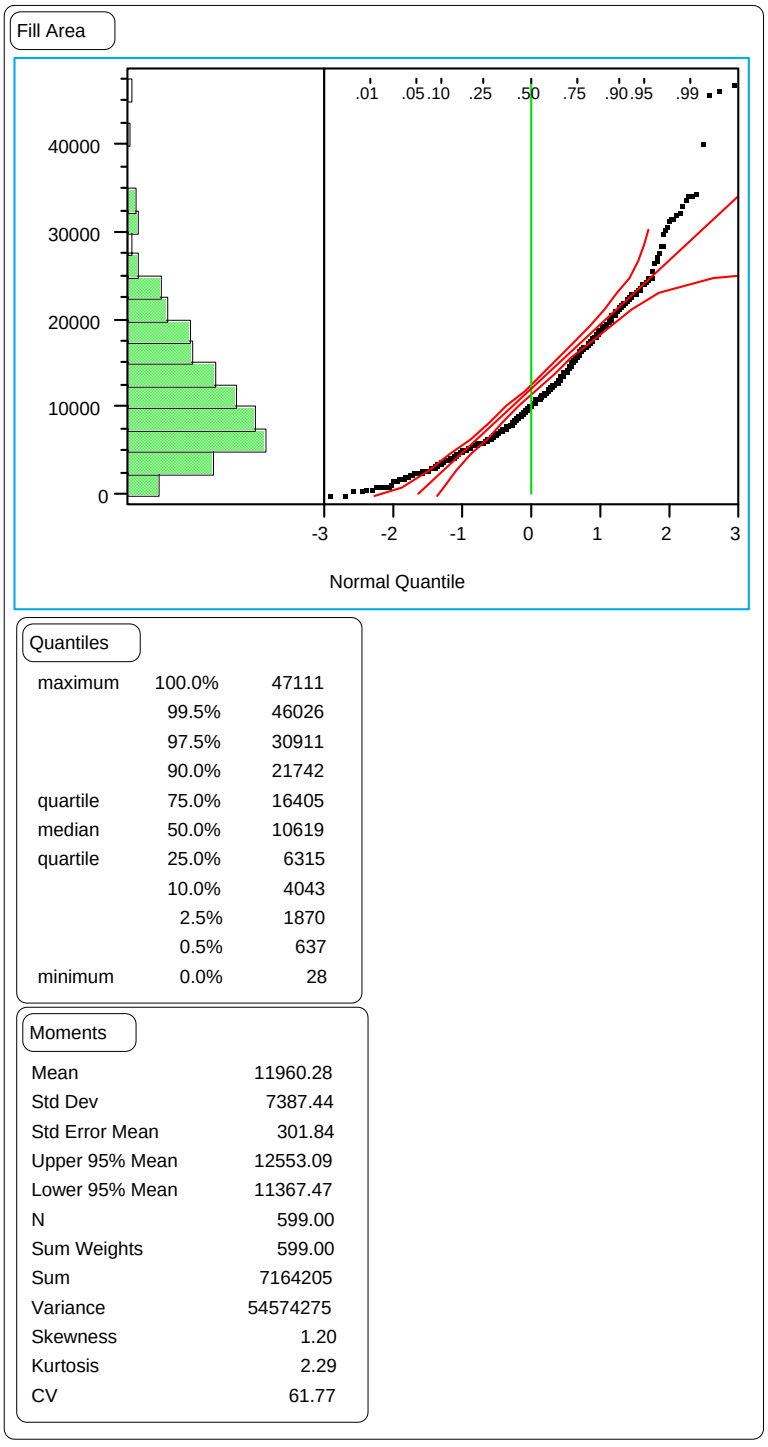

Figure 82. Distribution of the section means of the fill area index on GPS-2 test sections.

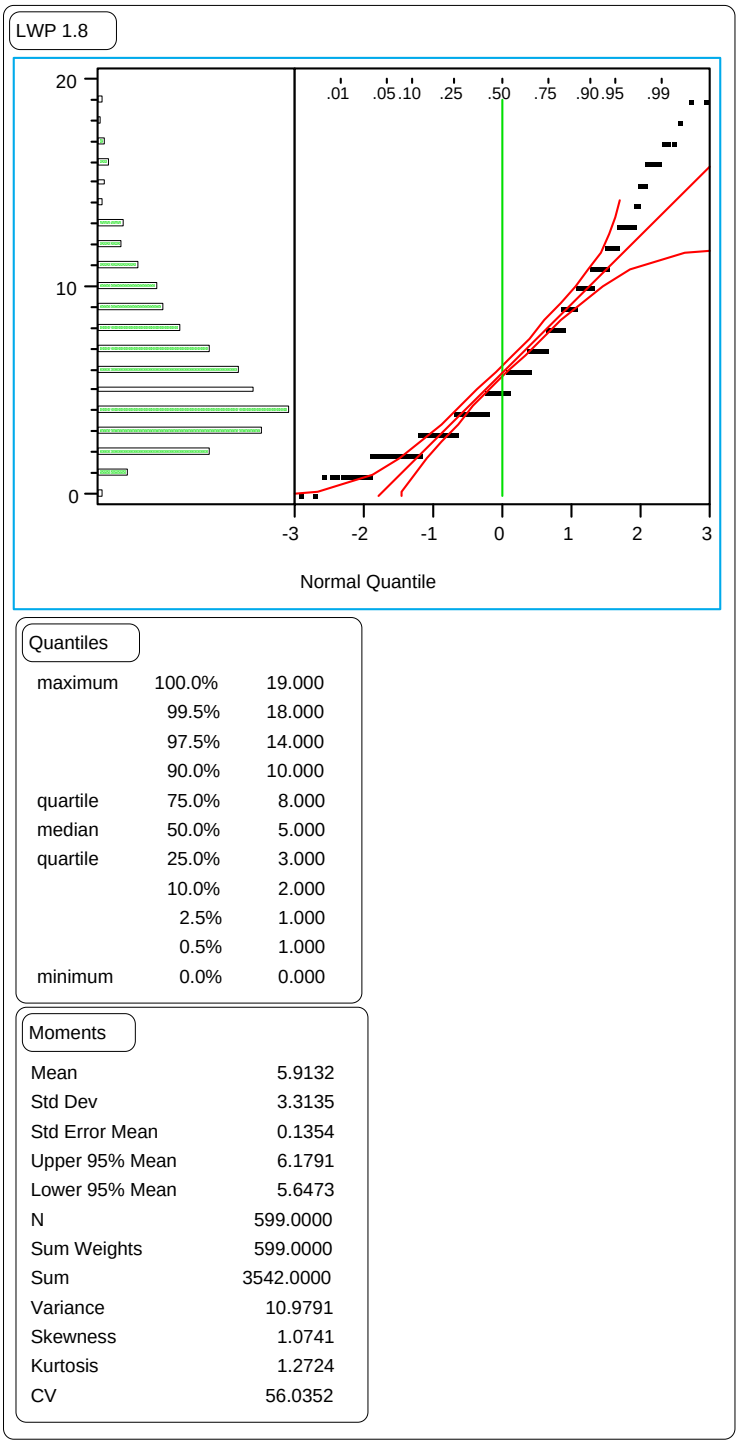

Quantiles

maximum	100.0%	19.000
	99.5%	18.000
	97.5%	14.000
	90.0%	10.000
quartile	75.0%	8.000
median	50.0%	5.000
quartile	25.0%	3.000
	10.0%	2.000
	2.5%	1.000
	0.5%	1.000
minimum	0.0%	0.000

Moments

Mean	5.9132
Std Dev	3.3135
Std Error Mean	0.1354
Upper 95% Mean	6.1791
Lower 95% Mean	5.6473
N	599.0000
Sum Weights	599.0000
Sum	3542.0000
Variance	10.9791
Skewness	1.0741
Kurtosis	1.2724
CV	56.0352

Figure 83. Distribution of the section means of the LWP 1.8-m rut depths on GPS-2 test sections.

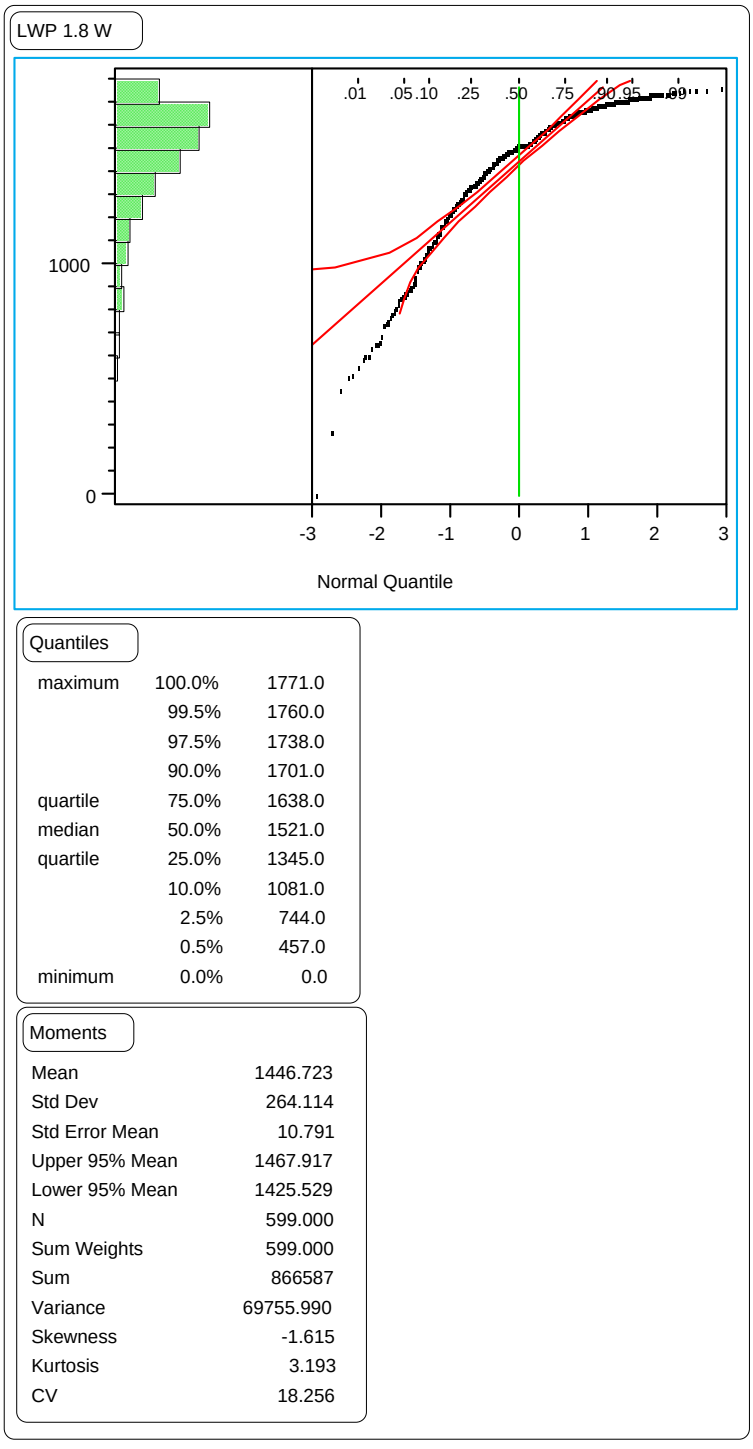

Figure 84. Distribution of the section means of the LWP 1.8-m rut widths on GPS-2 test sections.

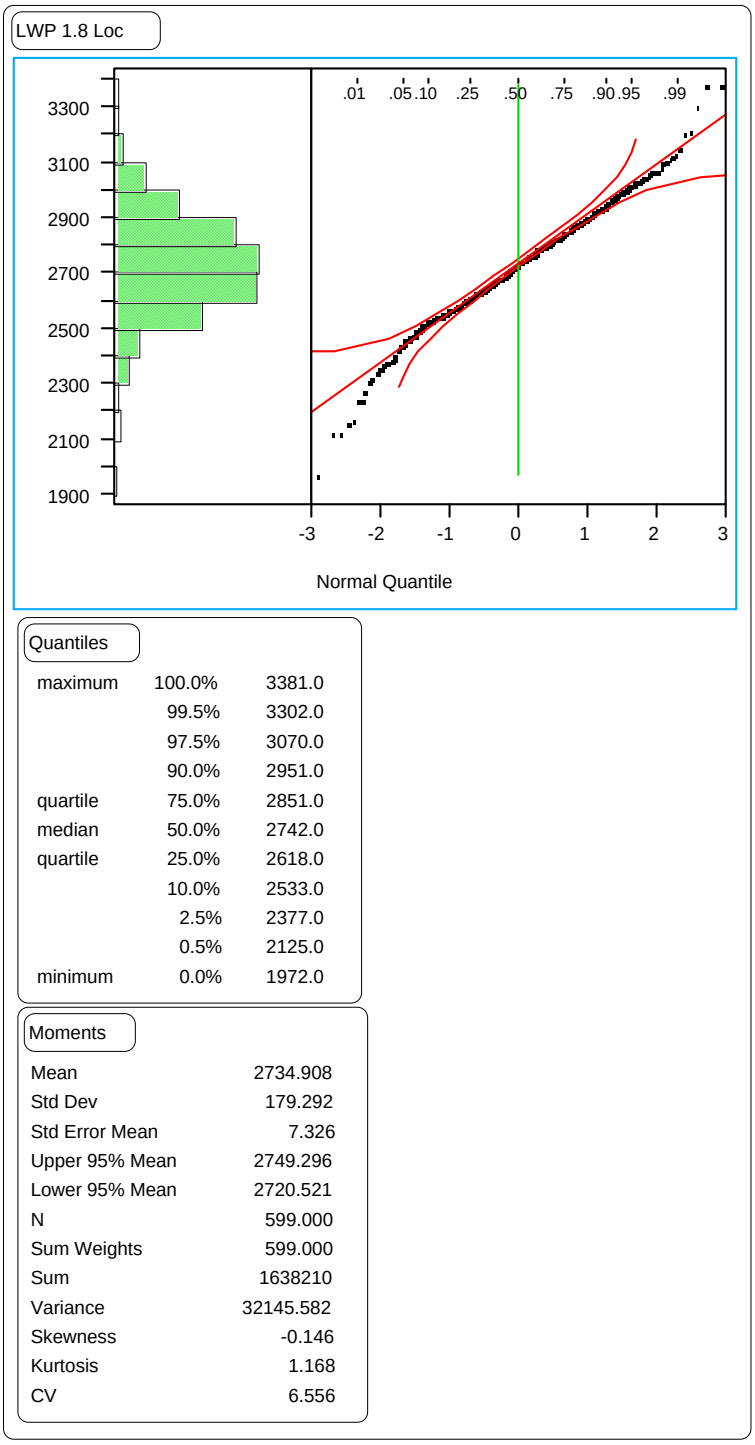

Figure 85. Distribution of the section means of the LWP 1.8-m rut locations on GPS-2 test sections.

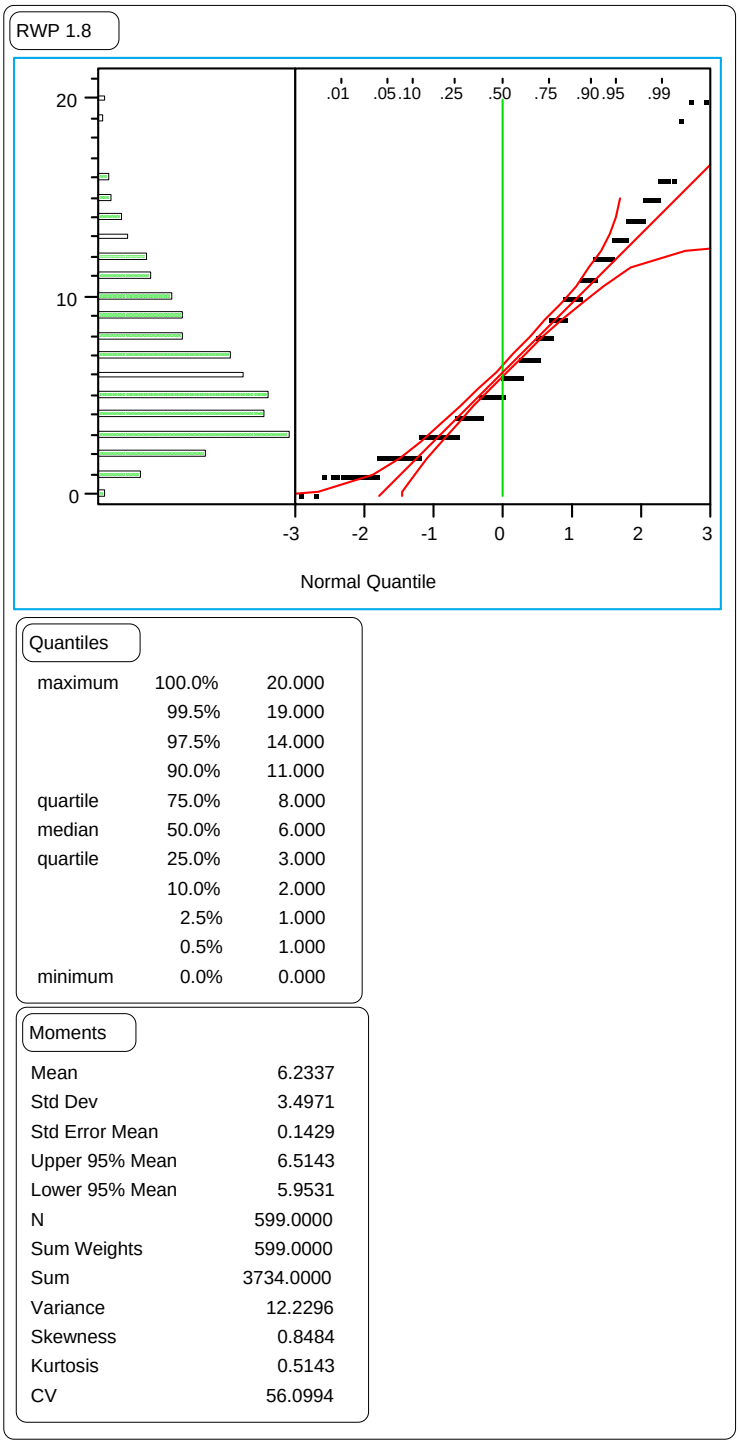

Figure 86. Distribution of the section means of the RWP 1.8-m rut depths on GPS-2 test sections.

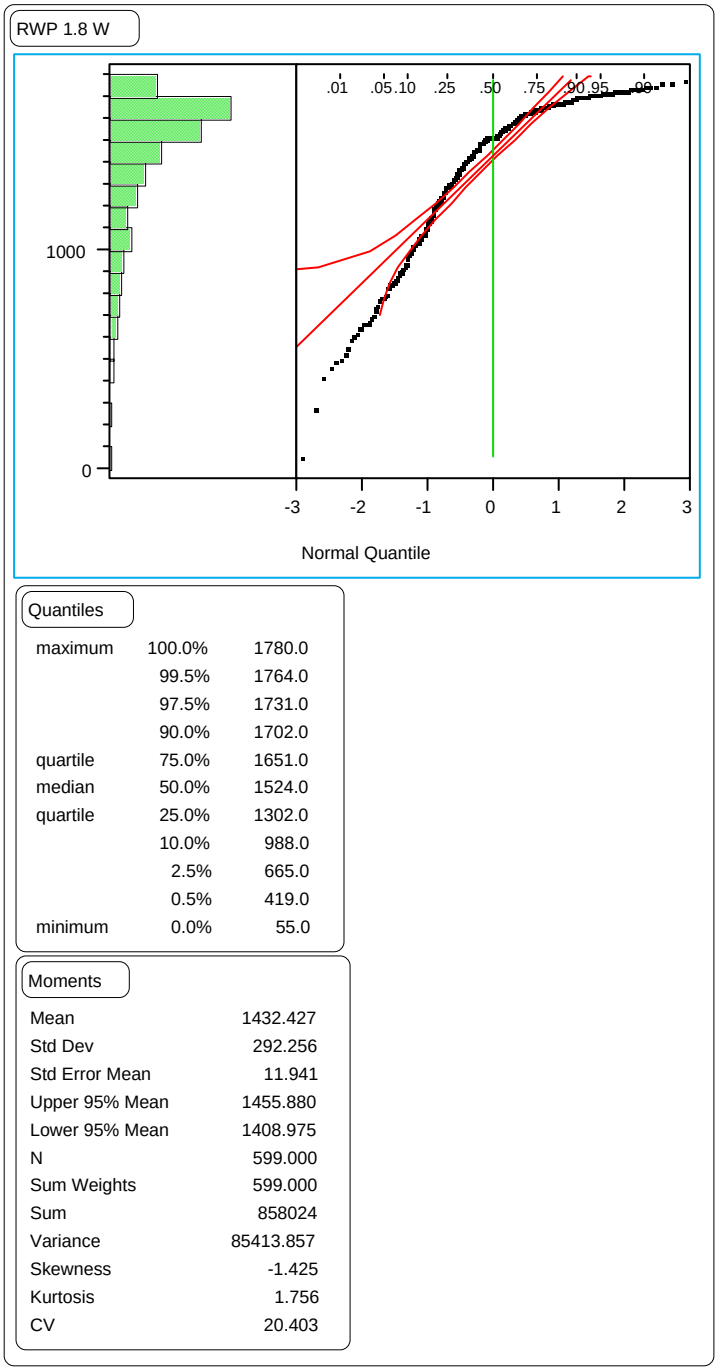

Figure 87. Distribution of the section means of the RWP 1.8-m rut widths on GPS-2 test sections.

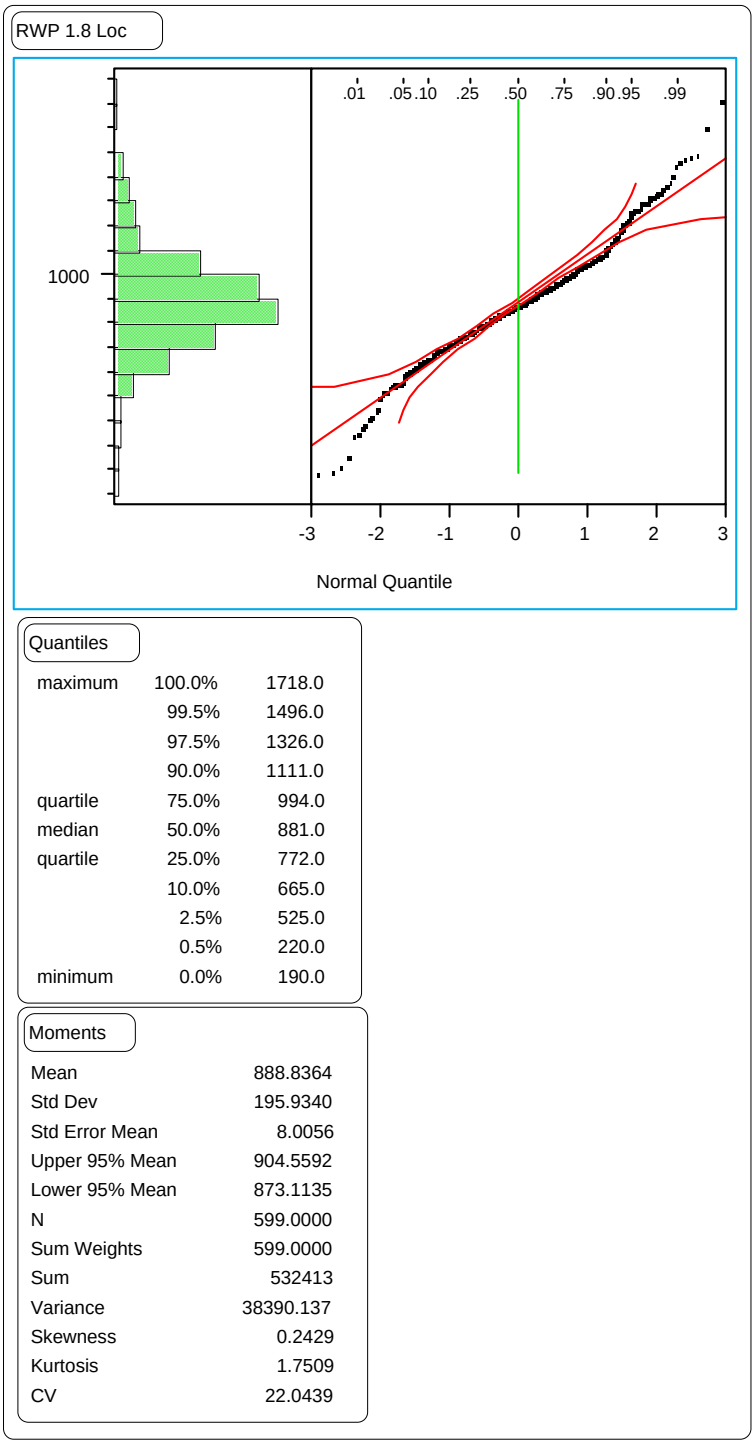

Figure 88. Distribution of the section means of the RWP 1.8-m rut locations on GPS-2 test sections.

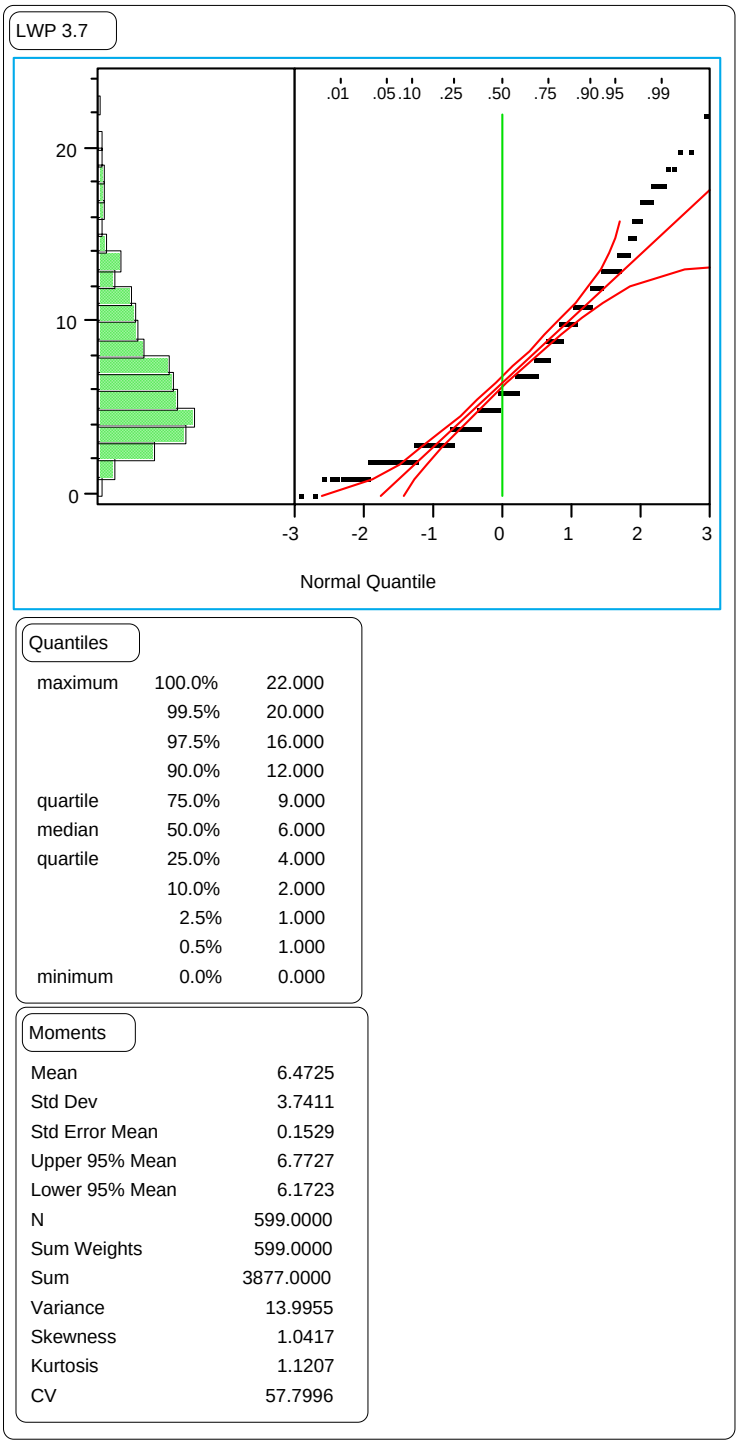

Figure 89. Distribution of the section means of the LWP wire line rut depths on GPS-2 test sections.

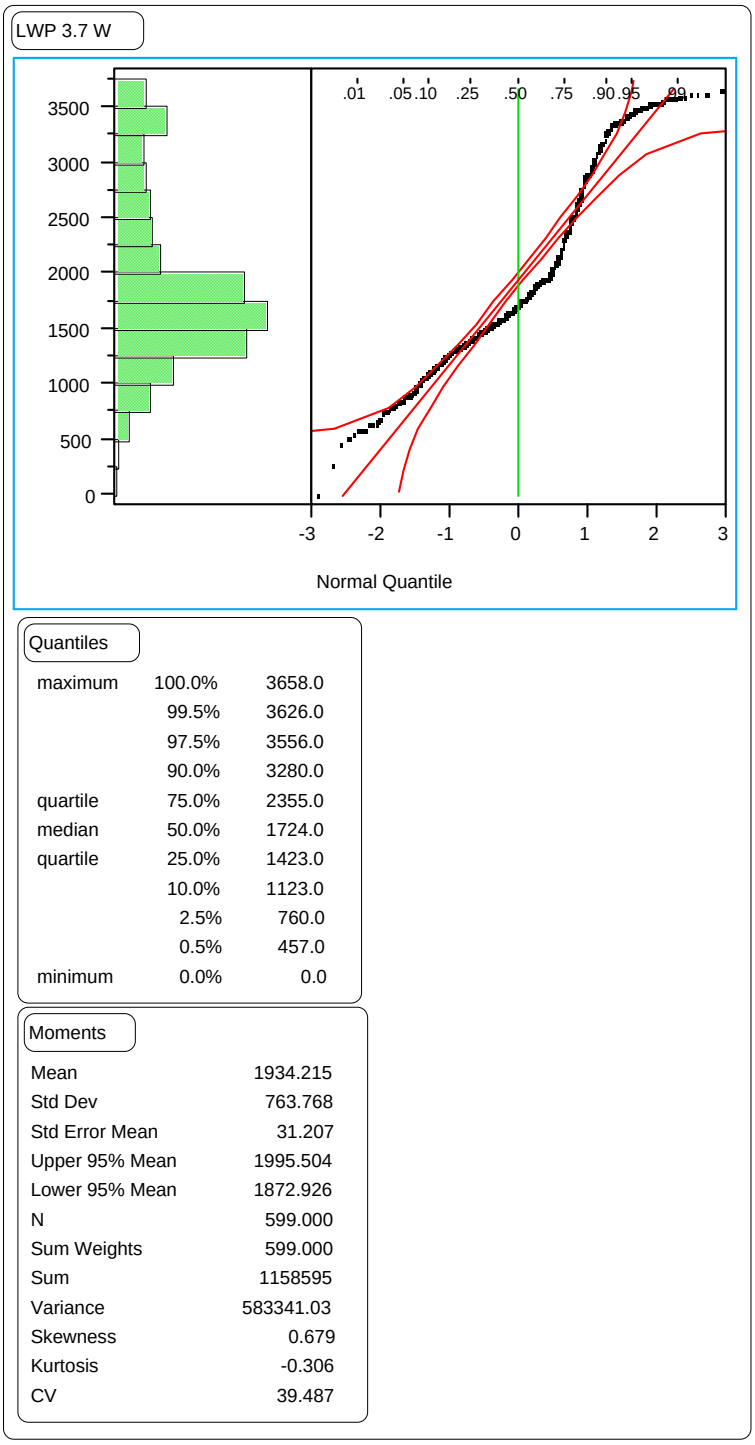

Figure 90. Distribution of the section means of the LWP wire line rut widths on GPS-2 test sections.

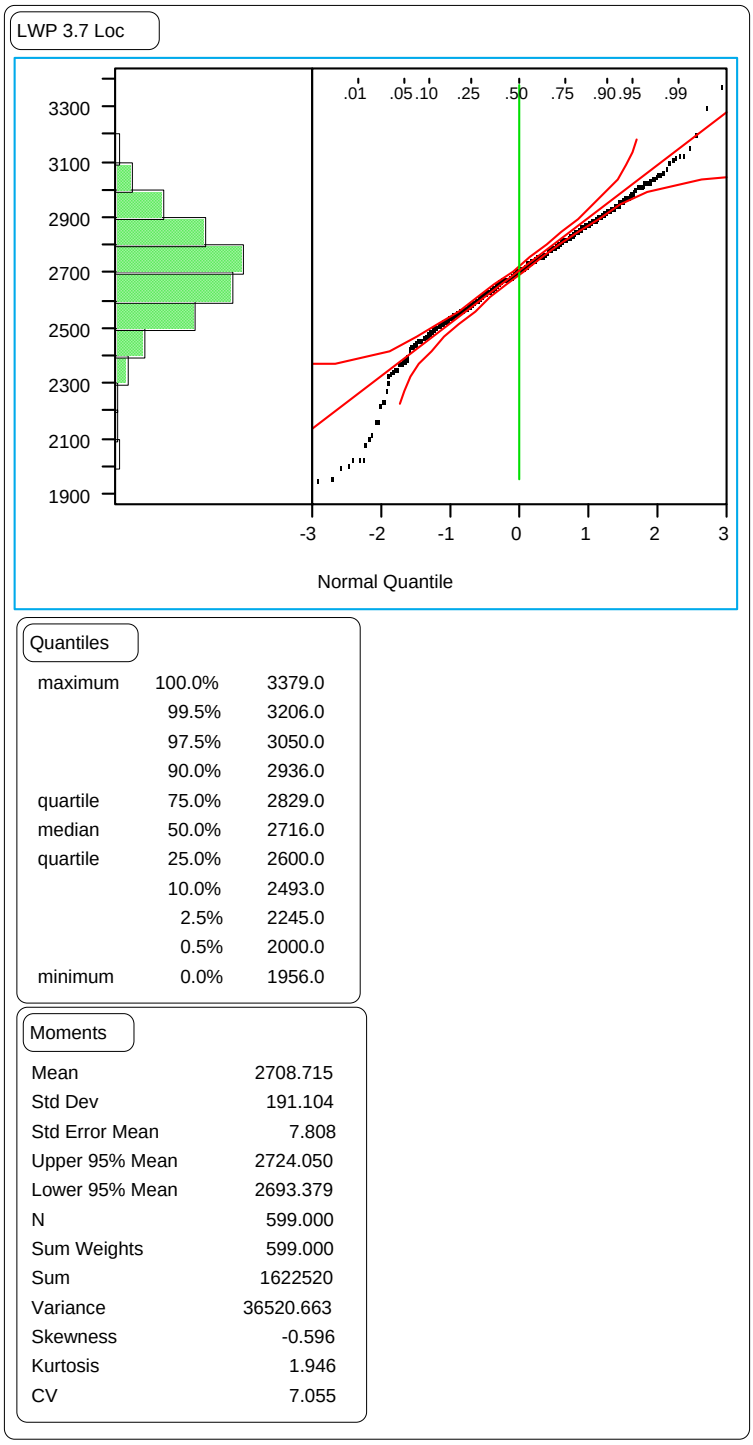

Figure 91. Distribution of the section means of the LWP wire line rut locations on GPS-2 test sections.

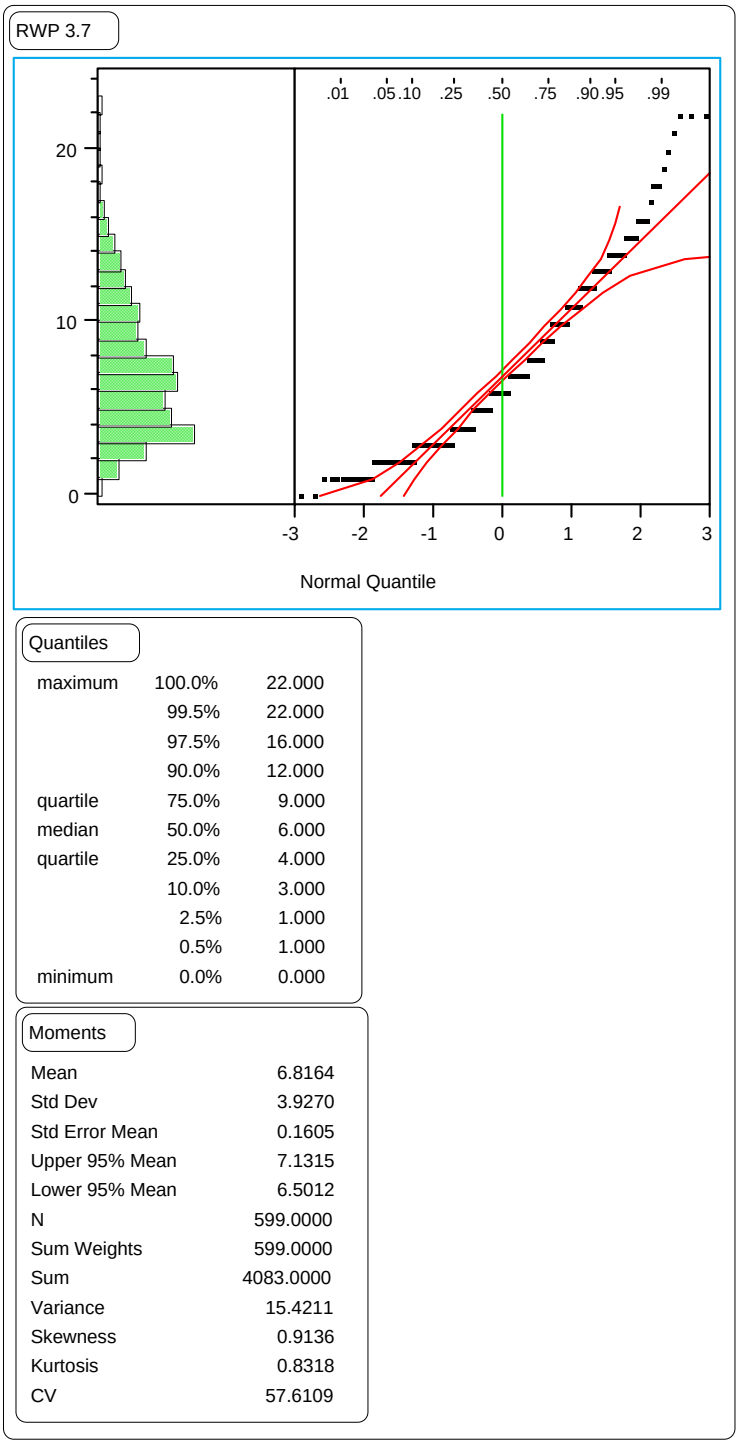

Figure 92. Distribution of the section means of the RWP wire line rut depths on GPS-2 test sections.

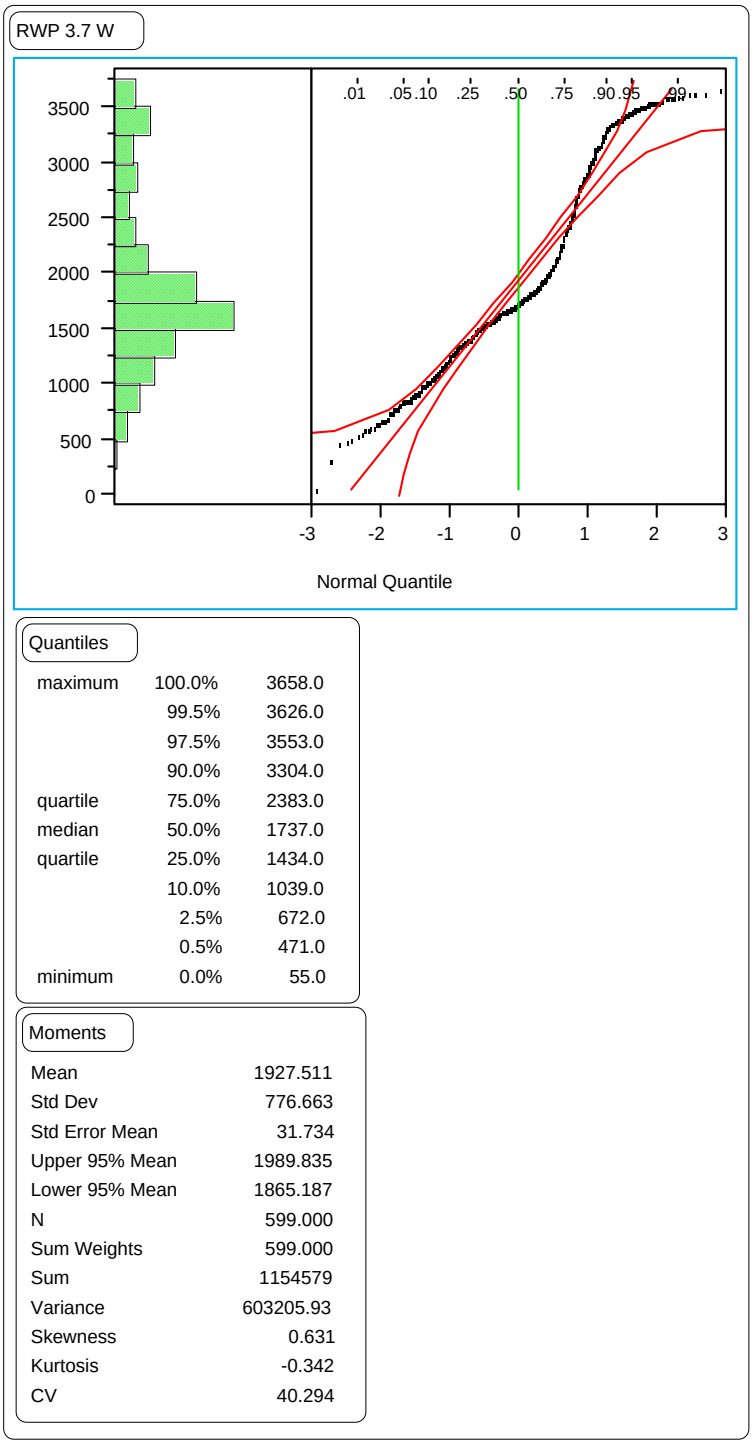

Figure 93. Distribution of the section means of the RWP wire line rut widths on GPS-2 test sections.

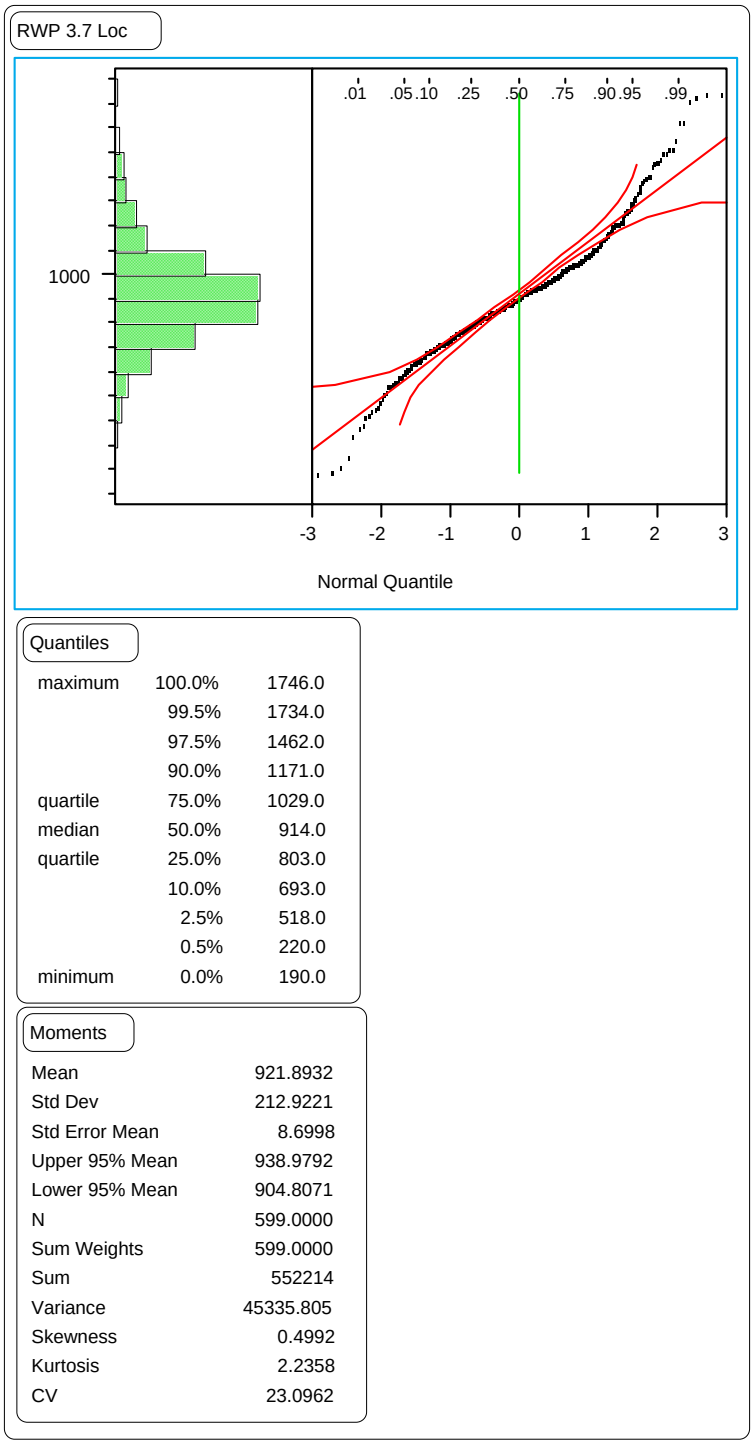

Figure 94. Distribution of the section means of the RWP wire line rut locations on GPS-2 test sections.

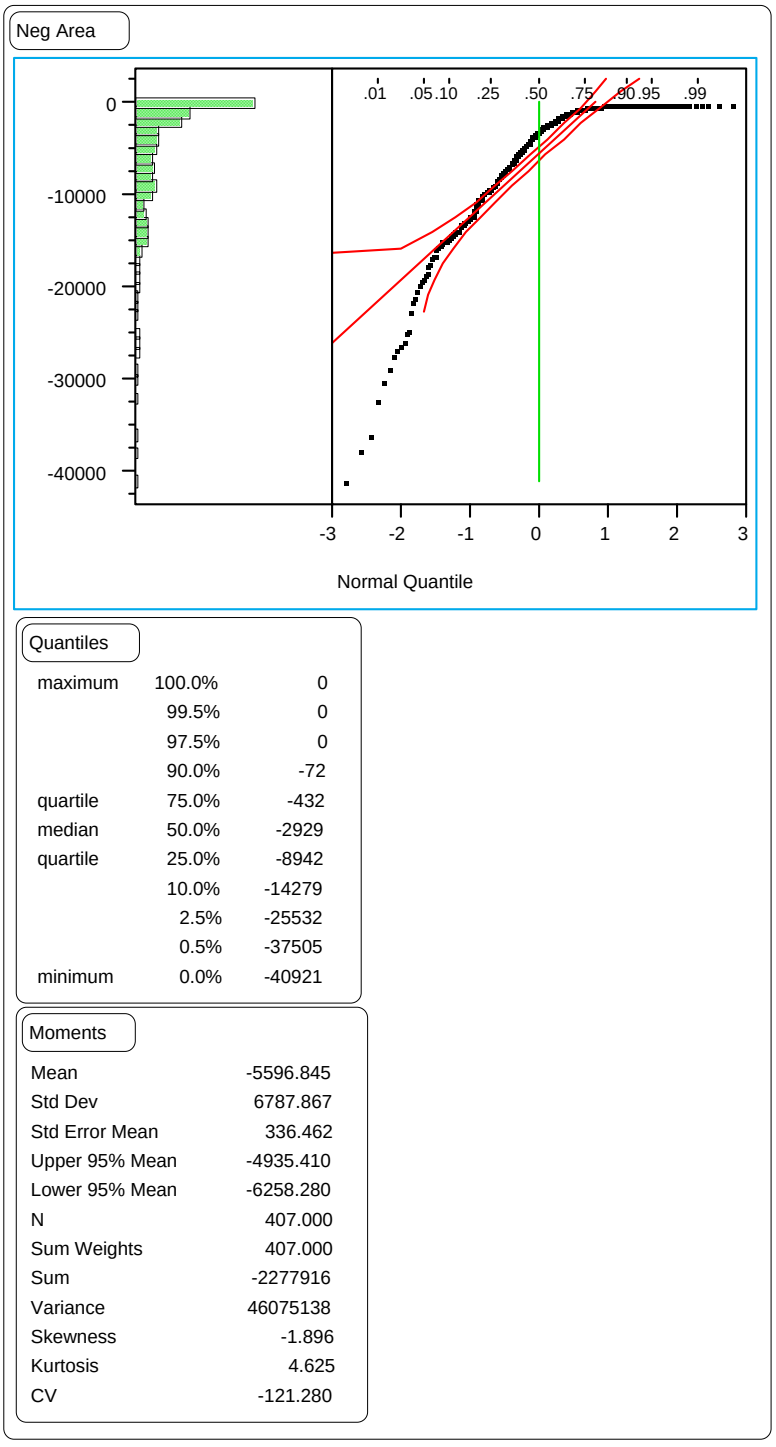

Figure 95. Distribution of the section means of the negative area index on GPS-6 test sections.

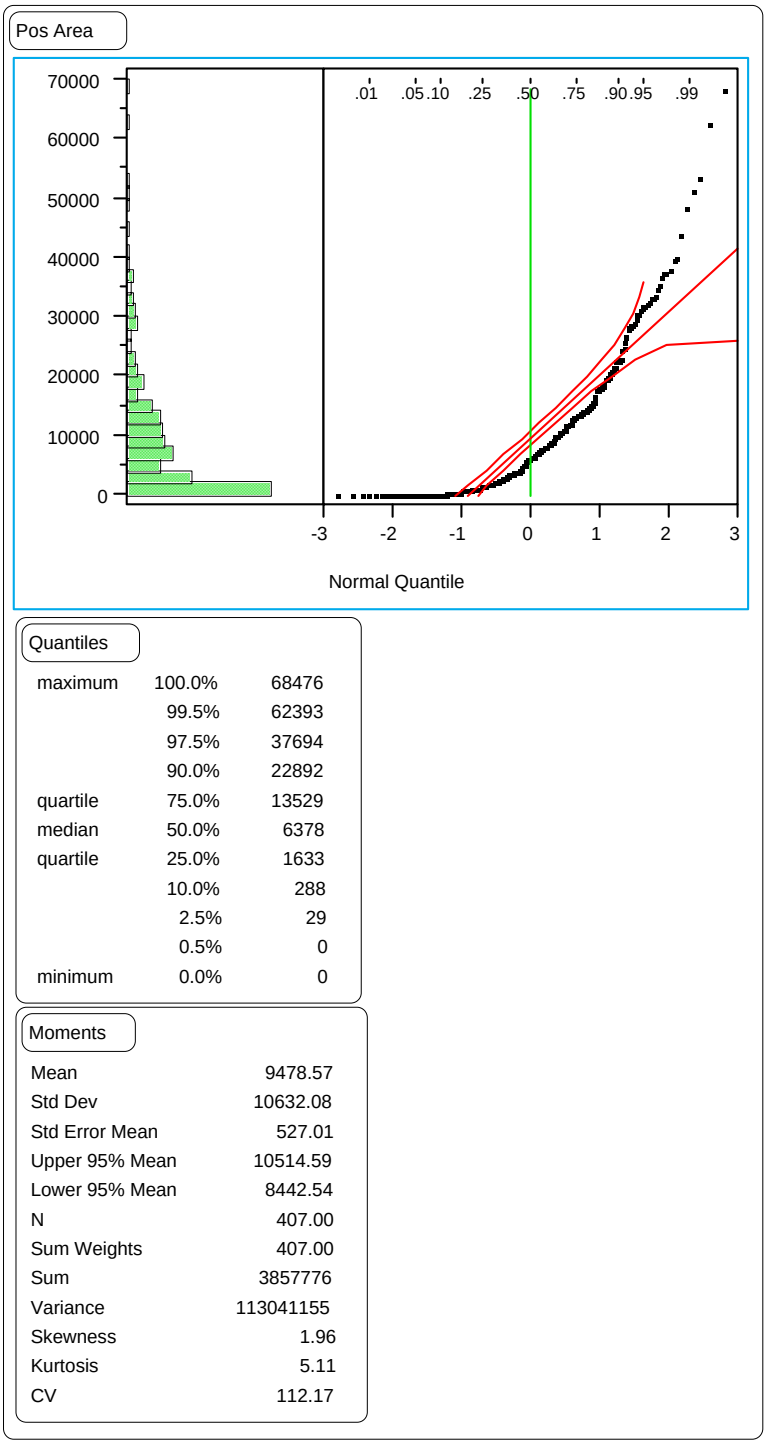

Figure 96. Distribution of the section means of the positive area index on GPS-6 test sections.

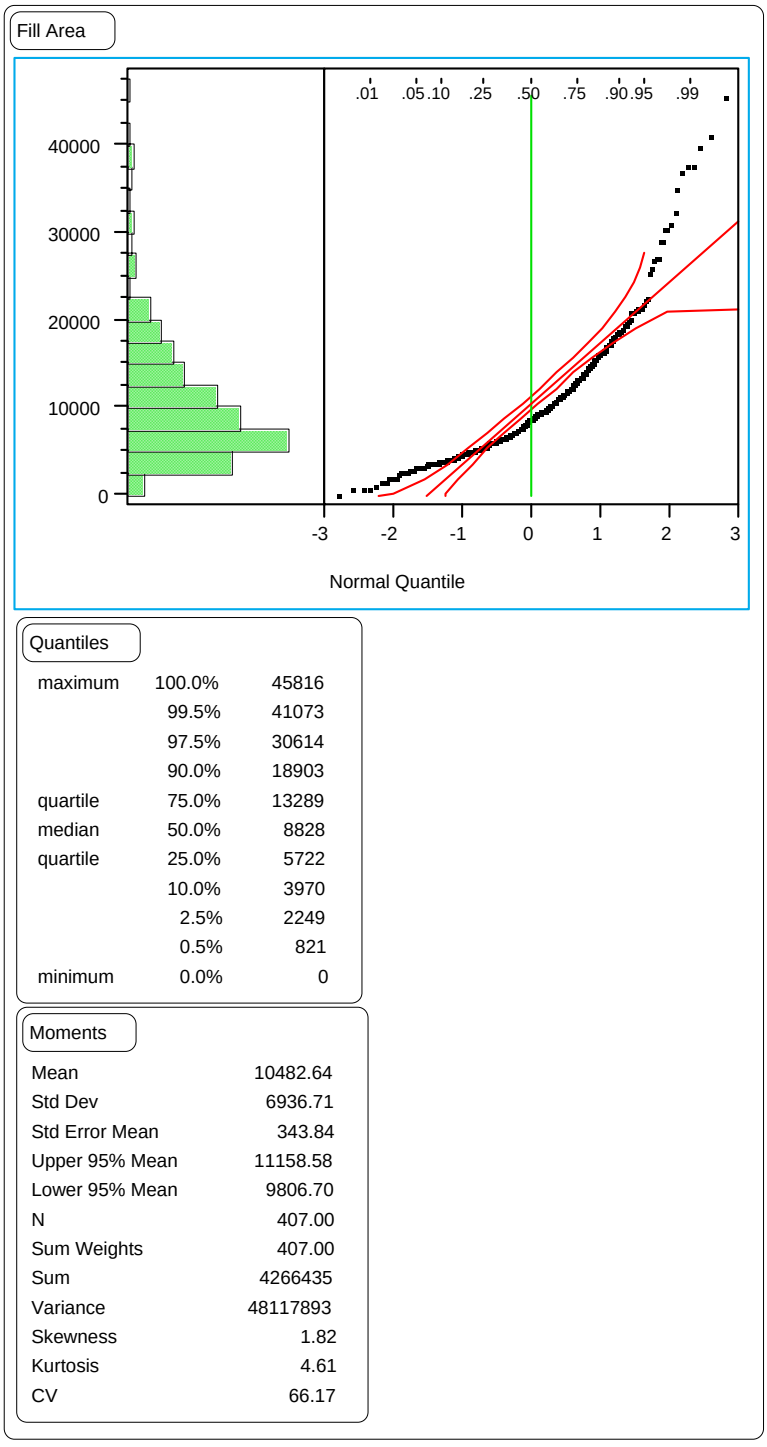

Figure 97. Distribution of the section means of the fill area index on GPS-6 test sections.

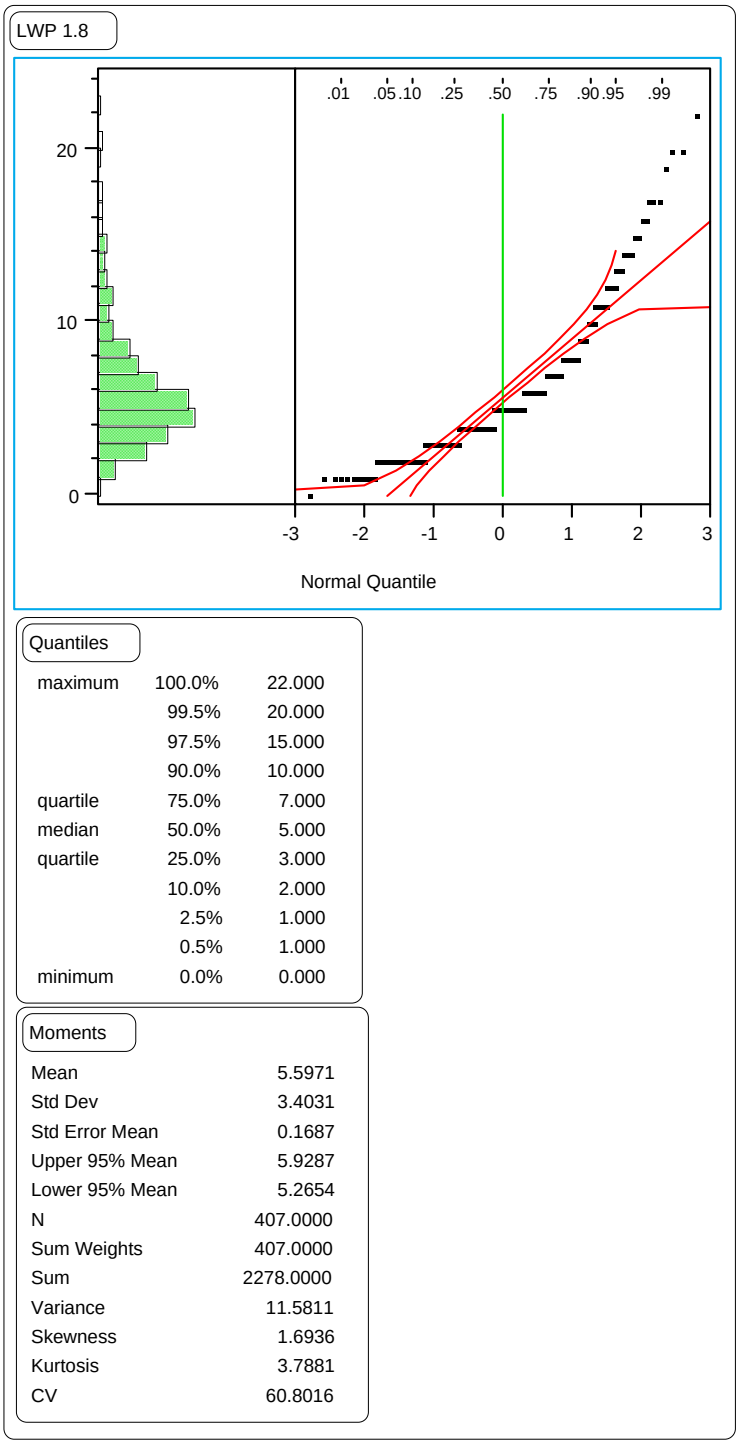

Figure 98. Distribution of the section means of the LWP 1.8-m rut depths on GPS-6 test sections.

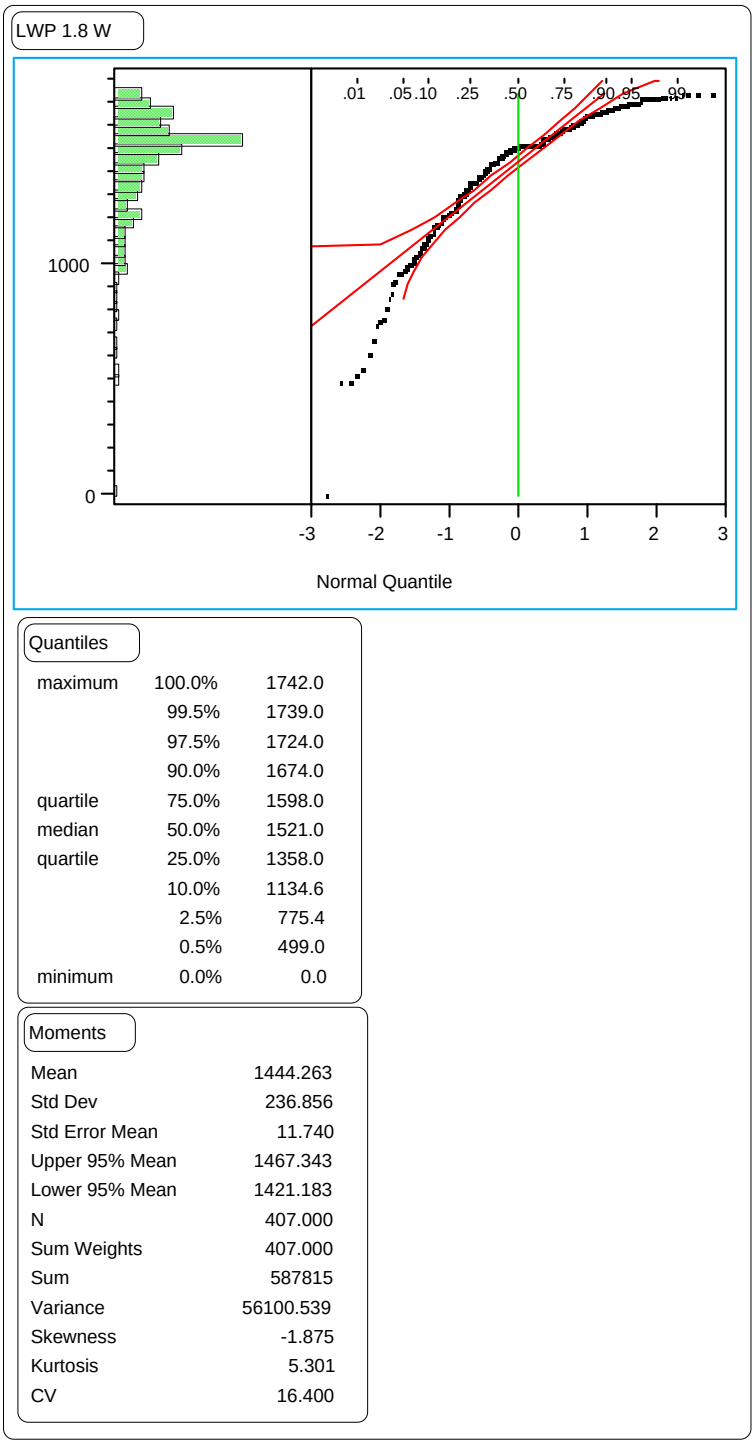

Figure 99. Distribution of the section means of the LWP 1.8-m rut widths on GPS-6 test sections.

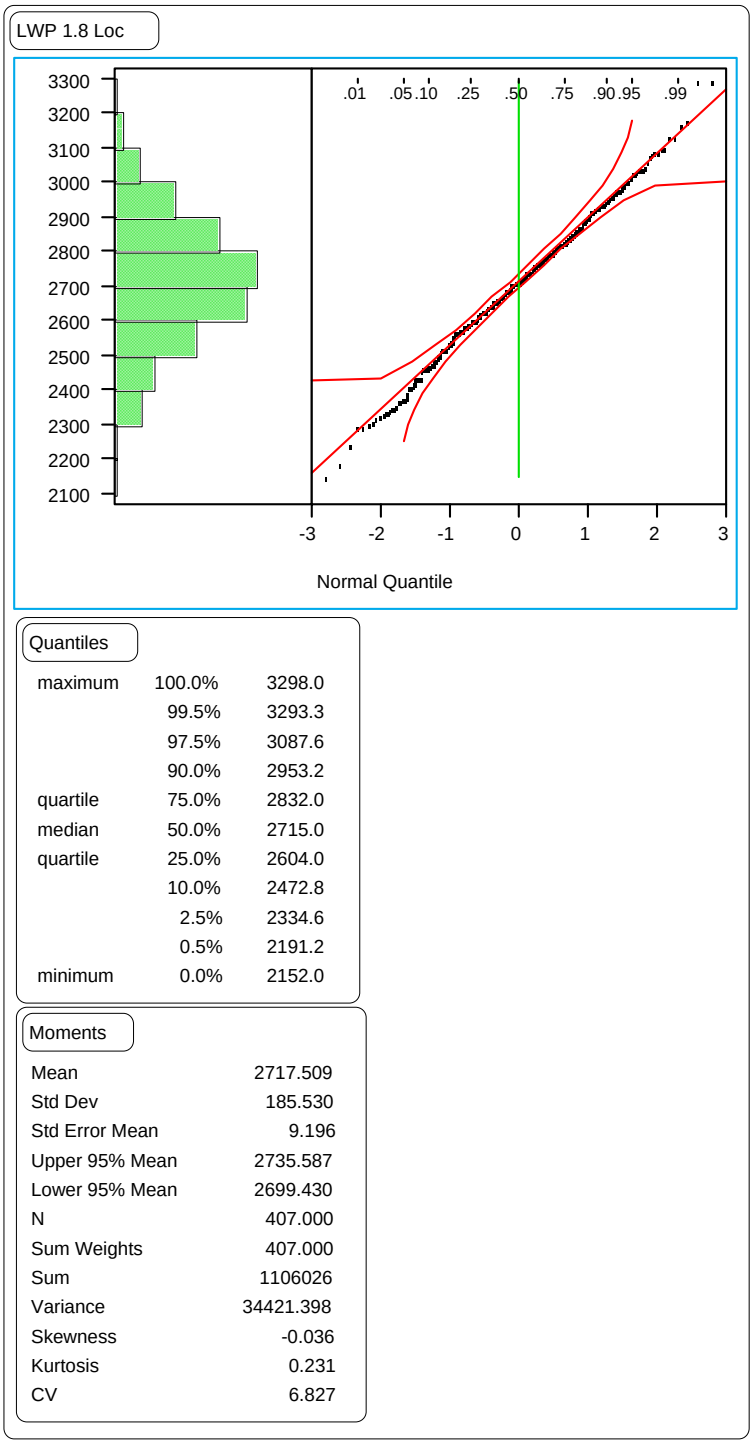

Figure 100. Distribution of the section means of the LWP 1.8-m rut locations on GPS-6 test sections.

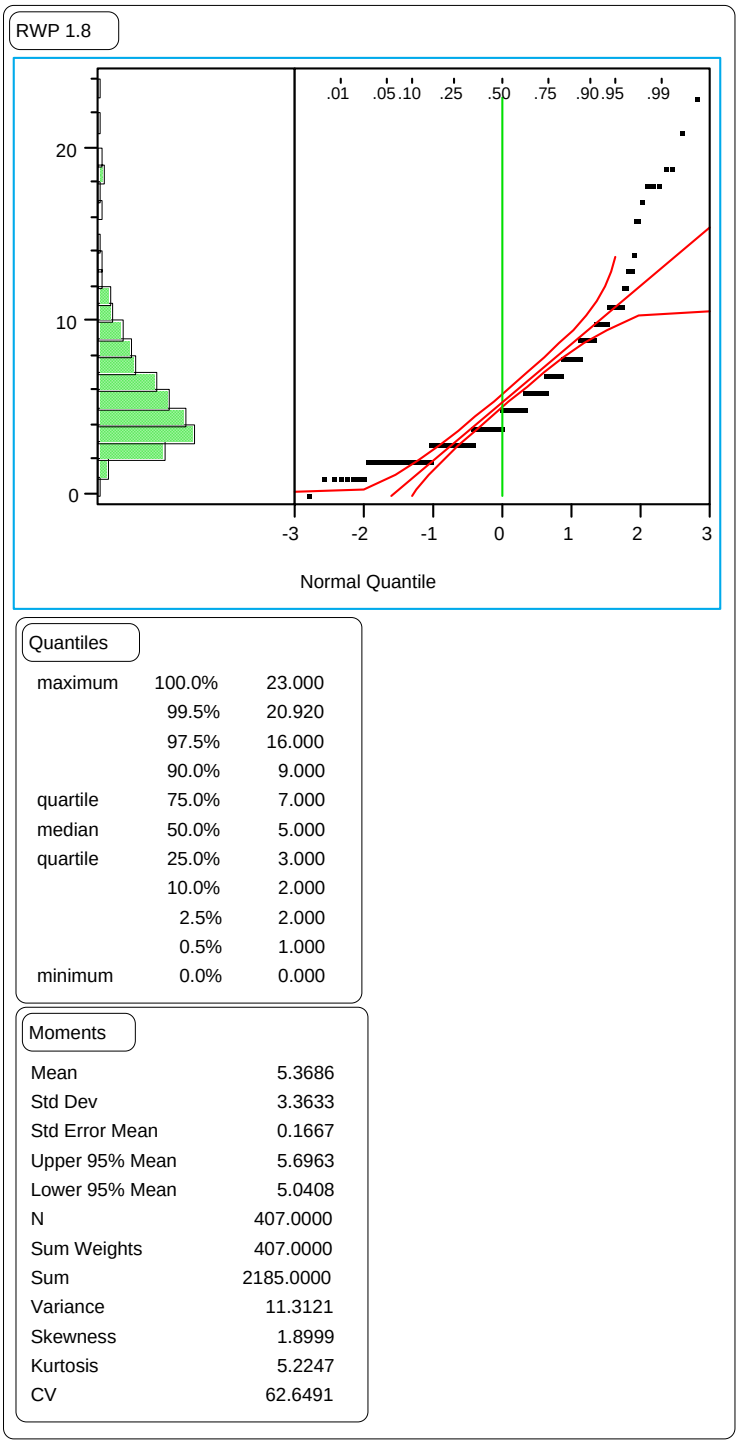

Figure 101. Distribution of the section means of the RWP 1.8-m rut depths on GPS-6 test sections.

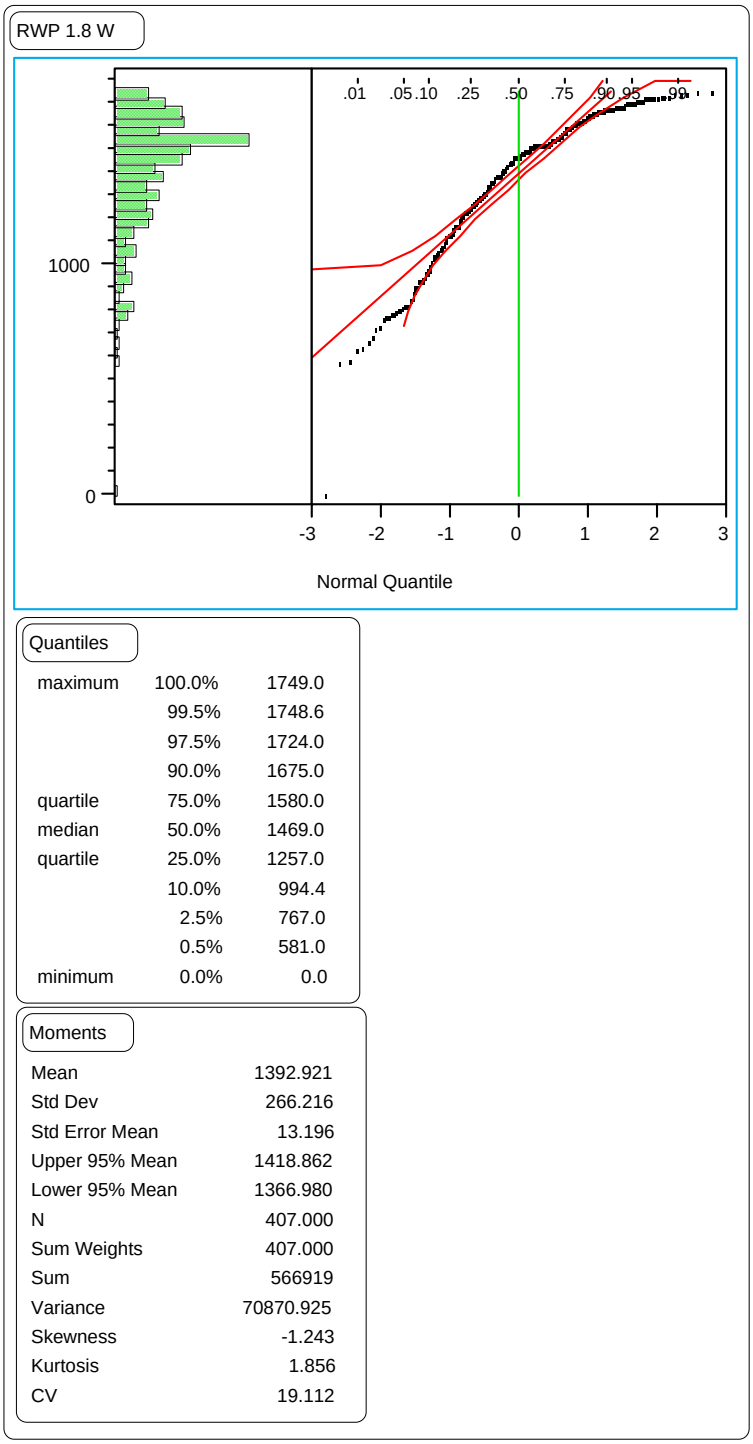

Figure 102. Distribution of the section means of the RWP 1.8-m rut widths on GPS-6 test sections.

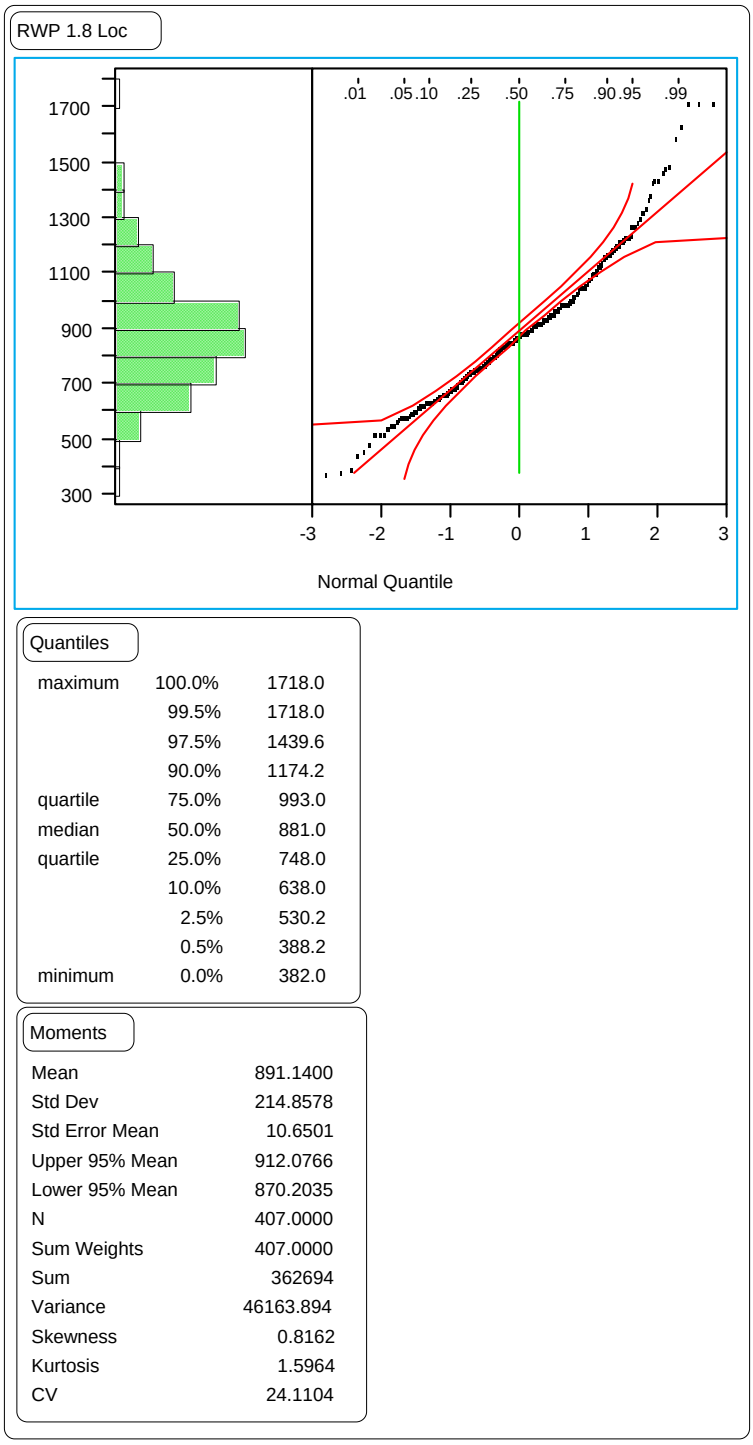

Figure 103. Distribution of the section means of the RWP 1.8-m rut locations on GPS-6 test sections.

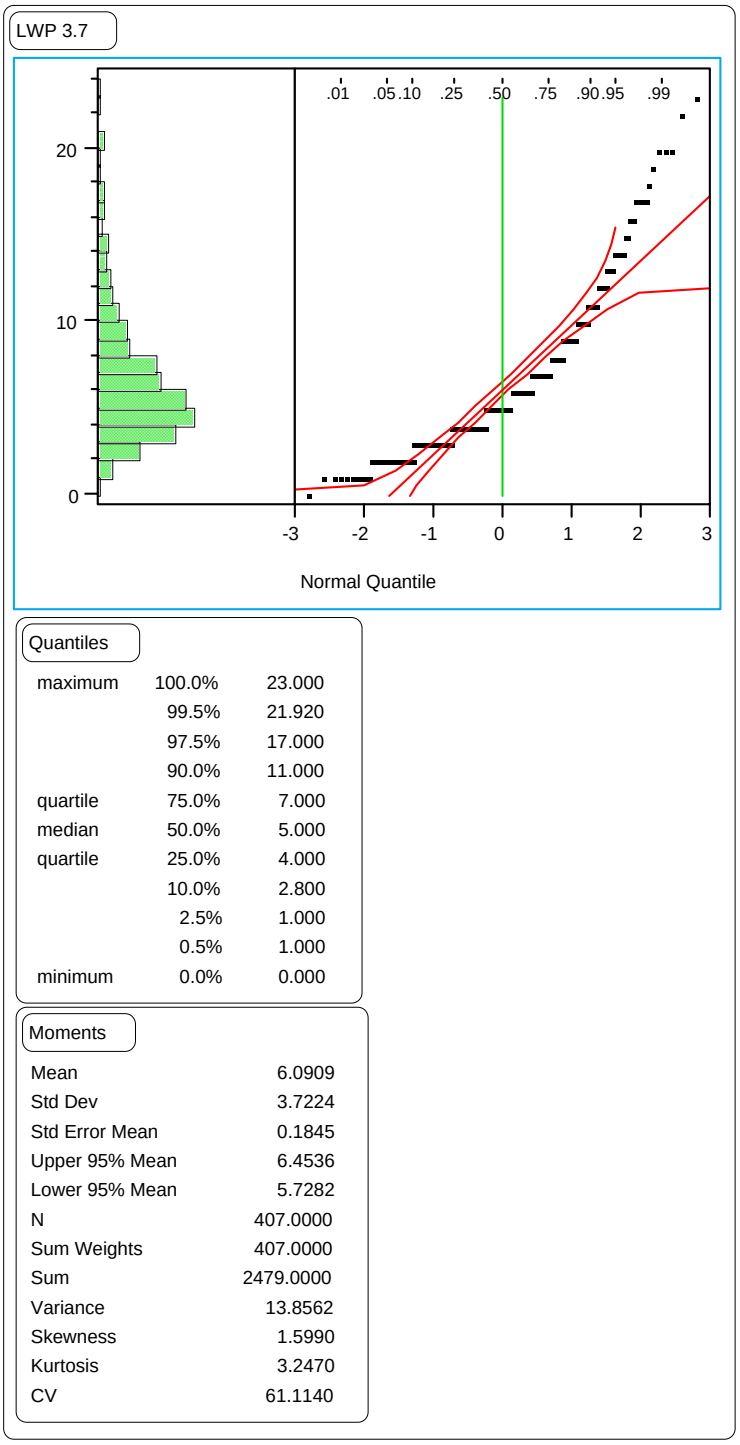

Figure 104. Distribution of the section means of the LWP wire line rut depths on GPS-6 test sections.

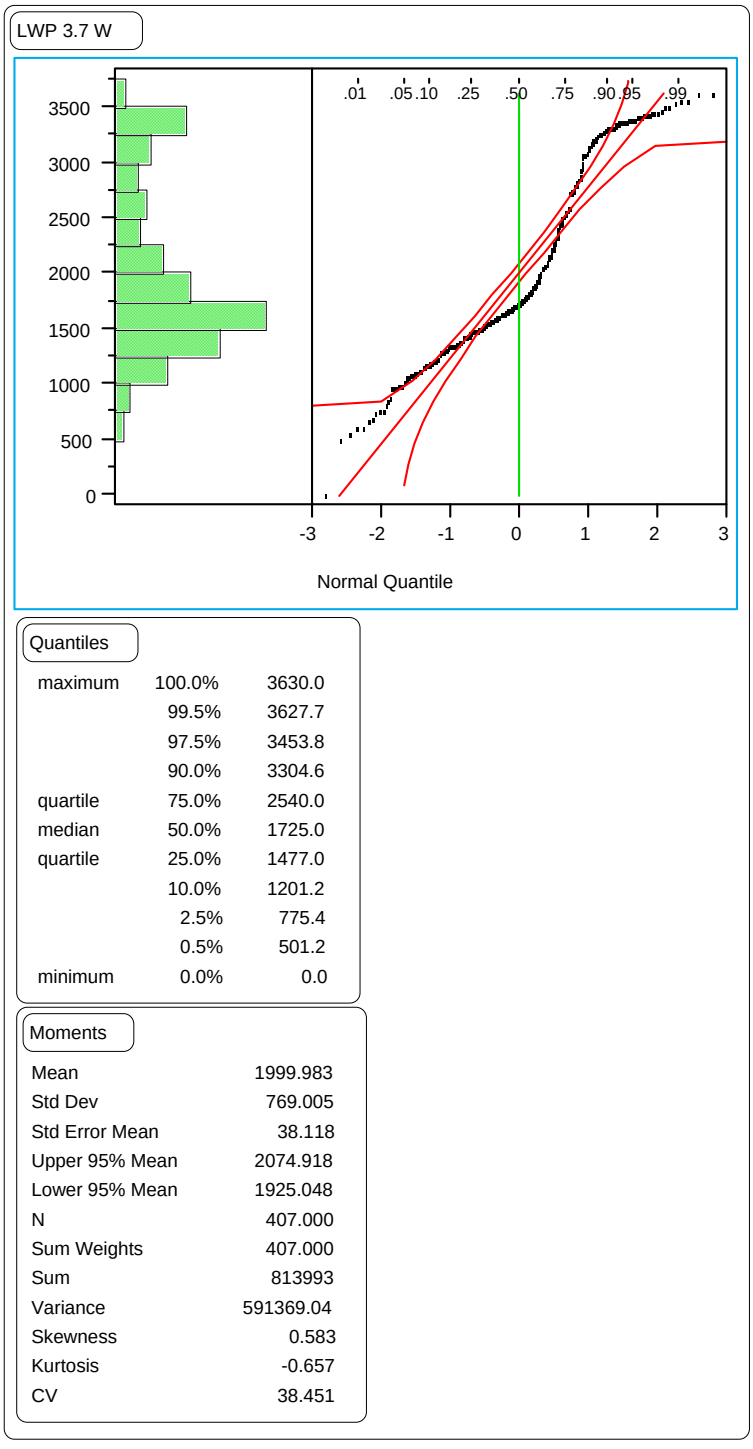

Figure 105. Distribution of the section means of the LWP wire line rut widths on GPS-6 test sections.

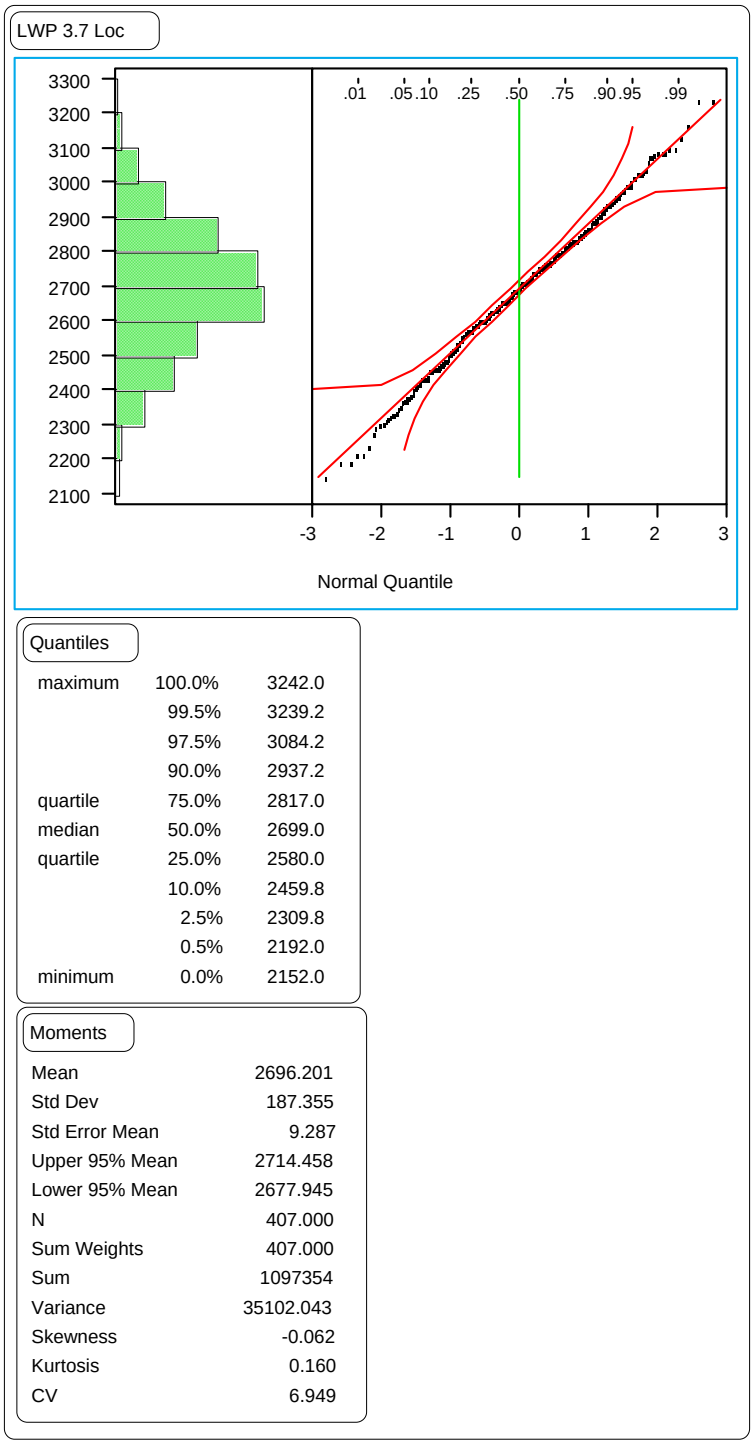

Figure 106. Distributions of the section means of the LWP wire line rut locations on GPS-6 test sections.

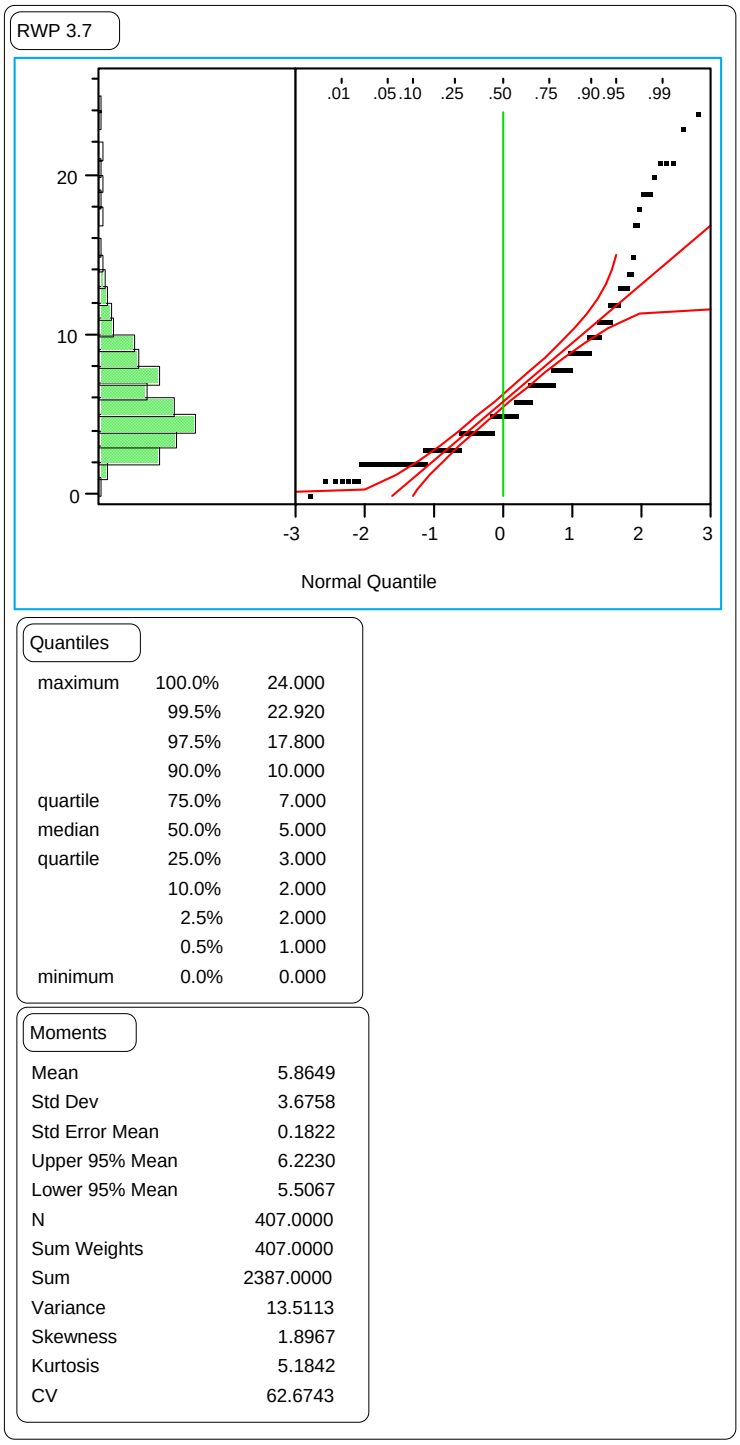

Figure 107. Distribution of the section means of the RWP wire line rut depths on GPS-6 test sections.

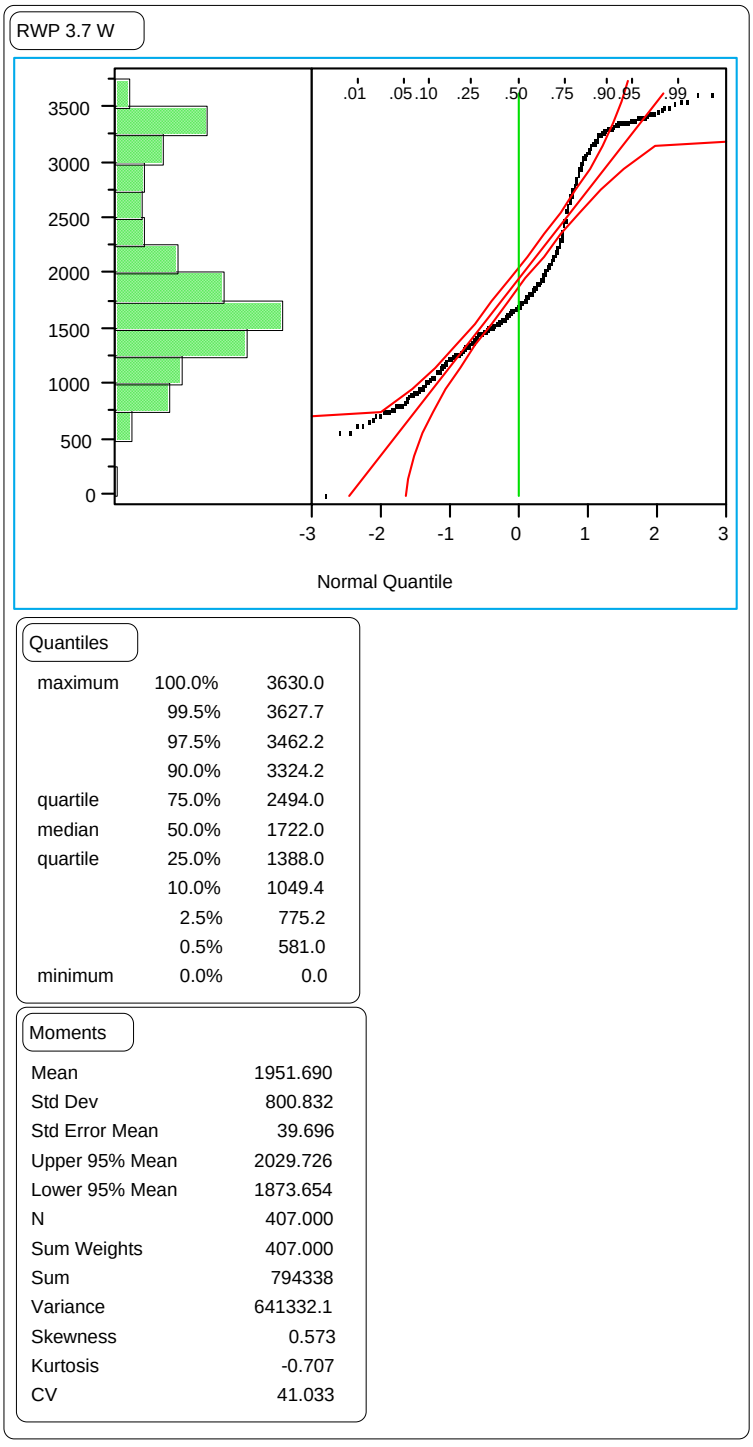

Figure 108. Distribution of the section means of the RWP wire line rut widths on GPS-6 test sections.

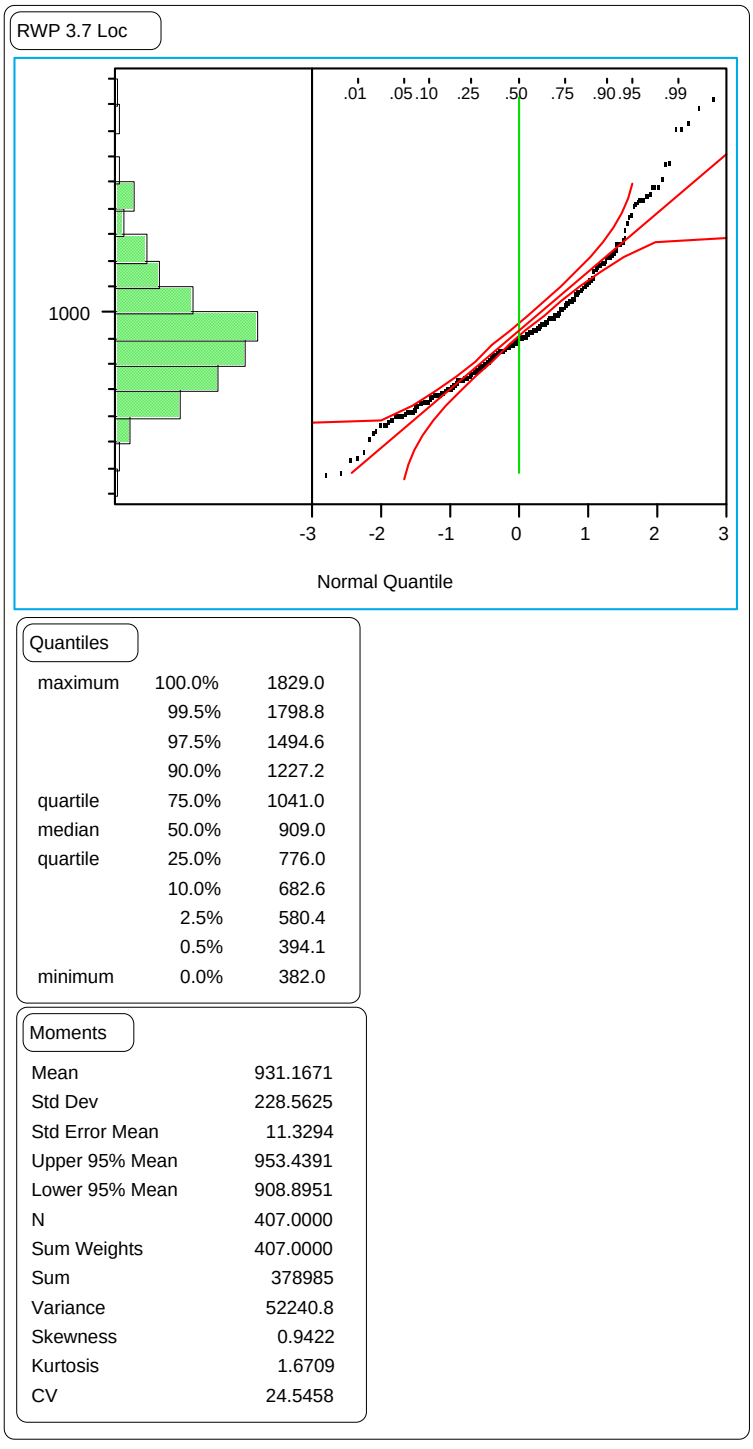

Figure 109. Distribution of the section means of the RWP wire line rut locations on GPS-6 test sections.

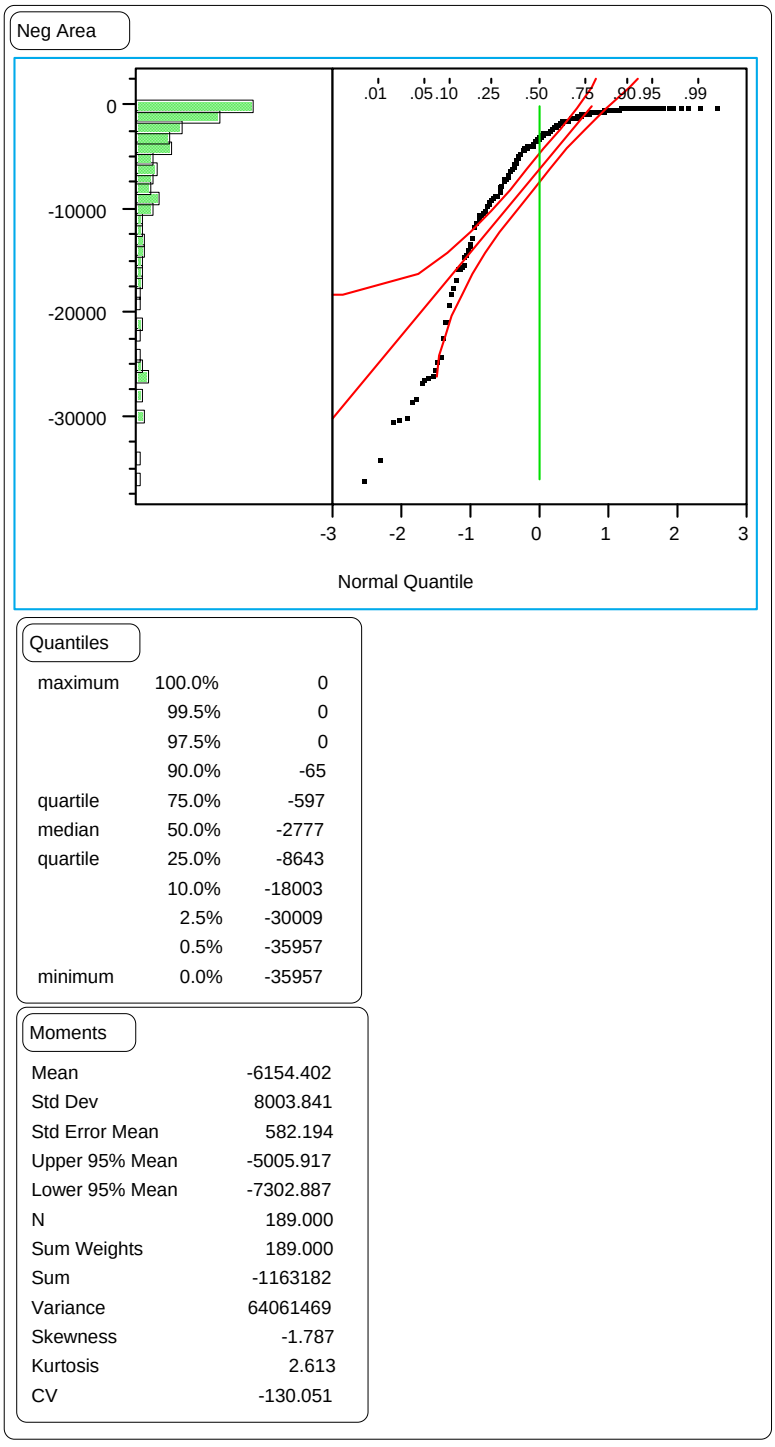

Figure 110. Distribution of the section means of the negative area index on GPS-7 test sections.

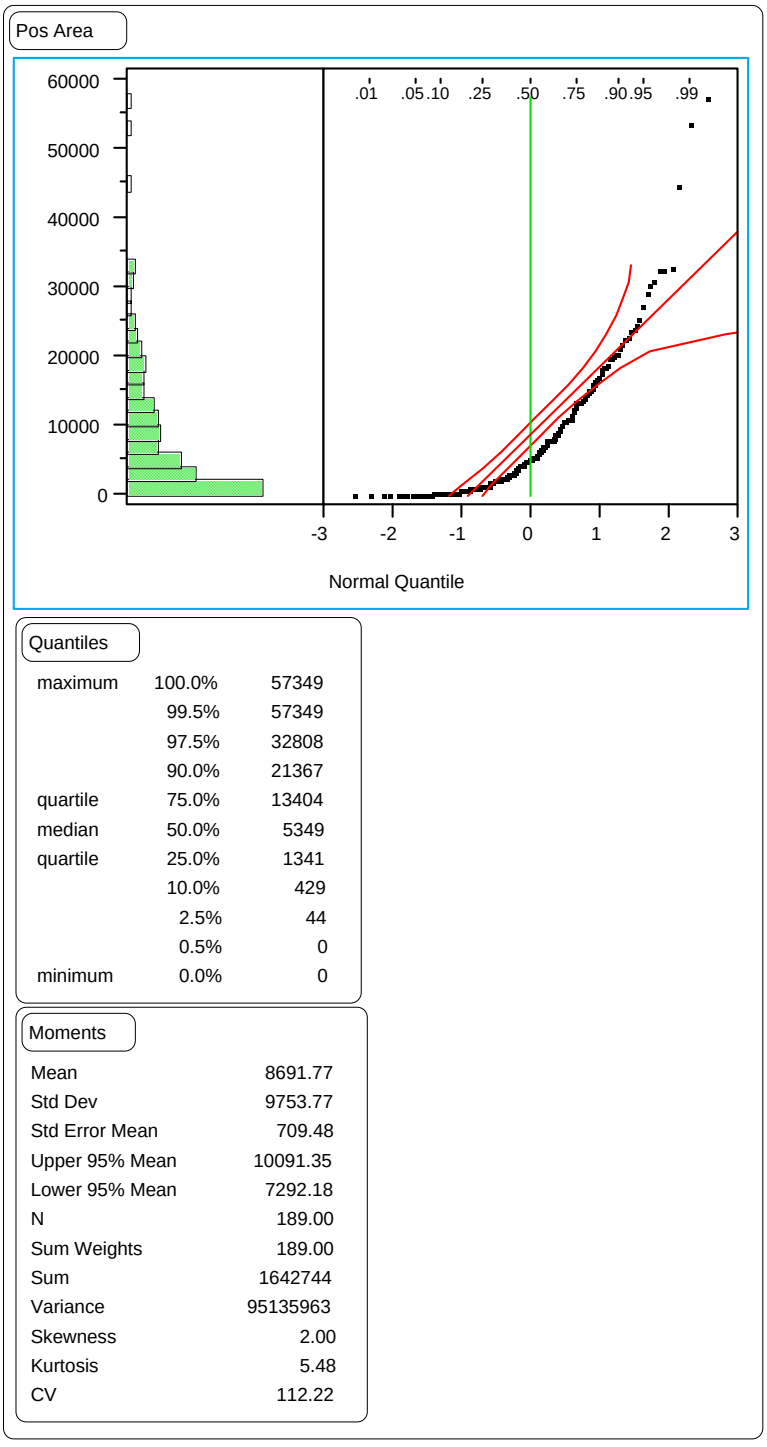

Figure 111. Distribution of the section means of the positive area index on GPS-7 test sections.

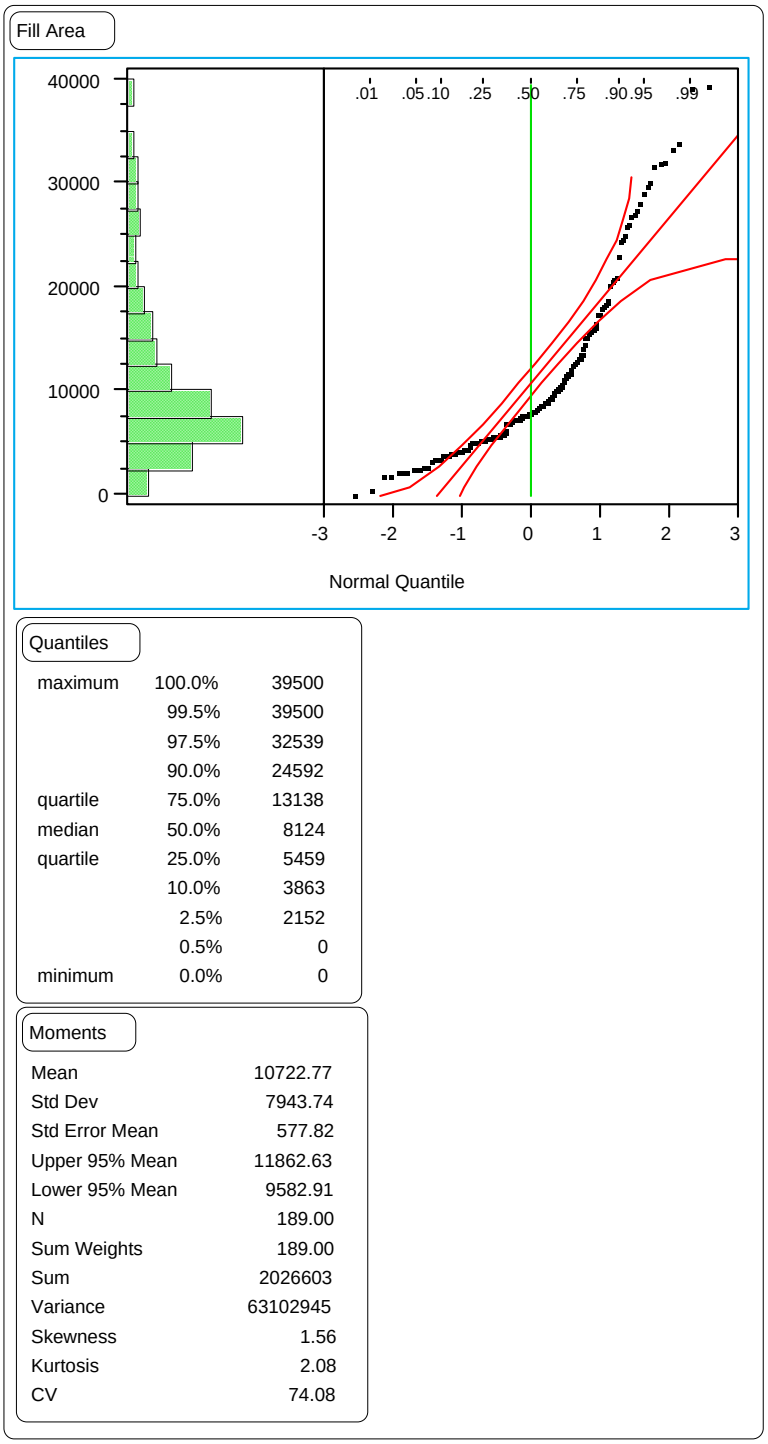

Figure 112. Distribution of the section means of the fill area index on GPS-7 test sections.

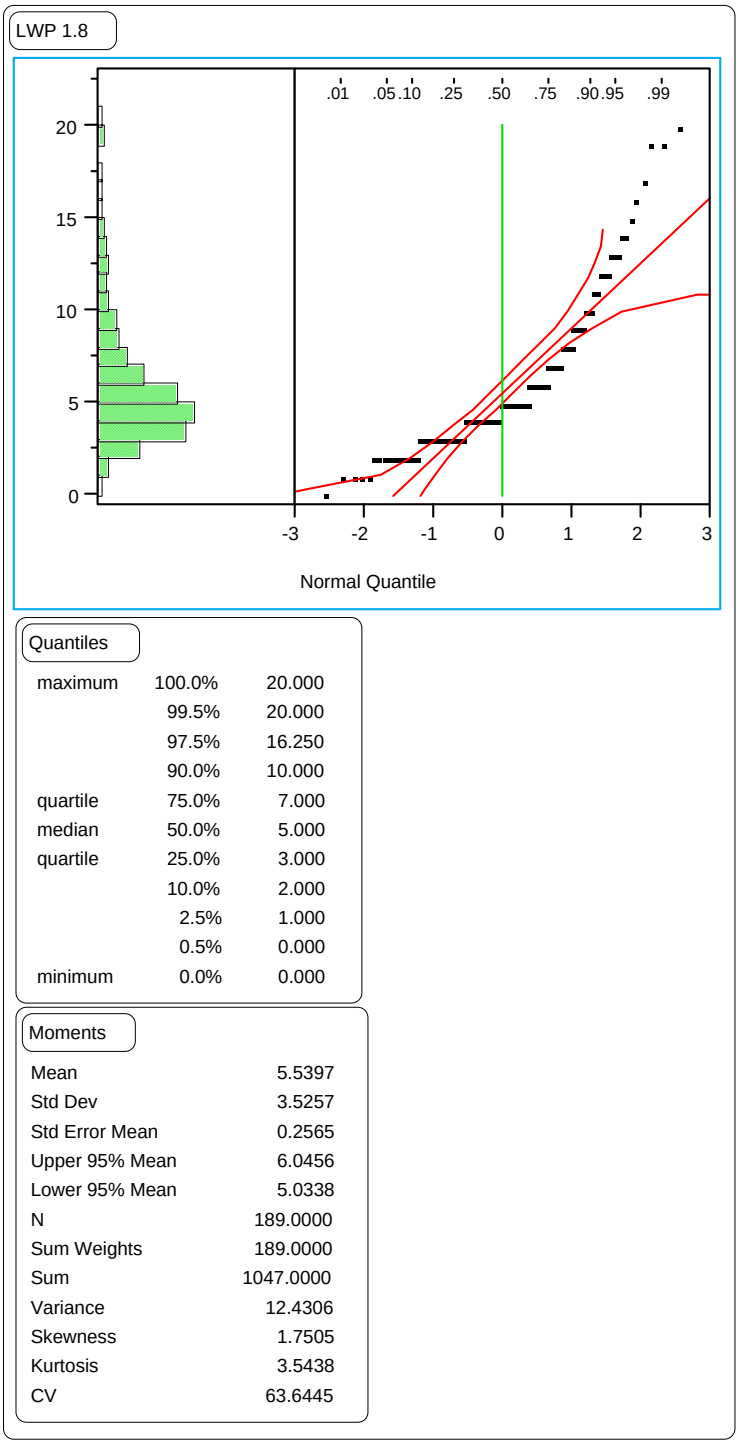

Figure 113. Distribution of the section means of the LWP 1.8-m rut depths on GPS-7 test sections.

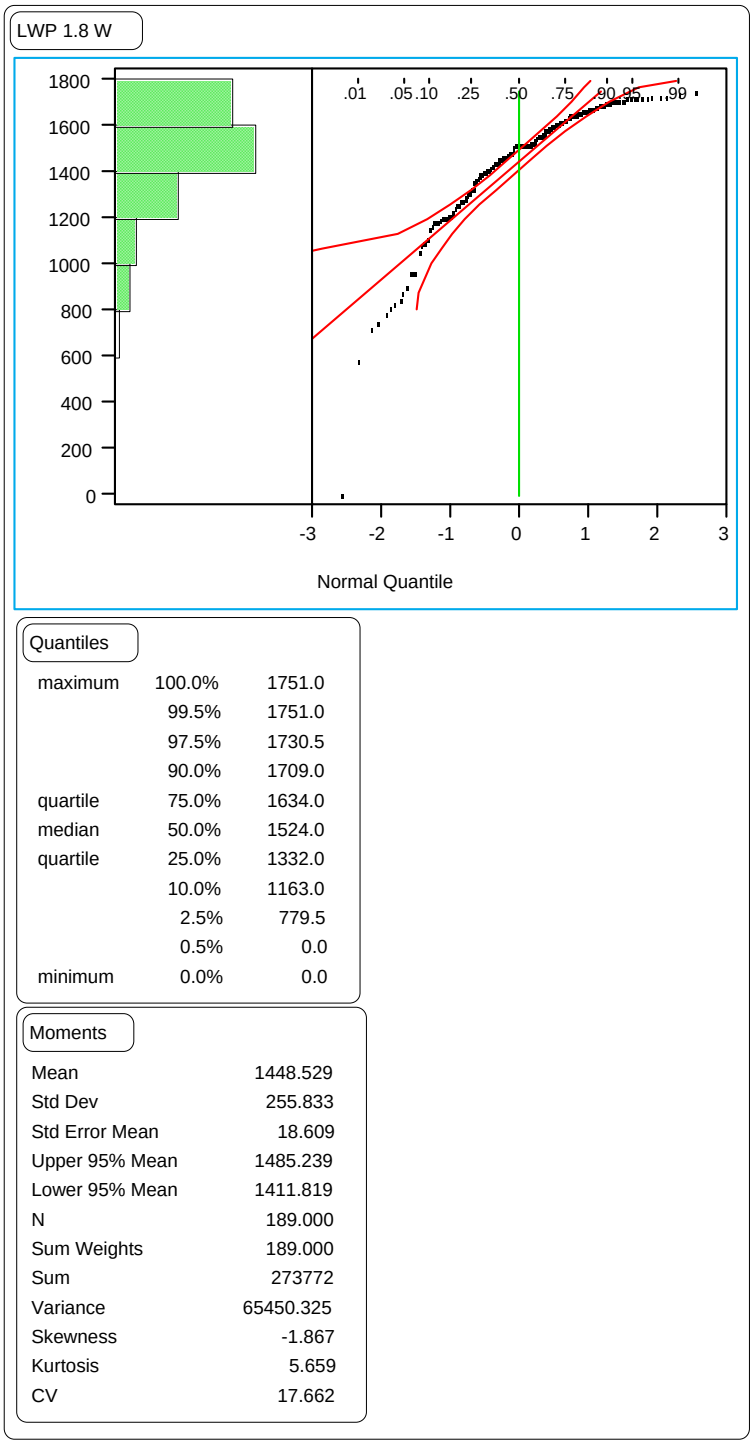

Figure 114. Distribution of the section means of the LWP 1.8-m rut widths on GPS-7 test sections.

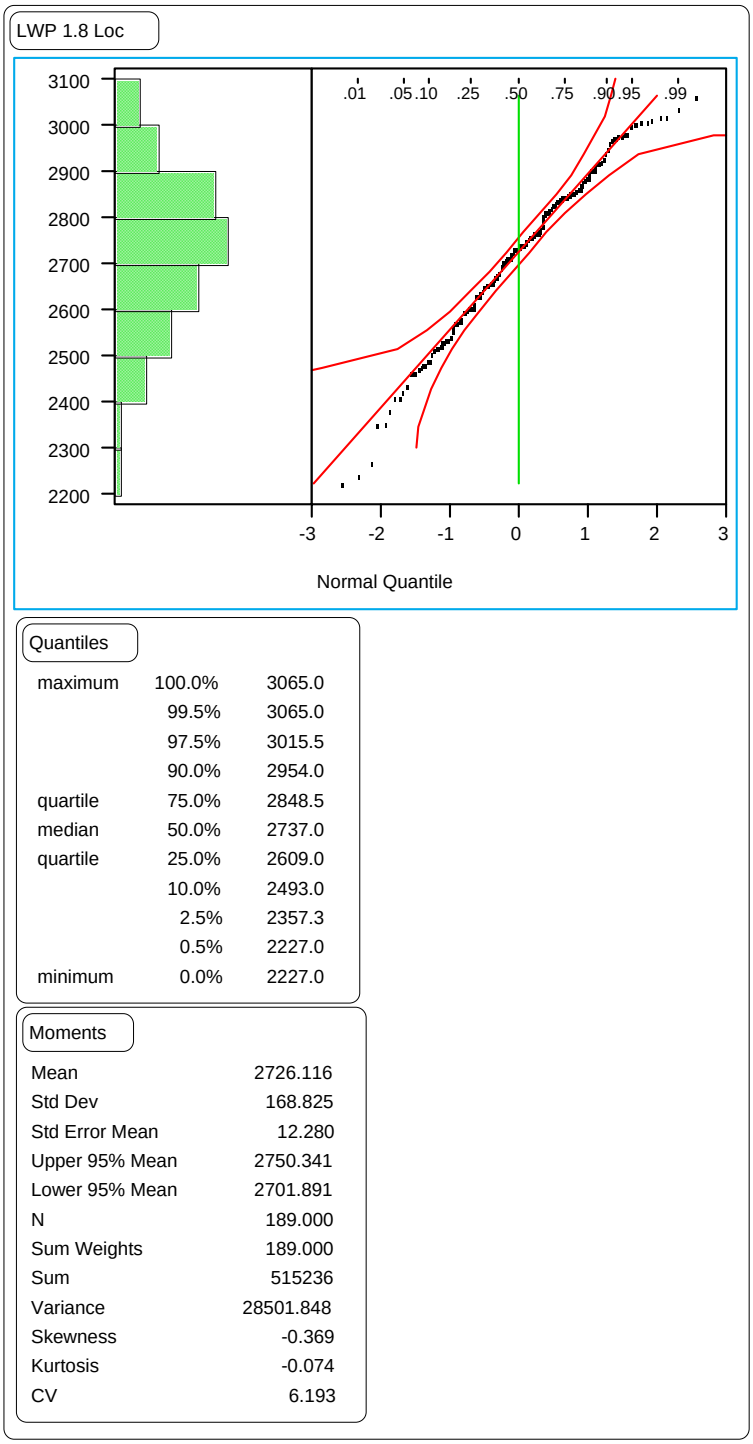

Figure 115. Distribution of the section means of the LWP 1.8-m rut locations on GPS-7 test sections.

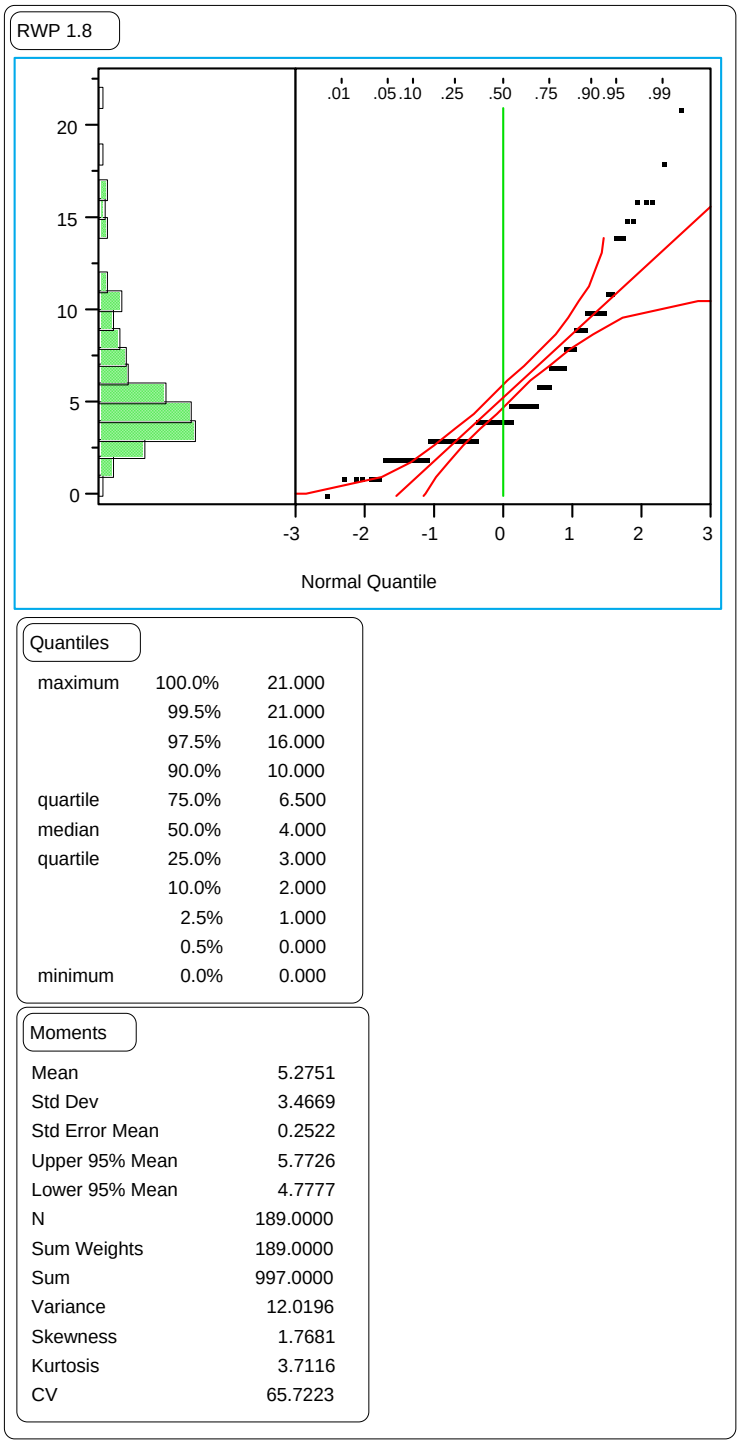

Figure 116. Distribution of the section means of the RWP 1.8-m rut depths on GPS-7 test sections.

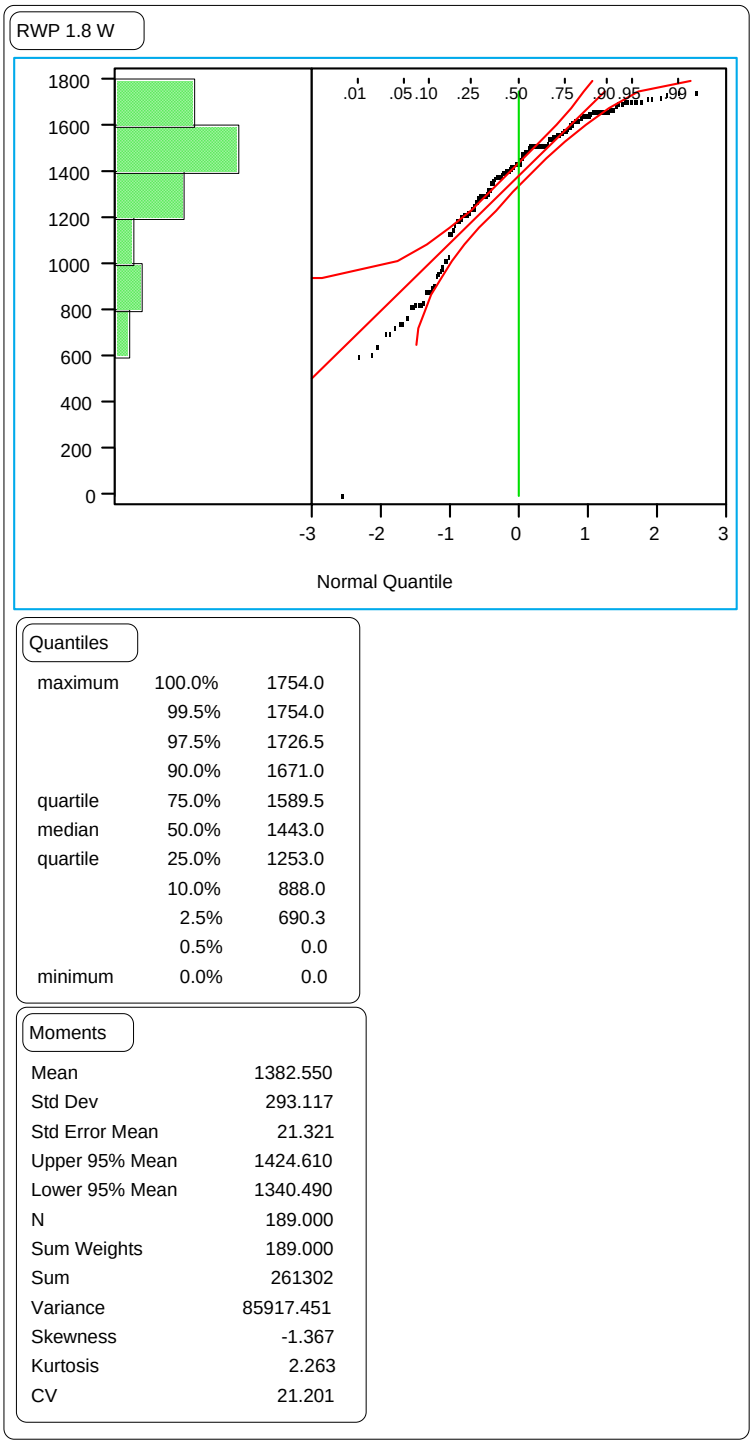

Figure 117. Distribution of the section means of the RWP 1.8-m rut widths on GPS-7 test sections.

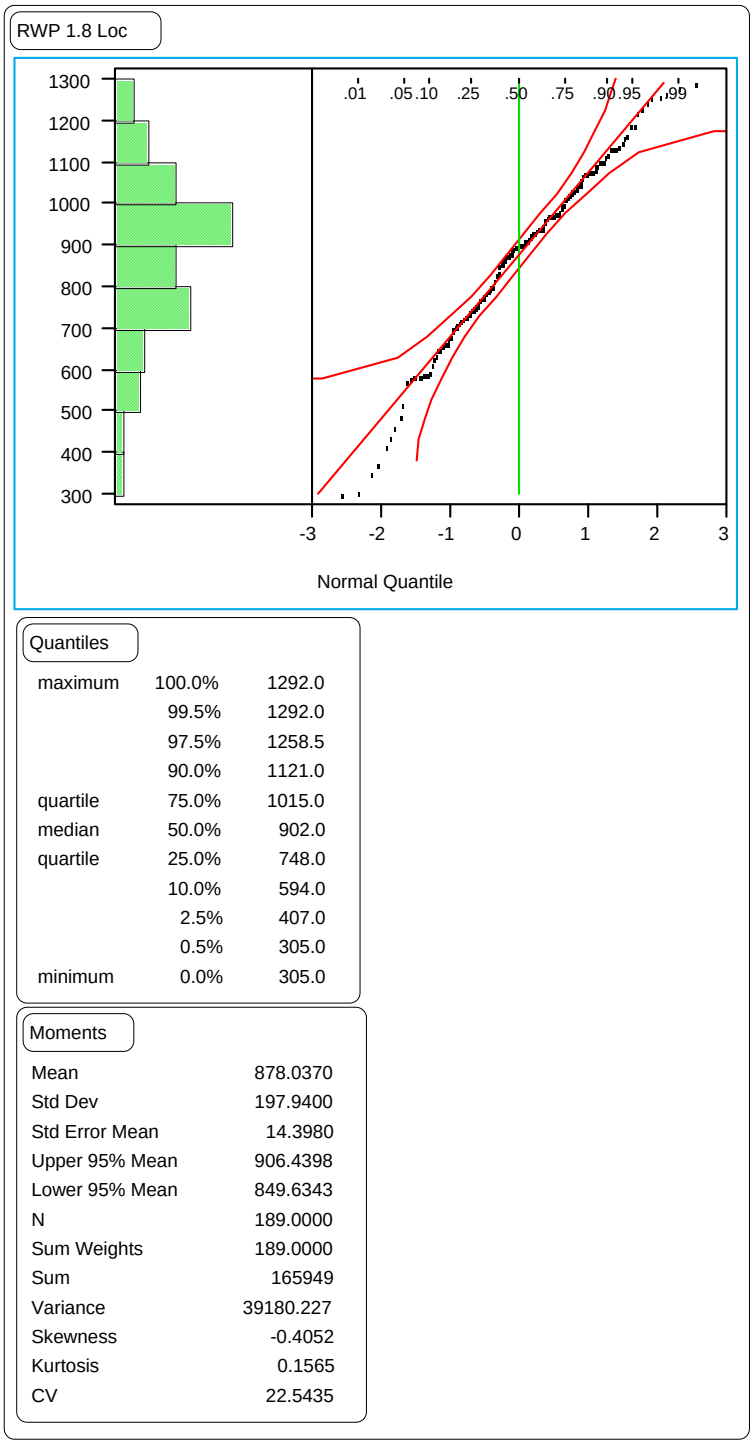

Figure 118. Distribution of the section means of the RWP 1.8-m rut locations on GPS-7 test sections.

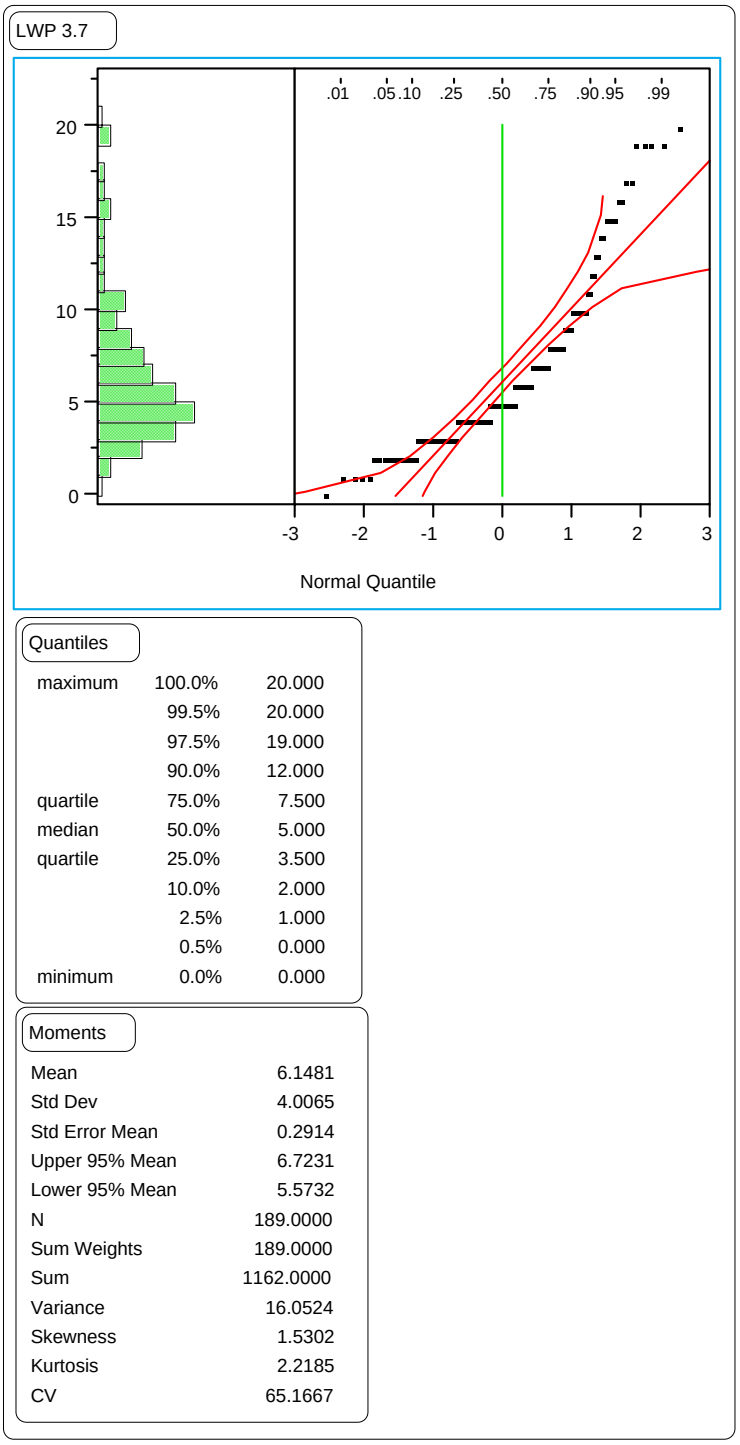

Quantiles

maximum	100.0%	20.000
	99.5%	20.000
	97.5%	19.000
	90.0%	12.000
quartile	75.0%	7.500
median	50.0%	5.000
quartile	25.0%	3.500
	10.0%	2.000
	2.5%	1.000
	0.5%	0.000
minimum	0.0%	0.000

Moments

Mean	6.1481
Std Dev	4.0065
Std Error Mean	0.2914
Upper 95% Mean	6.7231
Lower 95% Mean	5.5732
N	189.0000
Sum Weights	189.0000
Sum	1162.0000
Variance	16.0524
Skewness	1.5302
Kurtosis	2.2185
CV	65.1667

Figure 119. Distribution of the section means of the LWP wire line rut depths on GPS-7 test sections.

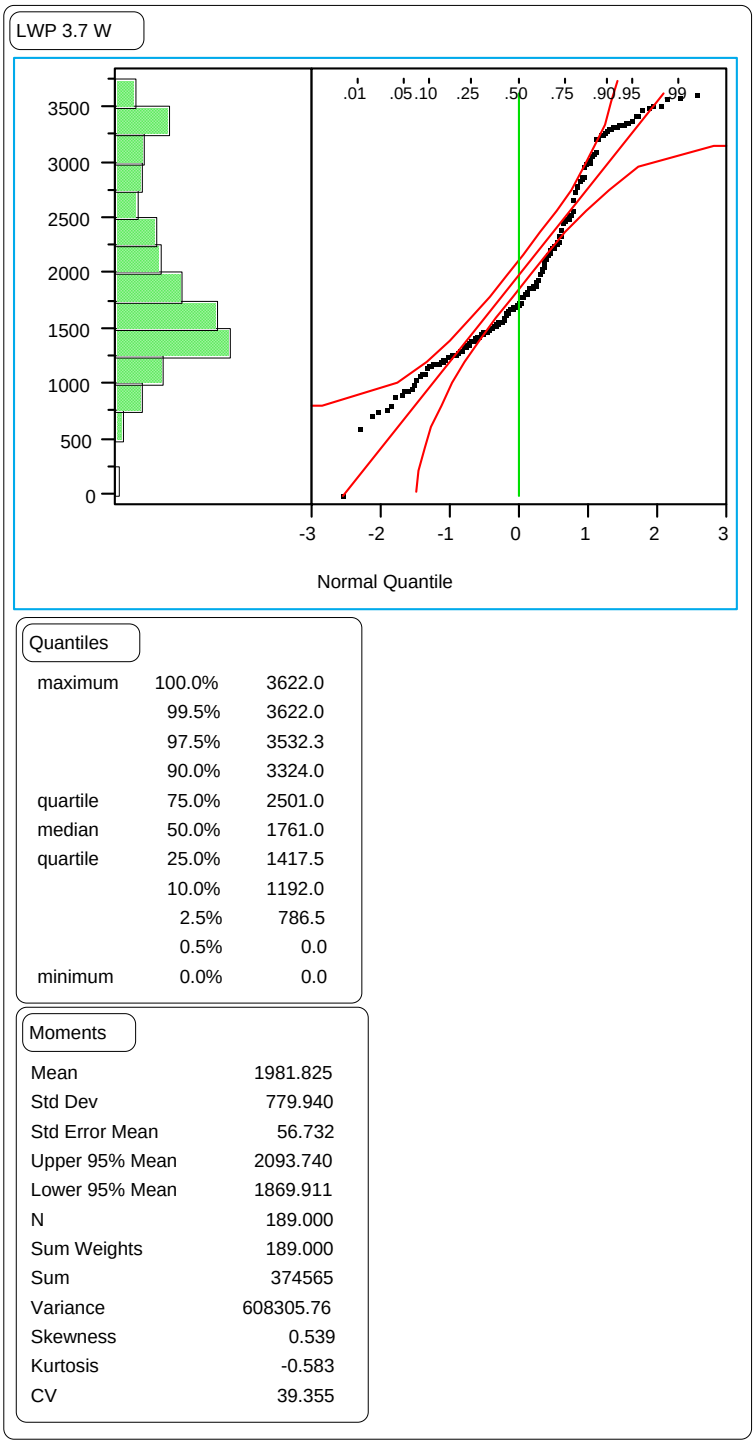

Figure 120. Distribution of the section means of the LWP wire line rut widths on GPS-7 test sections.

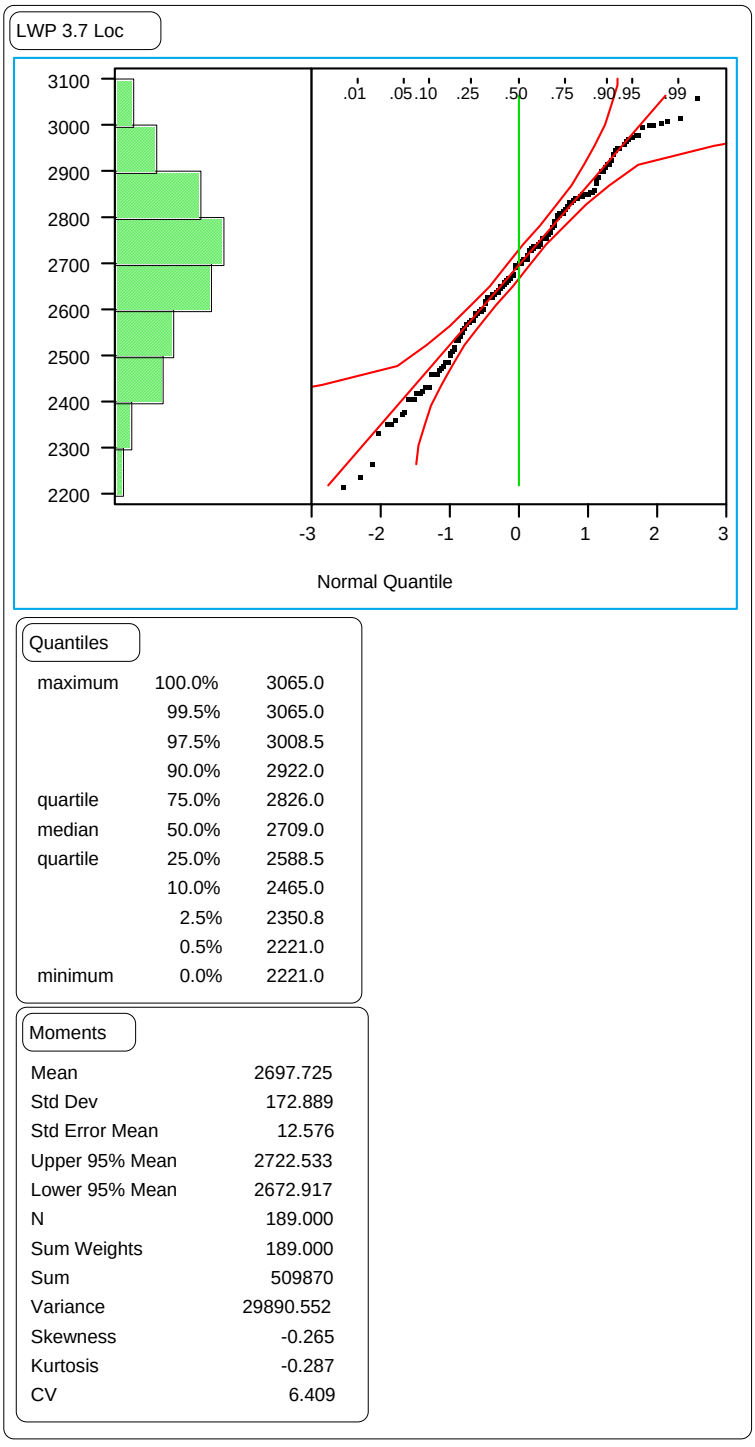

Figure 121. Distribution of the section means of the LWP wire line rut locations on GPS-7 test sections.

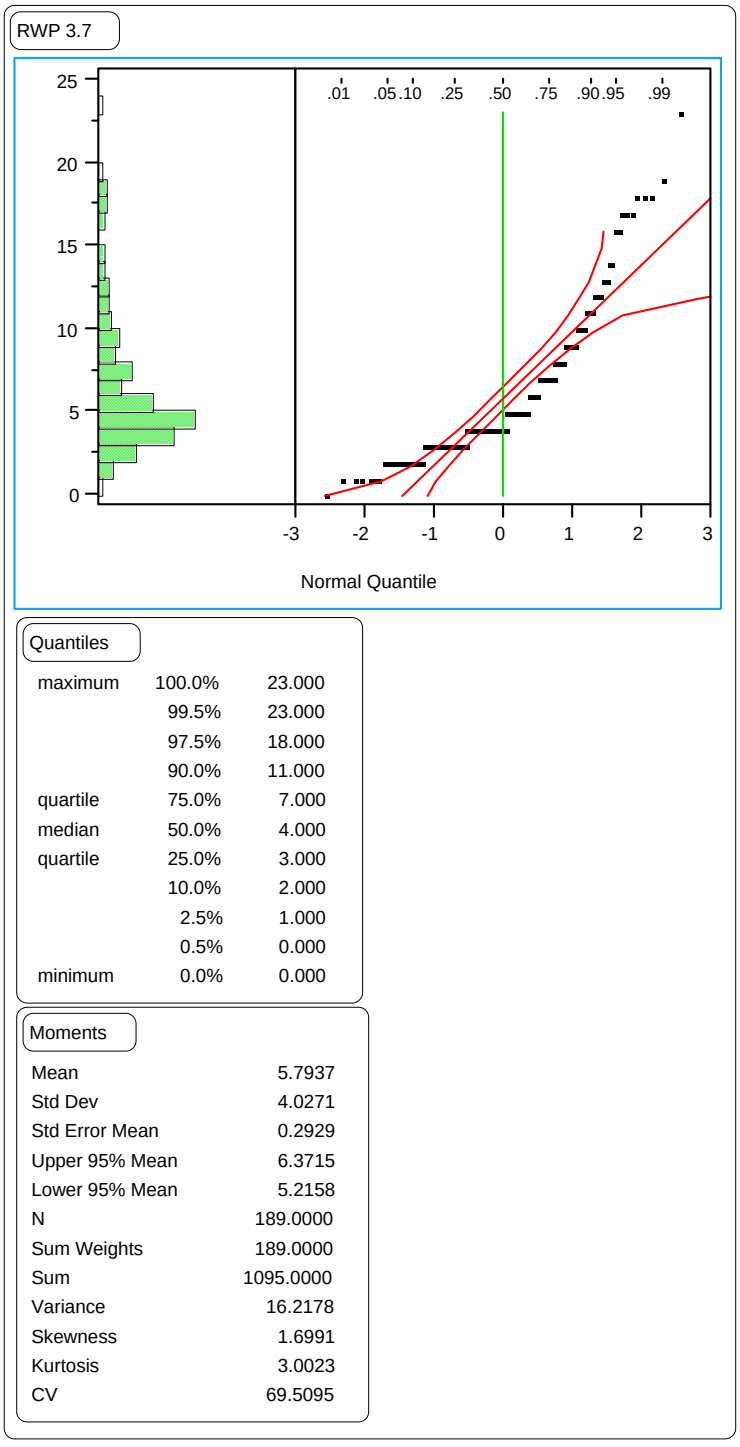

Figure 122. Distribution of the section means of the RWP wire line rut depths on GPS-7 test sections.

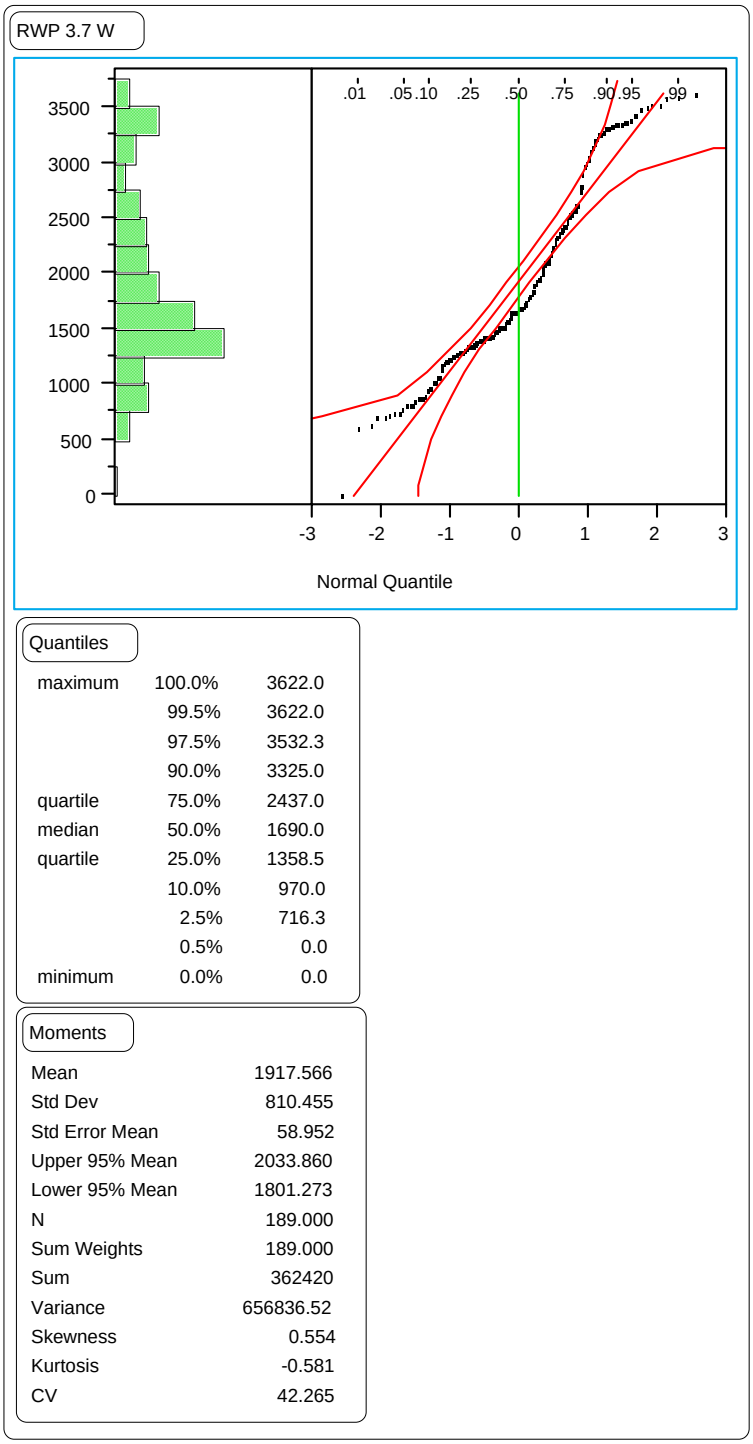

Figure 123. Distribution of the section means of the RWP wire line rut widths on GPS-7 test sections.

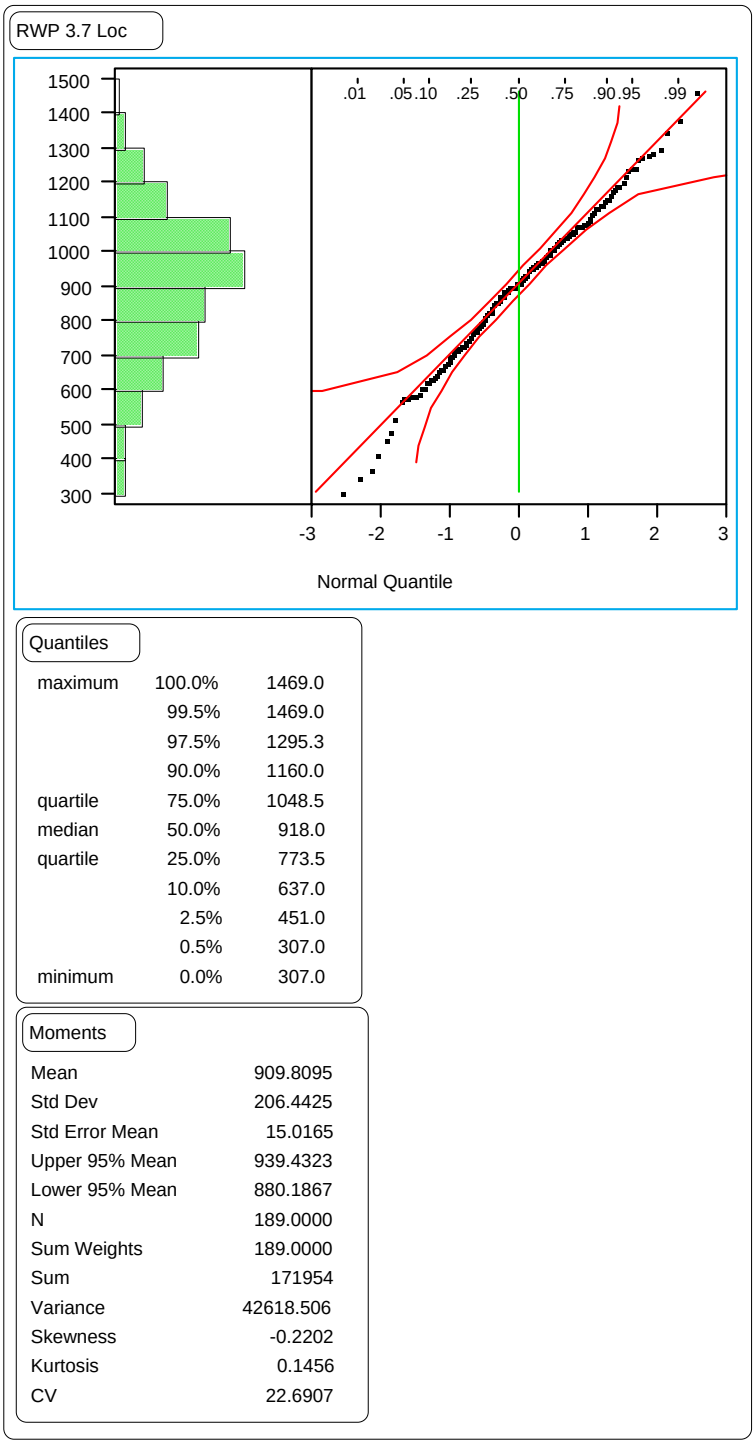

Figure 124. Distribution of the section means of the RWP wire line rut locations on GPS-7 test sections.

APPENDIX C.
COMPARISONS OF SECTION MEANS TO DETERMINE NUMBER OF TRANSVERSE PROFILES NECESSARY

Comparisons were made to determine the number of profiles necessary to accurately predict the mean. Figures 125 through 146 provide the results from these comparisons. In each of these figures, the axis labeled "All" used all of the available profiles to determine the section mean for a given survey date. The axis labeled "Whole" used data from every 30 m to determine the section mean on a given survey date. Pairwise comparisons were then made between the "All" means and the "Whole" means. Figures 125 through 135 used all of the available data to make these comparisons. Figures 136 through 146 used only the data obtained by Dipstick® for these comparisons. The difference between the "All" value and the "Whole" value was determined for each data pair. The mean of these differences is presented as the mean difference. If the value labeled "Prob>|t|" is less than 0.05, the test is statistically significant, which indicates that the two values from each pair of values are from two different populations with a 95 percent level of confidence.

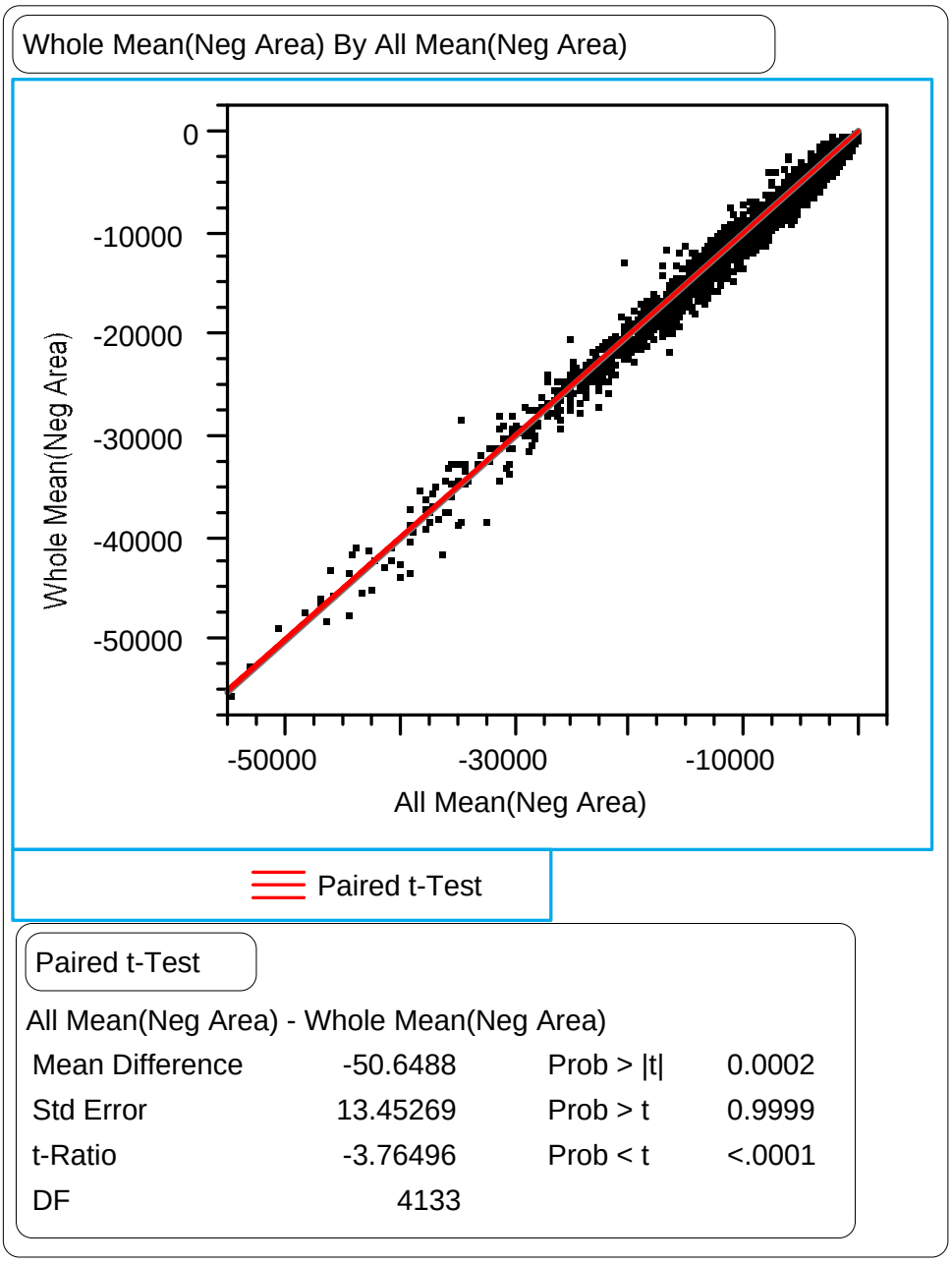

Figure 125. Paired t-test comparing section means from all of the profiles versus those from profiles taken every 30 m for the negative area index.

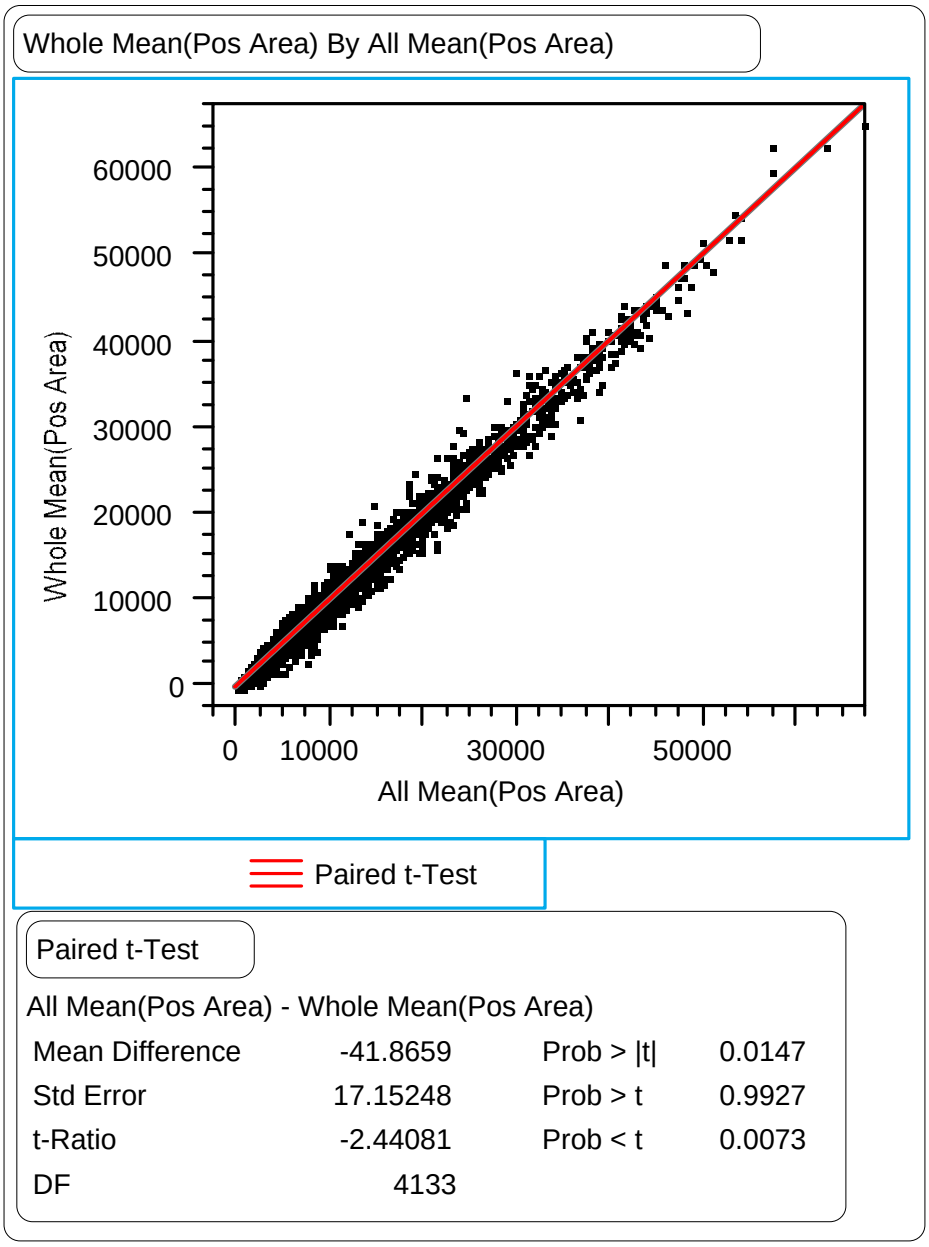

Figure 126. Paired t-test comparing section means from all of the profiles versus those from profiles taken every 30 m for the positive area index.

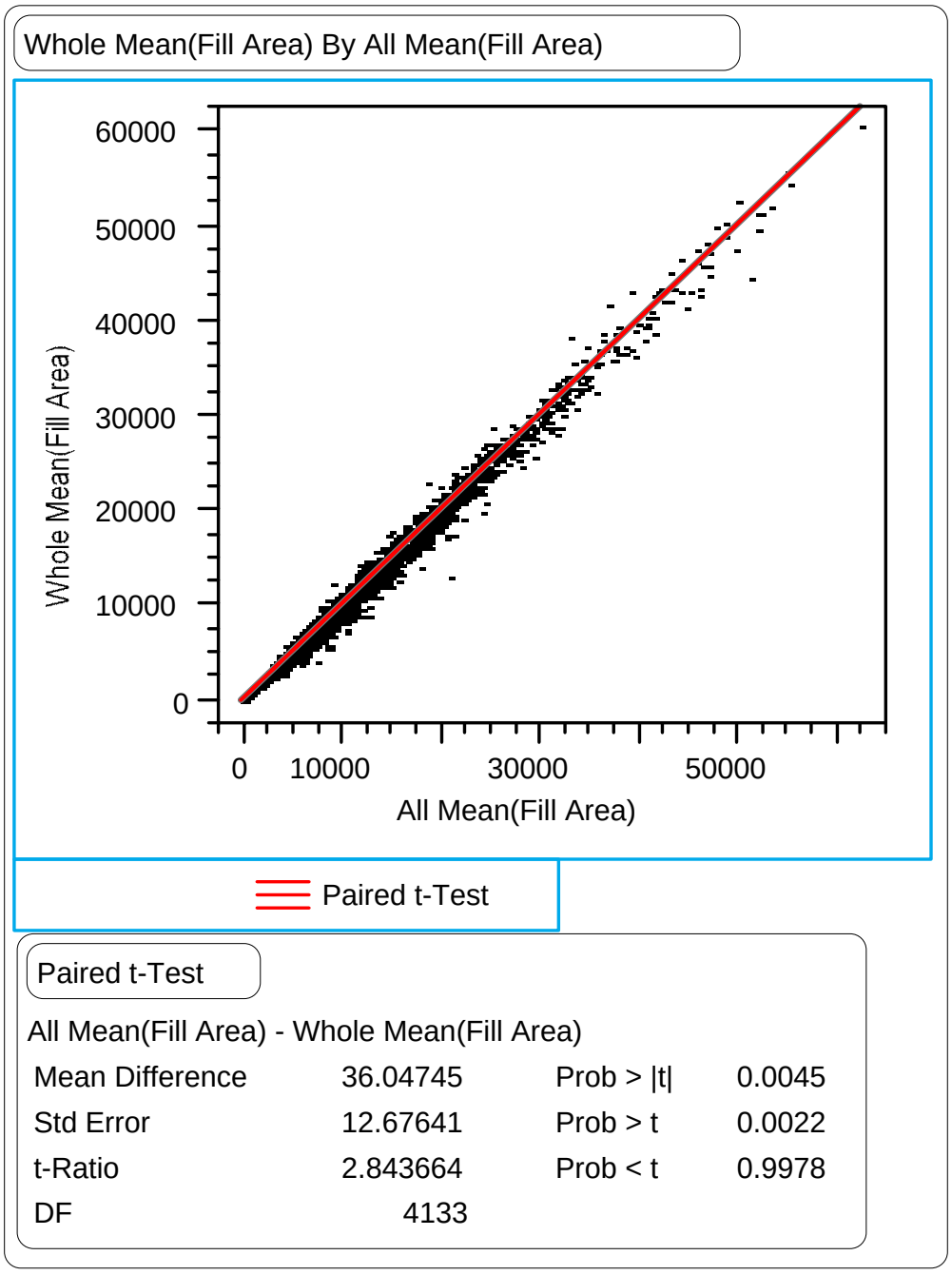

Figure 127. Paired t-test comparing section means from all of the profiles versus those from profiles taken every 30 m for the fill area index.

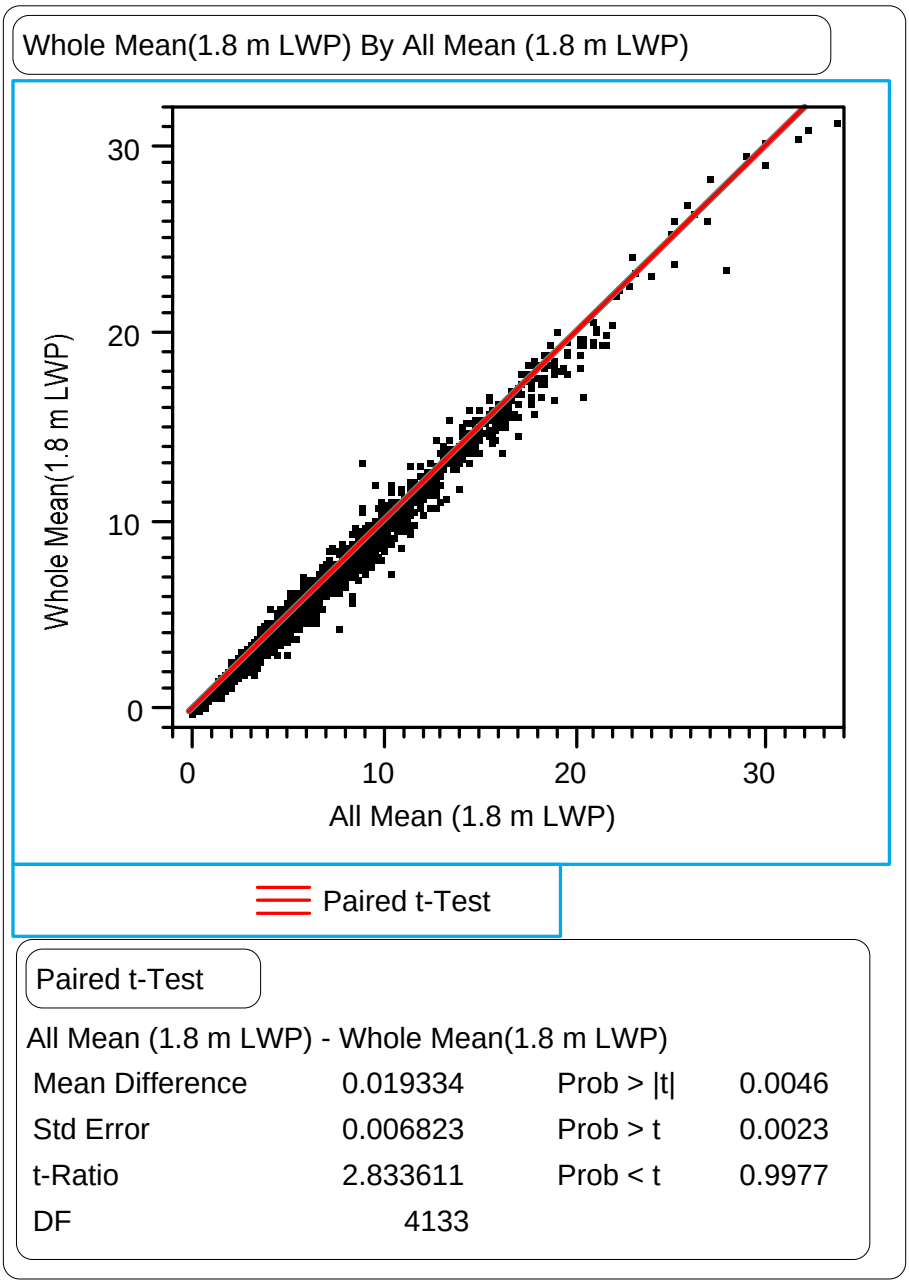

Figure 128. Paired t-test comparing section means from all of the profiles versus those from profiles taken every 30 m for the LWP 1.8-m rut depths.

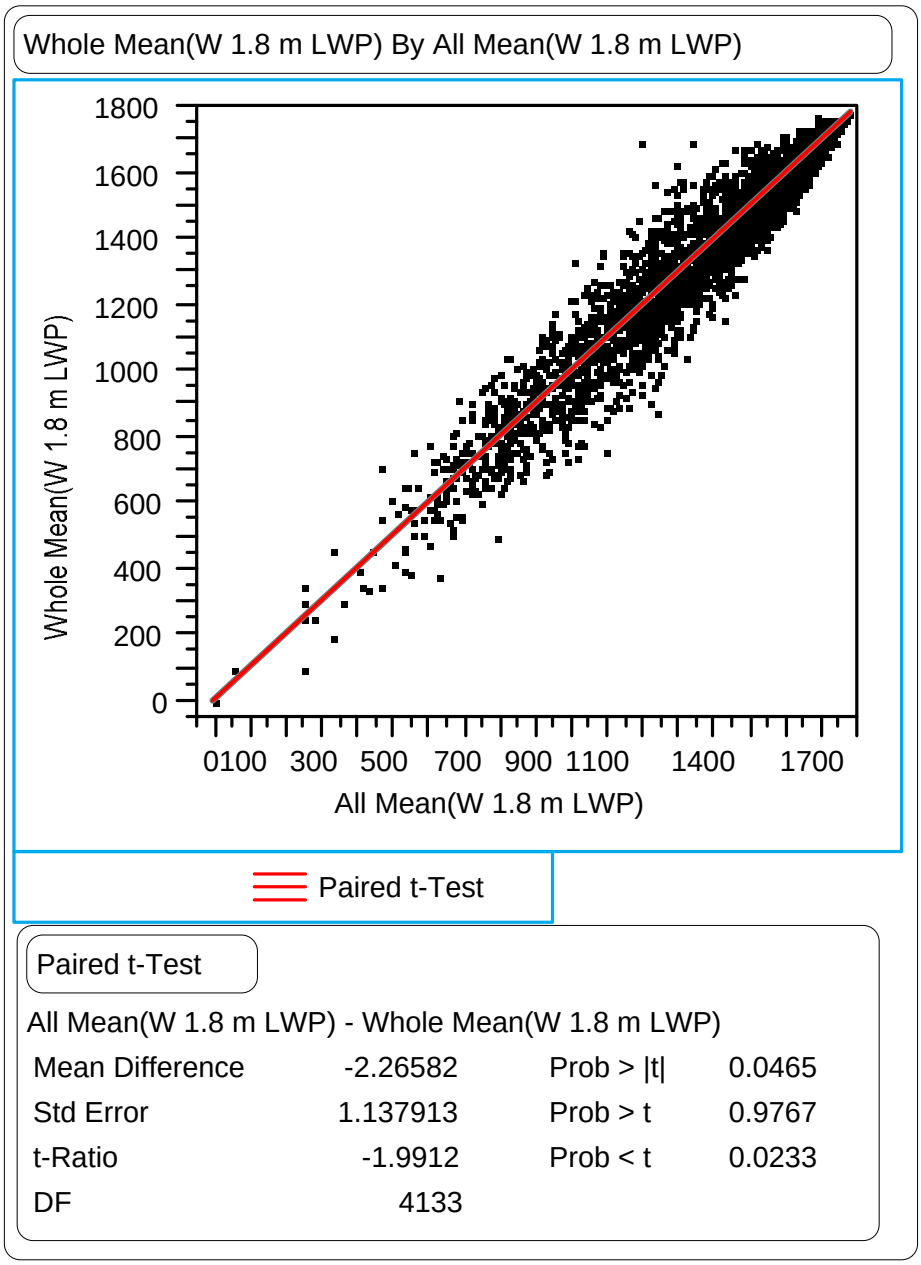

Figure 129. Paired t-test comparing section means from all of the profiles versus those from profiles taken every 30 m for the LWP 1.8-m rut widths.

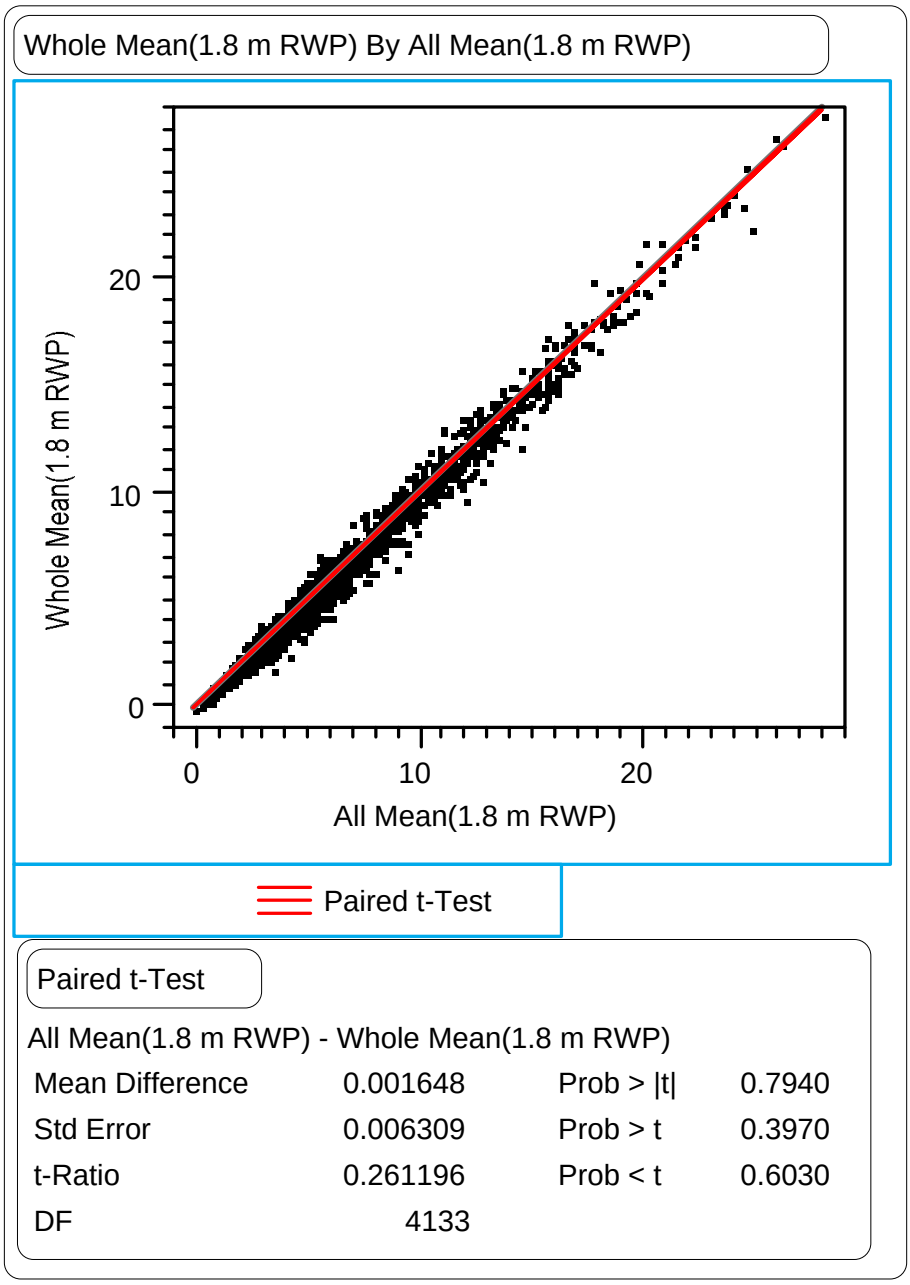

Figure 130. Paired t-test comparing section means from all of the profiles versus those from profiles taken every 30 m for the RWP 1.8-m rut depths.

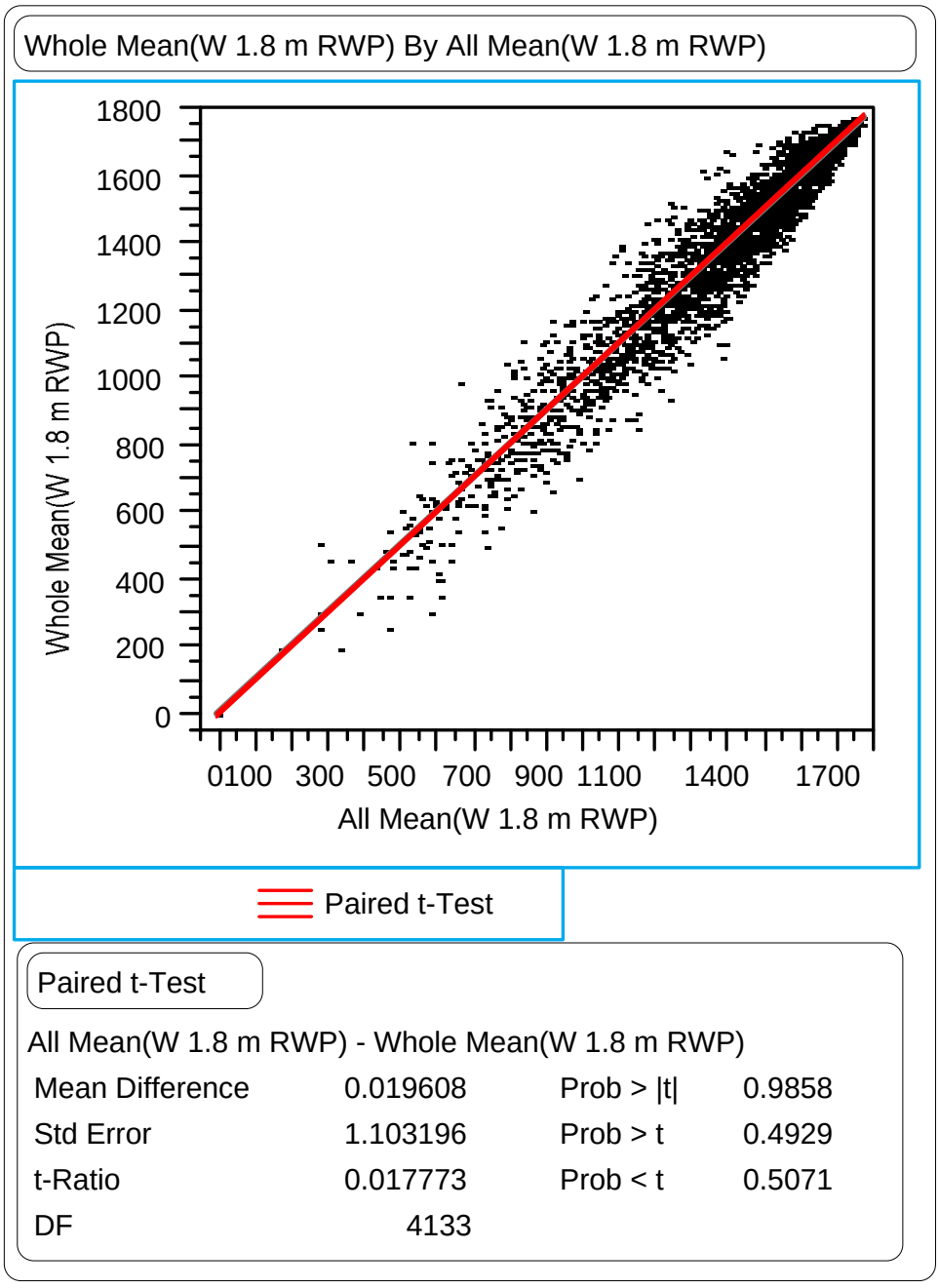

Figure 131. Paired t-test comparing section means from all of the profiles versus those from profiles taken every 30 m for the RWP 1.8-m rut widths.

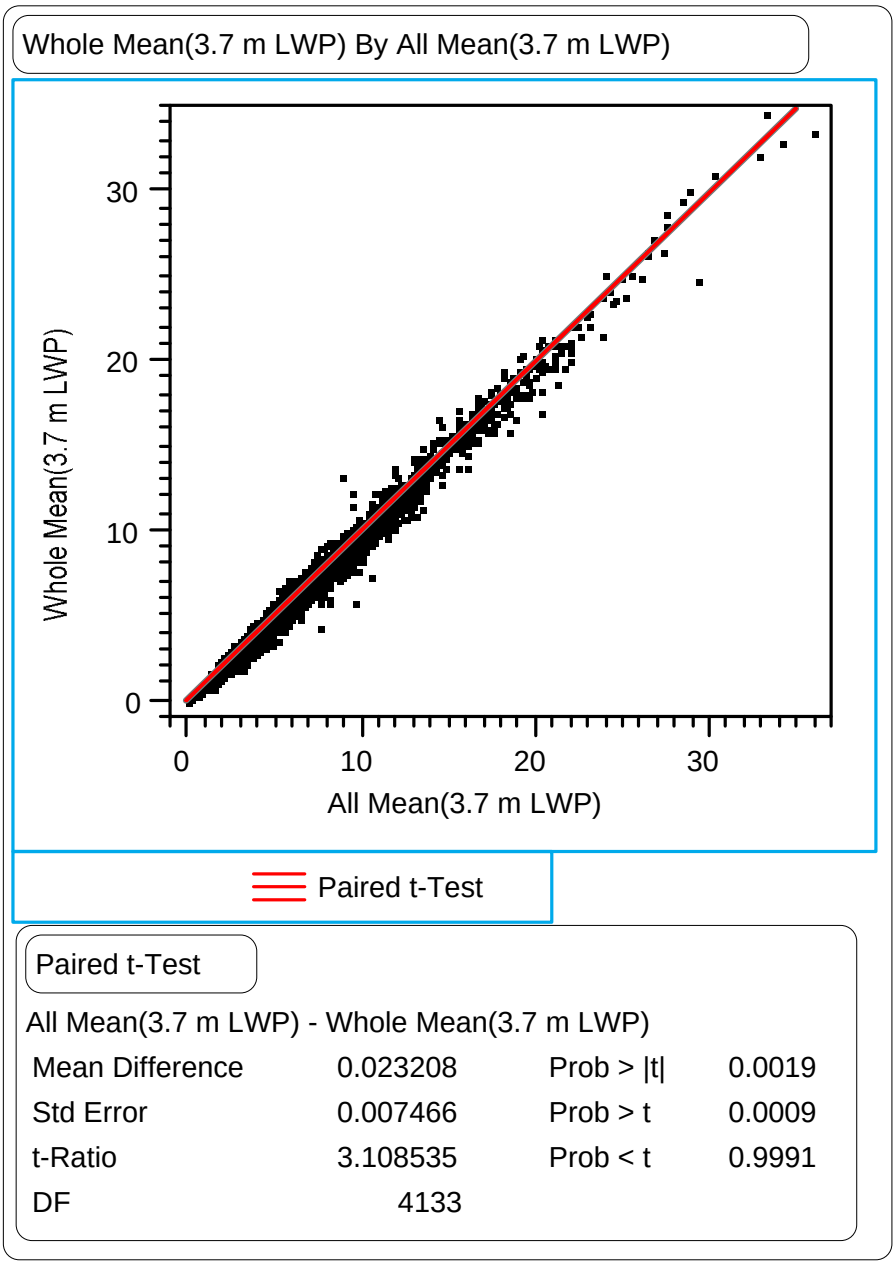

Figure 132. Paired t-test comparing section means from all of the profiles versus those from profiles taken every 30 m for the LWP wire line rut depths.

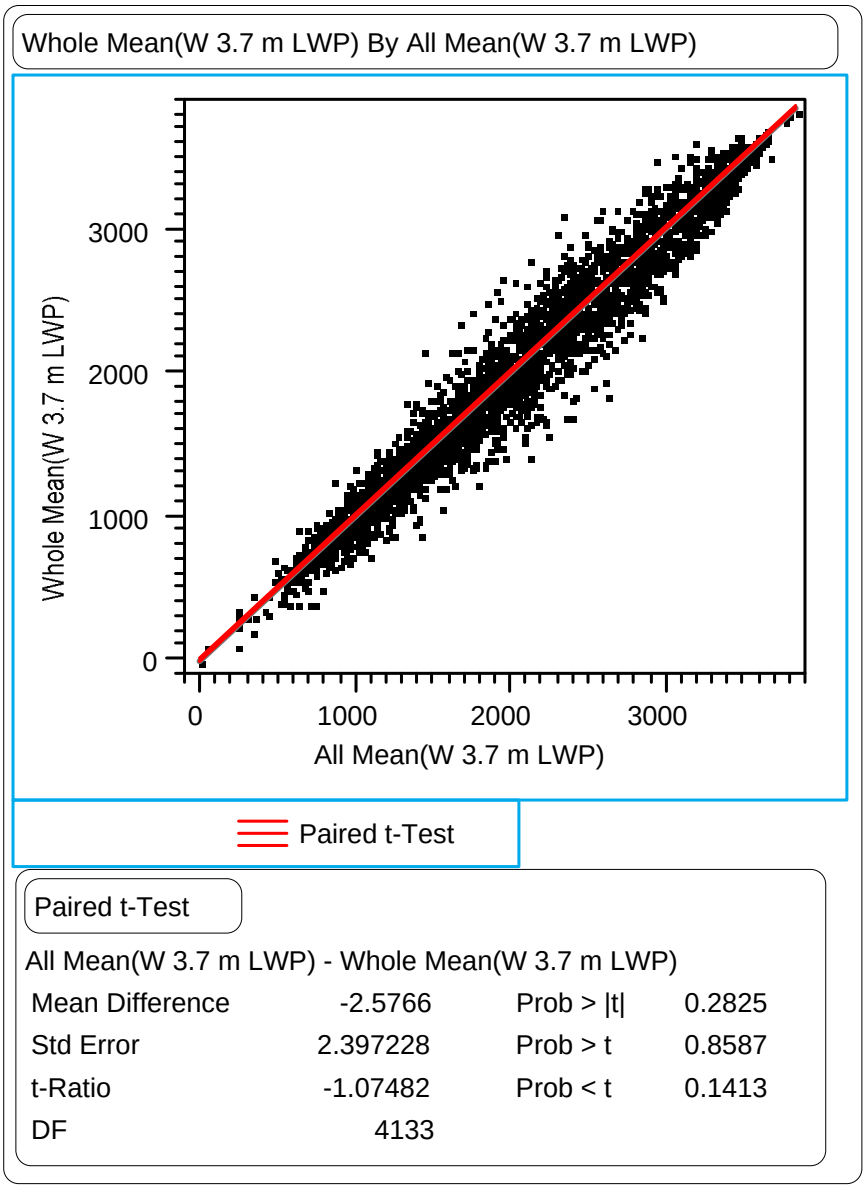

Figure 133. Paired t-test comparing section means from all of the profiles versus those from profiles taken every 30 m for the LWP wire line rut widths.

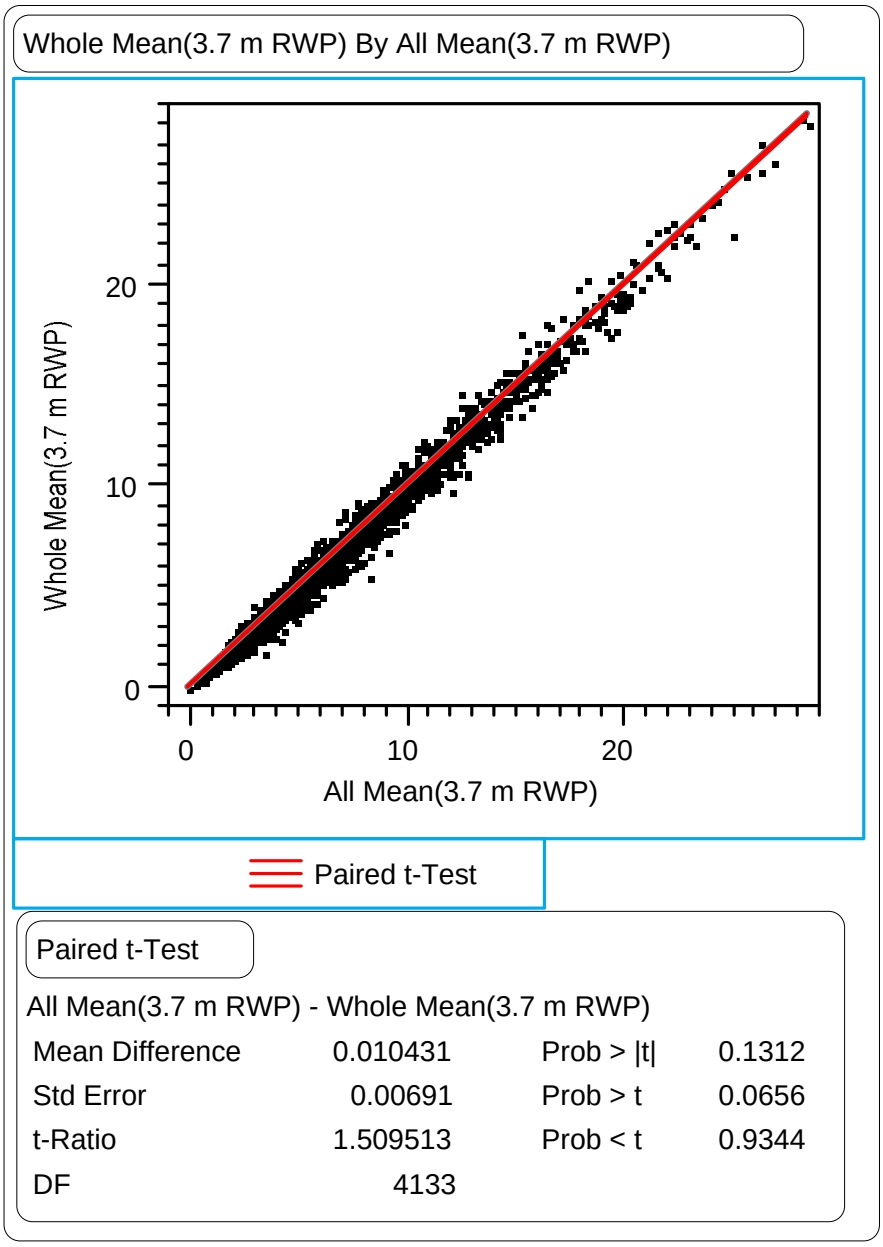

Figure 134. Paired t-test comparing section means from all of the profiles versus those from profiles taken every 30 m for the RWP wire line rut depths.

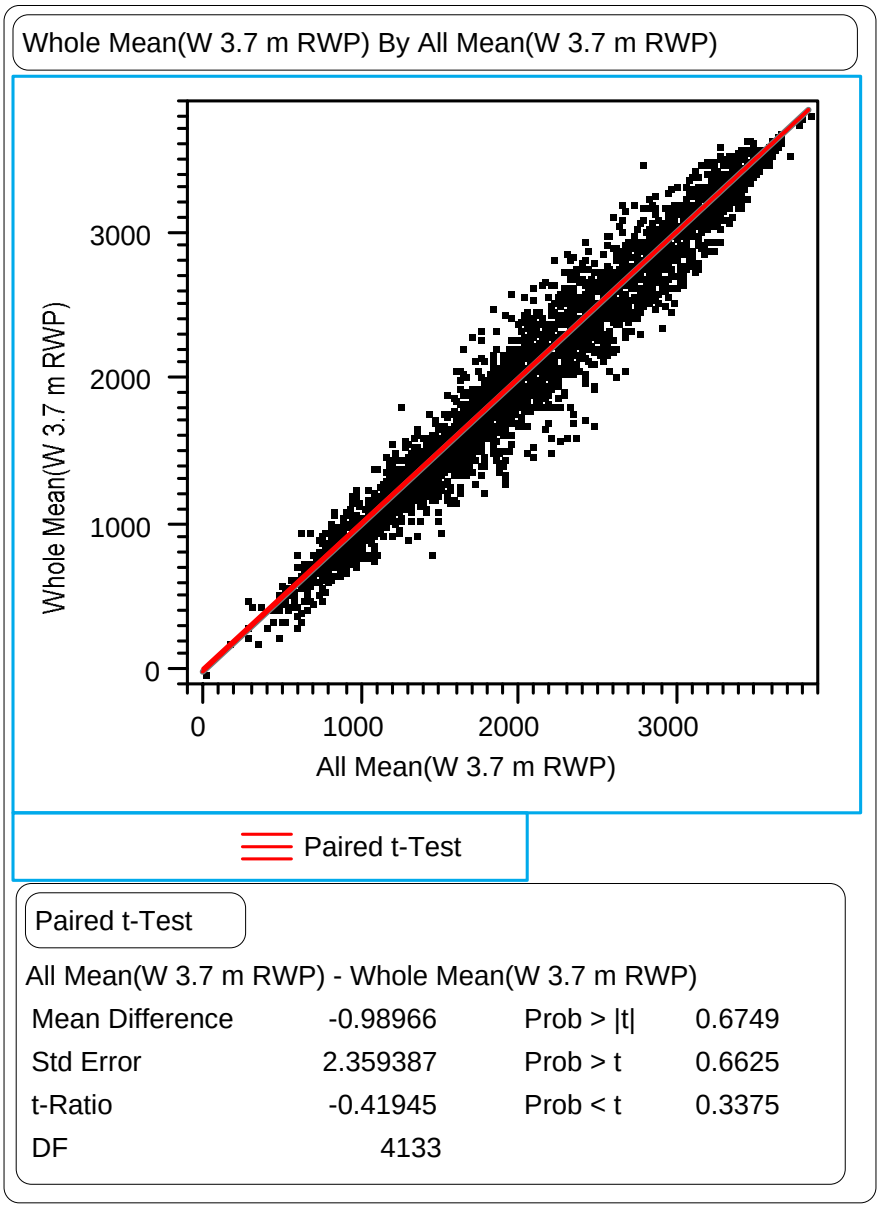

Figure 135. Paired t-test comparing section means from all of the profiles versus those from profiles taken every 30 m for the RWP wire line rut widths.

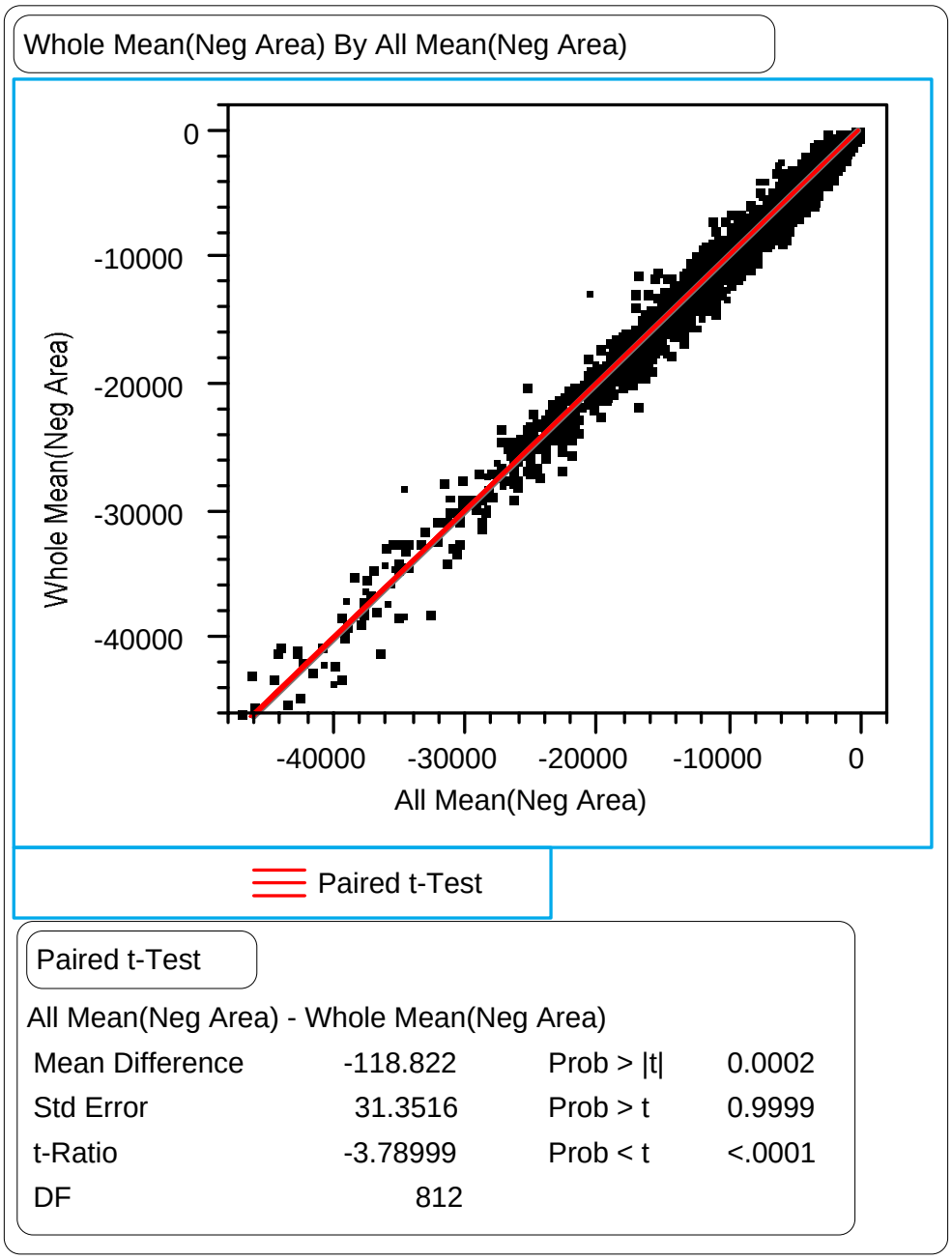

Figure 136. Paired t-test comparing section means from all of the profiles versus those from profiles taken every 30 m for data collected by Dipstick® for the negative area index.

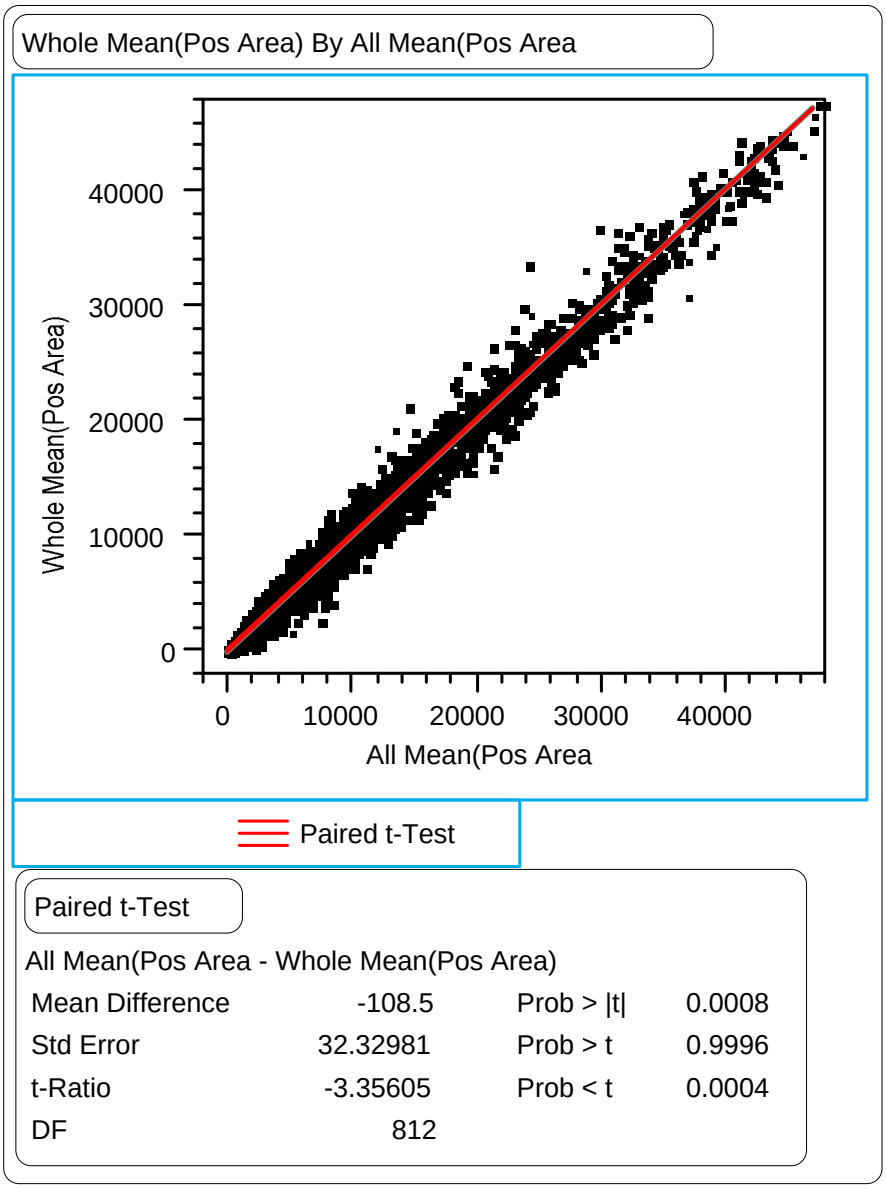

Figure 137. Paired t-test comparing section means from all of the profiles versus those from profiles taken every 30 m for data collected by Dipstick® for the positive area index.

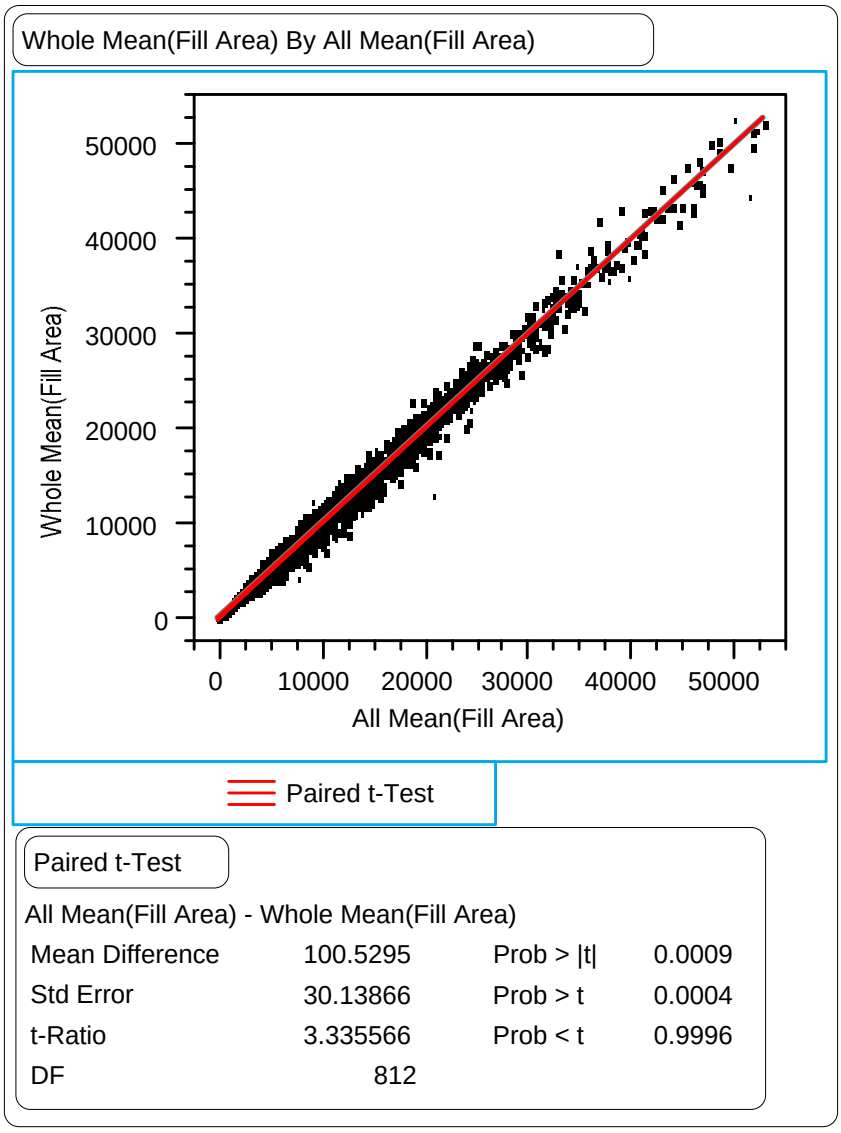

Figure 138. Paired t-test comparing section means from all of the profiles versus those from profiles taken every 30 m for data collected by Dipstick® for the fill area index.

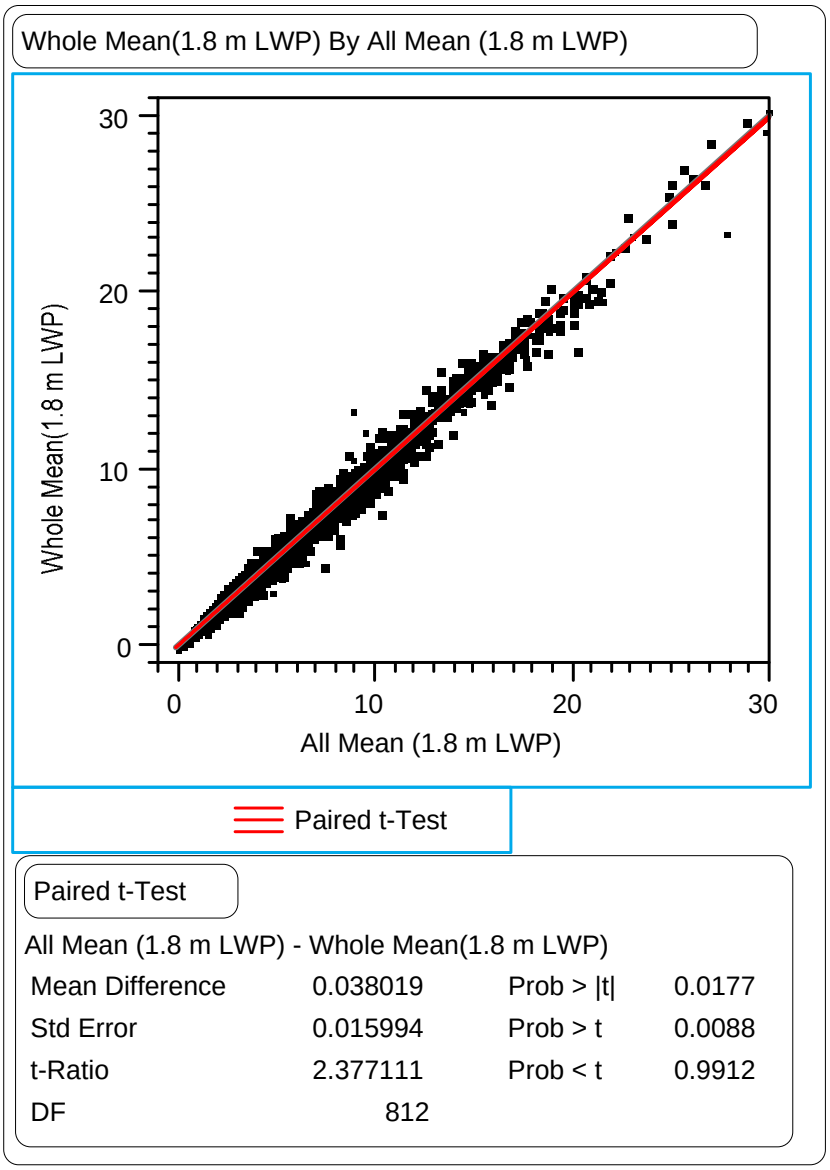

Figure 139. Paired t-test comparing section means from all of the profiles versus those from profiles taken every 30 m for data collected by Dipstick® for the LWP 1.8-m rut depths.

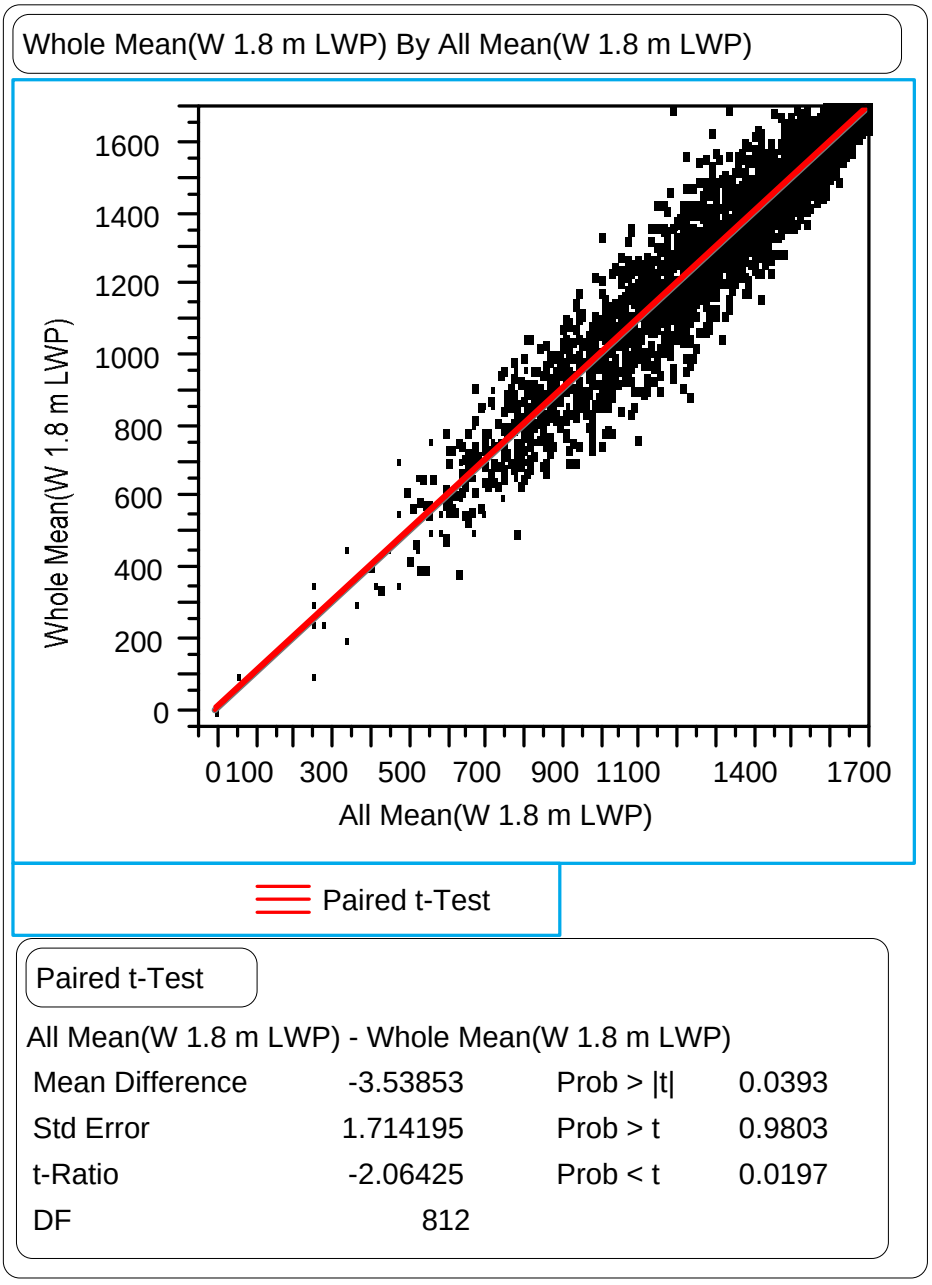

Figure 140. Paired t-test comparing section means from all of the profiles versus those from profiles taken every 30 m for data collected by Dipstick® for the LWP 1.8-m rut widths.

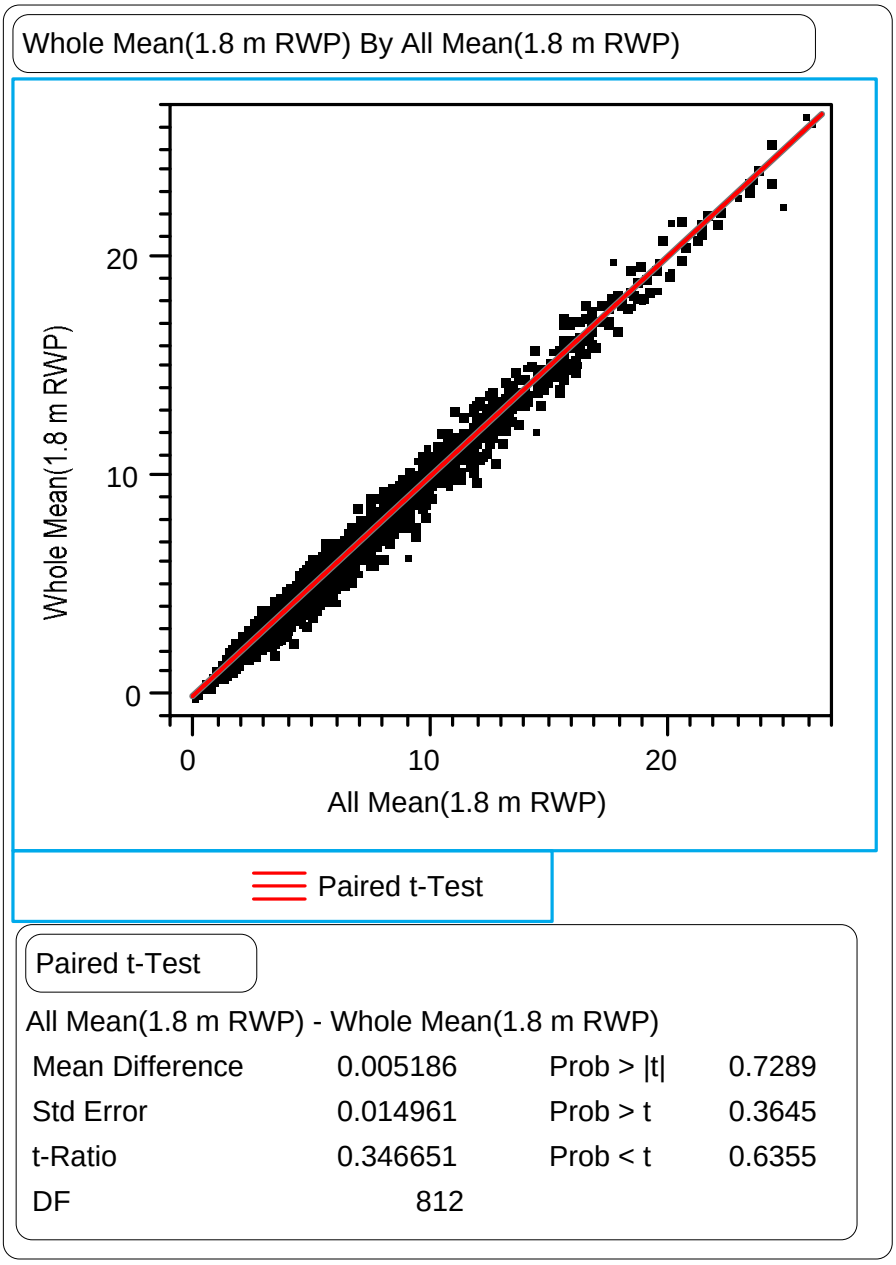

Figure 141. Paired t-test comparing section means from all of the profiles versus those from profiles taken every 30 m for data collected by Dipstick® for the RWP 1.8-m rut depths.

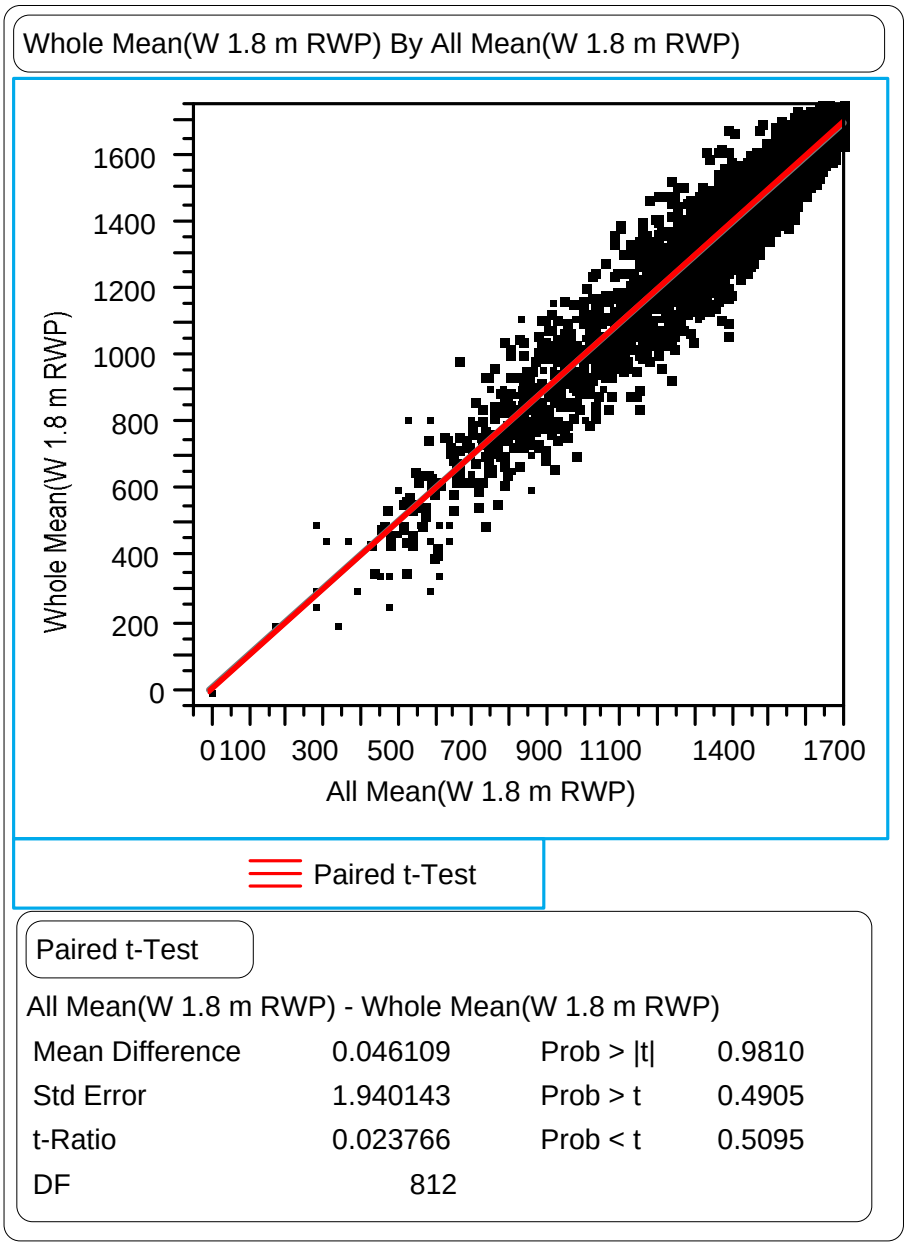

Figure 142. Paired t-test comparing section means from all of the profiles versus those from profiles taken every 30 m for data collected by Dipstick® for the RWP 1.8-m rut widths.

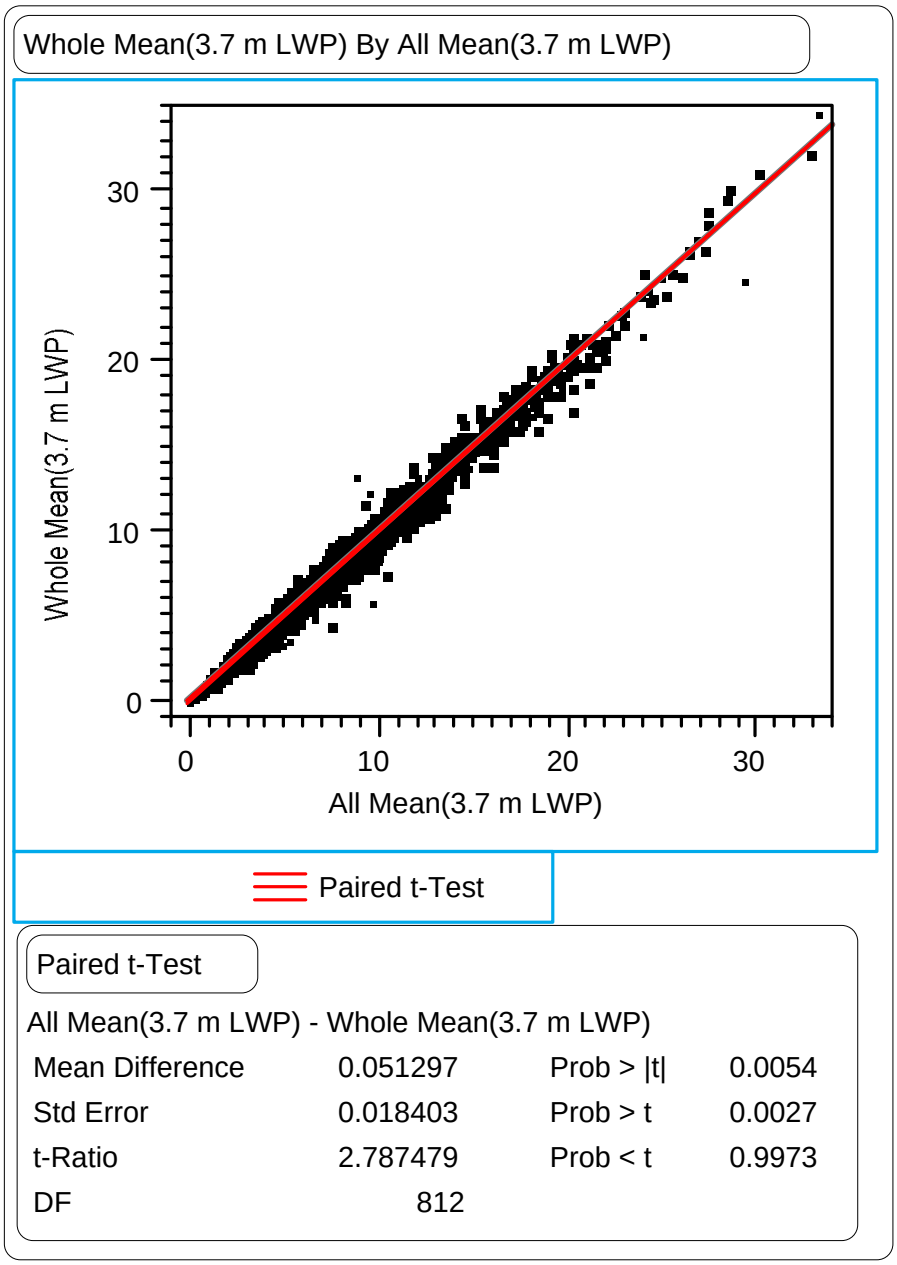

Figure 143. Paired t-test comparing section means from all of the profiles versus those from profiles taken every 30 m for data collected by Dipstick® for the LWP wire line rut depths.

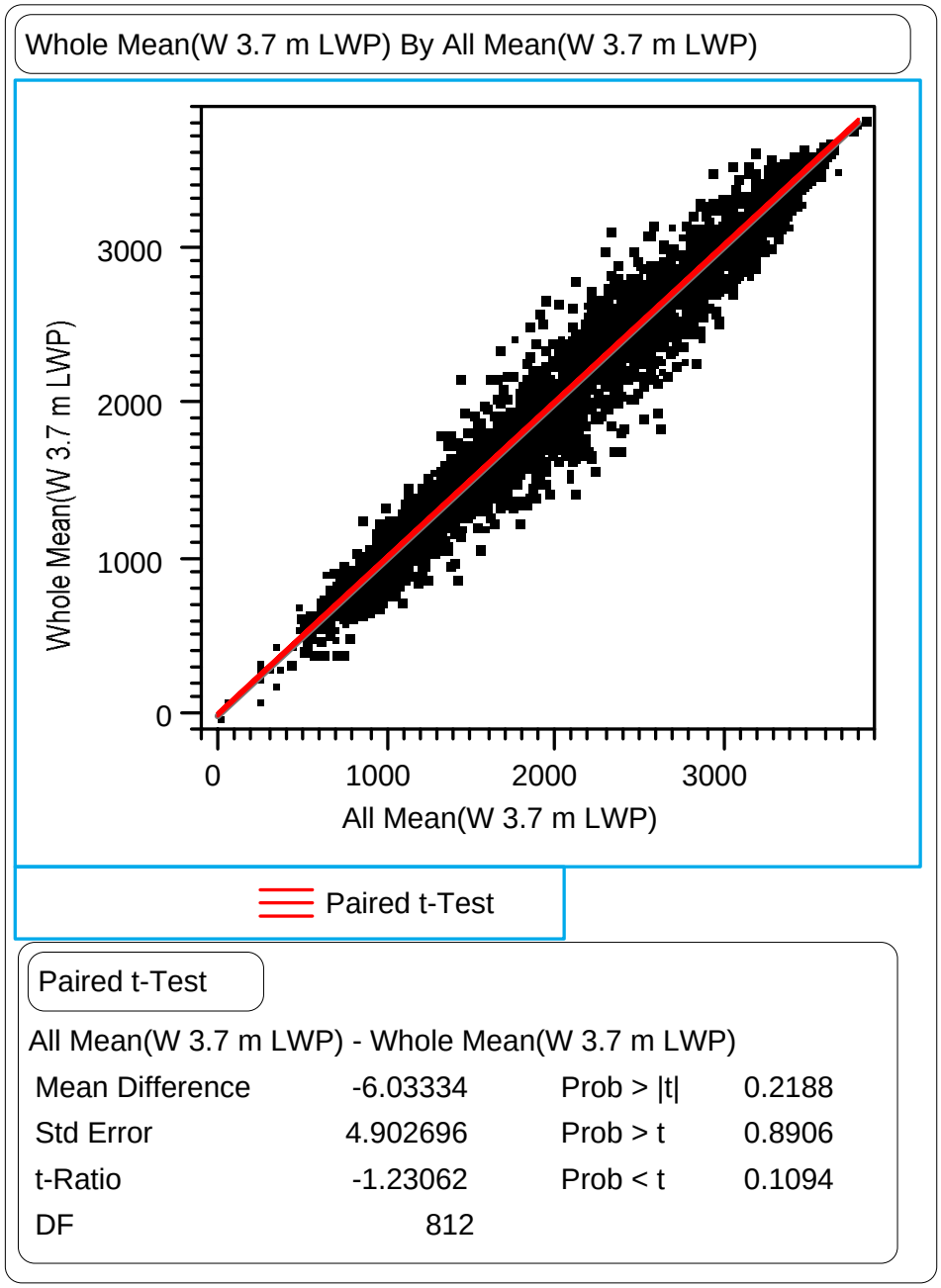

Figure 144. Paired t-test comparing section means from all of the profiles versus those from profiles taken every 30 m for data collected by Dipstick® for the LWP wire line rut widths.

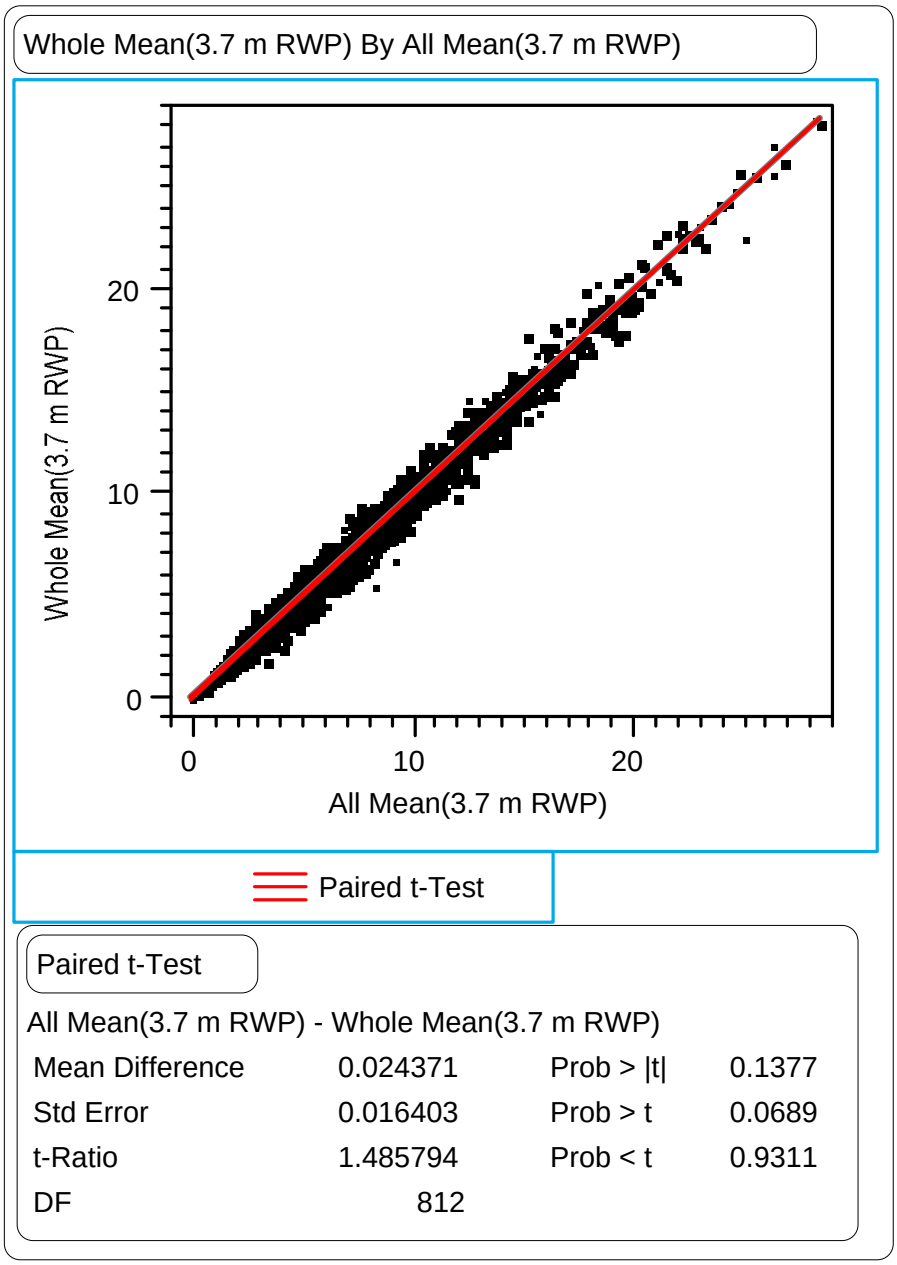

Figure 145. Paired t-test comparing section means from all of the profiles versus those from profiles taken every 30 m for data collected by Dipstick® for the RWP wire line rut depths.

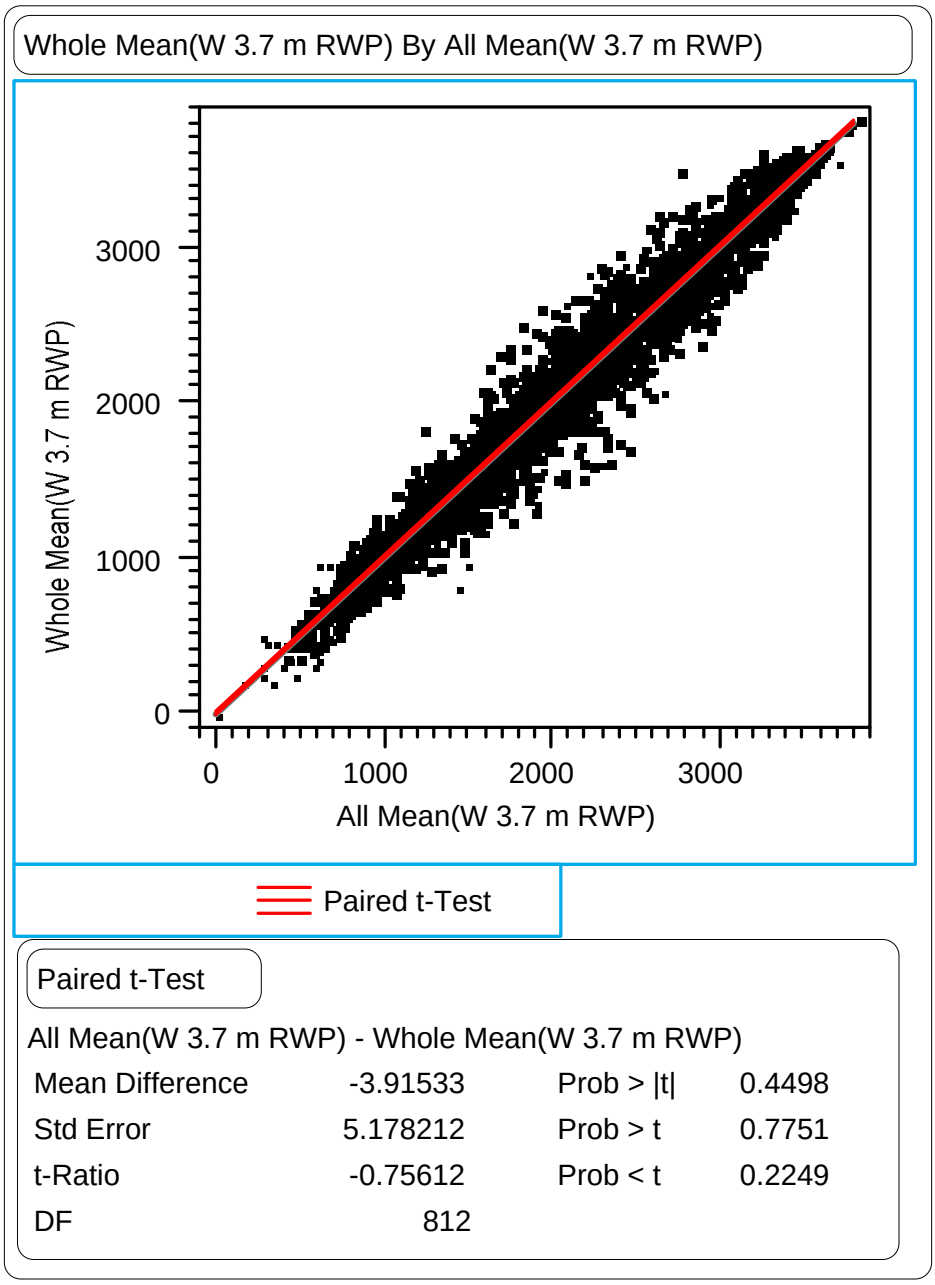

Figure 146. Paired t-test comparing section means from all of the profiles versus those from profiles taken every 30 m for data collected by Dipstick® for the RWP wire line rut widths.

APPENDIX D.
t-TESTS COMPARING VARIOUS PAVEMENT PARAMETERS

These are the comparisons that were performed in chapter 4. Figures 147 through 157 provide the results of the comparisons of each index for the GPS-1 (HMAC over granular base) section means and the GPS-7 (HMAC overlay of PCC) section means. The top box of each figure provides a graphical review of the results. The middle box provides the results from a t-test for comparing means with equal variances at an α-level of 5 percent. The bottom box provides the results of a comparison of the variances between the groups and an ANOVA test in case the variances are not equal. Figures 158 through 168 provide the results of the comparisons of the GPS-1 (HMAC over granular base) and GPS-2 (HMAC over stabilized base) sections by surface thickness. Figures 169 through 179 provide the results of the comparisons of granular versus stabilized base types for GPS-1 and GPS-2 sections with less than 127 mm of HMAC surface. Figures 180 through 190 provide the results of the comparisons of asphalt stabilized bases to cement stabilized bases for GPS-1 and GPS-2 sections with less than 127 mm of HMAC surface. Figures 191 through 201 provide the results of the comparisons between the freeze (F) zone and the no freeze (NF) zone for the GPS-7 test sections. The bottom half of the upper box of numbers provides the results of the t-tests comparing each set of values. If the value in the table is positive, the difference is statistically significant, which means that the data sets are from two different populations with a 95 percent level of confidence. The bottom box provides a comparison of the standard deviations. The column of numbers provided under the heading "Prob>F" are the probabilities of getting an F-ratio that large given that the standard deviations are the same. A value of 0.05 or less is statistically significant.

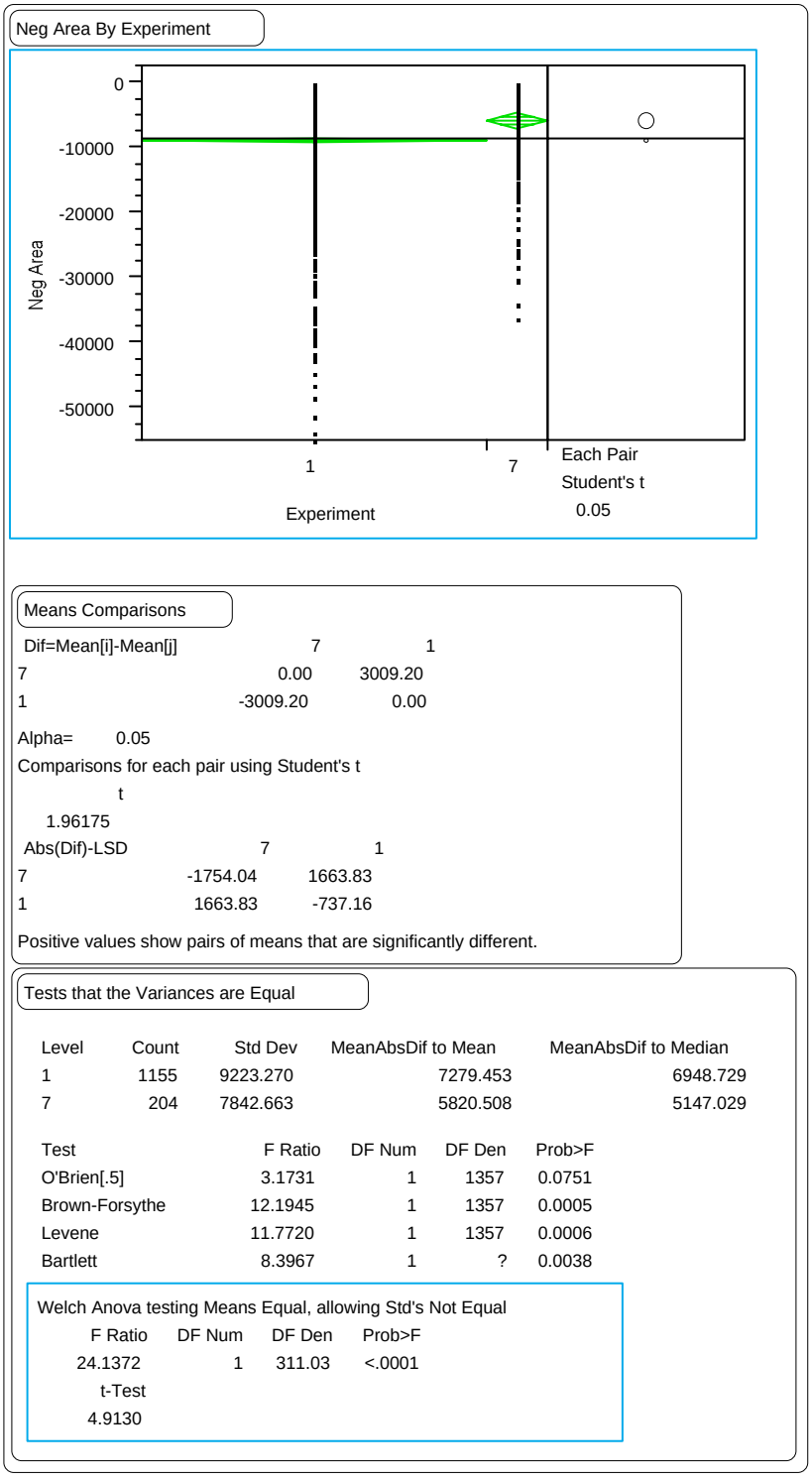

Means Comparisons

Dif=Mean[i]-Mean[j]	7	1
7	0.00	3009.20
1	-3009.20	0.00

Alpha= 0.05

Comparisons for each pair using Student's t

t

1.96175

Abs(Dif)-LSD	7	1
7	-1754.04	1663.83
1	1663.83	-737.16

Positive values show pairs of means that are significantly different.

Tests that the Variances are Equal

Level	Count	Std Dev	MeanAbsDif to Mean	MeanAbsDif to Median
1	1155	9223.270	7279.453	6948.729
7	204	7842.663	5820.508	5147.029

Test	F Ratio	DF Num	DF Den	Prob>F
O'Brien[.5]	3.1731	1	1357	0.0751
Brown-Forsythe	12.1945	1	1357	0.0005
Levene	11.7720	1	1357	0.0006
Bartlett	8.3967	1	?	0.0038

Welch Anova testing Means Equal, allowing Std's Not Equal

F Ratio	DF Num	DF Den	Prob>F
24.1372	1	311.03	<.0001

t-Test

4.9130

Figure 147. Paired t-test comparing GPS-1 section means versus GPS-7 section means for the negative area index.

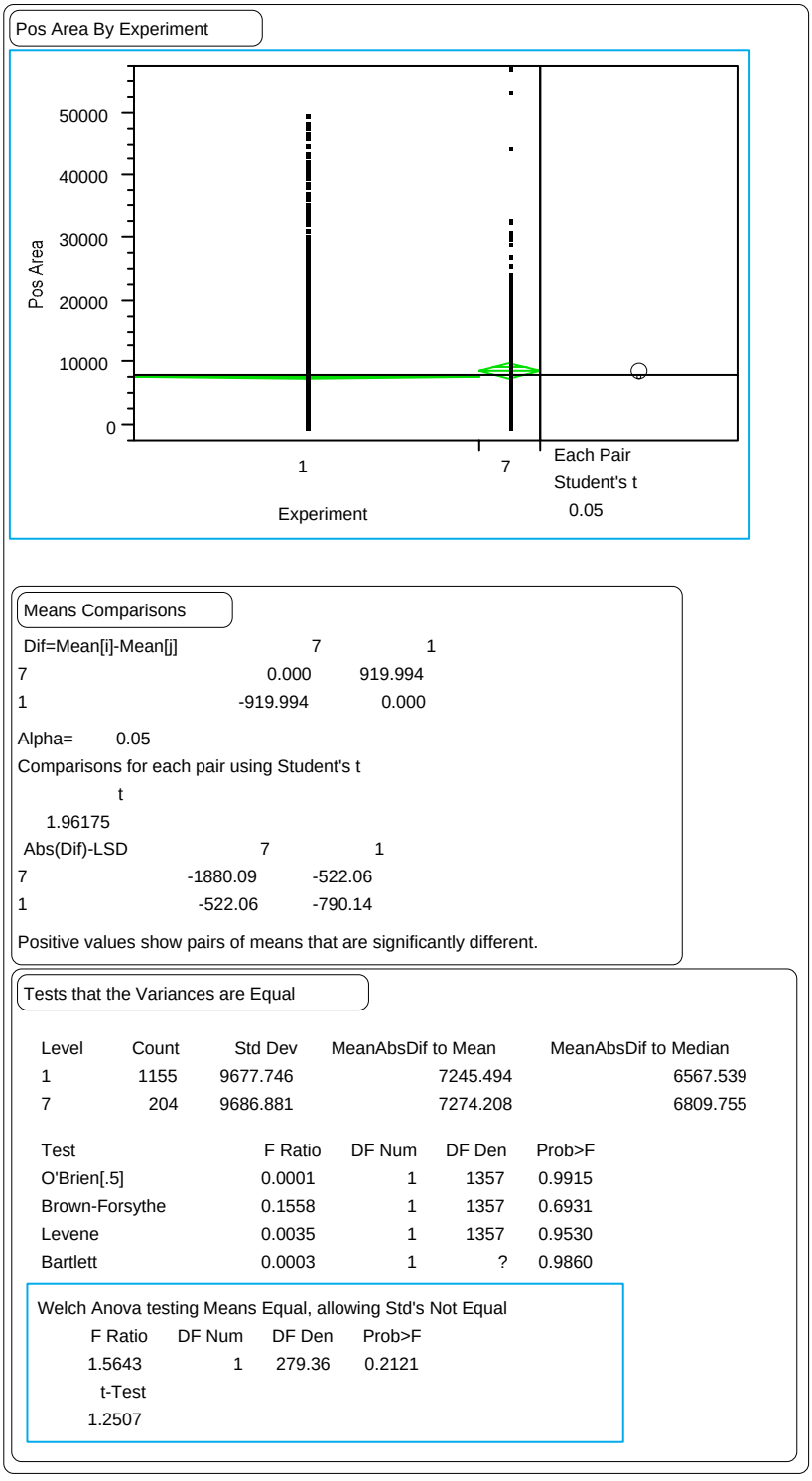

Figure 148. Paired t-test comparing GPS-1 section means versus GPS-7 section means for the positive area index.

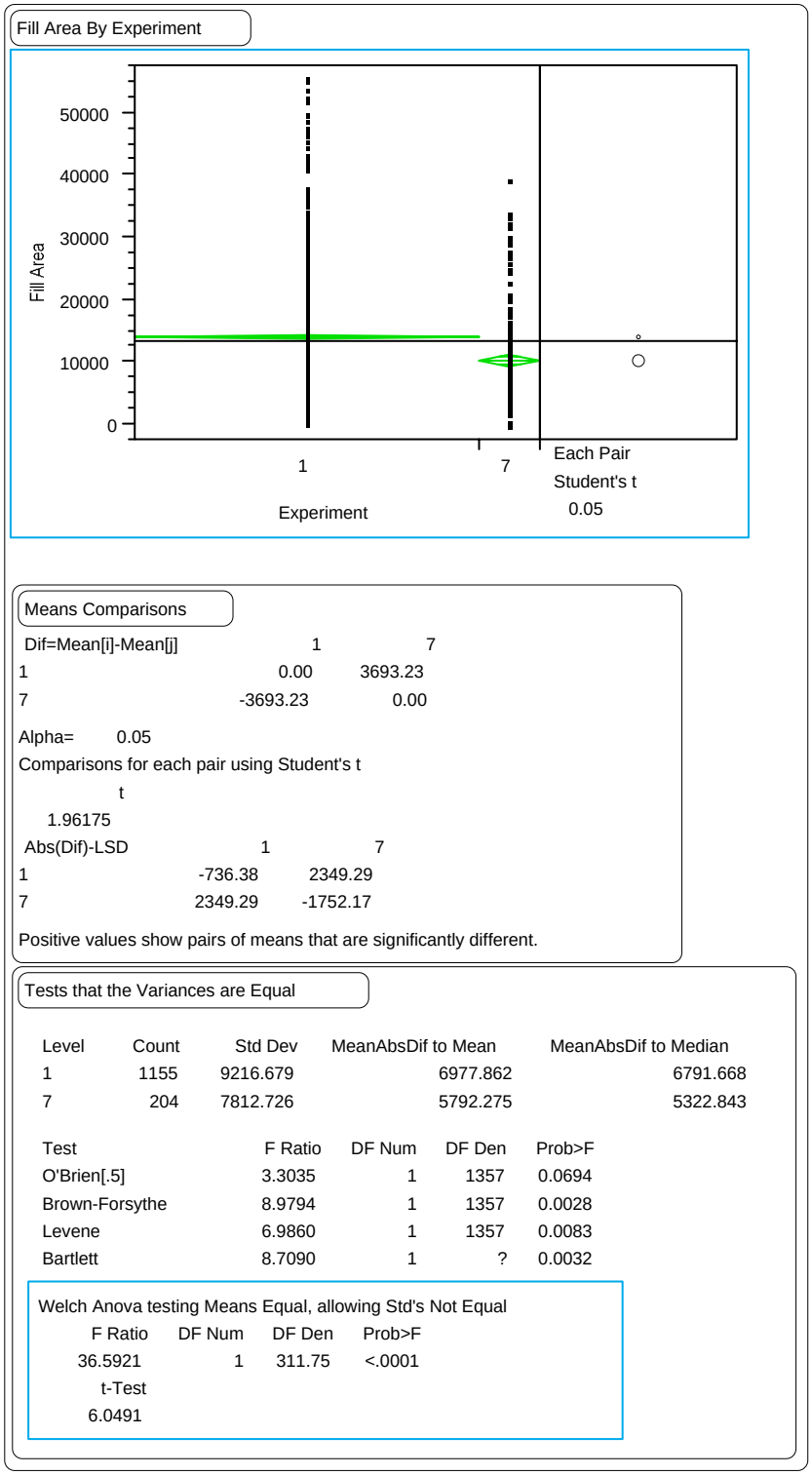

Figure 149. Paired t-test comparing GPS-1 section means versus GPS-7 section means for the fill area index.

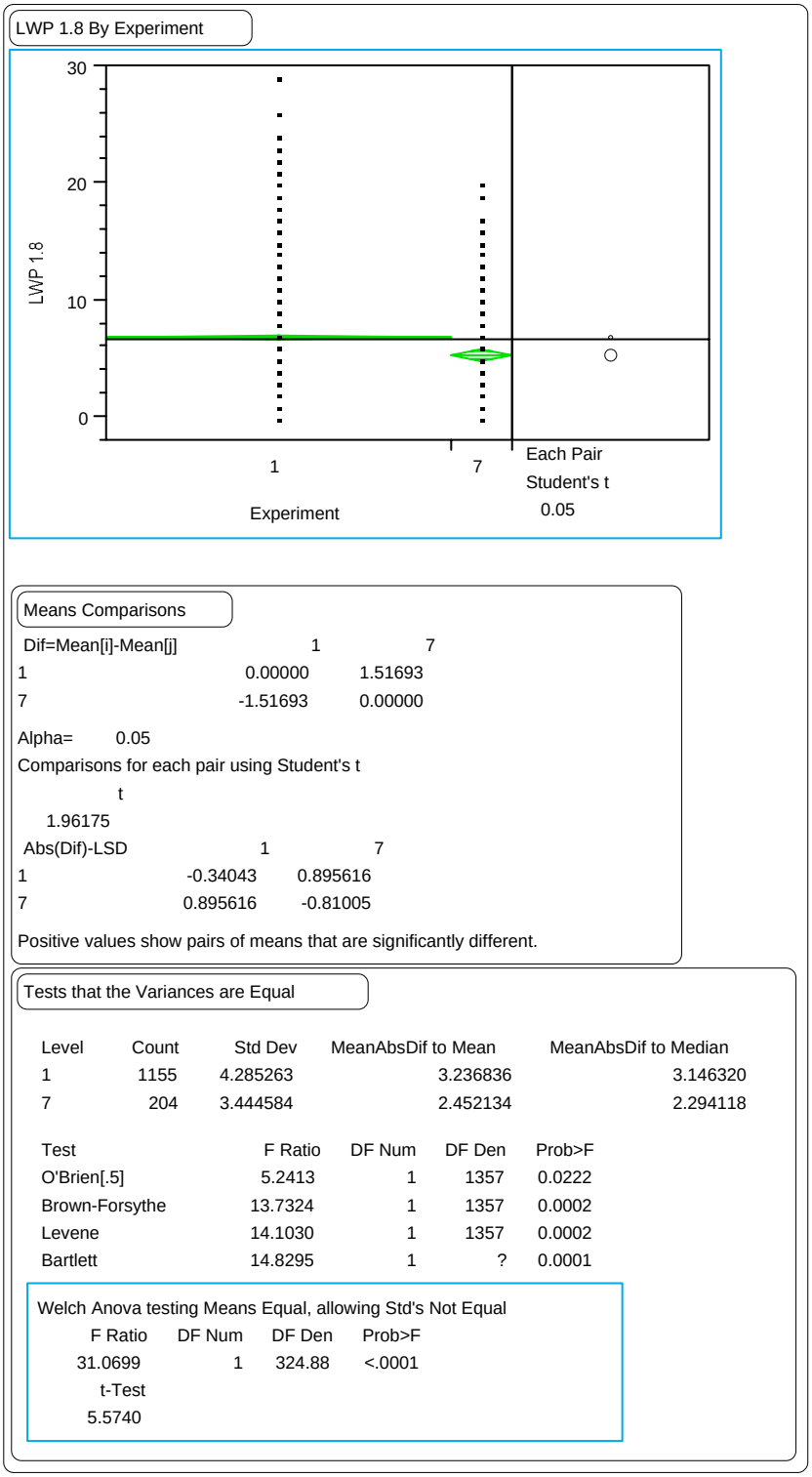

Figure 150. Paired t-test comparing GPS-1 section means versus GPS-7 section means for the LWP 1.8-m rut depths.

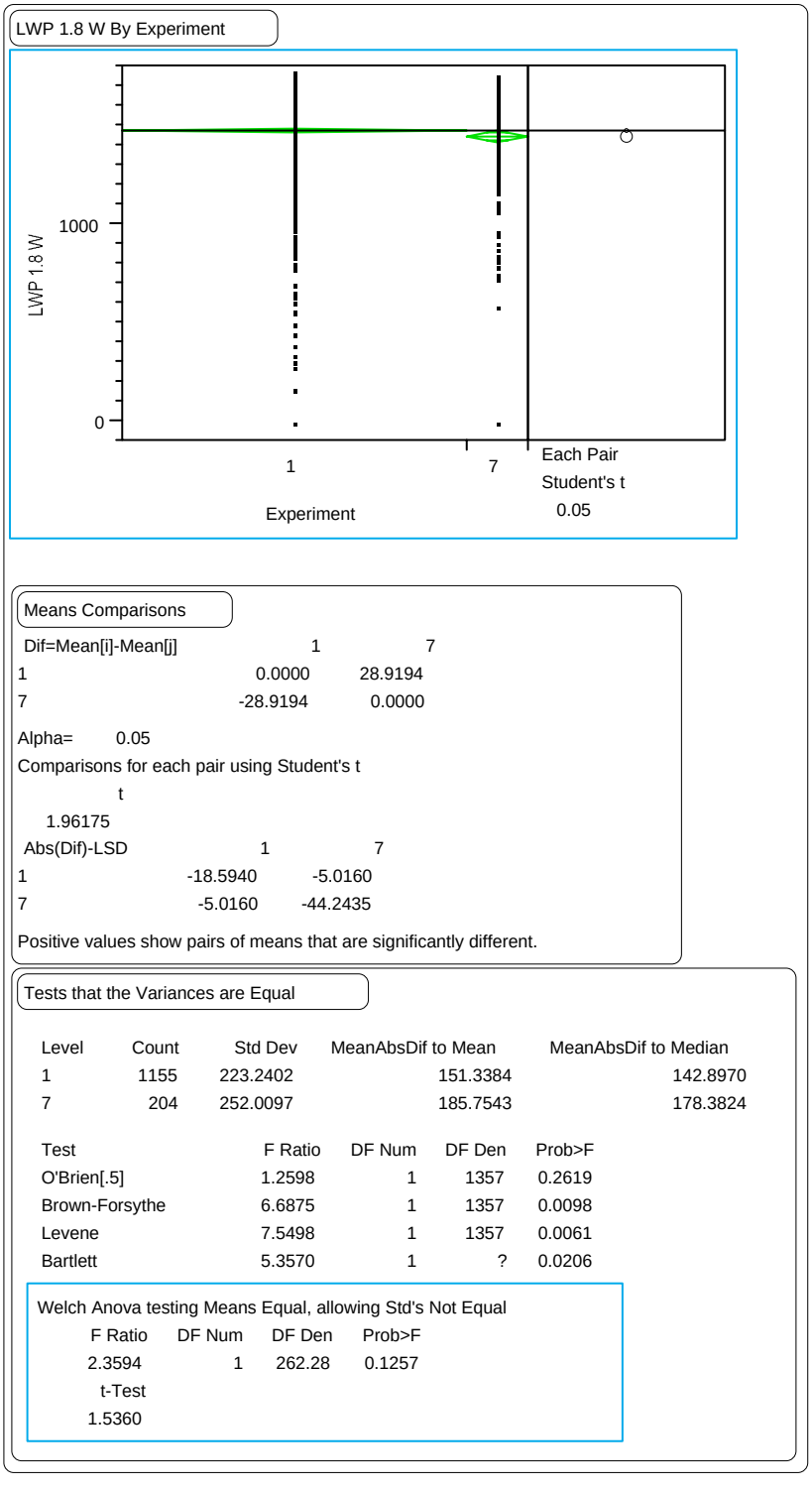

Means Comparisons

Dif=Mean[i]-Mean[j]	1	7
1	0.0000	28.9194
7	-28.9194	0.0000

Alpha= 0.05

Comparisons for each pair using Student's t

t

1.96175

Abs(Dif)-LSD	1	7
1	-18.5940	-5.0160
7	-5.0160	-44.2435

Positive values show pairs of means that are significantly different.

Tests that the Variances are Equal

Level	Count	Std Dev	MeanAbsDif to Mean	MeanAbsDif to Median
1	1155	223.2402	151.3384	142.8970
7	204	252.0097	185.7543	178.3824

Test	F Ratio	DF Num	DF Den	Prob>F
O'Brien[.5]	1.2598	1	1357	0.2619
Brown-Forsythe	6.6875	1	1357	0.0098
Levene	7.5498	1	1357	0.0061
Bartlett	5.3570	1	?	0.0206

Welch Anova testing Means Equal, allowing Std's Not Equal

F Ratio	DF Num	DF Den	Prob>F
2.3594	1	262.28	0.1257

t-Test

1.5360

Figure 151. Paired t-test comparing GPS-1 section means versus GPS-7 section means for the LWP 1.8-m rut widths.

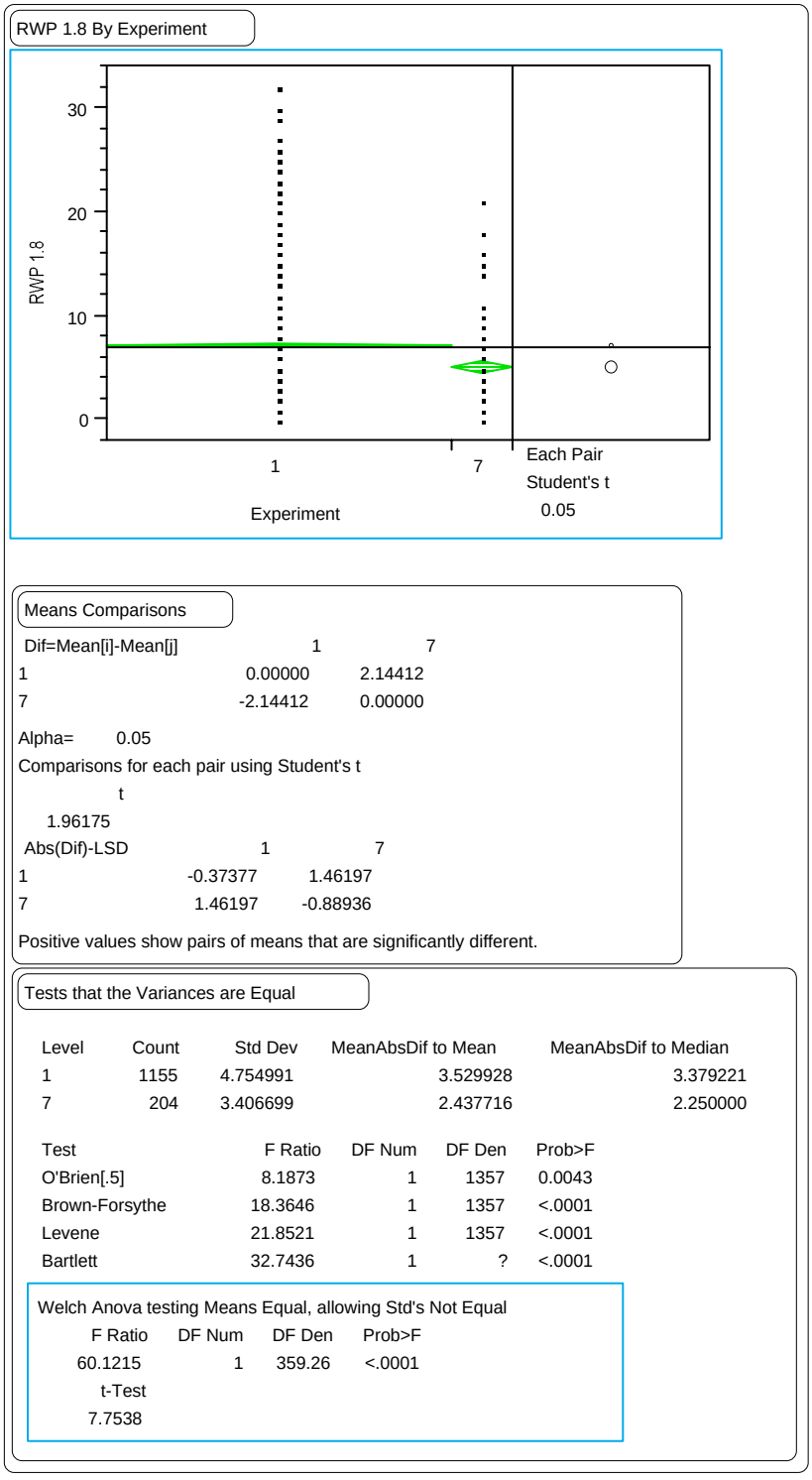

Figure 152. Paired t-test comparing GPS-1 section means versus GPS-7 section means for the RWP 1.8-m rut depths.

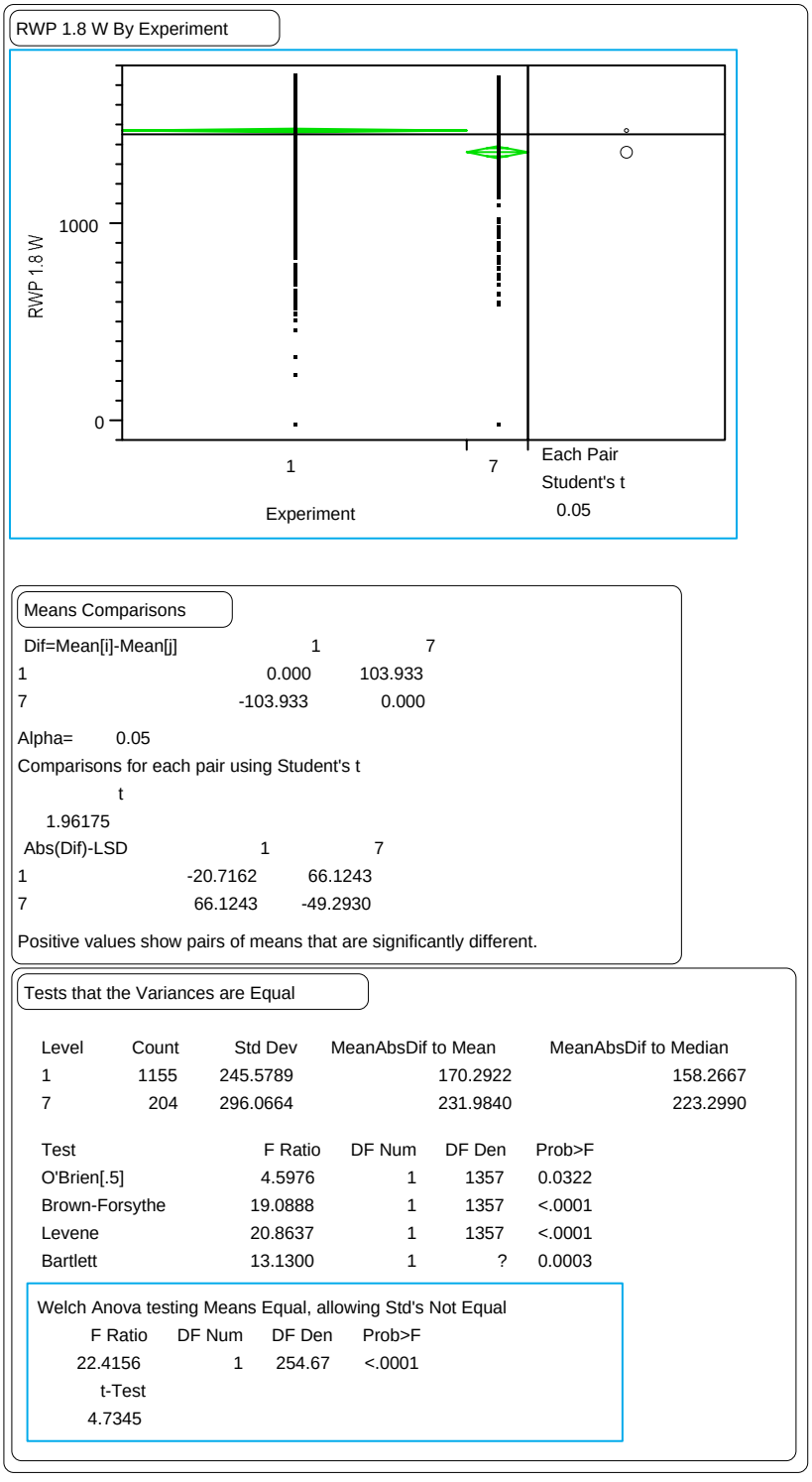

Figure 153. Paired t-test comparing GPS-1 section means versus GPS-7 section means for the RWP 1.8-m rut widths.

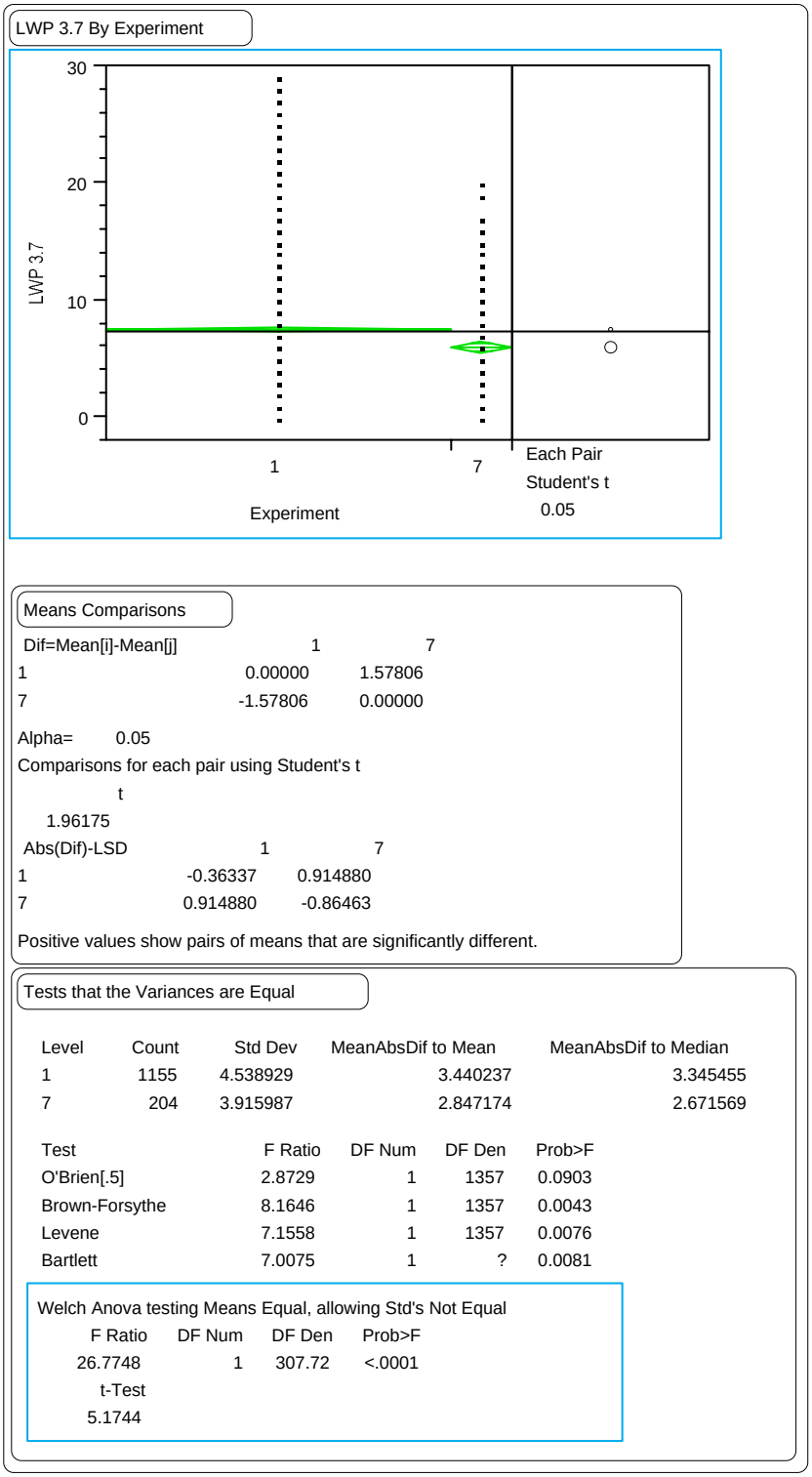

Figure 154. Paired t-test comparing GPS-1 section means versus GPS-7 section means for the LWP wire line rut depths.

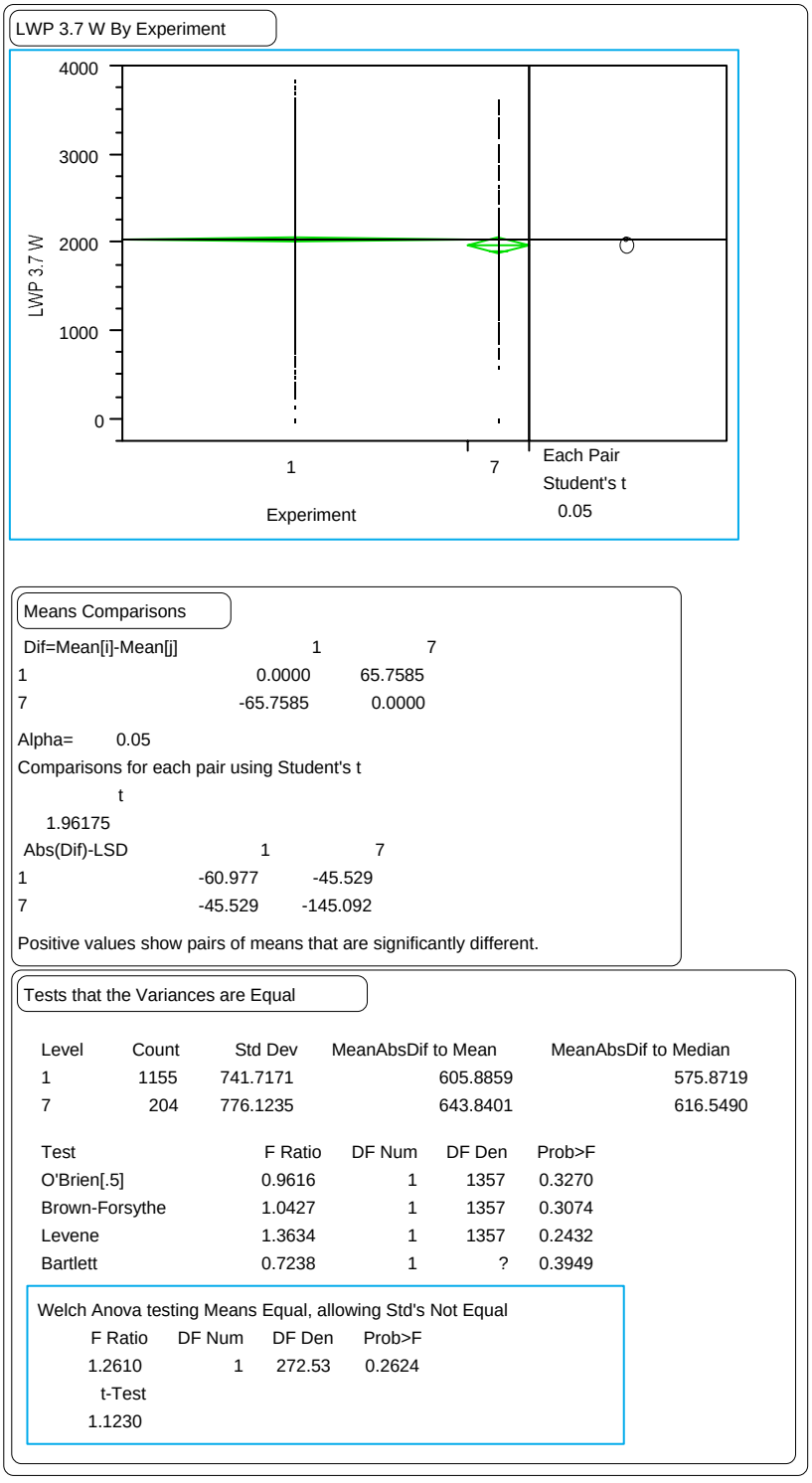

Figure 155. Paired t-test comparing GPS-1 section means versus GPS-7 section means for the LWP wire line rut widths.

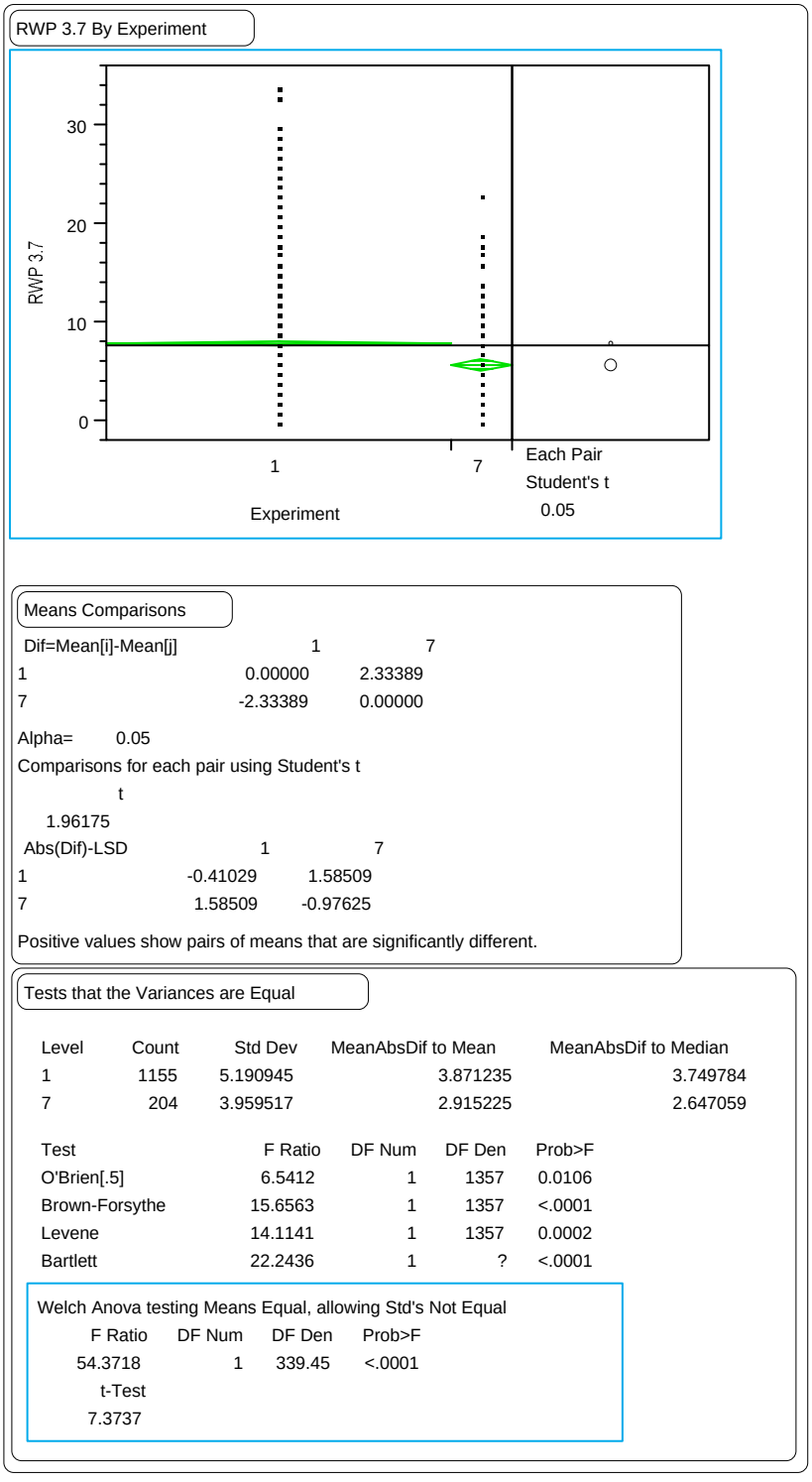

Figure 156. Paired t-test comparing GPS-1 section means versus GPS-7 section means for the RWP wire line rut depths.

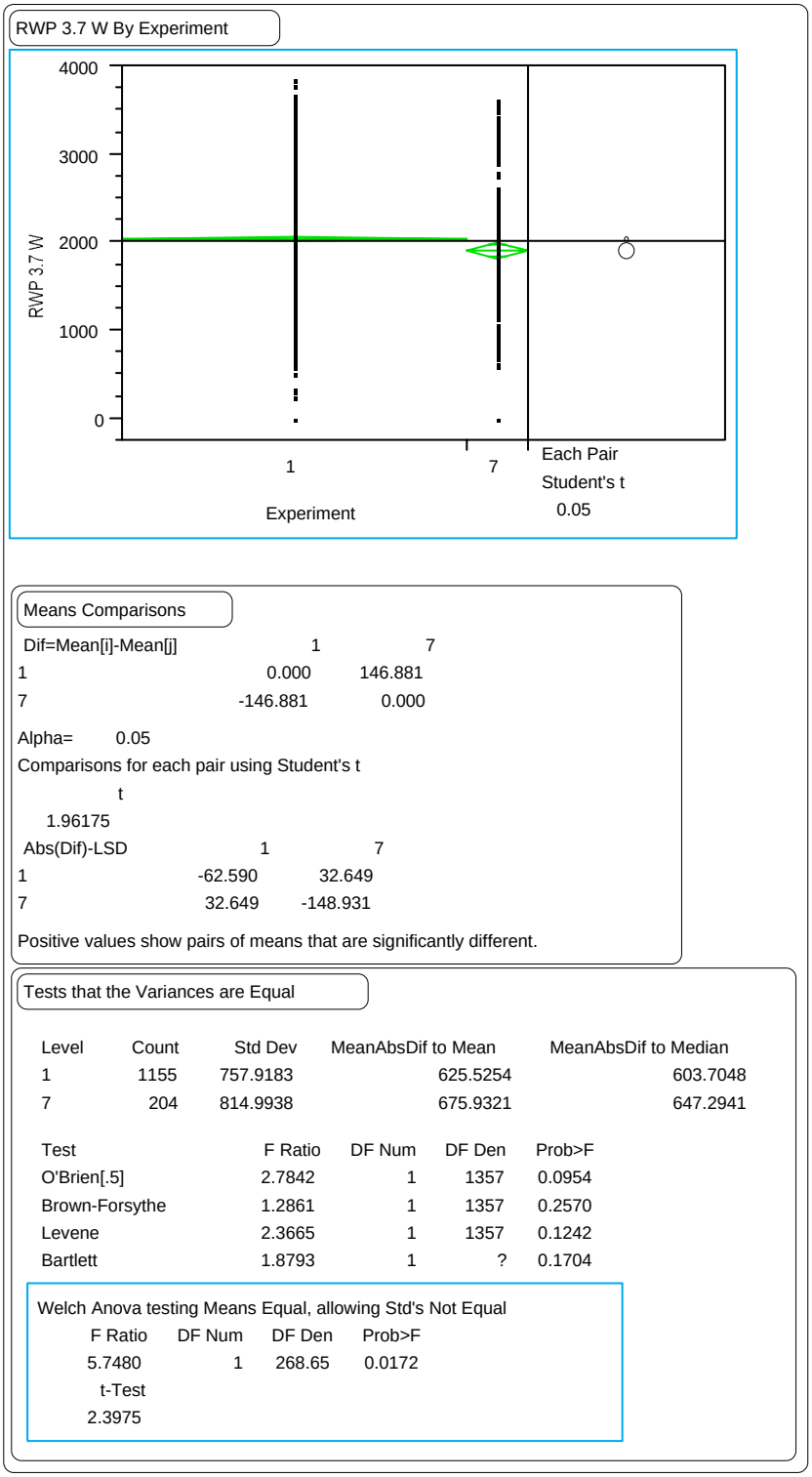

Figure 157. Paired t-test comparing GPS-1 section means versus GPS-7 section means for the RWP wire line rut widths.

Neg Area By Surface Thickness

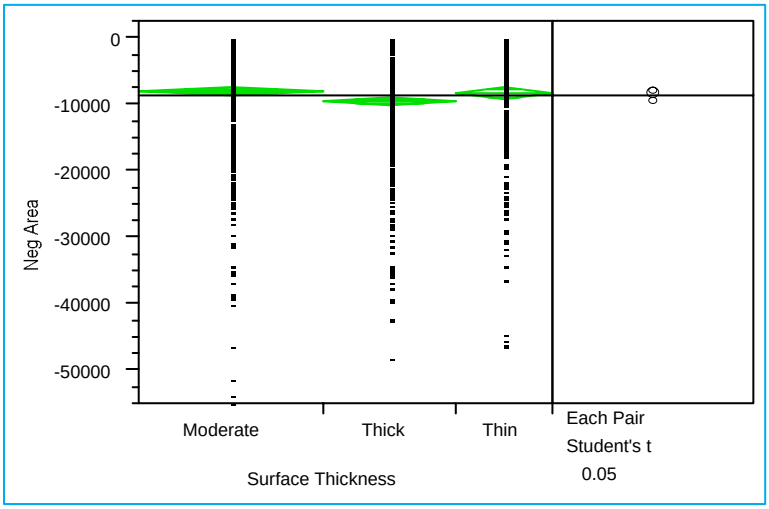

Means Comparisons

Dif=Mean[i]-Mean[j]	Moderate	Thin	Thick
Moderate	0.00	242.78	1655.20
Thin	-242.78	0.00	1412.42
Thick	-1655.20	-1412.42	0.00

Alpha= 0.05

Comparisons for each pair using Student's t

t

1.96166

Abs(Dif)-LSD	Moderate	Thin	Thick
Moderate	-985.92	-955.54	574.69
Thin	-955.54	-1378.37	135.15
Thick	574.69	135.15	-1167.46

Positive values show pairs of means that are significantly different.

Tests that the Variances are Equal

Level	Count	Std Dev	MeanAbsDif to Mean	MeanAbsDif to Median
Moderate	645	8609.324	6451.552	6057.938
Thick	460	9319.431	7508.581	7233.920
Thin	330	9398.057	7246.181	6652.897

Test	F Ratio	DF Num	DF Den	Prob>F
O'Brien[.5]	0.9604	2	1432	0.3830
Brown-Forsythe	3.9709	2	1432	0.0191
Levene	5.1061	2	1432	0.0062
Bartlett	2.4234	2	?	0.0886

Welch Anova testing Means Equal, allowing Std's Not Equal

F Ratio	DF Num	DF Den	Prob>F
4.7230	2	791.72	0.0091

Figure 158. Paired t-test comparing GPS-1 and GPS-2 section means for the negative area index versus surface thickness.

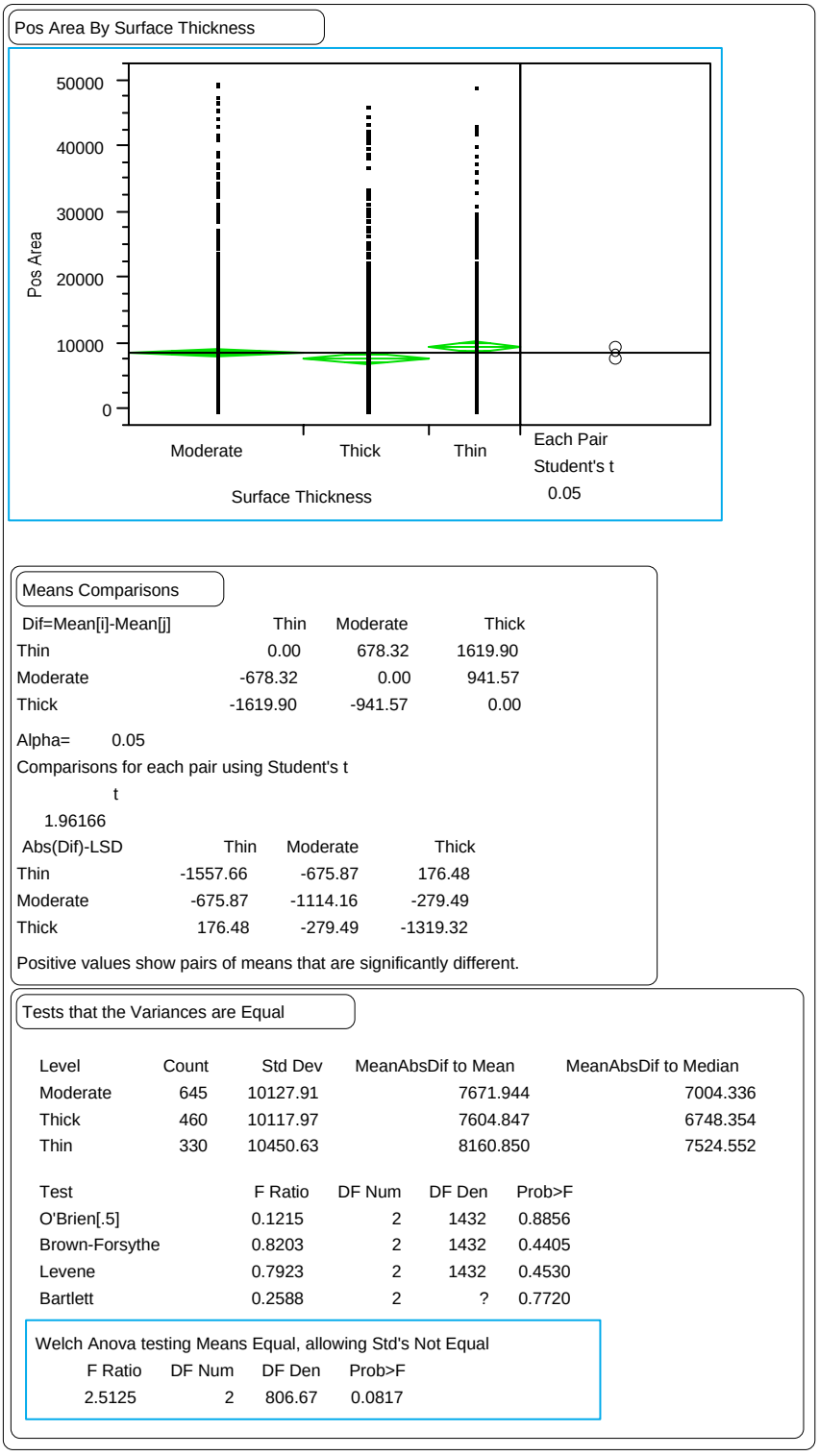

Means Comparisons

Dif=Mean[i]-Mean[j]	Thin	Moderate	Thick
Thin	0.00	678.32	1619.90
Moderate	-678.32	0.00	941.57
Thick	-1619.90	-941.57	0.00

Alpha= 0.05

Comparisons for each pair using Student's t

t

1.96166

Abs(Dif)-LSD	Thin	Moderate	Thick
Thin	-1557.66	-675.87	176.48
Moderate	-675.87	-1114.16	-279.49
Thick	176.48	-279.49	-1319.32

Positive values show pairs of means that are significantly different.

Tests that the Variances are Equal

Level	Count	Std Dev	MeanAbsDif to Mean	MeanAbsDif to Median
Moderate	645	10127.91	7671.944	7004.336
Thick	460	10117.97	7604.847	6748.354
Thin	330	10450.63	8160.850	7524.552

Test	F Ratio	DF Num	DF Den	Prob>F
O'Brien[.5]	0.1215	2	1432	0.8856
Brown-Forsythe	0.8203	2	1432	0.4405
Levene	0.7923	2	1432	0.4530
Bartlett	0.2588	2	?	0.7720

Welch Anova testing Means Equal, allowing Std's Not Equal

F Ratio	DF Num	DF Den	Prob>F
2.5125	2	806.67	0.0817

Figure 159. Paired t-test comparing GPS-1 and GPS-2 section means for the positive area index versus surface thickness.

Fill Area By Surface Thickness

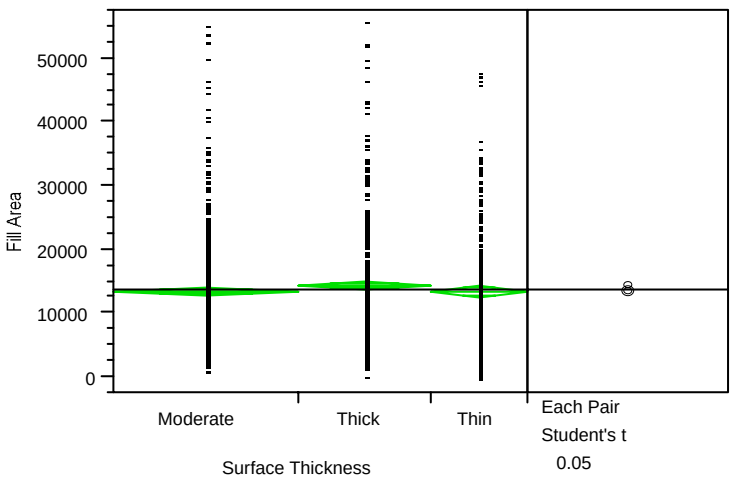

Means Comparisons

Dif=Mean[i]-Mean[j]	Thick	Thin	Moderate
Thick	0.00	1008.11	1102.48
Thin	-1008.11	0.00	94.37
Moderate	-1102.48	-94.37	0.00

Alpha= 0.05
Comparisons for each pair using Student's t
t
1.96166

Abs(Dif)-LSD	Thick	Thin	Moderate
Thick	-1155.36	-255.92	33.17
Thin	-255.92	-1364.07	-1091.53
Moderate	33.17	-1091.53	-975.70

Positive values show pairs of means that are significantly different.

Tests that the Variances are Equal

Level	Count	Std Dev	MeanAbsDif to Mean	MeanAbsDif to Median
Moderate	645	8582.128	6546.949	6328.358
Thick	460	9362.227	7181.002	6990.104
Thin	330	8989.305	6991.482	6766.818

Test	F Ratio	DF Num	DF Den	Prob>F
O'Brien[.5]	0.9104	2	1432	0.4026
Brown-Forsythe	1.5649	2	1432	0.2095
Levene	1.7801	2	1432	0.1690
Bartlett	2.0612	2	?	0.1273

Welch Anova testing Means Equal, allowing Std's Not Equal

F Ratio	DF Num	DF Den	Prob>F
2.1531	2	800.04	0.1168

Figure 160. Paired t-test comparing GPS-1 and GPS-2 section means for the fill area index versus surface thickness.

LWP 1.8 By Surface Thickness

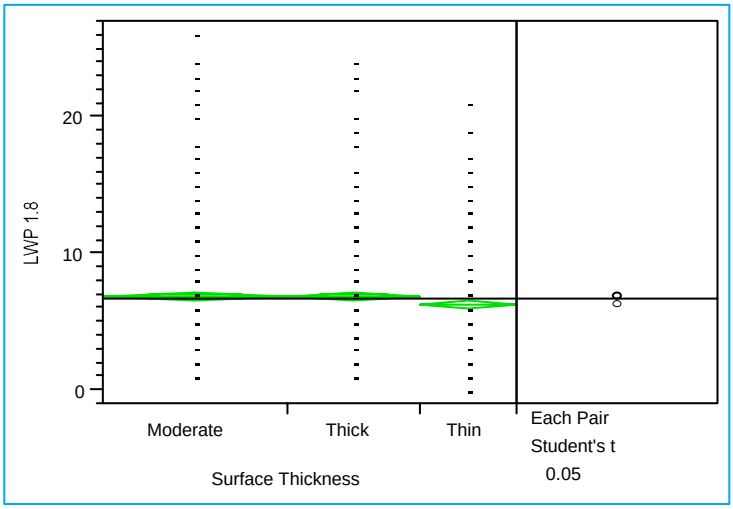

Means Comparisons

Dif=Mean[i]-Mean[j]	Thick	Moderate	Thin
Thick	0.000000	0.094203	0.630567
Moderate	-0.0942	0.000000	0.536364
Thin	-0.63057	-0.53636	0.000000

Alpha= 0.05

Comparisons for each pair using Student's t

t

1.96166

Abs(Dif)-LSD	Thick	Moderate	Thin
Thick	-0.51487	-0.38232	0.067273
Moderate	-0.38232	-0.4348	0.007891
Thin	0.067273	0.007891	-0.60788

Positive values show pairs of means that are significantly different.

Tests that the Variances are Equal

Level	Count	Std Dev	MeanAbsDif to Mean	MeanAbsDif to Median
Moderate	645	4.120192	3.147907	3.031008
Thick	460	4.024786	3.011172	2.965217
Thin	330	3.624049	2.885271	2.821212

Test	F Ratio	DF Num	DF Den	Prob>F
O'Brien[.5]	1.5743	2	1432	0.2075
Brown-Forsythe	0.6239	2	1432	0.5360
Levene	1.2041	2	1432	0.3003
Bartlett	3.5598	2	?	0.0284

Welch Anova testing Means Equal, allowing Std's Not Equal

F Ratio	DF Num	DF Den	Prob>F
3.1003	2	841.98	0.0455

Figure 161. Paired t-test comparing GPS-1 and GPS-2 section means for the LWP 1.8-m rut depths versus surface thickness.

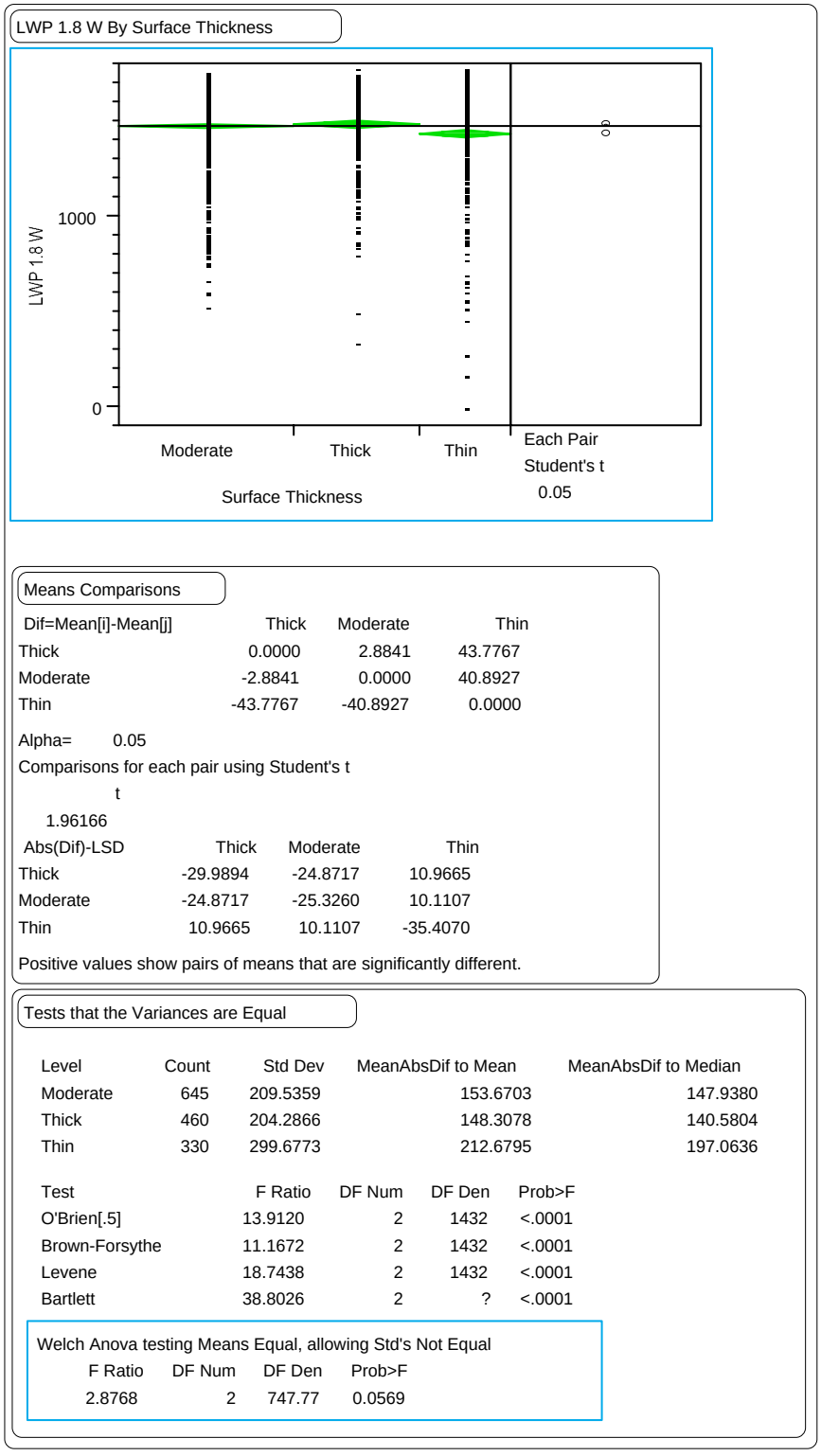

Means Comparisons

Dif=Mean[i]-Mean[j]	Thick	Moderate	Thin
Thick	0.0000	2.8841	43.7767
Moderate	-2.8841	0.0000	40.8927
Thin	-43.7767	-40.8927	0.0000

Alpha= 0.05

Comparisons for each pair using Student's t

t

1.96166

Abs(Dif)-LSD	Thick	Moderate	Thin
Thick	-29.9894	-24.8717	10.9665
Moderate	-24.8717	-25.3260	10.1107
Thin	10.9665	10.1107	-35.4070

Positive values show pairs of means that are significantly different.

Tests that the Variances are Equal

Level	Count	Std Dev	MeanAbsDif to Mean	MeanAbsDif to Median
Moderate	645	209.5359	153.6703	147.9380
Thick	460	204.2866	148.3078	140.5804
Thin	330	299.6773	212.6795	197.0636

Test	F Ratio	DF Num	DF Den	Prob>F
O'Brien[.5]	13.9120	2	1432	<.0001
Brown-Forsythe	11.1672	2	1432	<.0001
Levene	18.7438	2	1432	<.0001
Bartlett	38.8026	2	?	<.0001

Welch Anova testing Means Equal, allowing Std's Not Equal

F Ratio	DF Num	DF Den	Prob>F
2.8768	2	747.77	0.0569

Figure 162. Paired t-test comparing GPS-1 and GPS-2 section means for the LWP 1.8-m rut widths versus surface thickness.

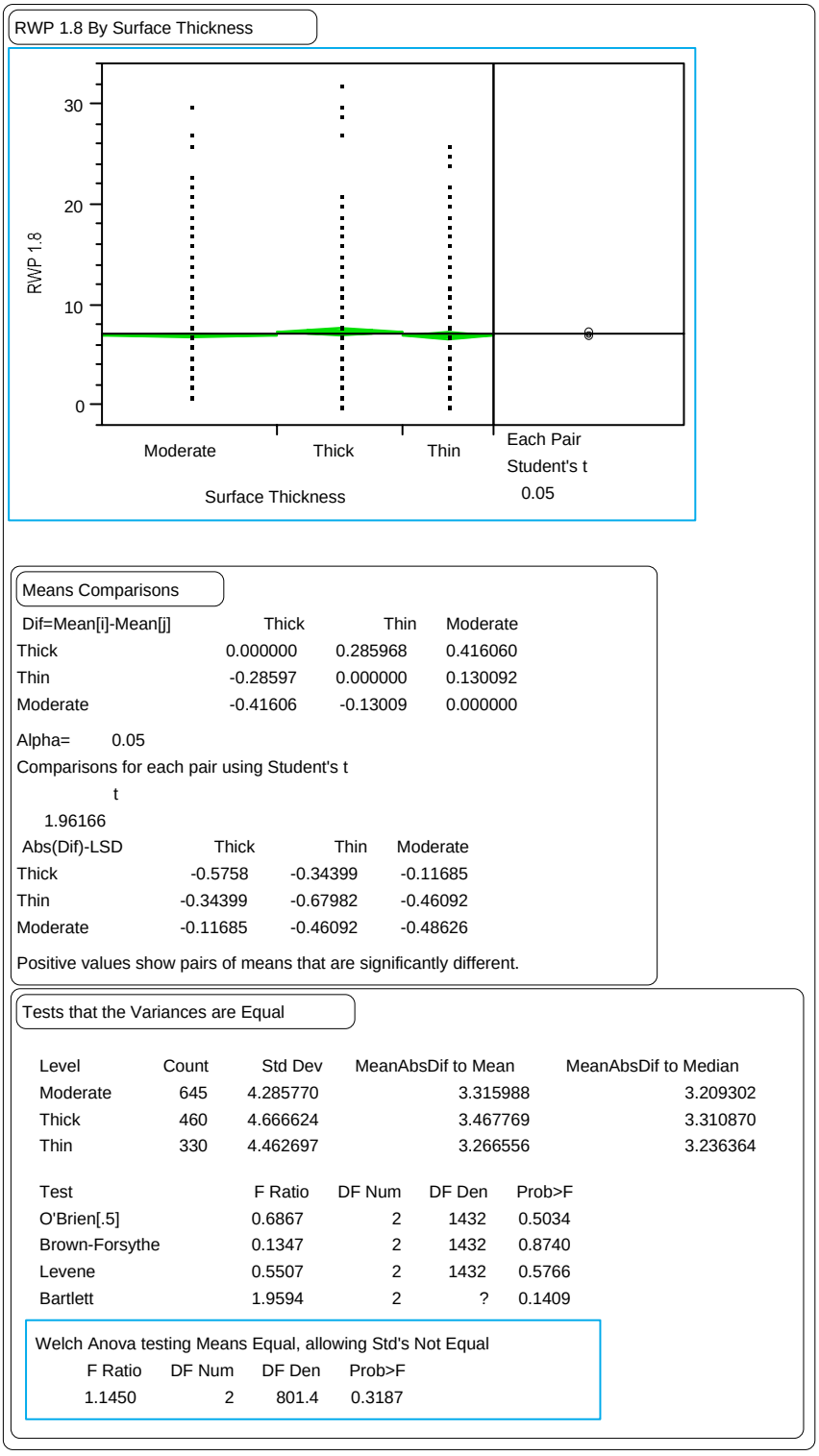

Means Comparisons

Dif=Mean[i]-Mean[j]	Thick	Thin	Moderate
Thick	0.000000	0.285968	0.416060
Thin	-0.28597	0.000000	0.130092
Moderate	-0.41606	-0.13009	0.000000

Alpha= 0.05

Comparisons for each pair using Student's t

t

1.96166

Abs(Dif)-LSD	Thick	Thin	Moderate
Thick	-0.5758	-0.34399	-0.11685
Thin	-0.34399	-0.67982	-0.46092
Moderate	-0.11685	-0.46092	-0.48626

Positive values show pairs of means that are significantly different.

Tests that the Variances are Equal

Level	Count	Std Dev	MeanAbsDif to Mean	MeanAbsDif to Median
Moderate	645	4.285770	3.315988	3.209302
Thick	460	4.666624	3.467769	3.310870
Thin	330	4.462697	3.266556	3.236364

Test	F Ratio	DF Num	DF Den	Prob>F
O'Brien[.5]	0.6867	2	1432	0.5034
Brown-Forsythe	0.1347	2	1432	0.8740
Levene	0.5507	2	1432	0.5766
Bartlett	1.9594	2	?	0.1409

Welch Anova testing Means Equal, allowing Std's Not Equal

F Ratio	DF Num	DF Den	Prob>F
1.1450	2	801.4	0.3187

Figure 163. Paired t-test comparing GPS-1 and GPS-2 section means for the RWP 1.8-m rut depths versus surface thickness.

RWP 1.8 W By Surface Thickness

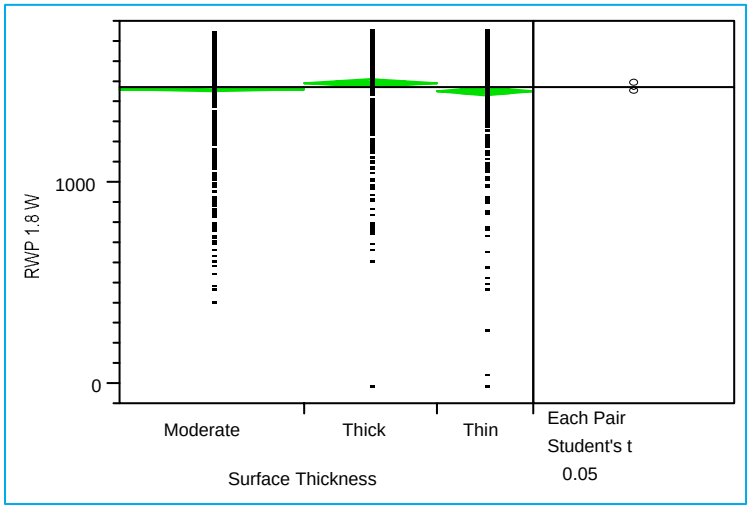

Means Comparisons

Dif=Mean[i]-Mean[j]	Thick	Moderate	Thin
Thick	0.0000	32.7824	38.0128
Moderate	-32.7824	0.0000	5.2304
Thin	-38.0128	-5.2304	0.0000

Alpha= 0.05

Comparisons for each pair using Student's t

t

1.96166

Abs(Dif)-LSD	Thick	Moderate	Thin
Thick	-33.1446	2.1064	1.7506
Moderate	2.1064	-27.9906	-28.7902
Thin	1.7506	-28.7902	-39.1322

Positive values show pairs of means that are significantly different.

Tests that the Variances are Equal

Level	Count	Std Dev	MeanAbsDif to Mean	MeanAbsDif to Median
Moderate	645	251.0544	184.6521	169.1147
Thick	460	237.0325	167.7991	160.7391
Thin	330	289.8882	213.2006	198.2212

Test	F Ratio	DF Num	DF Den	Prob>F
O'Brien[.5]	3.0730	2	1432	0.0466
Brown-Forsythe	3.7677	2	1432	0.0233
Levene	6.4590	2	1432	0.0016
Bartlett	8.3514	2	?	0.0002

Welch Anova testing Means Equal, allowing Std's Not Equal

F Ratio	DF Num	DF Den	Prob>F
3.0760	2	785.2	0.0467

Figure 164. Paired t-test comparing GPS-1 and GPS-2 section means for the RWP 1.8-m rut widths versus surface thickness.

LWP 3.7 By Surface Thickness

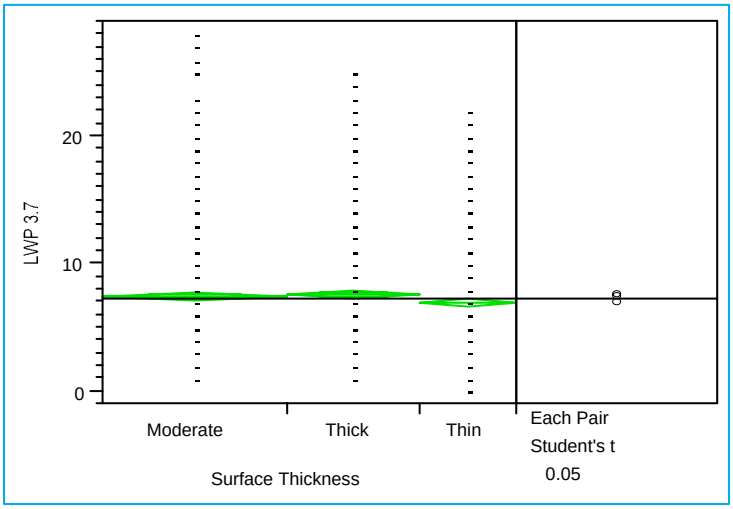

Means Comparisons

Dif=Mean[i]-Mean[j]	Thick	Moderate	Thin
Thick	0.000000	0.251230	0.710145
Moderate	-0.25123	0.000000	0.458915
Thin	-0.71014	-0.45891	0.000000

Alpha= 0.05

Comparisons for each pair using Student's t

t

1.96166

Abs(Dif)-LSD	Thick	Moderate	Thin
Thick	-0.56311	-0.26994	0.094071
Moderate	-0.26994	-0.47554	-0.11908
Thin	0.094071	-0.11908	-0.66483

Positive values show pairs of means that are significantly different.

Tests that the Variances are Equal

Level	Count	Std Dev	MeanAbsDif to Mean	MeanAbsDif to Median
Moderate	645	4.418299	3.384210	3.286822
Thick	460	4.412186	3.359093	3.269565
Thin	330	4.137652	3.278384	3.187879

Test	F Ratio	DF Num	DF Den	Prob>F
O'Brien[.5]	0.5129	2	1432	0.5989
Brown-Forsythe	0.1166	2	1432	0.8899
Levene	0.1612	2	1432	0.8511
Bartlett	1.0466	2	?	0.3511

Welch Anova testing Means Equal, allowing Std's Not Equal

F Ratio	DF Num	DF Den	Prob>F
2.7175	2	827.68	0.0666

Figure 165. Paired t-test comparing GPS-1 and GPS-2 section means for the LWP wire line rut depths versus surface thickness.

LWP 3.7 W By Surface Thickness

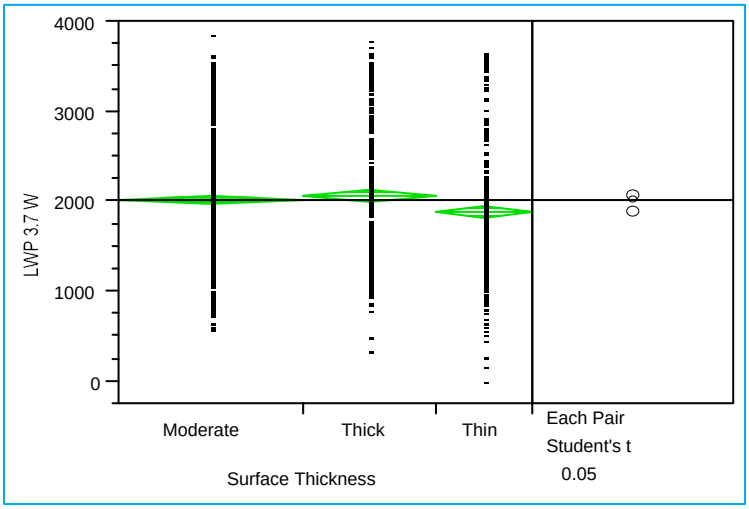

Means Comparisons

Dif=Mean[i]-Mean[j]	Thick	Moderate	Thin
Thick	0.000	35.609	170.667
Moderate	-35.609	0.000	135.058
Thin	-170.667	-135.058	0.000

Alpha= 0.05

Comparisons for each pair using Student's t

t

1.96166

Abs(Dif)-LSD	Thick	Moderate	Thin
Thick	-95.755	-53.014	65.905
Moderate	-53.014	-80.865	36.771
Thin	65.905	36.771	-113.054

Positive values show pairs of means that are significantly different.

Tests that the Variances are Equal

Level	Count	Std Dev	MeanAbsDif to Mean	MeanAbsDif to Median
Moderate	645	706.7583	584.6481	564.6698
Thick	460	758.8254	622.5829	589.8630
Thin	330	777.3502	599.0490	567.5303

Test	F Ratio	DF Num	DF Den	Prob>F
O'Brien[.5]	2.9581	2	1432	0.0522
Brown-Forsythe	0.3571	2	1432	0.6998
Levene	1.0352	2	1432	0.3554
Bartlett	2.4361	2	?	0.0875

Welch Anova testing Means Equal, allowing Std's Not Equal

F Ratio	DF Num	DF Den	Prob>F
5.0935	2	790.56	0.0063

Figure 166. Paired t-test comparing GPS-1 and GPS-2 section means for the LWP wire line rut widths versus surface thickness.

RWP 3.7 By Surface Thickness

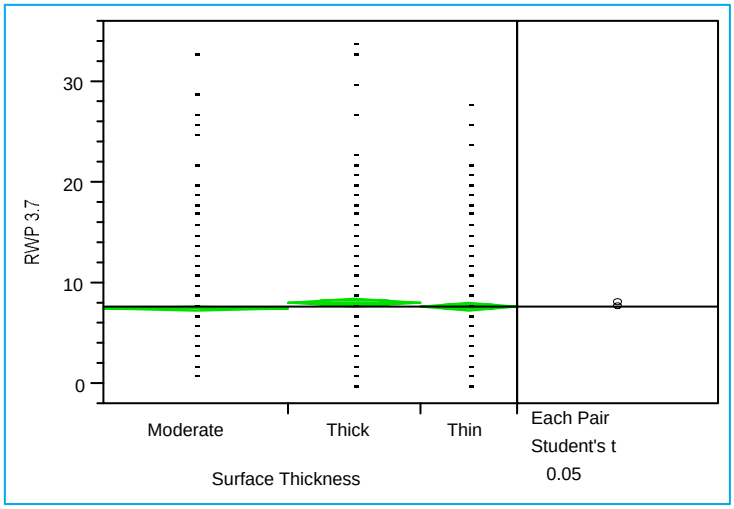

Means Comparisons

Dif=Mean[i]-Mean[j]	Thick	Thin	Moderate
Thick	0.000000	0.396179	0.585608
Thin	-0.39618	0.000000	0.189429
Moderate	-0.58561	-0.18943	0.000000

Alpha= 0.05

Comparisons for each pair using Student's t

t

1.96166

Abs(Dif)-LSD	Thick	Thin	Moderate
Thick	-0.63504	-0.29859	-0.00214
Thin	-0.29859	-0.74976	-0.4624
Moderate	-0.00214	-0.4624	-0.53629

Positive values show pairs of means that are significantly different.

Tests that the Variances are Equal

Level	Count	Std Dev	MeanAbsDif to Mean	MeanAbsDif to Median
Moderate	645	4.679577	3.610797	3.513178
Thick	460	5.135985	3.905312	3.773913
Thin	330	5.024666	3.732525	3.636364

Test	F Ratio	DF Num	DF Den	Prob>F
O'Brien[.5]	0.9634	2	1432	0.3818
Brown-Forsythe	0.7323	2	1432	0.4810
Levene	1.1505	2	1432	0.3168
Bartlett	2.5747	2	?	0.0762

Welch Anova testing Means Equal, allowing Std's Not Equal

F Ratio	DF Num	DF Den	Prob>F
1.8807	2	794.47	0.1532

Figure 167. Paired t-test comparing GPS-1 and GPS-2 section means for the RWP wire line rut depths versus surface thickness.

RWP 3.7 W By Surface Thickness

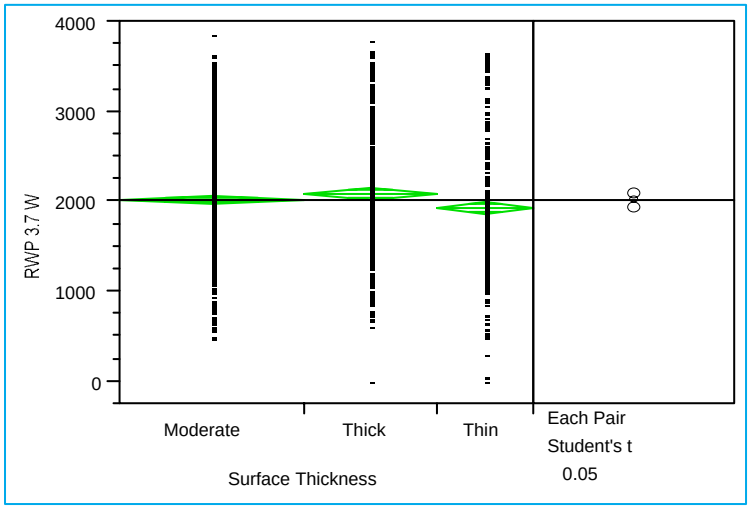

Means Comparisons

Dif=Mean[i]-Mean[j]	Thick	Moderate	Thin
Thick	0.000	70.659	159.422
Moderate	-70.659	0.000	88.763
Thin	-159.422	-88.763	0.000

Alpha= 0.05

Comparisons for each pair using Student's t

t

1.96166

Abs(Dif)-LSD	Thick	Moderate	Thin
Thick	-96.975	-19.093	53.325
Moderate	-19.093	-81.895	-10.775
Thin	53.325	-10.775	-114.493

Positive values show pairs of means that are significantly different.

Tests that the Variances are Equal

Level	Count	Std Dev	MeanAbsDif to Mean	MeanAbsDif to Median
Moderate	645	728.9054	602.9505	582.3690
Thick	460	768.1865	634.0347	607.5804
Thin	330	763.6867	588.9161	566.8970

Test	F Ratio	DF Num	DF Den	Prob>F
O'Brien[.5]	1.1370	2	1432	0.3211
Brown-Forsythe	0.6653	2	1432	0.5143
Levene	1.1738	2	1432	0.3095
Bartlett	0.8899	2	?	0.4107

Welch Anova testing Means Equal, allowing Std's Not Equal

F Ratio	DF Num	DF Den	Prob>F
4.1669	2	801.57	0.0158

Figure 168. Paired t-test comparing GPS-1 and GPS-2 section means for the RWP wire line rut widths versus surface thickness.

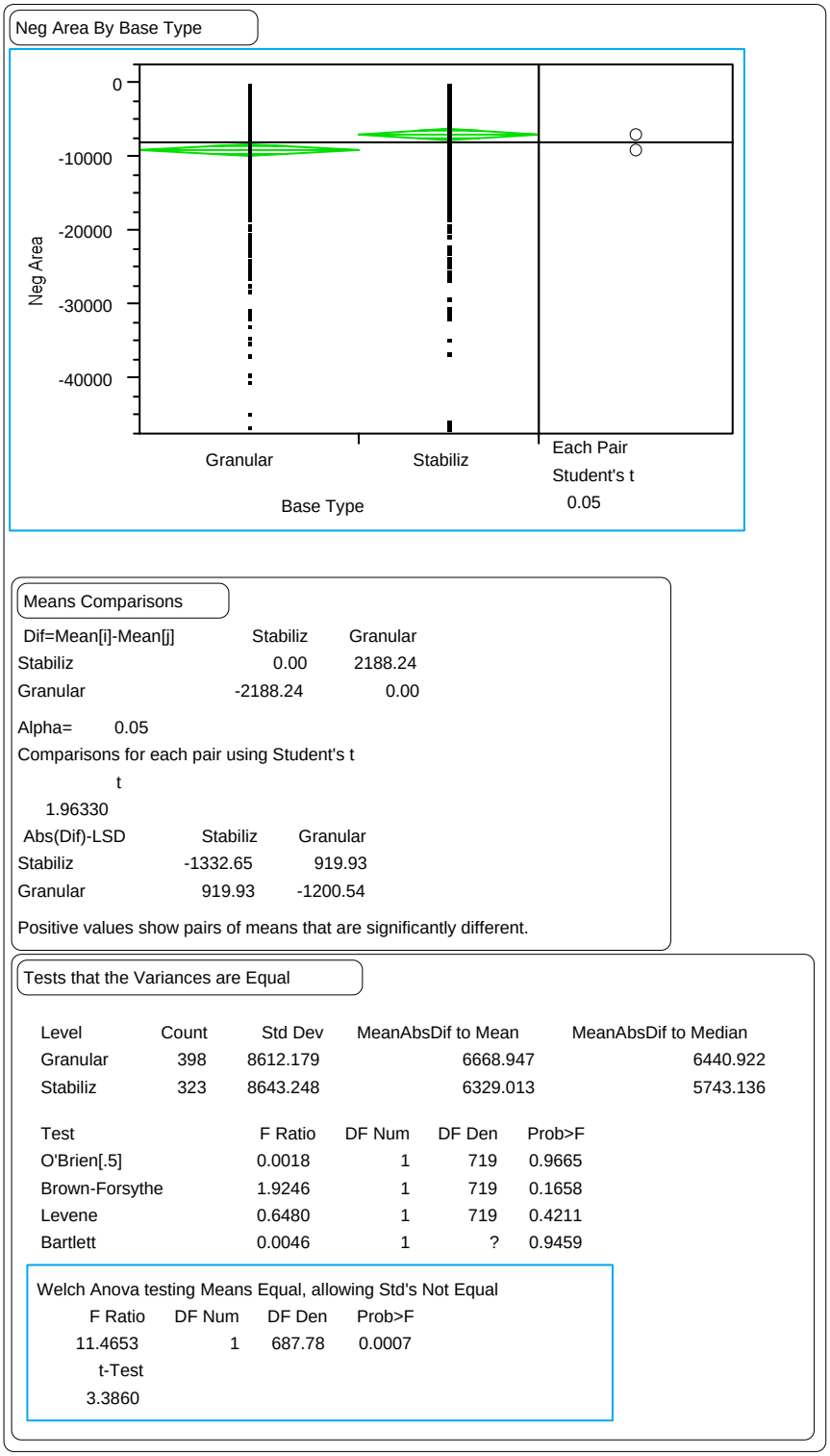

Figure 169. Paired t-test comparing thin-surfaced GPS-1 and GPS-2 section means for the negative area index versus base type.

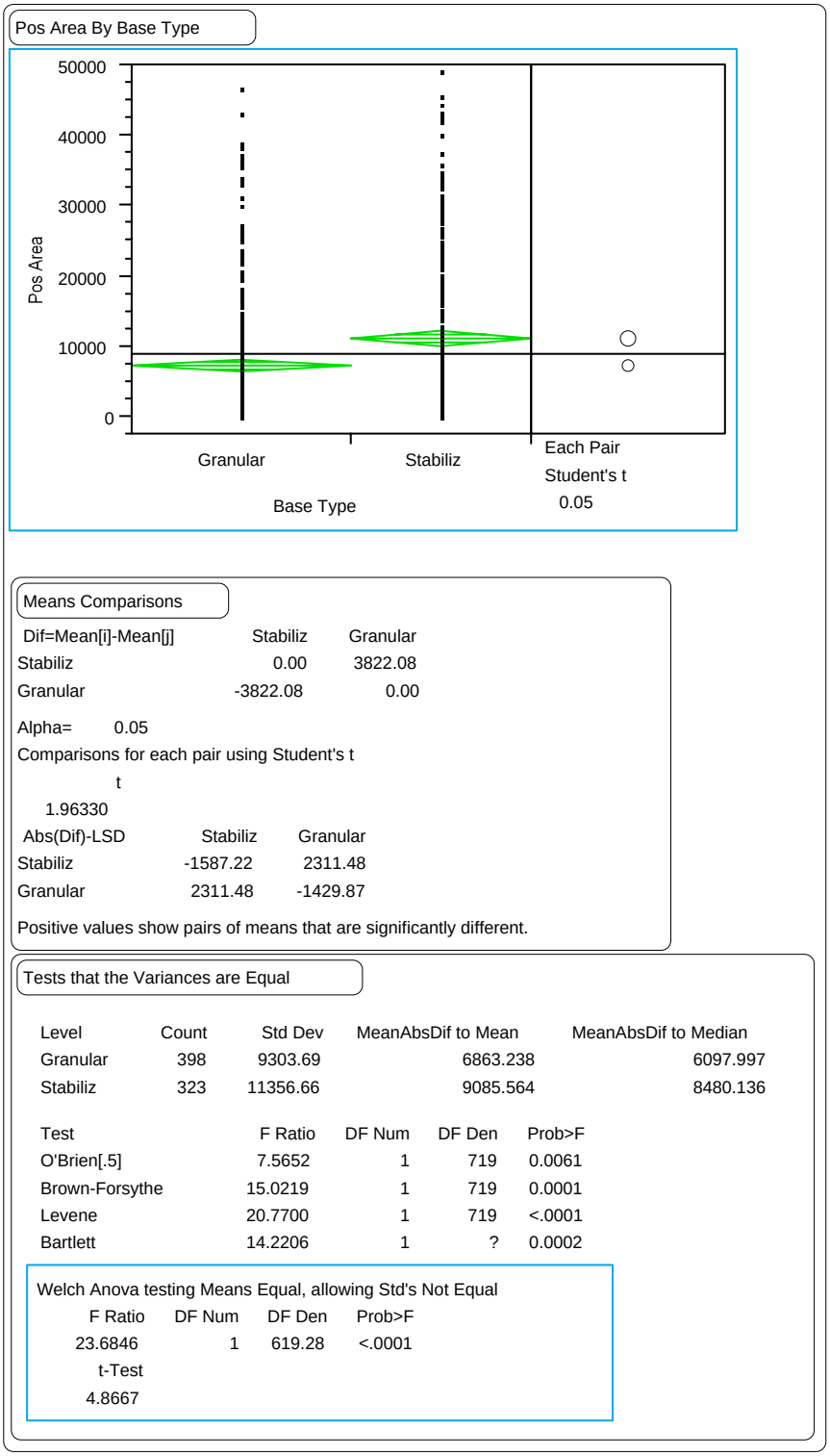

Figure 170. Paired t-test comparing thin-surfaced GPS-1 and GPS-2 section means for the positive area index versus base type.

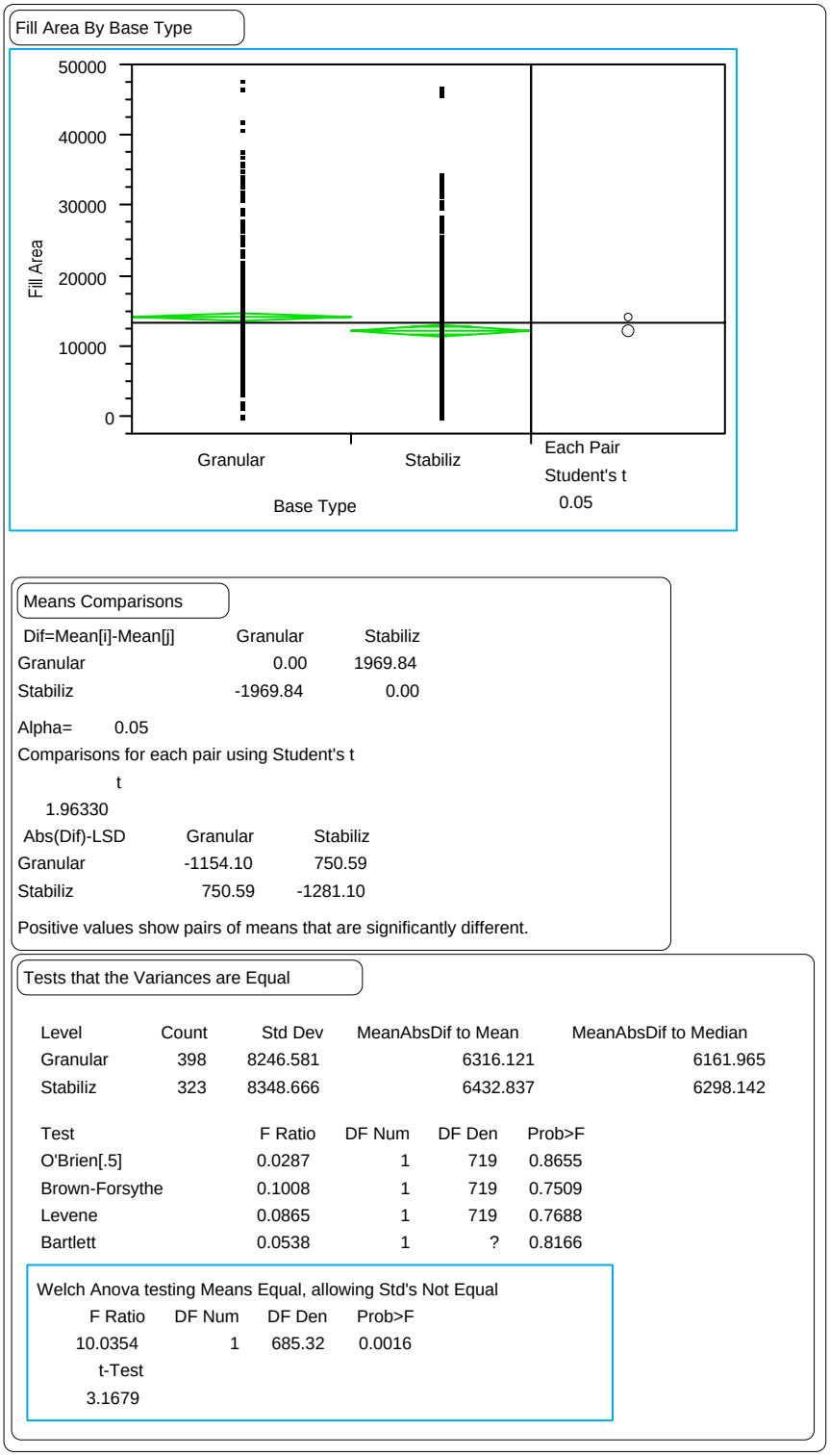

Figure 171. Paired t-test comparing thin-surfaced GPS-1 and GPS-2 section means for the fill area index versus base type.

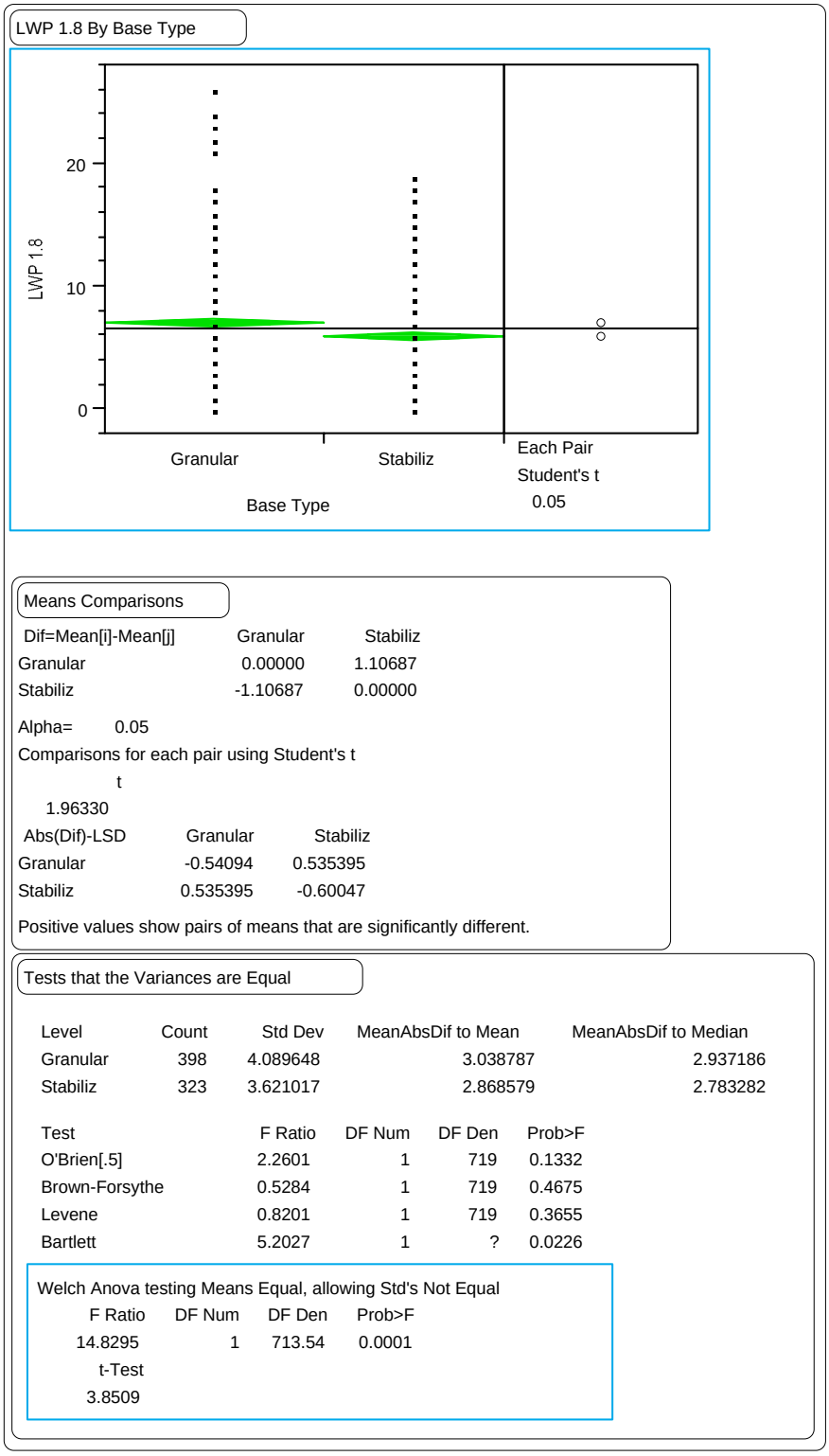

Figure 172. Paired t-test comparing thin-surfaced GPS-1 and GPS-2 section means for the LWP 1.8-m rut depths versus base type.

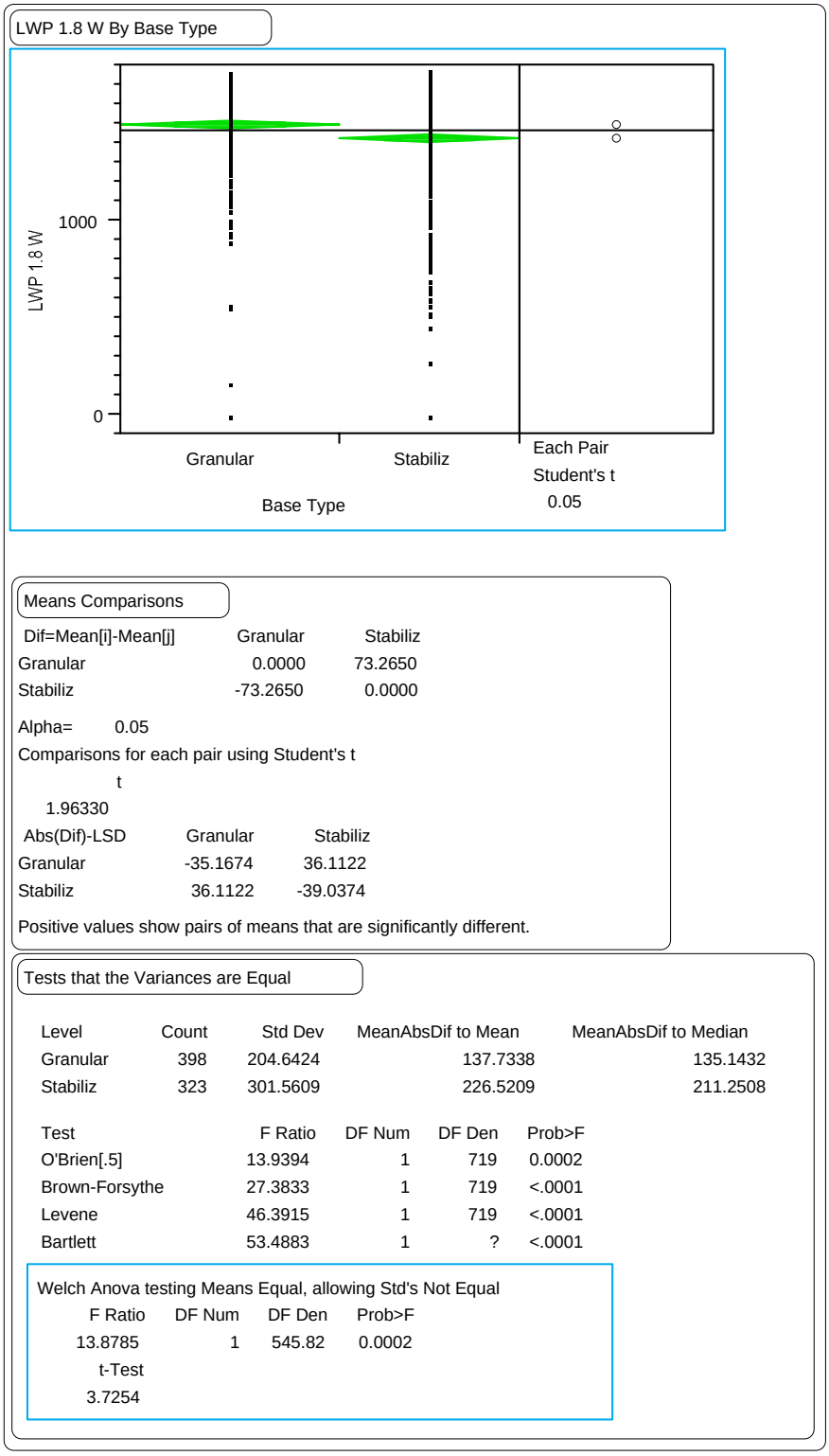

Figure 173. Paired t-test comparing thin-surfaced GPS-1 and GPS-2 section means for the LWP 1.8-m rut widths versus base type.

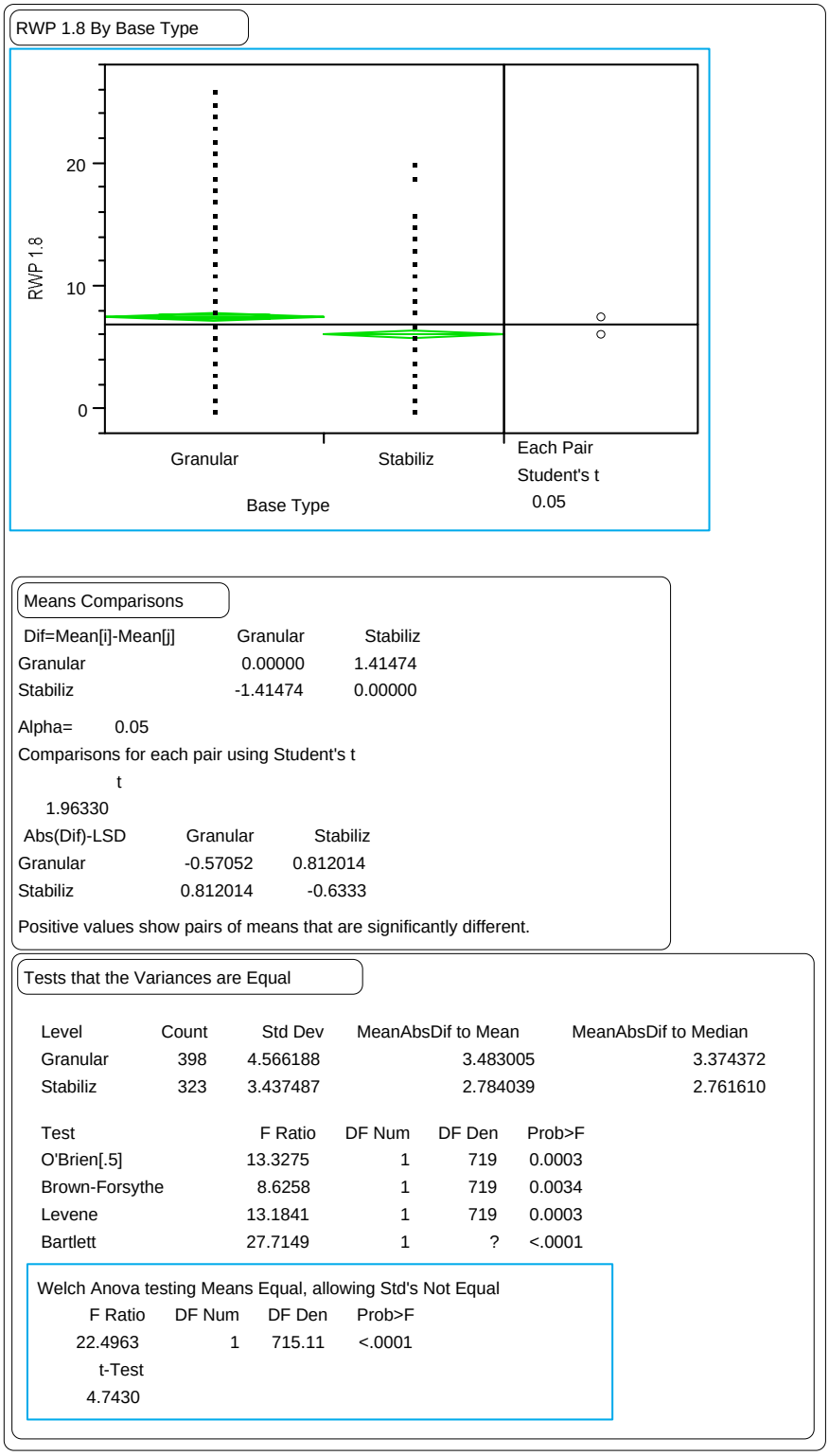

Figure 174. Paired t-test comparing thin-surfaced GPS-1 and GPS-2 section means for the RWP 1.8-m rut depths versus base type.

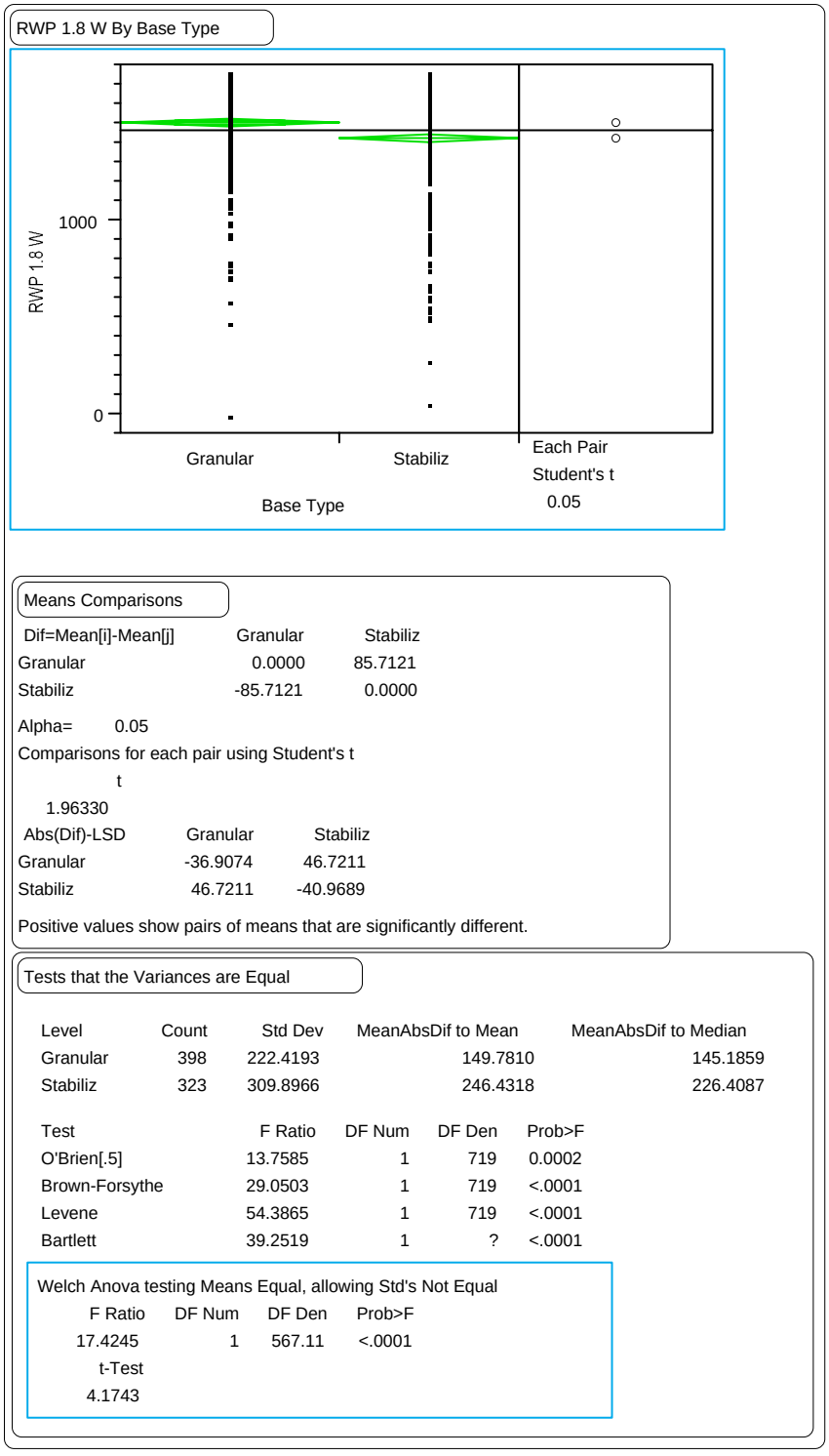

Figure 175. Paired t-test comparing thin-surfaced GPS-1 and GPS-2 section means for the RWP 1.8-m rut widths versus base type.

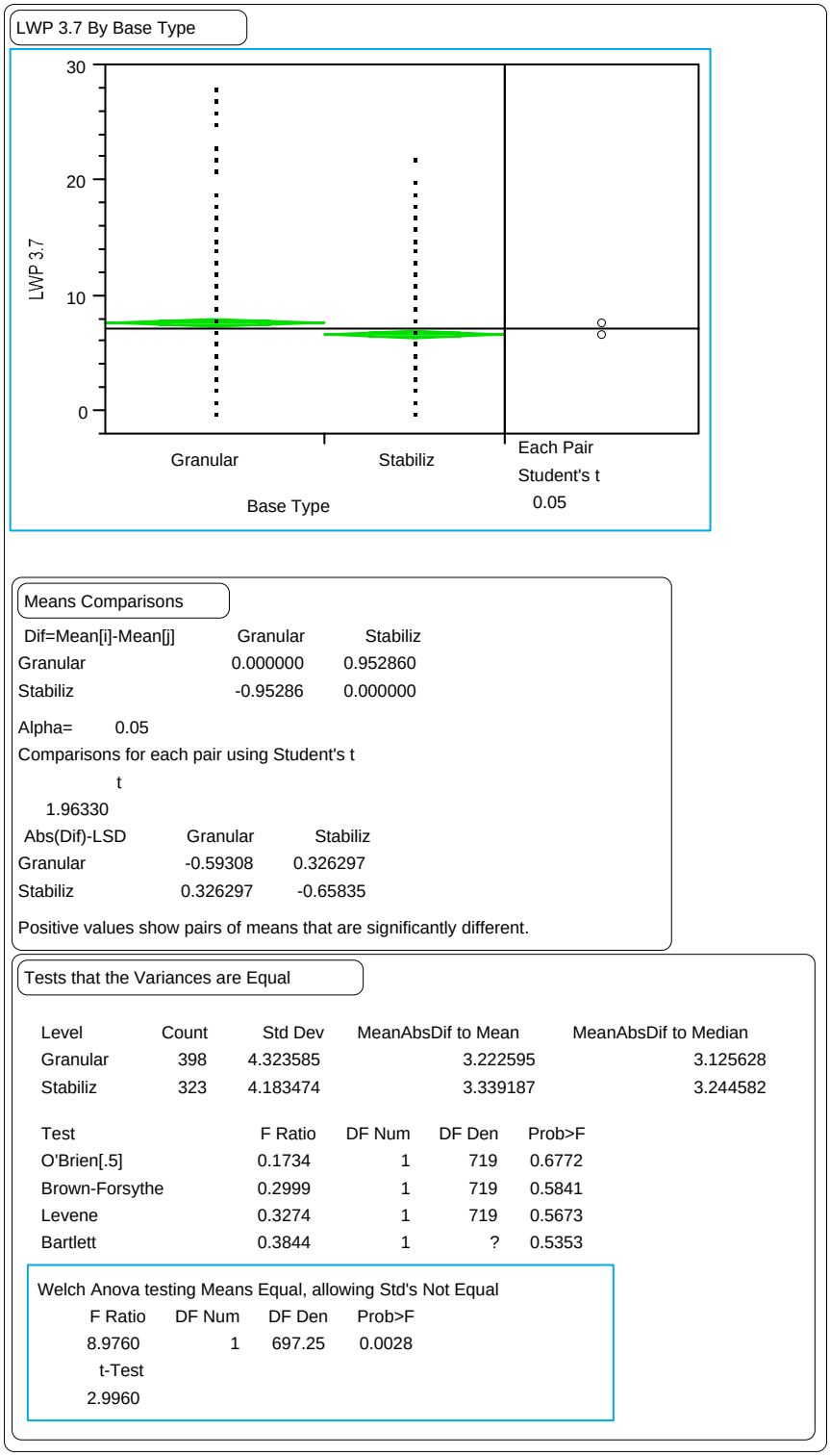

Figure 176. Paired t-test comparing thin-surfaced GPS-1 and GPS-2 section means for the LWP wire line rut depths versus base type.

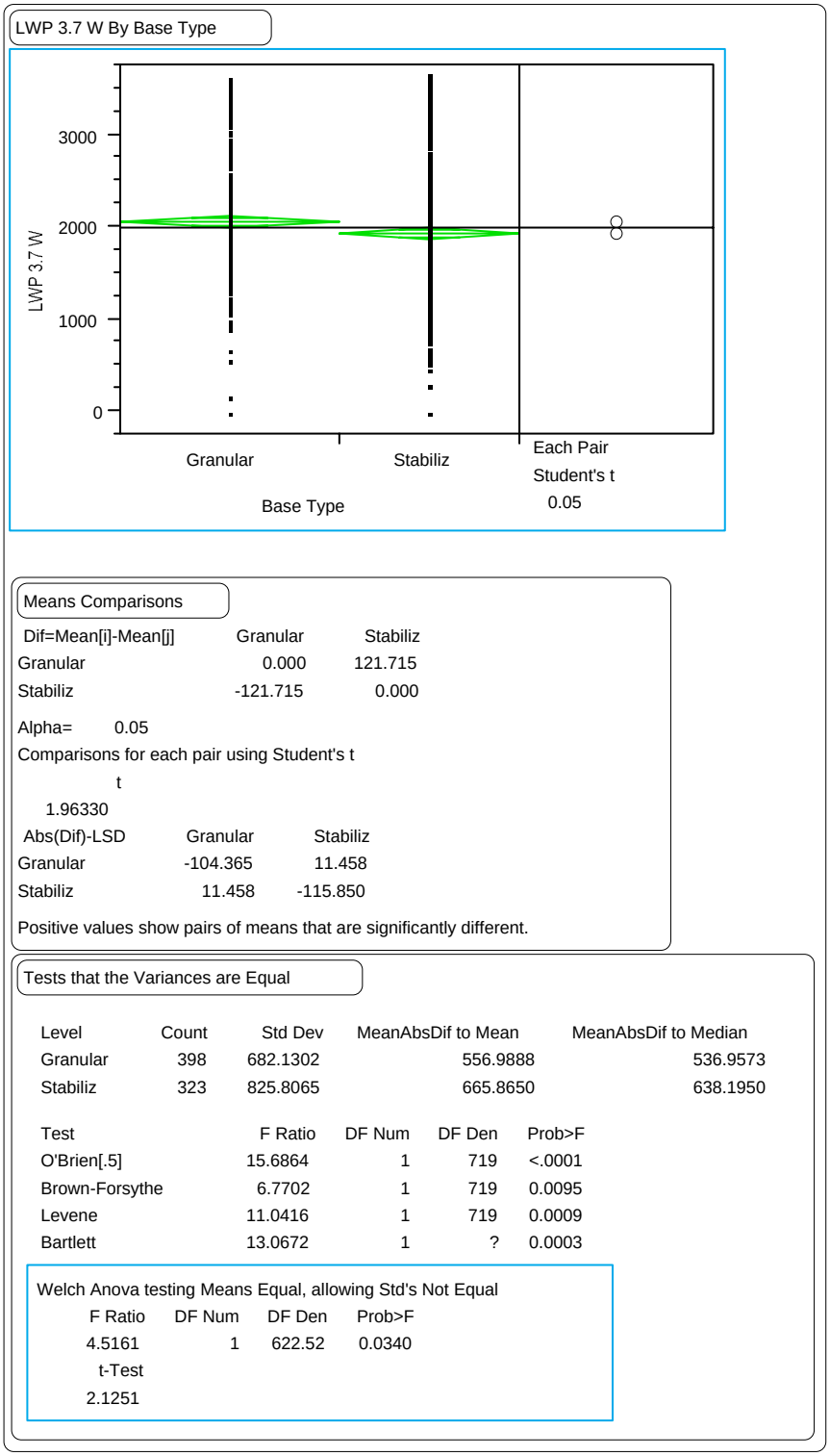

Figure 177. Paired t-test comparing thin-surfaced GPS-1 and GPS-2 section means for the LWP wire line rut widths versus base type.

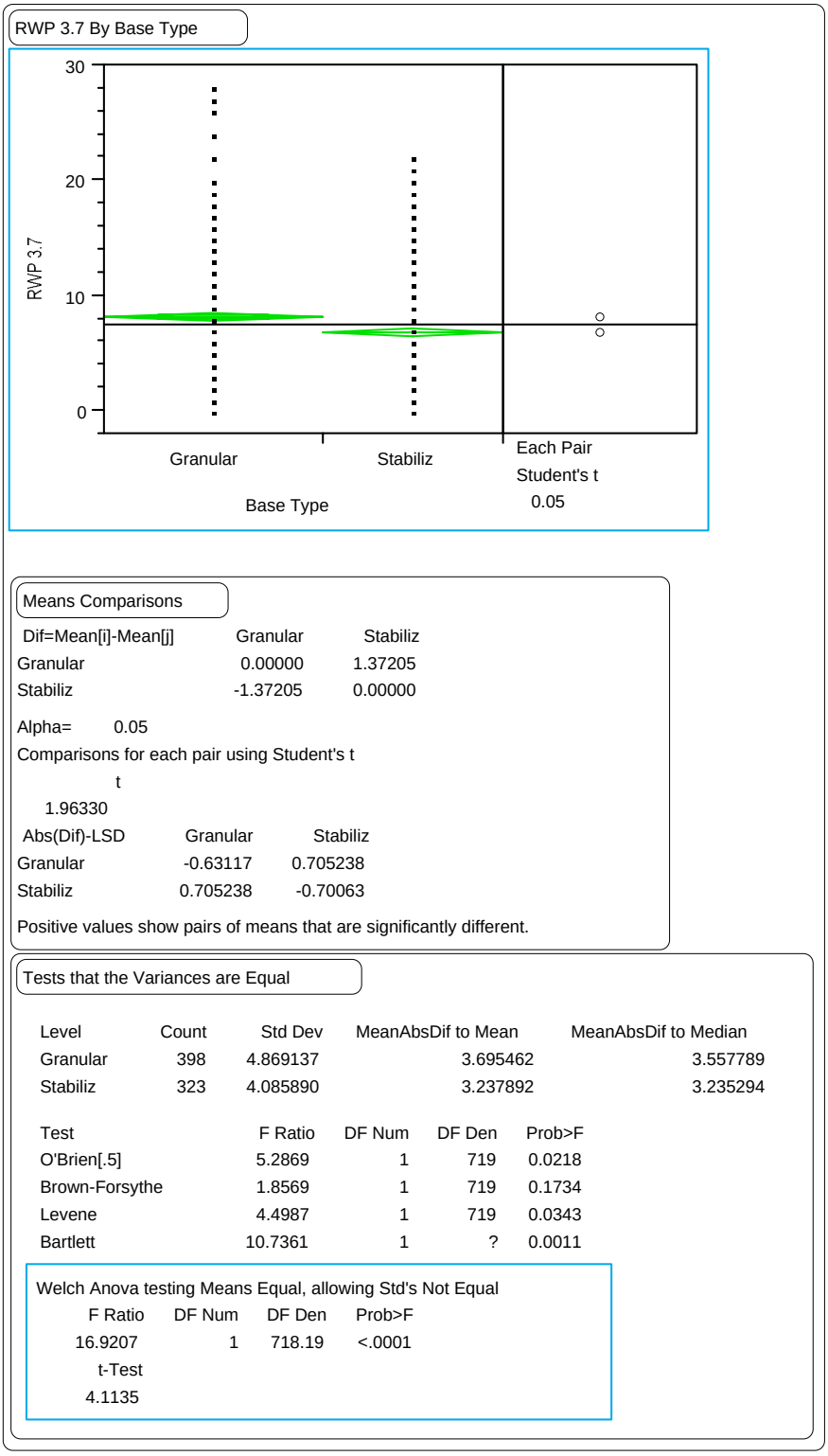

Figure 178. Paired t-test comparing thin-surfaced GPS-1 and GPS-2 section means for the RWP wire line rut depths versus base type.

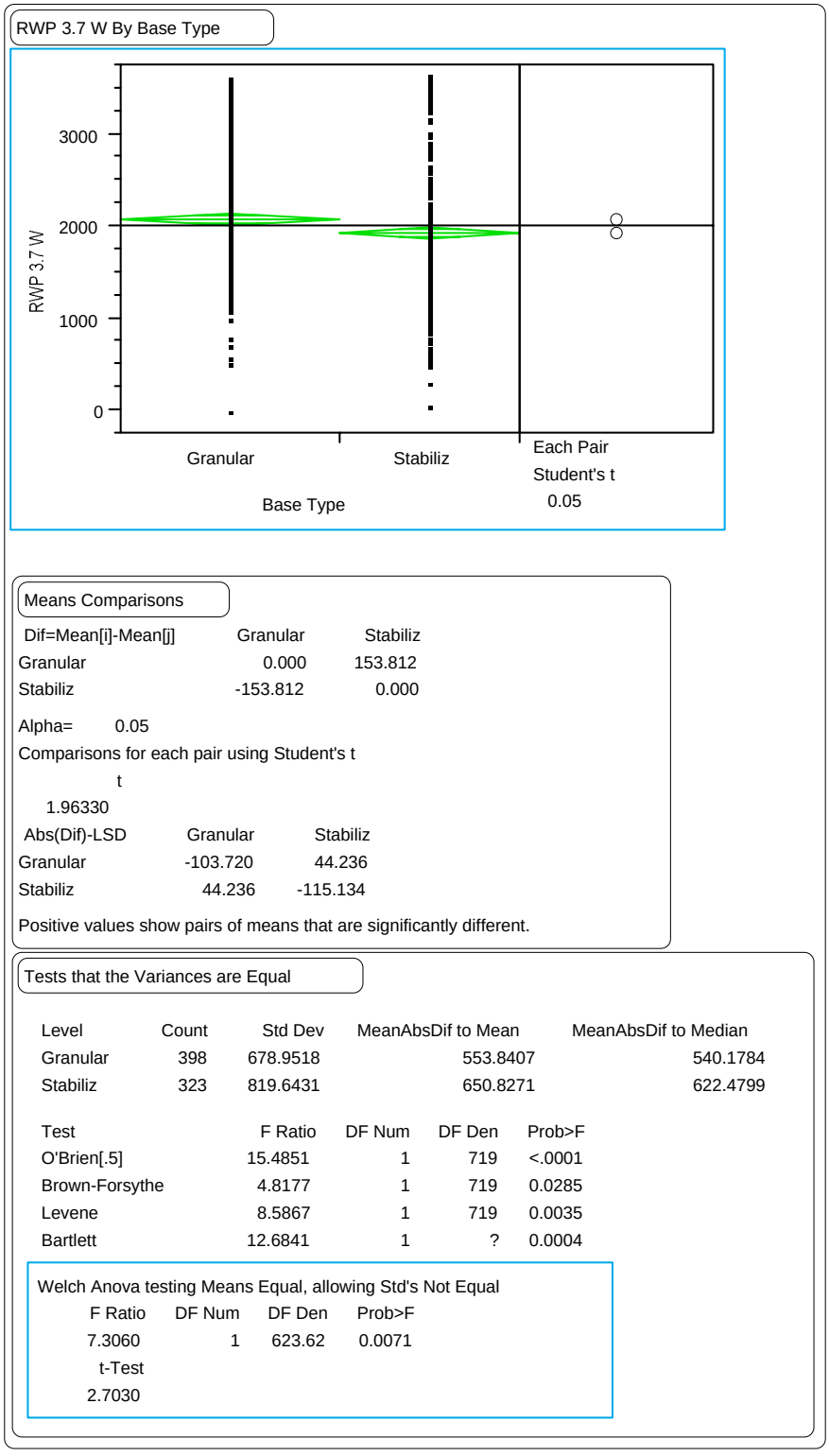

Figure 179. Paired t-test comparing thin-surfaced GPS-1 and GPS-2 section means for the RWP wire line rut widths versus base type.

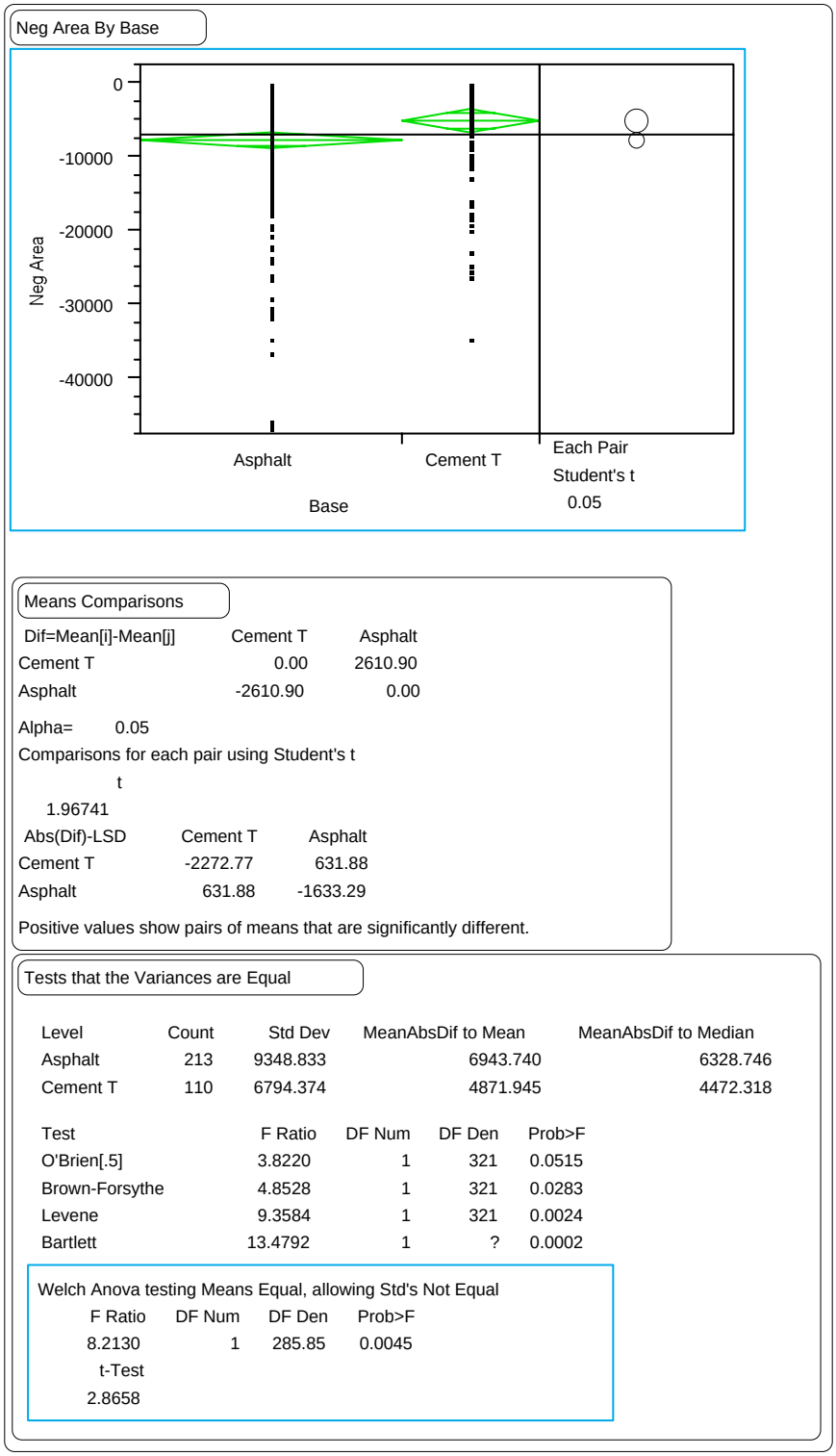

Figure 180. Paired t-test comparing thin-surfaced GPS-2 section means for the negative area index versus base type.

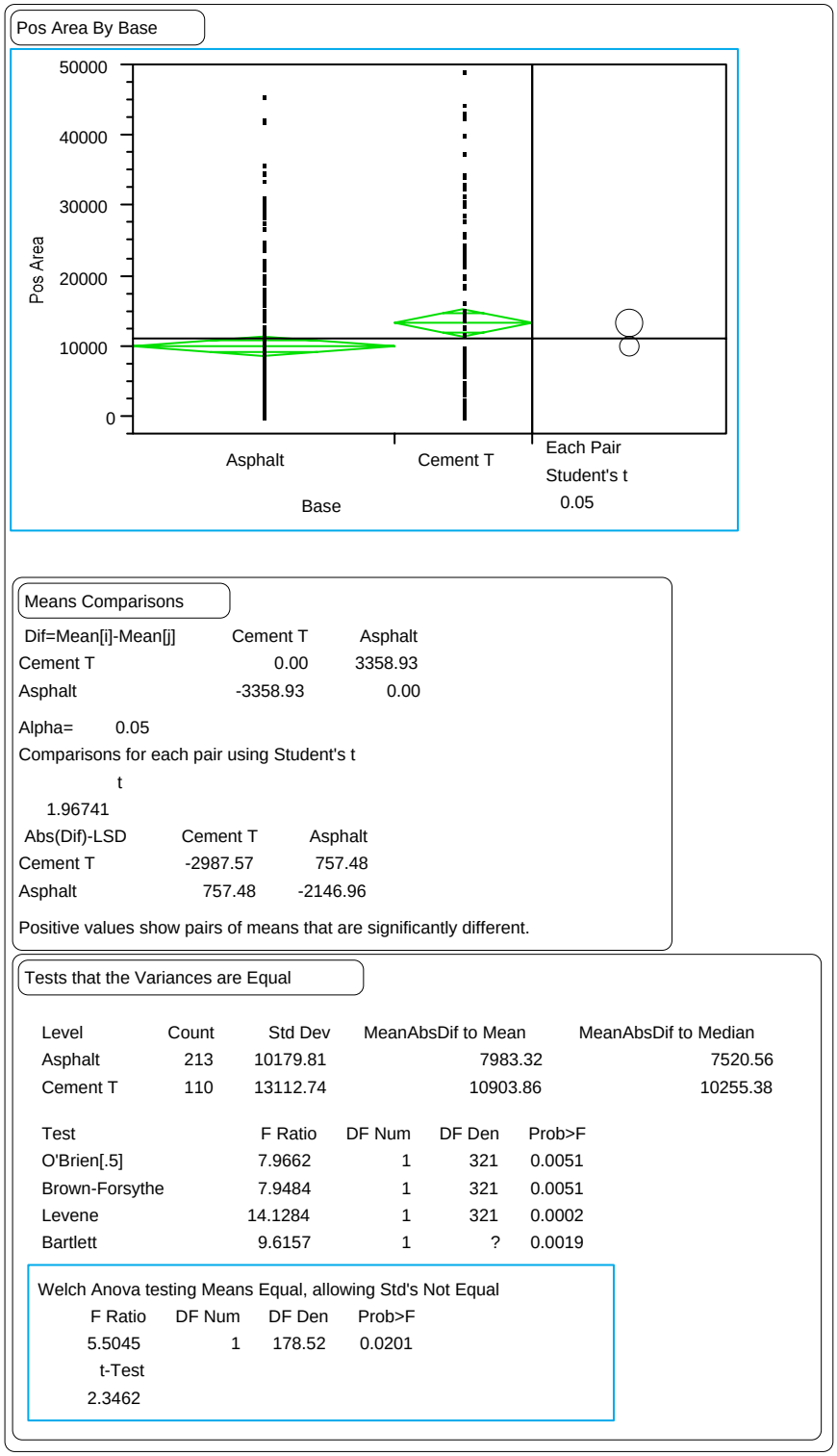

Figure 181. Paired t-test comparing thin-surfaced GPS-2 section means for the positive area index versus base type.

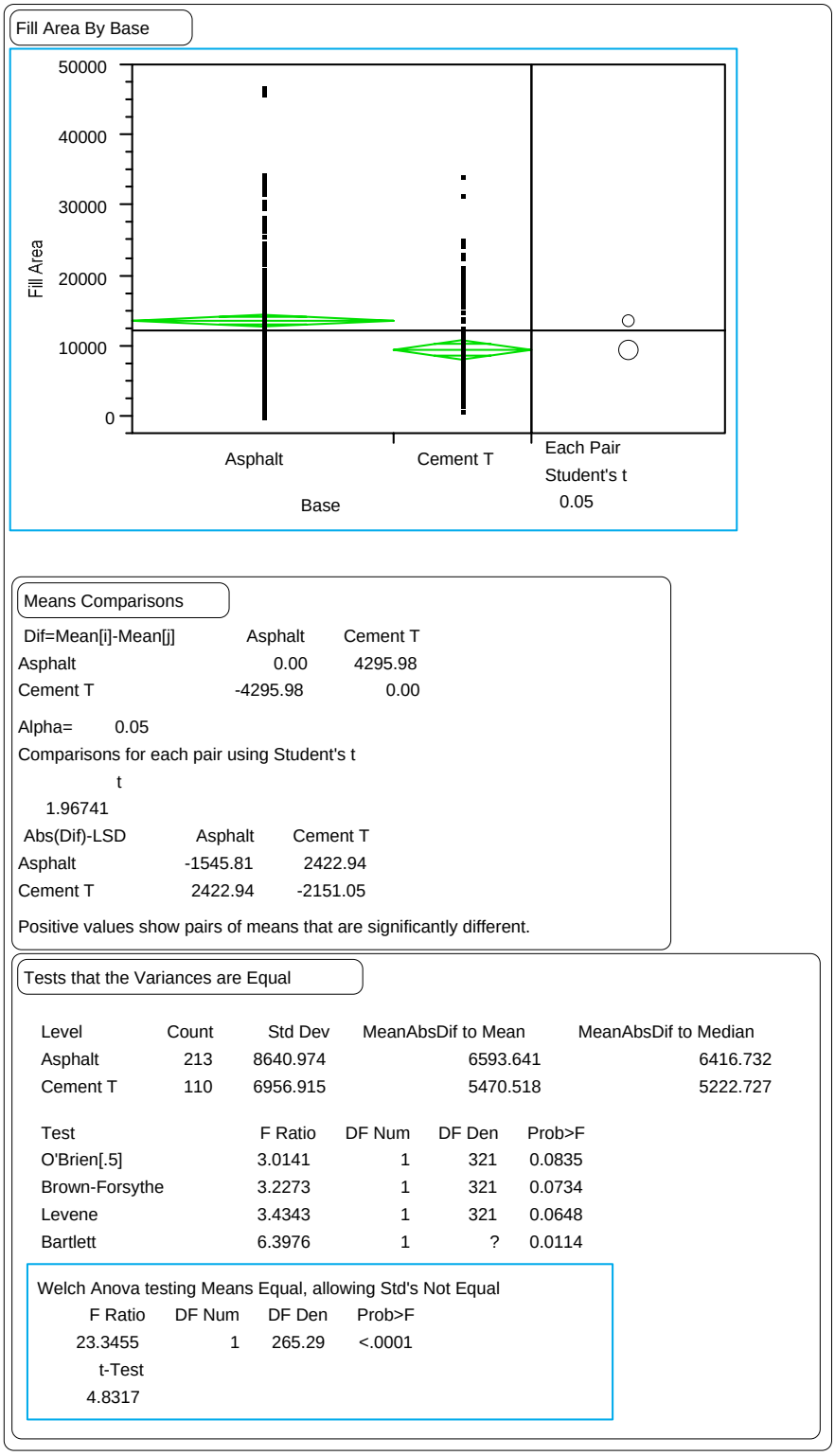

Figure 182. Paired t-test comparing thin-surfaced GPS-2 section means for the fill area index versus base type.

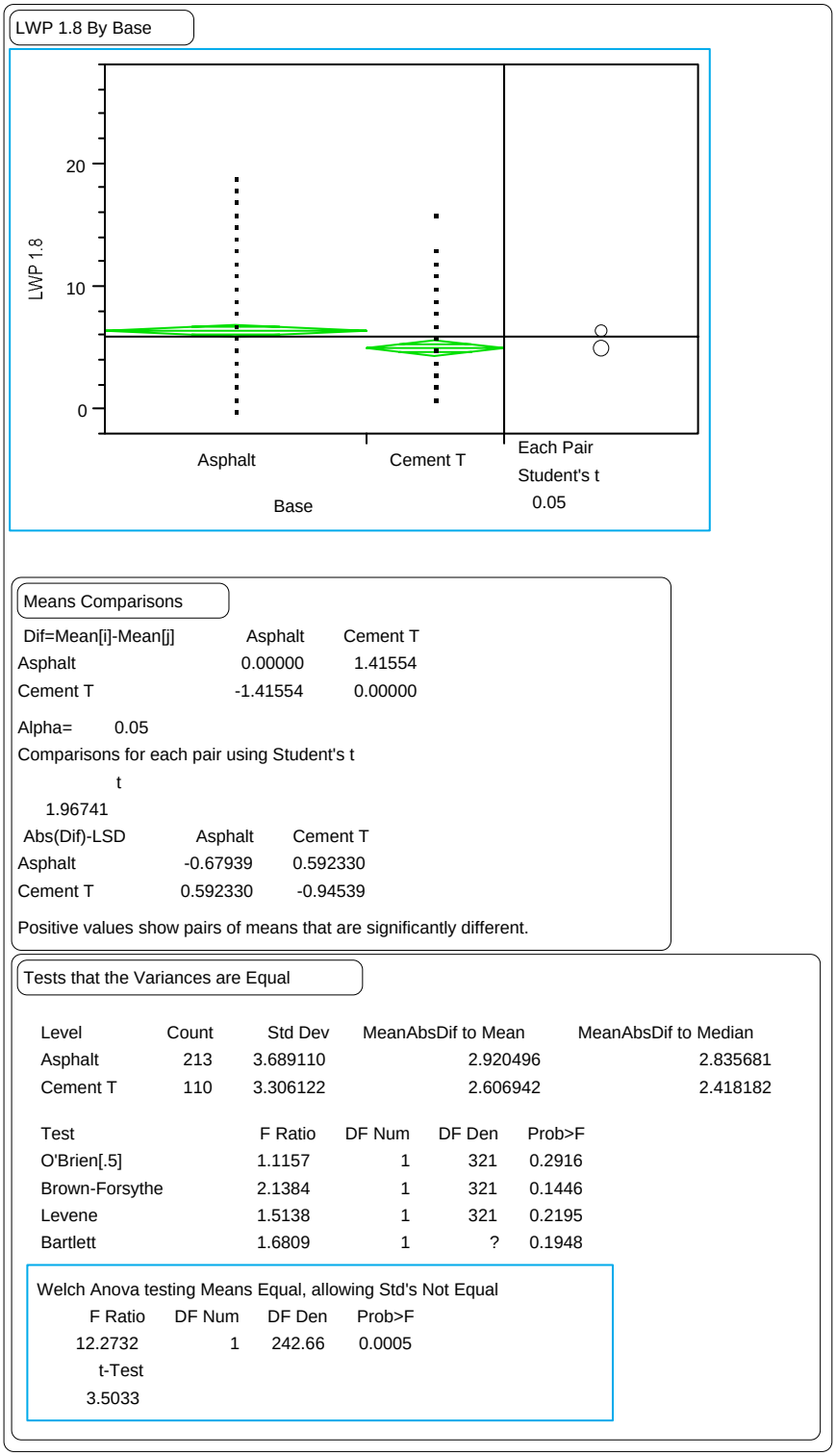

Figure 183. Paired t-test comparing thin-surfaced GPS-2 section means for the LWP 1.8-m rut depths versus base type.

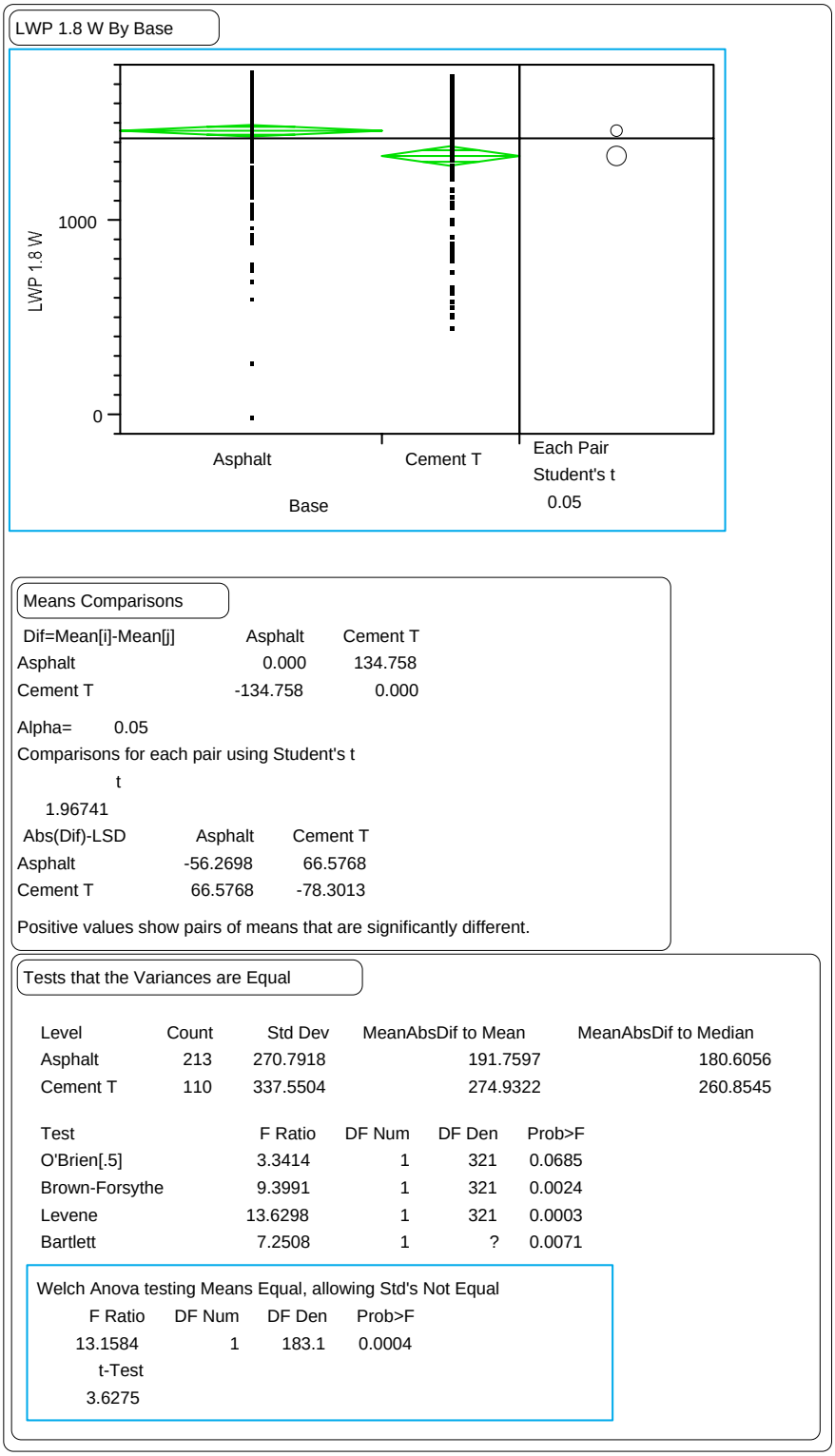

Figure 184. Paired t-test comparing thin-surfaced GPS-2 section means for the LWP 1.8-m rut widths versus base type.

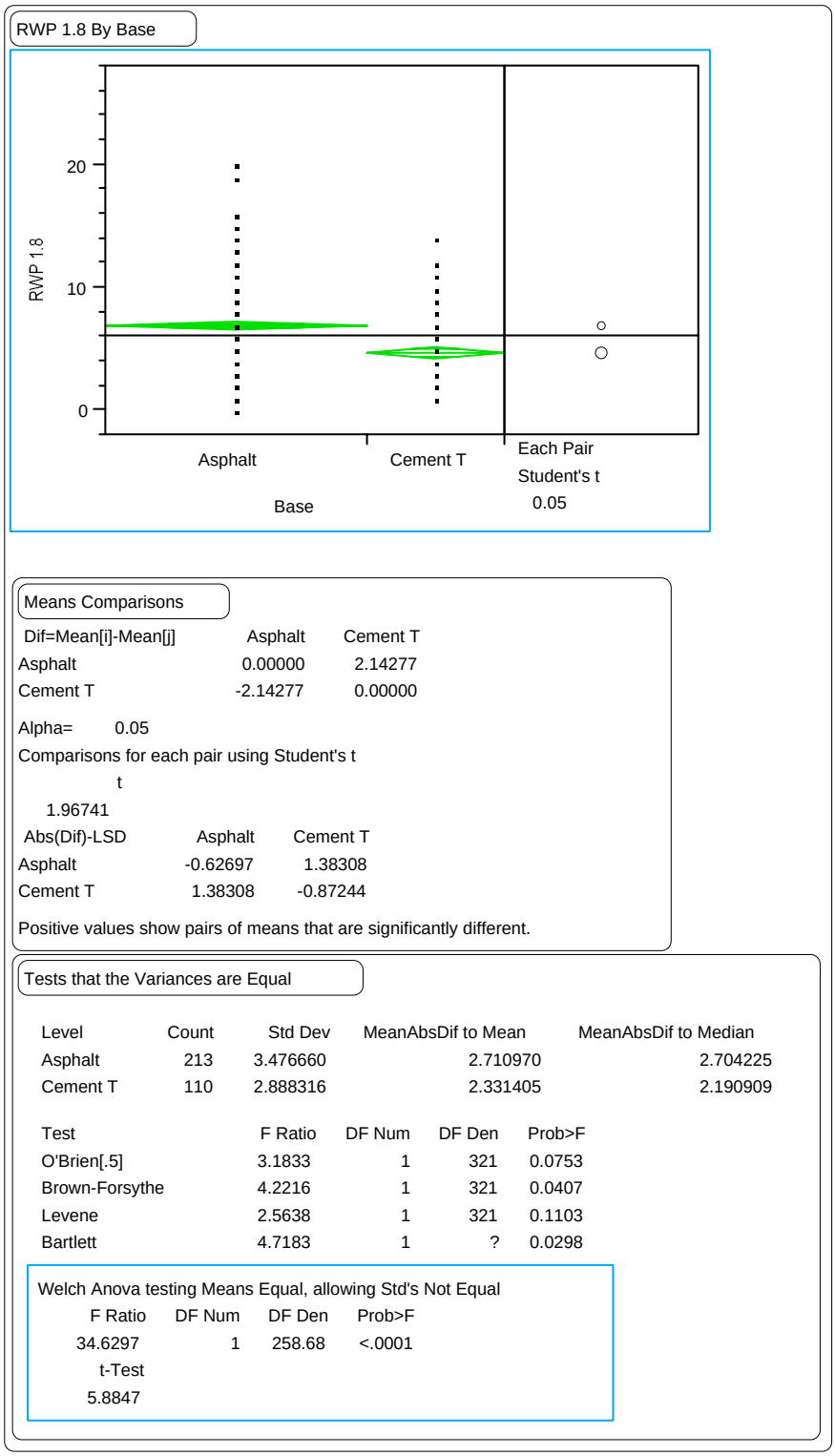

Figure 185. Paired t-test comparing thin-surfaced GPS-2 section means for the RWP 1.8-m rut depths versus base type.

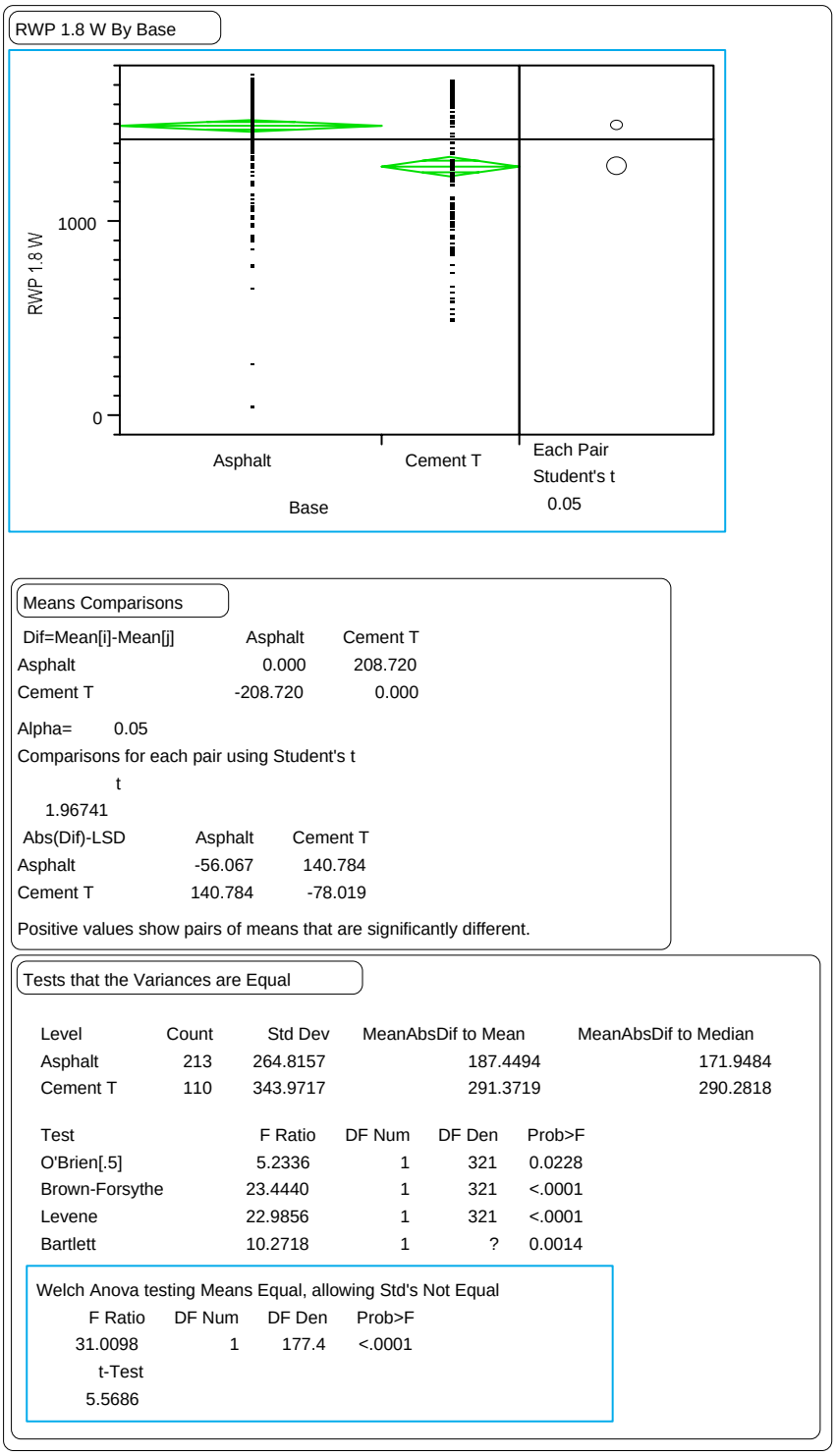

Figure 186. Paired t-test comparing thin-surfaced GPS-2 section means for the RWP 1.8-m rut widths versus base type.

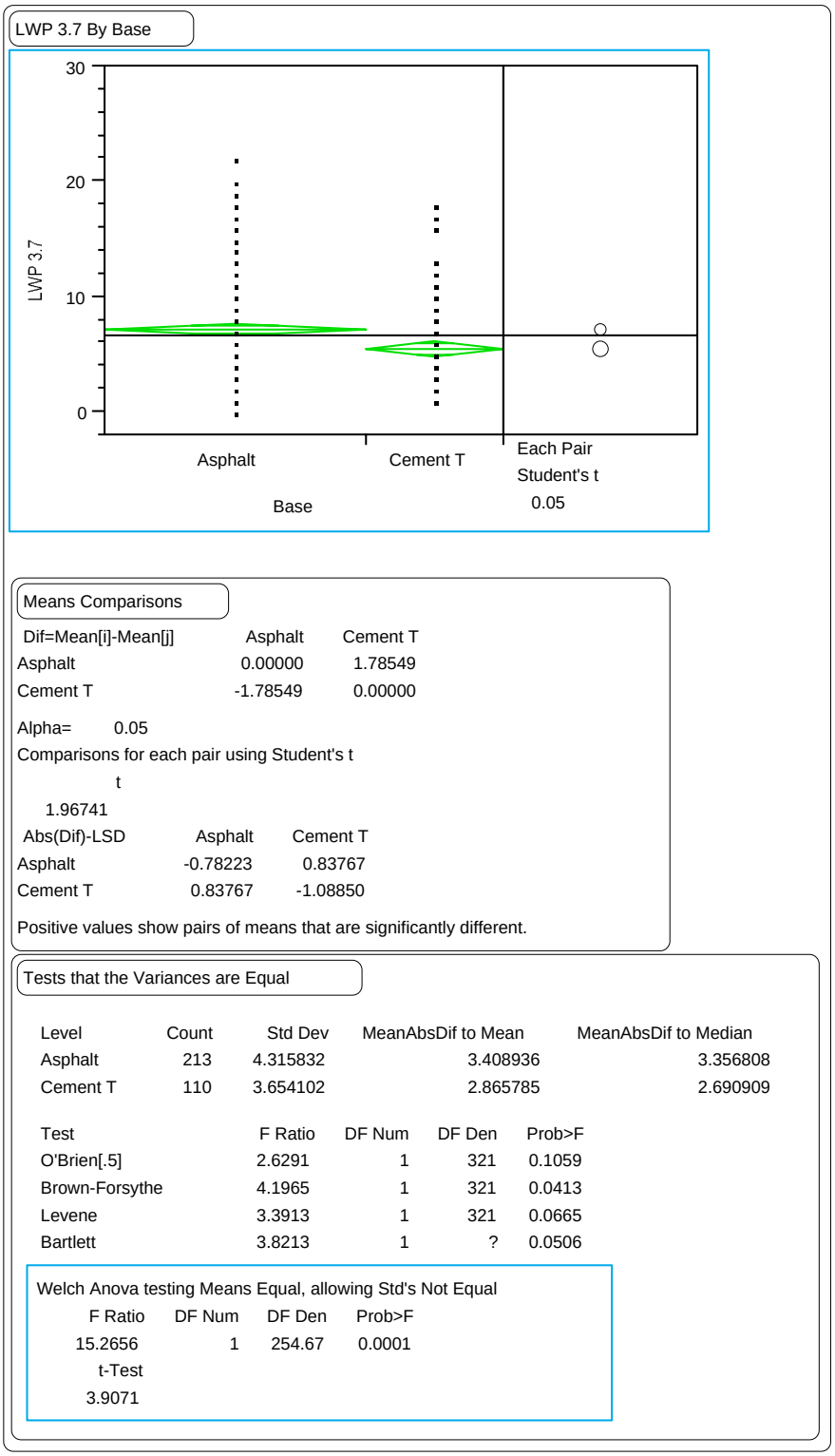

Figure 187. Paired t-test comparing thin-surfaced GPS-2 section means for the LWP wire line rut depths versus base type.

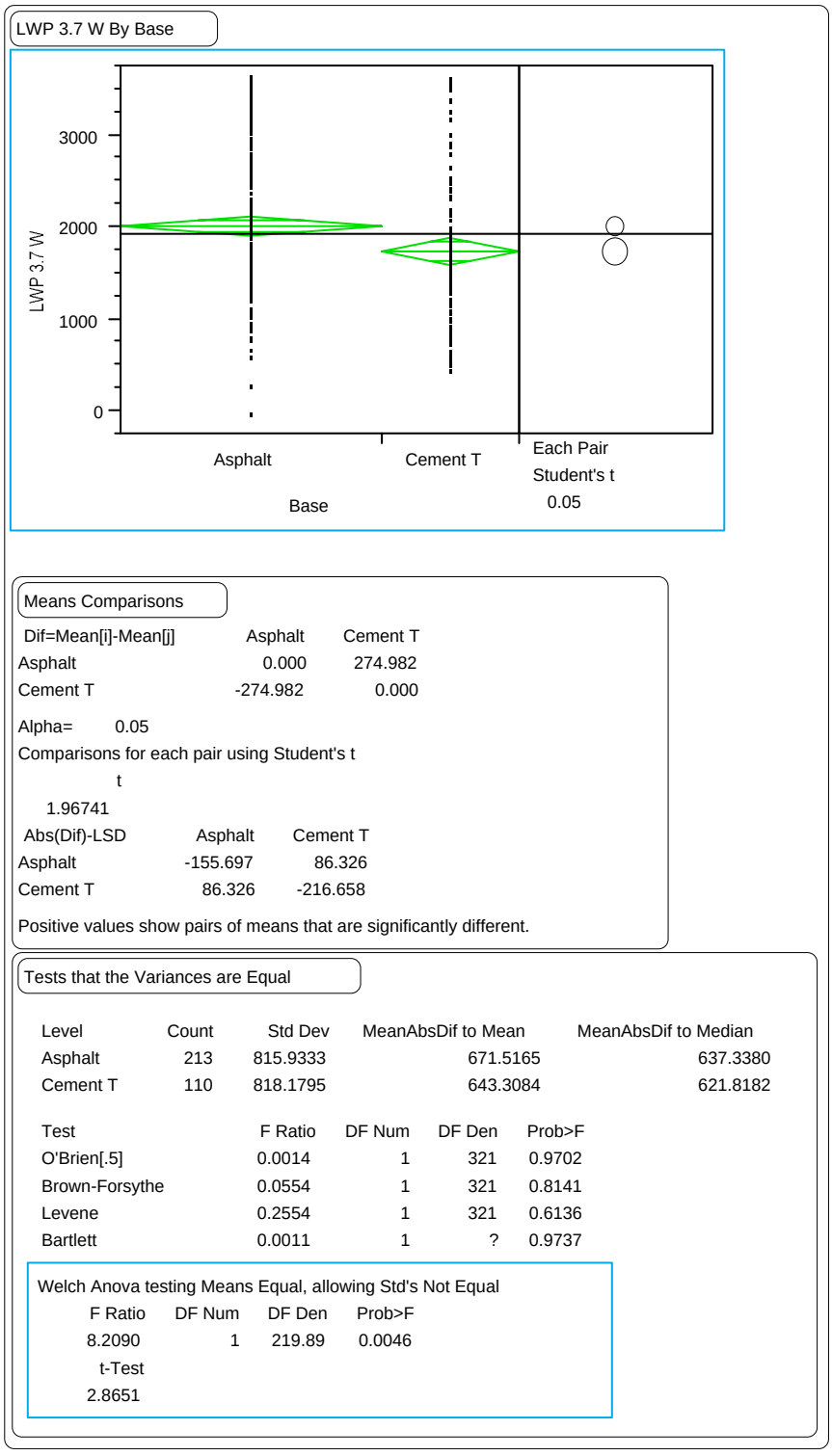

Figure 188. Paired t-test comparing thin-surfaced GPS-2 section means for the LWP wire line rut widths versus base type.

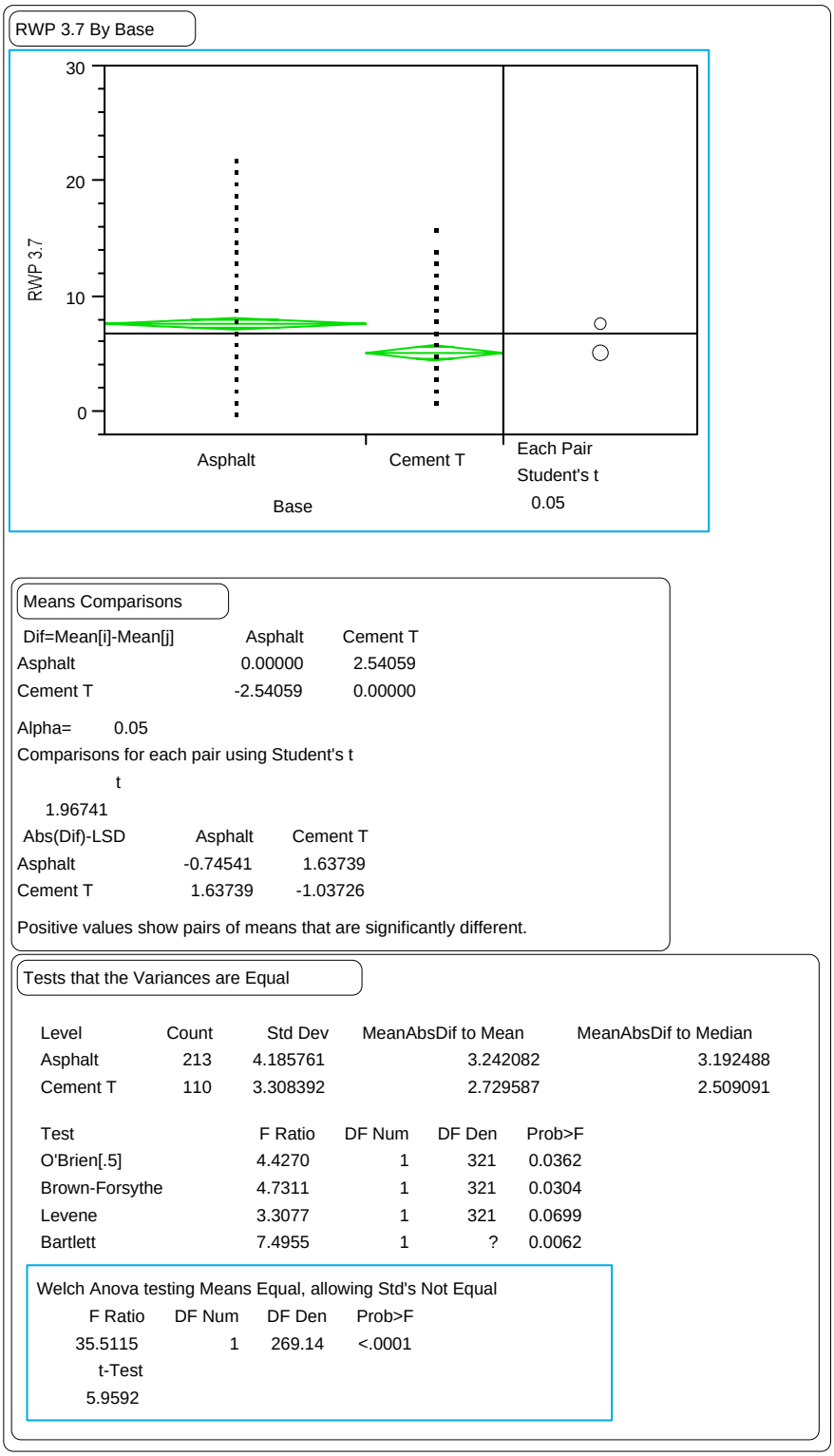

Figure 189. Paired t-test comparing thin-surfaced GPS-2 section means for the RWP wire line rut depths versus base type.

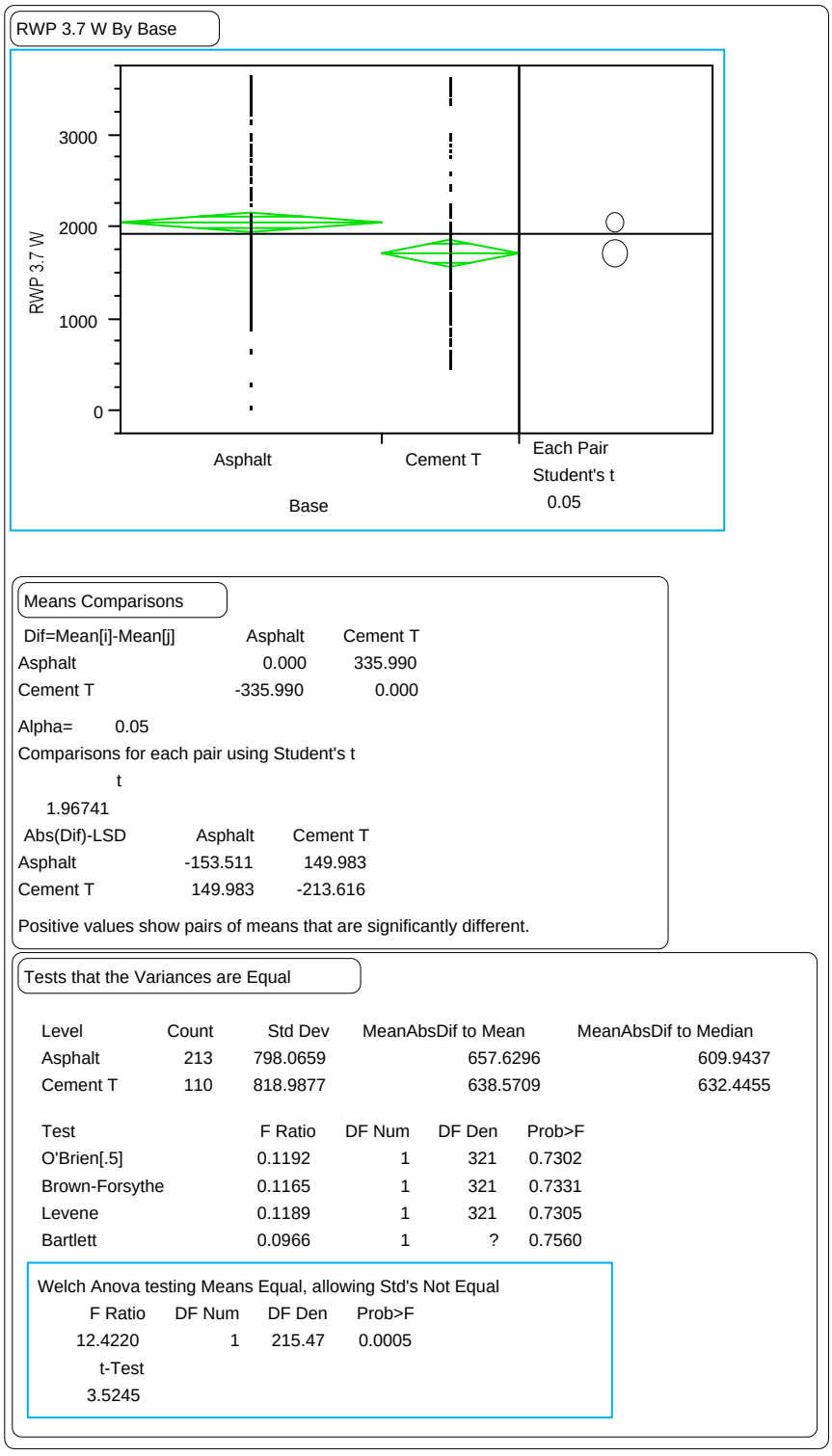

Figure 190. Paired t-test comparing thin-surfaced GPS-2 section means for the RWP wire line rut widths versus base type.

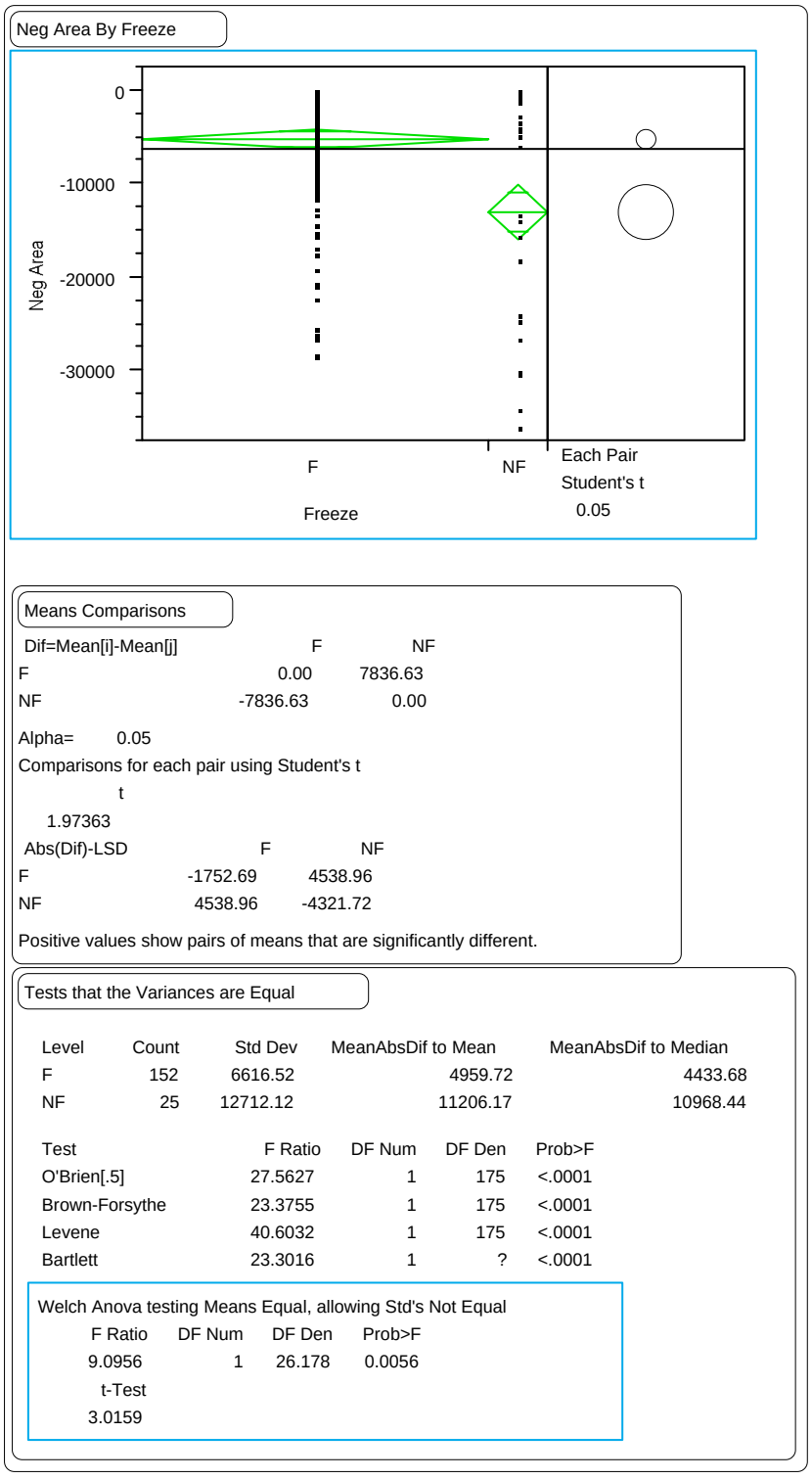

Figure 191. Paired t-test comparing climate for the GPS-7 section means of the negative area index.

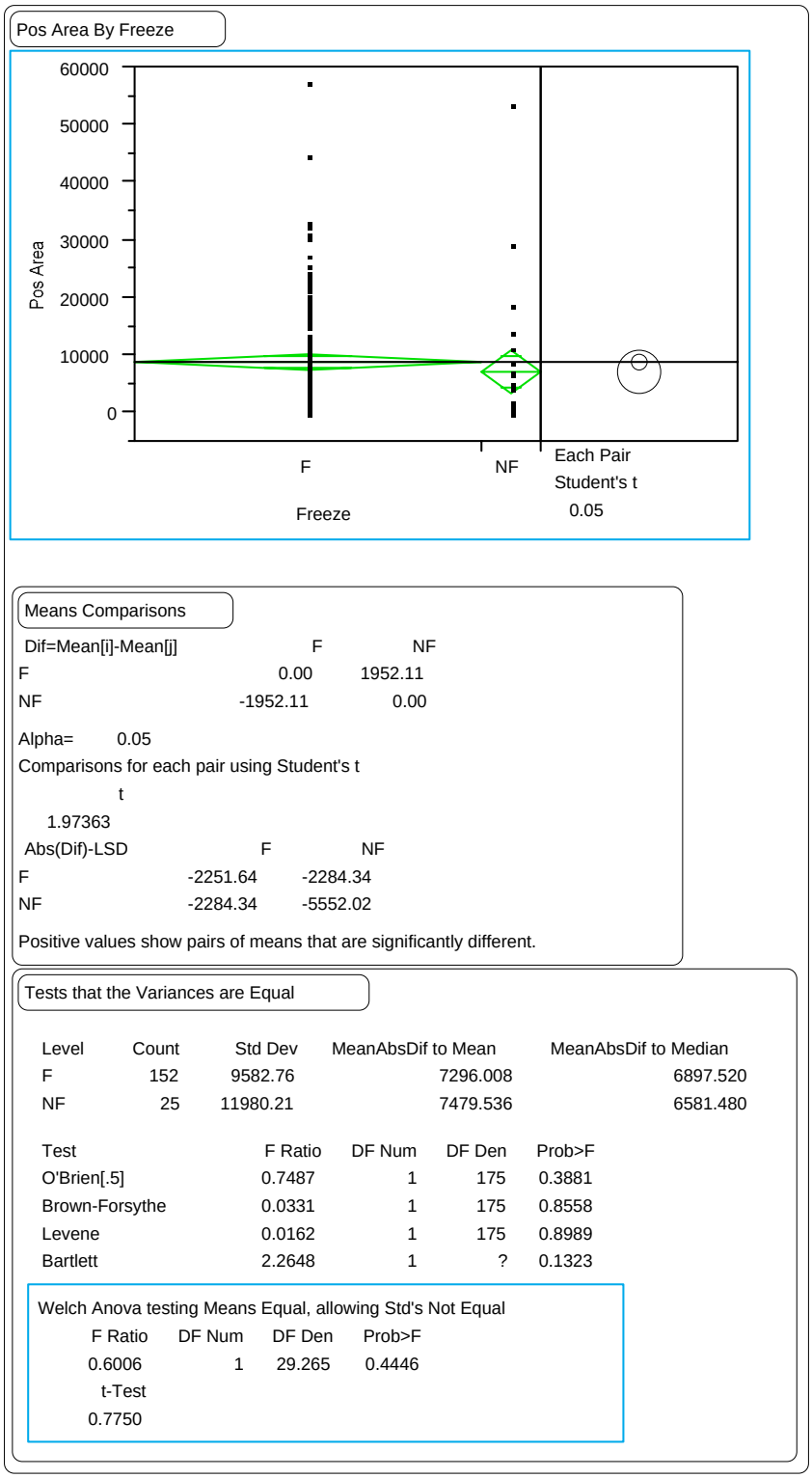

Figure 192. Paired t-test comparing climate for the GPS-7 section means of the positive area index.

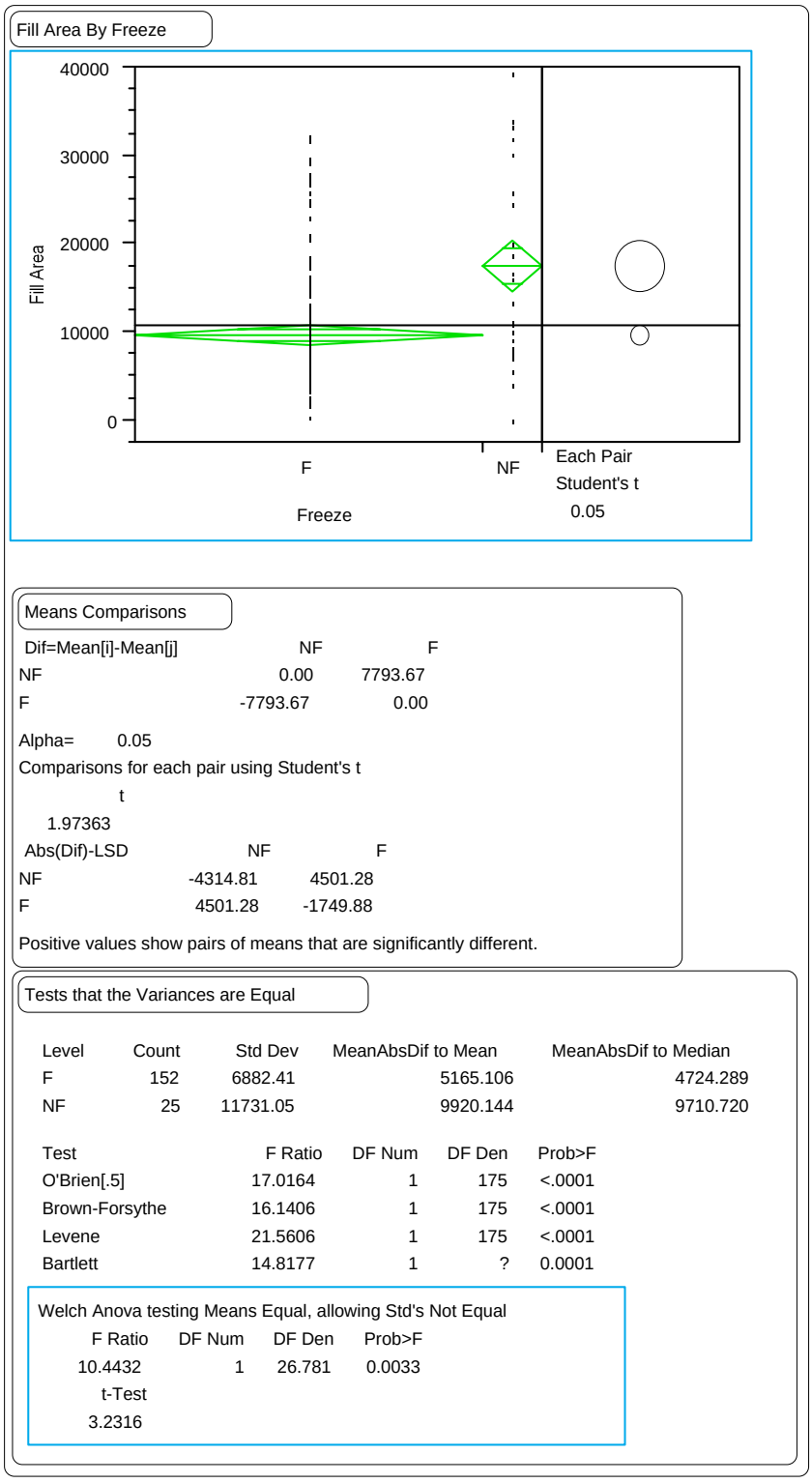

Figure 193. Paired t-test comparing climate for the GPS-7 section means of the fill area index.

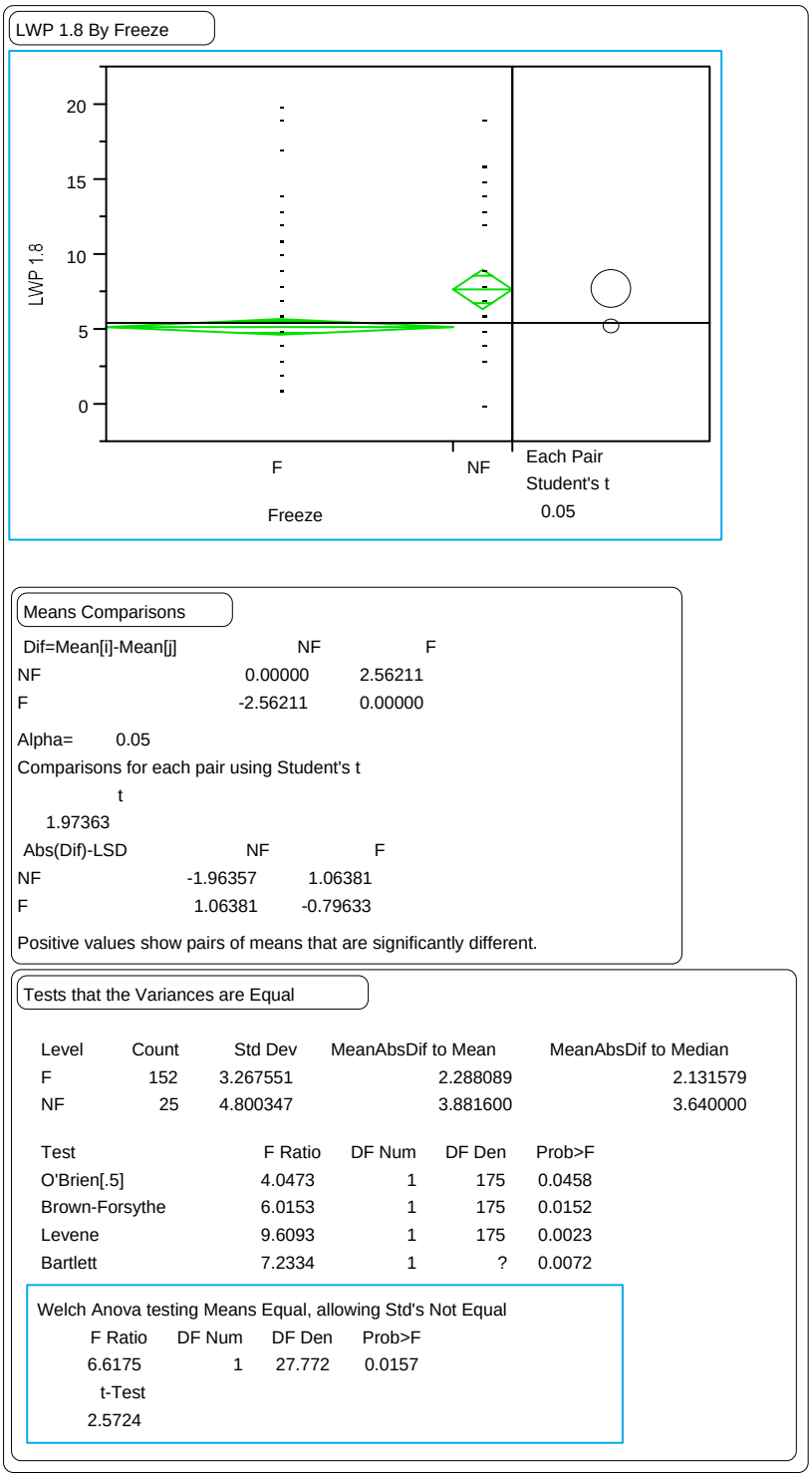

Figure 194. Paired t-test comparing climate for the GPS-7 section means of the LWP 1.8-m rut depths.

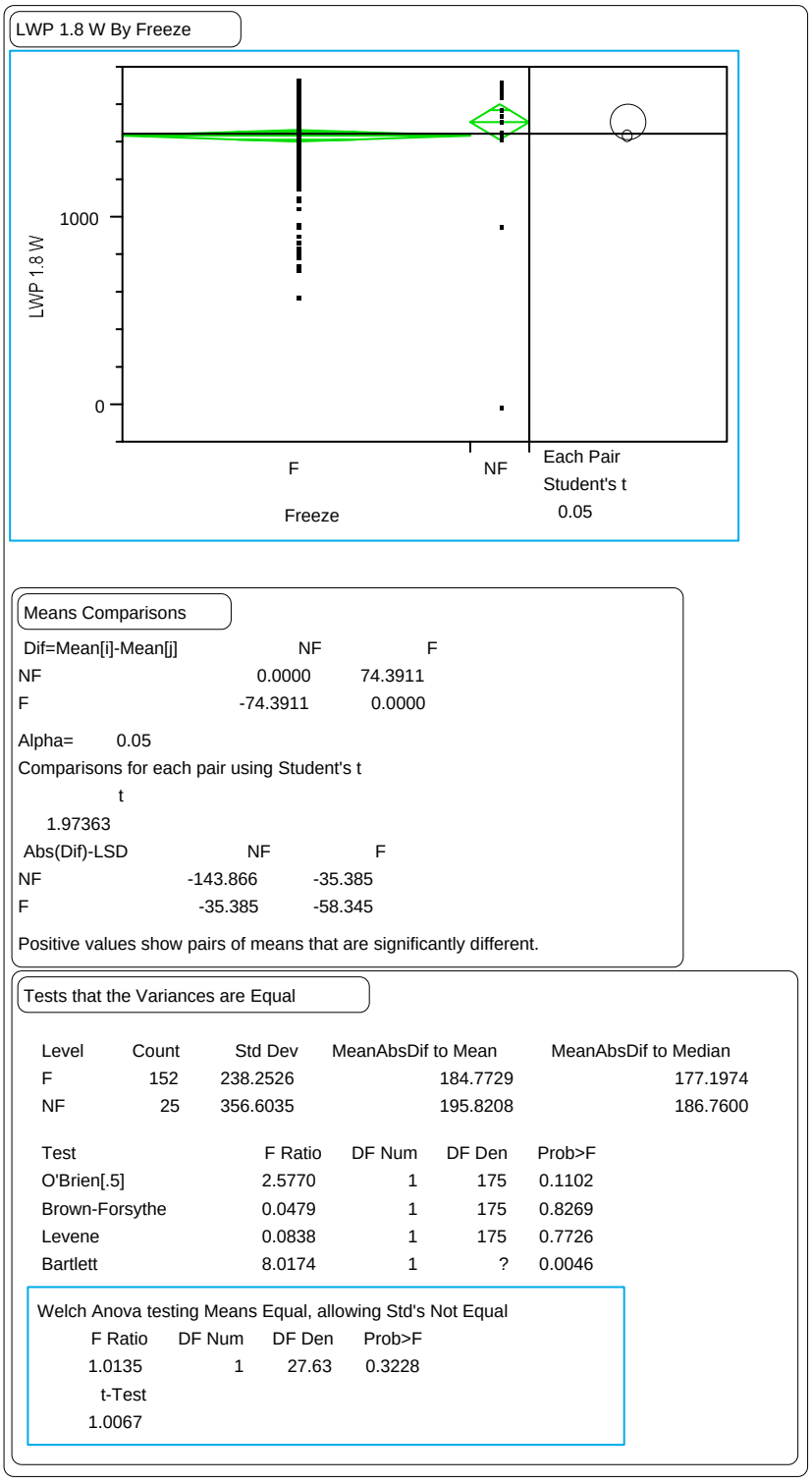

Figure 195. Paired t-test comparing climate for the GPS-7 section means of the LWP 1.8-m rut widths.

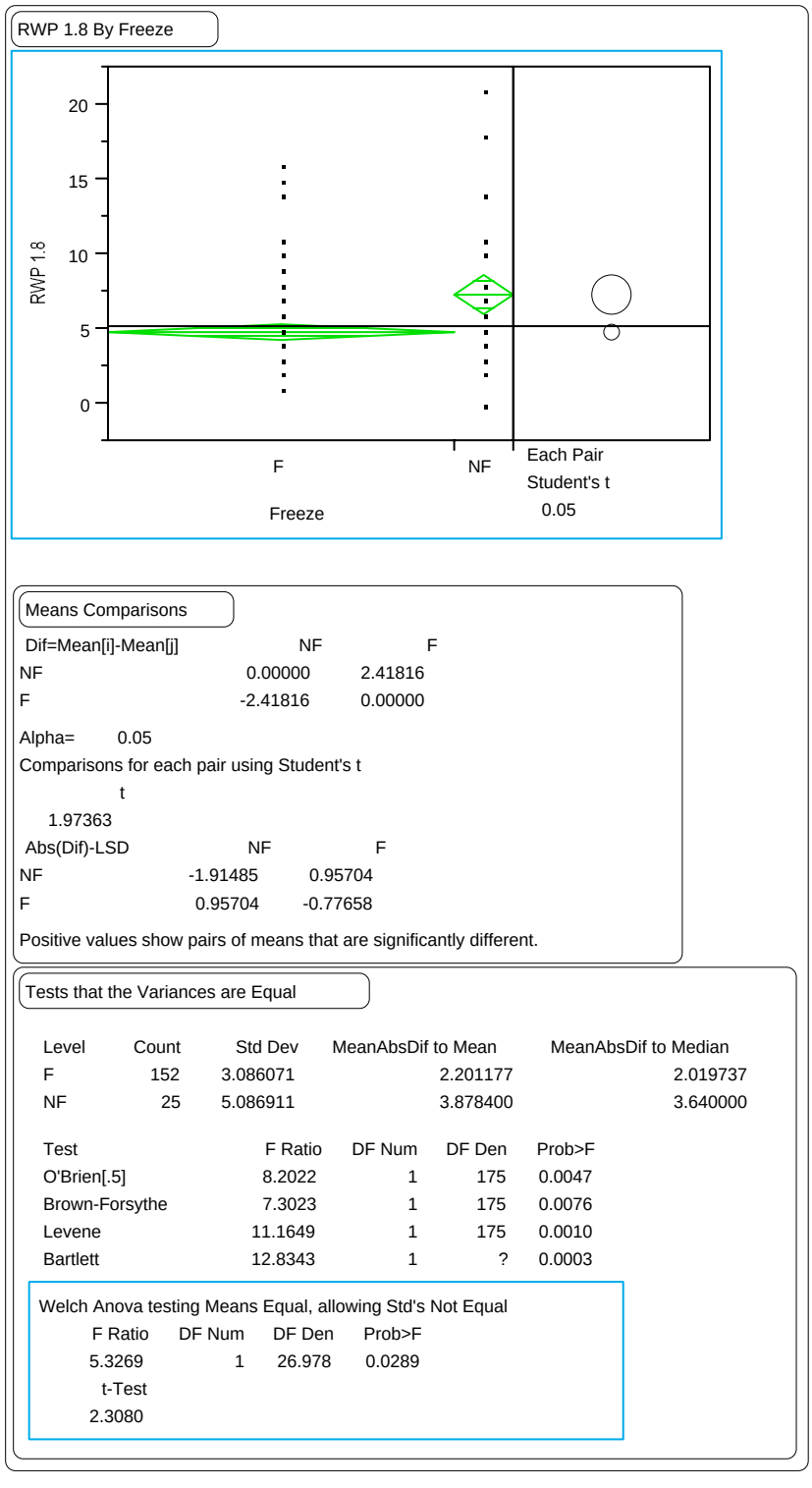

Figure 196. Paired t-test comparing climate for the GPS-7 section means of the RWP 1.8-m rut depths.

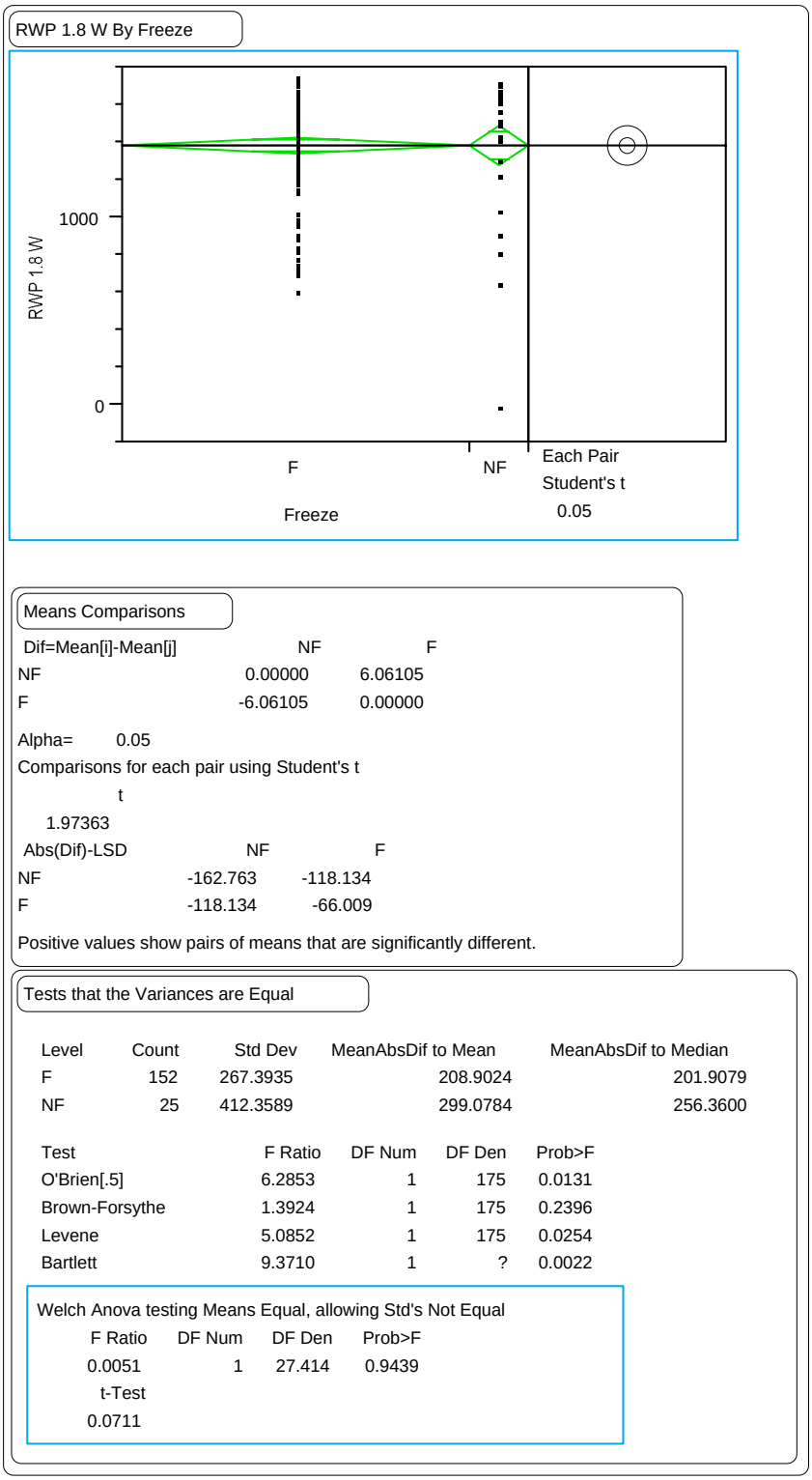

Figure 197. Paired t-test comparing climate for the GPS-7 section means of the RWP 1.8-m rut widths.

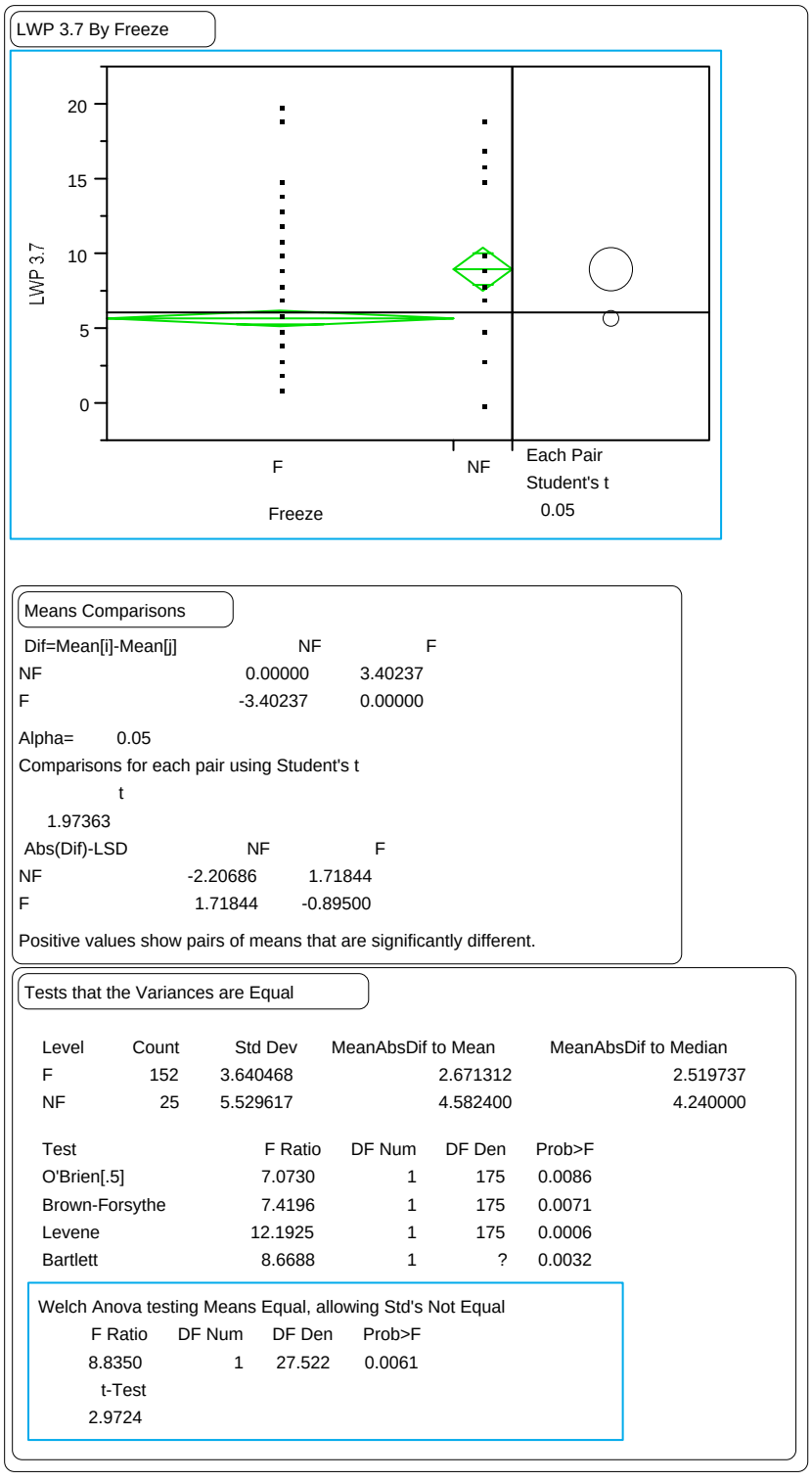

Figure 198. Paired t-test comparing climate for the GPS-7 section means of the LWP wire line rut depths.

LWP 3.7 W By Freeze

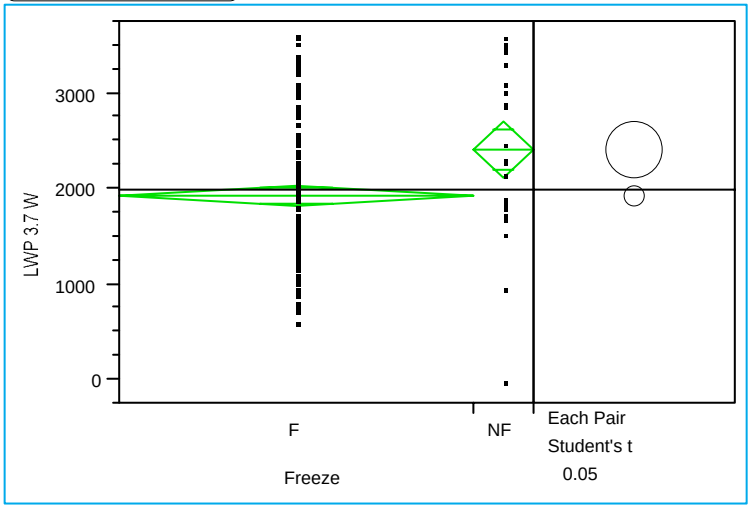

Means Comparisons

Dif=Mean[i]-Mean[j]	NF	F
NF	0.000	476.202
F	-476.202	0.000

Alpha= 0.05
Comparisons for each pair using Student's t
t
1.97363

Abs(Dif)-LSD	NF	F
NF	-437.046	142.717
F	142.717	-177.245

Positive values show pairs of means that are significantly different.

Tests that the Variances are Equal

Level	Count	Std Dev	MeanAbsDif to Mean	MeanAbsDif to Median
F	152	761.4174	632.8072	603.1382
NF	25	906.5596	745.9136	742.0800

Test	F Ratio	DF Num	DF Den	Prob>F
O'Brien[.5]	2.0283	1	175	0.1562
Brown-Forsythe	1.5290	1	175	0.2179
Levene	1.4793	1	175	0.2255
Bartlett	1.3514	1	?	0.2450

Welch Anova testing Means Equal, allowing Std's Not Equal

F Ratio	DF Num	DF Den	Prob>F
6.1810	1	29.828	0.0187

t-Test
2.4862

Figure 199. Paired t-test comparing climate for the GPS-7 section means of the LWP wire line rut widths.

RWP 3.7 By Freeze

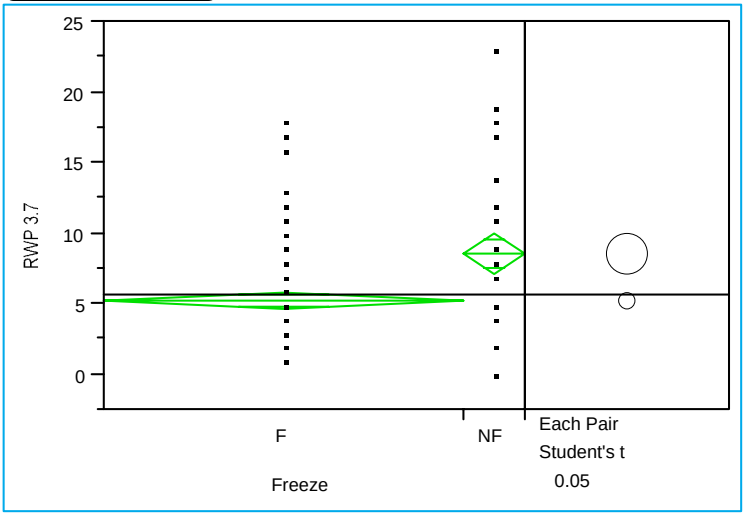

Means Comparisons

Dif=Mean[i]-Mean[j]	NF	F
NF	0.00000	3.28368
F	-3.28368	0.00000

Alpha= 0.05

Comparisons for each pair using Student's t

t

1.97363

Abs(Dif)-LSD	NF	F
NF	-2.20828	1.59867
F	1.59867	-0.89557

Positive values show pairs of means that are significantly different.

Tests that the Variances are Equal

Level	Count	Std Dev	MeanAbsDif to Mean	MeanAbsDif to Median
F	152	3.525118	2.546918	2.289474
NF	25	5.993608	4.796800	4.600000

Test	F Ratio	DF Num	DF Den	Prob>F
O'Brien[.5]	11.5847	1	175	0.0008
Brown-Forsythe	11.6526	1	175	0.0008
Levene	16.1536	1	175	<.0001
Bartlett	14.6645	1	?	0.0001

Welch Anova testing Means Equal, allowing Std's Not Equal

F Ratio	DF Num	DF Den	Prob>F
7.0999	1	26.795	0.0129

t-Test

2.6646

Figure 200. Paired t-test comparing climate for the GPS-7 section means of the RWP wire line rut depths.

RWP 3.7 W By Freeze

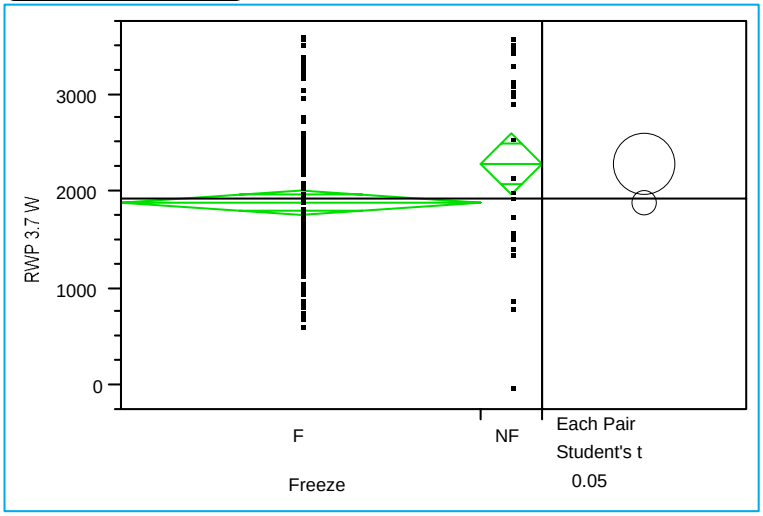

Means Comparisons

Dif=Mean[i]-Mean[j]	NF	F
NF	0.000	408.883
F	-408.883	0.000

Alpha= 0.05

Comparisons for each pair using Student's t

t

1.97363

Abs(Dif)-LSD	NF	F
NF	-454.253	62.267
F	62.267	-184.224

Positive values show pairs of means that are significantly different.

Tests that the Variances are Equal

Level	Count	Std Dev	MeanAbsDif to Mean	MeanAbsDif to Median
F	152	775.050	635.1389	602.9211
NF	25	1024.175	896.7232	896.6800

Test	F Ratio	DF Num	DF Den	Prob>F
O'Brien[.5]	6.5846	1	175	0.0111
Brown-Forsythe	6.7601	1	175	0.0101
Levene	7.4601	1	175	0.0070
Bartlett	3.6204	1	?	0.0571

Welch Anova testing Means Equal, allowing Std's Not Equal

F Ratio	DF Num	DF Den	Prob>F
3.6416	1	28.694	0.0664

t-Test

1.9083

Figure 201. Paired t-test comparing climate for the GPS-7 section means of the RWP wire line rut widths.

APPENDIX E.
COMPARISONS OF TIME-SERIES SLOPES

The slopes for the time-series data for each test section were determined for each of the indices. The distributions of the slopes are provided in figures 202 through 212. The signs of the slopes for each of the indices were compared to the signs for the LWP 1.8-m rut depth. These results are provided in figures 213 through 222. The top block in each figure is a graphical presentation of the results. The second block is a contingency table that provides a count for each cell in the table. A "-1" indicates a negative slope, a "0" indicates a zero slope, and a "1" indicates a positive slope. The bottom block provides the statistical results for each analysis.

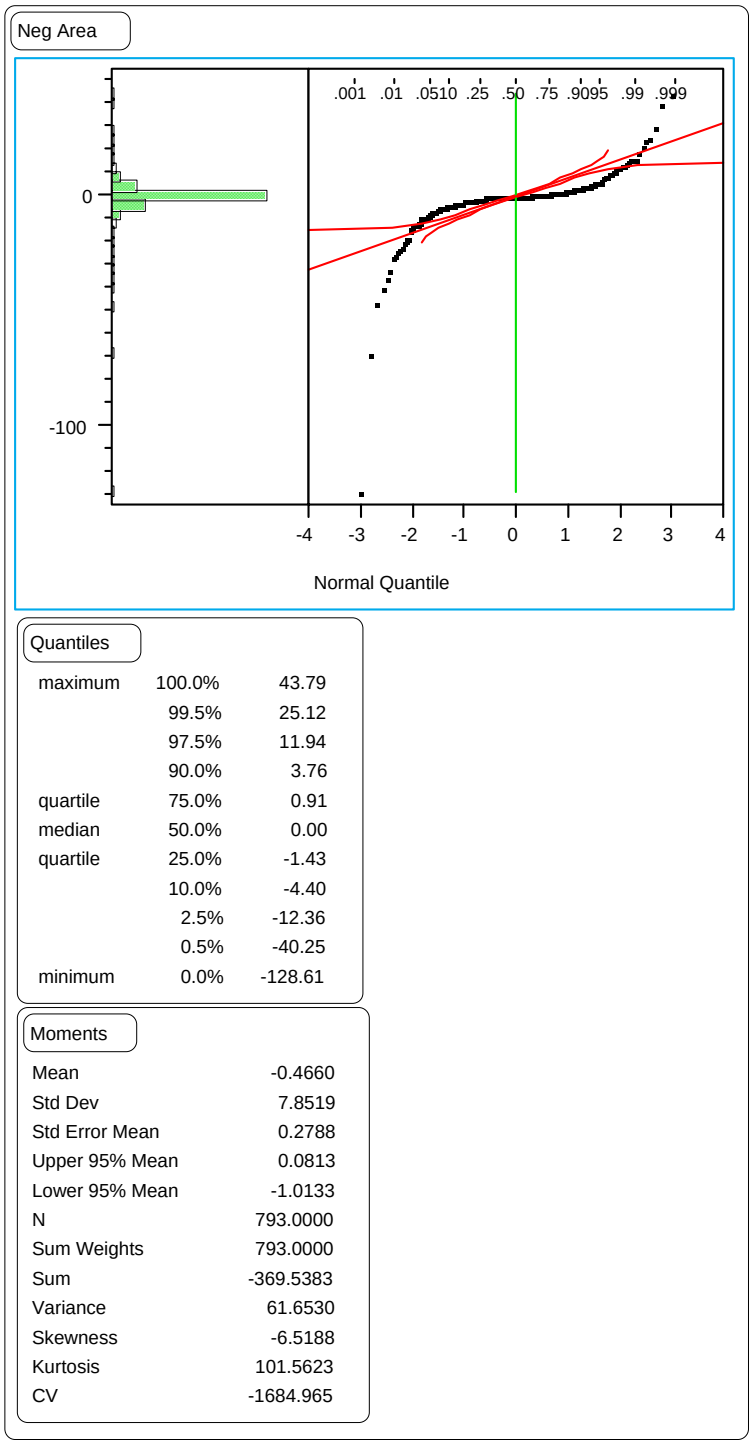

Figure 202. Distribution of the time-series slopes for the negative area index.

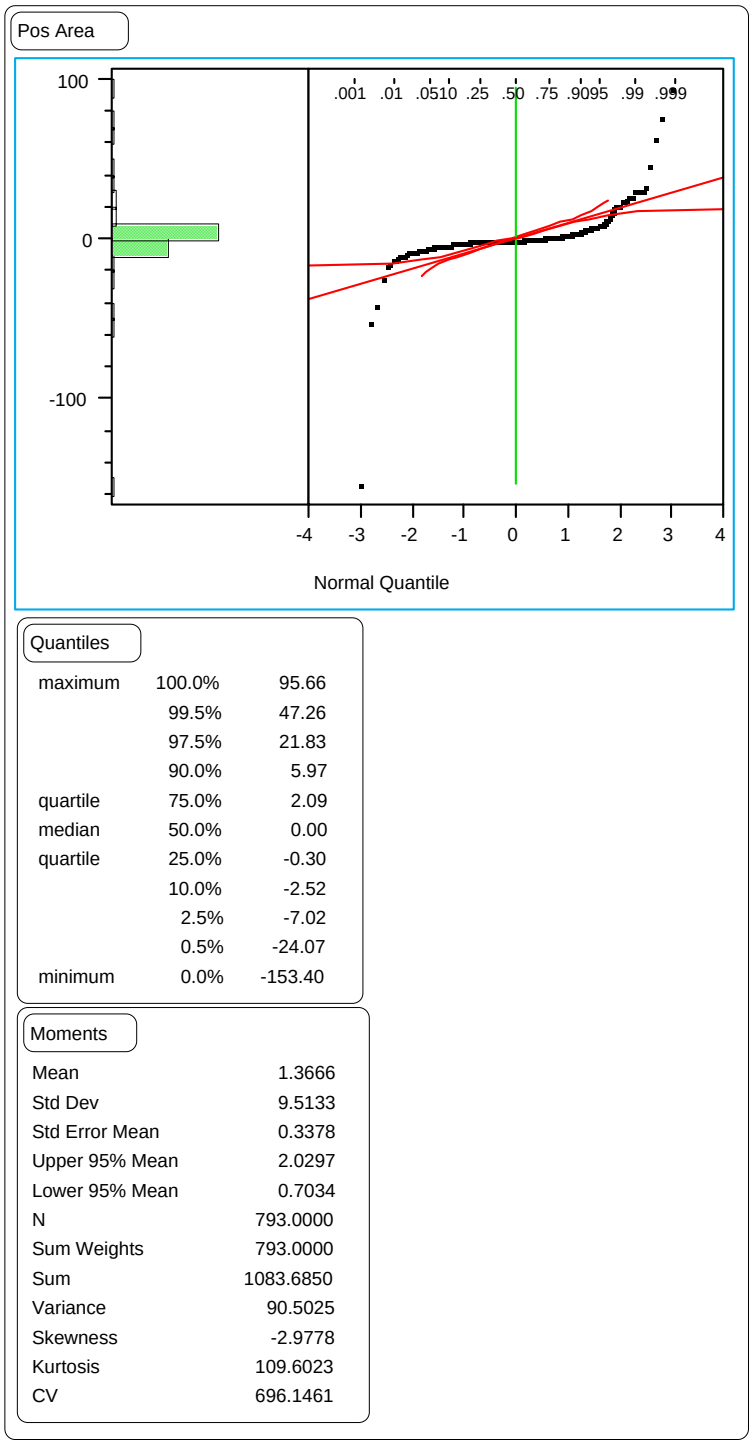

Figure 203. Distribution of the time-series slopes for the positive area index.

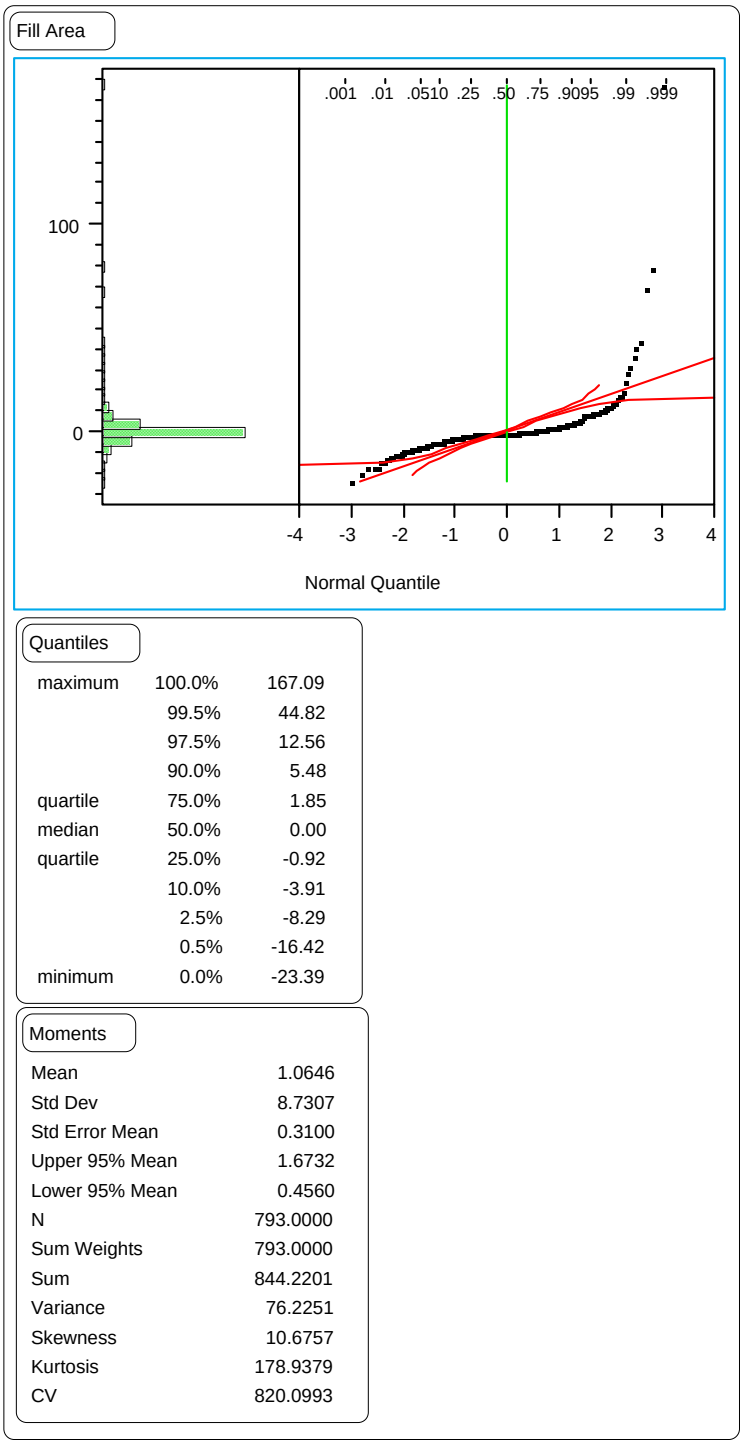

Figure 204. Distribution of the time-series slopes for the fill area index.

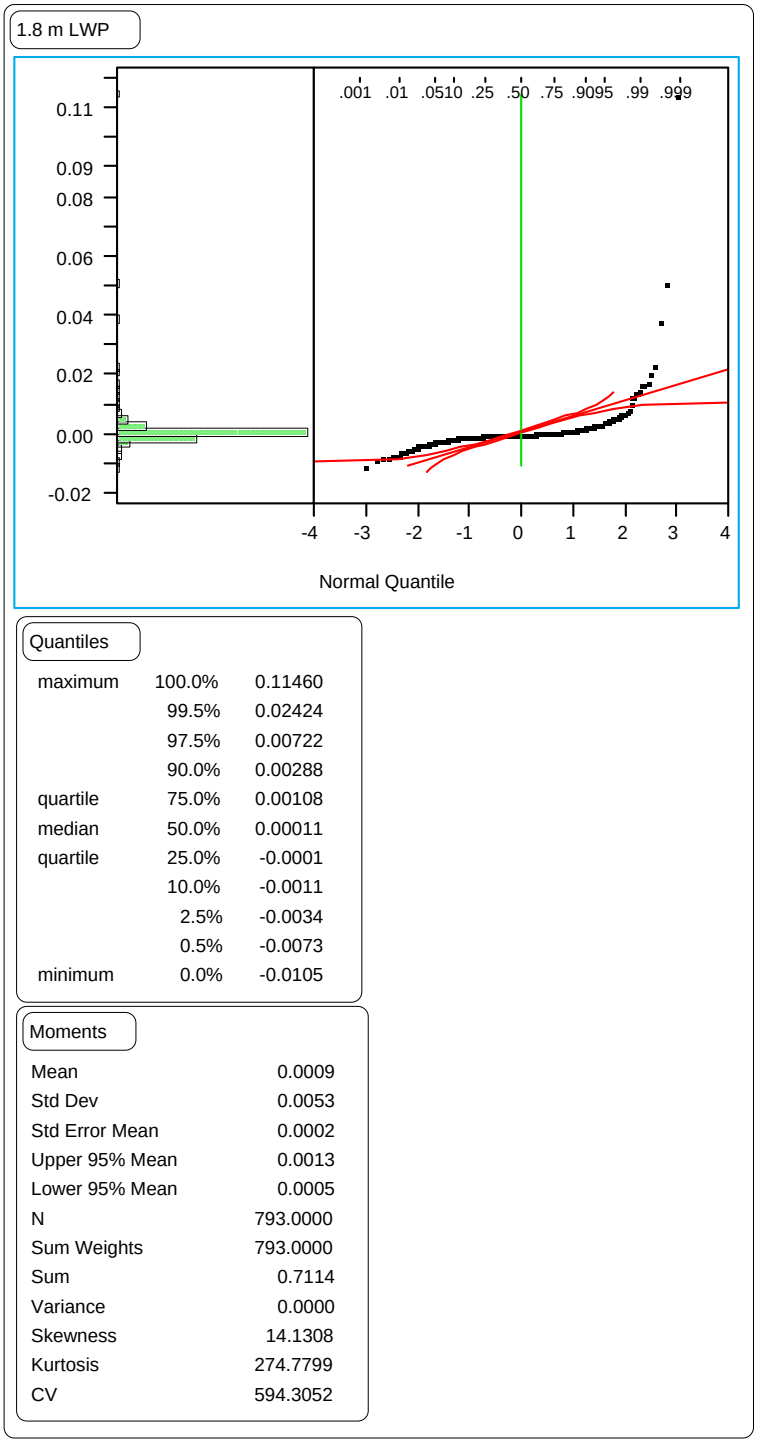

Figure 205. Distribution of the time-series slopes for the LWP 1.8-m rut depths.

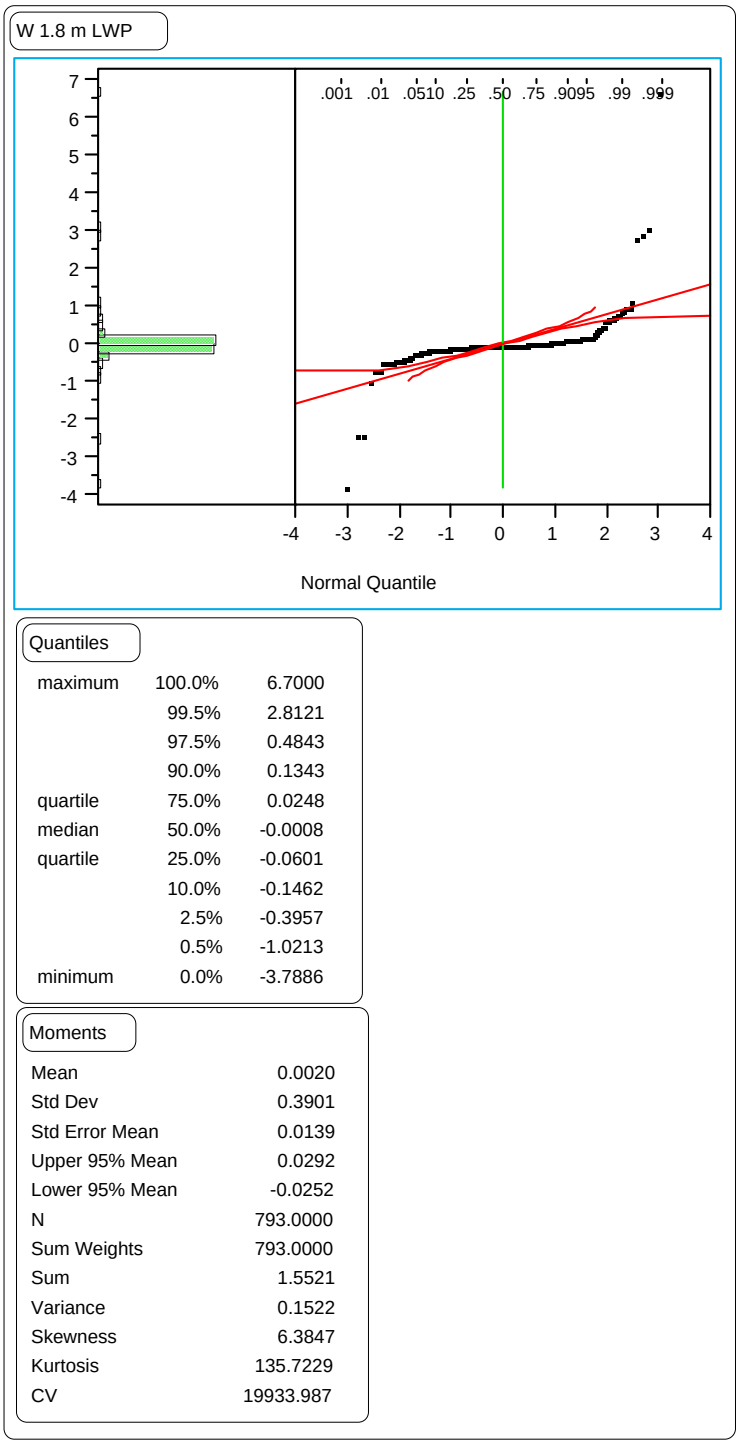

Figure 206. Distribution of the time-series slopes for the LWP 1.8-m rut widths.

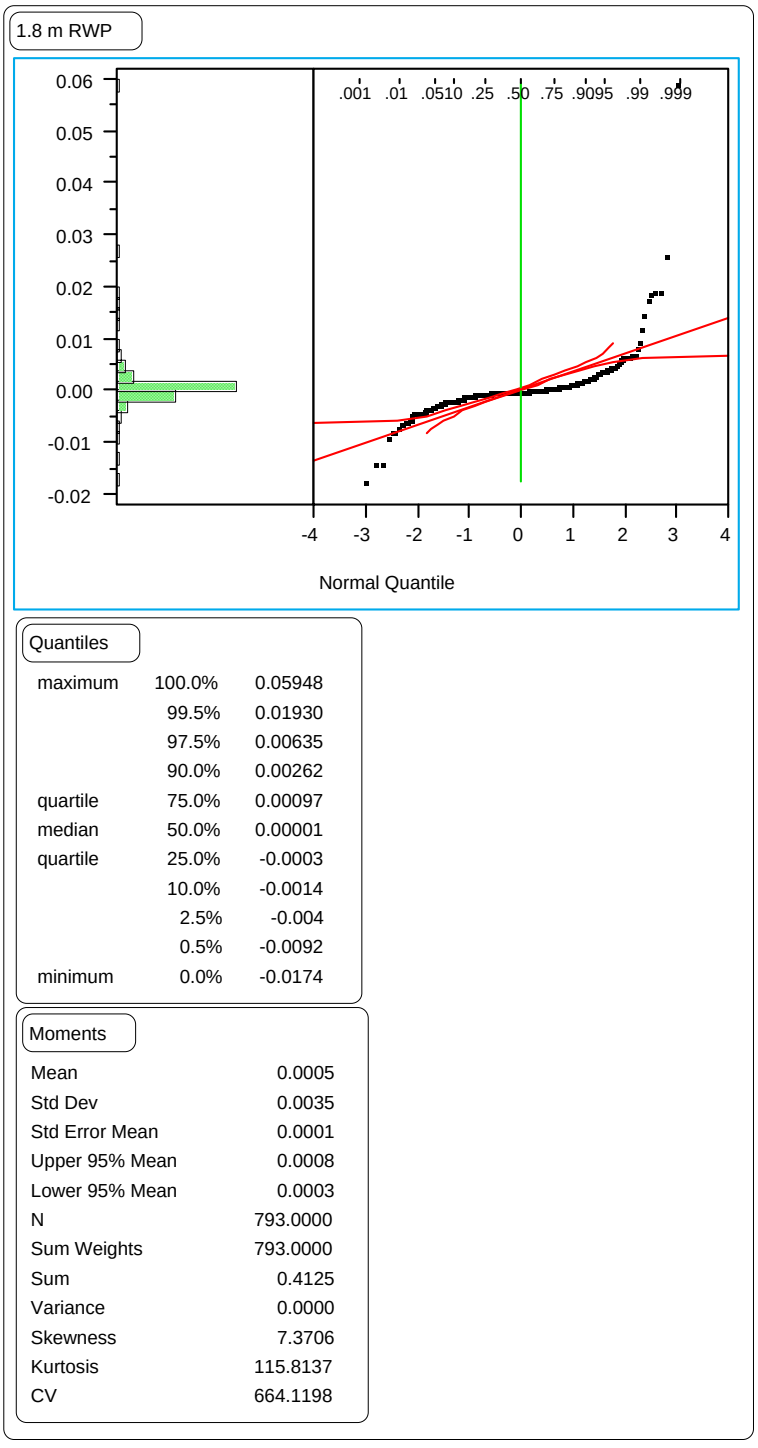

Figure 207. Distribution of the time-series slopes for the RWP 1.8-m rut depths.

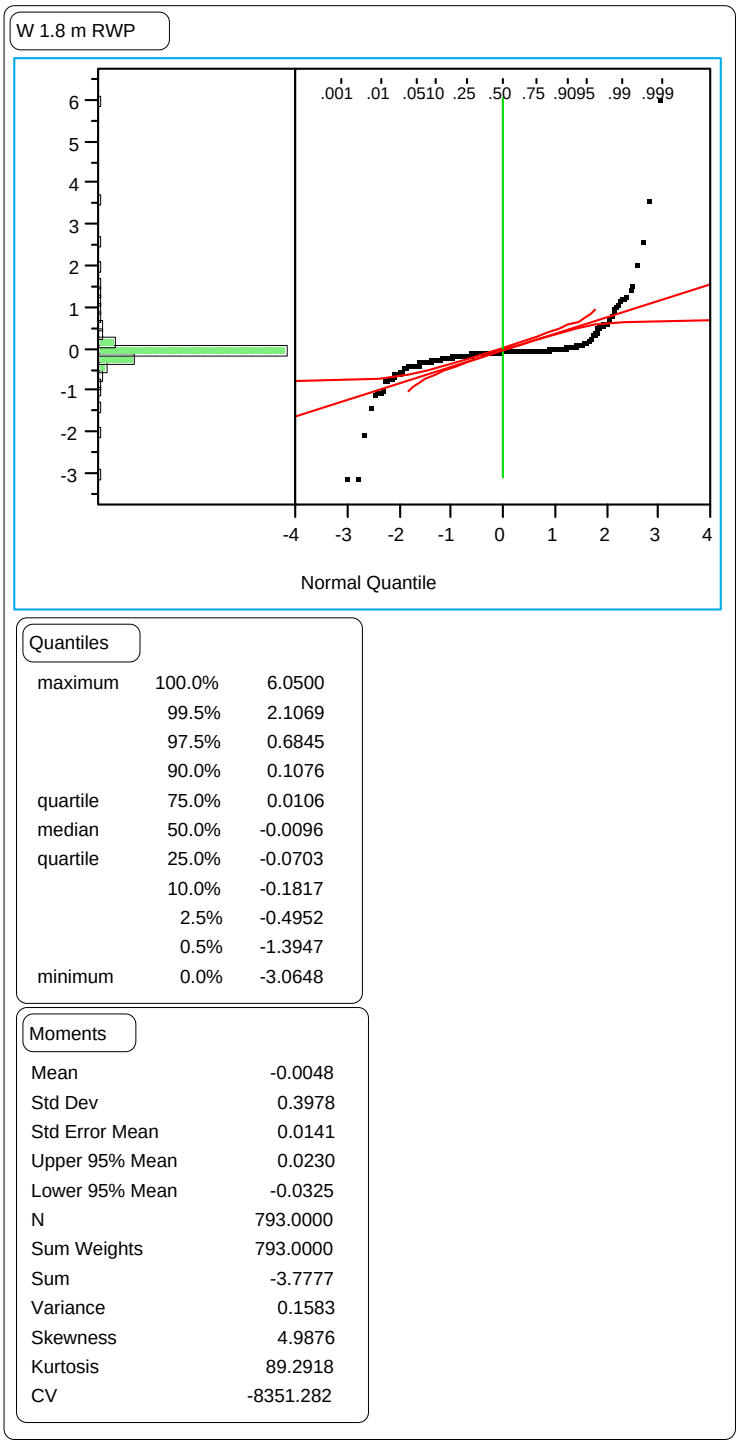

Figure 208. Distribution of the time-series slopes for the RWP 1.8-m rut widths.

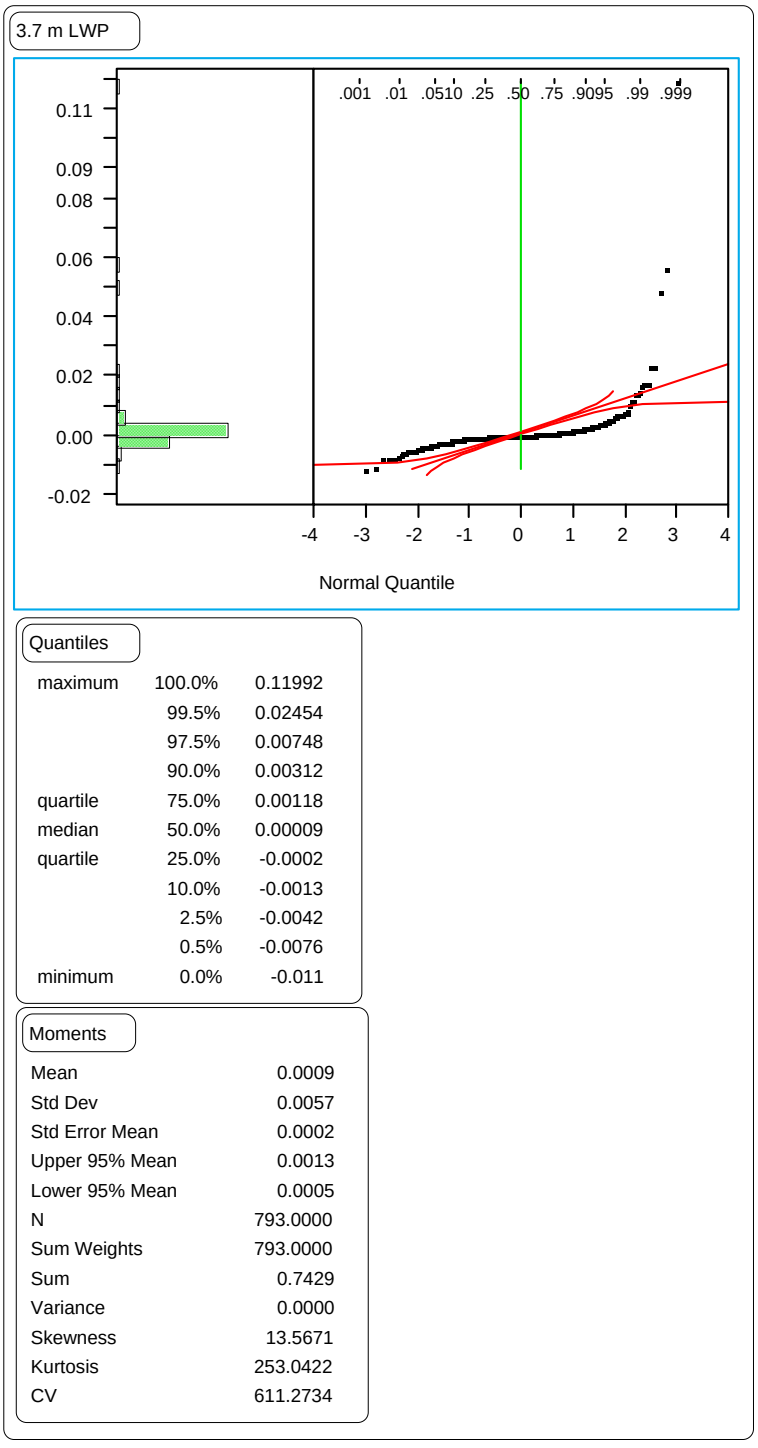

Figure 209. Distribution of the time-series slopes for the LWP wire line rut depths.

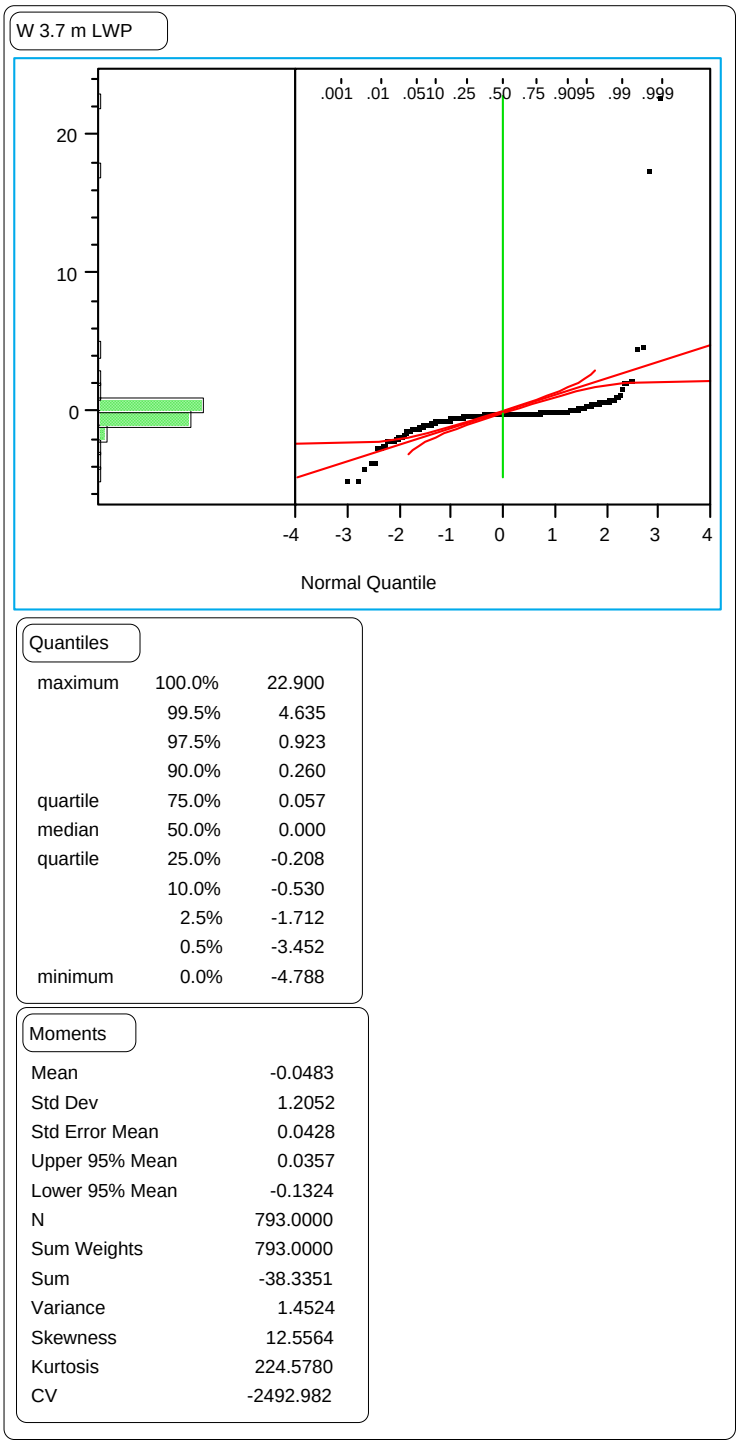

Figure 210. Distribution of the time-series slopes for the LWP wire line rut widths.

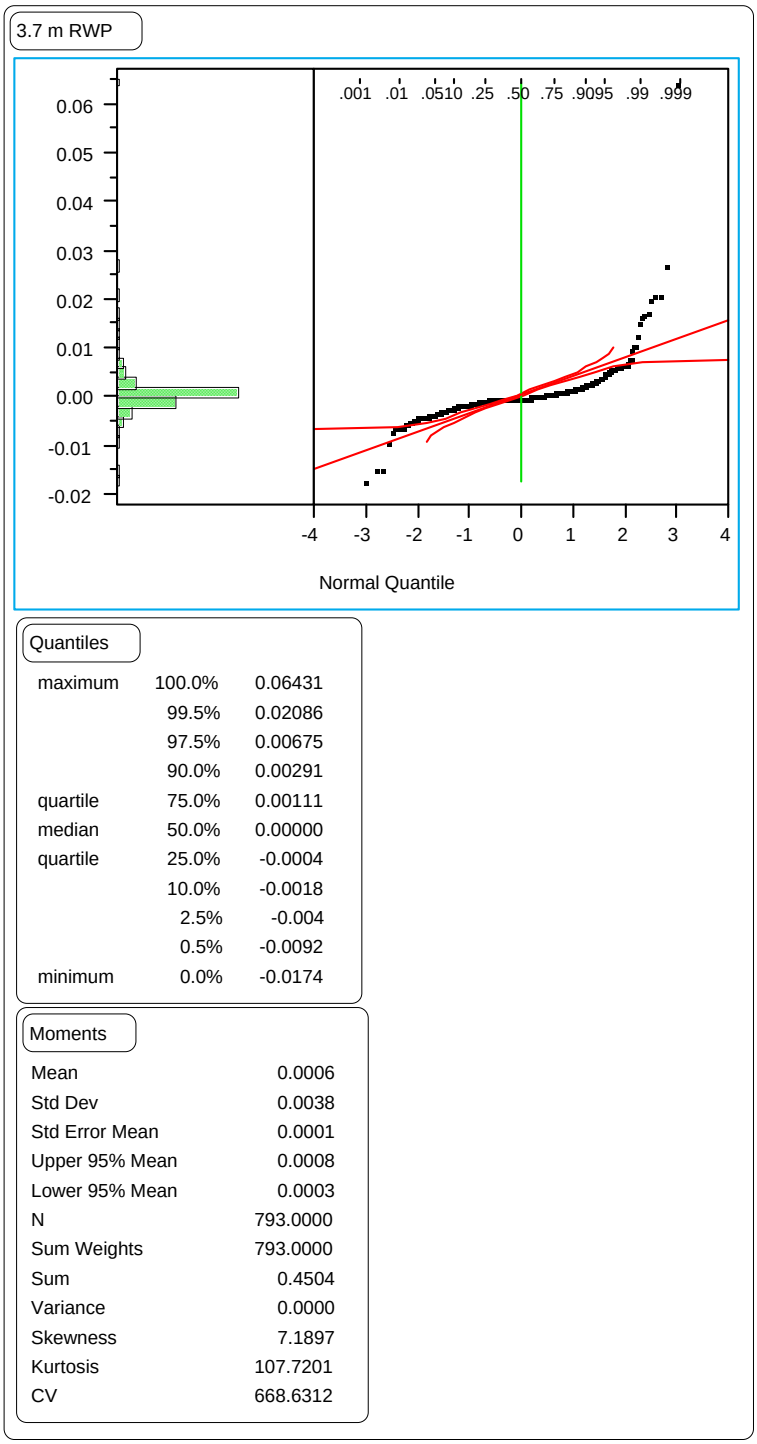

Figure 211. Distribution of the time-series slopes for the RWP wire line rut depths.

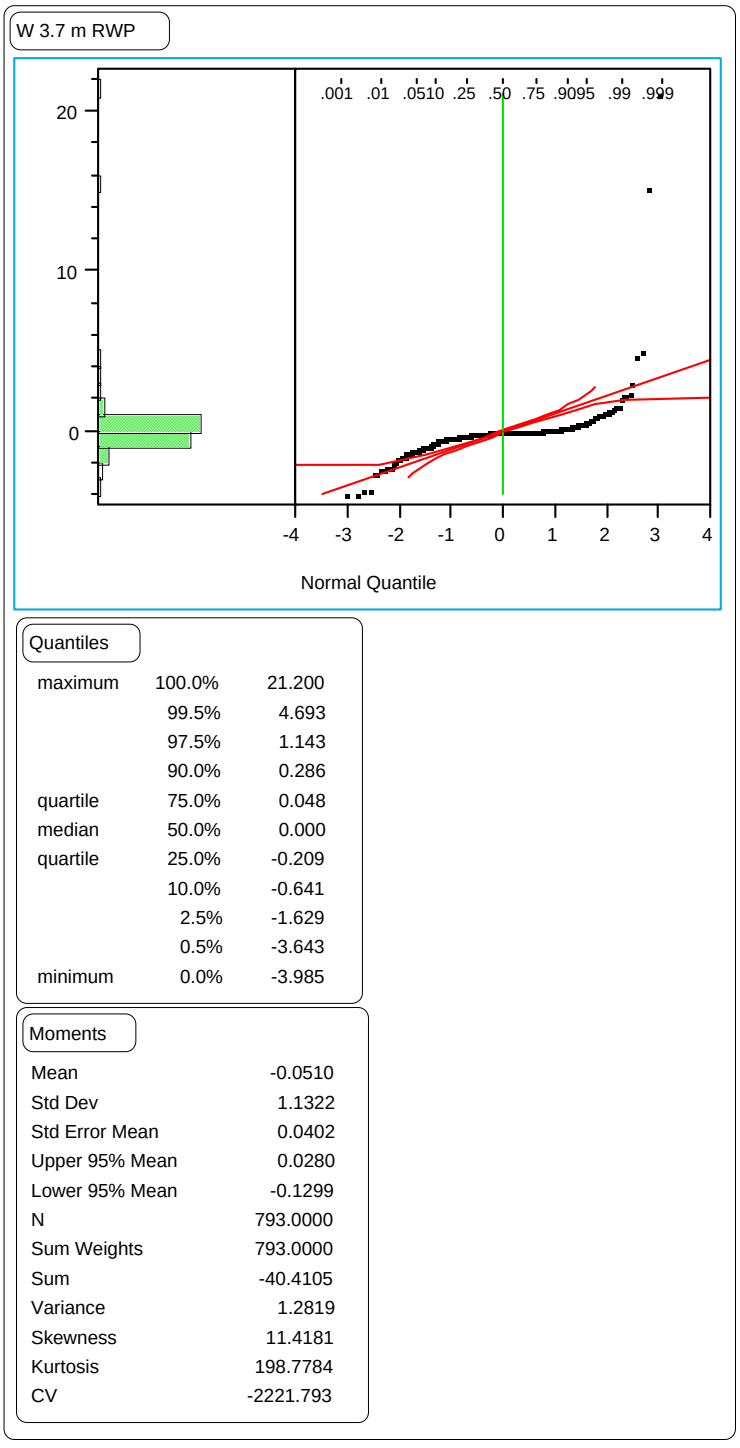

Figure 212. Distribution of the time-series slopes for the RWP wire line rut widths.

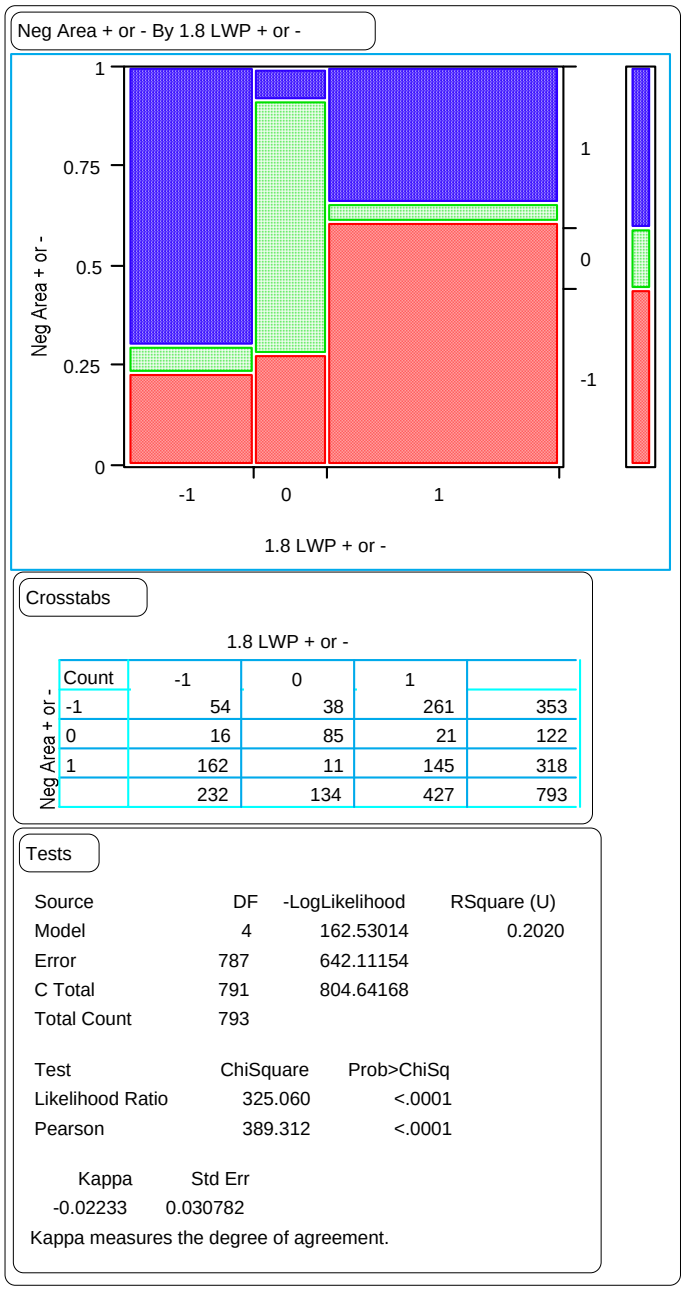

Figure 213. Comparison of the signs of the slopes for the negative area index versus those for the LWP 1.8-m rut depths.

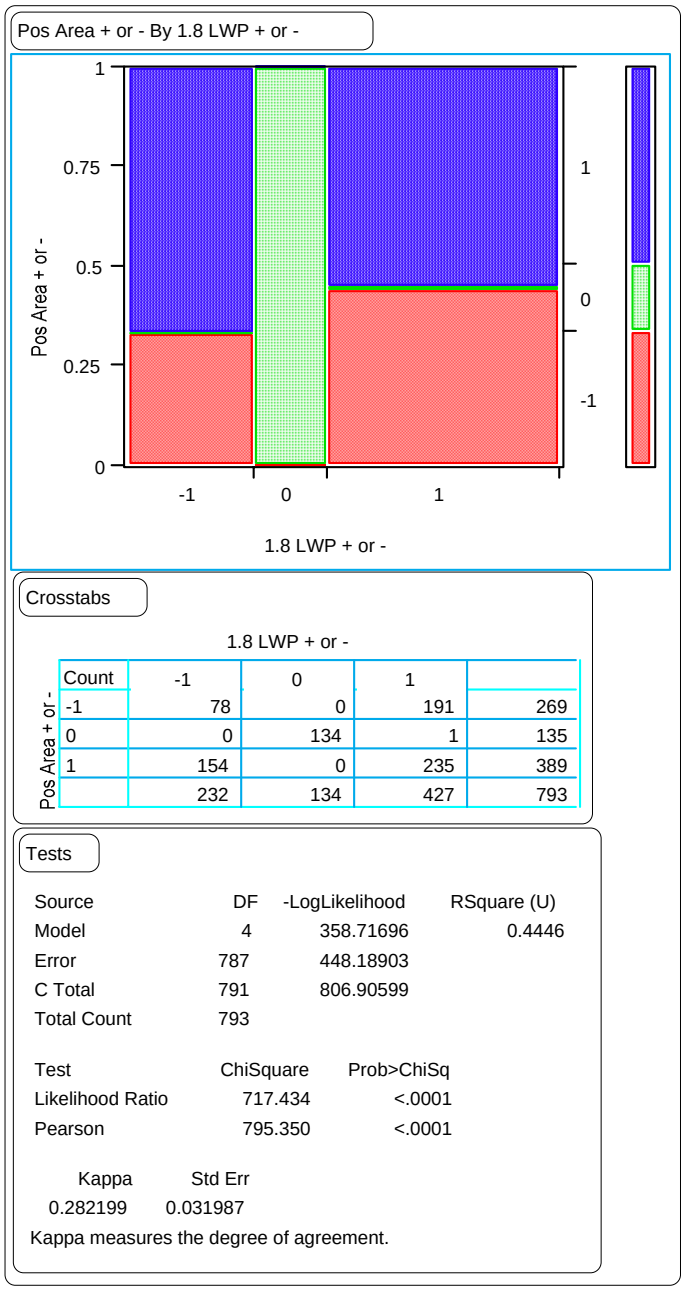

Figure 214. Comparison of the signs of the slopes for the positive area index versus those for the LWP 1.8-m rut depths.

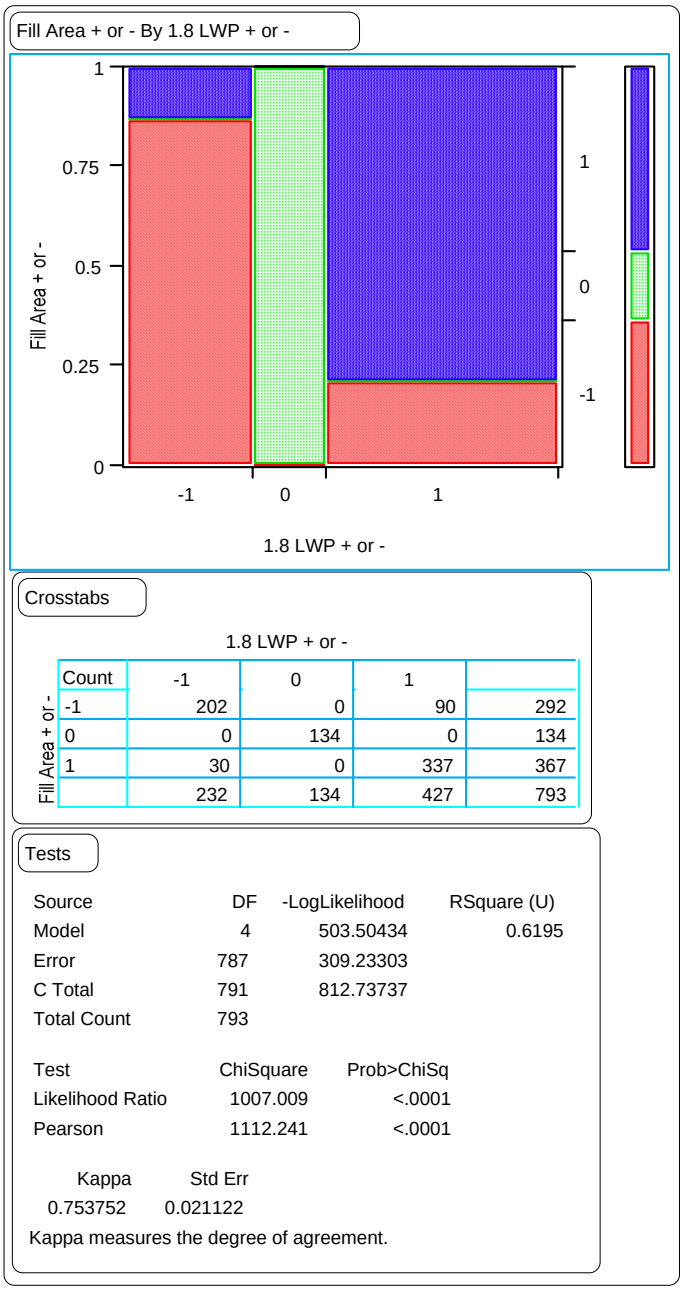

Figure 215. Comparison of the signs of the slopes for the fill area index versus those for the LWP 1.8-m rut depths.

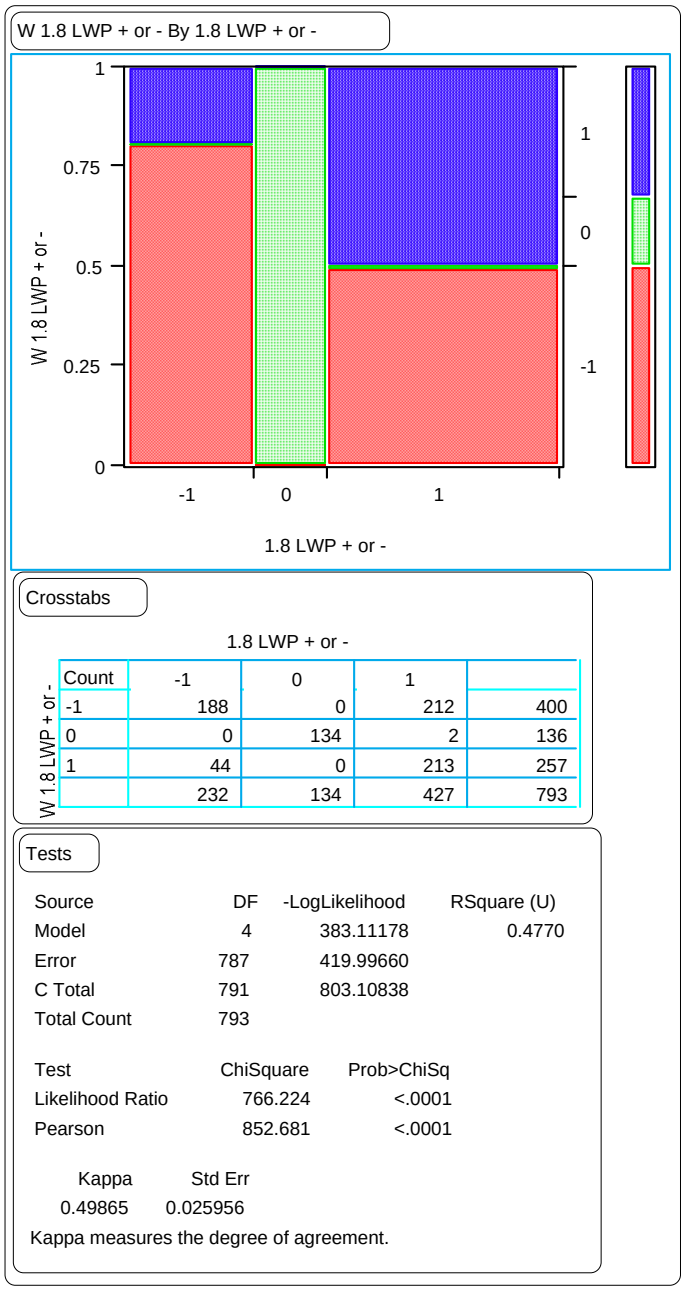

Crosstabs

1.8 LWP + or -

W 1.8 LWP + or -	Count	-1	0	1	
	-1	188	0	212	400
	0	0	134	2	136
	1	44	0	213	257
		232	134	427	793

Tests

Source	DF	-LogLikelihood	RSquare (U)
Model	4	383.11178	0.4770
Error	787	419.99660	
C Total	791	803.10838	
Total Count	793		

Test	ChiSquare	Prob>ChiSq
Likelihood Ratio	766.224	<.0001
Pearson	852.681	<.0001

Kappa	Std Err
0.49865	0.025956

Kappa measures the degree of agreement.

Figure 216. Comparison of the signs of the slopes for the LWP 1.8-m rut widths versus those for the LWP 1.8-m rut depths.

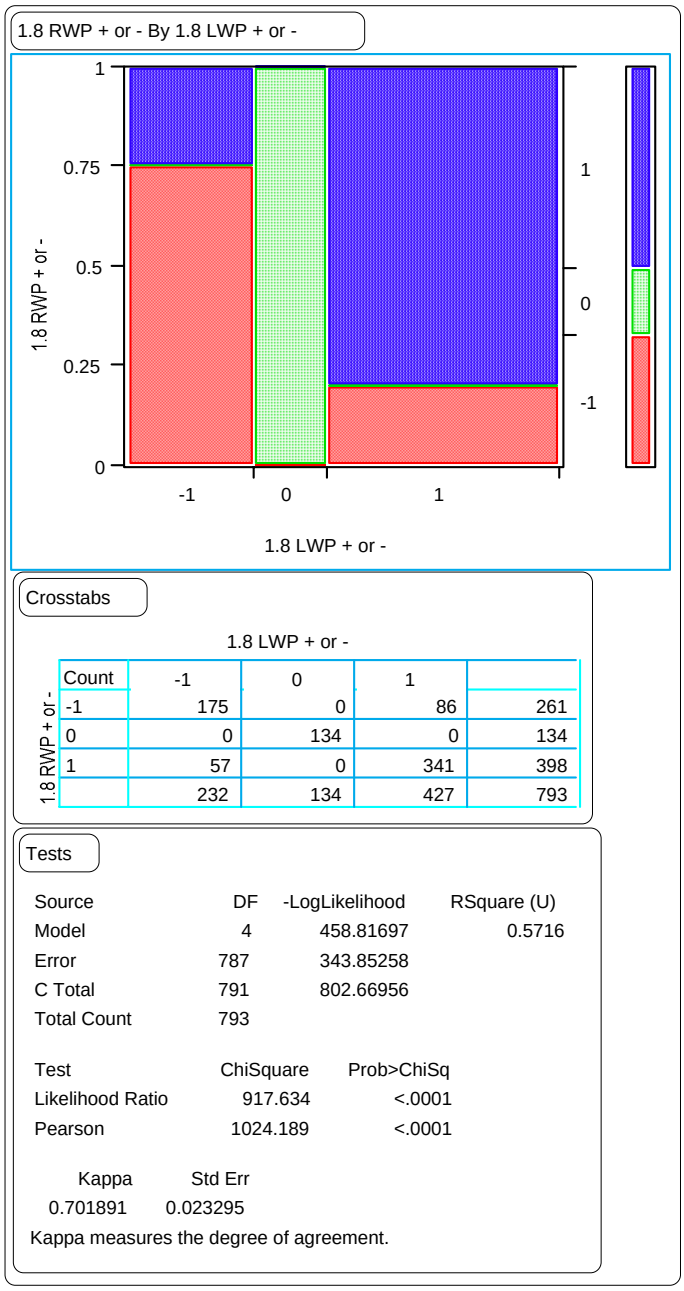

Figure 217. Comparison of the signs of the slopes for the RWP 1.8-m rut depths versus those for the LWP 1.8-m rut depths.

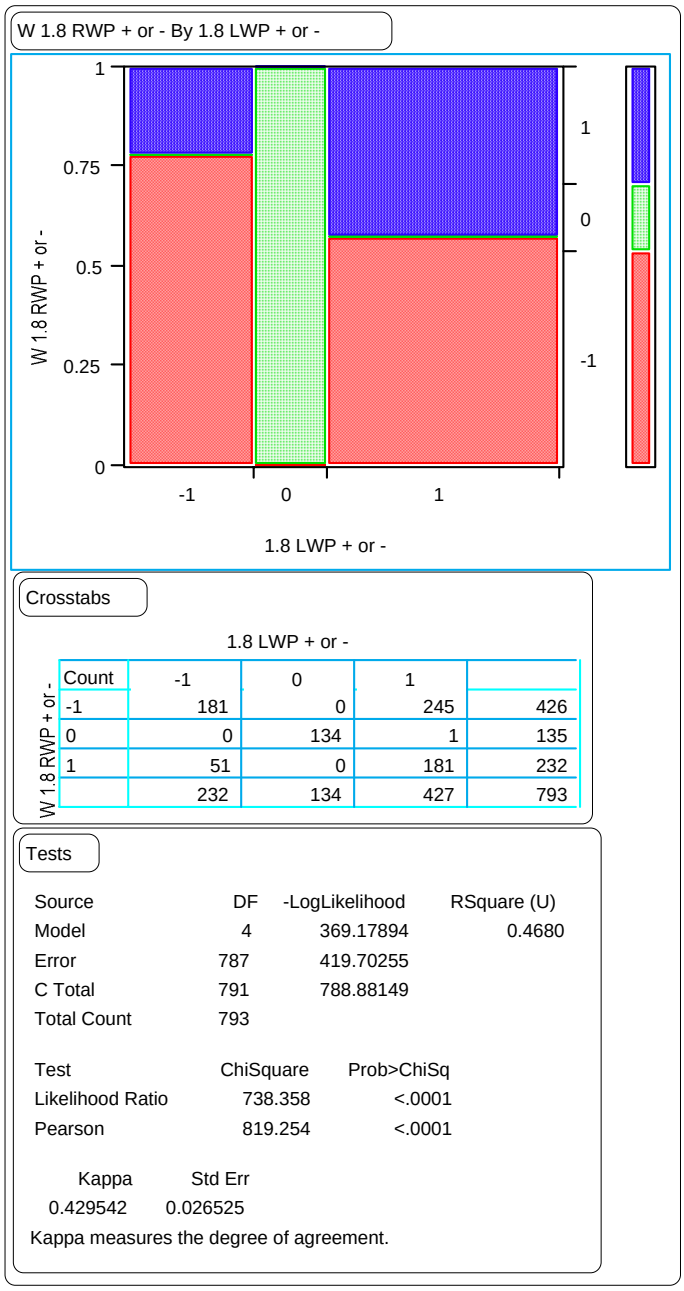

Figure 218. Comparison of the signs of the slopes for the RWP 1.8-m rut widths versus those for the LWP 1.8-m rut depths.

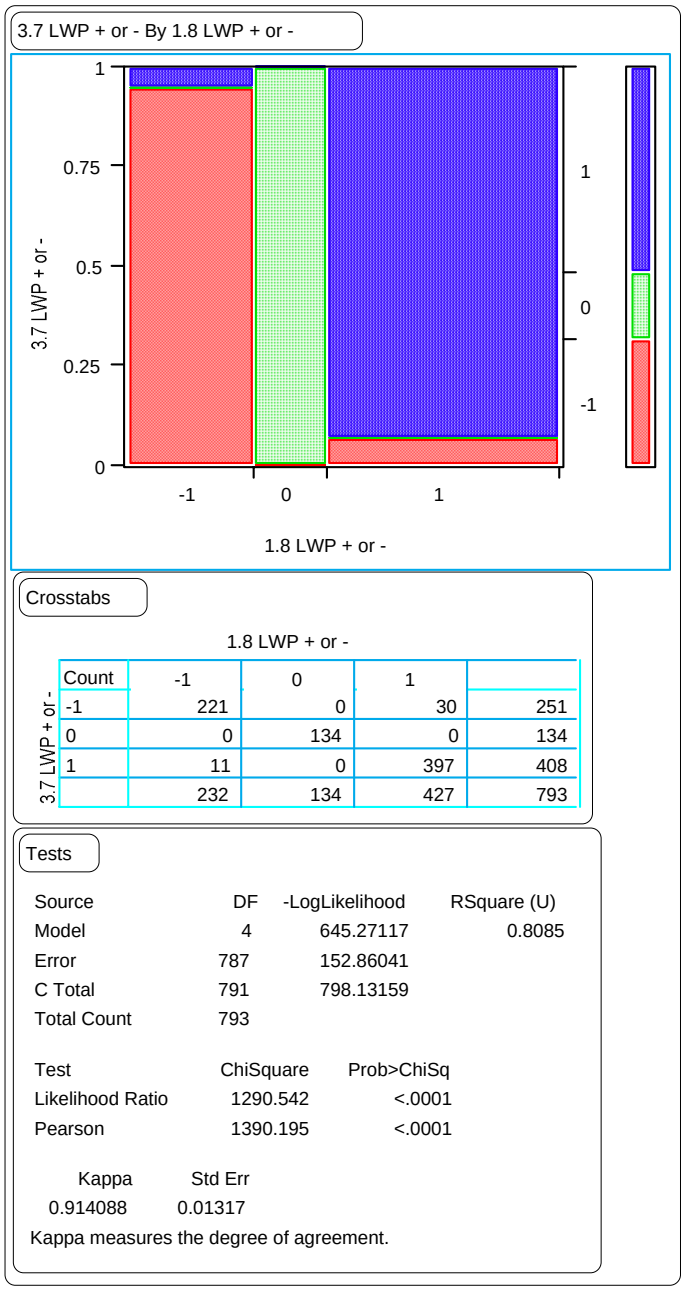

Figure 219. Comparison of the sign of the slopes for the LWP wire line rut depths versus those for the LWP 1.8-m rut depths.

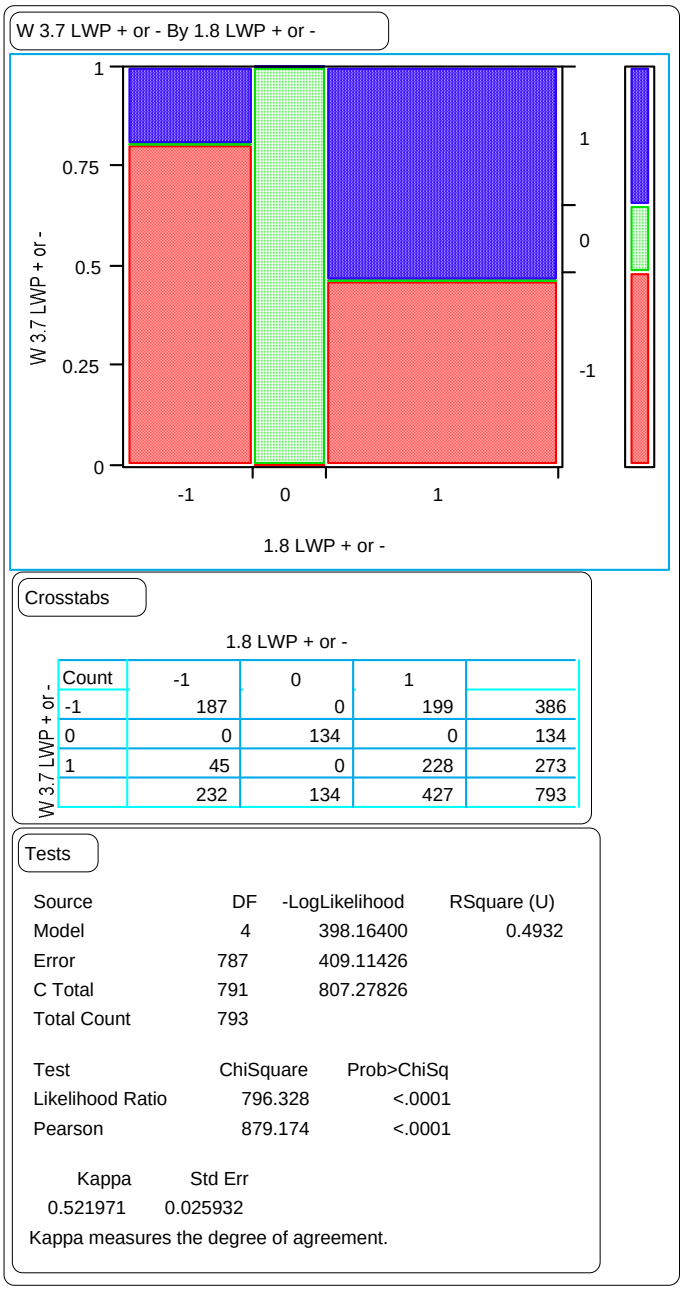

Figure 220. Comparison of the signs of the slopes for the LWP wire line rut widths versus those for the LWP 1.8-m rut depths.

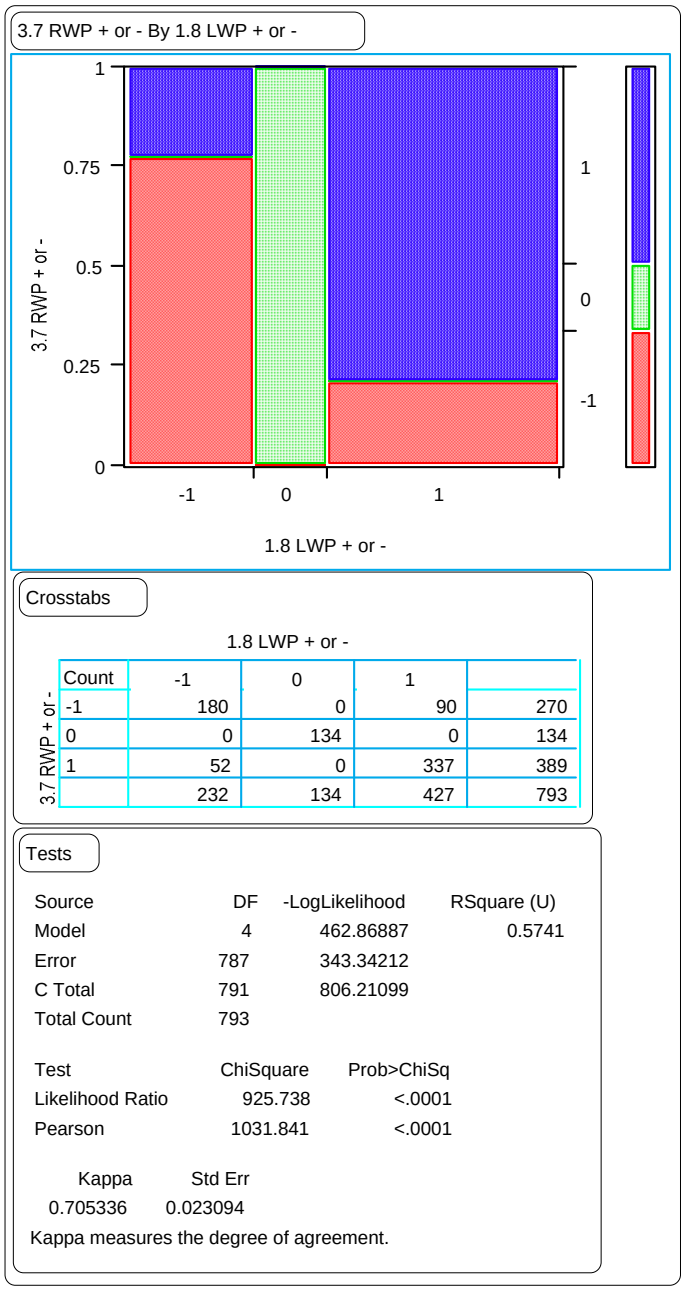

Figure 221. Comparison of the signs of the slopes for the RWP wire line rut depths versus those for the LWP 1.8-m rut depths.

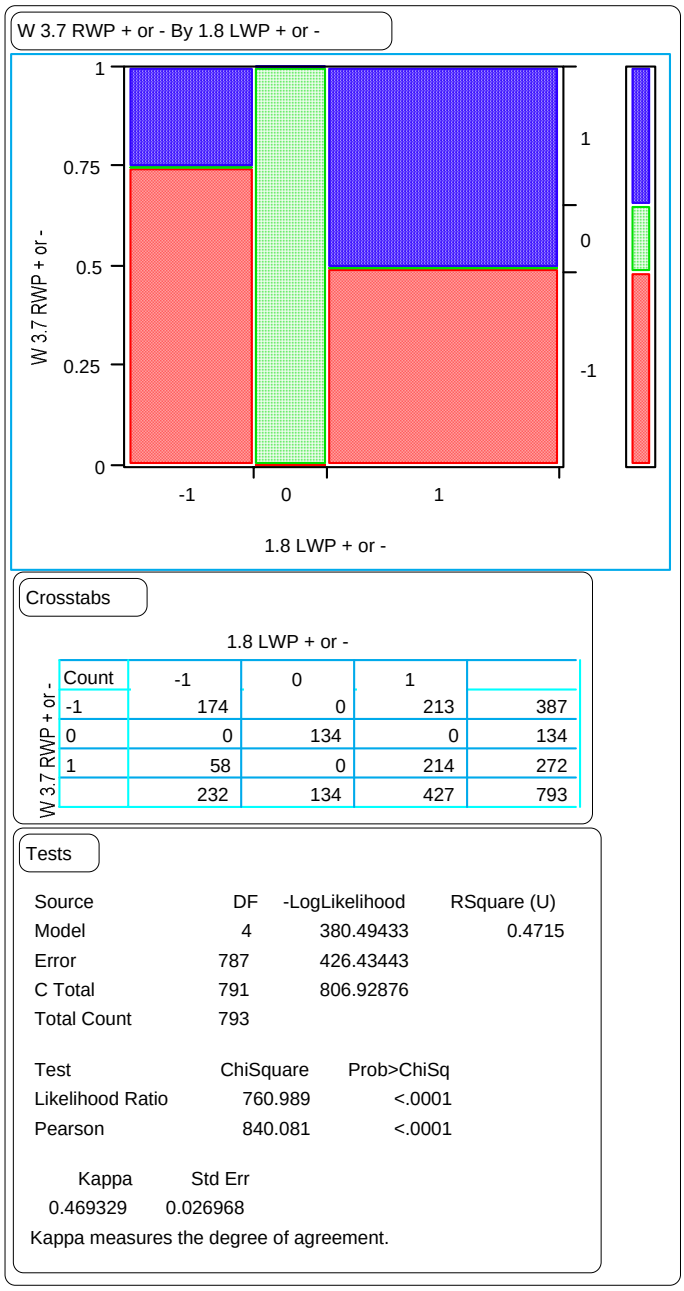

Figure 222. Comparison of the signs of the slopes for the RWP wire line rut widths versus those for the LWP 1.8-m rut depths.

REFERENCES

1. Gramling, W.L. and Hunt, J.E. *Photographic Pavement Distress Record Collection and Transverse Profile Analysis*, Report No. SHRP-P-600, National Research Council, Washington, D.C., 1993, unpublished.

2. *Distress Identification Manual for the Long-Term Pavement Performance Project*, Report No. SHRP-P-338, National Research Council, Washington, D.C., 1993.

3. Henderson, B. and Abukhater, B. *Long Term Pavement Performance PROQUAL V2.08 Users Documentation*, June 1998, Publication No. FHWA-TS-98-00-01, Federal Highway Administration, McLean, Virginia, June 1998.

4. *The AASHO Road Test, Report 5 Pavement Research*, Special Report 61E, Highway Research Board, Washington, D.C., 1962.

5. Simpson, A.L.; Rauhut, J.B.; Jordahl, P.J.; Owusu-Antwi, E.; Darter, M.I.; Ahmad, R.; Pendleton, O.J.; and Lee, Y.H. *Sensitivity Analyses for Selected Pavement Distresses*, Report No. SHRP-P-393, National Research Council, Washington, D.C., 1994.

6. Von Quintus, H. and Killingsworth, B. *Analyses Relating to Pavement Material Characterizations and Their Effects on Pavement Performance*, Report No. FHWA-RD-97-085, Federal Highway Administration, McLean, Virginia, 1998.

7. Thomas, G.B., Jr. and Finney, R.L. *Calculus and Analytic Geometry*, Sixth Edition, Addison-Wesley Publishing Company, Reading, Massachusetts, 1984.

8. Rosner, B. *Fundamentals of Biostatistics*, Third Edition, PSW-Kent Publishing Company, Boston, Massachusetts, 1990.

9. ASTM C670-96, "Standard Practice for Preparing Precision and Bias Statements for Test Methods for Construction Materials," *ASTM Standards on Precision and Bias for Various Applications*, Fifth Edition, American Society for Testing and Materials, West Conshohocken, Pennsylvania, 1997.